PO Box 2345, Beijing 100023, China
Fax: +86-10-85381893
E-mail: wjg@wjgnet.com www.wjgnet.com

World J Gastroenterol 2004;10(19):2773-2774
World Journal of Gastroenterology
Copyright © 2004 by The WJG Press ISSN 1007-9327

• EDITORIAL •

Why a *World Journal of Gastroenterology*?

Pelayo Correa

Pelayo Correa, Boyd Professor, Department of Pathology, Louisiana State University, LSU Health Sciences Center, 1901 Perdido Street, Box P5-1, New Orleans, LA 70112, USA
Correspondence to: Pelayo Correa, Boyd Professor, Department of Pathology, Louisiana State University, LSU Health Sciences Center, 1901 Perdido Street, Box P5-1, New Orleans, LA 70112, USA. correa@lsuhsc.edu
Teleohone: +1-504-568-6035 **Fax:** +1-504-599-1278
Received: 2004-06-11 **Accepted:** 2004-06-22

Correa P. Why a *World Journal of Gastroenterology*? *World J Gastroenterol* 2004; 10(19): 2773-2774
http://www.wjgnet.com/1007-9327/10/2773.asp

When a new medical journal is launched, the reaction is frequent: Why? Do we have already so much to read that we feel overwhelmed? But, the litmus test of a good new journal is: Does it find its way into the reading time of physicians and medical scientists? The new *World Journal of Gastroenterology* has the opportunity to pass that litmus test.

We already have excellent journals of gastroenterology. All have originated as local publications. Some have reached an international status because of the quality of the published materials. Clear examples in the Western world are journals originated in Great Britain, Scandinavia and the United States of America. But they all keep their original flavor which permeates their published materials and reflects mostly the experience and the interest of physicians in the countries they represent.

Gastroenterologists, as most clinicians, tend to draw conclusions from their own experience, which they tend to generalize to "the world". That experience represents the pattern of diseases in their community. But gastrointestinal diseases display radically different patterns in different populations. In the case of cancer, for instance, the incidence of cancers of the colon, liver, biliary system, and stomach displayed rates in some populations that were several times higher than in other populations, as regularly published and illustrated by the International Agency for Research on Cancer[1].

The phenomenon is well illustrated by gastric cancer and its precursor lesions. Their morphologic characteristics were first masterfully described and illustrated by European pioneers such as Faber, Fenwick, Magnus and Kupfer approximately a century ago[2-5]. In those days pernicious anemia was a major medical problem in Europe and was, with good reasons, linked to gastric carcinogenesis. At the present time pernicious anemia has drastically decreased in frequency perhaps due to improved nutrition and sanitation. However, the genes for the predisposition to the syndrome remain in the population. The type of gastric adenocarcinoma originally described in association with pernicious anemia (the papillary type, located in the corpus) has become very rare[6]. But it is entirely possible that the genes that predispose to pernicious anemia in one set of environmental conditions may manifest themselves as a different disease in another set of conditions. It has been suggested in populations susceptible to pernicious anemia, the initial trigger for chronic gastritis may be *Helicobacter pylori* infection. In such populations gastritis may be severe in the corpus leading to atrophy of the oxyntic mucosa[7].

Most clinicians attending only populations of non-European extraction have never seen a case of pernicious anemia. The genes linked to that disease are either rare or not present in their population and gastritis associated with *Helicobacter pylori* in their patients is multifocal but antral predominant, with minimal or absent corpus involvement. Some medical writers concentrated on corpus atrophy as a cancer precursor and ignore the gastric antrum[8]. They might not appreciate that outside Europe, most gastric cancer precursors were predominantly in the antrum, not in the corpus.

Some publications insist that the high cancer risk gastritis phenotype depends on the grade and activity of gastritis in the corpus. The general experience presently showed that the antrum and the antrum-corpus transition zones (mostly the area of the incisura) were the sites of the most advanced lesions, including intestinal metaplasia, dysplasia and carcinoma[9].

The Jarvi-Lauren classification of tumors as "intestinal" or "diffuse" has been challenged. Some reports have concluded that gastric carcinomas may arise as "gastric type" and later convert to a mixed type, expressing gastric and intestinal mucins. It has been suggested that stem cells, from which carcinomas are supposed to arise, are "primarily gastric type" (meaning they encode for gastric mucins only)[10]. Normal stem cells have a minimal amount of acid (intestinal) mucins, indicating repressed genes and explaining their multi-potential characteristics[11]. Obviously the ultimate mechanism of carcinogenesis is not well understood. An attractive hypotheses has been recently discussed by Kirchner *et al.*[12]. They presented scientific evidence in support of a mechanism of carcinogenesis based on atrophy (loss of differentiated cells) followed by re-differentiation of stem cells, which may be abnormal. This would explain the carcinogenic process of the gastric and cardiac mucosae. After atrophy, the so-called complete intestinal metaplasia expresses preferentially small intestinal (sialic) mucins. Later the so called "incomplete" metaplasia appears and expresses several types of mucins, including gastric MUC-5AC and MUC-6, small intestinal MUC-2 and large intestinal DAS-1[13]. These findings do not support gastric carcinoma classification based on mucin expressions as "gastric", "intestinal" or "mixed". Mucins expressed by pre-neoplastic and neoplastic cells represent abnormal re-differentiation which is not a permanent but rather a represent dynamic expression of mucin genes present in stem cells.

We hope that the *World Journal of Gastroenterology* will minimize the "provincial" bias and inspire the authors to be less dogmatic and more eclectic. We also hope that future authors adopt some of the basic teachings of epidemiology. For example, (1) Disease patterns are strongly influenced by the geographic and demographic characteristics of the populations under study. The local experience may not be applicable to all populations. Frequently, more than one demographic group share the same geography, comparison of such groups offers opportunities for etiologic research. (2) Disease frequency determines population risk and there are clear rules to assign causality. As an example, cancer frequency is often measured in the number of cases per 100 000 populations. Invasive gastric carcinoma is the final stage of a prolonged precancerous process involving chronic gastritis, atrophy, metaplasia and dysplasia. As in precancerous processes in other organs, the earlier stages are very frequent but less predictive of eventual neoplastic outcomes. Later stages have a lower prevalence in the population but are better indicators of cancer risk. Let us

remember that the skin of all people is exposed to the effects of sun rays which may lead to several degrees of actinic damage. But very few develop skin cancer. Large cohorts observed for many years may provide more valid data than small cohorts followed-up for a few years. Large cohorts have been reported in Finland, Yugoslavia and Japan[14-16]. (3) As in all medical sciences, epidemiologic observations may be biased. But epidemiologists have figured out how to deal with bias. Causal *vs* non-causal associations are distinguished by epidemiologic criteria such as strength, consistency, temporality, and plausibility of the associations.

Recent advances in medicine and biology have made it possible to depend less on experimental animals to test causality. Molecular changes can be traced in human cells, tissues and fluids, but molecular techniques are not an end in themselves. Clinicians and medical scientists should remember that these new techniques are merely tools to explore causality in human beings. The new science of molecular epidemiology in some way should make molecular biologists use the epidemiologic techniques to analyze their findings. Similarly, classical epidemiologists need to become acquainted with the new powerful tools provided by molecular biologists. More than ever, multidisciplinary teams are needed to make real progresses in our understanding of the complex processes of carcinogenesis.

REFERENCES

1 **Parkin DM**, Whelan S, Ferlay S. Cancer incidence in five continents. Vol. VII. International Agency for Research on Cancer Publication. *Lyon, France* 1993: 143

2 **Faber K**, Block CE. Uber die pathologischen Verenderungen am digestion tractus bei die perniciosen anemia und ulcer die Sogennante. *Dermat Z Klin Med* 1900; **40**: 98

3 **Fenwick S**. On atrophy of the stomach. *Lancet* 1870; **2**: 78-80

4 **Kupfer C**. Festschrift. *Arz Verein Munch* 1883: 7

5 **Magnus HA**. A re-assessment of the gastric lesion in pernicious anaemia. *J Clin Path* 1958; **11**: 289-295

6 **Elsborg L**, Mosbech J. Pernicious anemia as a risk factor in gastric cancer. *Acta Medica Scandinavica* 1979; **206**: 315-318

7 **Carmel R**, Perez-Perez G, Blaser MJ. *Helicobacter pylori* infection and food cobalamine malabsorption. *Dig Dis Sci* 1994; **39**: 309-314

8 **Meining A**, Morgner A, Miehlke S, Bayerdorffer E, Stolte M. Atrophy-metaplasia-dysplasia-carcinoma sequence in the stomach: a reality or merely a hypotheses? *Best Pract Res Clin Gastroenterol* 2001; **15**: 983-998

9 **Rugge M**, Cassaro M, Pennelli G. Atrophic gastritis: pathology and endoscopy in the reversibility assessment. *Gut* 2003; **52**: 1387-1388

10 **Endoh Y**, Sakata K, Tamura G, Ohmura K, Ajioka Y, Watanabe H, Motoyama T. Cellular phenotypes of differentiated type adenocarcinoma and precancerous lesions of the stomach are dependent on the genetic path ways. *J Path* 2000; **191**: 257-263

11 **Jass JR**, Filipe MI. The mucin profiles of normal gastric mucosa, intestinal metaplasia and its variants and gastric carcinoma. *Histochem J* 1981; **13**: 931-939

12 **Kirchner T,** Muller S, Hattori T, Mukaisyo K, Papadopoulos T, Brabletz T, Jung A. Metaplasia, intraepithelial neoplasia and early cancer of the stomach are related to dedifferentiated epithelial cells defined by cytokeration - 7 expressions in gastritis. *Virchow's Arch* 2001; **439**: 512-522

13 **Piazuelo MB**, Haque S, Delgado A. Phenotypic differences between esophageal and gastric intestinal metaplasia. *Mod Pathol* 2004; **19**: 62-74

14 **Siurala M**, Isokoski M, Varis K. Prevalence of gastritis in a rural population. *Scand J Gastroenterol* 1968; **3**: 211-223

15 **Filipe MI**, Munoz N, Matko I, Kato I, Pompe-Kirn V, Jutersek A, Teuchmann S, Benz M, Prijon T. Intestinal metaplasia types and the risk of gastric cancer: a cohort study in Slovenia. *In J Cancer* 1994; **57**: 324-329

16 **Ohata H**, Kitauchi S, Yoshimura N, Mugitani K, Iwane M, Nakamura H, Yoshikawa A, Yanaoka K, Arii K, Tamai H, Shimizu Y, Takeshita T, Mohara O, Ichinose M. Progression of chronic atrophic gastritis associated with *Helicobacter pylori* infection increases risk of gastric cancer. *Int J Cancer* 2004; **109**: 138-143

Edited by Xu XQ, Wang XL and Zhang JZ **Proofread by** Xu FM

PO Box 2345, Beijing 100023, China
Fax: +86-10-85381893
E-mail: wjg@wjgnet.com www.wjgnet.com

World J Gastroenterol 2004;10(19):2775-2778
World Journal of Gastroenterology
Copyright © 2004 by The WJG Press ISSN 1007-9327

• ESOPHAGEAL CANCER •

p53 polymorphism in human papillomavirus-associated Kazakh's esophageal cancer in Xinjiang, China

Xiao-Mei Lu, Yue-Ming Zhang, Ren-Yong Lin, Xiao-Hui Liang, Ya-Lou Zhang, Xing Wang, Yan Zhang, Yan Wang, Hao Wen

Xiao-Mei Lu, Ren-Yong Lin, Xiao-Hui Liang, Ya-Lou Zhang, Xing Wang, Yan Zhang, Yan Wang, Hao Wen, Medical Research Center, 1st Teaching Hospital, Xinjiang Medical University, Urumqi 830054, Xinjiang Uygur Autonomous Region, China
Yue-Ming Zhang, Public and Health College, Xinjiang Medical University, Urumqi 830054, Xinjiang Uygur Autonomous Region, China
Supported by Xinjiang Key Laboratory Foundation, No. XJDX0202-2003-05
Correspondence to: Hao Wen, Ph.D., Professor, Medical Research Center, 1st Teaching Hospital, Xinjiang Medical University, No.1 Liyushan Road, Urumqi 830054, Xinjiang Uygur Autonomous Region, China. wenhao2002@hotmail.com
Telephone: +86-991-4362844 **Fax:** +86-991-4324139
Received: 2004-03-26 **Accepted:** 2004-04-05

Abstract

AIM: To investigate the relationship between *p53* codon 72 polymorphism and human papillomavirus (HPV) type 16 infection in Kazakh's esophageal cancer (EC) in Xinjiang, China.

METHODS: Encoding regions of *p53* codon 72 and HPV-16 *E6* were amplified by polymerase chain reaction-restriction fragment length polymorphism (PCR-RFLP) and polymerase chain reaction (PCR) methods using pairs of primary esophageal squamous cell carcinoma (SCC) tissue and corresponding normal mucosa, which were collected from 104 patients of Kazakh in Xinjiang, China.

RESULTS: Only arginine allele was detected in 70.1% (39/55) of HPV-16-*E6*- positive cases but only in 40.8% (20/49) of HPV-16-*E6*-negative cases ($P<0.05$; *OR*, 3.53; 95% *CI*, 1.57-7.98). In contrast, such a significant correlation between *p53* polymorphism and HPV infection was not evident in corresponding normal mucosae. The allele frequency of *Arg* allele in cancer cases (0.68) was higher than that in normal mucosa samples (0.54) ($P<0.05$; *OR*, 1.80; 95% *CI*, 1.21-2.69).

CONCLUSION: *p53* codon 72 *Arg* homozygous genotype is one of the high-risk genetic factors for HPV-associated SCC of Kazakh. Individuals carrying *Arg* allele compared to those with *Pro* allele have an increased risk for esophageal SCC.

Lu XM, Zhang YM, Lin RY, Liang XH, Zhang YL, Wang X, Zhang Y, Wang Y, Wen H. *p53* polymorphism in human papillomavirus-associated Kazakh's esophageal cancer in Xinjiang, China. *World J Gastroenterol* 2004; 10(19): 2775-2778
http://www.wjgnet.com/1007-9327/10/2775.asp

INTRODUCTION

Esophageal cancer is common in several areas of central Asia, including Xinjiang Uygur Autonomous Region,China. The incidence of Kazakh's EC is the highest among population in Xinjiang and its age-adjusted mortality rate up to 91/100 000 has been reported in Kazakh's population[1]. The population size of Kazakh was estimated to be 13 million around the world and 10 million Kazakh distributed in Kazakhstan and 2 million in Xinjiang, China. The population in the present study was a Kazakh isolated community located at the Northeast of Xinjiang. The genetic homogeneity and geography stability of the population, along with shared exposure to common environmental variables, provide an excellent opportunity for the study of genetic influence on EC. These cancers are mostly SCC , and show a high frequency of mutation in the *p53* tumor suppressor[2]. Epidemiological studies have suggested that a number of risk factors are involved in the carcinogenesis of Kazakh's SCC, including deficiencies in vitamins and minerals, consumption of pickled foods and environmental exposure to specific nitrosamines, *etc* [3,4]. Viral infections, in particular HPV infection, have been reported in esophageal cancers from China, and HPV DNA has been detected in 0-60.0% of cancer tissues by polymerase chain reaction analysis[5,6]. HPV is implicated in the pathogenesis of squamous cell carcinoma of the cervix and esophagus. HPV-16 encodes *E6* protein, which binds to cellular tumor-suppresser protein *p53* and directs degradation through the ubiquitin pathway[7]. This event is mediated by another cellular protein termed *E6*-AP, a component of the ubiquitin pathway[8,9]. The arginine allele at codon 72 of *p53* was found to be more susceptible to degradation by HPV *E6* protein than the proline allele *in vivo*, thus resulting in a high frequency of esophageal SCC in individuals homozygous for arginine at the codon[8]. On the basis of these experiments, it has been widely assumed that *p53* is functionally inactivated by the viral *E6* protein in HPV-associated cancer cells and that infection with high-risk HPV types leads to the same phenotype as a loss of *p53* function because of *p53* gene mutations or direct degradation[9].The association of *p53* codon 72 polymorphism with HPV-16-associated esophagus SCC risk has been studied by several groups but with inconsistent results. Kawaguchi *et al*.[10] reported that the form of *p53* protein carrying an *Arg* residue at this position in HPV-16/18 positive samples was found to be significantly more susceptible to degradation by *E6* protein than that in HPV-16/18 negative samples. There are controversial results from several clinical studies of esophagus SCC[11,12]. A part of Kazakh's esophageal SCC correlated with the presence of HPV-16/18[13]. To our knowledge, *p53* polymorphism in Kazakh's esophageal SCC has apparently not been documented. In this study, we investigated the genotypic frequency of *p53* codon 72 polymorphism and HPV-16 *E6* in Kazakh's esophageal SCC patients in Xinjiang, China. The data we obtained seemed to be the first regarding the association of this polymorphism with HPV-associated risk for cancer of the esophagus.

MATERIALS AND METHODS

Tissue specimens

Pairs of primary Kazakh's esophageal SCC tissue and corresponding normal mucosa were obtained from 63 patients who underwent surgery in the Department of Surgery, 1st Teaching Hospital of Xinjiang Medical University, from 1999 to 2003, and from 41 patients who underwent surgery in

Department of Surgery, the People's Hospital of Xinjiang Uygur Autonomous Region, China, between 1998 and 2000. No patient had been given treatment prior to the study. In all cases the histopathological type of tumors was squamous cell carcinoma. Cancer tissues and well-separated normal esophageal mucosae obtained from surgically resected esophageal SCC patients were fixed in 40 g/L formaldehyde and embedded in paraffin. Genomic DNA was prepared by proteinase K digestion and phenol/chloroform extraction, followed by ethanol precipitation, as described by Greer *et al*.[14].

HPV detection and identification

First, as a control, purified genomic DNA was successfully amplified by PCR using primers specific for the β-globin gene, indicating a suitable quality and quantity of DNA. PCR analysis was then performed using HPV-16 *E6* oligodeoxynucleotide primers as follows: HPV-16*E6* forward, 5'-GCAAGCAACAGTTACTGCGA-3' and reverse, 5'-CAACAAGACATACATCGACC-3'. Amplified PCR products were then determined by electrophoresis on 15 g/L agarose gels stained with ethidium bromide. Finally, the gels were analyzed by DC-2000 image system (Bio-Rad, USA).

Analysis of codon 72 polymorphism

p53 exon 4 (codons 33-125) containing codon 72 was amplified by PCR using oligodeoxynucleotide primers 5'-TGAGG*ACC*TGGTCCTCTGAC-3' (forward) and 5'-AGAGGAATCCCAAAGTTCCA-3' (reverse), under the following conditions: denaturation at 94 ℃ for 30 s, primary annealing at 54 ℃ for 30 s, and extension at 72 ℃ for 30 s for 35 cycles. PCR products (412 bp) were digested overnight at 37 ℃ with *Acc* II, which was cut within the sequence corresponding to the *Arg* codon (CGC) at position 72 to generate two fragments of 252 bp and 160 bp[15]. The DNA fragments were then resolved by electrophoresis on 30 g/L agarose gels stained with ethidium bromide. Presence of uncut (412 bp) DNA was indicative of the *Pro* allele and heterozygous for *Arg*/*Pro* genotypes showed three fragments of 412, 252 and 160 bp.

Statistical analysis

Chi-square test was used to examine the correlation between the *p53* codon 72 polymorphism of the esophageal SCC patients and the presence of HPV-16*E6* by SPSS software(12.0).

RESULTS

Frequency of HPV-16E6 among Kazakh's esophageal SCC patients

Pairs of 104 DNA sample from primary Kazakh's esophageal SCC tissues and corresponding normal mucosae were analyzed for the presence of oncogenic HPV-16-*E6* using PCR methods (Figure 1). The frequency of HPV-16-*E6* gene in cancer cases (52.9%) was higher than that in corresponding normal mucosae (39.4%) (Tables 1, 2). These results were similar to previous reports[16].

Table 1 *Arg* and *Pro* alleles of *p53* in SCCs of Kazakh's esophagus (*n*, %)

	Pro	*Pro*/*Arg*	*Arg*
Esophageal SCC (*n* = 104)	21 (20.2)	25 (24.0)	58 (55.8)
HPV16*E6* positive (*n*=55)	8 (14.5)	8 (14.5)	39 (71.0)[a]
HPV16*E6* negative (*n*=49)	13 (26.5)	16(32.7)	20 (40.8)

[a]$P<0.05$ *vs* negative.

Arg allele at the codon 72 in HPV-associated esophageal SCC

PCR-RFLP was carried out on 104 DNA samples from primary Kazakh's esophageal SCC tissues and corresponding normal mucosae to analyze the association between the *p53* codon 72 polymorphism and HPV-associated esophageal SCC by DC-2000 image system (Figure 2). It showed a typical pattern of codon 72 evaluated by restriction analysis. Presence of the *Pro* allele resulted in resistance of the PCR amplified DNA fragment to digestion by *Acc* II. The comparision between the distribution of *p53* alleles at codon 72 in HPV-positive esophageal SCC with the HPV-negative group is shown in Table 1. The frequency of presence of *Arg* allele alone from the Kazakh's esophageal cancer specimens was similar (55.8%, 58 of 104) to other population cases of esophageal cancer[10]. Moreover, there was a marked difference in the frequency of *Pro*/*Arg* alleles between HPV-positive and HPV-negative groups. *p53 Arg* allele alone was detected in 71.0% (39/55) in the HPV-positive group, whereas in 40.8% (20/49) in the HPV-negative group ($P<0.05$; *OR*, 3.53; 95% *CI*, 1.57-7.98) (Table 1). The allele frequency of *Arg* alleles in cancer cases (0.68) was higher than that in normal mucosa samples (0.54) ($P<0.05$; *OR*, 1.80; 95% *CI*, 1.21-2.69).

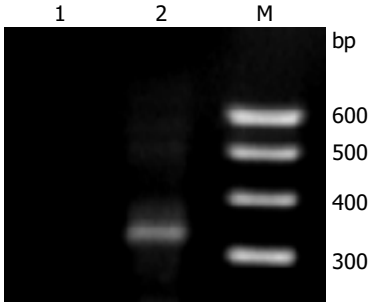

Figure 1 Agarose gel electrophoresis of HPV-16 E6 PCR-amplified fragments. Lane M: 100 bp DNA ladder marker; Lane 1: negative sample; and Lane 2: positive sample.

Table 2 *Arg* and *Pro* alleles of *p53* in normal mucosae of Kazakh's esophagus (*n*, %)

	Pro	*Pro*/*Arg*	*Arg*
Normal mucosa (*n* = 104)	28 (26.9)	40 (38.5)	36 (34.6)
HPV16*E6* positive (*n* = 41)	10 (24.4)	18 (43.9)	13 (31.7)
HPV16*E6* negative (*n* = 63)	10 (15.9)	30 (47.6)	23 (36.5)

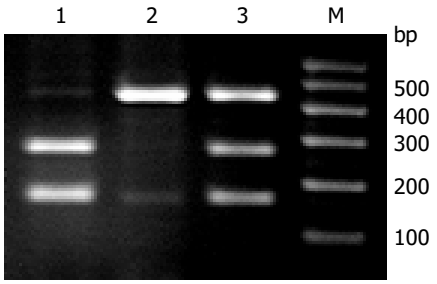

Figure 2 Restriction analysis of *p53* codon 72 polymorphism. The PCR product from the proline alleles had a single band with a fragment of 412 bp in length. The arginine was cleaved by *Acc* II, yielding two small fragments (252 and 160 bp). Lane M: 100 bp DNA ladder marker; Lane 1: homozygous for arginine; Lane 2: homozygous for proline; and Lane 3: digested sample, heterozygous for the polymorphism.

Arg allele at the codon 72 in surrounding normal mucosae in HPV-associated esophageal cancer

Differences in *p53* polymorphism in the corresponding normal mucosae were not significant between HPV-positive and -negative tissues ($P>0.05$; *OR*, 0.81; 95% *CI*, 0.35-1.86) (Table 2).

DISCUSSION

Infection with human papilloma virus is an important etiological factor in the development of SCC and it has been proposed that individuals homozygous for *Arg*/*Arg* at codon 72 of *p53* are several times more susceptible to HPV-mediated cancer[10,17]. In agreement with the result, studies in India and Mexico also found a strong increase in SCC risk associated with *p53* polymorphism and the presence of HPV infection[18,19]. In China similar research has been carried out on esophageal SCC, ovarian carcinoma, and breast carcinoma[20]. However, several studies conducted in different countries failed to reproduce this observation[21-25].This polymorphism has been shown to vary with ethnic and geographical distribution.However, its influence has not been elucidated in the Kazakh population.

In the present study, the frequency of HPV-16-*E6* gene in Kazakh's esophageal SCC cases was higher than that in corresponding normal mucosae, suggesting that there is a trend towards an association between the carcinogenesis of Kazakh's esophageal SCC and the presence of HPV-16 infection. These results were similar to previous report[16], which suggested that infection with HPV-16 might be involved in carcinogenesis of Kazakh's esophageal SCC. In addition, the distribution of *p53* codon 72 *Arg* homozygous genotype in Kazaks's esophageal SCC was significantly higher than that in corresponding normal mucosae, indicating that an individual homozygous for *p53 Arg* would be more likely to develop esophageal SCC than a *Pro*/*Arg* heterozygote or a *Pro* homozygote. Furthermore, it is noteworthy that the distribution of *p53* codon 72 *Arg* homozygous genotype in HPV positive samples of Kazakh's esophageal SCC was at a 3.53-folds higher risk for the development of esophageal SCC compared with HPV negative samples. In contrast, such a significant correlation between *p53* polymorphism and HPV infection was not evident in corresponding normal mucosae. From the above analyses, when stratified with HPV infection, the frequency of *p53* codon 72 *Arg* homozygous genotype was at a 1.48-folds increased risks for developing Kazakh's esophageal SCC compared with *p53 Arg* homozygosity (*Arg*/*Arg*) solely. Therefore, this implied *p53* codon 72 *Arg* polymorphism in combination with HPV infection could increase the risk of development of SCC in Kazakhs.

p53 tumor-suppresser protein accmulates rapidly through post-transcriptional mechanisms and is also activated as a transcriptional factor, thus leading to growth arrest or apoptosis when DNA damage has occurred[26]. The ubiquitin-dependent proteolytic pathway plays a major role in selective protein deregulation. *E6* oncoprotein of oncogenic HPV-16/18 might use this cellular proteolytic system to target *p53* protein[7] and bind to a cellular protein of *E6*-AP, and the *E6-AP* complex might interact with *p53*, resulting in the rapid ubiquitin-dependent degradation of *p53*[27]. The level and half-life of *p53* in *E6* immortalized cell lines or in HPV-positive cervical carcinoma cells have been reported to be generally decreased[28,29]. Certain HPV types such as HPV-16/18 found in SCC of esophagus suggested a model by which *E6* degraded cell growth control by elimination of the *p53* tumor suppresser protein and led to HPV-associated esophageal SCC[10,30].

In conclusion, the current study reveals the potential role of the polymorphism of *p53* at codon 72 in HPV-associated carcinogenesis of esophageal SCC in Kazakh population. Individuals carrying *Arg* alleles compared to those with *Pro* alleles have an increased risk for esophageal SCC.

ACKNOWLEDGMENTS

We thank Professor Zhen-Zhu Sun (Department of Pathology, the People's Hospital of Xinjiang Uygur Autonomous Region, China) for providing the samples of Kazakh's esophageal SCC.

REFERENCES

1 **Zhang YM**. The distribution of esophageal cancer in Xinjiang. *Xinjiang Yixueyuan Xuebao* 1988; **11:** 139-144

2 **Liang YY,** Esteve A, Martel-Planche G, Takahashi S, Lu SH, Montesano R, Hollstein M. *p53* mutations in esophageal tumors from high-incidence areas of China. *Int J Cancer* 1995; **61:** 611-614

3 **Munoz N,** Wahrendorf J, Bang LJ, Crespi M, Thurnham DI, Day NE, Ji ZH, Grassi A, Yan LW, Lin LG. No effect of riboflavine, retinol, and zinc on prevalence of precancerous lesions of oesophagus. Randomised double-blind intervention study in high-risk population of China. *Lancet* 1985; **2:** 111-114

4 **Lin K,** Shen W, Shen Z, Cai S, Wu Y. Estimation of the potential for nitrosation and its inhibition in subjects from high- and low-risk areas for esophageal cancer in southern China. *Int J Cancer* 2003; **10**: 891-895

5 **He D,** Zhang DK, Lam KY, Ma L, Ngan HY, Liu SS, Tsao SW. Prevalence of HPV infection in esophageal squamous cell carcinoma in Chinese patients and its relationship to the p53 gene mutation. *Int J Cancer* 1997; **72:** 959–964

6 **Chen B,** Yin H, Dhurandhar N. Detection of human papilloma-virus DNA in esophageal squamous cell carcinomas by the polymerase chain reaction using general consensus primers. *Hum Pathol* 1994; **25:** 920-923

7 **Scheffner M**, Werness BA, Huibregtse JM, Levine AJ, Howley PM. The E6 oncoprotein encoded by human papillomavirus types 16 and 18 promotes the degradation of p53. *Cell* 1990; **63:** 1129–1136

8 **Huibregtse JM,** Scheffner M, Howley PM. A cellular protein mediates association of p53 with the E6 oncoprotein of human papillomavirus types 16 or 18. *EMBO J* 1991; **10:** 4129–4135

9 **Huibregtse JM,** Scheffner M, Howley PM. Localization of the E6-AP regions that direct human papillomavirus E6 binding, association with p53, and ubiquitination of associated proteins. *Mol Cell Biol* 1993; **13:** 4918–4927

10 **Kawaguchi H,** Ohno S, Araki K, Miyazaki M, Saeki H, Watanabe M, Tanaka S, Sugimachi K. p53 polymorphism in human papillomavirus-associated esophageal cance. *Cancer Research* 2000; **60:** 2753-2755

11 **Peixoto Guimaraes D,** Hsin Lu S, Snijders P, Wilmotte R, Herrero R, Lenoir G, Montesano R, Meijer CJ, Walboomers J, Hainaut P. Absence of association between HPV DNA, TP53 codon 72 polymorphism, and risk of oesophageal cancer in a high-risk area of China. *Cancer Lett* 2001; **162:** 231-235

12 **Lu ZM,** Chen KN, Guo M. Detection of HPV in human esophageal cancer in high-incidence area and its correlation with *p53* expression. *Zhonghua Zhongliu Zazhi* 2001; **23**: 220-223

13 **Zou SY,** Si JY, Liu XM, Tang XP. PCR in detdction of human papillomavirus DNA in esophageal carcinoma in Xingjiang. *Aizheng* 1998; **17:** 32-34

14 **Greer CE,** Whee Le CM, Manos MM. PCR Primer A Laboratory Manual. *Cold Spring Harbor Laboratory Press* 1995: 64-69

15 **de la Calle-Martin O**, Fabregat V, Romero M, Soler J, Vives J, Yague J. AccII Polymorphism of the *p53* gene. *Nucleic Acids Res* 1990; **18:** 4963

16 **Chang F,** Syrjanen S, Shen Q, Cintorino M, Santopietro R, Tosi P, Syrjanen K. Human papillomavirus involvement in esophageal carcinogenesis in the high-incidence area of China. A study of 700 cases by screening and type-specific in situ hybridization. *Scand J Gastroenterol* 2000; **35**: 123-130

17 **Ojeda JM,** Ampuero S, Rojas P, Prado R, Allende JE, Barton SA, Chakraborty R, Rothhammer F. *p53* codon 72 polymorphism and risk of cervical cancer. *Biol Res* 2003; **36:** 279-283

18 **Saranath D,** Khan Z, Tandle AT, Dedhia P, Sharma B, Contractor R, Shrivastava S, Dinshaw K. HPV16/18 prevalence in cervical lesions/cancers and *p53* genotypes in cervical cancer patients from India. *Gynecol Oncol* 2002; **86**: 157-162

19 **Sifuentes Alvarez A,** Reyes Romero M. Risk factors for cervicouterine cancer associated to HPV: *p53* codon 72 polymorphism in women attending hospital care. *Ginecol Obstet Mex* 2003; **71**: 12-15

20 **Li T,** Lu ZM, Guo M, Wu QJ, Chen KN, Xing HP, Mei Q, Ke Y. *p53* codon 72 polymorphism (C/G) and the risk of human papillomavirus-associated carcinomas in China. *Cancer* 2002; **95**: 2571-2576

21 **Humbey O,** Cairey-Remonnay S, Guerrini JS, Algros MP, Mougin C, Bittard H, Aubin F. Detection of the human papillomavirus and analysis of the TP53 polymorphism of exon 4 at codon 72 in penile squamous cell carcinomas. *Eur J Cancer* 2003; **39**: 684-690

22 **Inserra P,** Abrahamsen M, Papenfuss M, Giuliano AR. Ethnic variation of the *P53* codon 72 polymorphism, HPV persistence, and cervical cancer risk. *Int J STD AIDS* 2003; **14**: 800-804

23 **Comar M,** Molin GD, Guaschino S, Campello C. *p53* at codon 72 polymorphism, human papillomavirus infection and cervical lesions: a cross-sectional study from northeastern Italy. *Eur J Obstet Gynecol Reprod Biol* 2004; **114**: 210-214

24 **Tanara G,** Falugi C, Cesario A, Margaritora S, Russo P, Cosimi A. TP53 codon 72 polymorphism does not affect risk of cervical cancer in patients from The Gambia. *Int J Biol Markers* 2003; **18**: 280-283

25 **Ngan HY,** Liu VW, Liu SS, Cheng DK, Ng TY, Wong LC. Homozygous arginine at codon 72 of *p53* has no prognostic significance in cervical cancer. *Tumour Biol* 2000; **21**: 135-138

26 **Levine AJ.** *p53*, the cellular gatekeeper for growth and division. *Cell* 1997; **88:** 323–331

27 **Scheffner M,** Huibregtse JM, Vierstra RD, Howley PM. The HPV-16 E6 and E6-AP complex functions as a ubiquitin-Protein ligase in the ubiquitination of *p53*. *Cell* 1993; **75:** 495–505

28 **Scheffner M,** Munger K, Byrne JC, Howley PM. The state of the *p53* and retinoblastoma genes in human cervical carcinoma cell lines. *Proc Natl Acad Sci U S A* 1991; **88:** 5523–5527

29 **Hengstermann A,** Linares LK, Ciechanover A, Whitaker NJ, Scheffner M. Complete switch from Mdm2 to human papillomavirus E6-mediated degradation of *p53* in cervical cancer cells. *Proc Natl Acad Sci U S A* 2001; **98**: 1218-1223

30 **Vos M,** Adams CH, Victor TC, van Helden PD. Polymorphisms and mutations found in the regions flanking exons 5 to 8 of the TP53 gene in a population at high risk for esophageal cancer in South Africa. *Cancer Genet Cytogenet* 2003; **140**: 23-30

Edited by Kumar M and Wang XL **Proofread by** Xu FM

PO Box 2345, Beijing 100023, China
Fax: +86-10-85381893
E-mail: wjg@wjgnet.com www.wjgnet.com

World J Gastroenterol 2004;10(19):2779-2784
World Journal of Gastroenterology
Copyright © 2004 by The WJG Press ISSN 1007-9327

• ESOPHAGEAL CANCER •

Inhibitory effect of ubiquitin-proteasome pathway on proliferation of esophageal carcinoma cells

Wei-Guo Zhang, Jie-Ping Yu, Qing-Ming Wu, Qiang Tong, Sheng-Bao Li, Xiao-Hu Wang, Guo-Jian Xie

Wei-Guo Zhang, Qing-Ming Wu, Qiang Tong, Sheng-Bao Li, Xiao-Hu Wang, Guo-Jian Xie, Digestive Department, Taihe Hospital, Yunyang Medical College, Shiyan 442000, Hubei Province, China
Jie-Ping Yu, Digestive Department, Renmin Hospital of Wuhan University, Wuhan 430060, Hubei Province, China
Correspondence to: Wei-Guo Zhang, Digestive Department, Taihe Hospital, Yunyang Medical College, Shiyan 442000, Hubei Province, China. zwg789@sina.com
Telephone: +86-719-8801431
Received: 2004-02-02 **Accepted:** 2004-02-18

Abstract

AIM: To investigate the inhibitory effect of ubiquitin-proteasome pathway (UPP) on proliferation of esophageal carcinoma cells.

METHODS: Esophageal carcinoma cell strain EC9706 was treated with MG-132 to inhibit its UPP specificity. Cell growth suppression was evaluated with 3-(4,5-dimethylthiazole-2-yl)-2,5-diphenyl tetrazolium bromide (MTT) assay. DNA synthesis was evaluated by ^{3}H-thymidine (^{3}H-TdR) incorporation. Morphologic changes of cells were observed under microscope. Activity of telomerase was examined by telomeric repeat amplification protocol (TRAP) of PCR-ELISA. Cell cycle and apoptosis were detected by flow cytometry (FCM). DNA fragment analysis was used to confirm the presence of apoptosis. Expression of p27^{kip1} was detected by immunocytochemical technique.

RESULTS: After exposed to MG-132, the growth and value of ^{3}H-TdR incorporation of EC9706 cells were obviously inhibited. Cells became round, small and exfoliative under microscope. TRAP PCR-ELISA showed that light absorption of cells gradually decreased after exposed to 5 μmol/L of MG-132 for 24, 48, 72 and 96 h (P<0.01). The percentage of cells at G_0/G_1 phase was increased and that at S and G_2/M was decreased (P<0.01). The rate of apoptotic cells treated with 5 μmol/L of MG-132 for 48 and 96 h was 31.7% and 66.4%, respectively. Agarose electrophoresis showed marked ladders. In addition, the positive signals of p27^{kip1} were located in cytoplasm and nuclei in MG-132 group in contrast to cytoplasm staining in control group.

CONCLUSION: MG-132 can obviously inhibit proliferation of EC9706 cells and induce apoptosis. The mechanisms include upregulation of p27^{kip1} expression, G_1 arrest and depression of telomerase activity. The results indicate that inhibiting UPP is a novel strategy for esophageal carcinoma therapy.

Zhang WG, Yu JP, Wu QM, Tong Q, Li SB, Wang XH, Xie GJ. Inhibitory effect of ubiquitin-proteasome pathway on proliferation of esophageal carcinoma cells. *World J Gastroenterol* 2004; 10 (19): 2779-2784
http://www.wjgnet.com/1007-9327/10/2779.asp

INTRODUCTION

Esophageal carcinoma is common in China. Previous studies have shown that its occurrence and progression are complicated, and are associated with the changes of multi-genes and molecules[1-3]. The ubiquitin-proteasome pathway (UPP) is the major system employed by eukaryotes for the selective degradation of cellular proteins that play key roles in cellular processes such as cell cycle regulation, differentiation, signal transduction, gene transcription, antigen presenting and transmembrance localization of proteins[4,5]. In this study, we investigated the inhibitory effect of UPP on proliferation of esophageal carcinoma cells by using specific ubiquitin proteasome to find a new strategy for esophageal carcinoma therapy.

MATERIALS AND METHODS

Materials

Esophageal carcinoma cell strain EC9706 was presented by professor Ming-Rong Wang, China Academy of Medical Sciences. MG-132 was purchased from Calbiochem Co. Ltd (USA), and dissolved in dimethylsulfoxide (DMSO) as a 40 mmol/L stock solution and stored at -20 ℃. 3-(4,5-dimethylthiazole-2-yl)-2,5-diphenyl tetrazolium bromide (MTT) and DMSO were bought from Sigma Co. Ltd (USA). ^{3}H-thymidine (^{3}H-TdR) was provided by Beijing Atomic Power Research Institute. Telomeric repeat amplification protocol (TRAP) ELISA telomerase detection kit was obtained from Intergen Company (USA). Monoclonal mouse antibody of p27^{kip1}, ultra sensitive S-P kit, and 3,3-diaminobenaidine (DAB) kit were purchased from Fuzhou Maixin Biotechnology Co. Ltd. RPMI 1640 medium was obtained from GIBCOBRL Company (USA). Low melting-temperature agarose was obtained from Promega Company (USA). DNA-PREP™ LPR and DNA-PREP™ stain were obtained from America Beckman Coulter Company.

Cell culture

Human esophageal carcinoma cell strain EC9706 was maintained in RPMI 1640 medium supplemented with 100 mL/L fetal calf serum (FCS), 100 kU/L penicillin, 100 mg/L streptomycin and 2 mmol/L *l*-glutamine in a humidified incubator containing 50 mL/L CO_2 at 37 ℃, the medium was changed every 2-3 d.

MTT assay

EC9706 cells growing exponentially were chosen. Cell density in the suspension was adjusted to 2×10^5 cells/mL. After addition of 200 mL/well of the final cell suspension, 96-well plates were incubated for 24 h. Then the cells were treated with 0.5, 1.0, 2.5, 5.0, 10, 15, 20 μmol/L (DMSO⩽0.5 g/L) of MG-132, respectively, as the different observation groups. The cells treated with an equal amount of DMSO instead of MG-132 served as the control. The background was conducted using only cell-free culture medium. After cultivated for 24, 48, 72 and 96 h, 10 μL of stock MTT solution (5 g/L) was added to the cells in each well, followed by a further incubation at 37 ℃ for 4 h. The culture medium was carefully removed, 100 μL of DMSO was added to each well and culture was vibrated for 20 min. The absorbance

of samples was measured three times for each group with three wells at a wavelength of 550 nm with the enzyme linked immunosorbent assay meter (PR 2100, SANOFI company, France). The inhibitory rate (IR) was calculated according to the formula: IR = [1-(absorbance of MG-132 group-absorbance of background group)/(absorbance of control group-absorbance of background group)]×100%.

Incorporation test of ^{3}H-TdR

As described above, experimental group and control group were cultured for 3 h with 100 mL/L FCS RPMI 1640, and then for 12 h with FCS-free RPMI 1640. MG-132 and 1 μ Ci ^{3}H-TdR were added to each group, which was rinsed with PBS after 24, 48, 72 and 96 h and fixed with methyl alcohol and absolute ethyl alcohol for 10 min each. Finally, 200 μL of 0.1mol/L NaOH was added, then 200 μL of each was taken after blowing, and mixed in 5 mL scintillation liquid for overnight. On the following day, the count per minute (CPM) of ^{3}H was tested three times for each group with three wells.

Morphologic changes of cells

Morphologic changes of EC9706 cells were observed under microscope 24, 48, 72 and 96 h after treated with MG-132 (5 μmol/L).

Telomerase assay

The cells (10^5-10^6) treated with MG-132 (5 μmol/L) for 24, 48, 72 and 96 h were collected, respectively. After addition of 300 μL telomerase assay lysis buffer (1×CHAPS), the cells were lysed on ice. The lysate was incubated on ice for 30 min and then centrifuged at 13 000 *g* for 25 min at 4 ℃. The supernatant (2 μL) was added to reaction solution containing 10 μL of TRAP buffer, 2 units of Taq polymerase and 48 μL of DH_2Oqs. PCR was carried out through 33 amplification cycles, each cycle consisting of denaturation at 94 ℃ for 30 s, primer annealing at 55 ℃ for 30 s, and extension at 72 ℃ for 30 s. The amplified product was added to block/dilution buffer (250 μL), and incubated at 37 ℃ for 30 min, and 5 μL of TRAP reactant was then added and mixed. After incubated at 37 ℃ for 60 min, 100 μL working solution of anti-DNP Ab was added and incubated for 30 min, then 100 μL of 3,3',5,5'-tetramethylbenzidine (TMB) substrate solution and 100 μL of stop reagent were added. The absorbance value in each well was read at the wave lengths of 450 nm and 690 nm on an enzyme linked immunosorbent assay meter. Telomerase activity was considered positive when the absorbance value of a sample was at least 0.8 units. When those were lower than 0.2 units, they were regarded as negative.

Flow cytometry detection

After cell cycle was synchronic, the cells of experiment group were treated with MG-132 (5 μmol/L) for 48 h and 96 h. The collected cells were added with DNA-PREP™ LPR and DNA-PREP™ stain, respectively, after they were washed with PBS and centrifuged. Cell cycle and apoptosis were detected by flow cytometry (Epics XL, Beckman Coulter Company, USA) and SYSTEM II™ software was used to dispose the data.

DNA ladder demonstration

As described above, the cells (7×10^6/sample, both attached and detached cells) were lyzed with hypotonic lysis buffer (10 mmol/L edetic acid, 5 g/L Triton X-100, Tris-HCl, pH 7.4) for 15 min on ice and precipitated with 25 g/L polyethylene glycol and 1 mol/L NaCl for 15 min at 4 ℃. After centrifugation at 16 000 *g* for 10 min at room temperature, the supernatant was treated with proteinase K (0.3 g/L) at 37 ℃ for 1 h and precipitated with isopropanol. After centrifugation, each pellet was dissolved in 10 μL of Tris-EDTA (pH 7.6) and electrophoresed on a 17 g/L agarose gel containing ethidium bromide. DNA ladder pattern was identified under ultraviolet light.

Immunocytochemical staining

EC9706 cells cultured with MG-132 (5 μmol/L) for 48 h were fixed with dimethyl ketone at 4 ℃. The cells carrying the detected antigen were stained following SP immunocytochemical staining method using anti-p27*kip1* as primary antibody[6]. PBS was substituted for primary antibody as negative control.

Statistics

The data were expressed as mean±SD. The difference between each group was analyzed by *t*-test. $P<0.05$ was considered statistically significant.

RESULTS

Inhibitory effect of MG-132 on EC9706 cell growth

The growth of EC9706 cells treated with 0.5-20 μmol/L of MG-132 was significantly inhibited compared with that of control group. While the cells exposed to MG-132 for 24 h produced a certain inhibitory effect, but only exceeding 48 h did MG-132 show significant effect. When the dose of MG-132 exceeded 5 μmol/L, only slight increases in IR of the cells were observed (Figure 1).

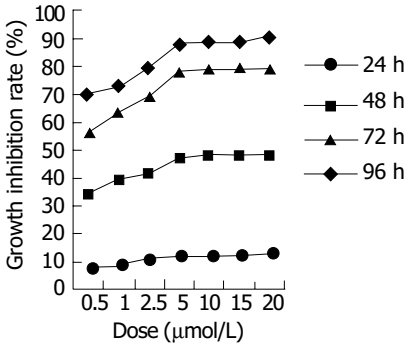

Figure 1 MTT assay of EC9706 cells after exposed to MG-132.

Table 1 Evaluation of DNA synthesis by ^{3}H-TdR incorporation (mean±SD)

Group	24 h	48 h	72 h	96 h
Control MG-132 (μmol/L)	4 295.52±136.32	5 236.17±221.36	5 642.92±105.41	5 863.43±206.58
0.5	3 764.68±97.37[a]	2 879.83±86.25[b]	1 918.73±76.49[b]	1 759.29±89.23[b]
1.0	3 526.14±101.42[a]	2 643.29±79.38[b]	1 547.25±68.94[b]	1 366.18±52.49[b]
2.5	3 402.34±93.44[a]	2 567.76±68.21[b]	1 260.37±51.27[b]	910.25±45.37[b]
5.0	3 324.78±65.43[a]	2 411.56±69.34[b]	840.79±41.17[b]	517.83±41.26[b]
10.0	3 301.29±59.28[a]	2 360.40±49.28[b]	820.56±39.76[b]	498.71±40.14[b]
15.0	3 294.12±67.33[a]	2 324.25±47.30[b]	810.17±45.61[b]	485.26±37.56[b]
20.0	3 280.54±62.46[a]	2 320.60±46.83[b]	804.63±51.34[b]	476.90±38.41[b]

[a]$P<0.05$, [b]$P<0.01$ *vs* control.

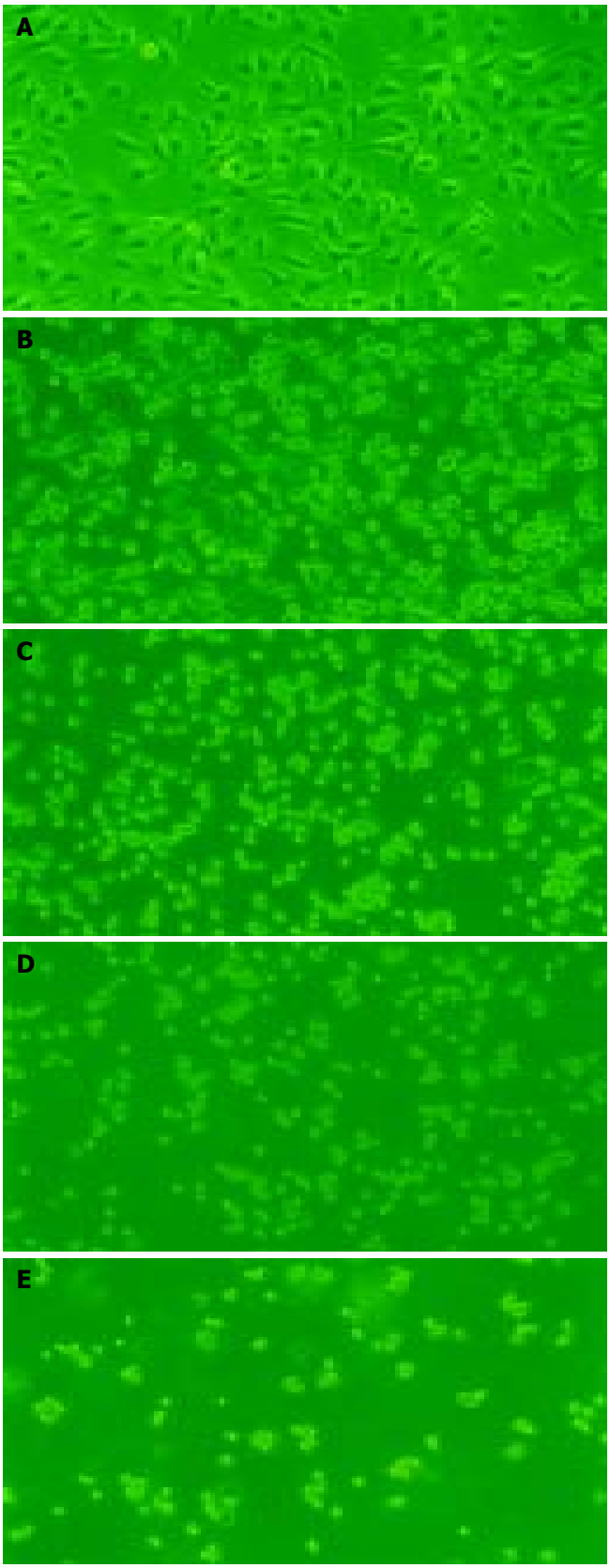

Figure 2 Morphologic changes of EC9706 cells observed under microscope after treated with 5 μmol/L of MG-132. A: control group; B: EC9706 cells treated with MG-132 for 24 h; C: EC9706 cells treated with MG-132 for 48 h; D: EC9706 cells treated with MG-132 for 72 h; E: EC9706 cells treated with MG-132 for 96 h (×200).

Inhibition of DNA synthesis

The values of ^{3}H-TdR incorporation of MG-132 group were decreased compared with the control group (Table 1).

Morphologic changes of cells

EC9706 cells became round, small and exfoliative after exposed to MG-132 under microscope (Figure 2).

Inhibition of telomerase activity

After treated with MG-132 (5 μmol/L) for 24, 48, 72 and 96 h, respectively, EC9706 cells showed a gradual decrease in values of *A* compared with the control group (P<0.01). Furthermore, telomerase activity was negative (Table 2).

Table 2 Effect of MG-132 on telomerase activity of EC9706 cells (mean±SD)

Groups	Light absorption (*A*)			
	24 h	48 h	72 h	96 h
Control	1.871±0.061	2.234±0.092	2.907±0.113	3.025±0.120
MG-132	0.154±0.008^b	0.085±0.006^b	0.072±0.004^b	0.067±0.003^b

^{b}P<0.01 *vs* control group.

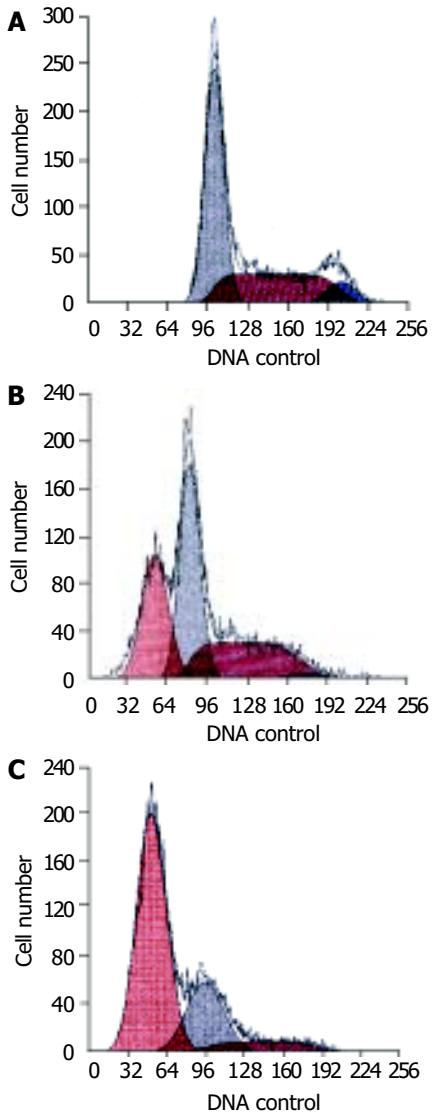

Figure 3 Cell cycle and apoptosis of EC9706 cells exposed to 5 μmol/L of MG-132. A: control group. Apoptotic sub-G_1 peak was not found; B: EC9706 cells exposed to MG-132 for 48 h. The ratio of apoptotic cells was 31.7%; C: EC9706 cells exposed to MG-132 for 96 h. The ratio of apoptotic cells was 66.4%.

Changes of cell cycle and apoptosis

The percentage of cells at G_0/G_1 phase was increased and that

at G_2/M and S was decreased (P<0.01). The rate of apoptotic cells treated with 5 μmol/L of MG-132 for 48 and 96 h was 31.7% and 66.4%, respectively (Table 3, Figure 3).

Table 3 Effect of MG-132 on cell cycle of EC9706 cells (mean±SD, %)

Groups	48 h			96 h		
	G_0/G_1	S	G_2/M	G_0/G_1	S	G_2/M
Control	40.4±3.9	46.5±4.3	13.1±1.0	44.6±4.1	40.9±2.3	14.5±1.4
MG-132	67.5±5.1[b]	29.3±2.8[b]	3.2±0.2[b]	73.1±5.2[b]	24.6±2.1[b]	2.3±0.1[b]

[b]P<0.01 *vs* control group.

DNA ladder

Agarose electrophoresis showed marked ladders in MG-132 group, while the ladder was not detected in control group. Furthermore, DNA fragmentation was more apparent at 96 h (Figure 4).

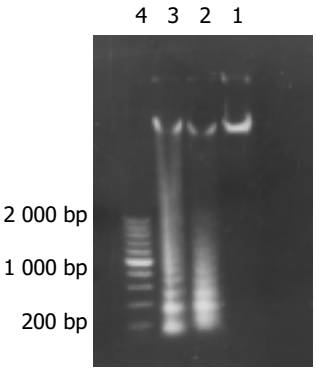

Figure 4 Results of DNA agarose electrophoresis. Lane1: control group; Lane 2: EC9706 cells exposed to 5 μmol/L of MG-132 for 48 h; Lane 3: EC9706 cells exposed to 5 μmol/L of MG-132 for 96 h; Lane 4: 200, 400, 600, 800, 1 000, 1 200, 1 400, 1 600, 1 800, 2 000 bp ladder markers.

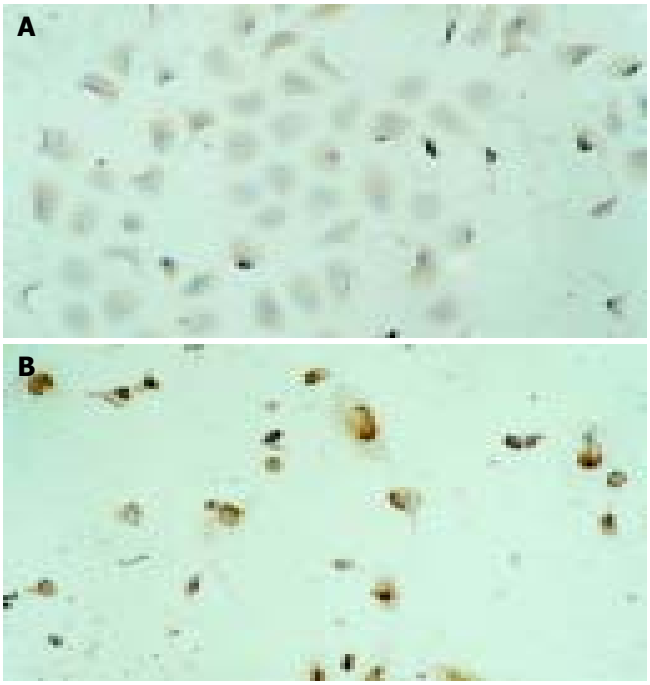

Figure 5 Results of immunohistochemical staining of EC9706 cells. A: control group. Immunohistochemical staining of p27^{kip1} protein located in cytoplasm of EC9706 cells; B: MG-132 group. Immunohistochemical staining of p27^{kip1} protein located in cytoplasm and nuclei (×200).

Expression of p27kip1

In the control group, the cytoplasm was stained in brownish yellow and the nuclei were stained in blue. In the experiment group, both the cytoplasm and nuclei were stained in brownish yellow, indicating that the expression of p27^{kip1} in EC9706 cells was increased after treated with MG-132 (Figure 5).

DISCUSSION

Proteolytic degradation by ubiquitin-proteasome system involves ATP-dependent covalent attachment of a macromolecular chain of ubiquitin (Ub) molecules to the target protein, followed by degradation through the multicatalytic 26s proteasome. The conjugation of Ub, a highly conserved 8.6 kDa protein, to its target protein is mediated by the serial actions of three enzymes. E1, the Ub-activating enzyme, activates Ub in an ATP-dependent manner. E2, the Ub-conjugating enzyme, catalyzes the attachment of Ub to the substrate protein. E3, the Ub-ligase, serves as a scaffold between E2 and the substrate and provides recognition specificity of the substrate[7-10]. A protein tagged with a polyubiquitin chain is recognized and degraded by the 26S proteasome complex. This complex is composed of a 19S regulatory subcomplex and two 20S catalytic subcomplexes. UPP is extensively involved in physiological and biochemical processes. Some experiments showed that the low expression of some anti-oncogene including p53, p27^{kip1} in tumor cells was associated with the increasing activity of ubiquitin proteasome which leads to degradation of expression products of anti-oncogene, and have proved that deubiquitination of p53 is an important pathway for p53 stabilization[11,12]. Moreover, the degradation accommodation of some transcription factors was regulated by UPP, such as *NF-κB*, *c-fos*, *c-jun*, *c-mos*, *c-myc* and *MATa*[13-17]. So UPP is closely associated with the occurrence and development of malignant tumor.

Ubiquitin proteasome inhibitors include peptide aldehyde, borofax peptide and 3, 4-dichloro isocoumarin. MG-132, also known as carbobenzoxy-L-leucyl-L-leucyl-L-leucinal, a reversible, effective and specific peptide aldehyde inhibitor of ubiquitin-proteasome, could block UPP through inhibiting ubiquitin-mediated proteolysis by binding to and inactivating 20S and 26S proteasomes[18-22].

In our study, esophageal cancer cell line EC9706 was exposed to MG-132 to observe whether UPP could be inhibited. We found that the proliferation of cells was obviously inhibited in a dose- and time-dependent manner. The results also revealed some anti-tumor mechanisms of MG-132. First, MG-132 could up-regulate the expression of p27^{kip1}. p27^{kip1} was recently found[23] as a anti-oncogene with function of negative regulation of cell cycle, getting involved in the inhibitive reaction of cytokines, inducing cell differentiation and apoptosis, enhancing cell's adherence and regulating the resistance to medicines for noumenal tumors. p27^{kip1} protein is a cyclin dependent kinase inhibitor (CDKI) that could block G_1/S transition of cell cycle by inhibiting the action of cyclin E-CDK2 complex and cyclin D-CDK4 complex[24-26]. p27^{kip1} expression decreases in esophageal cancer and it may correlate with the histologic differentiation. Reduction of p27^{kip1} has been considered to be an independent prognostic indicator of esophageal cancer[27-30]. The nuclear localization signal of p27^{kip1} contains a protein kinase B (PKB/Akt) consensus site at threonine 157, and phosphorylation of p27^{kip1} by PKB/Akt has been found to impair its nuclear import[31,32], which is a key procedure to play its functional role[33]. We found that p27^{kip1} protein localized in cytoplasm of EC9706 cells showed low expression, but that localized both in cytoplasm

and nuclei of EC9706 cells showed high expression after treated with MG-132. Our previous studies[6,34] demonstrated that the growth of EC9706 cells and tumors implanted in nude mice was obviously inhibited, apoptosis was induced and cell cycle was arrested in G_1 phase by up-regulating $p27^{kip1}$. Second, MG-132 could depress telomerase activity. The activation of telomerase was closely associated with cyclin. It has been reported that inhibition of UPP could not only increase the expression of $p27^{kip1}$, but also increase the expression of p53[35]. Moreover $p27^{kip1}$ and p21 regulated by p53 could inhibit cyclin and result in decreased telomerase activity[36,37]. Third, MG-132 could cause G_1 arrest, which may be involved in changes of cell cycle regulatory factors such as $p27^{kip1}$. Fan *et al*.[38] obtained the same results as ours. But Ling *et al*.[39] tended to consider ubiquitin proteasome inhibitors to cause G_2 arrest. The difference may be involved in the different types of cells. The last, MG-132 could induce apoptosis, which may be closely associated with the functions mentioned above.

In conclusion, MG-132 can obviously inhibit proliferation of EC9706 cells and induce apoptosis. The mechanisms include upregulation of $p27^{kip1}$ expression, G_1 arrest and depression of telomerase activity. The results indicate that inhibiting UPP is a novel strategy for esophageal carcinoma therapy.

REFERENCES

1 **Zhang WG**, Wu QM, Wang XH, Xie GJ, Yu JP. Relationship between expression of survivin gene and biological characteristics in human esophageal carcinoma. *J Chinese Physician* 2003; **5**: 1378-1380

2 **Wu QM**, Li SB, Wang Q, Wang DH, Li XB, Liu CZ. The expression of COX-2 in esophageal carcinoma and its relation to clinicopathologic characteristics. *Shijie Huaren Xiaohua Zazhi* 2001; **9**: 11-14

3 **Li SB**, Wu QM, Wang Q, Wang XH, Xie GJ. Effects of adenovirus-mediated human COX-2 antisense RNA on synthesis of DNA and proteins in esophgeal carcinoma cell line. *Shijie Huaren Xiaohua Zazhi* 2003; **11**: 517-521

4 **King RW**, Deshaies RJ, Peters JM, Kirschner MW. How proteolysis drives the cell cycle. *Science* 1996; **274**: 1652-1659

5 **Fuchs SY**. The role of ubiquitin-proteasome pathway in oncogenic signaling. *Cancer Biol Ther* 2002; **1**: 337-341

6 **Wu QM**, Yu JP, Tong Q, Wang XH, Xie GJ. Inhibition of adenovirus-mediated p27*kip1* gene on growth of esophageal carcinoma cell strain. *World J Gastroenterol* 2003; **9**: 2404-2408

7 **Hellmann H**, Estelle M. Plant development: regulation by protein degradation. *Science* 2002; **297**: 793-797

8 **Whitehouse AS**, Tisdale MJ. Increased expression of the ubiquitin-proteasome pathway in murine myotubes by proteolysis-inducing factor (PIF) is associated with activation of the transcription factor NF-kappaB. *Br J Cancer* 2003; **89**: 1116-1122

9 **von der Lehr N**, Johansson S, Larsson LG. Implication of the ubiquitin/proteasome system in Myc-regulated transcription. *Cell Cycle* 2003; **2**: 403-407

10 **Yun J**, Lee WH. Degradation of transcription repressor ZBRK1 through the ubiquitin-proteasome pathway relieves repression of Gadd45a upon DNA damage. *Mol Cell Biol* 2003; **23**: 7305-7314

11 **Lim MS**, Adamson A, Lin Z, Perez-Ordonez B, Jordan RC, Tripp S, Perkins SL, Elenitoba-Johnson KS. Expression of Skp2, a p27*kip1* ubiquitin ligase, in malignant lymphoma: correlation with p27*kip1* and proliferation index. *Blood* 2002; **100**: 2950-2956

12 **Li M**, Chen D, Shiloh A, Luo J, Nikolaev AY, Qin J, Gu W. Deubiquitination of p53 by HAUSP is an important pathway for p53 stabilization. *Nature* 2002; **416**: 648-653

13 **McDade TP**, Perugini RA, Vittimberga FJ Jr, Callery MP. Ubiquitin-proteasome inhibition enhances apoptosis of human pancreatic cancer cells. *Surgery* 1999; **126**: 371-377

14 **Salvat C**, Aquaviva C, Jariel-Encontre I, Ferrara P, Pariat M, Steff AM, Carillo S, Piechaczyk M. Are there multiple proteolytic pathways contributing to c-Fos, c-Jun and p53 protein degradation *in vivo*? *Mol Biol Rep* 1999; **26**: 45-51

15 **Lafarga M**, Berciano MT, Pena E, Mayo I, Castano JG, Bohmann D, Rodrigues JP, Tavanez JP, Carmo-Fonseca M. Clastosome: a subtype of nuclear body enriched in 19S and 20S proteasomes, ubiquitin, and protein substrates of proteasome. *Mol Biol Cell* 2002; **13**: 2771-2782

16 **Gregory MA**, Hann SR. c-Myc proteolysis by the ubiquitin-proteasome pathway: stabilization of c-Myc in Burkitt's lymphoma cells. *Mol Cell Biol* 2000; **20**: 2423-2435

17 **von der Lehr N**, Johansson S, Wu S, Bahram F, Castell A, Cetinkaya C, Hydbring P, Weidung I, Nakayama K, Nakayama KI, Soderberg O, Kerppola TK, Larsson LG. The F-box protein Skp2 participates in c-Myc proteosomal degradation and acts as a cofactor for c-Myc-regulated transcription. *Mol Cell* 2003; **11**: 1189-1200

18 **Mailhes JB**, Hilliard C, Lowery M, London SN. MG-132, an inhibitor of proteasomes and calpains, induced inhibition of oocyte maturation and aneuploidy in mouse oocytes. *Cell Chromosome* 2002; **1**: 2

19 **Steinhilb ML**, Turner RS, Gaut JR. The protease inhibitor, MG132, blocks maturation of the amyloid precursor protein Swedish mutant preventing cleavage by beta-Secretase. *J Biol Chem* 2001; **276**: 4476-4484

20 **Bonuccelli G**, Sotgia F, Schubert W, Park DS, Frank PG, Woodman SE, Insabato L, Cammer M, Minetti C, Lisanti MP. Proteasome inhibitor (MG-132) treatment of mdx mice rescues the expression and membrane localization of dystrophin and dystrophin-associated proteins. *Am J Pathol* 2003; **163**: 1663-1675

21 **Shibata T**, Imaizumi T, Tamo W, Matsumiya T, Kumagai M, Cui XF, Yoshida H, Takaya S, Fukuda I, Satoh K. Proteasome inhibitor MG-132 enhances the expression of interleukin-6 in human umbilical vein endothelial cells: Involvement of MAP/ERK kinase. *Immunol Cell Biol* 2002; **80**: 226-230

22 **Banerjee D**, Liefshitz A. Potential of the proteasomal inhibitor MG-132 as an anticancer agent, alone and in combination. *Anticancer Res* 2001; **21**: 3941-3947

23 **Polyak K**, Kato JY, Solomon MJ, Sherr CJ, Massague J, Roberts JM, Koff A. p27*kip1*, a cyclin-CdK inhibitor, links transforming growth factor-beta and contact inhibition to cell cycle arrest. *Genes Dev* 1994; **8**: 9-22

24 **Manne U**, Jhala NC, Jones J, Weiss HL, Chatla C, Meleth S, Suarez-Cuervo C, Grizzle WE. Prognostic significance of p27*kip-1* expression in colorectal adenocarcinomas is associated with tumor stage. *Clin Cancer Res* 2004; **10**: 1743-1752

25 **Center DM**, Cruikshank WW, Zhang Y. Nuclear pro-IL-16 regulation of T cell proliferation: p27(*kip1*)-dependent G0/G1 arrest mediated by inhibition of Skp2 transcription. *J Immunol* 2004; **172**: 1654-1660

26 **Wang G**, Reisdorph R, Clark RE Jr, Miskimins R, Lindahl R, Miskimins WK. Cyclin dependent kinase inhibitor p27(*kip1*) is upregulated by hypoxia via an ARNT dependent pathway. *J Cell Biochem* 2003; **90**: 548-560

27 **Yasunaga M**, Tabira Y, Nakano K, Iida S, Ichimaru N, Nagamoto N, Sakaguchi T. Accelerated growth signals and low tumor-infiltrating lymphocyte levels predict poor outcome in T4 esophageal squamous cell carcinoma. *Ann Thorac Surg* 2000; **70**: 1634-1640

28 **Shamma A**, Doki Y, Tsujinaka T, Shiozaki H, Inoue M, Yano M, Kawanishi K, Monden M. Loss of p27(*kip1*) expression predicts poor prognosis in patients with esophageal squamous cell carcinoma. *Oncology* 2000; **58**: 152-158

29 **Shibata H**, Matsubara O, Wakiyama H, Tanaka S. The role of cyclin-dependent kinase inhibitor p27 in squamous cell carcinoma of the esophagus. *Pathol Res Pract* 2001; **197**: 157-164

30 **Taniere P**, Martel-Planche G, Saurin JC, Lombard-Bohas C, Berger F, Scoazec JY, Hainaut P. TP53 mutations, amplification of P63 and expression of cell cycle proteins in squamous cell carcinoma of the oesophagus from a low incidence area in Western Europe. *Br J Cancer* 2001; **85**: 721-726

31 **Liang J**, Zubovitz J, Petrocelli T, Kotchetkov R, Connor MK, Han K, Lee JH, Ciarallo S, Catzavelos C, Beniston R, Franssen E, Slingerland JM. PKB/Akt phosphorylates p27, impairs nuclear import of p27 and opposes p27-mediated G1 arrest. *Nat Med* 2002; **8**: 1153-1160

32 **Viglietto G**, Motti ML, Bruni P, Melillo RM, D'Alessio A, Califano D, Vinci F, Chiappetta G, Tsichlis P, Bellacosa A, Fusco A, Santoro M. Cytoplasmic relocalization and inhibition of the cyclin-dependent kinase inhibitor p27*kip1* by PKB/Akt-mediated phosphorylation in breast cancer. *Nat Med* 2002; **8**: 1136-1144

33 **Singh SP**, Lipman J, Goldman H, Ellis FH Jr, Aizenman L, Cangi MG, Signoretti S, Chiaur DS, Pagano M, Loda M. Loss or altered subcellular localization of p27 in Barrett's associated adenocarcinoma. *Cancer Res* 1998; **58**: 1730-1735

34 **Zhang WG**, Wu QM, Tong Q, Yu JP. Inhibitory effect of p27*kip1* mediated by adenovirus on model of esophageal carcinoma in nude mice. *Shijie Huaren Xiaohua Zazhi* 2003; **11**: 512-516

35 **Fan XM**, Wong BC, Wang WP, Zhou XM, Cho CH, Yuen ST, Leung SY, Lin MC, Kung HF, Lam SK. Inhibition of proteasome function induced apoptosis in gastric cancer. *Int J Cancer* 2001; **93**: 481-488

36 **Liu XJ**, Wu QM, Tong Q, Zhang WG, Liu CZ, Yu JP. The effect of p27*kip1* cDNA on the telomerase activity and cell cycle of SGC7901 cells. *Shiyong Aizheng Zazhi* 2003; **18**: 253-256

37 **Harada K**, Kurisu K, Sadatomo T, Tahara H, Tahara E, Ide T, Tahara E. Growth inhibition of human glioma cells by transfection-induced P21 and its effects on telomerase activity. *J Neurooncol* 2000; **47**: 39-46

38 **Fan XM**, Wong BC, Wang WP, Zhou XM, Cho CH, Yuen ST, Leung SY, Lin MC, Kung HF, Lam SK. Inhibition of proteasome function induced apoptosis in gastric cancer. *Int J Cancer* 2001; **93**: 481-488

39 **Ling YH**, Liebes L, Ng B, Buckley M, Elliott PJ, Adams J, Jiang JD, Muggia FM, Perez-Soler R. PS-341, a novel proteasome inhibitor, induces Bcl-2 phosphorylation and cleavage in association with G2-M phase arrest and apoptosis. *Mol Cancer Ther* 2002; **1**: 841-849

Edited by Kumar M and Wang XL **Proofread by** Xu FM

PO Box 2345, Beijing 100023, China
Fax: +86-10-85381893
E-mail: wjg@wjgnet.com www.wjgnet.com

World J Gastroenterol 2004;10(19):2785-2790
World Journal of Gastroenterology
Copyright © 2004 by The WJG Press ISSN 1007-9327

• LIVER CANCER •

Are gap junction gene connexins 26, 32 and 43 of prognostic values in hepatocellular carcinoma? A prospective study

I-Shyan Sheen, Kuo-Shyang Jeng, Po-Chuan Wang, Shou-Chuan Shih, Wen-Hsing Chang, Horng-Yuan Wang, Chung-Chu Chen, Li-Rung Shyung

I-Shyan Sheen, Division of Hepatogastroenterology, Chang Gung Memorial Hospital, Taipei, Taiwan, China
Kuo-Shyang Jeng, Departments of Surgery, Mackay Memorial Hospital, Taipei, Taiwan, China
Po-Chuan Wang, Shou-Chuan Shih, Wen-Hsing Chang, Horng-Yuan Wang, Chung-Chu Chen, Li-Rung Shyung, Department of Internal Medicine, Mackay Memorial Hospital, Taipei, Taiwan, China
Kuo-Shyang Jeng, Mackay Junior School of Nursing, Taipei, Taiwan, China
Supported by grants from Department of Health, National Science Council, Executive Yuan, Taiwan, China NSC-89-2314-B-195-027
Correspondence to: Kuo-Shyang Jeng, M.D., F.A.C.S., Department of Surgery, Mackay Memorial Hospital, No.92, Sec 2,Chung-San North Road, Taipei, Taiwan, China. issheen.jks@msa.hinet.net
Telephone: +886-2-25433535 **Fax:** +886-2-27065704
Received: 2004-02-02 **Accepted:** 2004-02-23

Abstract

AIM: To investigate the prognostic value of the expression of connexin (Cx) 26, 32 and 43 messenger RNA (mRNA) in hepatocellular carcinoma (HCC) tissues.

METHODS: Using a reverse-transcriptase polymerase chain reaction (RT-PCR), Cx 26, Cx 32 and Cx 43 mRNAs were determined in the liver tissues of 15 controls and in HCC tissues of 25 patients undergoing curative hepatic resection. The patients were followed up clinically.

RESULTS: Cx 26 and Cx 32 mRNAs were significantly lower in HCC tissues compared with controls (both $P<0.01$). By multivariate analysis, a lower level of Cx 26 and Cx 32 mRNA correlated significantly with a risk of HCC recurrence ($P = 0.033$) and recurrence-related mortality ($P = 0.031$, $P = 0.031$). Cx 43 mRNA was higher in HCC tissues compared with controls but did not correlate with postoperative recurrence or recurrence-related mortality. Other significant predictors of HCC recurrence included cellular dedifferentiation ($P = 0.033$), less encapsulation ($P = 0.050$), vascular permeation ($P = 0.046$), and daughter nodules ($P = 0.046$). Significant variables related to recurrence-related mortality consisted of cell dedifferentiation ($P = 0.031$), vascular permeation ($P = 0.048$), and daughter nodules ($P = 0.048$). The levels of Cx 26 and Cx 32 mRNAs correlated significantly with cell differentiation ($P = 0.031$).

CONCLUSION: A low expression of Cx 26 and Cx 32 mRNAs in HCC tissues is predictive of postoperative recurrence of HCCs.

Sheen IS, Jeng KS, Wang PC, Shih SC, Chang WH, Wang HY, Chen CC, Shyung LR. Are gap junction gene connexins 26, 32 and 43 of prognostic values in hepatocellular carcinoma? A prospective study. *World J Gastroenterol* 2004; 10(19): 2785-2790
http://www.wjgnet.com/1007-9327/10/2785.asp

INTRODUCTION

Hepatocellular carcinoma (HCC) is a leading cause of death in Taiwan and many Asian countries, where hepatitis B and C have a high prevalence. During the last 10 years, efforts have been made worldwide toward early detection and curative surgical resection of HCC. However, despite diagnostic and therapeutic advances, postoperative recurrence is still common[1-7]. Predicting which patients are likely to have a recurrence is a challenge.

Gap junctional intercellular communication (GJIC) occurs via intercellular hemichannels, which are formed by six basic protein subunits expressed in neighboring cells. These subunits are called connexins (Cx)[8]. Six connexins locate around a central pore, through which adjacent cells directly exchange low weight molecules providing information or energy. GJIC plays important roles in embryonic development, metabolic cooperation, growth control, cell proliferation, and differentiation[9-12]. Many authors believed that disorders of GJIC were involved in carcinogenesis[12-21].

Connexin 32 (Cx 32) and connexin 26 (Cx 26) are the major gap junction proteins in hepatocytes. Some authors have reported that Cx 32 and Cx 43 mRNAs and their proteins were significantly decreased in HCC tissues and cell lines. In contrast, Cx 43 protein was increased in the hepatoma cell line SMMC-7721[22-25].

To the best of our knowledge, little is known about the prognostic significance of connexin mRNA expression in the prediction of postresection recurrence of HCCs. We conducted this prospective study to investigate the correlation between connexin mRNA expression in HCC tissues and postoperative recurrence of the tumor.

MATERIALS AND METHODS

Study population

From July 1999 to August 2000, 25 (18 men and 7 women, with a mean age of 56.4±12.6 years) of 34 consecutive patients with HCC undergoing curative hepatectomy were enrolled in this prospective study. The 9 patients who were excluded had a previous hepatectomy, preoperative neoadjuvant ethanol injection, hepatic arterial chemoembolization (TACE), or surgical morbidity. The surgical procedures performed included 23 major resections (6 extended right lobectomies, 10 right lobectomies, 3 left lobectomies and 4 double segmentectomies) and 2 minor resections (single segmentectomy). Clinical details were available from medical records on all patients (Table 1). Connexins were assayed in both cancerous and noncancerous liver tissues obtained at the time of resection. A control group including 5 healthy volunteers, 5 individuals with chronic active hepatitis without HCCs, and 5 individuals with liver cirrhosis but no HCC also underwent liver biopsies during exploratory laparotomies for other reasons. The surgically removed liver samples were immediately transferred to the pathology laboratory, dissected, frozen in liquid nitrogen, and stored at -80 ℃ until RNA extraction. Frozen and formalin-fixed samples of the dissected tumor and surrounding tissues were also studied by routine pathology. No obvious ischemic change

was observed in the surrounding tissues, suggesting that the time between removal and freezing of samples did not result in problematic artifacts.

After discharge, the patients were assessed regularly to detect tumor recurrence with abdominal ultrasonography (every 2-3 mo during the first 5 years, then every 4-6 mo thereafter), serum alpha fetoprotein (AFP) and liver biochemistry (every 2 mo during the first 2 years, then every 4 mo during the following 3 years, and every 6 mo thereafter), abdominal computed tomography (CT) (every 6 mo during the first 5 years, then annually), and chest X-ray and bone scans (every 6 mo). Hepatic arteriography was obtained if the other studies suggested possible recurrences. A recurrence was defined as detection of a tumor on any imaging study.

Clinicopathologic parameters analyzed included sex (male *vs* female), age, presence of liver cirrhosis, hepatitis B virus (HBV) infection (hepatitis B surface antigen-positive), hepatitis C virus (HCV) infection (anti-hepatitis C virus antibody-positive), serum AFP level (<20 ng/mL *vs* 20 to 1 000 ng/mL *vs* >1 000 ng/mL), cirrhosis, Child-Pugh class of liver functional reserve (A *vs* B), tumor size (<3 cm *vs* 3 to 10 cm *vs* >10 cm in diameter), tumor encapsulation (complete *vs* incomplete or absent), presence of daughter nodules, vascular permeation (including vascular invasion and/or tumor thrombi in either the portal or hepatic vein), and cell differentiation grade (Edmondson and Steiner grades I to IV) (Table 1).

Table 1 Demographic, clinical and pathological variables in patients with HCC undergoing curative resections (n = 25)

Variables	Patients (n, %)
Age (mean, yr)	56.4±12.6
Male	18 (72)
Child- Pugh class A	
Serum AFP <20 ng/mL	3 (12)
20-10^3 ng/mL	10 (40)
>10^3 ng/mL	12 (48)
HBsAg (+)	12 (48)
Anti-HCV (+)	10 (40)
Diameter of HCC <3 cm	2 (8)
3-10 cm	10 (40)
>10 cm	13 (52)
Cirrhosis	20 (80)
Edmondson-Steiner's grade I	11 (44)
grade II	
grade III	14 (56)
grade IV	
Complete capsule	9 (36)
Vascular permeation	14 (56)
Daughter nodules	13 (52)
Multinodular HCC	5 (20)
Tumor necrosis	5 (20)
Tumor hemorrhage	1 (4)

AFP: serum alpha fetoprotein; HBsAg (+): positive hepatitis B surface antigen; Anti-HCV(+): positive hepatitis C virus antibody; Edmondson Steiner grade: differentiation grade.

Detection of connexin mRNA in liver tissues

We chose measuring connexin mRNA instead of measuring protein because RT-PCR was thought to provide better quantification method than immunohistochemistry.

Extraction of RNA Resected tissues were completely homogenized in 1 mL of RNA-bee™ (Tel-Test, Protech Technology Enterprises Co., Ltd, Friendswood, TX, USA), 0.2 mL chloroform was added, and the mixture was shaken vigorously for 15 to 30 s. The samples were stored on ice for 5 min and then centrifuged at 12 000 *g* for 15 min. The supernatant was transferred to a new 1.5 mL Eppendorf tube, precipitated with 0.5 mL of isopropanol for 5 min at 4 ℃, and centrifuged at 12 000 *g* for 5 min at 4 ℃. The supernatant was removed and the RNA pellet was washed with 1 mL of isopropanol and shaken to dislodge the pellet from the side of the tube. The pellet was centrifuged again at 12 000 *g* for 5 min at 4 ℃, the supernatant was removed, and the RNA pellet was washed once again with 750 mL/L ethanol. The pellet was resuspended in at least 1 mL of 750 mL/L ethanol and centrifuged at 7 500 r/min for 5 min at 4 ℃, after which the ethanol was carefully removed. The RNA was allowed to dry in air and then dissolved in DEPC-H_2O (50 to 100 μL) and stored at -80 ℃.

Reverse transcription The RNA sample was heated at 55 ℃ for 10 min and chilled on ice. The following reagents were then added: (1) 4 μL 5×RT buffer containing Tris-HCl (pH 8.3), 75 mmol/L KCl, 3 mmol/L $MgCl_2$, and 10 mmol/L DTT (dithiothreitol), (2) 3 μL 10 mmol/L dNTP (deoxyribonucleoside triphosphate), (3) 1.6 μL Oligo-d$(T)_{18}$ and 0.4 μL random hexamers (N) 6 (1 μg/μL), (4) 0.5 μL RNase inhibitor (40 U/μL), (5) 3 μL 25 mmol/L $MnCl_2$, (6) 6 μL RNA in DEPC-H_2O, and (7) 0.5 μL DEPC-H_2O. The mixture was incubated at 70 ℃ for 2 min and then chilled to 23 ℃ to anneal the primer to the RNA. We then added 1 μL of M-MLV RTase (moloney murine leukemia virus reverse transcriptase, 200 U/μL, Promega) and the mixture was incubated for 10 min at 23 ℃ followed by 60 min at 40 ℃. It was heated at 94 ℃ for 5 min, then chilled on ice. The cDNA was stored -20 ℃.

Amplification of connexins 26, 32, 43, and GAPDH cDNA by PCR First-strand cDNA synthesis was carried out using 2 μg of total RNA purified from 50 mg tissue. Reverse transcription was performed in a final volume of 20 μL containing 2 μg of random hexamer (Gene Teks Bioscience Inc., Taipei), and 1.5 mmol/L each of dATP, dCTP, dGTP, and dTTP. Each reaction mixture was incubated for 8 min at 23 ℃ with 20 U of rRNasin (RNase inhibitor; Promega, Madison, WI) followed by incubation with 200 U of moloney murine leukemia virus reverse transcriptase (Gibco-BRL, Paisley, UK) for 60 min at 40 ℃, followed by 5 min at 94 ℃. PCR was performed in a final volume of 50 μL, by using 2 μL of cDNA solution in a mixture containing 0.4 mmol/L deoxynucleotide triphosphates, 40 pmol/L of both sense and antisense oligonucleotide primers for Cx 26, Cx 32 or Cx 43, 2.5 mmol/L $MgCl_2$, 2.5U of Taq DNA polymerase (Promega) and 5 μL of 10x Taq DNA polymerase reaction buffer (500 mmol/L KCl, 100 mmol/L Tris-HCl (pH9.0), 10 g/L Triton-X-100). PCR primer sequences of the sense and antisense oligonucleotides for Cx 26, Cx 32 and Cx 43 as well as the direction, size and reaction conditions are shown in Table 2. For example, Cx 26 anti-sense oligonucleotide (5'-CCGAAGTTCATGAAGGGAGA GAT-3') and its related scrambled sequence (5'-GGTCTTTTGG ACTTCCCTGAGCA -3') were synthesized (by Sigma-Genosys Ltd, Woodlands, TX, USA). GAPDH was used as a control, with the quantities of the other mRNA products reported as their intensity as a fraction of that of GAPDH mRNA. To eliminate any possibility of genomic DNA contamination, PCR amplification reaction was carried out on each sample from the RNA extraction. As another internal contamination control, PCR amplification was also carried out on a sample of reaction mixture in the absence of cDNA.

The intensity of bands was measured using Fujifilm Science Lab 98 (Image Gauge V3.12). The sensitivity of our assay was assessed using human hepatocytes. A HepG2 (hepatoblastoma) cell line served as a positive control for connexin mRNA expression. For negative controls, we used EDTA-treated water (filtered and vaporized).

Statistical analysis

A statistical software package (SPSS for windows, version 8.0, Chicago, Illinois) was used. Student's *t*-test was used to analyze continuous variables and chi-square or Fisher's exact test was used for categorical variables. A Cox proportional hazards model was used for multivariate stepwise analysis to identify the significant factors predicting recurrence and mortality. Significance was taken as a *P* value <0.05.

Table 2 Nucleotide sequences of the primer sets and specific oligonucleotide probes to each type of connexin 5'-noncoding mRNA

Type of connexin mRNA	Primer probes	Nucleotide sequences
Cx 26	Sense	5' CCGAAGTTCATGAAGGGAGAGAT
	Antisense	5' GGTCTTTTGGACTTCCCTGAGCA
Cx 32	Sense	5' CTGCTCTACCCGGGCTATGC
	Antisense	5' CAGGCTGAGCATCGGTCGCTCTT
Cx 43	Sense	5' TACCATGCGACCAGTGGTGCGCT
	Antisense	5'GAATTCTGGTTATCATCGTCGGGGAA

RESULTS

RT-PCR analysis of connexin transcripts in liver and HCC tissues

The mean values of Cx 26 mRNA and Cx 32 mRNA in HCC tissues were significantly lower than those in the control samples (*P*<0.01, *P*<0.01 respectively). There was no significant difference in Cx 43 mRNA between cancerous and control tissues (Table 3).

Table 3 Correlation of Cx 26, Cx 32, and Cx 43 mRNAs in cancerous and noncancerous liver tissues of 25 patients with HCC and liver tissues of 15 control patients

Tissues	mRNA (mean value)		
	Connexin 26	Connexin 32	Connexin 43
HCC patients			
Cancerous liver[1]	0.745	0.775	0.241
Controls[2]	1.205	1.225	0.100

P<0.01 for connexin 26 mRNA; *P*<0.01 for connexin 32 mRNA; *P*>0.05 for connexin 43 mRNA.

Correlation of connexin mRNA expression and tumor recurrence

Patients were followed up for a median of 45 mo (range 38 to 51 mo). Fourteen (56%) had clinically detectable recurrences, of whom 6 died. A low Cx 26 mRNA correlated significantly with tumor recurrences by both univariate (*P*<0.001, *P*<0.001) and multivariate analyses (*P* = 0.033, *P* = 0.033). No such correlation was found with Cx 43 mRNA. By multivariate analyses, other significant predictors of recurrences included poor cell differentiation (*P* = 0.033), less encapsulation (*P* = 0.050), vascular permeation (*P* = 0.046) and the presence of daughter nodules (*P* = 0.046) (Table 4).

Correlation of connexin mRNA expression and recurrence-related death

A low level of Cx 26 mRNA and Cx 32 mRNA in HCC tissues was significantly correlated with death from recurrent tumors by both univariate (*P*<0.001, *P*<0.001) and multivariate analyses (*P* = 0.031, *P* = 0.031) (Table 5). By multivariate analyses, poor cell differentiation, vascular permeation, and daughter nodules correlated significantly with mortality (*P* = 0.031, 0.048, and 0.048 respectively), and less encapsulation correlated with mortality with a marginal significance (*P* = 0.053).

Table 4 Predictors of HCC recurrence

Variable	*P* values	
	UV	MV
Sex	1.000	-
Age (yr)	0.030	0.071
Tumor diameter (<3 cm, >10 cm)	0.250	-
Liver cirrhosis	0.009	0.067
Child-Pugh class	0.528	-
Serum AFP	0.744	-
HBsAg (+)	1.000	-
Anti-HCV (+)	1.000	-
Edmondson Steiner grade	<0.001	0.033
Capsule	<0.001	0.050
Vascular permeation	<0.001	0.046
Daughter nodules	<0.001	0.046
Tumor necrosis	0.046	-
Tumor hemorrhage	0.046	-
Connexin 26 mRNA	<0.001	0.033
Connexin 32 mRNA	<0.001	0.033
Connexin 43 mRNA	0.280	0.071

UV: univariate analysis; MV: multivariate analysis; AFP: serum alpha fetoprotein; HbsAg(+): positive hepatitis B surface antigen; Anti-HCV(+): positive hepatitis C virus antibody; Edmondson Steiner grade: differentiation grades I, II *vs* III, IV.

Table 5 Correlation between clinical and pathological variables and recurrence-related mortality

Parameters	*P* values	
	UV	MV
Sex	0.888	-
Age (yr)	0.005	0.356
Tumor diameter (<3 cm, >10 cm)	0.324	-
Liver cirrhosis	0.030	0.324
Child-Pugh class	0.548	
HBsAg (+)	0.956	-
Anti-HCV (+)	0.785	-
Edmondson Steiner grade	0.000	0.031
Capsule	0.000	0.053
Vascular permeation	0.000	0.048
Daughter nodules	0.039	0.048
Multinodular HCC	0.007	0.324
Tumor necrosis	0.373	-
Tumor hemorrhage	0.356	-
Connexin 26 mRNA	<0.001	0.031
Connexin 32 mRNA	<0.001	0.031
Connexin 43 mRNA	0.461	-

UV: univariate analysis; MV: multivariate analysis; AFP: serum alpha fetoprotein; HBsAg (+): positive hepatitis B surface antigen; Anti-HCV(+): positive hepatitis C virus antibody; Edmondson Steiner grade: differentiation grades I, II *vs* III, IV; n.s: not significant.

Correlation between connexin mRNA expression and clinical and histopathologic features

Cx 26 and Cx 32 mRNAs were significantly correlated with cell differentiation but not with gender, age, serum AFP level, chronic HBV or HCV carriage, tumor size, coexisting cirrhosis, encapsulation, vascular permeation, daughter nodules, tumor necrosis, or tumor hemorrhage (all $P>0.05$).

DISCUSSION

Our study showed that a low value of Cx 26 and Cx 32 mRNAs in resected HCC tissues was significantly associated with an increased risk of postoperative recurrences and death. While increased Cx 43 mRNA was not significantly predictive of outcomes.

Most tumors studied had a reduction in either homologous or heterologous GJIC. This presumably contributed to neoplastic progression by allowing tumor cells to escape intercellular signals involved in regulation of cell proliferation, differentiation, and apoptosis[8,10,12,13]. Cx 32 and Cx 26, the components of hepatocyte gap junctions, were also found in a variety of other cell types. Cx 43 (or α1) was prominent in the liver capsule and between other types of liver cells, including Ito (fat-storing) cells, cholangiocytes, and endothelial cells lining the venules. We speculated that, because the Cx 32 and Cx 26 genes were expressed in normal liver tissues, they might serve as tumor suppressor genes. Other authors have suggested Cx 32 and Cx 43 for this role[16]. Eghbali *et al*.[18] found that transfection of tumor cells with Cx 32 cDNA retarded tumor growth *in vivo*. They demonstrated that the growth rate of tumor cells correlated negatively with the strength of intercellular communication.

Since Lowenstein *et al*.[12] used electrophysiologic techniques to demonstrate a lack of communication between rat liver cancer cells, an interest has been attracted to changes in cell-to-cell communications in carcinoma tissues. In studies of rat hepatocarcinogenesis, several laboratories have found that a significant decrease in the major liver gap junction protein Cx 32 at the mRNA or protein level occurred in preneoplastic nodules and HCCs induced by chemicals[14,17,19,21]. Loss of GJIC due to down-regulated expression of Cx genes appears to be an important event in cell transformation and is associated with uncontrolled tumor cell growth. Transformed cells *in vitro* and *in vivo* had a decreased GJIC capacity between themselves or with surrounding normal cells[18,20]. Disruption of GJIC activity could contribute to the multi-step process of carcinogenesis.

Oyamada *et al*.[25] reported that GJIC was altered in human HCCs by molecular mechanisms different from those in rat hepatocarcinogenesis. It is possible that defects in post-translational processing of Cx 32 and Cx 43 proteins may be an obstacle in their transportation to cell membranes. Some studies suggested that multiple mechanisms could likely contribute to block of GJIC, including decreased expressions of gap junction proteins and abnormal pathways of signal transduction resulted from decreased levels of intracellular Ca^{2+}, phosphorylation of the tyrosine of Cx proteins[19]. Other potential mechanisms included control of cell recognition and gating of established gap junctions[19,20,24].

Different authors have proposed various mechanisms by which changes in connexin mRNA might contribute to the biological behaviors of HCC. These include rapid proliferation of tumor cells, changes in the interaction between host and tumors, aberrant localization of connexins, and change in connexin expression during tumor differentiation. Whether the rapid growth of preneoplastic tissues is the cause or the effect of a decrease in connexin mRNA remains unknown.

Some authors have found a great decrease in the number of gap junctions after partial hepatectomy. A reciprocal correlation between the expression of Cx32 and the mitotic activities of hepatocytes during liver regeneration was noted. Based on their findings of a significant reduction of Cx 32 expression in S-phase cells, it seems that quantitative changes in gap junction expression may play an important role in the control of proliferation of liver cells. Since neoplastic liver tissues had a higher proliferation rate than the surrounding tissues, it might have fewer gap junctions. It was found that the partial loss of gap junctions provided a selective advantage for those preneoplastic liver cells which developed into rapidly proliferating tumor cells. It is possible that preneoplastic cells with a reduced number of gap junctions might have an increased capability of proliferating and are therefore more likely to develop into HCC[14].

With regard to changes in the interaction between host and tumors, Krutovskikh *et al*.[24] highlighted the role such an interaction might play in natural host resistance against neoplastic growth, with an emphasis on the underlying mechanisms of both connexin function and impairment.

Some other authors attributed the possible contribution of connexins to aberrant localization of the gap junction proteins. Some studies showed that the levels of Cx 32 and Cx 43 mRNAs were not decreased in HCCs compared with normal liver tissues, but the proteins were aberrantly located in HCCs[25]. Krutovskikh *et al*.[26] thought abnormal location of Cx 32 was more important than its translational disregulation. Omori *et al*.[17] drew a similar conclusion regarding Cx 32.

Another mechanism leading to a loss of heterologous host-cancer cell coupling is a change in the expression of connexin species in tumors during differentiation. According to Markert *et al*.[27] three important characteristics of cell differentiation were the rate of cell division, the adhesive properties of the cell membrane that determine the capacity of the cell of migrating or metastasizing, and specific patterns of cell metabolism. Connexins are likely related to adhesive properties. An altered pattern of adhesion molecules on the surface of tumorigenic hepatocytes may influence the distribution of gap junctions in neoplastic tissues.

A characteristic feature of a cancerous phenotype is dedifferentiation. In some tissues, cells at different stages of differentiation express different sets of connexin proteins. HCC cells may express the same connexins as surrounding normal hepatocytes and therefore adhere well to each other. However, because of the inability of Cx 32 hemichannels expressed by normal hepatocytes to assemble functional gap junctional channels with Cx 43 hemichannels in neoplastic cells, they failed to communicate with each other[28,29].

The high recurrence rate after resection is the main cause of the poor outcomes of HCC. Variables correlated with tumor recurrence included high serum AFP, hepatitis, vascular permeation, grade of cell differentiation, infiltration or absence of capsule, tumor size, coexisting cirrhosis, presence of daughter nodules, and multiple lesions[1-7, 30-33]. According to our study, connexin was significantly correlated with the grade of cell differentiation. In our series, tumors with higher levels of Cx26 and Cx32 mRNAs, that were closer to normal, were more likely to be well-differentiated (Edmondson and Steiner grade I) and less likely to recur than those tumors of grade II to IV. The association between the grade of anaplasia and connexin positivity also varied in other reports. We attribute these differences to the possibility that different histologic grades may coexist within a particular HCC. Additionally, the regulation of connexin may be complex, particularly at different grades of dedifferentiation.

There is also discrepancy in the expression of Cx 43 in human HCCs. Ma *et al*.[34] suggested that decreased expression of Cx 32 and Cx 43 might be closely related to liver carcinogenesis.

We found a similar decrease in Cx32 mRNA, but Cx 43 mRNA was increased. The discrepancy might be due to a difference in study samples and examination methods, as well as the background liver diseases. Furthermore, it should be noted that the benign liver tissue surrounding HCC was not normal. Oyamada *et al*.[25] studied 6 patients with HCC and found various abnormalities in the surrounding tissues, including cholestasis in 2, fatty liver in 1, chronic persistent hepatitis in 1, cirrhosis in 1, and possible hemochromatosis in 1. In our 25 patients, we found a different distribution of background liver diseases, including cirrhosis in 20 (80%), hepatitis B virus hepatitis in 12 (48%) and hepatitis C virus hepatitis in 10 (40%); 3 patients had both hepatitis B and C hepatitis. We used RT-PCR and Northern and Southern blot analyses. Oyamada *et al*.[25] found no decrease in Cx 32 mRNA, while the level of Cx 43 mRNA was higher than that in the surrounding nontumorous tissues but without any amplification of Cx 43 gene. They attributed the increased expression of Cx 43 to a large amount of connective tissues in HCC.

However, another possible explanation for elevated expression of Cx 43 is the stem cell concept of tumor cell origins. This theory proposes that the target cells in carcinogenesis are stem cells present in normal tissues. Assuming that a stem cell that expresses Cx 43 is the target cell in human hepatocarcinogenesis, the resulting neoplasm would be expected to express connexin 43. The mechanism of switching on the Cx 43 gene in human HCC remains to be investigated, which may include DNA methylation, a stablization of RNA, or positive or negative trans-acting factors[25].

Carcinogenesis is believed to result from block, arrest, or derangement in differentiation. Based on this concept, we could explain the increased expression of Cx 43 by the appearance of isozymes, for example, aldolase and γ-glutamyl transpeptidase, in human HCC.

We proposed that not all HCCs contained connexin mutations, in another word, there might be both connexin-dependent and connexin-independent pathways leading to liver cancer. The selective advantage conferred on liver cells by a mutant connexin gene seems to be significant in later steps of tumorigenesis, after the accumulation of additional genetic changes. The identification of genetic alterations related to connexin changes remains a considerable challenge in the field of liver cancer research.

Surgery remains the best possible therapy for patients with HCC. Examination of connexin mRNA in HCC tissues may provide information about the risk of postoperative recurrences, and our results support this hypothesis. Addition of neoadjuvant therapy after surgery, might be considered for the risk patients. Furthermore, serial measurement of circulating connexin mRNAs after surgery to monitor the effects of therapy or screen for recurrences needs further investigation.

REFERENCES

1 **Poon RT**, Fan ST, Lo CM, Liu CL, Wong J. Intrahepatic recurrence after curative resection of hepatocellular carcinoma. Long-term results of treatment and prognostic factors. *Ann Surg* 1999; **229**: 216–222

2 **Yamamoto J**, Kosuge T, Takayama T, Shimada K, Yamasaki S, Ozaki H, Yamaguchi N, Makuuchi M. Recurrence of hepatocellular carcinoma after surgery. *Br J Surg* 1996; **83:** 1219–1222

3 **Lee PH,** Lin WJ, Tsang YM. Clinical management of recurrent hepatocellular carcinoma. *Ann Surg* 1995; **222:** 670–676

4 **Jeng KS,** Sheen IS, Chen BF, Wu JY. Is the p53 gene mutation of prognostic value in hepatocellular carcinoma after resection? *Arch Surg* 2000; **135:** 1329–1333

5 **Jeng JS**, Sheen IS, Tsai YC. Gamma glutamyl transpeptidase messenger RNA may serve as a diagnostic aid in hepatocellular carcinoma. *Br J Surg* 2001; **88**: 986–987

6 **Jeng KS**, Chen BF, Lin HJ. En bloc resection for extensive hepatocellular carcinoma. Is it advisable? *World J Surg* 1994; **18:** 834–849

7 **Jeng K**, Yang FS, Chiang HJ, Ohta I. Is it advisable to perform a second operation for nodular recurrent hepatocellular carcinoma within the cirrhotic liver remnant? A comparison with TACE. *World J Surg* 1992; **16:** 1188–1191

8 **Bennett MV**, Barrio LC, Bargiello TA, Spray DC, Hertzberg E, Saez JC. Gap junctions: new tools, new answers, new questions. *Neuron* 1991; **6:** 305-320

9 **Robenek H**, Rassat J, Themann H. A quantitative freeze-fracture analysis of gap and tight junctions in the normal and cholestatic human liver. *Virchows Arch B Cell Pathol Incl Mol Pathol* 1981; **38:** 39-56

10 **Wilson MR**, Close TW, Trosko JE. Cell population dynamics (apoptosis, mitosis, and cell-cell communication) during disruption of homeostasis. *Exp Cell Res* 2000; **254:** 257-268

11 **Yamaoka K**, Nouchi T, Kohashi T, Marumo F, Sato C. Expression of gap junction protein connexin 32 in chronic liver diseases. *Liver* 2000; **20:** 104-107

12 **Loewenstein WR**, Kanno Y. Intercellular communication and the control of tissue growth: lack of communication between cancer cells. *Nature* 1966; **209:** 1248-1249

13 **Niessen H**, Willecke K. Strongly decreased gap junctional permeability to inositol 1,4,5-triphosphate in connexin32 deficient hepatocytes. *FEBS Lett* 2000; **466:** 112-114

14 **Janssen-Timmen U**, Traub O, Dermietzel R, Rabes HM, Willecke K. Reduced number of gap junctions in rat hepatocarcinomas detected by monoclonal antibody. *Carcinogenesis* 1986; **7:** 1475-1482

15 **Lee SW**, Tomasetto C, Paul D, Keyomarsi K, Sager R. Transcriptional downregulation of gap-junction proteins blocks junctional communication in human mammary tumor cell lines. *J Cell Biol* 1992; **118:** 1213-1221

16 **Hirschi KK**, Xu CE, Tsukamoto T, Sager R. Gap junction genes Cx26 and Cx43 individually suppress the cancer phenotype of human mammary carcinoma cells and restore differentiation potential. *Cell Growth Differ* 1996; **7:** 861-870

17 **Omori Y**, Krutovskikh V, Mironov N, Tsuda H, Yamasaki H. Cx32 gene mutation in a chemically induced rat liver tumour. *Carcinogenesis* 1996; **17:** 2077-2080

18 **Eghbali B**, Kessler JA, Reid LM, Roy C, Spray DC. Involvement of gap junctions in tumorigenesis: transfection of tumor cells with connexin 32 cDNA retards growth *in vivo*. *Proc Natl Acad Sci U S A* 1991; **88:** 10701-10705

19 **Krutovskikh VA**, Mesnil M, Mazzoleni G, Yamasaki H. Inhibition of rat liver gap junction intercellular communication by tumor-promoting agents *in vivo*. Association with aberrant localization of connexin proteins. *Lab Invest* 1995; **72:** 571-577

20 **Rose B**, Mehta PP, Loewenstein WR. Gap-junction protein gene suppresses tumorigenicity. *Carcinogenesis* 1993; **14:** 1073-1075

21 **Iwai M**, Harada Y, Muramatsu A, Tanaka S, Mori T, Okanoue T, Katoh F, Ohkusa T, Kashima K. Development of gap junctional channels and intercellular communication in rat liver during ontogenesis. *J Hepatol* 2000; **32:** 11-18

22 **Rahman S**, Carlile G, Evans WH. Assembly of hepatic gap junctions. Topography and distribution of connexin 32 in intracellular and plasma membranes determined using sequence-specific antibodies. *J Biol Chem* 1993; **268**: 1260-1265

23 **Zhang JT**, Nicholson BJ. Sequence and tissue distribution of a second protein of hepatic gap junctions, Cx26, as deduced from its cDNA. *J Cell Biol* 1989; **109:** 3391-3401

24 **Krutovskikh V**, Mazzoleni G, Mironov N, Omori Y, Aguelon AM, Mesnil M, Berger F, Partensky C, Yamasaki H. Altered homologous and heterologous gap-junctional intercellular communication in primary human liver tumors associated with aberrant protein localization but not gene mutation of connexin 32. *Int J Cancer* 1994; **56:** 87-94

25 **Oyamada M**, Krutovskikh VA, Mesnil M, Partensky C, Berger F, Yamasaki H. Aberrant expression of gap junction gene in primary human hepatocellular carcinomas: increased expres-

sion of cardiac-type gap junction gene connexin 43. *Mol Carcinog* 1990; **3:** 273-278

26 **Krutovskikh VA**, Mesnil M, Mazzoleni G, Yamasaki H. Inhibition of rat liver gap junction intercellular communication by tumor-promoting agents *in vivo*. Association with aberrant localization of connexin proteins. *Lab Invest* 1995; **72:** 571-577

27 **Markert CL.** Neoplasia: a disease of cell differentiation. *Cancer Res* 1968; **28:** 1908-1914

28 **Shimoyama Y**, Hirohashi S. Cadherin intercellular adhesion molecule in hepatocellular carcinomas: loss of E-cadherin expression in an undifferentiated carcinoma. *Cancer Lett* 1991; **57:** 131-135

29 **Yamaoka K**, Nouchi T, Tazawa J, Hiranuma S, Marumo F, Sato C. Expression of gap junction protein connexin 32 and E-cadherin in human hepatocellular carcinoma. *J Hepatol* 1995; **22:** 536-539

30 **Ng IO**, Lai EC, Fan ST, Ng MM, So MK. Prognostic significance of pathologic features of hepatocellular carcinoma. A multivariate analysis of 278 patients. *Cancer* 1995; **76:** 2443–2448

31 **Sakamoto M**, Ino Y, Fujii T, Hirohashi S. Phenotype changes in tumor vessels associated with the progression of hepatocellular carcinoma. *Jpn J Clin Oncol* 1993; **23:** 98-104

32 **Terada T**, Nakanuma Y. Arterial elements and perisinusoidal cells in borderline hepatocellular nodules and small hepatocellular carcinomas. *Histopathology* 1995; **27:** 333–339

33 **Nakashima O**. Pathological diagnosis of hepatocellular carcinoma. *Nippon Rinsho* 2001; **59**(Suppl 6): 333–341

34 **Ma XD**, Ma X, Sui YF, Wang WL, Wang CM. Signal transduction of gap junctional genes, connexin32, connexin43 in human hepatocarcinogenesis. *World J Gastroenterol* 2003; **9:** 946-950

Edited by Zhu LH and Wang XL **Proofread by** Xu FM

PO Box 2345, Beijing 100023, China
Fax: +86-10-85381893
E-mail: wjg@wjgnet.com www.wjgnet.com

World J Gastroenterol 2004;10(19):2791-2794
World Journal of Gastroenterology
Copyright © 2004 by The WJG Press ISSN 1007-9327

• LIVER CANCER •

Postoperative adjuvant arterial chemoembolization improves survival of hepatocellular carcinoma patients with risk factors for residual tumor: A retrospective control study

Zheng-Gang Ren, Zhi-Ying Lin, Jing-Lin Xia, Sheng-Long Ye, Zeng-Chen Ma, Qing-Hai Ye, Lun-Xiu Qin, Zhi-Quan Wu, Jia Fan, Zhao-You Tang

Zheng-Gang Ren, Zhi-Ying Lin, Jing-Lin Xia, Sheng-Long Ye, Zeng-Chen Ma, Qing-Hai Ye, Lun-Xiu Qin, Zhi-Quan Wu, Jia Fan, Zhao-You Tang, Liver Cancer Institute and Zhongshan Hospital, Fudan University, Shanghai 200032, China
Correspondence to: Dr. Zhao-You Tang, Liver Cancer Institute and Zhongshan Hospital, Fudan University, Shanghai 200032, China. zytang@srcap.stc.sh.cn
Telephone: +86-21-64037181 **Fax:** +86-21-64037181
Received: 2003-10-09 **Accepted:** 2003-12-06

Ren ZG, Lin ZY, Xia JL, Ye SL, Ma ZC, Ye QH, Qin LX, Wu ZQ, Fan J, Tang ZY. Postoperative adjuvant arterial chemoembolization improves survival of hepatocellular carcinoma patients with risk factors for residual tumor: A retrospective control study. *World J Gastroenterol* 2004; 10(19): 2791-2794
http://www.wjgnet.com/1007-9327/10/2791.asp

Abstract

AIM: To evaluate the effect of postoperative adjuvant transcatheter arterial chemoembolization (TACE) on the prognosis of hepatocellular carcinoma (HCC) patients with or without risk factors for the residual tumor.

METHODS: From January 1995 to December 1998, 549 consecutive HCC patients undergoing surgical resection were included in this research. There were 185 patients who underwent surgical resection with adjuvant TACE and 364 patients who underwent surgical resection only. Tumors with a diameter more than 5 cm, multiple nodules, and vascular invasion were defined as risk factors for residual tumor and used for patient stratification. Kaplan-Meier method was used to analyze survival curve and Cox proportional hazard model was used to evaluate the prognostic significance of adjuvant TACE.

RESULTS: In the patients without any risk factors for the residual tumor, the 1-, 3-, 5-year survival rates were 93.48%, 75.85%, 62.39% in the control group and 97.39%, 70.37%, 50.85% in the adjuvant TACE group, respectively. There was no significant difference in the survival between two groups (P = 0.3956). However, in the patients with risk factors for residual tumor, postoperative adjuvant TACE significantly prolonged the patients' survival. There was a statistically significant difference in survival between two groups (P = 0.0216). The 1-, 3-, 5-year survival rates were 69.95%, 49.86%, 37.40% in the control group and 89.67%, 61.28%, 44.36% in the adjuvant TACE group, respectively. Cox proportional hazard model showed that tumor diameter and cirrhosis, but not the adjuvant TACE, were the significantly independent prognostic factors in the patients without risk factors for residual tumor. However, in the patients with risk factors for residual tumor adjuvant TACE, and also tumor diameter, AFP level, vascular invasion, were the significantly independent factors associated with the decreasing risk for patients' death from HCC.

CONCLUSION: Postoperative adjuvant TACE can prolong the survival of patients with risk factors for residual tumor, but can not prolong the survival of patients without risk factors for residual tumor.

INTRODUCTION

Hepatocellular carcinoma is the fifth most common malignant death in the world and is estimated to cause half a million deaths annually[1]. In China, primary liver cancer mortality ranked second after stomach cancer. The age-standardized mortality rate (adjusted by the world population) was 33.7 per 100 000 in male Chinese and 12.3 per 100 000 in female Chinese[2]. Surgical resection is a major treatment for hepatocellular carcinoma (HCC)[3]. However, postoperative recurrence is still high and the main death cause after resection of HCC[4]. The overall recurrence was 30.1%, 62.3% and 79.0% in 1, 3, 5 years after resection of HCC, respectively[5]. Adjuvant therapies were used to prolong the survival and decrease the recurrence of HCC in different centers, such as transcatheter arterial chemoembolization (TACE)[6-13], polyprenoic acid[14], adoptive immunotherapy[15], interferon[16], and iodine-131-labeled lipiodol[17-19]. TACE was one of the most commonly used adjuvant managements for preventing recurrence and prolonging the survival of patients postoperatively. However, the benefits of adjuvant TACE were controversial. From January 1995 to December 1998, a consecutive series of 549 HCC patients with partially hepatectomy were included in this study. Of them, 185 patients received adjuvant TACE and 364 patients received surgical resection only. The aim of this research was to evaluate the benefits of adjuvant TACE in our series and to determine whether the characteristics of HCC such as diameter of tumor size, tumor nodules and vascular invasion could affect the benefits of adjuvant TACE to the patients' survival.

MATERIALS AND METHODS

Patients

This study included 549 patients with HCC who underwent partial hepatectomy. The entry criteria included: 1) All the tumor lesions were removed, which were judged by surgeon's gross inspection; 2) no lymphonode involvement; and 3) no distant metastasis. For all the 549 patients, hepatectomy was performed in Liver Cancer Institute, Zhonghan Hospital, Fudan University from January 1995 to December 1998. There were 465 males and 84 females with a median age of 50 years. According to the UICC TNM classification, 48 patients were in stage I, 382 in stage II, 86 in stage IIIA, and 33 in stage IVA. For their liver function defined by Child-Pugh classification, 539 patients were in class A, 10 in class B, and no patients in class C.

Adjuvant TACE

In the entire series, 185 patients underwent adjuvant TACE and 364 patients who did not undergo adjuvant TACE were assigned as control. Adjuvant TACE was performed 2 mo after hepatectomy. Hepatic arterial angiography was performed and then preventive or therapeutic chemoembolization was done depending on the patients with or without tumor stain in the remnant liver, respectively. The regimen for preventive adjuvant TACE consisted of 5-fluorouracil (5-FU) 0.75 g, cisplatin (DDP) 60 mg, and the emulsion mixed with mitomycin C (MMC) 16 mg and lipiodol 5 mL. Two months later a repeated preventive adjuvant TACE was performed and the regimen was finished. For therapeutic adjuvant TACE, the regimen consisted of 5-FU 1.0 g, DDP 80 mg, and the emulsion of MMC 20 mg and lipiodol 5-10 mL (the volume of lipiodol used for a patient depending on the tumor volume in the patient). TACE was repeated every one and a half month. The interval and times of repeated TACE depended on the response of the patients.

Patient stratification and grouping

The patients were retrospectively stratified into patients without risk factors for the residual tumor and patients with any risk factors for the residual tumor. These risk factors were evaluated according to preoperative ultrosonography, CT scan and postoperative pathological examination. Risk factors were defined as tumor diameter >5 cm, multiple nodules or vascular invasion. These factors were reported to have a close relation with residual tumor or recurrence in the remnant liver of HCC patients[4,20-23]. After stratification, there were 251 patients without risk factors for the residual tumor and 298 patients with risk factors for the residual tumor. After stratification, the patients were further grouped as the adjuvant TACE group and the control group.

Follow-up and statistics

The patients were followed up every 2 to 3 mo with ultrasonography and alpha-fetoprotein (AFP) during the first 2 years after HCC resection and every 3-6 mo afterwards. If the patients were unable to undergo this procedure, they were followed up with telephone or letter every year. The follow-up termination time for all patients was December 31, 2002. The significance of differences in clinical and pathological characteristics between groups was examined with Chi-square test and Student *t* test. Cumulative survival rates were obtained by the Kaplan-Meier method. Cumulative survival comparison between groups was performed with log-rank test. Multivariate analysis for the independent prognostic factors was determined by Cox proportional hazards model. *P* values <0.05 were considered statistically significant.

RESULTS

Clinical and pathological characteristics of adjuvant TACE and control groups

Clinical and pathological characteristics of the patients with or without risk factors for residual tumor in adjuvant TACE and control groups were summarized in Tables 1 and 2, respectively. There were no significant differences in their age, HBsAg positive rate, Child-Pugh class, AFP level, TNM class between two groups, except that the ratio of female *vs* male patients was lower in the adjuvant TACE group than that in control group ($P = 0.005$) without risk factor for residual tumor.

Survival of patients in adjuvant TACE group and control group

Figure 1A presents the Kaplan-Meier survival analysis comparing the patients in control group and adjuvant TACE group without risk factors for the residual tumor. There were no differences in their survival curves between two groups ($P = 0.3956$). The 1-, 3-, 5-year survival rates were 93.48%, 75.85%, 62.39% in the control group and 97.39%, 70.37%, 50.85% in the adjuvant TACE group, respectively. However, for the patients with risk factors for the residual tumor improved survival rates were observed in the adjuvant TACE group, as showed by Figure 2B. There were significant differences between two groups ($P = 0.0216$). The 1-, 3-, 5-year survival rates were 69.95%, 49.86%, 37.40% in the control group and 86.67%, 61.28%, 44.36% in the adjuvant TACE group.

Table 1 Clinical and pathological characteristics in control and adjuvant TACE groups patients without risk factors for residual tumor

Characteristics	Control (n = 174)	Adjuvant TACE group (n = 77)	P value
Gender			
Female	34	5	0.009
Male	140	72	
Age (mean±SD)	50.86±11.61	49.35±10.04	0.323
HBsAg			
Positive	43	11	0.135
Negative	131	66	
Cirrhosis			
Absent	22	6	0.130
Mild	53	33	
Severe	99	38	
Child-pugh Class			
A	165	77	0.134
B	5	0	
AFP (mean±SD, ug/L)	333.91±529.92	406.04±735.16	0.381
TNM classification			
I	28	19	0.108
II	146	58	

Table 2 Clinical and pathological characteristics in control and adjuvant TACE groups patients with risk factors for residual tumor

Characteristics	Control (n = 190)	Adjuvant TACE group (n = 108)	P value
Gender			
Female	33	12	0.147
Male	157	96	
Age (mean±SD)	51.50±11.72	49.63±10.07	0.105
HBsAg			
Positive	47	27	0.588
Negative	143	81	
Cirrhosis			
Absent	41	24	0.563
Mild	69	45	
Severe	80	39	
Child-pugh Class			
A	187	106	0.860
B	3	2	
AFP (mean±SD, ug/l)	501.39±807.14	518.25±707.99	0.856
TNM classification			
II	113	66	0.926
IIIA	55	31	
IVA	22	11	

Multivariates analysis

Cox proportional hazards models were constructed to predict the survival of the patients with adjuvant TACE and other variables including sex, age, HBsAg, cirrhosis, Child-Pugh class, AFP levels, tumor diameter, tumor nodules, and vascular invasion. In the patients without risk factors for residual tumor, the tumor diameter and cirrhosis were statistically significant independent factors associated with an increased risk of death from HCC, but adjuvant TACE had no effect on the survival of patients (Table 3). However, in the patients with risk factors for residual tumor, adjuvant TACE was statistically significant independent factor associated with a decreased risk of the death of patients with HCC. Tumor diameter, AFP level and vascular invasion were significantly independent factors associated with death of patients with HCC (Table 4). These results indicated that adjuvant TACE could improve the survival of patients with risk factors for residual tumor, but did not affect the survival of patients without risk factors for residual tumor.

Table 3 Multivariate Cox proportional hazard analysis to evaluate independent variables in patients without risk factors for residual tumor

Variables	B	Wald	Significance	HR	95% CI lower	95% CI upper
Cirrhosis	0.689	14.443	0.000	1.991	1.396	2.841
Absent = 1						
Mild = 2						
Severe = 3						
Tumor diameter (cm)	0.235	6.019	0.014	1.264	1.048	1.525

Table 4 Multivariate Cox proportional hazard analysis to evaluate independent variables in patients with risk factors for residual tumor

Variables	B	Wald	Significance	HR	95% CI lower	95% CI upper
AFP (μg/L)	0.212	5.333	0.021	1.236	1.033	1.480
<20 = 1						
21-400 = 2						
>400 = 3						
Adjuvant TACE	-0.406	6.041	0.014	0.666	0.482	0.921
Without = 1						
With = 2						
Tumor diameter (cm)	0.076	16.327	0.000	1.079	1.040	1.119
Vascular invasion	0.245	7.691	0.006	1.278	1.075	1.520
Absent = 1						
Present = 2						

DISCUSSION

The frequent postoperative recurrence was a main obstacle for long survival after resection of HCC and intrahepatic metastasis was thought to have a close relation with the postoperative recurrence[24]. However, it is difficulty to detect the minimal intrahepatic metastasis before or during operation and the existence of this minimal intrahepatic metastasis contributes to intrahepatic recurrence. Theoretically, treatment of this minimal intrahepatic metastasis should play an important role in preventing of postoperative recurrence of HCC. However, though TACE has been widely used in unresectable HCC patients[25-27], the clinical trial showed there was no confirmed evidence supporting the benefits of adjuvant TACE to patients with resectable HCC[6]. Tanaka and Izumi showed that postoperative adjuvant TACE improved the survival of HCC patients[28,29]. The patients selected in their clinical trials had advanced stages (TNM III or TNM IV) or characteristics of uncompleted encapsulated, intrahepatic metastasis, or vascular invasion which was thought to have a close relation with residual tumor and earlier massive recurrence[22,30]. For these patients postoperative adjuvant TACE played a role in earlier therapy of the residual tumor and could decrease the earlier recurrence and prolong survival. However, TACE has been known to damage remnant liver and deteriorate liver function. This adverse impact is possible to affect long survival of patients with resectable HCC if the resection is truly curative. One of the clinical trials showed that adjuvant chemembolization using the regimen of intravenous epirubicin in combination with transarterial infusion of an emulsion of iodized oil and cisplatin, was even associated with more frequent extrahepatic recurrences and a worse outcome in their group of patients[31]. In that clinical trial, all the patients had no demonstrable evidence of residual disease on ultrasonography and hepatic angiography 1 mo after surgery. These evidences suggested that the benefits of adjuvant TACE depended on the selection of patients. In patients who had high risks of residual tumor or intrahepatic metastasis in remnant liver, adjuvant TACE could improve their survival due to therapeutic actions on the residual tumor. However, in patients with lower risks of residual tumor or intrahepatic metastasis, adjuvant TACE might have less usefulness or even worse actions due to deterioration of remnant liver function.

Our results showed that postoperative adjuvant TACE could improve the survival of patients with risk factors for the residual tumor but not the survival of patients without risk factors for the residual tumor. For further evaluation of the effect of adjuvant TACE on patients with resectable HCC, Cox proportional hazards models were constructed to study if adjuvant TACE was the significantly independent factor associated with the survival. The results showed that in patients without risk factors for residual tumor, the significantly independent prognostic factors

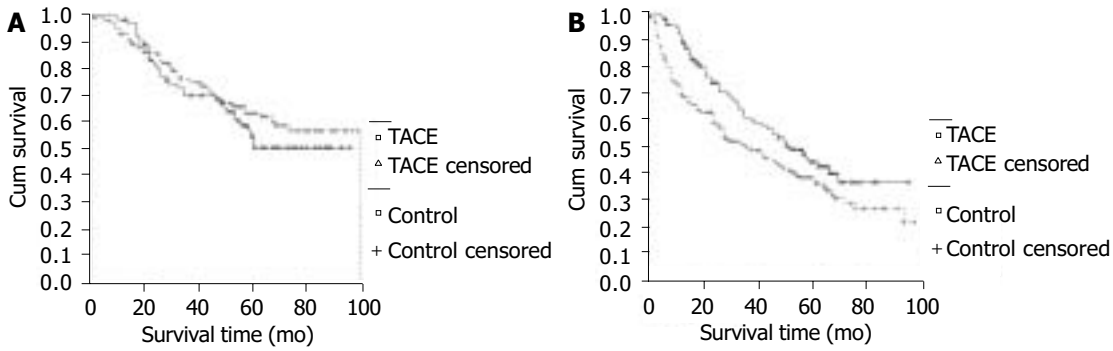

Figure 1 Survival curves of patients in control group and adjuvant TACE group without or with risk factors for residual tumor. A: Survival curve of patients in control group and adjuvant TACE group without risk factor for residual tumor.B: Survival curve of patients in control group and adjuvant TACE group with risk factors for residual tumor.

were tumor diameter and cirrhosis but not the adjuvant TACE. However, in patients with risk factors for residual tumor, adjuvant TACE was the significant prognostic factor. This result suggested that the benefits of adjuvant TACE to patients with resectable HCC depended on the selected patients with or without risk factors for the residual tumor. Therefore adjuvant TACE should be used in patients with higher risks of residual tumor but not in patients with lower risks of residual tumor.

REFERENCES

1 **El-Serag HB.** Hepatocellular carcinoma: an epidemiologic view. *J Clin Gastroenterol* 2002; **35**(5 Suppl 2): S72-78

2 **Zhang S,** Li L, Lu F. Mortality of primary liver cancer in China from 1990 through 1992. *Zhonghua Zhongliu Zazhi* 1999; **21:** 245-249

3 **Tang ZY.** Hepatocellular carcinoma. *J Gastroenterol Hepatol* 2000; **15**(Suppl): G1-7

4 **Cha C,** Fong Y, Jarnagin WR, Blumgart LH, DeMatteo RP. Predictors and patterns of recurrence after resection of hepatocellular carcinoma. *J Am Coll Surg* 2003; **197:** 753-758

5 **Imamura H,** Matsuyama Y, Tanaka E, Ohkubo T, Hasegawa K, Miyagawa S, Sugawara Y, Minagawa M, Takayama T, Kawasaki S, Makuuchi M. Risk factors contributing to early and late phase intrahepatic recurrence of hepatocellular carcinoma after hepatectomy. *J Hepatol* 2003; **38:** 200-207

6 **Schwartz JD,** Schwartz M, Mandeli J, Sung M. Neoadjuvant and adjuvant therapy for resectable hepatocellular carcinoma: review of the randomised clinical trials. *Lancet Oncol* 2002; **3:** 593-603

7 **Fukuda S,** Okuda K, Imamura M, Imamura I, Eriguchi N, Aoyagi S. Surgical resection combined with chemotherapy for advanced hepatocellular carcinoma with tumor thrombus: report of 19 cases. *Surgery* 2002; **131:** 300-310

8 **Ono T,** Yamanoi A, Nazmy El Assal O, Kohno H, Nagasue N. Adjuvant chemotherapy after resection of hepatocellular carcinoma causes deterioration of long-term prognosis in cirrhotic patients: metaanalysis of three randomized controlled trials. *Cancer* 2001; **91:** 2378-2385

9 **Shimoda M,** Bando T, Nagata T, Shirosaki I, Sakamoto T, Tsukada K. Prophylactic chemolipiodolization for postoperative hepatoma patients. *Hepatogastroenterology* 2001; **48:** 493-497

10 **Huang YH,** Wu JC, Lui WY, Chau GY, Tsay SH, Chiang JH, King KL, Huo TI, Chang FY, Lee SD. Prospective case-controlled trial of adjuvant chemotherapy after resection of hepatocellular carcinoma. *World J Surg* 2000; **24:** 551-555

11 **Kohno H,** Nagasue N, Hayashi T, Yamanoi A, Uchida M, Ono T, Yukaya H, Kimura N, Nakamura T. Postoperative adjuvant chemotherapy after radical hepatic resection for hepatocellular carcinoma (HCC). *Hepatogastroenterology* 1996; **43:** 1405-1409

12 **Yamamoto M,** Arii S, Sugahara K, Tobe T. Adjuvant oral chemotherapy to prevent recurrence after curative resection for hepatocellular carcinoma. *Br J Surg* 1996; **83:** 336-340

13 **Takenaka K,** Yoshida K, Nishizaki T, Korenaga D, Hiroshige K, Ikeda T, Sugimachi K. Postoperative prophylactic lipiodolization reduces the intrahepatic recurrence of hepatocellular carcinoma. *Am J Surg* 1995; **169:** 400-404

14 **Muto Y,** Moriwaki H, Ninomiya M, Adachi S, Saito A, Takasaki KT, Tanaka T, Tsurumi K, Okuno M, Tomita E, Nakamura T, Kojima T. Prevention of second primary tumors by an acyclic retinoid, polyprenoic acid, in patients with hepatocellular carcinoma. Hepatoma Prevention Study Group. *N Engl J Med* 1996; **334:** 1561-1567

15 **Takayama T,** Sekine T, Makuuchi M, Yamasaki S, Kosuge T, Yamamoto J, Shimada K, Sakamoto M, Hirohashi S, Ohashi Y, Kakizoe T. Adoptive immunotherapy to lower postsurgical recurrence rates of hepatocellular carcinoma: a randomised trial. *Lancet* 2000; **356:** 802-807

16 **Kubo S,** Nishiguchi S, Hirohashi K, Tanaka H, Shuto T, Kinoshita H. Randomized clinical trial of long-term outcome after resection of hepatitis C virus-related hepatocellular carcinoma by postoperative interferon therapy. *Br J Surg* 2002; **89:** 418-422

17 **Lau WY,** Leung TW, Ho SK, Chan M, Machin D, Lau J, Chan AT, Yeo W, Mok TS, Yu SC, Leung NW, Johnson PJ. Adjuvant intra-arterial iodine-131-labelled lipiodol for resectable hepatocellular carcinoma: a prospective randomised trial. *Lancet* 1999; **353:** 797-801

18 **Partensky C**, Sassolas G, Henry L, Paliard P, Maddern GJ. Intra-arterial iodine 131-labeled lipiodol as adjuvant therapy after curative liver resection for hepatocellular carcinoma: a phase 2 clinical study. *Arch Surg* 2000; **135:** 1298-1300

19 **Boucher E,** Corbinais S, Rolland Y, Bourguet P, Guyader D, Boudjema K, Meunier B, Raoul JL. Adjuvant intra-arterial injection of iodine-131-labeled lipiodol after resection of hepatocellular carcinoma. *Hepatology* 2003; **38:** 1237-1241

20 **Lee WC,** Jeng LB, Chen MF. Estimation of prognosis after hepatectomy for hepatocellular carcinoma. *Br J Surg* 2002; **89:** 311-316

21 **Sun HC,** Tang ZY. Preventive treatments for recurrence after curative resection of hepatocellular carcinoma-A literature review of randomized control trials. *World J Gastroenterol* 2003; **9**: 635-640

22 **Lin Z,** Ren Z, Xia J. Appraisal of postoperative transcatheter arterial chemoembolization (TACE) for prevention and treatment of hepatocellular carcinoma recurrence. *Zhonghua Zhongliu Zazhi* 2000; **22:** 315-317

23 **Poon RT,** Ng IO, Fan ST, Lai EC, Lo CM, Liu CL, Wong J. Clinicopathologic features of long-term survivors and disease-free survivors after resection of hepatocellular carcinoma: a study of a prospective cohort. *J Clin Oncol* 2001; **19:** 3037-3044

24 **Ouchi K,** Sugawara T, Fujiya T, Kamiyama Y, Kakugawa Y, Mikuni J, Yamanami H, Nakagawa K. Prediction of recurrence and extratumor spread of hepatocellular carcinoma following resection. *J Surg Oncol* 2000; **75:** 241-245

25 **Tzoracoleftherakis EE,** Spiliotis JD, Kyriakopoulou T, Kakkos SK. Intra-arterial versus systemic chemotherapy for non-operable hepatocellular carcinoma. *Hepatogastroenterology* 1999; **46:** 1122-1125

26 **Rose DM,** Chapman WC, Brockenbrough AT, Wright JK, Rose AT, Meranze S, Mazer M, Blair T, Blanke CD, Debelak JP, Pinson CW. Transcatheter arterial chemoembolization as primary treatment for hepatocellular carcinoma. *Am J Surg* 1999: **177:** 405-410

27 **Wallace S,** Kan Z, Li C. Hepatic chemoembolization: clinical and experimental correlation. *Acta Gastroenterol Belg* 2000; **63:** 169-173

28 **Tanaka K,** Shimada H, Togo S, Takahashi T, Endo I, Sekido H, Yoshida T. Use of transcatheter arterial infusion of anticancer agents with lipiodol to prevent recurrence of hepatocellular carcinoma after hepatic resection. *Hepatogastroenterology* 1999; **46:** 1083-1088

29 **Izumi R,** Shimizu K, Miyazaki I. Postoperative adjuvant locoregional chemotherapy in patients with hepatocellular carcinoma. *Hepatogastroenterology* 1996; **43:** 1415-1420

30 **Yamanaka J,** Yamanaka N, Nakasho K, Tanaka T, Ando T, Yasui C, Kuroda N, Takata M, Maeda S, Matsushita K, Uematsu K, Okamoto E. Clinicopathologic analysis of stage II-III hepatocellular carcinoma showing early massive recurrence after liver resection. *J Gastroenterol Hepatol* 2000; **15:** 1192-1198

31 **Lai EC,** Lo CM, Fan ST, Liu CL, Wong J. Postoperative adjuvant chemotherapy after curative resection of hepatocellular carcinoma: a randomized controlled trial. *Arch Surg* 1998; **133:** 183-188

Edited by Wang XL and Xu FM

PO Box 2345, Beijing 100023, China
Fax: +86-10-85381893
E-mail: wjg@wjgnet.com www.wjgnet.com

World J Gastroenterol 2004;10(19):2795-2799
World Journal of Gastroenterology
Copyright © 2004 by The WJG Press ISSN 1007-9327

• LIVER CANCER •

Heparanase mRNA expression and point mutation in hepatocellular carcinoma

Xiao-Peng Chen, Yin-Bib Liu, Jing Rui, Shu-You Peng, Cheng-Hong Peng, Zi-Yan Zhou, Liang-Hui Shi, Hong-Wei Shen, Bin Xu

Xiao-Peng Chen, Jing Rui, Zi-Yan Zhou, Liang-Hui Shi, Department of Surgery, Affiliated Yijishan Hospital, Wannan Medical College, Wuhu 241001, Anhui Province, China
Yin-Bib Liu, Shu-You Peng, Cheng-Hong Peng, Hong-Wei Shen, Bin Xu, Department of Surgery , Second Affiliated Hospital, Medical School of Zhejiang University, Hangzhou 310009, Zhejiang Province, China
Correspondence to: Dr. Xiao-Peng Chen, Department of Surgery, Affilicated Yijishan Hospital, Wannan Medical College, Wuhu 241001, Anhui Province, China. drcxp@sohu.com
Telephone: +86-553-5866103 **Fax:** +86-10-85381893
Received: 2003-06-05 **Accepted:** 2003-08-16

Abstract

AIM: To explore the expression of heparanase mRNA and point mutation in hepatocellular carcinoma (HCC).

METHODS: Reverse transcription polymerase chain reaction was used to measure the expression of heparanase mRNA in the primary tumor tissues and surrounding liver tissues of 33 HCC patients. T-A cloning and sequencing were used to detect whether there was any mutation in the amplified PCR products.

RESULTS: The expression of heparanase mRNA was positive in 16 primary tumor tissues of HCC, and the positive rate was 48.5%, which was significantly higher than that in the surrounding liver parenchyma (P<0.01). The positive rate for heparanase gene in high-tendency to metastatic recurrence group (71.4%, 10/14) was obviously higher than that in low-tendency to metastatic recurrence group (31.6%, 6/19) (P = 0.023). The positive rate for heparanase gene in patients with metastatic recurrence during postoperative follow-up (78.6%, 11/14) was also significantly higher than that in those without metastatic recurrence (21.4%, 3/14) (P = 0.003). Sequence analysis of the HPA PCR products was made in 7 patients, and 2-point mutations were found in 4 patients, one of which was sense mutation, neither base insertion nor deletion was detected. The mutation rate was 57.1% (4/7).

CONCLUSION: The expression rate of heparanase mRNA increases in HCC, and HPA mRNA may be one of the reliable markers for the metastatic activity gained by the liver tumor cells and could be used clinically in predicting metastatic recurrence of HCC. Point mutation may be one of the causes for enhanced heparanase mRNA expression.

Chen XP, Liu YB, Rui J, Peng SY, Peng CH, Zhou ZY, Shi LH, Shen HW, Xu B. Heparanase mRNA expression and point mutation in hepatocellular carcinoma. *World J Gastroenterol* 2004; 10(19): 2795-2799
http://www.wjgnet.com/1007-9327/10/2795.asp

INTRODUCTION

Primary hepatocellular carcinoma (HCC) is a common malignant tumor, especially in China and southeast Asia. Although the resection rate of HCC has improved in recent 20 years, the general therapeutic efficacy is still not satisfactory yet. The death rate of HCC ranks second in all malignant tumors in China, due to postoperative metastatic recurrence as the main cause. Tumor invasion and metastasis can break through the tissue barriers, which are formed of extracellular matrix (ECM) and basement membranes (BMs) and are composed of structural proteins, including collagen, laminin and vitronectin,*etc*. and glycosaminoglycans (GSGs). The chief components of GSG are heparan sulfate proteoglycans (HSPGs) that are principally composed of a core protein covalently linked to several heparan sulfate side chains[1]. Over the past ten years, most studies about neoplasm metastasis including HCC, focused on some proteases, such as matrix metalloproteinases (MMPs)[2-4], u-PA[5,6], serine and cysteine protease[7,8] whose substrates were structural proteins, but heparanase (HPA), whose substrate was GSGs, was ignored. In recent years, mammalian HPA gene has successfully been cloned and sequenced in Israel and U.S.A[9-13], and HPA was found to play an important role in tumor invasion and metastasis. El-Assal *et al*.[14] found that HPA mRNA expression in HCC patients was related to the tumor sizes, staging, classification, infection of hepatitis C virus (HCV), vascularization, postoperative metastasis and prognosis. However, in their studies, over half of HCC patients (52.7%, 29/55) were accompanied with HCV infection, and few were associated with hepatitis B virus (HBV). Ikeguchi *et al*.[15] found that relative heparanase mRNA expression level in HCC was significantly lower than that in noncancerous liver tissues (P<0.001), and that tumor heparanase expression did not correlate to tumor differentiation, tumor stage, or patient prognosis. They concluded that enhanced heparanase mRNA expression might not be a good biological marker for HCC. In addition, the possible mechanism of HPA expression has not been explored in both studies. It is well known that most HCCs in China are HBV-associated, which is different from the HCCs reported in Japan, but whether there is some difference of HPA expression in HCCs between in China and Japan or other regions is still unknown. In the present study, we tried to find out whether HPA mRNA expression was related to the clinicopathological indexes, including infection of HBV and postoperative metastatic recurrence of Chinese HCC patients, whether there was mutation in HPA gene, and whether the mutation of HPA gene was associated with HPA mRNA expression.

MATERIALS AND METHODS

Patients

Thirty-three patients (28 men and 5 women) undergoing curative hepatic resection for HCC between October 2000 and April 2001, were included in the present study. None of the patients received preoperative chemo- or embolic therapy. The patients' ages ranged from 27 to 73 years (49±7 years, mean±SD). Among the 33 patients, the biggest diameter of tumors was >5 cm in 25 cases and ⩽5 cm in 8. Tumor capsules were integrated in 14 and disintegrated in 19 cases. Serum AFP was positive in 21 and negative in 12; HBsAg was positive in 24 and negative in 9. Liver cirrhosis was detected in 18 cases. Thirteen patients

belonged to Edmondson grade I or II, and the remaining 20 patients to Edmondson grade III or IV. Eighteen patients belonged to TNM staging I or II,and 15 to TNM staging III or IV. According to the operative records and postoperative pathologic data, 14 HCC patients with cancer emboli, intrahepatic dissemination (satellite foci or multiple nodules) and/or lymph node metastasis were demarcated to high-tendency to metastatic recurrence group, and the other 19 patients without emboli, dissemination and/or metastasis belonged to low-tendency to metastatic recurrence group. A total of 28 patients were followed up 6-16 mo after operation, during which neoplasm metastasis or recurrence was found in 14 patients.

Tissue selection

After the neoplasm was resected, HCC tissues from all the patients were selected from the most viable areas of the tumors immediately. This aimed at excluding areas of tissue necrosis and hemorrhages, which might influence the quality and the quantity of the extracted RNA. For selection of surrounding non-tumor liver tissues, specimens were obtained from tissues at a clear distance from the edge of tumors (>1cm), if there was no evidence of nearby tumor invasion. Tissues were at once preserved in liquid nitrogen after the resection and kept at -80 ℃ until the experiment began.

RNA extraction and cDNA synthesis

About 100 mg tumor or liver tissue was used for total RNA isolation using TRIzol reagent (Gibco-BRL), according to the instructions of the manufacturer. First-strand cDNA was synthesized using 5 L total RNA with oligo $(dT)_{16}$ primer in a 50-L reverse transcription mixture containing 10 L of 5× first-strand buffer, 2.5 L dNTP mixture containing 25 mmoL/L each deoxynucleotide triphosphate base (Pharmacia Biotech, Tokyo, Japan), 2.5 L ribonuclease inhibitor (TaKaRa Biochemicals, Ohotsu, Japan), 25 L ddH_2O (managed with DEPC in advance), and 2.5 L avian myeloblastosis virus reverse transciptase (TaKaRa Biochemicals, Ohotsu, Japan).

PCR amplification of HPA and β-actin genes

The resulting cDNA was used for PCR amplification using Taq polymerse (TaKaRa Biochemicals, Ohotsu, Japan). The primers for HPA PCR amplification were designed according to the literature[9]. The sequences of the oligonucleotides were: forward,5'-TTCGATCCCAAGAAGGAATCAAC-3'; and reverse, 5'-GATTCAGTTACATGGCATCACTAC-3'. The first and final bases of the amplified HPA segment were at the 409th and 993rd positions of the HPA cDNA, respectively, and the amplified segment should be 585 bp in length. The primers used for β-actin had the following sequences: forward, 5'-TTCCAGCCTTCCTTCCTGG-3',and reverse, 5'-ATTGCTCCTCCTGAGCGCAA-3', as generated by Oligo 4.0 S computer software. The amplified β-actin segment was 224 bp in length. The PCR conditions included initial denaturation at 94 ℃ for 4 min, followed by 35 cycles of amplification with subsequent denaturation at 94 ℃ for 30 s, annealing at 57 ℃ for 45 s, and extension for 1 min at 72 ℃. Ten μL PCR products underwent electrophoresis using 12 g/L agarose and was visualized by UV absorption and ethidium bromide.

T-A cloning and sequencing

By using *Escherichia coli*, competent cell DH5α was routinely prepared and stored at -80 ℃. One hundred μL liquid HPA PCR products was used for purification. Five liters of purified preparation, 1 L pGEM-Teasy vector (3 015 bp in length) and 1 L T4-DNA ligase (Promega, New York, U.S.A) were mixed and incubated overnight at 4 ℃ for ligation reaction. After 200 L competent cell suspension was thawed at room temperature, 5 L ligated products was added for transformation test. The recombinant plasmid was screened, and the plasmid DNA was extracted by the alkaline lysis method. Five liters plasmid DNA was digested with 0.5 L restriction endonuclease *Eco*R I for 2-3 h at 37 ℃, then the enzyme digestion products were identified by electrophoresis. Results of enzyme digestion analysis were essentially identical with expected ones. Using the recombinant plasmid DNA as a template, DNA sequencing for both strands was performed on an ALF express DNA automatic sequencer (Pharmacia Co.) by the dideoxy terminal termination method. The sequenced HPA segment was 585 bp in length. The sequence of amplified HPA segment was compared with the gene bank database and analyzed for homogeneity using BLAST program at NCBI.

Statistical analysis

The significance of difference between two groups was tested with Chi-square analysis or exact probabilities in fourfold table. A *P* value less than 0.05 was considered statistically significant.

RESULTS

Expression of HPA mRNA in HCC

HPA mRNA was amplified in the tumor tissues from 16 patients. Electrophoretic analysis showed a bright band about 550-600 bp in length in these patients. No amplification strand was found in the other 17 patients (Figure 1). The HPA mRNA expression rate in the tumor tissues of HCC was 48.5% (16/33) and significantly higher than that in the surrounding non-tumor liver tissues ($P<0.01$) in which HPA mRNA was positive in only one patient.

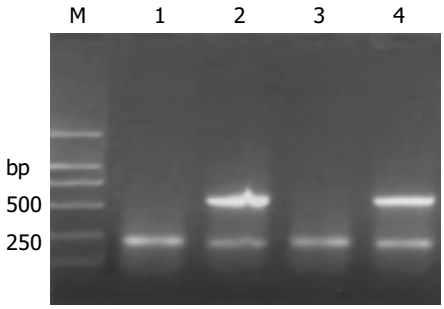

Figure 1 Expression of HPA mRNA in HCC. M: molecular mass markers (DL2 000); lanes 1 and 3: the noncancerous liver tissue; lanes 2 and 4: the HPA positive samples of cancer tissues both with a bright band at 585 bp.

Relationship between HPA expression and clinicopathological indexes

By statistical analysis, no significant difference in HPA mRNA expression was found among the tumor size, capsule, AFP, HBsAg and liver cirrhosis groups ($P>0.05$) (Table 1). HPA expression rate in Edmondson grade I or II group was significantly lower than that in Edmondson grade III or IV group ($P = 0.019$), and the rate in TNM staging I or II group was also obviously lower than that in TNM staging III or IV group ($P = 0.047$) (Table 1).

Relationship between HPA expression and metastatic recurrence of HCC

HPA mRNA expression rate in high-tendency to metastatic recurrence group was obviously higher than that in low-tendency to metastatic recurrence group ($P = 0.023$), and the rate in metastatic recurrence group was also significantly higher than that in non-metastatic recurrence group ($P=0.003$) (Table 2).

Table 1 Relationship between the HPA expression and the clinicopathological parameters of HCC

Items	Number	HPA positive	HPA negative	*P* value
Size of tumor				
>5 cm	25	13	12	0.250
≤5 cm	8	3	5	
Tumor capsule				
Integrated	14	5	9	0.130
Disintegrated	19	11	8	
AFP				
Positive	21	12	9	0.125
Negative	12	4	8	
HBsAg				
Positive	24	12	12	0.292
Negative	9	4	5	
Liver cirrhosis				
Yes	18	8	10	0.241
No	15	8	7	
Edmondson grade				
I, II	13	3	10	0.019
III, IV	20	13	7	
TNM staging				
I, II	18	6	12	0.047
III, IV	15	10	5	

Point mutation

After the recombinant plasmid DNA was digested by *Eco*R I and run in 10 g/L agarose gel electrophoresis, 2 bright bands could be seen, which were about 750 and 2 900 bp in length, respectively, according to the markers. The recombinant plasmid that was not digested by the enzyme showed only one band about 3 600 bp in length, and the pure HPA RT-PCR products only produced one strip about 550-600 bp in length in the same agarose gel. These results proved that it was successful to purify HPA RT-PCR products, ligate them with plasmid DNA to be digested by restriction endonuclease (Figure 2). Seven samples of HPA mRNA positive PCR products were cDNA sequenced, and the results confirmed that the target gene segment in all the 7 samples of PCR products was human HPA cDNA. Two point mutations (at the 513th and 878th base of the HPA cDNA, respectively) were observed in 4 samples, and no insertion or deletion was found. The mutation rate was 57.1%(4/7). One of the point mutations of G to A transversion was at the third base position of codon 138. Because the varied codon was still translated to glutamic acid resulting in no alternation of amino acid residues, the mutation belonged to nonsense mutation. The other point mutation of A to G transversion at nucleotide 878 corresponded to the second base position of codon 260. After transversion, the codon became AGU from AAU, resulting in alternation of amino acid residues (asparamide to serine), it was therefore sense mutation (Table 3, Figure 3).

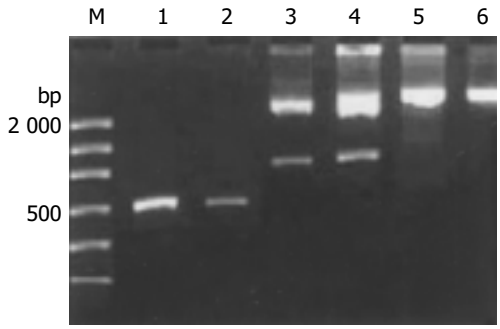

Figure 2 Electrophoretogram of the recombinant plasmid DNA digested by *Eco*RI. M: molecular mass markers (DL2 000); lanes 1 and 2: the pure HPA RT-PCR products; lanes 3 and 4: the products of digestion; lanes 5 and 6: the products without digestion.

Table 2 Relationship between HPA expression and metastatic recurrence of HCC

Items	Number	HPA positive	HPA negative	*P* value
Tendency to metastatic recurrence				
High	14	10	4	0.023
Low	19	6	13	
Metastatic recurrence				
Yes	14	11	3	0.003
No	14	3	11	

Table 3 Sequencing and corresponding series number

Number	Nucleotide sequence						Remarks
	TTGG	GCCCGACGTC	GCATGCTCCC	GGCCGCCATG	GCGGCCGCGG	GAATTCGATT	Plasmid DNA
409-468	***TTCGATCCCA***	***AGAAGGAATC***	***AA***[1]CCTTTGAA	GAGAGAAGTT	ACTGGCAATC	TCAAGTCAAC	HPA cDNA
469-528	CAGGATATTT	GCAAATATGG	ATCCATCCCT	CCTGATGTGG	AGGA**A**[3,5]AAGTT	ACGGTTGGAA	HPA cDNA
529-588	TGGCCCTACC	AGGAGCAATT	GCTACTCCGA	GAACACTACC	AGAAAAAGTT	CAAGAACAGC	HPA cDNA
589-648	ACCTACTCAA	GAAGCTCTGT	AGATGTGCTA	TACACTTTTG	CAAACTGCTC	AGGACTGGAC	HPA cDNA
649-708	TTGATCTTTG	GCCTAAATGC	GTTATTAAGA	ACAGCAGATT	TGCAGTGGAA	CAGTTCTAAT	HPA cDNA
709-768	GCTCAGTTGC	TCCTGGACTA	CTGCTCTTCC	AAGGGGTATA	ACATTTCTTG	GGAACTAGGC	HPA cDNA
769-828	AATGAACCTA	ACAGTTTCCT	TAAGAAGGCT	GATATTTTCA	TCAATGGGTC	GCAGTTAGGA	HPA cDNA
829-888	GAAGATTTTA	TTCAATTGCA	TAAACTTCTA	AGAAAGTCCA	CCTTCAAA**A**G[4]	T[6]GCAAAACTC	HPA cDNA
889-948	TATGGTCCTG	ATGTTGGTCA	GCCTCGAAGA	AAGACGGCTA	AGATGCTGAA	GAGCTTCCTG	HPA cDNA
949-993	AAGGCTGGTG	GAGAAGTGAT	T***GATTCAGTT***	***ACATGGCATC***	***ACTAC***[2]		HPA cDNA
	AATCACTAGT	GAATTCGCGG	CCGCCTGCAG	GTCGACCATA	TGGGAGAGCT	CCCAACGCGT	Plasmid DNA
	TGAATCACTA	GTGAATTCGC	GGCCGCCTGC	AGGTCGACCA	TATGGGAGAG	CTCCCAACGC	Plasmid DNA
	GTTG						Plasmid DNA

[1,2]The segments with italics and boldface corresponded to the primers used in RT-PCR. [3,4]The letters represented the mutated bases. [5,6]The parts with underline represented the codons.

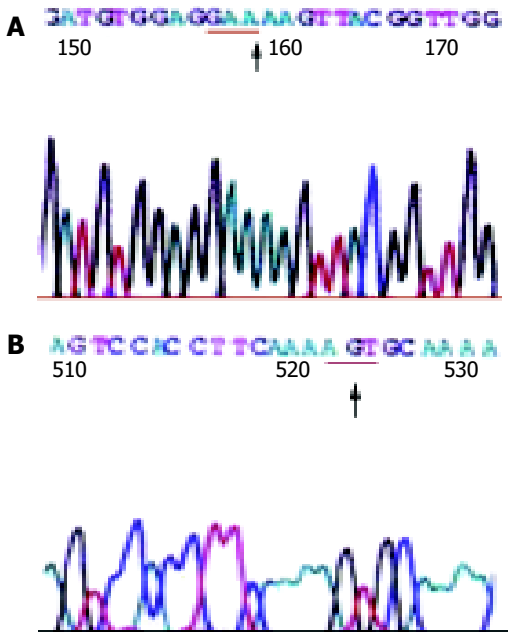

Figure 3 The sequencing map 1(A) and map 2(B) ↑, the mutated base; the parts with underline, the codons.

DISCUSSION

Mammalian genes including human HPA gene have been cloned and identified in recent years[9-13]. It is known that the gene is on chromosome 4q22[16] and includes 14 exons separated by 13 introns. The complete cDNA of HPA is 1 758[9] or 1 629 bp in length[10], and contains an open reading frame encoding a polypeptide of 543 amino acids, with a calculated molecular weight of 61 192 daltons. The HPA enzymes of about 50 ku isolated from human placenta and hepatoma cell line (SK-hep-1) may represent a processed or mature form of the native protein. In normal state, HPA is mainly identified in placenta, fetus liver, thymus gland, spleen, platelets, neutrophils, and activated T- and B-lymphocytes. HPA plays important physiological roles in embryonic morphogenesis, wound healing, inflammatory and autoimmune conditions by degrading GAGs. Many tumors and their stroma cells also produce or secrete HPA and use the same molecular machinery to induce neoplasm metastasis. RT-PCR analysis showed that most highly metastatic tumor cells expressed higher levels of HPA mRNA or HPA activity, but nonmetastatic carcinoma cells and low metastatic cells expressed no or only very weak HPA activity. HPA expression correlates with the metastatic potential of breast cancers[17], and antisense-mediated suppression of human heparanase gene expression may inhibit pleural dissemination of human cancer cells[18]. It has been found that high levels of HPA can be detected in a variety of malignant tissues or cells with high malignance or powerfully metastatic potential, among which are lymphoma, fibrosarcoma[9,19],oral cancer cell lines and oral cancer[20], esophageal carcinomas[21], lung cancer[18,22],malignant melanoma [19,23,24],breast cancer[9,25],gastric carcinoma and carcinoma of colon[26,27], pancreatic carcinoma[28,29], prostate cancer[30],bladder carcinoma[31], pheochromocytoma and ovarian cancer, and that no or only very weak HPA could be observed in some tumor cells with low or no metastatic potential. We detected the HPA mRNA expression of cancerous tissues in 33 HCC patients, and found that it was positive in 16 HCC samples (48.5%, 16/33). The expression rate of HPA mRNA in our study was similar to that of El-Assal *et al*. (47%)[14]. In addition, we detected the HPA mRNA expression in the surrounding non-tumor liver tissues, and found that it was positive in only one sample. These results showed that about half of HCC tissues could synthesize or secrete HPA, and the surrounding non-tumor liver tissues could hardly produce the enzyme on the whole.

HPA could degrade HSPG by cleaving the glycosidic linkages[24] with a hydrolase mechanism, destroy and degrade the ECM and BM barricade in coordination with other proteases to promote the invasion and metastasis of tumor cells[9,24]. Moreover, HPA could not only activate plasminogen and MMPs by means of promoting the release of urokinase-type plasminogen activator (u-PA) and tissue-type plasminogen activator (t-PA) but also facilitate the release of HS-banding active basic fibroblast growth factor (bFGF) and vascular endothelial growth factor (VEGF) to deliver its effect of enhancing cell metastasis and angiogenesis. It has been proved that HPA in cancerous tissues is closely related to tumor invasion, metastasis and angiogenesis[9,10]. Both metastatic recurrence and tumor microvessel density (MVD) in tumors might significantly increase with high levels of HPA. By analyzing statistically the relationship between HPA mRNA and clinicopathological parameters in HCC patients, El-Assal *et al*.[14] found that HPA mRNA expression was related to the tumor size, staging, classification, infection of HCV, vascularization, postoperative metastasis and prognosis, but was not related to other clinicopathological parameters. In this study, the expression rate in HCC was 48.5%, and HPA expression was associated with the pathological classification and TNM staging, which were similar to the conclusions drawn by El-Assal *et al*.[14] The obvious difference in HPA expression between low- and high-tendency to metastatic recurrence groups in our study preliminarily indicated that HPA was associated with the invasion and metastasis of HCC. The significant difference between metastatic recurrence group and nonmetastatic recurrence group in our study was also similar to that of El-Assal[14], and further proved that HPA expression was associated with metastatic recurrence, and that there were stronger invasiveness and tendency of postoperative recurrence in patients with positive HPA compared with HPA negative patients, and that HPA might provide a potential and valuable index to predict clinically postoperative metastatic recurrence.

No relationship was found between HPA expression and the integrity of tumor size or capsule in this study, which was different from the study of El-Assal *et al*.[14]. We speculate that the probable cause is that there were relatively fewer patients with tumors ≤5 cm in diameter (only 8 cases). In addition, HPA expression was not found to be associated with AFP, HBsAg and liver cirrhosis in this study perhaps because the types of causative viruses were different. Patients in the study of El-Assal *et al*.[14] were mainly infected with HCV, but most HCCs in China were related to HBV infection and posthepatitic cirrhosis, few were infected with HCV. In addition, our conclusions are different from those of Ikeguchi *et al*.[15], in which relative heparanase mRNA expression level in HCC was significantly lower than that in noncancerous liver tissues, and tumor heparanase expression did not correlate with tumor differentiation, tumor stage, or patient prognosis. Both the discrepancy of hepatitis virus and experimental methods could contribute to the different results. The surrounding non-tumor liver tissues in our study were at a clear distance from the edge of tumors (>1 cm), but they could be close to the tumor tissues in the study of keguchi *et al*.

Both the positive rates of HPA mRNA in the study of El-Assal *et al*.[14] and ours were close to 50% (47% and 48.5%, respectively), but very few HPAs were expressed in the surrounding non-tumor liver tissues. To our knowledge, no concrete mechanism of enhanced HPA mRNA expression in tumor tissues has been evaluated so far. To explore the probable mechanism of enhanced HPA expression in cancerous tissues, the positive PCR products of 7 patients were randomly selected and sequenced by T-A cloning. Two-point mutations including

a G to A transversion at nucleotide 513 and a A to G at nucleotide 878 of the HPA cDNA were found in 4 cases. By sequence analysis, we did not find base insertion and deletion, and the mutation rate was 57.1%. The point mutation of G to A transversion at nucleotide 513 resulting in GAG to GAA at condon 138 was a nonsense mutation because the amino acid residue was still glutamic acid after translation. The other point mutation of A to G transversion at nucleotide 878 leading to AAU to AGU at condon 260 belonged to sense mutation because it resulted in the alteration of amino acid residue (asparamide to serine), which may cause HPA structure to change and HPA activity to increase, resulting in the acceleration of ECM and BM barrier degrading and the final metastasis of tumor cells. Therefore, we guess that the point mutation at HPA gene might be one of the important mechanisms of increased HPA expression and enhanced metastasis of carcinoma cells, and it deserves further study.

REFERENCES

1 **Eccles SA.** Heparanase: breaking down barriers in tumors. *Nat Med* 1999; **5**: 735-736

2 **Airola K,** Karonen T, Vaalamo M, Lehti K, Lohi J, Kariniemi AL, Keski-Oja J, Saarialho-Kere UK. Expression of collagenases-1 and -3 and their inhibitors TIMP-1 and–3 correlates with the level of invasion in malignant melanomas. *Br J Cancer* 1999; **80**: 733-743

3 **Fan YZ,** Zhang JT, Yang HC, Yang YQ. Expression of MMP-2, TIMP-2 protein and the ratio of MMP-2/TIMP-2 in gallbladder carcinoma and their significance. *World J Gastroenterol* 2002; **8**: 1138-1143

4 **Tang Z,** Zhou X, Lin Z, Yang B, Ma Z, Ye S, Wu Z, Fan J, Liu Y, Liu K, Qin L, Tian J, Sun H, He B, Xia J, Qiu S, Zhou J. Surgical treatment of hepatocellular carcinoma and related basic research with special reference to recurrence and metastasis. *Chin Med J* 1999; **112**: 887-891

5 **Zheng Q,** Tang ZY, Xue Q, Shi DR, Song HY, Tang HB. Invasion and metastasis of hepatocellular carcinoma in relation to urokinase-type plasminogen activator, its receptor and inhibitor. *J Cancer Res Clin Oncol* 2000; **126**: 641-646

6 **Morita Y**, Hayashi Y, Wang Y, Kanamaru T, Suzuki S, Kawasaki K, Ohta K, Yamamoto M, Saitoh Y, Itoh H, Doe WF. Expression of urokinase-type plasminogen activator receptor in hepatocellular carcinoma. *Hepatology* 1997; **25**: 856-861

7 **Herszenyi L**, Plebani M, Carraro P, De Paoli M, Roveroni G, Cardin R, Tulassay Z, Naccarato R, Farinati F. The role of cysteine and serine proteases in colorectal carcinoma. *Cancer* 1999; **86**: 1135-1142

8 **Liu Y,** Xiao S, Shi Y, Wang L, Ren W, Sloane BF. Cathepsin B on invasion and metastasis of gastric carcinoma. *Chin Med J* 1998; **111**: 784-788

9 **Vlodavsky I,** Friedmann Y, Elkin M, Aingorn H, Atzmon R, Ishai-Michaeli R, Bitan M, Pappo O, Peretz T, Michal I, Spector L, Pecker I. Mammalian heparanase: gene cloning, expression and function in tumor progression and metastasis. *Nat Med* 1999; **5**: 793-802

10 **Hulett MD,** Freeman C, Hamdorf BJ, Baker RT, Harris MJ, Parish CR. Cloning of mammalian heparanase, an important enzyme in tumor invasion and metastasis. *Nat Med* 1999; **5**: 803-809

11 **Toyoshima M,** Nakajima M. Human heparanase. Purification, characterization, cloning, and expression. *J Biol Chem* 1999; **274**: 24153-24160

12 **Kussie PH,** Hulmes JD, Ludwig DL, Patel S, Navarro EC, Seddon AP, Giorgio NA, Bohlen P. Cloning and functional expression of a human heparanase gene. *Biochem Biophys Res Commun* 1999; **261**: 183-187

13 **Miao HQ,** Navarro E, Patel S, Sargent D, Koo H, Wan H, Plata A, Zhou Q, Ludwig D, Bohlen P, Kussie P. Cloning, expression, and purification of mouse heparanase. *Protein Expr Purif* 2002; **26**: 425-431

14 **El-Assal ON,** Yamanoi A, Ono T, Kohno H, Nagasue N. The clinicopathological significance of heparanase and basic fibroblast growth factor expressions in hepatocellular carcinoma. *Clin Cancer Res* 2001; **7**: 1299-1305

15 **Ikeguchi M,** Ueta T, Yamane Y, Hirooka Y, Kaibara N. Quantitative analysis of heparanase messenger RNA expression in hepatocellular carcinoma. *J Surg Oncol* 2002; **81**: 148-154

16 **Dong J,** Kukula AK, Toyoshima M, Nakajima M. Genomic organization and chromosome localization of the newly identified human heparanase gene. *Gene* 2000; **253**: 171-178

17 **Maxhimer JB,** Quiros RM, Stewart R, Dowlatshahi K, Gattuso P, Fan M, Prinz RA, Xu X. Heparanase-1 expression is associated with the metastatic potential of breast cancer. *Surgery* 2002; **132**: 326-333

18 **Uno F,** Fujiwara T, Takata Y, Ohtani S, Katsuda K, Takaoka M, Ohkawa T, Naomoto Y, Nakajima M, Tanaka N. Antisense-mediated suppression of human heparanase gene expression inhibits pleural dissemination of human cancer cells. *Cancer Res* 2001; **61**: 7855-7860

19 **Nakajima M,** Irimura T, Di Ferrante D, Di Ferrante N, Nicolson GL. Heparan sulfate degradation: relation to tumor invasive and metastatic properties of mouse B16 melanoma sublines. *Science* 1983; **220**: 611-613

20 **Ikuta M,** Podyma KA, Maruyama K, Enomoto S, Yanagishita M. Expression of heparanase in oral cancer cell lines and oral cancer tissues. *Oral Oncol* 2001; **37**: 177-184

21 **Mikami S,** Ohashi K, Usui Y, Nemoto T, Katsube K, Yanagishita M, Nakajima M, Nakamura K, Koike M. Loss of syndecan-1 and increased expression of heparanase in invasive esophageal carcinomas. *Jpn J Cancer Res* 2001; **92**: 1062-1073

22 **Sasaki M,** Ito T, Kashima M, Fukui S, Izumiyama N, Watanabe A, Sano M, Fujiwara Y, Miura M. Erythromycin and clarithromycin modulation of growth factor-induced expression of heparanase mRNA on human lung cancer cells *in vitro*. *Mediators Inflamm* 2001; **10**: 259-267

23 **Staquicini FI,** Moreira CR, Nascimento FD, Tersariol IL, Nader HB, Dietrich CP, Lopes JD. Enzyme and integrin expression by high and low metastatic melanoma cell lines. *Melanoma Res* 2003; **13**: 11-18

24 **Marchetti D,** Li J, Shen R. Astrocytes contribute to the brain-metastatic specificity of melanoma cells by producing heparanase. *Cancer Res* 2000; **60**: 4767-4770

25 **Zcharia E,** Metzger S, Chajek-Shaul T, Friedmann Y, Pappo O, Aviv A, Elkin M, Pecker I, Peretz T, Vlodavsky I. Molecular properties and involvement of heparanase in cancer progression and mammary gland morphogenesis. *J Mammary Gland Biol Neoplasia* 2001; **6**: 311-322

26 **Endo K,** Maejara U, Baba H, Tokunaga E, Koga T, Ikeda Y, Toh Y, Kohnoe S, Okamura T, Nakajima M, Sugimachi K. Heparanase gene expression and metastatic potential in human gastric cancer. *Anticancer Res* 2001; **21**: 3365-3369

27 **Friedmann Y,** Vlodavsky I, Aingorn H, Aviv A, Peretz T, Pecker I, Pappo O. Expression of heparanase in normal dysplastic, and neoplastic human colonic mucosa and stroma. Evidence for its role in colonic tumorigenesis. *Am J Pathol* 2000; **157**: 1167-1175

28 **Koliopanos A,** Friess H, Kleeff J, Shi X, Liao Q, Pecker I, Vlodavsky I, Zimmermann A, Buchler MW. Heparanase expression in primary and metastatic pancreatic cancer. *Cancer Res* 2001; **61**: 4655-4659

29 **Rohloff J,** Zinke J, Schoppmeyer K, Tannapfel A, Witzigmann H, Mossner J, Wittekind C, Caca K. Heparanase expression is a prognostic indicator for postoperative survival in pancreatic adenocarcinoma. *Br J Cancer* 2002; **86**: 1270-1275

30 **Kosir MA**, Wang W, Zukowski KL, Tromp G, Barber J. Degradation of basement membrane by prostate tumor heparanase. *J Surg Res* 1999; **81**: 42-47

31 **Gohji K,** Okamoto M, Kitazawa S, Toyoshima M, Dong J, Katsuoka Y, Nakajima M. Heparanase protein and gene expression in bladder cancer. *J Urol* 2001; **166**: 1286-1290

Edited by Ma JY and Wang XL **Proofread by** Xu FM

PO Box 2345, Beijing 100023, China
Fax: +86-10-85381893
E-mail: wjg@wjgnet.com www.wjgnet.com

World J Gastroenterol 2004;10(19):2800-2804
World Journal of Gastroenterology
Copyright © 2004 by The WJG Press ISSN 1007-9327

• COLORECTAL CANCER •

Lymphatic metastasis and nm23H$_1$ genetic instability in Chinese colon cancer patients

Zhi-Hong Su, Ji-Cheng Li

Zhi-Hong Su, Ji-Cheng Li, Department of Histology and Embryology, Zhejiang University Medical College, Hangzhou 310031, Zhejiang Province, China
Correspondence to: Dr. Ji-Cheng Li, Department of Histology and Embryology, Zhejiang University Medical College, Hangzhou 310031, Zhejiang Province, China. lijc@mail.hz.zj.cn
Telephone: +86-571-87217451 **Fax:** +86-571-87217139
Received: 2004-02-02 **Accepted:** 2004-02-21

Abstract

AIM: To investigate the pathogenic mechanism of colon cancer at the molecular level and to elucidate the relationship between intercellular adhesion molecule-1 (ICAM-1) and nm23H$_1$ genes and Chinese patients with colon cancer.

METHODS: DNA was extracted from paraffin-embedded materials. Polymerase chain reaction-single strand conformation polymorphism (PCR-SSCP) was used to analyze MSI and LOH. Expression of ICAM-1 was detected by Envision immunohistochemistry. Experimental results were analyzed with Leica-Qwin computer imaging techniques and SPSS software of statistics.

RESULTS: ICAM-1 expression of lymphatic endothelium was negative in normal colon and positive in colon cancer respectively. The number of lymphatics positive for ICAM-1 was gradually increased with degree of cancer invasion (P<0.01). In the group with metastasis of colon cancer, the number of lymphatics positive for ICAM-1 in lymph nodes was more than that in the group with no metastasis (P<0.01). The frequency of MSI, LOH and nm23H$_1$ protein was 26.67%, 20.00% and 53.33% in colon cancer, respectively. In TNM staging, MSI (43.75%) and nm23H$_1$ protein (81.25%) in stages I+II were detected more easily than the corresponding indexes (MSI: 7.14%, P<0.05 and nm23H$_1$: 21.43%, P<0.01) in stages III+IV. By comparison, the frequency of LOH (35.71%) in stages III+IV was more than that of LOH (6.25%, P<0.05) in stages I+II. LOH exhibited a rising trend along with the Duke's staging. nm23H$_1$ protein in the group of tubular adenocarcinoma (60.00%) was higher expressed than that in the group of mucoid adenocarcinoma (20.00%) (P<0.01), and exhibited a rising trend with the differentiation degrees of tubular adenocarcinoma. nm23H$_1$ protein in MSI positive group was higher expressed (75%) than that in MSI negative group (45.45%, P<0.05).

CONCLUSION: The expression of ICAM-1 in lymphatic vessels is beneficial to the judgement of the invasion and metastasis ability of colon cancer and the anti-tumor immunity function, and shows an important clinical significance in predicting lymphatic metastasis of colon cancer. MSI and LOH may separately control the development of sporadic colon cancer with different pathways. LOH mostly arises in the late period of sporadic colon cancer and endows a high aggressive and poor prognostic phenotype. By compassion, MSI may be an early period molecule marker for sporadic colon cancer, enhanced expression of nm23H$_1$ protein can effectively inhibit colon cancer metastasis and improve prognosis of sporadic colon cancer patients.

Su ZH, Li JC. Lymphatic metastasis and nm23H$_1$ genetic instability in Chinese colon cancer patients. *World J Gastroenterol* 2004; 10(19): 2800-2804
http://www.wjgnet.com/1007-9327/10/2800.asp

INTRODUCTION

Colon cancer is one of the common malignant tumors. A series of investigations have revealed that the main reason why it gives rise to death of patients lies in its invasiveness and metastasis[1]. Therefore, preventing colon deterioration and decreasing the death rate of colon cancer is of great significance. So far, it has been known that many factors may have an influence on colon cancer, such as anti-oncogenes, adhesion molecular E-selectin and E-cadherin, vascular endothelial growth factor and matrix metal protein (MMP-2)[2-5]. Among these factors, anti-oncogene and adhesion molecules have become the "hot spots" in research of colon cancer[6-8].

Intercellular adhesion molecule-1 (ICAM-1), an important transmembrane glycoprotein, is negatively expressed on endothelial cells of lymphatic vessels in normal conditions[9, 10]. ICAM-1 could induce attachment of cells such as lymphocytes to endothelial cells of blood vessels, and traverse blood vessels, aggregate antigens and take part in immune and inflammatory reactions. When tumors appeared in the body, lymphatic vessels became the main pathway for tumor cells to be transferred as a result of their own permeability[11]. In the process, recognition, adhesion, morphologic change and penetration between cells were involved. Vasse *et al*.[12]. reported that breast cancer cells could over-express the specific ligands of ICAM-1 (lymphocyte function associated antigen 1, LFA-1). With the development of cancer, the expression of LFA-1 went to an ascending trend on cancer cells. All the results indicated that ICAM-1 might take part in the metastasis. How endothelial cells of lymphatic vessels express ICAM-1? Few reports are available about whether endothelial cells of lymphatics express ICAM-1 or not in cancer tissue and whether ICAM-1/LFA-1 take part in the process of cancer cells attached to endothelial cells of lymphatics and metastasis.

nm23H$_1$ is one of the main anti-oncogenes. A great number of experiments indicated that inactivation of these genes, that is, genetic instability, resulted in metastasis[13,14]. However, there were few researches of these genes on colon cancers[15]. In order to further investigate the pathogenic mechanism of colon, we examined the instability of D17S396 of nm23H$_1$ in unrelated patients with the single strand conformation polymorphism analysis of polymerase chain reaction products (PCR-SSCP).

MATERIALS AND METHODS

Case selection and extraction of DNA

Thirty-two specimens were obtained during 2000 to 2002. There were 21 males and 11 females, aged 27-77 years. Twenty-seven cases were patients with tubular adenocarcinoma, 5 cases were

patients with mucoid adenocarcinoma in histological types. A senior pathologist made the final diagnosis on the basis of histological examination. No patient received radioactive therapy, chemotherapy before operation. Fresh surgical tissue samples were fixed immediately in formaldehyde solution for 12-24 h and paraffin-embedded for PCR-SSCP and immunohistochemical assay.

DNA extraction

DNA was extracted according to the standard protocols.

PCR amplification

Designed primers were synthesized by Shanghai Shengyou Biology Company. The primer sequences were (sense) 5'- TTGA CCGGGGTAGAGAACTC -3', (antisense) 5'- TCTCAGTACTT CCCGTGACC -3'. PCR mixture contained 200 ng of template-DNA and PCR reaction buffer containing 50 mmol/L KCl, 10 mmol/L Tris-HCl (pH 8.4), 1.5 mmol/L $MgCl_2$, 0.5 μmol/L each of two fragment-specific primers, 100 μmol/L each of dATP, dGTP, dTTP and dCTP, and 2 units of Taq DNA polymerase (Shanghai Shengyou Biology Company) for a reaction volume of 50 μL. The conditions for all PCR amplifications were at 94 ℃ for 5 min for pre-denaturation, at 94 ℃ for 45 s, at 62 ℃ for 45 s and at 72 ℃ for 45 s. Amplification was carried out for 35 cycles with a final extension for 10 min at 72 ℃. The amplified fragments were run in 1% agarose gel.

SSCP analysis

SSCP analysis of fragments was performed on a mini electrophoresis Unit (Bio-Rad Company, USA). Ten microlitre of the PCR product was diluted with 10 μL of sample buffer containing 90% formamide, 0.05% bromphenol blue dye and 0.05% xylene cyanol. The samples were heated at 100 ℃ for 8 min, transferred into an ice-cold water bath for 3 min, and analysed by 8% PAGE in 45 mmol/L-Tris-borate (pH8.0)/1 mmol/L-EDTA (TBE) buffer under 13 v/cm at 10 ℃.

DNA silver staining

Gels were stained with silver as follows. Gels were firstly fixed in 100 mL/L alcohol for 10 min and then oxidized in 100 mL/L nitric acid for 3 min. After washed for 1 min with double distilled water, they were stained in 2 g/L silver nitric acid for 5 min and washed for 1 min with double distilled water. Gels showed appropriate color in 15 g/L anhydrous sodium carbonate and 4 mL/L formalin and then the reaction was terminated by 7.5 mL/L glacial acetic acid. Finally they were washed with double distilled water.

Immunohistochemical assay

Immunohistochemical study was performed using Envision method. Briefly, 5 μm thick sections of the tissue were deparaffinized and rehydrated. Endogenous peroxidase activity was blocked with 3% hydrogen peroxide for 20 min. After three times of rinsing with 0.01 mol/L phosphate-buffered saline (PBS) (pH = 7.4), the slides were incubated with 10% normal goat serum at room temperature for 10 min to block the nonspecific reaction, and incubated for two hours with anti-ICAM-1 antibody. After rinsed in PBS for five min, they were incubated with Envision complex for two hours at room temperature, and stained with DAB after washed in PBS.

Statistical analyses

The experimental results were expressed as mean±SD. The correlation was analyzed with SPSS 8.0 software. *P* value less than 0.05 was regarded as statistically significant.

RESULTS

Expression of ICAM-1 in lymphatic endothelial cells

In the submucosa of normal colon, there existed a few lymphatic vessels with large, irregular cavities and thin walls. Simple squamous epithelia lined on them had no expression of ICAM-1 (Figure 1A). But in the submucosa and peripheral area of colon cancer, the number of lymphatic vessels was increased. Significant differences existed between them ($P<0.01$) (Table1). The expression of lymphatic endothelial cell was positive for ICAM-1 in colon cancer (Figure 1B). With the degree of cancer invasion, lymphatic vessels positive for ICAM-1 showed an increasing trend ($P<0.01$) (Table 2). When cancer metastasis appeared in the peripheral lymph node, ICAM-1 was strongly expressed in endothelial cells of their peripheral lymphatic vessels, and the number of lymphatic vessels positive for ICAM-1 was to the highest (Table 2).

Table 1 Comparison of ICAM-1 expression between colon cancer and normal colon (mean±SD)

Group	Cases	ICAM-1/15HPF
Normal colon	5	11.001±1.58
Colon cancer	32	26.131±9.19[b]

[a]$P<0.05$, [b]$P<0.01$, *vs* normal colon group.

Genetic instability at D17S396 of nm23H1

Microsatellite fragments of D17S396 were amplified. The positive rate of D17S396 MSI (Figures 2A, B), LOH (Figure 2C) and nm23H$_1$ protein (Figure 2D) was 26.67%, 20.00% and 53.33% respectively in 30 cases of colon cancer (Table 3).

MSI and LOH were independent of the histological type of colon cancer, the degree of differentiation and Duke's stage were related to the clinical TNM stage. In TNM staging, the frequency of MSI (43.75%) in stages I+II was more than that in stages III+IV (7.14%, $P<0.05$). In contrast, LOH (35.71%) in stages III+IV was detected more easily than that (6.25%, $P<0.05$) in stages I+II. In addition, LOH exhibited an ascending trend with the Duke's stage ($P<0.01$).

Expression of nm23H$_1$ protein

The positive rate of nm23H$_1$ protein was related with the histological type of colon cancer, differentiation degree and

Table 2 ICAM-1 expression in colon cancer (mean±SD)

Dukes stage	Cases	ICAM-1		ICAM-1/15HPF	*P* Value
		Low-expression	High-expression		
A	5	3	2	19.671±5.59	
B	15	6	9	23.571±9.65	
C	10	3	7	25.591±8.07	<0.01
D	2	0	2	35.681±2.51	
Metastasis	12	3	9	28.091±8.33	
No metastasis	20	11	9	22.621±8.99	

Table 3 Relationship between clinical pathological parameter and nm23H$_1$ genetic instability in colon cancer (mean±SD)

	Cases	MSI(%)	LOH(%)	nm23(%)	nm23 expression
Histological types	30	8 (26.67)	6 (20.00)	16 (53.33)	40.21±3.29
Tubular adenocarcinoma	25	7 (28.00)	5 (20.00)	15 (60.00)	40.76±2.74
High differentiation	8	2 (25.00)	1 (12.50)	8 (100.00)	41.49±2.01
Intermediate differentiation	13	5 (38.46)	2 (15.38)	6 (46.15)	40.41±1.98
Poor differentiation	4	0 (0.00)	2 (50.00)	1 (25.00)[d]	40.18±2.17
Mucoid adenocarcinoma	5	1 (20.00)	1 (20.00)	1 (20.00)[b]	39.53±2.61
TNM stage					
Stage I+II	16	7 (43.75)	1 (6.25)	13 (81.25)	42.42±1.08
Stage III+IV	14	1 (7.14)[e]	5 (35.71)[e]	3 (21.43)[f]	39.49±2.57
Dukes stage					
A	5	2 (40.00)	0 (0.00)	4 (80.00)	41.32±2.18
B	15	5 (33.33)	3 (20.00)	8 (53.33)	40.69±2.11
C	8	1 (12.50)	1 (12.50)	4 (50.00)	42.32±1.66
D	2	0 (0.00)	2 (100.0)[h]	0 (0.00)	39.24±2.32

[a]P<0.05, [b]P<0.01, *vs* tubular adenocarcinoma group; [c]P<0.05, [d]P<0.01 *vs* high differentiation group; [e]P<0.05, [f]P<0.01, *vs* stage I+II group; [g]P<0.05, [h]P<0.01 *vs* A, B, C groups respectively.

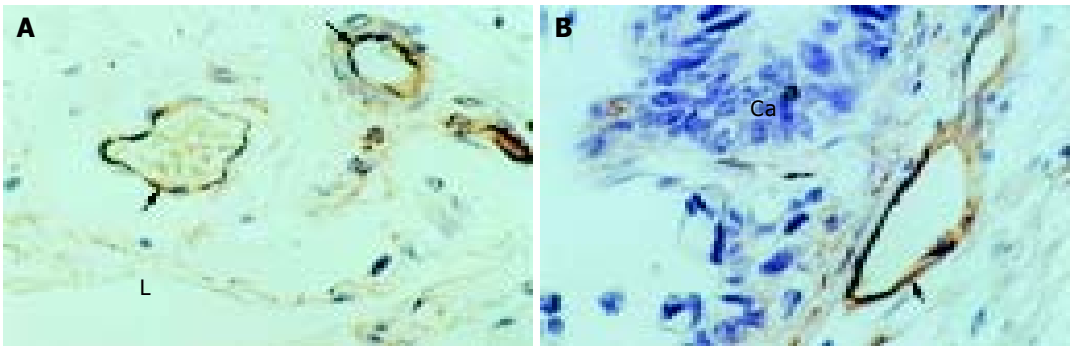

Figure 1 Expression of ICAM-1 in lymphatic endothelial cells. A: Negative expression of ICAM-1 in the lymphatic endothelium (L) of normal colon and positive expression of ICAM-1 in blood vessel endothelium (arrow) (Envision, original magnification ×400); B: Positive expression of ICAM-1 in the lymphatic endothelium (arrow) of colon cancer (Ca) (Envision, original magnification ×400).

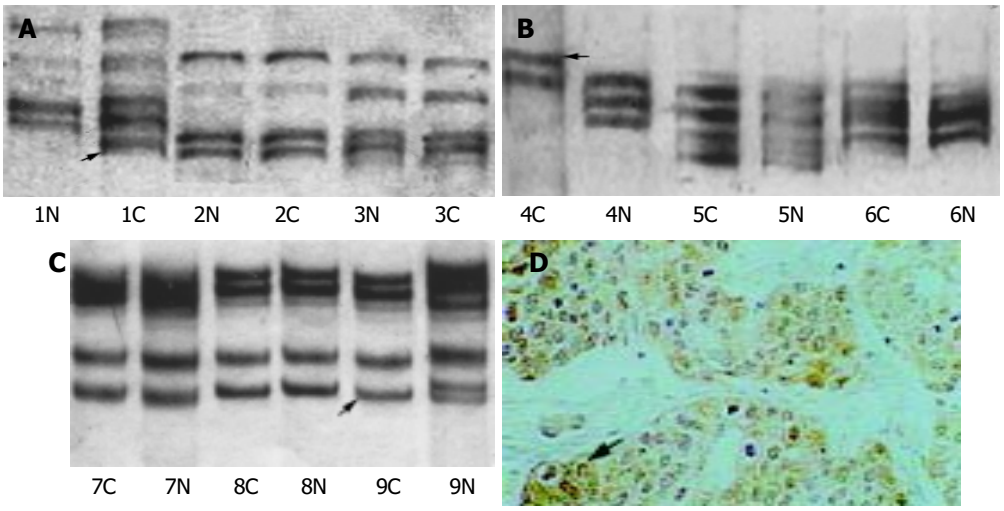

Figure 2 Positive D17S396 MSI, LOH and nm23H$_1$ in 30 cases of colon cancer. A: Positive MSI (arrow-headed) with an additional allele band (1C) compared with normal tissue (1N); B: Positive MSI (arrow-headed) with a removed allele band (4C) compared with normal tissue (4N); C: Positive LOH (arrow-headed) with a lacked allele band (9C) compared with normal tissue (9N); D: Positive nm23H$_1$ protein (arrow-headed) in cytoplasm, and nucleoli and membranes (Envision, original magnification ×200).

clinical stage. The expression of nm23H$_1$ protein in the group of tubular adenocarcinoma (60.00%) was apparently higher than that in the group of mucoid adenocarcinoma (20.00%, P<0.01), and exhibited a rising trend with the differentiation degrees of tubular adenocarcinoma (P<0.01). The positive rate of nm23H$_1$ in stages I+II (81.25%) was greater than that in stages III+IV (21.43%) (P<0.01). The same phenomenon occurred between the group positive for MSI (75%) and the group negative for MSI (45.45%) (P<0.05) (Table 4). However, LOH had no effect on the expression of nm23H$_1$ protein (Table 4). Computer imaging analysis showed that there was a difference among the groups in nm23H$_1$ protein expression level.

Table 4 Relationship between LOH, MSI and nm23 protein expression (mean±SD)

Groups	Cases	Expression of nm23 protein(%)	Intensity of nm23 protein
Positive to MSI	8	6/8 (75.00)	39.06±2.14
Negative to MSI	22	10/22(45.45)	41.14±2.36
Positive to LOH	6	2/6 (33.33)	41.23±2.27
Negative to LOH	24	14/24 (58.33)	39.44±2.52

DISCUSSION

Metastasis, the spread of cells from primary neoplasms to distant sites and their growth at that location, is the most harmful aspect of cancer. Despite great improvements in early diagnosis, surgical techniques, general patient care, local and systemic adjuvant therapies, most deaths from cancer are attributable to metastases that are resistant to conventional therapies. During metastatic cascade, tumor cells interact with various host cells as well as extracellular matrices and basement membrane components including laminin, fibronectin, and type I collagen through certain adhesion molecules such as integrins. Such adhesive interactions may lead to the enhancement of survival, arrest, or invasiveness of tumor cells and is one of the most important events in the metastatic process[14-17].

Intercellular adhesion molecule-1 (ICAM-1) is a single transmembrane glycoprotein and has two patterns in the body. One is located on the endothelial cells of blood vessels and is consisted of outmembrane region, transmembrane region and cytoplasmic region. The other (sICAM-1) is soluble in serum and is consisted of extracellular domains and originates from leucocytes, endothelial cells and hepatocytes[18-20]. The specific ligand of ICAM-1, LFA-1, can be expressed on the surfaces of leucocytes and lymphocytes. In normal conditions, ICAM-1/LFA-1 plays an important role in various immune responses.

How ICAM-1 expresses when tumors appear in the body? In the present case, ICAM-1 was expressed on endothelial cells of lymphatic vessels in colon cancer. With the degree of cancer invasion, lymphatic vessels positive for ICAM-1 showed an increasing trend. When cancer metastasis appeared in peripheral lymph nodes, ICAM-1 was strongly expressed on endothelial cells of peripheral lymphatic vessels, and the number of lymphatic vessels positive for ICAM-1 was the highest. The results might give a hint that cancer cells can be transferred into lymphatic vessels in combination with LFA-1. Furthermore, sICAM-1 transformed from ICAM-1 could inhibit natural killer cells, which could activate lymphocytes and restrict major histocompatibility complex (MHC) to react with T cells and tumor cells, thus promoting tumor cells to escape[21-23]. Therefore, sICAM-1 could strengthen and promote cancer cells to survive and transfer in lymphatic vessels when tumor metastasis occurred.

Genetic instability is the main reason why tumors appear and transfer[24-31]. MSI and LOH could induce canceration in the body. MSI was firstly found in hereditary non-polyposis colorectal cancer (HNPCC), and then in some kinds of sporatic tumors such as colon cancer, gastric cancer, uterus cancer, breast cancer, prostate cancer and pancreatic cancer. Our results showed that DNA from thirty Chinese patients at the site of D17S396 appeared microsatellite instability, the incidence was 26.67%. Subsequent experiments indicated that the incidence of MSI at the site of D17S396 in the stage of TNM I+II was greater than that in the stage of TNM III+IV, suggesting that MSI might be one of the markers for early colon cancer.

In contrast to MSI, the incidence of LOH at the site of D17S396 increased with the degree of Duke stage. Therefore, our results made it clear that LOH of nm23H$_1$ appeared at the later stage of colon cancer, which endowed colon cancer with a high invasiveness and a poor prognosis.

The expression of nm23H$_1$ has a negative relationship with tumor metastasis. Leone *et al*.[32] found that nm23H$_1$ had a function on the prevention of tumor metastasis by inhibiting the ability of cancer cells to clone. With the degree of tumor stage, the expression of nm23H$_1$ decreased. Our results indicate that with the development of colon cancer, the expression of nm23H$_1$ decreases.

REFERENCES

1 **Bodey B,** Bodey B Jr, Siegel SE, Kaiser HE. Failure of cancer vaccines: the significant limitations of this approach to immunotherapy. *Anticancer Res* 2000; **20**: 2665-2676

2 **Dudda JC,** Simon JC, Martin S. Dendritic cell immunization route determines CD8$^+$ T cell trafficking to inflamed skin: role for tissue microenvironment and dendritic cells in establishment of T cell-homing subsets. *J Immunol* 2004; **172**: 857-863

3 **Launay D,** Peyrat JP, Verdiere A, Hornez L, Hatron PY, Hachulla E, Devulder B, Hebbar M. Multiplex reverse transcription polymerase chain reaction assessment of sialyltransferase expression in peripheral blood mononuclear cells in systemic sclerosis. *J Rheumatol* 2004; **31**: 88-95

4 **Perdikogianni CH,** Dimitriou H, Stiakaki E, Markaki EA, Kalmanti M. Adhesion molecules, endogenous granulocyte colony-stimulating factor levels and replating capacity of progenitors in autoimmune neutropenia of childhood. *Acta Paediatr* 2003; **92**: 1277-1283

5 **Kwei S,** Stavrakis G, Takahas M, Taylor G, Folkman MJ, Gimbrone MA Jr, Garcia-Cardena G. Early adaptive responses of the vascular wall during venous arterialization in mice. *Am J Pathol* 2004; **164**: 81-89

6 **Benkoel L,** Dodero F, Hardwigsen J, Benoliel AM, Bongrand P, Botta-Fridlund D, Le Treut YP, Chamlian A, Lombardo D. Expression of intercellular adhesion molecule-1 (ICAM- 1) during ischemia-reperfusion in human liver tissue allograft: image analysis by confocal laser scanning microscopy. *Dig Dis Sci* 2003; **48**: 2167-2172

7 **Nyska A,** Moomaw CR, Ezov N, Shabat S, Levin-Harrus T, Nyska M, Redlich M, Mittelman M, Yedgar S, Foley JF. Ocular expression of vascular cell adhesion molecule (VCAM-1) in 2-butoxyethanol-induced hemolysis and thrombosis in female rats. *Exp Toxicol Pathol* 2003; **55**: 231-236

8 **Somersalo K,** Anikeeva N, Sims TN, Thomas VK, Strong RK, Spies T, Lebedeva T, Sykulev Y, Dustin ML. Cytotoxic T lymphocytes form an antigen-independent ring junction. *J Clin Invest* 2004; **113**: 49-57

9 **Chattopadhyay R,** Taneja T, Chakrabarti K, Pillai CR, Chitnis CE. Molecular analysis of the cytoadherence phenotype of a Plasmodium falciparum field isolate that binds intercellular adhesion molecule-1. *Mol Biochem Parasitol* 2004; **133**: 255-265

10 **Einstein O,** Karussis D, Grigoriadis N, Mizrachi-Kol R, Reinhartz E, Abramsky O, Ben-Hur T. Intraventricular transplantation of neural precursor cell spheres attenuates acute experimental allergic encephalomyelitis. *Mol Cell Neurosci* 2003; **24**: 1074-1082

11 **Toyama H,** Takada M, Suzuki Y, Kuroda Y. Brain death-induced expression of ICAM-1 and VCAM-1 on rat hepatocytes. *Hepatogastroenterology* 2003; **50**: 1854-1856

12 **Vasse M,** Thibout D, Paysant J, Legrand E, Soria C, Crepin M. Decrease of breast cancer cell invasiveness by sodium phenylacetate (NaPa) is associated with an increased expression of adhesive molecules. *Br J Cancer* 2001; **84**: 802-807

13 **Soufir N,** Daya-Grosjean L, de La Salmoniere P, Moles JP, Dubertret L, Sarasin A, Basset-Seguin N. Association between INK4a-ARF and p53 mutations in skin carcinomas of xeroderma pigmentosum patients. *J Natl Cancer Inst* 2000; **92**: 1841-1847

14 **Berney CR,** Fisher RJ, Yang J, Russell PJ, Crowe PJ. Genomic alterations (LOH, MI) on chromosome 17q21-23 and prognosis of sporadic colorectal cancer. *Int J Cancer* 2000; **89**: 1-7

15 **Chow NH,** Liu HS, Chan SH. The role of nm23H1 in the progression of transitional cell bladder cancer. *Clin Cancer Res* 2000; **6**: 3595-3599

16 **Kawamura A,** Miura S, Murayama T, Iwata A, Zhang B, Nishikawa H, Tsuchiya Y, Matsuo K, Tsuji E, Saku K. Increased Expression of Monocyte CD11a and intracellular adhesion molecule-1 in patients with initial atherosclerotic coronary stenosis. *Circ J* 2004; **68**: 6-10
17 **Burns S,** Hardy SJ, Buddle J, Yong KL, Jones GE, Thrasher AJ. Maturation of DC is associated with changes in motile characteristics and adherence. *Cell Motil Cytoskeleton* 2004; **57**: 118-132
18 **DesJardin LE,** Kaufman TM, Potts B, Kutzbach B, Yi H, Schlesinger LS. Mycobacterium tuberculosis-infected human macrophages exhibit enhanced cellular adhesion with increased expression of LFA-1 and ICAM-1 and reduced expression and/or function of complement receptors, FcgammaRII and the mannose receptor. *Microbiology* 2002; **148**(Pt 10): 3161-3171
19 **Masamune A,** Sakai Y, Kikuta K, Satoh M, Satoh A, Shimosegawa T. Activated rat pancreatic stellate cells express intercellular adhesion molecule-1 (ICAM-1) *in vitro*. *Pancreas* 2002; **25**: 78-85
20 **Becker A,** van Hinsbergh VW, Jager A, Kostense PJ, Dekker JM, Nijpels G, Heine RJ, Bouter LM, Stehouwer CD. Why is soluble intercellular adhesion molecule-1 related to cardiovascular mortality? *Eur J Clin Invest* 2002; **32**: 1-8
21 **Rescigno M,** Valzasina B, Bonasio R, Urbano M, Ricciardi-Castagnoli P. Dendritic cells, loaded with recombinant bacteria expressing tumor antigens, induce a protective tumor-specific response. *Clin Cancer Res* 2001; **7**(3 Suppl): 865S-870S
22 **Zhou Y,** Bosch ML, Salgaller ML. Current methods for loading dendritic cells with tumor antigen for the induction of antitumor immunity. *J Immunother* 2002; **25**: 289-303
23 **Ishigami S,** Natsugoe S, Tokuda K, Nakajo A, Xiangming C, Iwashige H, Aridome K, Hokita S, Aikou T. Clinical impact of intratumoral natural killer cell and dendritic cell infiltration in gastric cancer. *Cancer Lett* 2000; **159**: 103-108
24 **Storchova Z,** Pellman D. From polyploidy to aneuploidy, genome instability and cancer. *Nat Rev Mol Cell Biol* 2004; **5**: 45-54
25 **Ko EC,** Wang X, Ferrone S. Immunotherapy of malignant diseases. Challenges and strategies. *Int Arch Allergy Immunol* 2003; **132**: 294-309
26 **Kleist B,** Junghans D, Lorenz G, Bankau A, Poetsch M. The supplementary diagnostic power of selected immunohistochemical, molecular genetic and infective parameters in epithelial hyperplastic laryngeal lesions. *Oncology* 2003; **65**: 347-354
27 **Kovesi G,** Szende B. Changes in apoptosis and mitotic index, p53 and ki67 expression in various types of oral leukoplakia. *Oncology* 2003; **65**: 331-336
28 **Hayashi H,** Furihata M, Kuwahara M, Kagawa S, Shuin T, Ohtsuki Y. Infrequent alteration in the P53R2 gene in human transitional cell carcinoma of the urinary tract. *Pathobiology* 2004; **71**: 103-106
29 **Bai Y,** Murnane JP. Telomere instability in a human tumor cell line expressing NBS1 with mutations at sites phosphorylated by ATM. *Mol Cancer Res* 2003; **1**: 1058-1069
30 **Alexander J,** Watanabe T, Wu TT, Rashid A, Li S, Hamilton SR**.** Histopathological identification of colon cancer with microsatellite instability. *Am J Pathol* 2001; **158**: 527-535
31 **Rouba A,** Kaisi N, Al-Chaty E, Badin R, Pals G, Young C, Worsham MJ. Patterns of allelic loss at the BRCA1 locus in Arabic women with breast cancer. *Int J Mol Med* 2000; **6**: 565-569
32 **Leone A**, Flatow U, van Houtte K, Steeg PS. Transfection of human nm23-H1 into the human MDA-MB-435 breast carcinoma cell line: effects on tumor metastatic potential, colonization and enzymatic activity. *Oncogene* 1993; **8**: 2325-2333

Edited by Wang XL and Zhang JZ **Proofread by** Xu FM

PO Box 2345, Beijing 100023, China
Fax: +86-10-85381893
E-mail: wjg@wjgnet.com www.wjgnet.com

World J Gastroenterol 2004;10(19):2805-2808
World Journal of Gastroenterology
Copyright © 2004 by The WJG Press ISSN 1007-9327

• VIRAL HEPATITIS •

Cytochrome C oxidase III interacts with hepatitis B virus X protein *in vivo* by yeast two-hybrid system

Dan Li, Xiao-Zhong Wang, Jie-Ping Yu, Zhi-Xin Chen, Yue-Hong Huang, Qi-Min Tao

Dan Li, Jie-Ping Yu, Department of Gastroenterology, Renmin Hospital of Wuhan University, Wuhan 430060, Hubei Province, China
Xiao-Zhong Wang, Zhi-Xin Chen, Yue-Hong Huang, Department of Gastroenterology, Union Hospital of Fujian Medical University, Fuzhou 350001, Fujian Province, China
Qi-Min Tao, Research Institute of Hepatology, Beijing University, Beijing 100044, China
Supported by Science and Technology Program of Fujian Province, No. 2001Z157
Correspondence to: Dr. Dan Li, Department of Gastroenterology, Renmin Hospital of Wuhan University, Wuhan 430060, Hubei Province, China. lidan2006@hotmail.com
Telephone: +86-27-88043424-8508
Received: 2003-12-10 **Accepted:** 2004-02-01

Abstract

AIM: To screen and identify the proteins which interact with hepatitis B virus (HBV) X protein in hepatocytes by yeast two-hybrid system and to explore the effects of X protein in the development of hepatocellular carcinoma (HCC).

METHODS: With HBV X gene amplified by polymerase chain reaction (PCR), HBV X bait plasmid, named pAS2-1-X, was constructed by yeast-two hybridization system3 and verified by auto-sequencing assay. pAS2-1-X was transformed into the yeast AH109, and X-BD fusion protein expressed in the yeast cells was detected by Western blotting. The yeast cells cotransformed with pAS2-1-X and normal human liver cDNA library were grown in selective SC/-trp-leu-his-ade medium. The second screen was performed with β-gal activity detection, and false positive clones were eliminated by segregation analysis, true positive clones were amplified, sequenced and analyzed with bioinformatics. Mating experiment was peformed to confirm the binding of putative proteins to X protein in the yeast cells.

RESULTS: Bait plasmid pAS2-1-X was successfully constructed and pAS2-1-X correctly expressed BD-X fusion protein in yeast AH109. One hundred and three clones grew in the selective SC/-trp-leu-his-ade medium, and only one clone passed through β-gal activity detection and segregation analysis. The inserted cDNA fragment showed high homology with Homo sapiens cytochrome C oxidase III (COXIII). Furthermore, mating experiment identified that the binding of COXIII to X protein was specific.

CONCLUSION: COXIII protein is a novel protein that can interact with X protein *in vivo* by yeast two-hybrid system, and may contribute to the development of HCC through the interaction with X protein.

Li D, Wang XZ, Yu JP, Chen ZX, Huang YH, Tao QM. Cytochrome C oxidase III interacts with hepatitis B virus X protein *in vivo* by yeast two-hybrid system. *World J Gastroenterol* 2004; 10(19): 2805-2808
http://www.wjgnet.com/1007-9327/10/2805.asp

INTRODUCTION

Hepatitis B virus (HBV) belongs to the family hepadnaviridae which replicate their genome by reverse transcription, and causes acute and chronic hepatitis and is strongly associated with the development of primary hepatocellular carcinoma (HCC)[1,2]. HBV has a unique open reading frame, with the sequence being highly conserved among different mammalian hepadnaviruses, coding for a 16.5 kDa protein known as hepatitis B virus X protein (HBx). X gene is a multifunctional regulatory factor which has been identified as a potential oncogene. Transcriptional activation of diverse cellular genes by the HBx has been suggested as one of the mechanisms for HBV-associated HCC[2]. HBx has been shown to activate a wide variety of cellular and viral genes in trans activation including the HBV enhancers, tumor suppressor *p53*[3,4], and proto-oncogenes *c-jun*, *c-fos* and *c-myc*[5,6]. HBx-responsive elements also include nuclear factor kappa B (NF-κB), activator protein-1 (AP-1), activator protein-2 (AP-2) and cAMP-response element (CRE)[7,8]. Since HBx has no ability to bind to dsDNA, protein-protein interaction seems to be crucial for HBx transactivation. The interaction of HBx with cellular proteins may trigger a cascade of phosphorylation and dephosohorylation events which might lead to a general up-regulation of gene expression[9]. Identification of cellular X-interactive proteins would provide insights into the mechanism of HBV celluar effects. Several technigues have been used to study possible protein-protein interaction with HBx. Using these approaches, HBx has been discovered to interact with many proteins[9]. Nonetheless, to the author's knowledge, the functional significance of these interactions has not yet been elucidated. In the present study, we screened a clone encoding a novel X-interactive protein which was homologous to Homo sapiens cytochrome C oxidase III (COXIII) from normal human liver cDNA library by the *Saccharomyces cerevisiae* two-hybrid system.

MATERIALS AND METHODS

Plasmids and cells

Plasmids pAS2-1, PCL1, PLAM5'-1, normal human liver pACT2-cDNA library and *Saccharomyces cerevisiae* AH109 were purchased from Clontech, USA. *Saccharomyces cerevisiae* AH109 was grown in YPD medium (10 g/L yeast extract, 20 g/L peptone, 20 g/L dextrose). This yeast strain carried LacZ, HIS3 and ADE2 reporter genes under the control of Gal4-binding site and was used to screen the liver cDNA library. *Escherichia coli* JM105 was provided as a gift from Research Institute of Hepatology, Beijing University, China.

Reagents

Restriction enzymes (*Eco*RI and *Pst* I), TaqDNA polymerase and T4 DNA ligase were purchased from Promega, USA. DNA gel extraction kit was provided by Jingmei Company, China. Gal4 DNA-BD monoclonal antibody, matchmaker AD LD-insert screening amplimers and yeast culture medium were purchased from Clontech, USA. Glass beads (acid-washed) were purchased from Sigma, USA. Alkaline phosphatase-conjugated goat anti-mouse IgG was purchased from Wuhan Boster Biological Technology Company, China.

pAS2-1-X construction

The X region of the HBV genome was amplified by PCR with XF and XR as forward and reverse primers which contained an *Eco*RI site and a *Pst*I site, respectively, for convenience of cloning. The sequences of the primers with the restriction enzyme sites underlined were: XF, 5'-*ACGGAATTCATGGCTGCTAGGCTGTG*-3'; XR, 5'-*ATCCTGCAGAGGTGAAAAAGTTGCAT*-3'. The fragment amplified was from nucleotides 1 374 to 1 838 on HBV genome. The template for this reaction was extracted from sera of HBV DNA-positive patients. The reaction mixture was subjected to 30 cycles of PCR amplification. Each cycle included denaturation at 94 ℃ for 30 s, annealing at 58 ℃ for 1 min, and extension at 72 ℃ for 30 s , and a final extension for 7 min at 72 ℃. The approximate 464 bp fragment was digested by *Eco*RI and *Pst* I, and recombined into the plasmid pAS2-1 by T4 DNA ligase. The reconstructed plasmid was subsequently named pAS2-1-X and identified by PCR and auto-sequencing assay. Auto-sequencing assay was performed in Bioasia Biologic Technology Company and the resulting sequence was analyzed in the database of EMBL\GeneBank by the BLAST program.

Transformation of pAS2-1-X into AH109

Yeast AH109 was transformed with pAS2-1-X by lithium acetate-mediated method demonstrated by Gietz *et al.*[10] and plated in selective SC/-trp medium. Plasmids were isolated from transformants and X gene was amplified. Filter assay was used to exclude the auto-activation function of pAS2-1-X in AH109. Expressed X-BD fusion protein in yeasts transformed with PAS2-1-X was detected by Western blotting. The cells were collected by centrifugation and yeast protein extract was prepared according to urea/SDS method. SDS-polyacrylamide gel electrophoresis was performed and protein extracts were electroblotted onto nitrocellulose membrane. After being blocked with nonfat milk, the membrane was added to 1:3 000 diluted Gal4 DNA-BD monoclonal antibodies and incubated for 1 h, after washed with TBST. Then, the secondary alkaline phosphatase-conjugated goat anti-mouse IgG was added and incubated for 2 h. The proteins were visualized with 5-bromo-4-chloro-3-indolyl phosphate and nitro blue tetrazolium. Protein extracts of untransformed yeast cells were used as negative control.

Screening of human liver cDNA library by the yeast two-hybrid system

The screening procedure used here was a modification of the method described by Gietz *et al.*[10]. Yeast cells were transformed with pAS2-1-X and pACT2-cDNA library by lithium acetate-mediated method , plated in selective SC/-trp-leu-his-ade medium, incubated at 30 ℃ for 7 d and selected for histidine, leucine and tryptophan prototrophy. The freshly growing clones were assayed for β-gal activity by replicaplating the yeast transformants onto Whatman filter paper. The filters were then snap frozen twice in liquid nitrogen for 10 s and incubated in a buffer containing 5-bromo-4-chloro-3-indolyl-β-D-galactopyranoside solution at 30 ℃ for 1-8 h. Positive interactions were detected by appearance of blue clones. Plasmids PCL1 and PLAM5'-1 were transformated into AH109 as positive and negative controls, respectively. Segregation analysis was performed to eliminate false positive clones and thus true positive clones were obtained.

Analysis of positive clones

pACT2-cDNA plasmid genome was isolated following the method described by Gietz *et al.*[10]. Briefly, the true positive clones were incubated with SC/-leu liquid medium at 30 ℃ overnight, followed by spinning down the cells by centrifuging at 14 000 *g* for 5 min, and resuspension of pellets in lysis buffer (20 g/L Triton 100, 10 g/L SDS, 10 mmol/L NaCl, 10 mmol/ L Tris-HCl, pH8.0, 1 mmol/L Na_2EDTA) was added with phenol, chloroform and isoamyl alcohol (volume fraction 25:24:1). Then the suspension was vortexed vigorously with acid-washed glass beads, lysate was centrifugated and plasmid DNA was harvested. The pACT2-cDNA plasmid was purified by CsCl gradient centrifugation to permit PCR using the matchmaker AD LD-insert screening amplimers which annealed to GAL4-AD. The PCR reaction consisted 30 amplification cycles, each cycle included denaturation at 94 ℃ for 30 s, annealing at 68 ℃ for 3 min, and a final extension for 7 min at 72 ℃. Auto-sequencing assay was performed in Shanghai Sangon Biological Engineering Technology and Service Corporation, the resulting sequences were compared against the databases of EMBL\GenBank by the BLAST program.

Mating experiment

pAS2-1-X, pAS2-1, pLAM5'-1 transformed yeasts in SC/-trp medium and positive clones were incubated in SC/-leu medium at 30 ℃ for 2 d, respectively, then removed. Two types of transformants were incubated into YPD medium at 30 ℃ for 4 h. Finally, transformants were subcultured in SC/-leu-trp medium, incubated at 30 ℃ for 2 d and assayed for β-gal activity.

RESULTS

Identification of the pAS2-1-X

The fragment of approximately 460 bp was amplified from the reconstructed plasmid pAS2-1-X, and auto-sequencing assay confirmed the fragment inserted into plasmid pAS2-1 had a high identity (99.9%) with X gene.

Detection of the transformed yeast AH109

X gene was amplified from the plasmid isolated from the transformed yeast cells (Figure 1). Filter assay excluded the auto-activation function of pAS2-1-X in the cells. Staining for X-BD was obtained in yeast cells transformed with pAS2-1-X (Figure 2). pAS2-1-X could be used as a bait plasmid in yeast two-hybrid system.

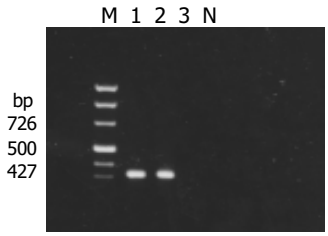

Figure 1 Result of detection of X gene in yeasts transformed with pAS2-1-X. M: PCR marker; lanes 1 and 2: transformed yeasts; lanes 3: untransformed yeasts; N: negative control.

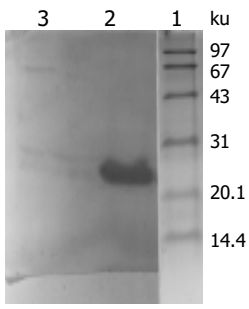

Figure 2 Western blot analysis of expressed fusion protein in yeasts transformed with PAS2-1-X. Lane 1: protein moclecular weight standard; lane 2: protein extracted from transformed yeasts; lane 3: protein extracted from untransformed yeasts.

Screening of the liver cell cDNA library

Of the 5×10^6 transformants screened, 103 were grown in the selective SC/-trp-leu-his-ade medium, 19 were positive for β-gal activity, and only 1 clone passed through the segregation analysis.

Analysis of positive clones

The fragment of approximately 900 bp was amplified from the true positive clones (Figure 3). DNA sequence analysis of the fragment revealed that the yeast plasmid insert had a high identity (98%) with the Homo sapiens COXIII gene (GeneBank ID:BC013930).

Mating experiment

The transformants containing pAS2-1-X and positive pACT2-cDNA gave a blue colour by filter assay, whereas the transformants containing pAS2-1 or pLAM5'-1 and positive pACT2-cDNA gave a white colour. Mating experiment confirmed the specific interaction between positive clones and HBx (Figure 4).

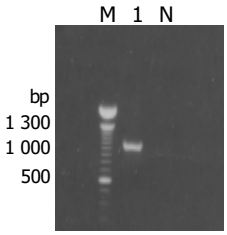

Figure 3 Results of amplification for cDNA fragment by PCR from the positive clones. M: 100 bp DNA ladder; lane1: positive clone; N: negative control.

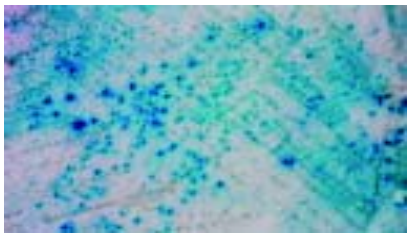

Figure 4 Mating experiment for the interaction between COXIII and X protein in yeast cells.

DISSCUSION

Chronic HBV infection is strongly associated with the development of HCC, but the mechanisms by which HBV induces events leading to the genesis of HCC remains unclear. Several studies have suggested a possible role of HBx in the process of HCC, a few studies have reported transformation of certain cell types *in vitro* by HBx[11] and initiation of HCC in HBx transgenic mice[12,13], but its direct oncogenicity seems to depend on the strength, and duration of protein expression and the genetic background of mice and cells. It is more likely that HBx causes transactivation of cell regulatory genes or interacts with one or more cellular proteins to initiate the development of human HCC through upregulation of cell growth and mutagenesis. The transactivation function of HBx has been shown to involve both direct interaction with transcriptional factors, such as RPB5 of RNA polymerases[14], TATA-binding protein[15] or activating transcription factor (ATF) /CRE-binding protein (CREB)[16] and activation of signal transduction pathways, such as ras/raf/MAP-kinase[17], protein kinase C (PKC)[18] and SAPK/JNK[19,20]. HBx is predominatly localized in the cytoplasm with a low level of nuclear distribution, whereas recent findings from two independent laboratories indicated that HBx could localize at the mitochondria. Confocal laser microscopy of hepatoma cells transfected with respective expression vectors showed colocalization of the third member of the family of human genes that encode the voltage-dependent anion channel (HVDAC3) and HBx in mitochondria. Moreover, stable cationic fluorophore dye showed that HBx expression in hepatoma cells led to alteration of mitochondrial transmembrane potential, an abnormal aggregation of mitochondrial structures, release of cytochrome C from mitochondria, decrease of mitochondrial membrane potential and membrane blebbing of cells, which are characteristics of cell death. These functional roles of HBx in affecting mitochondrial physiology are associated with HBV-induced liver injury and development of HCC[21,22].

Since HBx seems to accomplish its functions via protein-protein interaction, identification of the HBx- interactive cellular proteins represents a major goal in order to define the function of HBx in HBV replication and liver carcinogenesis. The yeast two-hybrid system using a genetic approach, offers a way to clone and identify genes that interact with a protein of interest through *in vivo* complementation in yeast cells[23,24]. In the present study, we screened and cloned a novel HBx-interactive protein from a normal human liver cDNA library. Sequence analysis revealed it was the homolog of Homo sapiens COXIII. The interaction of HBx with COXIII was confirmed by yeast-two hybridization system 3. The growth of yeast cells harboring both pAS-1-X and pACT2-COXIII recombinant plasmids in His-independent medium, formation of blue-colonies detected by the β-gal assay, and the behaviors of the cells in false-positive elimination tests suggested that the binding of COXIII was HBx specific. Mating experiment further identified the interaction between COXIII and HBx in yeast cells.

Cytochrome C oxidase (COX), the terminal enzyme of the mitochondrial respiratory chain, catalyzes the transfer of electrons from reduced cytochrome C to molecular oxygen. COXIII, which is encoded by the mitochondrial DNA and synthesized within the mitochondria, represents one of the large subunits of COX and acts as the catalytic core of the enzyme[25]. Defective COX activity resulting in deficient adenosine triphosphate generation may contribute to the development of Alzheimer's disease[26], cardiomyopathy[27], neonatal giant cell hepatitis[28] and other clinically heterogeneous diseases[29,30]. Incorrect assembly of the critical subunits incluing COXI,COXIIand COXIII, is a major mechanism leading to COX deficiencies. COX also plays a key role in inducing apoptosis in multiple cell types through transcriptional activation of the respective genes[31]. Mitochodrial dysfuction and transcriptional function changes have been identified to be associated with chronic liver disease and oncogenic processes[32]. Kuo *et al.*[33] reported the integration of HBV with human hepatoma cells might cause mitochondrial defects in the ATP synthase 6 and COXIII genes. Studies on the effects of HBx on apoptotic pathways indicated that HBx blocked the actirit, of caspases 8, 9 and 3 and the release of cytochrome c, it also upregulated PKC, extracellular signal-regulated kinase (ERK), phosphatidyl inositol-3-kinase (PI-3-K) and NF-κB activity[34]. The study of NF-κB and HBx expression in human HCC tissues detected by immunohistochemistry SP method strongly suggested that NF-κB was abnormally activated in HCC, which was probably related to HBx. The ability of HBx to induce the activation of NF-κB has been demonstrated by mobility shift and reporter gene expression assays with lysates from HBx-transfected HepG2 cells[35]. Furthermore, HBx was shown to bind to a voltage-dependent anion channel and alter the mitochondrial transmembrane potential and consequently induce activation of transcription factors, which include STAT-3 and NF-κB[21]. Cogswell *et al.*[36] reported that the NF-κB regulatory pathway existed in mitochondria and NF-κB could negatively regulate the expression of both COXIII and cytochrome B mRNAs. Whether and how the interaction of HBx with COXIII

regulates the activity of transcription factor NF-κB has remained obscure. However, based on our data, we hypothesize that HBx might impair mitochondrial respiration chain and energy metabolism by combining COXIII.

Future investigations will focus on the identification of COXIII properties and physiological significance of interaction of HBx with COXIII and probably with other mitochondrial proteins. Further inquiries in this area may pave the way for investigation of possible mechanisms leading to chronic infection and subsequent progression to HCC in the context of mitochondrial association of HBx.

REFERENCES

1 **Su Q,** Schroder CH, Hofmann WJ, Otto G, Pichlmayr R, Bannasch P. Expression of hepatitis B virus protein in HBV-infected human livers and hepatocellular carcinomas. *Hepatology* 1998; **27**: 1109-1120

2 **Koike K,** Tsutsumi T, Fujie H, Shintani Y, Kyoji M. Molecular mechanism of viral hepatocarcinogenesis. *Oncology* 2002; **62** (Suppl 1): 29-37

3 **Huo TI,** Wang XW, Forgues M, Wu CG, Spillare EA, Giannini C, Brechot C, Harris CC. Hepatitis B virus X mutants derived from human hepatocellular carcinoma retain the ability to abrogate p53-induced apoptosis. *Oncogene* 2001; **20**: 3620-3628

4 **Shiota G,** Oyama K, Udagawa A, Tanaka K, Nomi T, Kitamura A, Tsutsumi A, Noguchi N, Takano Y, Yashima K, Kishimoto Y, Suou T, Kawasaki H. Occult hepatitis B virus infection in HBs antigen-negative hepatocellular carcinoma in a Japanese population: involvement of HBx and p53. *J Med Virol* 2000; **62**: 151-158

5 **Sirma H,** Giannini C, Poussin K, Paterlini P, Kremsdorf D, Brechot C. Hepatitis B virus X mutants, present in hepatocellular carcinoma tissue abrogate both the antiproliferative and transactivation effects of HBx. *Oncogene* 1999; **18**: 4848-4859

6 **Natoli G,** Avantaggiati ML, Chirillo P, Puri PL, Ianni A, Balsano C, Levrero M. Ras- and Raf-dependent activation of c-jun transcriptional activity by the hepatitis B virus transactivator pX. *Oncogene* 1994; **9**: 2837-2843

7 **Cao XY,** Liu J, Lian ZR, Clayton M, Hu JL, Zhu MH, Fan DM, Feitelson M. Cloning of differentially expressed genes in human hepatocellular carcinoma and nontumor liver. *World J Gastroenterol* 2001; **7**: 579-582

8 **Shamay M,** Barak O, Doitsh G, Ben-Dor I, Shaul Y. Hepatitis B virus pX interacts with HBXAP, a PHD finger protein to coactivate transcription. *J Biol Chem* 2002; **277**: 9982-9988

9 **Yeh CT.** Hepatitis B virus X protein: searching for a role in hepatocarcinogenesis. *J Gastroenterol Hepatol* 2000; **15**: 339-341

10 **Gietz RD,** Triggs-Raine B, Robbins A, Graham KC, Woods RA. Identification of proteins that interact with a protein of interest: applications of the yeast two-hybrid system. *Mol Cell Biochem* 1997; **172**: 67-69

11 **Tarn C,** Bilodeau ML, Hullinger RL, Andrisani OM. Differential immediate early gene expression in conditional hepatitis B virus pX-transforming versus nontransforming hepatocyte cell lines. *J Biol Chem* 1999; **274**: 2327-2336

12 **Murakami S.** Hepatitis B virus X protein: a multifunctional viral regulator. *J Gastroenterol* 2001; **36**: 651-660

13 **Kim CM,** Koike K, Saito I, Miyamura T, Jay G. HBx gene of hepatitis B virus induces liver cancer in transgenic mice. *Nature* 1991; **351**: 317-320

14 **Cheong JH,** Yi M, Lin Y, Murakami S. Human RPB5, a subunit shared by eukaryotic nuclear RNA polymerases, binds human hepatitis B virus X protein and may play a role in X transactivation. *EMBO J* 1995; **14**: 143-150

15 **Haviv I,** Matza Y, Shaul Y. pX, the HBV-encoded coactivator, suppresses the phenotypes of TBP and TAFII250 mutants. *Genes Dev* 1998; **12**: 1217-1226

16 **Maguire HF,** Hoeffler JP, Siddiqui A. HBV X protein alters the DNA binding specificity of CREB and ATF-2 by protein-protein interactions. *Science* 1991; **252**: 842-844

17 **Chirillo P,** Falco M, Puri PL, Artini M, Balsano C, Levrero M, Natoli G. Hepatitis B virus pX activates NF-kappa B-dependent transcription through a Raf-independent pathway. *J Virol* 1996; **70**: 641-646

18 **Cong YS,** Yao YL, Yang WM, Kuzhandaivelu N, Seto E. The hepatitis B virus X-associated protein, XAP3, is a protein kinase C-binding protein. *J Biol Chem* 1997; **272**: 16482-16489

19 **Diao J,** Khine AA, Sarangi F, Hsu E, Iorio C, Tibbles LA, Woodgett JR, Penninger J, Richardson CD. X protein of hepatitis B virus inhibits Fas-mediated apoptosis and is associated with up-regulation of the SAPK/JNK pathway. *J Biol Chem* 2001; **276**: 8328-8340

20 **Arbuthnot P,** Capovilla A, Kew M. Putative role of hepatitis B virus X protein in hepatocarcinogenesis: effects on apoptosis, DNA repair, mitogen-activated protein kinase and JAK/STAT pathways. *J Gastroenterol Hepatol* 2000; **15**: 357-368

21 **Rahmani Z,** Huh KW, Lasher R, Siddiqui A. Hepatitis B virus X protein colocalizes to mitochondria with a human voltage-dependent anion channel, HVDAC3, and alters its transmembrane potential. *J Virol* 2000; **74**: 2840-2846

22 **Takada S,** Shirakata Y, Kaneniwa N, Koike K. Association of hepatitis B virus X protein with mitochondria causes mitochondrial aggregation at the nuclear periphery, leading to cell death. *Oncogene* 1999; **18**: 6965-6973

23 **Fields S,** Song O. A novel genetic system to detect protein-protein interactions. *Nature* 1989; **340**: 245-246

24 **Bartel PL**, Fields S. Analyzing protein-protein interactions using two-hybrid system. *Methods Enzymol* 1995; **254**: 241-263

25 **Lenka N,** Vijayasarathy C, Mullick J, Avadhani NG. Structural organization and transcription regulation of nuclear genes encoding the mammalian cytochrome c oxidase complex. *Prog Nucleic Acid Res Mol Biol* 1998; **61**: 309-344

26 **Maurer I,** Zierz S, Moller HJ. A selective defect of cytochrome c oxidase is present in brain of Alzheimer disease patients. *Neurobiol Aging* 2000; **21**: 455-462

27 **Quigley AF,** Kapsa RM, Esmore D, Hale G, Byrne E. Mitochondrial respiratory chain activity in idiopathic dilated cardiomyopathy. *J Card Fail* 2000; **6**: 47-55

28 **Muller-Hocker J,** Muntau A, Schafer S, Jaksch M, Staudt F, Pongratz D, Taanman JM. Depletion of mitochondrial DNA in the liver of an infant with neonatal giant cell hepatitis. *Hum Pathol* 2002; **33**: 247-253

29 **von Kleist-Retzow JC,** Vial E, Chantrel-Groussard K, Rotig A, Munnich A, Rustin P, Taanman JW. Biochemical, genetic and immunoblot analyses of 17 patients with an isolated cytochrome c oxidase deficiency. *Biochim Biophys Acta* 1999; **1455**: 35-44

30 **Aguilera I,** Garcia-Lozano JR, Munoz A, Arenas J, Campos Y, Chinchon I, Roldan AN, Bautista J. Mitochondrial DNA point mutation in the COI gene in a patient with McArdle's disease. *J Neurol Sci* 2001; **192**: 81-84

31 **Chandra D,** Liu JW, Tang DG. Early mitochondrial activation and cytochrome c up-regulation during apoptosis. *J Biol Chem* 2002; **277**: 50842-50854

32 **Valgimigli M,** Valgimigli L, Trere D, Gaiani S, Pedulli GF, Gramantieri L, Bolondi L. Oxidative stress EPR measurement in human liver by radical-probe technique. Correlation with etiology, histology and cell proliferation. *Free Radic Res* 2002; **36**: 939-948

33 **Kuo KW,** Yang PY, Huang YS, Shieh DZ. Variations in gene expression and genomic stability of human hepatoma cells integrated with hepatitis B virus DNA. *Biochem Mol Biol Int* 1998; **44**: 1133-1140

34 **Li J,** Xu Z, Zheng Y, Johnson DL, Ou JH. Regulation of hepatocyte nuclear factor 1 activity by wild-type and mutant hepatitis B virus X proteins. *J Virol* 2002; **76**: 5875-5881

35 **Waris G,** Huh KW, Siddiqui A. Mitochondrially associated hepatitis B virus X protein constitutively activates transcription factors STAT-3 and NF-kappa B via oxidative stress. *Mol Cell Biol* 2001; **21**: 7721-7730

36 **Cogswell PC,** Kashatus DF, Keifer JA, Guttridge DC, Reuther JY, Bristow C, Roy S, Nicholson DW, Baldwin AS Jr. NF-kappaB and I kappa B alpha are found in the mitochondria. Evidence for regulation of mitochondrial gene expression by NF-kappaB. *J Biol Chem* 2003; **278**: 2963-2968

Edited by Kumar M and Wang XL **Proofread by** Xu FM

PO Box 2345, Beijing 100023, China
Fax: +86-10-85381893
E-mail: wjg@wjgnet.com www.wjgnet.com

World J Gastroenterol 2004;10(19):2809-2813
World Journal of Gastroenterology
Copyright © 2004 by The WJG Press ISSN 1007-9327

• *H pylori* •

Roles of *Helicobacter pylori* infection and cyclooxygenase-2 expression in gastric carcinogenesis

Wei-Hao Sun, Qian Yu, Hong Shen, Xi-Long Ou, Da-Zhong Cao, Ting Yu, Cheng Qian, Feng Zhu, Yun-Liang Sun, Xi-Ling Fu, Han Su

Wei-Hao Sun, Department of Geriatrics, The First Affiliated Hospital of Nanjing Medical University, Nanjing 210029, Jiangsu Province, China
Qian Yu, Xi-Long Ou, Da-Zhong Cao, Ting Yu, Cheng Qian, Feng Zhu, Yun-Liang Sun, Xi-Ling Fu, Han Su, Department of Gastroenterology, Zhongda Hospital of Southeast University, Nanjing 210009, Jiangsu Province, China
Hong Shen, Department of Gastroenterology, Jiangsu Provincial Hospital of Traditional Chinese Medicine, Nanjing 210029, Jiangsu Province, China
Supported by the Scientific Research Foundation for the Returned Overseas Chinese Scholars, State Education Ministry, No. 9247342057
Correspondence to: Dr. Wei-Hao Sun, Department of Geriatrics, The First Affiliated Hospital of Nanjing Medical University, 300 Guangzhou Road, Nanjing 210029, China. weihaosun@hotmail.com
Telephone: +86-25-83718836-6044 **Fax:** +86-25-83783506
Received: 2003-10-20 **Accepted:** 2003-12-08

Abstract

AIM: Cyclooxygenase (COX)-2 is over expressed in gastrointestinal neoplasm. *Helicobacter pylori* (*H pylori*) infection is causally linked to gastric cancer. However, the expression of COX-2 in various stages of *H pylori*-associated gastric carcinogenesis pathway has not been elucidated. Therefore, the aim of this study was to clarify the role of *H pylori* induced COX-2 expression during carcinogenesis in the stomach.

METHODS: Gastric biopsies from 138 subjects [30 cases of chronic superficial gastritis (CSG), 28 cases of gastric glandular atrophy (GA), 45 cases of gastric mucosal intestinal metaplasia (IM), 12 cases of moderate gastric epithelial dysplasia and 23 cases of gastric cancer] were enrolled. *H pylori* infection was assessed by a rapid urease test and histological examination (modified Giemsa staining). The expression of COX-1 and COX-2 in human gastric mucosa was detected by immunohistochemical staining.

RESULTS: *H pylori* infection rate was 64.3% in GA and 69.5% in gastric cancer, which was significantly higher than that (36.7%) in CSG ($P<0.05$). The positive expression rates of COX-2 were 10.0%, 35.7%, 37.8%, 41.7% and 69.5% in CSG, GA, IM, dysplasia and gastric cancer, respectively. From CSG to GA, IM, dysplasia and finally to gastric cancer, expression of COX-2 showed an ascending tendency, whereas COX-1 expression did not change significantly in the gastric mucosa. The level of COX-2 expression in IM and dysplasia was significantly higher in *H pylori*-positive than in *H pylori*-negative subjects ($P<0.01$).

CONCLUSION: COX-2 expression induced by *H pylori* infection is a relatively early event during carcinogenesis in the stomach.

Sun WH, Yu Q, Shen H, Ou XL, Cao DZ, Yu T, Qian C, Zhu F, Sun YL, Fu XL, Su H. Roles of *Helicobacter pylori* infection and cyclooxygenase-2 expression in gastric carcinogenesis. *World J Gastroenterol* 2004; 10(19): 2809-2813
http://www.wjgnet.com/1007-9327/10/2809.asp

INTRODUCTION

Gastric cancer remains the world's second, and the Chinese first, commonest cause of cancer related deaths[1]. There is epidemiological evidence that *Helicobacter pylori* (*H pylori*) infection is causally linked to gastric cancer[2,3]. It has been classified as a class I biological carcinogen by the World Health Organization[4]. However, the exact mechanism responsible for the development of gastric cancer in *H pylori*-infected patients still remains obscure. According to Correa's [5] model, gastric cancer develops in a multistep process from chronic active gastritis, gastric glandular atrophy (GA), intestinal metaplasia (IM), dysplasia, and finally to gastric cancer. Recent studies have shown that *H pylori* infection induces cyclooxygenase-2 (COX-2) expression in human gastric mucosa[6-8]. COX-2, an inducible isoform of cyclooxygenase enzyme, which converts arachidonic acid to prostanoids, is strongly expressed in colorectal cancer[9,10], pancreatic cancer[11], hepatocellular carcinoma[12,13], esophageal cancer[14,15], and gastric cancer[16,17]. Several studies have also shown that COX-2 expression is increased in premalignant lesions including colonic adenoma[9], Barrett's esophagus[18,19], and gastric adenomas[20], indicating that this enzyme may be involved in the early process of carcinogenesis.

It is well known that *H pylori* infection causes inflammation, and COX-2 is involved in inflammatory responses and also related to carcinogenesis. However, COX-2 expression in various stages of *H pylori*-associated gastric carcinogenesis pathway has not been elucidated. To clarify the role of *H pylori* induced COX-2 expression during carcinogenesis in the stomach, COX-1 and COX-2 expression at different stages of gastric carcinogenesis from inflammation, premalignant lesions, to gastric cancer was investigated by using immunohistochemical analysis in the present study.

MATERIALS AND METHODS

Patients

A total of 138 patients were studied. Of these, 78 were males and 60 were females. The mean age was 52 years (range, 19-74). Endoscopies with biopsy were performed in all patients. Patients who took non-steroidal anti-inflammatory drugs (NSAIDs), H_2 receptor antagonists, proton pump inhibitors, antimicrobials, bismuth compounds, over last 4 wk prior to the examination, were excluded. The Medical Ethics Committee of Nanjing Medical University approved this study and written informed consent was obtained from all patients.

Endoscopy and histological assessment

All endoscopic examinations were performed under local anesthesia with lidocaine. Four biopsy specimens, 2 from the antrum within 2 cm of the pyloric channel and 2 from the corpus, were taken during the procedure. When lesions suspected to be cancerous were noted, additional biopsies were taken from the site of lesions. Of these specimens, 2 (each from antrum and corpus) were submitted to a rapid urease test (RUT), and the others were processed for hematoxylin and eosin (H&E) stain and modified Giemsa stain. The pathologic assessment

was performed by one pathologist according to the updated Sydney system[21]. GA was defined as loss of glandular tissue and fibrous replacement of lamina propria. IM or exchange of crypts by intestinal epithelium was recognized by the presence of goblet cells and absorptive cells.

Detection of H pylori infection

H pylori infection was identified by histological examination using modified Giemsa stain and RUT (CLO test, Delta West, Bentley, Australia). Patients were classified as *H pylori* positive if any of the two examinations yielded a positive result. Subjects were considered to be *H pylori* negative only when both assays were negative for the organism.

Immunohistochemistry

Immunohistochemical staining for COX-1 and COX-2 was performed by the avidin-biotin-peroxidase complex (ABC) method using a Vectastain kit (Vector Laboratories, Burlingame, CA). In brief, paraffin-embedded blocks were sectioned at about 4-μm thickness, deparaffinized, and rehydrated. After microwave pretreatment in citrate buffer (pH 6.0) for antigen retrieval, slides were immersed in 3 mL/L H_2O_2 in methanol for 30 min to block the endogenous peroxidase activity. Nonspecific binding was blocked with 50 mL/L rabbit serum (DAKO, Glostrup, Denmark) in phosphate-buffered saline (PBS), and the tissues were then incubated with goat polyclonal antibody against COX-1 or COX-2 (1:200, Santa Cruz Biotechnology, Inc. Santa Cruz, CA) in PBS containing 20 mL/L rabbit serum and 1 mL/L Triton 100 overnight at 4 ℃ in a humidity chamber. After being rinsed with PBS, the sections were subsequently incubated with biotinylated secondary rabbit anti-goat immunoglobulins (1:400) for 45 min and then with avidin-biotin-peroxidase complex for another 45 min. The color was developed in 3,3'-diaminobenzidine tetrahydrochloride (Sigma Chemical Co., St. Louis, MO) solution containing 0.3 mL/L H_2O_2. Nuclei were counterstained with Mayer's hematoxylin (Merck, Darmstadt, Germany). Tissues of part sections were incubated with PBS containing 20 mL/L rabbit serum and 1 mL/L Triton 100 without the primary antibody as a negative control.

Evaluation of COX-1 and COX-2 immunostaining

In each section, 5 high-power fields were selected, and a total of at least 1 000 cells were calculated. The percentage of positive staining cells was graded semiquantitatively, and each sample was assigned to one of the following categories: - (negative, 0% to 4%); + (weak, 5% to 29%); + + (moderate, 30% to 59%); or + + + (strong, more than 60%). All immunostained sections were evaluated independently by two investigators who were blind to the pathological and clinical data. Evaluations were similar among assessors, with less than 10% disagreement. A final consensus was achieved between the 2 assessors using a multihead microscope.

Statistical analysis

Expressions of COX-1 and COX-2 between the 5 study groups (CSG, GA, IM, dysplasia and gastric cancer) were compared by Kruskal-Wallis nonparametric analysis of variance test, using Dunn's multiple comparison tests for *post hoc* comparison. The association between COX-2 expression and *H pylori* infection was analyzed using Fisher's exact test. Statistical significance was taken at $P<0.05$.

RESULTS

Histopathologic characteristics and the prevalence of H pylori infection

Of the 138 patients, 63 were *H pylori*-positive and 75 were *H pylori*-negative. Table 1 shows the histopathologic characteristics and *H pylori* status. Histopathologic diagnosis in this population included CSG (n = 30), GA (n = 28), IM (n = 45), moderate dysplasia (n = 12) and gastric cancer (n = 23). The rates of *H pylori* infection in GA and gastric cancer were significantly higher than that in CSG.

Table 1 Rates of *H pylori* infection in various gastric mucosal lesions

Pathological diagnosis	n	*H pylori* rate (%)
CSG	30	36.7
GA	28	64.3[a]
IM	45	31.1
Dysplasia	12	33.3
Gastric cancer	23	69.5[a]

[a]$P<0.05$ *vs* CSG.

Expression of COX-1 and COX-2 in human gastric mucosa with various lesions

COX-1 was clearly detected in the gastric foveolar and glandular epithelium including parietal cells. Patchy cytoplasmic staining for COX-1 was also seen in the inflammatory mononuclear cells and macrophages, myofibroblasts, as well as endothelial cells in the lamina propria. Spotty cytoplasmic staining for COX-1 was seen in gastric cancer cells (Figure 1). Perinuclear and cytoplasmic staining for COX-2 was mainly seen in the foveolar and glandular epithelium, and mild staining in mononuclear inflammatory cells and macrophages in the lamina propria. Strong expression of COX-2 was also found on glandular epithelium of IM and dysplasia. Immunoreactivity of COX-2 protein showed diffuse staining in the cytoplasm of gastric cancer cells (Figure 2). Furthermore, scattered expression for COX-2 was detected in interstitial cells such as vascular endothelial cells and myofibroblasts. Table 2 shows the positive rates of COX-1 and COX-2 expression in the gastric mucosa with various lesions. From CSG to GA, IM, dysplasia and finally to gastric cancer, the expression of COX-2 showed an ascending tendency, whereas COX-1 expression did not change significantly in the gastric mucosa with various lesions.

Table 2 Expression of COX-1 and COX-2 in gastric mucosa with various lesions

Pathological diagnosis	n	COX-1 expression (%)	COX-2 expression (%)
CSG	30	56.6	10.0
GA	28	53.8	35.7[a]
IM	45	53.3	37.8[b]
Dysplasia	12	41.7	41.7[a]
Gastric cancer	23	43.4	69.5[bc]

[a]$P<0.05$; [b]$P<0.01$ *vs* CSG; [c]$P<0.05$ *vs* GA.

Relationship between H pylori infection and COX-2 expression in the gastric mucosa

COX-2 expression was found in 57% (36/63) *H pylori*-infected patients, including one case of CSG, eight cases of GA, twelve cases of IM, four cases of dysplasia, and eleven cases of gastric cancer, with intensity scoring ranged from + to +++ (Table 3). *H pylori*-associated gastritis exhibited strong expression of COX-2 in foveolar and glandular epithelium but with a lower intensity in mononuclear inflammatory cells. On the contrary, only 20% (15/75) of non-infected patients expressed COX-2 protein in the gastric biopsy. The intensity of COX-2 expression in IM and dysplasia was significantly higher in *H pylori*-

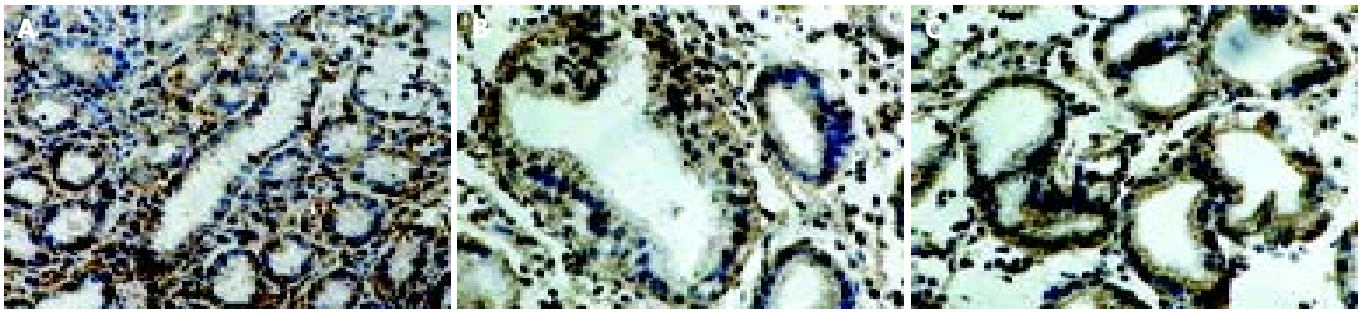

Figure 1 Immunostaining of cyclooxygenase-1 in the gastric mucosa with CSG (A), dysplasia (B) and gastric cancer (C) as shown by immunostaining. In the gastric biopsies of cases of CSG, GA, IM and dysplasia, COX-1 immunostaining was detected in the foveolar and glandular epithelium including parietal cells, and in the subepithelial mononuclear inflammatory cells. Spotty cytoplasmic staining for COX-1 was seen in the gastric cancer cells.

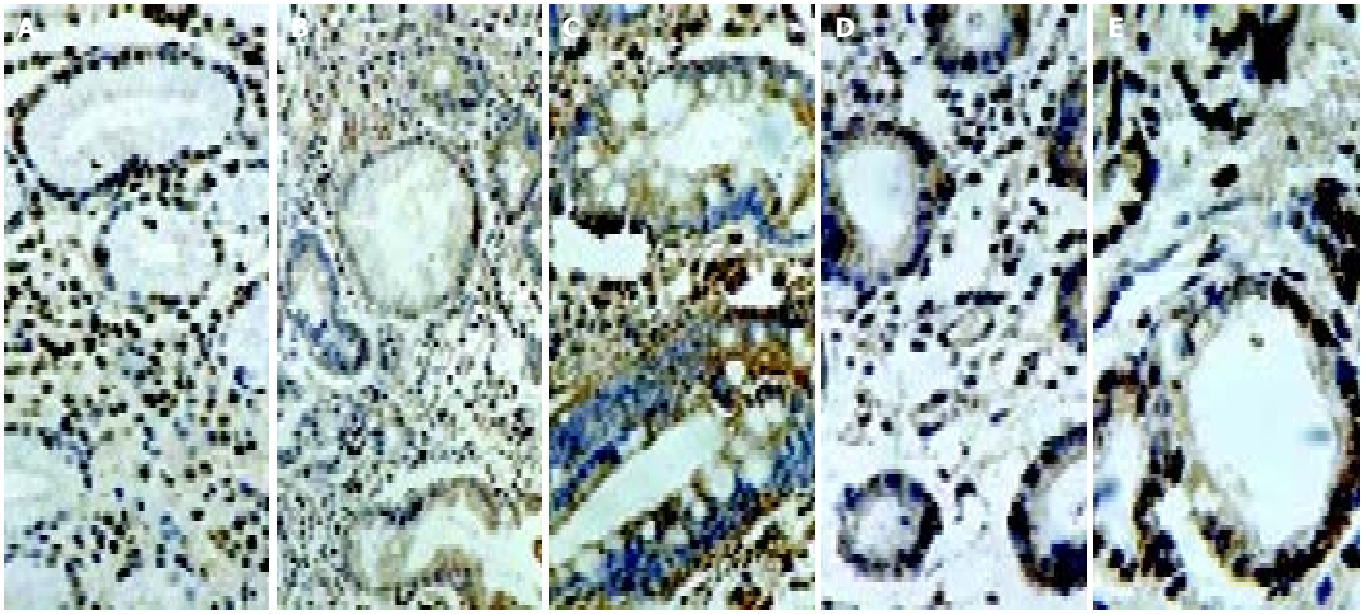

Figure 2 Immunostaining of cyclooxygenase-2 in the gastric mucosa with CSG (A), GA (B), IM (C), dysplasia (D) and gastric cancer (E). CSG showing strong expression in foveolar and glandular epithelium and weak expression in mononuclear inflammatory cells, myofibroblasts, and endothelial cells in the lamina propria; GA showing strong expression in the atrophic glands of the gastric mucosa; IM showing strong expression in intestinal epithelium and goblet cells; and gastric cancer showing strong expression in cancer cells.

Table 3 Relationship between *H pylori* infection and COX-1/COX-2 expression in the gastric mucosa with various lesions

Pathological diagnosis		*n*	COX-1				COX-2			
			–	+	++	+++	–	+	++	+++
CSG	*H pylori* (+)	11	5	1	3	2	10	0	0	1
	H pylori (-)	19	8	3	4	4	17	1	1	0
GA	*H pylori* (+)	18	9	2	4	3	10	1	3	4
	H pylori (-)	10	4	2	2	2	8	1	1	0
IM	*H pylori* (+)	14	6	3	2	3	2	2	4	6[b]
	H pylori (-)	31	15	5	5	6	26	3	2	0
Dysplasia	*H pylori* (+)	4	2	0	1	1	0	0	2	2[b]
	H pylori (-)	8	5	0	1	2	7	0	1	0
Gastric cancer	*H pylori* (+)	16	9	2	2	3	5	1	3	7
	H pylori (-)	7	4	2	0	1	2	1	2	2

[b]$P<0.01$ *vs H pylori* (-).

positive than in *H pylori*-negative subjects ($P<0.01$). However, there was no significant difference in COX-2 expression in CSG, GA and gastric cancer patients with or without *H pylori* infection (Table 3).

DISCUSSION

Epidemiological studies have shown that long-term use of NSAIDs reduces the risk of colon cancer development by 40%[22,23] and the risk of esophageal cancer development by up to 90%[24,25].

In addition, NSAIDs could induce regression of adenomatous polyps in patients with familial adenomatous polyposis[26,27], as well as in an Apc Min mouse model[28]. Although the exact mechanisms of NSAIDs on cancer prevention have not been clarified, one possible role of NSAIDs is via the inhibition of COX enzymes, leading to chemopreventive effect. COX exists in two isoforms, of which COX-1 is constitutively expressed in many tissues, including the stomach, and COX-2 showing 61% homology with COX-1 is expressed at low concentrations or is even undetectable in unstimulated cells or tissues, but is readily induced by various stimuli including mitogens, cytokines, growth factors, and tumor promoters in inflammatory and certain cell types, such as fibroblasts, macrophages and endothelial cells[29,30]. It is well known that COX-2 is strongly expressed in gastric cancer[17,20]. More than 90% of gastric cancers are adenocarcinomas, which are divided into intestinal and diffuse histological types. Pathogenesis of the intestinal-type gastric cancer has been connected to precursor changes such as GA, IM, and dysplasia. The present study clearly showed that COX-2 protein was expressed not only in gastric cancer cells but also in the glandular epithelium of IM and dysplasia as detected by immunohistochemistry. From CSG, GA to IM and dysplasia and finally to gastric cancer, the expression of COX-2 showed an ascending tendency, whereas COX-1 expression did not change significantly in premalignant and malignant gastric lesions. These results provided evidence that COX-2 might contribute to an early event in gastric carcinogenesis[31], and suggesting the possibility that the use of selective COX-2 inhibitors may provide a chemopreventive strategy against gastric carcinogenesis.

H pylori infection is an important risk factor for adenocarcinoma of the distal stomach in humans[2-5], but the mechanism whereby *H pylori* infection contributes to gastric carcinogenesis is still hypothetical. Recent studies have shown that *H pylori* infection induces COX-2 expression in human gastric mucosa[6-8]. Furthermore, McCarthy *et al.*[32] showed that COX-2 expression in antral mucosa was reduced but not eliminated in the epithelium after successful eradication of *H pylori*. Kimura *et al.*[33] reported that immunoreactivity of COX-2 was observed in all cases of IM even after the cure of *H pylori* infection. Thus, cure of *H pylori* infection may decrease the risk of gastric carcinogenesis due to COX-2-related compounds in gastric mucosa but not in those patients with IM. In this study, we demonstrated that COX-2 was expressed in epithelial lining of the stomach in the *H pylori*-associated gastric carcinogenesis pathway from CSG, to GA and IM and dysplasia, and finally to gastric cancer. The level of COX-2 expression in patients with IM and dysplasia was significantly higher in *H pylori*-positive than in *H pylori*-negative subjects. In contrast, COX-1 protein was constitutively expressed in different gastric mucosal lesions with or without *H pylori* infection. Thus, COX-1 is considered as a housekeeping gene, and prostanoids synthesized via the COX-1 pathway are thought to be responsible for cytoprotection of the stomach, for vasodilatation in the kidney, and for production of a proaggregative prostanoid, thromboxane, by the platelets. In contrast, COX-2 is an inducible immediate-early gene, and its role has been connected to inflammation, reproduction, and carcinogenesis. Although the exact mechanism of COX-2 expression in carcinogenesis is still unclear, some studies have suggested that overexpression of COX-2 is associated with cellular resistance to apoptosis whereas treatment with specific COX-2 inhibitors could suppress cell proliferation and induces apoptosis[14,34-36]. It has been hypothesized that the alteration of the balance between apoptosis and proliferation of gastric epithelial cells, induced by *H pylori* infection, contributes to either gastric injury or carcinogenesis of the stomach[37-39]. Although *H pylori* could decrease epithelial cell proliferation and induce apoptosis *in vitro*[40-43], *H pylori* infection *in vivo* was associated with both increased apoptosis and proliferation[44-46]. These differences between the *in vivo* and *in vitro* results suggest that *in vivo* factors including inflammatory cells, extracellular matrix proteins, cytokines, and adhesion molecules may also contribute to epithelial cell turnover. On the other hand, COX-2 expression has been reported to correlate with invasion of the lymphatic vessels, lymph node metastasis, and advanced tumor stage in gastric cancer[47,48].

In conclusion, COX-2 overex-pression plays an important role in the initiation of gastric carcinogenesis. The use of selective COX-2 inhibitors may provide a chemopreventive strategy against gastric carcinogenesis.

REFERENCES

1 **Stadtlander CT**, Waterbor JW. Molecular epidemiology, pathogenesis and prevention of gastric cancer. *Carcinogenesis* 1999; **20**: 2195-2208

2 **Wang RT**, Wang T, Chen K, Wang JY, Zhang JP, Lin SR, Zhu YM, Zhang WM, Cao YX, Zhu CW, Yu H, Cong YJ, Zheng S, Wu BQ. *Helicobacter pylori* infection and gastric cancer: evidence from a retrospective cohort study and nested case-control study in China. *World J Gastroenterol* 2002; **8**: 1103-1107

3 **Welin M**, Holmgren NM, Nilsson P, Enroth H. Statistical model of the interactions between *Helicobacter pylori* infection and gastric cancer development. *Helicobacter* 2003; **8**: 72-78

4 Infection with *Helicobacter pylori*. *IARC Monogr Eval Carcinog Risks Hum* 1994; **61**: 177-240

5 **Correa P**. *Helicobacter pylori* and gastric carcinogenesis. *Am J Surg Pathol* 1995; **19**(Suppl 1): S37-S43

6 **Fu S**, Ramanujam KS, Wong A, Fantry GT, Drachenberg CB, James SP, Meltzer SJ, Wilson KT. Increased expression and cellular localization of inducible nitric oxide synthase and cyclooxygenase 2 in *Helicobacter pylori* gastritis. *Gastroenterology* 1999; **116**: 1319-1329

7 **Tatsuguchi A**, Sakamoto C, Wada K, Akamatsu T, Tsukui T, Miyake K, Futagami S, Kishida T, Fukuda Y, Yamanaka N, Kobayashi M. Localisation of cyclooxygenase 1 and cyclooxygenase 2 in *Helicobacter pylori* related gastritis and gastric ulcer tissues in humans. *Gut* 2000; **46**: 782-789

8 **Chan FK**, To KF, Ng YP, Lee TL, Cheng AS, Leung WK, Sung JJ. Expression and cellular localization of COX-1 and -2 in *Helicobacter pylori* gastritis. *Aliment Pharmacol Ther* 2001; **15**: 187-193

9 **Eberhart CE**, Coffey RJ, Radhika A, Giardiello FM, Ferrenbach S, DuBois RN. Up-regulation of cyclooxygenase 2 gene expression in human colorectal adenomas and adenocarcinomas. *Gastroenterology* 1994; **107**: 1183-1188

10 **Sano H**, Kawahito Y, Wilder RL, Hashiramoto A, Mukai S, Asai K, Kimura S, Kato H, Kondo M, Hla T. Expression of cyclooxygenase-1 and -2 in human colorectal cancer. *Cancer Res* 1995; **55**: 3785-3789

11 **Tucker ON**, Dannenberg AJ, Yang EK, Zhang F, Teng L, Daly JM, Soslow RA, Masferrer JL, Woerner BM, Koki AT, Fahey TJ 3rd. Cyclooxygenase-2 expression is up-regulated in human pancreatic cancer. *Cancer Res* 1999; **59**: 987-990

12 **Koga H**, Sakisaka S, Ohishi M, Kawaguchi T, Taniguchi E, Sasatomi K, Harada M, Kusaba T, Tanaka M, Kimura R, Nakashima Y, Nakashima O, Kojiro M, Kurohiji T, Sata M. Expression of cyclooxygenase-2 in human hepatocellular carcinoma: relevance to tumor dedifferentiation. *Hepatology* 1999; **29**: 688-696

13 **Shiota G**, Okubo M, Noumi T, Noguchi N, Oyama K, Takano Y, Yashima K, Kishimoto Y, Kawasaki H. Cyclooxygenase-2 expression in hepatocellular carcinoma. *Hepatogastroenterology* 1999; **46**: 407-412

14 **Zimmermann KC**, Sarbia M, Weber AA, Borchard F, Gabbert HE, Schror K. Cyclooxygenase-2 expression in human esophageal carcinoma. *Cancer Res* 1999; **59**: 198-204

15 **Ratnasinghe D**, Tangrea J, Roth MJ, Dawsey S, Hu N, Anver M, Wang QH, Taylor PR. Expression of cyclooxygenase-2 in human squamous cell carcinoma of the esophagus; an immunohistochemical survey. *Anticancer Res* 1999; **19**: 171-174

16 **Sung JJ**, Leung WK, Go MY, To KF, Cheng AS, Ng EK, Chan FK. Cyclooxygenase-2 expression in *Helicobacter pylori*-associ-

ated premalignant and malignant gastric lesions. *Am J Pathol* 2000; **157**: 729-735
17 **Uefuji K**, Ichikura T, Mochizuki H, Shinomiya N. Expression of cyclooxygenase-2 protein in gastric adenocarcinoma. *J Surg Oncol* 1998; **69**: 168-172
18 **Wilson KT**, Fu S, Ramanujam KS, Meltzer SJ. Increased expression of inducible nitric oxide synthase and cyclooxygenase-2 in Barrett's esophagus and associated adenocarcinomas. *Cancer Res* 1998; **58**: 2929-2934
19 **Shirvani VN**, Ouatu-Lascar R, Kaur BS, Omary MB, Triadafilopoulos G. Cyclooxygenase 2 expression in Barrett's esophagus and adenocarcinoma: Ex vivo induction by bile salts and acid exposure. *Gastroenterology* 2000; **118**: 487-496
20 **Uefuji K**, Ichikura T, Mochizuki H. Expression of cyclooxygenase-2 in human gastric adenomas and adenocarcinomas. *J Surg Oncol* 2001; **76**: 26-30
21 **Dixon MF**, Genta RM, Yardley JH, Correa P. Classification and grading of gastritis. The updated Sydney System. International Workshop on the Histopathology of Gastritis, Houston 1994. *Am J Surg Pathol* 1996; **20**: 1161-1181
22 **Thun MJ**, Namboodiri MM, Heath CW Jr. Aspirin use and reduced risk of fatal colon cancer. *N Engl J Med* 1991; **325**: 1593-1596
23 **Rosenberg L**, Palmer JR, Zauber AG, Warshauer ME, Stolley PD, Shapiro S. A hypothesis: nonsteroidal anti-inflammatory drugs reduce the incidence of large-bowel cancer. *J Natl Cancer Inst* 1991; **83**: 355-358
24 **Thun MJ**, Namboodiri MM, Calle EE, Flanders WD, Heath CW Jr. Aspirin use and risk of fatal cancer. *Cancer Res* 1993; **53**: 1322-1327
25 **Funkhouser EM**, Sharp GB. Aspirin and reduced risk of esophageal carcinoma. *Cancer* 1995; **76**: 1116-1119
26 **Giardiello FM**, Hamilton SR, Krush AJ, Piantadosi S, Hylind LM, Celano P, Booker SV, Robinson CR, Offerhaus GJ. Treatment of colonic and rectal adenomas with sulindac in familial adenomatous polyposis. *N Engl J Med* 1993; **328**: 1313-1316
27 **Waddell WR**, Loughry RW. Sulindac for polyposis of the colon. *J Surg Oncol* 1983; **24**: 83-87
28 **Jacoby RF**, Marshall DJ, Newton MA, Novakovic K, Tutsch K, Cole CE, Lubet RA, Kelloff GJ, Verma A, Moser AR, Dove WF. Chemoprevention of spontaneous intestinal adenomas in the Apc Min mouse model by the nonsteroidal anti-inflammatory drug piroxicam. *Cancer Res* 1996; **56**: 710-714
29 **Lee SH**, Soyoola E, Chanmugam P, Hart S, Sun W, Zhong H, Liou S, Simmons D, Hwang D. Selective expression of mitogen-inducible cyclooxygenase in macrophages stimulated with lipopolysaccharide. *J Biol Chem* 1992; **267**: 25934-25938
30 **Mitchell JA**, Larkin S, Williams TJ. Cyclooxygenase-2: regulation and relevance in inflammation. *Biochem Pharmacol* 1995; **50**: 1535-1542
31 **Lim HY**, Joo HJ, Choi JH, Yi JW, Yang MS, Cho DY, Kim HS, Nam DK, Lee KB, Kim HC. Increased expression of cyclooxygenase-2 protein in human gastric carcinoma. *Clin Cancer Res* 2000; **6**: 519-525
32 **McCarthy CJ**, Crofford LJ, Greenson J, Scheiman JM. Cyclooxygenase-2 expression in gastric antral mucosa before and after eradication of *Helicobacter pylori* infection. *Am J Gastroenterol* 1999; **94**: 1218-1223
33 **Kimura A**, Tsuji S, Tsujii M, Sawaoka H, Iijima H, Kawai N, Yasumaru M, Kakiuchi Y, Okuda Y, Ali Z, Nishimura Y, Sasaki Y, Kawano S, Hori M. Expression of cyclooxygenase-2 and nitrotyrosine in human gastric mucosa before and after *Helicobacter pylori* eradication. *Prostaglandins Leukot Essent Fatty Acids* 2000; **63**: 315-322
34 **Sheng H**, Shao J, Morrow JD, Beauchamp RD, DuBois RN. Modulation of apoptosis and Bcl-2 expression by prostaglandin E2 in human colon cancer cells. *Cancer Res* 1998; **58**: 362-366
35 **Sawaoka H**, Kawano S, Tsuji S, Tsujii M, Gunawan ES, Takei Y, Nagano K, Hori M. Cyclooxygenase-2 inhibitors suppress the growth of gastric cancer xenografts via induction of apoptosis in nude mice. *Am J Physiol* 1998; **274**(6 Pt 1): G1061-G1067
36 **Erickson BA**, Longo WE, Panesar N, Mazuski JE, Kaminski DL. The effect of selective cyclooxygenase inhibitors on intestinal epithelial cell mitogenesis. *J Surg Res* 1999; **81**: 101-107
37 **Anti M**, Armuzzi A, Gasbarrini A, Gasbarrini G. Importance of changes in epithelial cell turnover during *Helicobacter pylori* infection in gastric carcinogenesis. *Gut* 1998; **43**(Suppl 1): S27-S32
38 **Correa P**, Miller MJ. Carcinogenesis, apoptosis and cell proliferation. *Br Med Bull* 1998; **54**: 151-162
39 **Mannick EE**, Bravo LE, Zarama G, Realpe JL, Zhang XJ, Ruiz B, Fontham ET, Mera R, Miller MJ, Correa P. Inducible nitric oxide synthase, nitrotyrosine, and apoptosis in *Helicobacter pylori* gastritis: effect of antibiotics and antioxidants. *Cancer Res* 1996; **56**: 3238-3243
40 **Chen G**, Sordillo EM, Ramey WG, Reidy J, Holt PR, Krajewski S, Reed JC, Blaser MJ, Moss SF. Apoptosis in gastric epithelial cells is induced by *Helicobacter pylori* and accompanied by increased expression of BAK. *Biochem Biophys Res Commun* 1997; **239**: 626-632
41 **Ricci V**, Ciacci C, Zarrilli R, Sommi P, Tummuru MK, Del Vecchio Blanco C, Bruni CB, Cover TL, Blaser MJ, Romano M. Effect of *Helicobacter pylori* on gastric epithelial cell migration and proliferation *in vitro*: role of VacA and CagA. *Infect Immun* 1996; **64**: 2829-2833
42 **Rudi J**, Kuck D, Strand S, von Herbay A, Mariani SM, Krammer PH, Galle PR, Stremmel W. Involvement of the CD95 (APO-1/Fas) receptor and ligand system in *Helicobacter pylori*-induced gastric epithelial apoptosis. *J Clin Invest* 1998; **102**: 1506-1514
43 **Wagner S**, Beil W, Westermann J, Logan RP, Bock CT, Trautwein C, Bleck JS, Manns MP. Regulation of gastric epithelial cell growth by *Helicobacter pylori*: offdence for a major role of apoptosis. *Gastroenterology* 1997; **113**: 1836-1847
44 **Fraser AG**, Sim R, Sankey EA, Dhillon AP, Pounder RE. Effect of eradication of *Helicobacter pylori* on gastric epithelial cell proliferation. *Aliment Pharmacol Ther* 1994; **8**: 167-173
45 **Peek RM Jr**, Wirth HP, Moss SF, Yang M, Abdalla AM, Tham KT, Zhang T, Tang LH, Modlin IM, Blaser MJ. *Helicobacter pylori* alters gastric epithelial cell cycle events and gastrin secretion in Mongolian gerbils. *Gastroenterology* 2000; **118**: 48-59
46 **Peek RM Jr**, Moss SF, Tham KT, Perez-Perez GI, Wang S, Miller GG, Atherton JC, Holt PR, Blaser MJ. *Helicobacter pylori* cagA+ strains and dissociation of gastric epithelial cell proliferation from apoptosis. *J Natl Cancer Inst* 1997; **89**: 863-868
47 **Murata H**, Kawano S, Tsuji S, Tsuji M, Sawaoka H, Kimura Y, Shiozaki H, Hori M. Cyclooxygenase-2 overexpression enhances lymphatic invasion and metastasis in human gastric carcinoma. *Am J Gastroenterol* 1999; **94**: 451-455
48 **Yamamoto H**, Itoh F, Fukushima H, Hinoda Y, Imai K. Overexpression of cyclooxygenase-2 protein is less frequent in gastric cancers with microsatellite instability. *Int J Cancer* 1999; **84**: 400-403

Edited by Xia HHX and Wang XL **Proofread by** Xu FM

PO Box 2345, Beijing 100023, China
Fax: +86-10-85381893
E-mail: wjg@wjgnet.com www.wjgnet.com

World J Gastroenterol 2004;10(19):2814-2817
World Journal of Gastroenterology
Copyright © 2004 by The WJG Press ISSN 1007-9327

• BASIC RESEARCH •

Lansoprazole ameliorates intestinal mucosal damage induced by ischemia-reperfusion in rats

Hiroshi Ichikawa, Norimasa Yoshida, Tomohisa Takagi, Naoya Tomatsuri, Kazuhiro Katada, Yutaka Isozaki, Kazuhiko Uchiyama, Yuji Naito, Takeshi Okanoue, Toshikazu Yoshikawa

Hiroshi Ichikawa, Department of Food Sciences and Nutritional Health, Faculty of Human Environment, Kyoto Prefectural University, 606-8522, Japan
Norimasa Yoshida, Yuji Naito, Takeshi Okanoue, Department of Molecular Gastroenterology and Hepatology, Graduate School of Medical Sciences, Kyoto Prefectural University of Medicine, 606-8522, Japan
Tomohisa Takagi, Naoya Tomatsuri, Kazuhiro Katada, Yutaka Isozaki, Kazuhiko Uchiyama, Toshikazu Yoshikawa, Department of Inflammation and Immunology, Graduate School of Medical Sciences, Kyoto Prefectural University of Medicine, 606-8522, Japan
Correspondence to: Dr. Norimasa Yoshida, Department of Molecular Gastroenterology and Hepatology, Graduate School of Medical Sciences, Kyoto Prefectural University of Medicine, 465 Kajii-cho, Kawaramachi-Hirokoji, Kamigyo-ku, Kyoto 602-8566, Japan. nyoshida@koto.kpu-m.ac.jp
Telephone: +81-75-251-5508 **Fax:** +81-75-252-3721
Received: 2004-03-18 **Accepted:** 2004-04-29

Abstract

AIM: To investigate the protective effect of lansoprazole on ischemia and reperfusion (I/R)-induced rat intestinal mucosal injury *in vivo*.

METHODS: Intestinal damage was induced by clamping both the superior mesenteric artery and the celiac trunk for 30 min followed by reperfusion in male Sprague-Dawley rats. Lansoprazole was given to rats intraperitoneally 1 h before vascular clamping.

RESULTS: Both the intraluminal hemoglobin and protein levels, as indices of mucosal damage, significantly increased in I/R-groups comparion with those of sham-operation groups. These increases in intraluminal hemoglobin and protein levels were significantly inhibited by the treatment with lansoprazole at a dose of 1 mg/kg. Small intestine exposed to I/R resulted in mucosal inflammation that was characterized by significant increases in thiobarbituric acid-reactive substances (TBARS), tissue-associated myeloperoxidase activity (MPO), and mucosal content of rat cytokine-induced neutrophil chemoattractant-1 (CINC-1). These increases in TBARS, MPO activities and CINC-1 content in the intestinal mucosa after I/R were all inhibited by pretreatment with lansoprazole at a dose of 1 mg/kg. Furthermore, the CINC-1 mRNA expression was increased during intestinal I/R, and this increase in mRNA expression was inhibited by treatment with lansoprazole.

CONCLUSION: Lansoprazole inhibits lipid peroxidation and reduces development of intestinal mucosal inflammation induced by I/R in rats, suggesting that lansoprazole may have a therapeutic potential for I/R injury.

Ichikawa H, Yoshida N, Takagi T, Tomatsuri N, Katada K, Isozaki Y, Uchiyama K, Naito Y, Okanoue T, Yoshikawa T. Lansoprazole ameliorates intestinal mucosal damage induced by ischemia-reperfusion in rats. *World J Gastroenterol* 2004; 10(19): 2814-2817
http://www.wjgnet.com/1007-9327/10/2814.asp

INTRODUCTION

Reactive oxygen species such as superoxide radicals, hydrogen peroxide, and hydroxyl radicals, have been implicated in the pathogenesis of ischemia-reperfusion (I/R) injury in a variety of organs, including the brain[1], large intestine[2], and heart[3]. Intestinal I/R is an especially grave condition resulted from acute mesenteric ischemia, small bowel transplantation, abdominal aortic aneurysm, hemorrhagic, traumatic, or septic shock, and severe burns[4,5]. I/R injury of the small intestine is characterized by a number of microvascular and mucosal alterations, including endothelial cell swelling, capillary plugging, prolonged reduction in intestinal blood flow, and mucosal barrier dysfunction[6-8]. Previous studies have demonstrated that neutrophils are critically involved in I/R injury. This hypothesis based on experiments shows that neutrophil depletion[9,10] and inhibition of neutrophil-endothelial cell interactions[11] could protect against injury after I/R.

Proton-pump inhibitors (PPIs)[12] such as omeprazole and lansoprazole are extensively used for therapeutic control of acid-related disorders, including gastroesophageal reflux disease and peptic-ulcer diseases caused by stress, nonsteroidal anti-inflammatory drugs and *Helicobacter pylori* infection[13-16]. PPIs are strong antisecretory agents that act on gastric (H^+/K^+) ATPase of parietal cells[17]. Recently, it has been suggested that PPIs inhibit neutrophil functions such as chemotaxis, superoxide production and degradation[18]. We have already reported that PPIs can attenuate neutrophil adherence to endothelial cells via inhibition of the expression of adhesion molecules[19]. These results have indicated that PPIs have anti-inflammatory effects and can inhibit acid secretion.

The present study was to evaluate anti-inflammatory effects of lansoprazole, which has dramatically influenced the management of acid-peptic disorders in recent years, using I/R-induced rat intestinal mucosal injury model unrelated to acid secretion.

MATERIALS AND METHODS

Experimental animals

Male Sprague-Dawley (SD) rats weighing 190-210 g were obtained from Keari Co. Ltd. (Osaka, Japan). The rats were housed in stainless steel cages with wire bottoms and maintained on a 12-h light and dark cycle, with the temperature and relative humidity of the animal room controlled at 21-23 ℃ and 55-65%, respectively. The rats were not fed for 18 h prior to the experiments, but allowed free access to water. All experimental procedures described below were approved by the Animal Care Committee of the Kyoto Prefectural University of Medicine (Kyoto, Japan).

Preparation of rats for intestinal ischemia-reperfusion

Intestinal ischemia was induced for 30 min by applying a small clamp to the superior mesenteric artery after ligating the celiac artery in rats given intraperitoneal urethane anesthesia (1 000 mg/kg). Reoxygenation was produced by removal of the clamp. Sixty minutes after reperfusion, the rats were killed by exsanguinations via the abdominal aorta under urethane anesthesia (1 000 mg/kg). 2-[[[3-methyl-4- (2,2,2-trifluoroethoxy)-2-pyridyl] methyl] sulfinyl] benzimidazole (Lansoprazole), a gift from Takeda Chemical Industries Ltd. Japan, was diluted with physiological saline at a dose of 0.3-1 mg/kg after dissolved in dimethylsulfoxide, and was given to rats intraperitoneally 1 h before the vascular clamping. In the control groups, rats received an equivalent volume of the vehicle.

Assessment of intestinal mucosal injury induced by ischemia-reperfusion

To estimate the severity of the intestinal mucosal damage by I/R, leakage of intraluminal protein and intraluminal hemoglobin levels were measured as mg/cm intestine.

The concentrations of thiobarbituric acid-reactive substances (TBARS) in the intestinal mucosa, an index of lipid peroxidation, were measured by the method of Ohkawa *et al*.[20]. In brief, the small intestine was opened by a longitudinal incision, and the intestinal mucosa was scraped off using two glass slides. Mucosal tissue was then homogenized with 10 mmol/L potassium phosphate buffer (pH 7.8) containing 30 mmol/L KCl in a Teflon Potter-Elvehjem homogenizer. The levels of TBARS in the mucosal homogenates were expressed as nmol of malondialdehyde per gram of wet weight using 1,1,3,3-tetramethoxypropane as the standard.

Myeloperoxidase (MPO) activity in the intestinal mucosa, an index of polymorphonuclear leukocyte accumulation, were determined by a modification of the method of Grisham *et al*.[21]. Two milliliters of mucosal homogenate was centrifuged at 20 000 *g* for 15 min at 4 ℃ to pellet the insoluble cellular debris. The pellet was then rehomogenized in an equivalent volume of 0.05 mol/L potassium phosphate buffer (pH 5.4) containing 5 g/L hexadecyltrimethylammonium bromide. Samples were centrifuged at 20 000 *g* for 15 min at 4 ℃, and the supernatants were saved. MPO activity was assessed by measuring the H_2O_2-dependent oxidation of 3,3',5,5'-tetramethylbenzidine. One unit of enzyme activity was defined as the amount of MPO that caused a change in the absorbance of 1.0/min at 655 nm and 25 ℃.

The content of cytokine-induced neutrophil chemoattractant-1 (CINC-1) in the intestinal mucosal homogenates was determined by enzyme-linked immunosorbent assay (ELISA) using a kit (Immuno Biological Laboratories, Gunma, Japan) according to the manufacturer's instructions. The absorbance of each well was read at 490 nm by a microplate reader (MPR-A4i; Tosoh, Tokyo, Japan).

The expression of intestinal CINC-1 was determined using the RT-PCR method. Samples of intestinal tissue for mRNA isolation were prepared from the whole intestine. Total RNA was isolated using the acid-guanidium-phenol-chloroform (AGPC) method with ISOGEN (NIPPON GENE). The concentration of RNA was determined by the absorbance at 260 nm in relation to that at 280 nm. The RNA was stored at -70 ℃ until used for RT-PCR. One microliter of RT-PCR products was added to 3 mmol/L of each primer, CINC-1 and β-actin (for internal standard purpose), and a solution of 0.5 U of *Taq* DNA polymerase (Takara Biochemicals) in a final volume of 50 L. The primers had the following sequences: for CINC-1, sense 5'-ACAGTGGCAGGGATTCACTT-3', and antisense 5'-CTAGCA CAGTGGTTGACACT-3'; for β-actin, sense 5'-TCCTGTGG CATCCATGAAACT-3', and antisense 5'-GAAGCATTTGCGG TGCACGAT-3'. The mixture was subjected to 30 cycles (1 min at 94 ℃, 1 min at 54 ℃, 1 min at 72 ℃) of amplification. Then the reaction products were separated by electrophoresis on 25 g/L agarose gel and stained with ethidium bromide.

Statistical analysis

All values were expressed as mean±SE. The data were compared by one-way analysis of variance (ANOVA) followed by Dunnett's multiple comparison test. All analyses were performed using the Stat View 5.0-J program (Abacus Concepts Inc. Berkeley, CA). $P<0.05$ was considered statistically significant.

RESULTS

Intraluminal protein and hemoglobin levels of the small intestine

Intraluminal hemoglobin and protein levels, the reflections of intestinal mucosal injury, were significantly increased above basal levels after 60 min of reperfusion. These increases in intraluminal protein and hemoglobin levels induced by I/R were significantly decreased by lansoprazole treatment at a dose of 1 mg/kg (Table 1).

TBARS in the intestinal mucosa

TBARS in the intestinal mucosa, an index of lipid peroxidation, significantly increased 60 min after reperfusion (13.0±2.5 nmoL/ 100 g wet wt). These levels were significantly decreased to 7.98±1.98 nmol/100 g wet wt after lansoprazole treatment at a dose of 1 mg/kg (Figure 1A).

MPO activity in the intestinal mucosa

The I/R group showed a significant increase in mucosal MPO activity (0.167±0.046 mU/mg wet wt) compared with the sham-operation group (0.014±0.001 mU/mg wet wt). However, this increase in MPO activity significantly decreased to 0.028±0.008 mU/mg wet wt after lansoprazole treatment at a dose of 1 mg/kg (Figure 1B).

Inflammatory cytokine in the intestinal mucosa

The content of mucosal CINC-1 in the I/R groups was significantly increased compared with the levels in sham-operated groups. This increase in the levels of inflammatory cytokines was significantly inhibited by lansoprazole at a dose of 1 mg/kg (Figure 1C).

Intestinal expression of CINC-1 mRNA during ischemia-reperfusion

The expression of CINC-1 mRNA in the intestinal mucosa was up-regulated by I/R injury. This increase in the expression of CINC-1 mRNA was also inhibited by lansoprazole at a dose of 1 mg/kg (Figure 2).

Table 1 Effect of lansoprazole on intraluminal hemoglobin and protein levels in small intestine of I/R-induced rats (mean±SE)

	Sham-operation (Normal)	Ischemia-reperfusion (Control)	Lansoprazole (mg/kg)	
			0.3	1
Intraluminal hemoglobin (mg/cm)	0.000043±0.000002	0.0043±0.0006[a]	0.0035±0.0007	0.0010±0.0004[c]
Intraluminal protein (mg/cm)	0.065±0.012	0.172±0.016[a]	0.156±0.022	0.087±0.010[c]

[a]$P<0.05$ *vs* normal; [c]$P<0.05$ *vs* control.

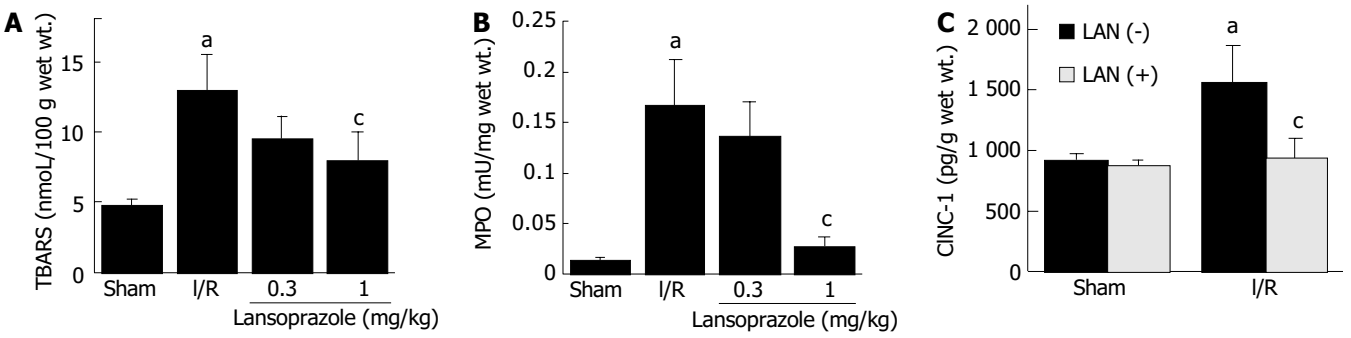

Figure 1 Effect of lansoprazole on the level of thiobarbituric-acid reactive substances (TBARS), mucosal mye-loperoxidase (MPO) activity, and cytolline induced meutrophil chemo-attracttant-1 (CINC-1) in intestinal mucosa of I/R-induced rats.A: Effect of lansoprazole on the level of TBARS in intestinal mucosa of I/R-induced rats. $^{a}P<0.05$ *vs* normal; $^{c}P<0.05$ *vs* control. Sham group and I/R group received an equivalent volume of vehicle instead of lansoprazole. B: Effect of lansoprazole on the level of mucosal myeloperoxidase (MPO) activities in intestinal mucosa of I/R-induced rats. $^{a}P<0.05$ *vs* normal; $^{c}P<0.05$ *vs* control. Sham group and I/R group received an equivalent volume of vehicle instead of lansoprazole. C: Effect of lansoprazole on cytokine induced neutrophil chemoattractant-1 (CINC-1) of intestinal mucosa of I/R-induced rats. $^{a}P<0.05$ *vs* normal; $^{c}P<0.05$ *vs* control. LAN(+): with lansoprazole; LAN(-): without lansoprazole.

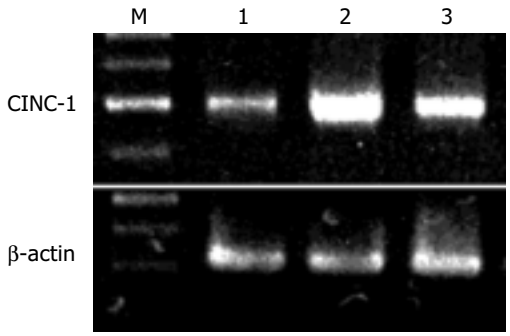

Figure 2 Intestinal CINC-1 mRNA expression during I/R in rats. M: Marker; Lane 1: Before ischemia; Lane 2: After I/R; Lane 3: I/R + lansoprazole.

DISCUSSION

Our results clearly showed that lansoprazole had a protective effect against reperfusion-induced intestinal mucosal injury in rats. In addition, increases in TBARS contents, MPO activity and CINC-1 contents were inhibited by the treatment of lansoprazole. In I/R-induced tissue injury, oxygen radicals have been suggested to be generated via several mechanisms, including the xanthine/xanthine oxidase reaction[22], NADPH oxidase and myeloperoxidase of activated leukocytes migrating into the previously ischemic area[23], and mitochondrial respiratory system[24]. We have already reported that oxygen-derived free radicals and lipid peroxidation played a role in the formation of gastrointestinal mucosal damage induced by I/R[25,26]. Furthermore, it is well known that neutrophils that adhere to post-capillary venules and subsequently emigrate into the interstitium are implicated in the I/R-related tissue injury[27,28]. Activated neutrophils release a variety of cytotoxic substances, including proteases, collagenases, cytokines, leukotrienes, and cationic proteins, thereby causing tissue damage. In addition, adhered and aggregated neutrophils can physically disturb capillary flow and induce a non-reflow phenomenon.

Little is known about the protective mechanism of lansoprazole against I/R injury. However, there have been some reports about the anti-inflammatory action of PPIs. We have shown that the expression of adhesion molecules on neutrophils and endothelial cells elicited by *H pylori* extract and IL-1 was inhibited by lansoprazole and omeprazole at clinical relevant doses[19]. Other reports have also revealed that PPIs could prevent the neutrophil-endothelial cell adhesion reaction[29,30]. Recently, some reports regarding the anti-oxidative effects of PPIs have also appeared. Suzuki *et al*.[31] reported that PPIs inhibited the production of oxygen-derived free radicals from neutrophils activated by chemotactic peptides or opsonized zymosan. Other studies have concluded that PPIs block stress-induced increased reactive oxygen intermediates and associated lipid peroxidation and protein oxidation, indicating that its antioxidant properties play a major role in preventing oxidative damage[32-34].

Lansoprazole has been widely used in the treatment of acid-related diseases including reflux esophagitis. This drug is thought to be transformed into two active species which inhibit acid secretion by (H+, K+)-ATPase within the parietal cell canaliculi. However, acid secretion was not directly involved in the pathogenesis of I/R-induced intestinal injury model we used. In the present study, lansoprazole was found to prevent lipid peroxidation and to reduce the development of intestinal mucosal inflammation via inhibition of the production of inflammatory cytokines such as CINC-1. These results suggest that lansoprazole may protect against I/R injury via an anti-inflammatory effect but not inhibition of acid secretion.

It was previously reported that CINC levels were increased during small intestinal I/R injury, and that CINC-1 was related with the extent of mucosal damage[35]. It was reported that CINC could be produced by many types of cells, including macrophages, monocytes, and endothelial cells[36]. In the present study, lansoprazole inhibited both CINC-1 protein and mRNA in the small intestine after I/R injury. These results suggest that lansoplazole may prevent CINC-1 production by scavenging active oxygen species that are related to signal transduction for the promotion of CINC-1 synthesis. Further study needs to be done to determine the molecular mechanisms involved in the inhibition of CINC-1 production by lansoprazole.

In conclusion, lansoprazole protects against acid-unrelated intestinal injury induced by I/R via inhibition of neutrophil-dependent inflammation. We suggest that lansoprazole has potential as a new therapeutic agent for reperfusion injury.

REFERENCES

1 **Walder CE**, Green SP, Darbonne WC, Mathias J, Rae J, Dinauer MC, Curnutte JT, Thomas GR. Ischemic stroke injury is reduced in mice lacking a functional NADPH oxidase. *Stroke* 1997; **28**: 2252-2258

2 **Panes J**, Granger DN. Leukocyte-endothelial cell interactions: molecular mechanisms and implications in gastrointestinal disease. *Gastroenterology* 1998; **114**: 1066-1090

3 **Jolly SR**, Kane WJ, Baile MB, Abrams GD, Lucchesi BR. Canine myocardial reperfusion injury. Its reduction by the combined administration of superoxide dismutase and catalase. *Circ Res* 1984; **54**: 277-285

4 **Cappell MS**. Intestinal (mesenteric) vasculopathy. I. Acute

superior mesenteric arteriopathy and venopathy. *Gastroenterol Clin North Am* 1998; **27**: 783-825
5 **Homer-Vanniasinkam S**, Crinnion JN, Gough MJ. Post-ischaemic organ dysfunction: a review. *Eur J Vasc Endovasc Surg* 1997; **14**: 195-203
6 **Schoenberg M**, Muhl E, Sellin D, Younes M, Schildberg F, Haglund U. Posthypotensive generation of superoxide free radicals: possible role in the pathogenesis of the intestinal mucosal damage. *Acta Chir Scand* 1984; **150**: 301-309
7 **Granger DN**, Hollwarth ME, Parks DA. Ischemia-reperfusion injury; role of oxygen-derived free radicals. *Acta Physiol Scand suppl* 1986; **548**: 47-53
8 **Haglund U**, Bulkley GB, Granger DN. On the pathophysiology of intestinal ischemic injury. Clinical review. *Acta Chir Scand* 1987; **153**: 321-324
9 **Hernandez LA**, Grisham MB, Twohig B, Arfors KE, Harlan JM, Granger DN. Role of neutrophils in ischemic-reperfusion-induced microvascular injury. *Am J Physiol* 1987; **253**: H699-H703
10 **Sisley AC**, Desai T, Harig JM, Gewertz BL. Neutrophil depletion attenuates human intestinal reperfusion injury. *J Surg Res* 1994; **57**: 192-196
11 **Kurose I**, Anderson DC, Miyasaka M, Tamatani T, Paulson JC, Todd RF, Rusche JR, Granger DN. Molecular determinants of reperfusion-induced leukocyte adhesion and vascular protein leakage. *Circ Res* 1994; **74**: 336-343
12 **Horn J**. The proton-pump inhibitors: similarities and differences. *Clin Ther* 2000; **22**: 266-280
13 **Langtry HD**, Wilde MI. Omeprazole. A review of its use in *Helicobacter pylori* infection, gastro-oesophageal reflux disease and peptic ulcers induced by nonsteroidal anti-inflammatory drugs. *Drugs* 1998; **56**: 447-486
14 **Garnett WR**. Lansoprazole: a proton pump inhibitor. *Ann Pharmacother* 1996; **30**: 1425-1436
15 **Zimmermann AE**, Katona BG. Lansoprazole: a comprehensive review. *Pharmacotherapy* 1997; **17**: 308-326
16 **Wolfe MM**, Sachs G. Acid suppression: optimizing therapy for gastroduodenal ulcer healing, gastroesophageal reflux disease, and stress-related erosive syndrome. *Gastroenterology* 2000; **118**: S9-31
17 **Fellenius E**, Berglindh T, Sachs G, Olbe L, Elander B, Sjostrand SE, Wallmark B. Substituted benzimidazoles inhibit gastric acid secretion by blocking (H+ + K+)ATPase. *Nature* 1981; **290**: 159-161
18 **Wandall JH**. Effects of omeprazole on neutrophil chemotaxis, super oxide production, degranulation, and translocation of cytochrome b-245. *Gut* 1992; **33**: 617-621
19 **Yoshida N**, Yoshikawa T, Tanaka Y, Fujita N, Kassai K, Naito Y, Kondo M. A new mechanism for anti-inflammatory actions of proton pump inhibitors-inhibitory effects on neutrophil-endothelial cell interactions. *Aliment Pharmacol Ther* 2000; **14**: 74-81
20 **Ohkawa H**, Ohnishi N, Yagi K. Assay for lipid peroxides for animal tissues by thiobarbituric acid reaction. *Anal Biochem* 1979; **95**: 351-358
21 **Grisham MB**, Hernandez LA, Granger DN. Xanthine oxidase and neutrophil infiltration in intestinal ischemia. *Am J Physiol* 1986; **251**: G567-G574
22 **McCord JM**. Oxygen-derived free radicals in post ischemic tissue injury. *N Engl J Med* 1985; **312**: 159-163
23 **Fantone JC**, Ward PA. Role of oxygen derived free radicals and metabolites in leukocyte dependent inflammatory reactions. *Am J Pathol* 1982; **107**: 395-418
24 **Chance B**, Sies H, Boveris A. Hydroperoxide metabolism in mammalian tissues. *Physiol Rev* 1979; **59**: 527-605
25 **Yoshikawa T**, Naito Y, Ueda S, Ichikawa H, Takahashi S, Yasuda M, Kondo M. Ischemia-reperfusion injury and free radical involvement in gastric mucosal disorders. *Adv Exp Med Biol* 1992; **316**: 231-238
26 **Yoshikawa T**, Ueda S, Naito Y, Takahashi S, Oyamada H, Morita Y, Yoneta T, Kondo M. Role of oxygen-derived free radicals in gastric mucosal injury induced by ischemia or ischemia-reperfusion in rats. *Free Rad Res Comms* 1989; **7**: 285-291
27 **Granger DN**. Role of xanthine oxidase and granulocytes in ischemia-reperfusion injury. *Am J Physiol* 1988; **255**: H1269-H1275
28 **Yoshida N**, Granger DN, Anderson DC, Rothlein R, Lane C, Kvietys PR. Anoxia/reoxygenation-induced neutrophil adherence to cultured endothelial cells. *Am J Physiol* 1992; **262**: H1891-H1898
29 **Suzuki M**, Mori M, Fukumura D, Suzuki H, Miura S, Ishii H. Omeprazole attenuates neutrophil-endothelial cell adhesive interaction induced by extracts of *Helicobacter pylori*. *J Gastroenterol Hepatol* 1999; **14**: 27-31
30 **Ohara T**, Arakawa T. Lansoprazole decreases peripheral blood monocytes and intercellular adhesion molecule-1-positive mononuclear cells. *Dig Dis Sci* 1999; **44**: 1710-1715
31 **Suzuki M**, Mori M, Miura S, Suematsu M, Fukumura D, Kimura H, Ishii H. Omeprazole attenuates oxygen-derived free radical production from human neutrophils. *Free Radic Biol Med* 1996; **21**: 727-731
32 **Biswas K**, Bandyopadhyay U, Chattopadhyay I, Varadaraj A, Ali E, Banerjee RK. A novel antioxidant and antiapoptotic role of omeprazole to block gastric ulcer through scavenging of hydroxyl radical. *J Biol Chem* 2003; **278**: 10993-11001
33 **Zedtwitz-Liebenstein K**, Wenisch C, Patruta S, Parschalk B, Daxbock F, Graninger W. Omeprazole treatment diminishes intra- and extracellular neutrophil reactive oxygen production and bactericidal activity. *Crit Care Med* 2002; **30**: 1118-1122
34 **Noble DW**. Proton pump inhibitors and stress ulcer prophylaxis: pause for thought? *Crit Care Med* 2002; **30**: 1175-1176
35 **Tsuruma T**, Yagihashi A, Tarumi K, Hirata K. Anti-rat IL-8 (CINC) monoclonal antibody administration reduces ischemia-reperfusion injury in small intestine. *Transplant Proc* 1998; **30**: 2644-2645
36 **Yagihashi A**, Tsuruma T, Tarumi K, Kameshima T, Yajima T, Yanai Y, Watanabe N, Hirata K. Prevention of small intestinal ischemia-reperfusion injury in rat by anti-cytokine-induced neutrophil chemoattractant monoclonal antibody. *J Surg Res* 1998; **78**: 92-96

Edited by Chen WW and Wang XL **Proofread by** Xu FM

PO Box 2345, Beijing 100023, China
Fax: +86-10-85381893
E-mail: wjg@wjgnet.com www.wjgnet.com

World J Gastroenterol 2004;10(19):2818-2822
World Journal of Gastroenterology
Copyright © 2004 by The WJG Press ISSN 1007-9327

• BASIC RESEARCH •

Hepatic differentiation capability of rat bone marrow-derived mesenchymal stem cells and hematopoietic stem cells

Sai-Nan Shu, Lai Wei, Jiang-Hua Wang, Yu-Tao Zhan, Hong-Song Chen, Yu Wang

Sai-Nan Shu, Lai Wei, Jiang-Hua Wang, Hong-Song Chen, Yu Wang, Institute of Hepatology, People's Hospital, Peking University, Beijing 100044, China
Yu-Tao Zhan, Gastroenterology Department, Tong-Ren Hospital, Capital Medical University, Beijing 100730, China
Supported by the National High Technology Research and Development Program of China (863 Program), No. 2001AA216031
Correspondence to: Dr. Lai Wei, Institute of Hepatology, People's Hospital, Peking University, 11 Xizhimen South Street, Beijing 100044, China. w1114@hotmail.com
Telephone: +86-10-68314422 Ext.5730 **Fax:** +86-10-68318386
Received: 2003-12-23 **Accepted:** 2004-01-12

Abstract

AIM: To investigate the different effects of mesenchymal stem cells (MSCs) and hematopoietic stem cells (HSCs) on hepatic differentiation.

METHODS: MSCs from rat bone marrow were isolated and cultured by standard methods. HSCs from rat bone marrow were isolated and purified by magnetic activated cell sorting. Both cell subsets were induced. Morphology, RT-PCR and immunocytochemistry were used to identify the hepatic differentiation grade.

RESULTS: MSCs exhibited round in shape after differentiation, instead of fibroblast-like morphology before differentiation. Albumin mRNA and protein were expressed positively in MSCs, without detection of alpha-fetoprotein (AFP). HSCs were polygonal in shape after differentiation. The expression of albumin signal decreased and AFP signal increased. The expression of CK18 was continuous in MSCs and HSCs both before and after induction.

CONCLUSION: Both MSCs and HSCs have hepatic differentiation capabilities. However, their capabilities are not the same. MSCs can differentiate into mature hepatocyte-like cells, never expressing early hepatic specific genes, while Thy-1.1$^+$ cells are inclined to differentiate into hepatic stem cell-like cells, with an increasing AFP expression and a decreasing albumin signal. CK18 mRNA is positive in Thy-1.1$^+$ cells and MSCs, negative in Thy-1.1$^-$ cells. It seems that CK18 has some relationship with Thy-1.1 antigen, and CK18 may be a predictive marker of hepatic differentiation capability.

Shu SN, Wei L, Wang JH, Zhan YT, Chen HS, Wang Y. Hepatic differentiation capability of rat bone marrow-derived mesenchymal stem cells and hematopoietic stem cells. *World J Gastroenterol* 2004; 10(19): 2818-2822
http://www.wjgnet.com/1007-9327/10/2818.asp

INTRODUCTION

In recent years, liver related stem cells have become a hot spot of research. One of the important findings is that liver stem cells might be derived from bone marrow. Petersen *et al*.[1] first identified this phenomenon in rat model of liver injury. Later many researchers have reported similar *in vivo* and *in vitro* findings[2-8]. Bone marrow cells have been hypothesized as the third recruitment source in liver regeneration besides hepatocytes and endogenous liver stem cells[9].

Among bone marrow cells, there are two subsets, hematopoietic stem cells (HSCs) and mesenchymal stem cells (MSCs). Hepatic oval cells[10], well known endogenous liver stem cells, can express CD34[11], c-kit[12, 13], Thy-1[14] and flt-3 receptor mRNA[15], all of which are markers of HSCs. So HSCs are regarded as the exact source of hepatocytes. However, some studies have found that non-hematopoietic subsets (CD45$^-$ subsets) also play such a role[7]. In this paper, we isolated two subsets of stem cells from rat bone marrow. One was MSCs, isolated and cultured by standard methods, the other was Thy-1.1$^+$ cells, isolated and purified by magnetic activated cell sorting (MACS), which were recognized as HSCs of rats. We imitated the circumstances of liver development to define the different capacities of hepatic differentiation of the two subsets *in vitro*.

MATERIALS AND METHODS

Animals

Male Sprague-Dawley (SD) rats at 6-7 wk of age were obtained from Charles River China. All animal experiments were performed in accordance with the animal guidelines of Peking University Health Science Center.

Isolation and culture of MSCs from rat bone marrow

Rat bone marrow was harvested from rat femurs and tibias, and collected into Dulbecco's modified Eagle's medium (DMEM), filtered (40 μm), and centrifuged at 300 r/min to pellet cells. After rinsed in PBS, bone marrow cells were loaded onto 5 mL 57% Percoll (1.073 g/mL in 0.01 mol/L PBS) and centrifuged at 400 r/min for 30 min. Mononuclear cells were collected at the Percoll interface, rinsed twice in PBS, and seeded at 2×10^5/cm^2 in 600 g/L low glucose DMEM (DMEM-LG, Sigma-Aldrich), 400 g/L MCDB-201 (Sigma-Aldrich), with 100 mL/L fetal bovine serum (FBS; Hyclone, USA) and 1 000 U/mL rat leukemia inhibitory factor (rLIF; Chemicon, USA). Non-adherent cells were removed after 24 h and culture media were replaced every 3 d. After about 7 d, isolated colonies of MSCs were apparent. Then the cells were trypsinized and replated at 8 000/cm^2, and the cells from passage 3 were used for differentiation protocol.

Differentiation protocols

MSCs from passage 3 were seeded at 2×10^4/cm^2 on 10 ng/mL fibronectin (FN, Sigma-Aldrich, USA) in culture medium as above. After 12 h, media were removed and cells were cultured in 600 g/L DMEM-LG, 400 g/L MCDB-201 supplemented with 50 mL/L FBS, 10^{-6} mol/L dexamethasone (Dex, Sigma-Aldrich, USA), 10 ng/mL epithelial growth factor (EGF, R&D, USA), 1×insulin/transferrin/selenium (ITS, Sigma-Aldrich, USA). In some experiments, inducing growth factors were added into culture medium (20 ng/mL acid fibroblast growth factors, aFGF; 10 ng/mL basic fibroblast growth factors, bFGF; and 20 ng/mL hepatocyte growth factor, HGF). aFGF, bFGF, and HGF were all from R&D System Inc, USA.

Isolation, culture and differentiation of Thy-1.1$^+$ stem cells from rat marrow

After Percoll gradient centrifugation, bone marrow mononuclear cells were collected, then incubated with mouse anti-rat Thy-1.1 monoclonal antibody (Serotech, UK) at 4 ℃ for 30 min. Unbound antibodies were removed by washing twice. Secondary marking was done by incubation with rat-anti-mouse IgG bound magnetic microbeads (MiltenyiBiotec, Germany). The positive cells were absorbed in magnetic field by Mini-MACS columns (MiltenyiBiotec, Germany). The column was removed from the magnetic field and the Thy-1.1$^+$ cells were washed out.

Thy-1.1$^+$ cells were cultured in differentiation media, 600 g/L DMEM-LG, 400 g/L MCDB-201 supplemented with 150 mL/L FBS, 10^{-6} mol/L Dex, 10 ng/mL EGF, 1×ITS, 20 ng/mL aFGF, 10 ng/mL bFGF, and 20 ng/mL HGF. After about 7-10 d, apparent colonies of Thy-1.1$^+$ cells appeared.

Flow cytometry determination of cell-surface antigen

The cells were resuspended in washing buffer (10 mL/L bovine serum, 2 g/L sodium azide in PBS), and stained on ice according to the manufacturer's recommendations with the monoclonal antibodies as follows: R-PE conjugated mouse anti-rat-Thy1.1 (Pharmingen, USA), FITC conjugated mouse anti-rat-CD45 (HarlanSera-Lab, UK), PE conjugated mouse anti-rat-CD34 (Santa Cruz, USA). After washed three times with washing buffer, the stained cells were resuspended in 300 μL fixation buffer (20 g/L formaldehyde in PBS) and run on a flow cytometer (FACS Calibur, BectonDi-ckinson, USA). The results were analyzed by CellQuest software (BD, USA).

Reverse transcription-polymerase chain reaction (RT-PCR)

Total RNA was extracted by using TRIzol (Invitrogen, USA) according to the manufacturer's instructions and quantified by UV spectroscopy. To prepare RNA for PCR analysis, 2 μg total RNA was converted to the cDNA using SuperScript II reverse transcriptase (Invitrogen, USA) with oligo (dT) (Promega, USA) and random hexamer primers (Promega, USA). PCR was performed by using *Taq* DNA polymerase (Gibco BRL, USA). For each gene, the DNA primers were originated from different exons to ensure that the PCR products represented the specific mRNA species and not genomic DNA. All PCR experiments were performed using a GeneAmp PCR system 2 400 (Perkin-Elmer, USA).

The following specific oligonucleotide primers were used: albumin (5'-AAGGCACCCCGATTACTCCG-3' (sense), 5'-TGCGAAGTCACCCATCACCG-3' (antisense)), AFP (5' -AGGCTGTACTCATCATTAAACT-3' (sense), 5'-ATATTGTCC TGGCATTTCG-3' (antisense)), CK18 (5'-GGACCTCAGCAAG ATCATGGC-3' (sense), 5'-CCACGATCTTACGGGTAGTTG-3' (antisense)), β-actin (5'-AGAGGGAAATCGTGCGTGAC-3' (sense), 5'-AGGAGCCAGGGCAGTAATC-3' (anti-sense)).

Amplification reactions were carried out for 35 cycles (25 cycles for β-actin) at 94 ℃ for 1 min, 58 ℃ for 1 min, and at 72 ℃ for 1 min for albumin; at 94 ℃ for 45 s, at 51 ℃ for 45 s and at 72 ℃ for 45 s for AFP; at 94 ℃ for 1 min, at 60 ℃ for 1 min and at 72 ℃ for 1 min for CK18 and at 94 ℃ for 30 s, at 55 ℃ for 45 s, and at 72 ℃ for 45 s for β-actin. The reaction products were subjected to 12 g/L agarose gel electrophoresis and visualized by ethidium bromide staining. The reaction products were 649 bp (albumin), 484 bp (AFP), 515 bp (CK18), and 353 bp (β-actin), respectively. Housekeeping gene β-actin was used as an internal control. Adult liver tissue or newborn rat liver tissue was used as a positive control.

Immunocytochemistry

Cell cultures were washed with PBS twice and fixed with 95% alcohol/acetic acid (99:1) for 10 min at room temperature, then permeabilized with 2 g/L Triton X-100 for 10 min. After washed, cells were incubated overnight at 4 ℃ with primary antibodies, including mouse anti-human CK18 (Sigma, USA), mouse anti-human albumin (Dako, Denmark) and goat anti-human AFP (SantaCruz, USA). Subsequently, the cells were washed with PBS three times and incubated with fluorescence labeled second antibody, FITC labeled goat anti-mouse IgG1 and rhodamine labeled donkey anti-goat IgG at 37 ℃ for 1 h. After washed with PBS, cells were mounted with glycerol-PBS (9:1). The cells were visualized and photomicrographed by a fluorescence microscope (Olympus Provis AX80, Japan).

RESULTS

Cell yield and shape of MSC and Thy-1.1$^+$ cells before and after differentiation

The number of mononuclear cells by 57% Percoll gradient centrifugation was about 6.44×10^7 per rat. After MACS

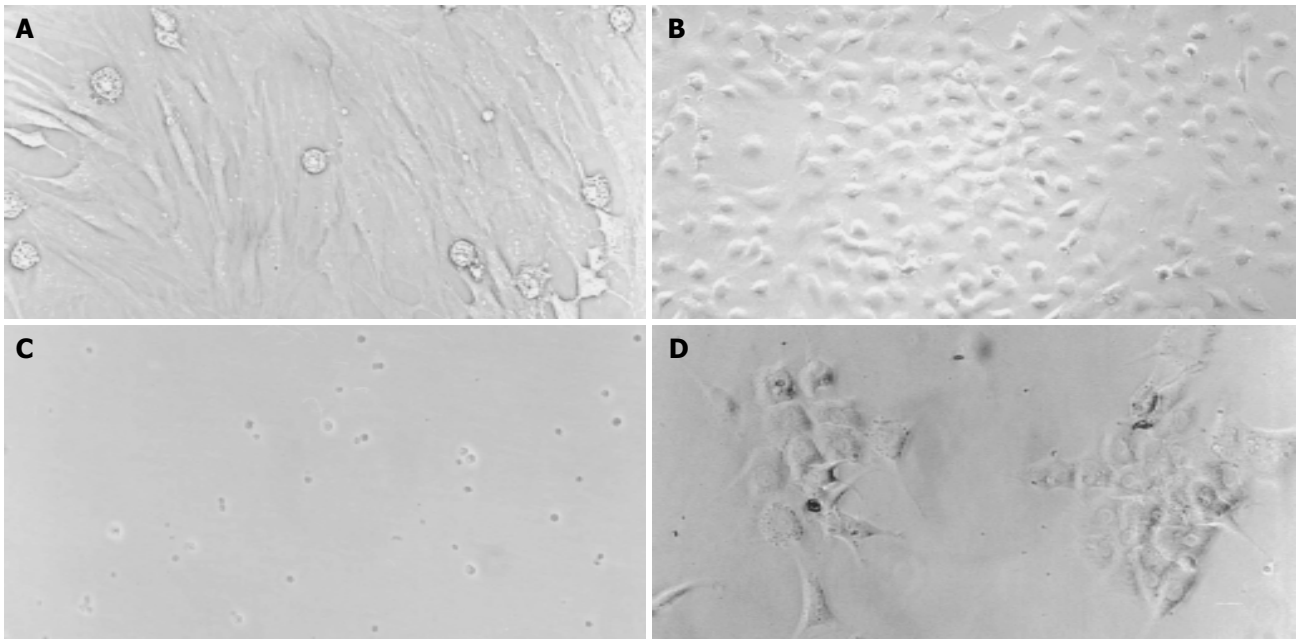

Figure 1 A-D Cell morphology before and after differentiation (Original magnification, 200×). A: Fibroblast-like MSC before differentiation, B: Round MSC after differentiation, C: Freshly isolated Thy1.1$^+$ cells, D: Thy1.1$^+$ cells 10 d after differentiation.

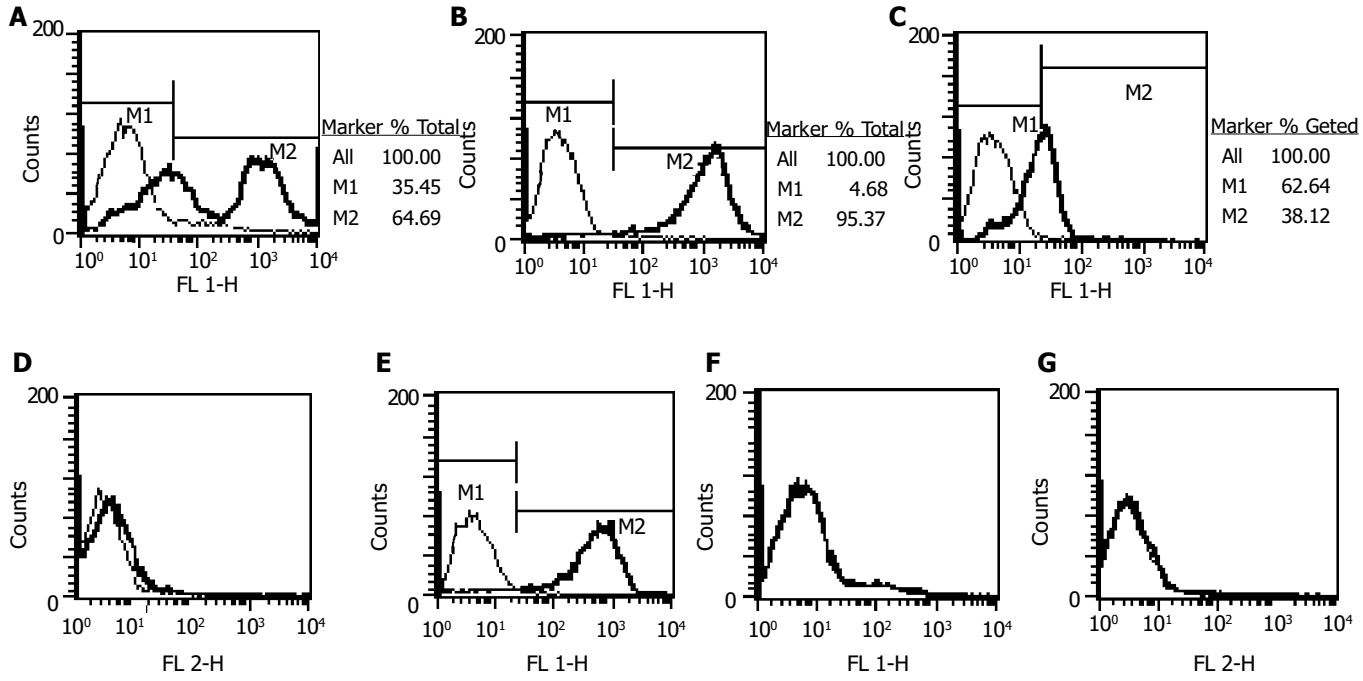

Figure 2 Phenotype analysis of MSCs and Thy-1.1$^+$ cells. A: Thy-1.1 of mononuclear bone marrow cells before MACS; B, C, D: Thy-1.1, CD45, CD34 after MACS purification; E, F, G: Thy-1.1, CD45, CD34 of MSCs.

purification, the number of Thy1.1$^+$ cells was about 2.36×10^7. The recovery rate of Thy1.1$^+$ cells from mononuclear bone marrow cells was 64.65%. Before differentiation, MSCs exhibited a fibroblastic morphology with spindle cell bodies (Figure 1A), while after differentiation, the cells contracted obviously and were inclined to be round in shape (Figure 1B). This change occurred early on d 4 after MSC differentiation protocol. Thy1.1$^+$ cells were small and round in shape when freshly isolated (Figure 1C), and became typical polygonal, much bigger in size after cultured in differentiation media (Figure 1D).

Quantitative analysis of cell-surface antigen expression

The percentage of Thy-1.1$^+$ of rat bone marrow mononuclear cells was 56.65%. After MACS, this percentage was 93.45% in positive subset (Figure 2A, B). Thy-1.1$^+$ subset was CD34$^-$, and partial CD45$^+$ (Figure 2C, D). The percentage of CD45 positivity in Thy-1.1$^+$ subset was 36.68%. As displayed in Figure 2E-2G, MSC was Thy-1.1$^+$, CD45$^-$, CD34$^-$.

RT-PCR analysis of hepatic gene expression of CK18, albumin, and AFP

We analyzed hepatic gene expression of the cells before and after differentiation protocol. Adult rat liver or newborn rat liver tissue

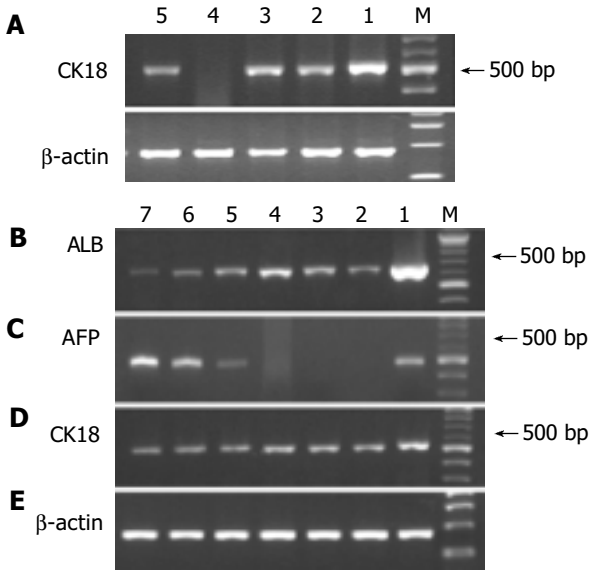

Figure 3 RT-PCR analysis of hepatic gene expression before and after differentiation. A: Analysis of CK18 mRNA before differentiation, lane 1: Adult liver, lane 2: Mononuclear BM cells.

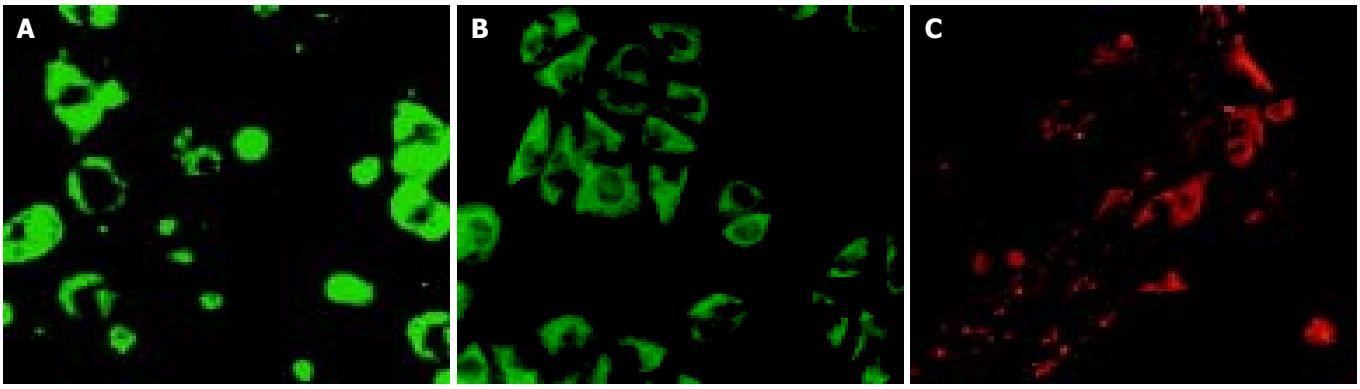

Figure 4 Immunocytofluorescence. A: MSCs-albumin, B: Thy1.1$^+$ cells-CK18, C: Thy1.1$^+$ cells-AFP.

was used as positive control. Before differentiation, Thy-1.1$^+$ cells showed a CK18 signal, so did MSCs. However, Thy-1.1$^-$ cells did not express CK18 (Figure 3A). After differentiation, Thy-1.1$^+$ cells were AFP mRNA positive and had decreased signals of albumin, while MSCs expressed albumin only and the signals of albumin increased with the extension of differentiation time (Figure 3B, C). Both cells had a continuous CK18 expression during the process of induction (Figure 3D).

Immunocytochemical analysis

MSCs showed positive staining for albumin (Figure 4A), and Thy1.1+ cells showed CK18 and AFP positive staining (Figure 4B, C).

DISCUSSION

As stromal cells of bone marrow, MSCs could differentiate into cells of all mesodermal origin, including adipocytes, osteocytes, chondrocytes and myocytes[16-19], *etc*. Besides these, MSCs are also capable of "transdifferentiation" into ectodermal cells, such as neural cells[20,21]. So MSCs are multipotential adult stem cells. Regarding hepatic differentiation of MSCs, there has been no specific report yet. Schwartz *et al*.[7] isolated a non-hematopoietic stem cell subset (CD45$^-$GlyA$^-$ in humans or CD45$^-$Ter119$^-$ in mice) from bone marrow, termed multipotent adult progenitor cells (MAPCs). MAPCs should be ascribed to MSCs, since they were copurified with MSCs at the same time[22]. Under serial conditions, Schwartz *et al*.[7] induced MAPCs into cells with morphological, phenotypic, and functional characteristics of hepatocytes *in vitro*. In our study, we tried to induce standard MSCs into hepatocytes, and found hepatic specific gene CK18 was already expressed by MSCs without differentiation protocol. After induction, MSCs also expressed albumin besides CK18. Albumin mRNA appeared early on d 4 after differentiation (data not shown), coinciding with the change of morphology. Albumin signals had a gradual increase with the extension of differentiation time. Immunocytochemical staining confirmed the results of the PCR analysis at protein-level. There were no early markers of hepatocytes before or during differentiation protocol. Morphologic change of MSCs was apparent. Cell shape changed from spindle and fibroblast-like to round and epithelia-like.

HSCs are another subset of stem cells from bone marrow. A large number of papers demonstrated that HSCs could differentiate into hepatocytes or hepatocyte-like cells. Among the papers, CD34, the most general marker of HSCs in humans and mice, was used. Theise *et al*.[2] reported 200 CD34$^+$ marrow cells produced the same degree of hepatic engraftment as 20 000 unfractionated bone marrow cells in gender mismatch bone marrow transplantation model of mice. Human investigations with G-CSF mobilized CD34$^+$ stem cells have shown that these cells were also able to transdifferentiate into hepatocytes[23]. Thy1.1 antigen has been a well-accepted marker of rat HSCs since 1978[24]. Recently, Avital *et al*.[25] identified a population of bone marrow-derived hepatocyte stem cells in rats, which were beta 2 microglobulin-negative and Thy-1-positive (β_2m$^-$/Thy-1$^+$). Moreover, according to Petersen *et al*.[26], Thy-1 is a new marker for identification of hepatic oval cells. Using Thy-1 would facilitate both *in vivo* and *in vitro* studies of hepatic oval cells. There was no colony-formation in Thy-1.1$^-$ bone marrow cells in our studies (data not shown). Thy-1.1$^-$ cells did not express CK18 mRNA when freshly isolated, while Thy-1.1$^+$ cells had a strong CK18 expression. During hepatic differentiation, Thy-1.1$^+$ cells expressed AFP mRNA and had a weak albumin signal. Expression of CK18 of Thy-1.1$^+$ cells continued. The cells were polygonal in shape, exhibiting epithelial morphology.

HSCs and MSCs are two separate stem cell subsets of bone marrow. They have different functions in hematopoiesis. Previous studies have explored the ability of hepatic differentiation of different subsets from bone marrow. However, what relationship they have or what similarity or difference exists among the two subsets is unknown. Our study combined two subsets for the first time, and investigated their different abilities of hepatic differentiation simultaneously. Our results indicated that both of them had hepatic differentiation ability, however, they were different. MSCs could differentiate into mature hepatocyte-like cells, not expressing early hepatic specific genes. Under a similar induction condition, Thy-1.1$^+$ cells were inclined to become hepatic stem cell-like cells, with a continuous AFP expression and weak albumin signal. To our interest, CK18 mRNA was positive in Thy-1.1$^+$ cells and MSCs, negative in Thy-1.1$^-$ cells. It seemed that CK18 had some relationship with Thy-1.1 antigen, and it would be an indicative marker of hepatic differentiation ability.

Hepatic stem cells, especially bone marrow-derived hepatic stem cells may be therapeutically useful for treating a variety of diseases that affect the liver. This has been proved in some animal models[3,27]. Compared with other liver-related stem cells, such as embryonic stem cells[28], pancreatic stem cells[29], and neural stem cells[30], bone marrow-derived stem cells provide several advantages: (1) Bone marrow can be obtained from living donors or recipients themselves using a moderately invasive procedure. There is no problem of limited donors, which restrict liver transplantation and hepatocyte transplantation greatly. (2) Based on its ability of high self-renewal, the amplification of bone marrow stem cells could be obtained. (3) Utilizing patients' own bone marrow or repopulation of both bone marrow and hepatic system from the same donor could avoid or reduce immunological rejection, which usually affects recipients for a life-long time.

REFERENCES

1 **Petersen BE**, Bowen WC, Patrene KD, Mars WM, Sullivan AK, Murase N, Boggs SS, Greenberger JS, Goff JP. Bone marrow as a potential source of hepatic oval cells. *Science* 1999; **284**: 1168-1170

2 **Theise ND,** Badve S, Saxena R, Henegariu O, Sell S, Crawford JM, Krause DS. Derivation of hepatocytes from bone marrow cells in mice after radiation-induced myeloablation. *Hepatology* 2000; **31**: 235-240

3 **Lagasse E**, Connors H, Al-Dhalimy M, Reitsma M, Dohse M, Osborne L, Wang X, Finegold M, Weissman IL, Grompe M. Purified hematopoietic stem cells can differentiate into hepatocytes *in vivo*. *Nat Med* 2000; **6**: 1229-1234

4 **Alison MR**, Poulsom R, Jeffery R, Dhillon AP, Quaglia A, Jacob J, Novelli M, Prentice G, Williamson J, Wright NA. Hepatocytes from non-hepatic adult stem cells. *Nature* 2000; **406**: 257

5 **Theise ND**, Nimmakayalu M, Gardner R, Illei PB, Morgan G, Teperman L, Henegariu O, Krause DS. Liver from bone marrow in humans. *Hepatology* 2000; **32**: 11-16

6 **Oh SH**, Miyazaki M, Kouchi H, Inoue Y, Sakaguchi M, Tsuji T, Shima N, Higashio K, Namba M. Hepatocyte growth factor induces differentiation of adult rat bone marrow cells into a hepatocyte lineage *in vitro*. *Biochem Biophys Res Commun* 2000; **279**: 500-504

7 **Schwartz RE**, Reyes M, Koodie L, Jiang Y, Blackstad M, Lund T, Lenvik T, Johnson S, Hu WS, Verfaillie CM. Multipotent adult progenitor cells from bone marrow differentiate into functional hepatocyte-like cells. *J Clin Invest* 2002; **109**: 1291-1302

8 **Fiegel HC**, Lioznov MV, Cortes-Dericks L, Lange C, Kluth D, Fehse B, Zander AR. Liver-specific gene expression in cultured human hematopoietic stem cells. *Stem Cells* 2003; **21**: 98-104

9 **Zhang Y,** Bai XF, Huang CX. Hepatic stem cells: existence and origin. *World J Gastroenterol* 2003; **9**: 201-204

10 **Theise ND**, Saxena R, Portmann BC, Thung SN, Yee H, Chiriboga L, Kumar A, Crawford JM. The canals of Hering and hepatic stem cells in humans. *Hepatology* 1999; **30**: 1425-1433

11 **Petersen BE**, Goff JP, Greenberger JS, Michalopoulos GK. Hepatic oval cells express the hematopoietic stem cell marker Thy-1 in the rat. *Hepatology* 1998; **27**: 433-435

12 **Baumann U**, Crosby HA, Ramani P, Kelly DA, Strain AJ. Expression of the stem cell factor receptor c-kit in normal and diseased pediatric liver: identification of a human hepatic progenitor cell? *Hepatology* 1999; **30**: 112-117
13 **Ma X,** Qiu DK, Peng YS. Immunohistochemical study of hepatic oval cells in human chronic viral hepatitis. *World J Gastroenterol* 2001; **7**: 238-242
14 **Omori N**, Omori M, Evarts RP, Teramoto T, Miller MJ, Hoang TN, Thorgeirsson SS. Partial cloning of rat CD34 cDNA and expression during stem cell-dependent liver regeneration in the adult rat. *Hepatology* 1997; **26**: 720-727
15 **Omori M**, Omori N, Evarts RP, Teramoto T, Thorgeirsson SS. Coexpression of flt-3 ligand/flt-3 and SCF/c-kit signal transduction system in bile-duct-ligated SI and W mice. *Am J Pathol* 1997; **150**: 1179-1187
16 **Pittenger MF**, Mackay AM, Beck SC, Jaiswal RK, Douglas R, Mosca JD, Moorman MA, Simonetti DW, Craig S, Marshak DR. Multilineage potential of adult human mesenchymal stem cells. *Science* 1999; **284**: 143-147
17 **Gerson SL**. Mesenchymal stem cells: no longer second class marrow citizens. *Nat Med* 1999; **5**: 262-264
18 **Jaiswal N**, Haynesworth SE, Caplan AI, Bruder SP. Osteogenic differentiation of purified, culture-expanded human mesenchymal stem cells *in vitro*. *J Cell Biochem* 1997; **64**: 295-312
19 **Wakitani S**, Saito T, Caplan AI. Myogenic cells derived from rat bone marrow mesenchymal stem cells exposed to 5-azacytidine. *Muscle Nerve* 1995; **18**: 1417-1426
20 **Woodbury D**, Schwarz EJ, Prockop DJ, Black IB. Adult rat and human bone marrow stromal cells differentiate into neurons. *J Neurosci Res* 2000; **61**: 364-370
21 **Sanchez-Ramos J**, Song S, Cardozo-Pelaez F, Hazzi C, Stedeford T, Willing A, Freeman TB, Saporta S, Janssen W, Patel N, Cooper DR, Sanberg PR. Adult bone marrow stromal cells differentiate into neural cells *in vitro*. *Exp Neurol* 2000; **164**: 247-256
22 **Reyes M**, Lund T, Lenvik T, Aguiar D, Koodie L, Verfaillie CM. Purification and ex vivo expansion of postnatal human marrow mesodermal progenitor cells. *Blood* 2001; **98**: 2615–2625
23 **Korbling M**, Katz RL, Khanna A, Ruifrok AC, Rondon G, Albitar M, Champlin RE, Estrov Z. Hepatocytes and epithelial cells of donor origin in recipients of peripheral-blood stem cells. *N Engl J Med* 2002; **346**: 738-746
24 **Goldschneider I**, Gordon LK, Morris RJ. Demonstration of Thy-1 antigen on pluripotent hemopoietic stem cells in the rat. *J Exp Med* 1978; **148**: 1351-1366
25 **Avital I**, Inderbitzin D, Aoki T, Tyan DB, Cohen AH, Ferraresso C, Rozga J, Arnaout WS, Demetriou AA. Isolation, characterization, and transplantation of bone marrow-derived hepatocyte stem cells. *Biochem Biophys Res Commun* 2001; **288**: 156-164
26 **Petersen BE**, Goff JP, Greenberger JS, Michalopoulos GK. Hepatic oval cells express the hematopoietic stem cell marker Thy-1 in the rat. *Hepatology* 1998; **27**: 433-445
27 **Zhan YT**, Wei L, Chen HS, Cong X, Fei R, Wang Y. Differentiation of bone marrow stem cells in rat hepatic fibrogenesis environment. *Zhonghua Ganzangbing Zazhi* 2003; **11**: 673-675
28 **Hamazaki T**, Iiboshi Y, Oka M, Papst PJ, Meacham AM, Zon LI, Terada N. Hepatic maturation in differentiating embryonic stem cells *in vitro*. *FEBS Lett* 2001, **497**: 15-19
29 **Wang X**, Al-Dhalimy M, Lagasse E, Finegold M, Grompe M. Liver repopulation and correction of metabolic liver disease by transplanted adult mouse pancreatic cells. *Am J Pathol* 2001; **158**: 571-579
30 **Clarke DL**, Johansson CB, Wilbertz J, Veress B, Nilsson E, Karlstrom H, Lendahl U, Frisen J. Generalized potential of adult neural stem cells. *Science* 2000; **288**: 1660-1663

Edited by Chen WW and Wang XL **Proofread by** Zhu LH and Xu FM

PO Box 2345, Beijing 100023, China
Fax: +86-10-85381893
E-mail: wjg@wjgnet.com www.wjgnet.com

World J Gastroenterol 2004;10(19):2823-2826
World Journal of Gastroenterology
Copyright © 2004 by The WJG Press ISSN 1007-9327

• BASIC RESEARCH •

Effects of Zuogui Wan on neurocyte apoptosis and down-regulation of TGF-β_1 expression in nuclei of arcuate hypothalamus of monosodium glutamate -liver regeneration rats

Han-Min Li, Xiang Gao, Mu-Lan Yang, Jia-Jun Mei, Liu-Tong Zhang, Xing-Fan Qiu

Han-Min Li, Xiang Gao, Hepatopathy Institute, Affiliated Hospital of Hubei Traditional Chinese Medicine College, Wuhan 430061, Hubei Province, China
Mu-Lan Yang, Ultramicropathology Laboratory, Tongji Medicine College, Huazhong Scientific University, Wuhan 430030, Hubei Province, China
Jia-Jun Mei, Liu-Tong Zhang, Xing-Fan Qiu, Hubei Traditional Chinese Medicine College, Wuhan 430061, Hubei Province, China
Supported by National Natural Science Foundation of China, No. 30271562 and Natural Science Foundation of Huibei Province, China, No.2001ABB171
Correspondence to: Han-Min Li, Hepatopathy Institute, Affiliated Hospital of Hubei Traditional Chinese Medicine College, Wuhan 430061, Hubei Province, China
Telephone: +86-27-88929180 **Fax:** +86-27-88929180
Received: 2003-08-08 **Accepted:** 2003-10-22

Abstract

AIM: To inquire into the effects and mechanism of Zuogui Wan (Pills for Kidney Yin) on neurocyte apoptosis in nuclei of arcuate hypothalamus (ARN) of monosodium glutamate (MSG)-liver regeneration rats, and the mechanism of liver regeneration by using optic microscope, electron microscope and *in situ* end labeling technology to adjust nerve-endocrine-immunity network.

METHODS: Neurocyte apoptosis in ARN of the experiment rats was observed by using optic microscope, electron microscope and *in situ* end labeling technology. Expression of TGF-β_1 in ARN was observed by using immunohistochemistry method.

RESULTS: The expression of TGF-β_1 in rats of model group was increased with the increase of ARN neurocyte apoptosis index (AI) (t = 8.3097, 12.9884, P<0.01). As compared with the rats of model group, the expression of TGF-β_1 in rats of Zuogui Wan treatment group was decreased with the significant decrease of ARN neurocyte apoptosis (t = 4.5624, 11.1420, P<0.01).

CONCLUSION: Brain neurocyte calcium ion overexertion and TGF-β_1 protein participate in the adjustment and control of ARN neurocyte apoptosis in MSG-liver regeneration-rats. Zuogui Wan can prevent ARN neurocyte apoptosis of MSG-liver regeneration in rats by down-regulating the expression of TGF-β_1, and influence liver regeneration through adjusting nerve-endocrine-immune network.

Li HM, Gao X, Yang ML, Mei JJ, Zhang LT, Qiu XF. Effects of Zuogui Wan on neurocyte apoptosis and down-regulation of TGF-β_1 expression in nuclei of arcuate hypothalamus of monosodium glutamate -liver regeneration rats. *World J Gastroenterol* 2004; 10(19): 2823-2826
http://www.wjgnet.com/1007-9327/10/2823.asp

INTRODUCTION

MSG-liver regeneration rat model is very useful in study about the correlative mechanism of liver regeneration with high-grade nerve center, hypothalami-hypophysis-liver axial and nerve-endocrine-immune network (NEIN). Experiment results showed that the process of liver regeneration in MSG-liver regeneration rats was disproportional, liver regeneration was faster in the initial stage (the postoperative 1st d), significantly restrained in the intermediate and advanced periods, finally the degree of liver regeneration, meiosis index of liver cells (MI) and the ratio of liver mass to body mass all could not recover the normal level[1-2], but the above mentioned indexes could be significantly improved after MSG-liver regeneration rats were treated with Zuogui Wan[2-5]. Functional disorder of NEIN is probably one of the important mechanisms of serious imbalance of liver regenerative process. In order to research the effects of Zuogui Wan on neurocyte apoptosis of MSG-liver regeneration in rat hypothalamus and the mechanism to interfere with liver regeneration by adjusting nerve-endocrine-immunity network, we studied the apoptosis of neurocytes on experimental rats' nuclei of arcuate hypothalami (ARN) and the expression of apoptosis related gene TGF-β_1 with *in situ* end-labeling technique (ISEL), optic microscope, electronic microscope and immunohistochemical method.

MATERIALS AND METHODS

Materials

Wistar rats were offered by the Animal Laboratory, Academy of Medical Sciences of Hubei Province, YDZ19-008. Monosodium glutamate (MSG) was provided by Sigma Co. ISEL apoptosis test kit was from Boehringer Mannheim Co. Strept avidin-biotin complex (SABC) was used to detect the expression of TGF-β_1 by immunohistochemical method (Wuhan Boshide Limited Company).

Establishment of MSG-liver regeneration-rat model

Wistar rats were divided into two groups: Treatment group which was given monosodium glutamate dissolved in saline solution, the other group which served as control was given the vehicle only. MSG 4 mg/g.b.mb was injected on d 2, 4, 6, 8, and 10 after birth. On the 28th d, pups were weaned and caged in 8 groups (4 groups were male rats, 4 groups were female rats). The rats were maintained in an air-conditioned (temperature 24±1 ℃) animal room with controlled lighting (12 h light, 12 h dark). They were provided with commercial diet and water. From the 6 th week to the experiment end, treatment group rats were treated by gastrogavage of Zuogui Wan (Radix Rehmanniae Praeparata, Rhizoma Dioscoreae, Fructus Lycii, Fructus Corni, Semen Cuscutae, Radix Cyathulae, Colla Cornus Cervi, and Colla Plastri Testudinis) 5 g/kg[1]. In the 8 wk, partial hepatectomy was performed by excision of the median and left hepatic lobes (occupying about 68% of whole liver) according to the method of Higgins and Anderson under pentobarbital anesthesia[1]. Shamly-operated rats (MSG-rats) were anesthetized, and their

livers were exposed but not removed. All operations above were clean operations. Rats were operated and killed between 8 and 12 h a.m. to avoid the effects of diurnal variation. Rats subjected to partial hepatectomy were killed on the 1st, 3rd, 5th, 11th d after operation, and 6 were taken randomly in each group per batch (3 males and 3 females).

Neurocyte apoptosis observation

Using *in situ* end labeling (ISEL) method, the nuclei of positively apoptotic neurocytes were stained into blue purple, the starches of cells were intact. Each slice was randomly taken under five fields of vision, the positively stained area was surveyed, and the positive cell number was calculated on the unit area. Then five fields of vision were averaged to calculate the proportion of positive cells in the slice. The percentage of positive cells (apoptosis index, AI) was used to show the apoptosis degree in the tissue.

Pathology-histology observation

Hypothalamus tissue specimens were fixed in 10% formalin, embedded in paraffin, cut into 4 μm thick sections, dewaxed and evaporated with routine procedures, stained with HE, observed with optic microscope. Hypothalamus specimens were embedded and sliced for observation under electron microscope (using ultramicrotome of AO type) and transmission electron microscope (EM10C, Germany OPTON).

Immunohistochemistry

We used SABC method. The cerebral nerve cells showing brown, homogeneous or fine grains were positive. These fine grains distributed all over the cell membranes and cytoplasm, mainly in cell membranes. Five visual fields were taken randomly in each microsection, then the number of stained areas was surveyed and the number of positive cells was calculated according to the total count of cells in unit area. Finally, the number of positive cells in five visual fields was averaged, and the proportion of positive cells in the microsection was obtained. The percentage of positive cells was used to show the content of fine grains in the tissue.

Statistical analysis

The experimental data were statistically analyzed with HPIAS-1000 high acuity colored pathology image measurement system and Microsoft's Excel.

RESULTS

Effect of Zuogui Wan on MSG-liver regeneration rat hypothalamus pathology-histology alteration

Under light microscope, the neurocytes in arcuatus hypothalami (ARN) of MSG-liver regeneration rats reduced significantly and astrocytes increased significantly. Under electron microscope, neurocyte nucleus chromatin collected at the edge was stained deeply, and nuclear membrane was not regular, cytoplasm was concentrated. Neurocyte nucleus shape factor (approach 1 was regular, and >1 was not regular), circularity (approach 1 was round, and <1 was not round) and heteromorphic index (approach 3 was low for the heterotype degree, >3 was high for the heterotype degree) had significant differences ($P<0.05$). Pathological changes in Zuogui Wan treatment group were distinguished (Table 1, Figure1).

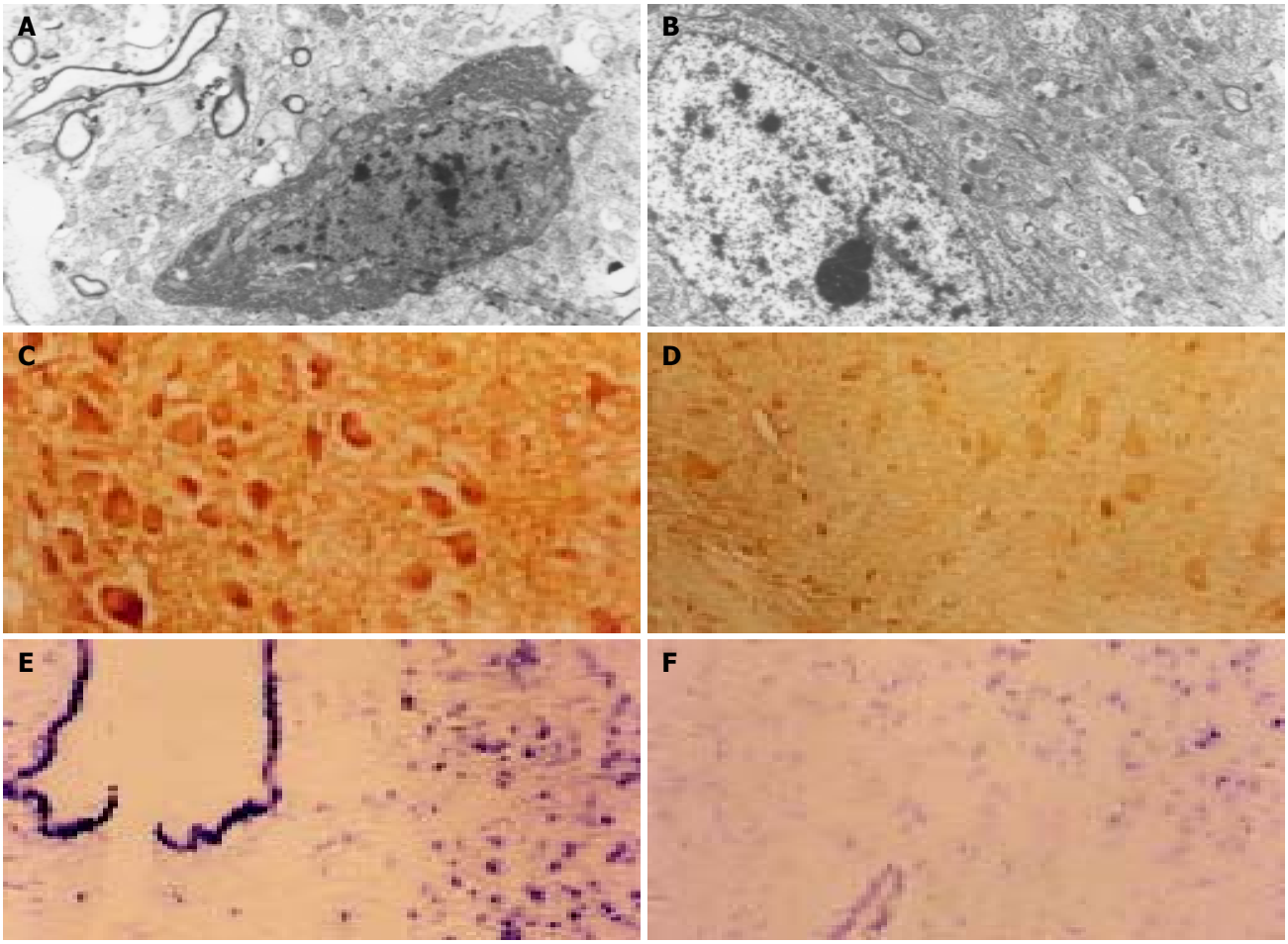

Figure 1 Effect of Zuogui Wan on alteration, apoptosis and TGF-β_1 expression in ARN of MSG-liver regeneration rats. A, B: Effect of Zuogui Wan on alteration in ARN of MSG-liver regeneration rats. C, D: Effect of Zuogui Wan on apoptosis in ARN of MSG-liver regeneration rats. E, F: Effect of Zuogui Wan on TGF-β_1 expression in ARN of MSG-liver regeneration rats.

Table 1 Effect of Zuogui Wan on alterations of ARN nuclei in MSG-liver regeneration rat on the postoperative 11th d (n = 10, mean±SD)

Group	Shape factor	Circular degree	Heteromorphic index
Normal saline	1.14±0.45	0.88±0.16	3.80±0.8
Model	3.10±1.14[b]	0.32±0.17[b]	6.24±1.83[b]
Zuogui Wan	1.68±0.33[d]	0.60±0.32[a]	4.60±0.74[a]

[1]t = 5.0572, 7.5856, 3.8633, [b]P<0.01 *vs* control (Normal saline); [2]t = 2.4436, 2.6273, [a]P<0.05, [3]t = 3.7836, [d]P<0.01 *vs* model.

Effect of Zuogui Wan on apoptosis index of MSG-liver regeneration rats in ARN

Apoptosis index (AI) of MSG-liver regeneration rats in ARN was higher than that of saline treated and shamly-operated MSG-rats, and the difference was significant (P<0.01 or P<0.05). AI of Zuogui Wan treated group reduced significantly on the postoperative 5th and 11th days compared to model group (P<0.01) (Table 2).

Table 2 Effect of Zuogui Wan on ARN neurocyte apoptosis in MSG-liver regeneration rats (positive cells %, n = 6, mean±SD)

Group	Postoperative 1st d	Postoperative 5th d	Postoperative 11th d
Normal saline	0.07±0.08	0.08±0.04	0.09±0.03
MSG-rats	2.45±0.32[d]	2.32±0.45[d]	2.56±0.59[d]
Model	2.62±0.72[d]	3.32±0.81[ad]	4.23±1.22[ad]
Zuogui Wan	1.62±0.65	1.43±0.75[f]	1.12±1.14[f]

[1]t = 2.6435, 3.0185, [a]P<0.05 *vs* MSG-rats; [2]t = 17.6741, 12.1451, 10.2414, 8.6222, 9.7860, 8.3097, [d]P<0.01 *vs* control (Normal saline); [3]t = 4.1938, 4.5624, [f]P<0.01 *vs* Model.

Effect of Zuogui Wan on expression of TGF-β1 in ARN of MSG-liver regeneration rats

Results indicated that, the expression of TGF-β_1 in ARN of MSG-liver regeneration rats was significantly higher than that in saline control group and shamly-operated group (MSG-rats) (P<0.01). Along with increased apoptotic index (AI) in ARN neurocytes, the expression of TGF-β_1 improved correspondingly, namely, the more the TGF-β_1 expressed, the larger the AI was. Besides, along with the weakened expression of TGF-β_1, AI of ARN in Zuogui Wan treatment group decreased significantly (P<0.01, Table 3).

DISCUSSION

Some studies found that neonate rats who were given high dose MSG on the 2nd, 4th, 6th, 8th, 10th days could destroy nucleus arcuatus hypothalami (ARN) selectively, and swelling and necrosis in ARN neurocytes were the main pathological lesions, and its mechanism in nervous poison might be concerned with the overexertion of calcium ions in cerebral neurocytes[6-11]. Our experiment results showed that MSG could induce neurocyte apoptosis in the intermediate and advanced stage after rats were injected with MSG, leading to acute swelling and necrosis in ARN neurocytes. We also could find apoptosis in cerebral neurocytes under electron microscopy and the number of apoptotic cells in model group is larger than that in control group, 8-10 wk after hypodermical injection of MSG. Furthermore, the shape factor, circularity and heteromorpic index that reflected the changes of neurocyte nuclei in ARN were different compared with saline control group. Quantitating apoptotic neurocytes in cerebra by *in situ* end-labeling technique also showed that cerebral IA was larger than that of control group. In ordinary physiological state, most neurons can survive all the life and do not renew, therefore, apoptosis can seldom be found. As a common secondary messenger of apoptosis, MSG could lead to overexertion of calcium ions in neuron cytoplasm, which may be one of the mechanisms underlying apoptosis in MSG-rats' and MSG-liver regeneration-rats' cerebral neurocytes. But the phenomenon that cerebral neurocyte apoptosis of MSG-liver regeneration rats was more conspicuous than that of MSG-rat group can not be explained completely with the mechanism, i.e. MSG leading to overexertion of calcium ions in neuron cytoplasm could induce neurocyte apoptosis. These studies showed that it probably involved other factors leading to cerebral neurocyte apoptosis, besides overexertion of calcium ions in neuron cytoplasm induced by MSG[4].

TGF-β_1 can enhance apoptosis, so the considerable expression of TGF-β_1 is an important signal that apoptosis takes place. TGF-β_1 expressed excessively in cerebral neurocytes of MSG-liver regeneration rats, and the quantity was larger than that in MSG-rat group and saline control group, and the differences were significant[12-22]. That overexertion of calcium ions in cerebral neurocytes induced by MSG and the considerable expression of TGF-β_1 induced by partial hepatectomy in ARN of MSG-liver regeneration rats hint that both of them have synergistic effects on inducing MSG-liver regeneration-rat cerebral neurocyte apoptosis. AI of MSG-liver regeneration rat cerebullar neurocytes is closely correlated with considerable expression of TGF-β_1. Neurocyte apoptosis in ARN of MSG-liver regeneration rats is one of the important mechanisms of functional disorder in nerve-endocrine-immune network. TGF-β_1 protein could participate in the regulation of neurocyte apoptosis in ARN of MSG-liver regeneration rats[2-5].

One of the major research achievements of the kidney's essence is deficiency of kidney-yang in hypothalamus, and deficiency of kidney-yang is closely correlated with functional disorder in nerve-endocrine-immune network[23-30]. Our results showed that deficiency of kidney-yin was located in hypothalamus also[2-5,27], and neurocyte apoptosis in ARN of MSG-liver regeneration rats significantly lessened and indexes such as shape factor, circularity, heteromorphism which reflect the changes of ARN neurocyte nuclei improved significantly by replenishing kidney-yin with Zuogui Wan. Meanwhile, its expression of TGF-β_1 was also less than that in model group.

In summary, Zuogui Wan could prevent cerebral neurocyte apoptosis MSG-liver regeneration rats and down-regulate the overexpression of TGF-β_1 and its acceptors. Thus Zuogui Wan

Table 3 Effect of Zuogui Wan on TGF-β_1 expression of ARN in MSG-liver regeneration-rats (positive cells %, n = 6, mean±SD)

Group	Postoperative 1st d	Postoperative 3rd d	Postoperative 5th d	Postoperative 11th d
Normal saline	10.9±2.7	13.7±2.5	16.8±2.9	12.6±1.6
MSG-rats	12.8±3.1	13.5±2.8	12.3±3.2	14.5±2.9
Model	19.4±2.4[bd]	21.3±2.6[bd]	25.1±2.9[bd]	29.7±2.8[bd]
Zuogui Wan	11.3±2.1[f]	12.9±3.2[f]	18.8±2.2[f]	14.8±1.7[f]

[1]t = 5.7635, 5.1612, 4.9573, 12.9884, [b]P<0.01 *vs* control (Normal saline); [2]t = 4.1237, 5.0003, 7.2602, 9.2362, [d]P<0.01 *vs* MSG-rats; [3]t = 6.2216, 4.9903, 4.2394, 11.1420, [f]P<0.01 *vs* Model.

can influence liver regeneration by adjusting nerve-endocrine-immune network.

REFERENCES

1 **Li HM**, Zhang LT, Mei JJ, Qiu XF, Wang P. The establishment of L-monosodium glutamate-liver regeneration-rat model. *Shijie Huaren Xiaohua Zazhi* 2000; **8**: 824-826

2 **Li HM**, Zhang LT, Qiu XF. Research of "liver and kidney are all origin from the same origin of brain" and the essence of liver and kidney. *Zhongyi Zazhi* 2000; **41**: 69-71

3 **Li HM**, Zhang LT, Qiu XF, Mei JJ, Wang P. Study about the effect and the mechanism of Zuogui Pill on the kidney-essence and liver-blood deficiency syndrome of model of MSG-regeneration-rats. *Hubei Zhongyixueyuan Xuebao* 2001; **3**: 30-33

4 **Li HM**, Yang ML, Mei JJ, Zhang LT, Qiu XF. Neurocyte apotosis and expression of TGF-β_1 in ARN of MSG-Regeneration-Rats. *China J Appl Physiol* 2003; **19**: 46-47

5 **Yang ML**, Li HM, Mei JJ, Zhang LT, Qiu XF. Dig marked probe *in situ* hybridization detected TGF-β_1 mRNA in MSG-liver regeneration-rats' nucleus arcuatus hypothalami. *Zhongguo Zuzhihuaxue Yu Xibaohuaxue Zazhi* 2002; **11**: 202-204

6 **Liu YF**, Cai DF. The effect of L-monosodium glutamate on nerve-endocrine-immune network. External medicine-endocrine fascicle. *Guowai Yixue Neifenmixie Fence* 1997; **17**: 143-145

7 **Olney JW**. Brain lesions, obesity, and other disturbances in mice treated with monosodium glutamate. *Science* 1969; **164**: 719-721

8 **Belluardo N,** Mudo G, Bindoni M. Effects of early destruction of the mouse arcuate nucleus by monosodium glutamate on age-dependent natural killer activity. *Brain Res* 1990; **534**: 225-233

9 **Kure S**, Tominaga T, Yoshimoto T, Tada K, Narisawa K. Glutamate triggers internucleosomal DNA cleavage in neuronal cells. *Biochem Biophys Res Commun* 1991; **179**: 39-45

10 **Terry LC**, Epelbaum J, Martin JB. Monosodium glutamate: acute and chronic effects on rhythmic growth hormone and prolactin secretion, and somatostatin in the undisturbed male rat. *Brain Res* 1981; **217**: 129-142

11 **Hu L**, Fernstrom JD, Goldsmith PC. Exogenous glutamate enhances glutamate receptor subunit expression during selective neuronal injury in the ventral arcuate nucleus of postnatal mice. *Neuroendocrinology* 1998; **68**: 77-88

12 **Yamamoto M**, Fukuda K, Miura N, Suzuki R, Kido T, Komatsu Y. Inhibition by dexamethasone of transforming growth factor beta1-induced apoptosis in rat hepatoma cells: a possible association with Bcl-xL induction. *Hepatology* 1998; **27**: 959-966

13 **Roberts RA**, James NH, Cosulich SC. The role of protein kinase B and mitogen-activated protein kinase in epidermal growth factor and tumor necrosis factor alpha-mediated rat hepatocyte survival and apoptosis. *Hepatology* 2000; **31**: 420-427

14 **Choi KS**, Lim IK, Brady JN, Kim SJ. ICE-like protease (caspase) is involved in transforming growth factor beta1-mediated apoptosis in FaO rat hepatoma cell line. *Hepatology* 1998; **27**: 415-421

15 **Tsukada T**, Eguchi K, Migita K, Kawabe Y, Kawakami A, Matsuoka N, Takashima H, Mizokami A, Nagataki S. Transforming growth factor beta 1 induces apoptotic cell death in cultured human umbilical vein endothelial cells with down-regulated expression of bcl-2. *Biochem Biophys Res Commun* 1995; **210**: 1076-1082

16 **Derynck R**, Zhang Y, Feng XH. Smads: transcriptional activators of TGF-beta responses. *Cell* 1998; **95**: 737-740

17 **Ribeiro A**, Bronk SF, Roberts PJ, Urrutia R, Gores GJ. The transforming growth factor beta 1 -inducible transcription factor, TIEG1, mediates apoptosis through oxidative stress. *Hepatology* 1999; **30**: 1490-1497

18 **Bissell DM**, Wang SS, Jarnagin WR, Roll FJ. Cell-specific expression of transforming growth factor-beta in rat liver. Evidence for autocrine regulation of hepatocyte proliferation. *J Clin Invest* 1995; **96**: 447-455

19 **Oberhammer F**, Bursch W, Tiefenbacher R, Fröschl G, Pavelka M, Purchio T, Schulte-Hermann R. Apoptosis is induced by transforming growth factor-beta 1 within 5 hours in regressing liver without significant fragmentation of the DNA. *Hepatology* 1993; **18**: 1238-1246

20 **Khosla S**, Oursler MJ, Schroeder MJ, Eberhardt NL. Transforming growth factor-beta 1 induces growth inhibition of a human medullary thyroid carcinoma cell line despite an increase in steady state *c-myc* messenger ribonucleic acid levels. *Endocrinology* 1994; **135**: 1887-1893

21 **Gruppuso PA**, Mead JE, Fausto N. Transforming growth factor receptors in liver regeneration following partial hepatectomy in the rat. *Cancer Res* 1990; **50**: 1464-1469

22 **Massague J.** TGFbeta signaling: receptors, transducers, and mad proteins. *Cell* 1996; **85**: 947-950

23 **Cai DF**, Shen ZY, Zhang LJ, Wang WJ. The effect of Yougui-ying on the hypothalamus-pituitary-adrenal thymus axis of rats inhibited by corticosterone. *Zhongguo Mianyixue Zazhi* 1994; **10**: 236-239

24 **Song CF**, Yin GS, Zhao JH, Sun SJ, Li En, Lü PY. The effect of tonifying kidney herbs on CaMPKII of hypothalamus-pituitry-adrenal axia in kidney-yang deficiency rats. *Zhongguo Zhongyi Jichuyixue Zazhi* 2001; **7**: 605-607

25 **Song CF**, Yin GS, Li E, Li XY. The effect of Yougui-ying on median eminenced ependymocytes of hypothalamus in Kidney-yang deficiency rats. *Zhongguo Zhongyi Jichu Yixue Zazhi* 2001; **7**: 19-22

26 **Gao B**, Yao YX, Zhang XY, Yin GS. Expression of NosmRNA in hypothalamus neuron on rats of kidney-yang deficiency and regulation of notifying kidney medicines. *Zhongguo Zhongyi Jichu Yixue Zazhi* 2001; **8**: 583-584

27 **Cai DF**, Liu YF, Cheng XH, Li WW, Bo J, Shen SY, Lin QW, Chen XQ, Ruan QM. The effect of Zuogui Pill on hypothalamus-pituitary-adrenal axia of MSG-rats. *Zhongguo Zhongyi Jichu Yixue Zazhi* 1999; **5**: 24-27

28 **Wu ZK**, Jiang BH, Li CJ, Chen SH, Liu FY, Cui JH, Chen YY, Zheng J, Huang XZ, Lü XX. Modern study on the theory of "kidney manufactures the marrow". *Zhongyi Zazhi* 1999; **10**: 626-628

29 **Shen ZY**. Contrasting research between kidney deficiency and senile in microcosmic. *Zhongyi Zazhi* 2002; **43**: 565-567

30 **Shen ZY**. Study on the localization of kidney-yang deficiency. *Zhongguo Zhongxiyi Jiehe Zazhi* 1997; **17**: 50-52

Edited by Wang XL **Proofread by** Xu FM

PO Box 2345, Beijing 100023, China
Fax: +86-10-85381893
E-mail: wjg@wjgnet.com www.wjgnet.com

World J Gastroenterol 2004;10(19):2827-2830
World Journal of Gastroenterology
Copyright © 2004 by The WJG Press ISSN 1007-9327

• BASIC RESEARCH •

Autocrine expression of hepatocyte growth factor and its cytoprotective effect on hepatocyte poisoning

Yong He, Jun Zhou, Ke-Feng Dou, Yong Chen, Qing-Guo Yan, Hai-Min Li

Yong He, Ke-Feng Dou, Yong Chen, Hai-Min Li, Department of Hepatobiliary Surgery, Xijing Hospital, the Fourth Military Medical University, Xi'an 710032, Shaanxi Province, China
Jun Zhou, Department of Pathology, Qindu Hospital, the Fourth Military Medical University, Xi'an 710032, Shaanxi Province, China
Qing-Guo Yan, Department of Pathology, the Fourth Military Medical University, Xi'an 710032, Shaanxi Province, China
Supported by National Natural Science Foundation of China, No. 30170927 and No. 3007021
Correspondence to: Dr. Yong He, Department of Hepatobiliary Surgery, Xijing Hospital, the Fourth Military Medical University, 127 ChangLe West Road, Xi'an 710032, Shaanxi Province, China. heyong007@yahoo.com
Telephone: +86-29-83375259 **Fax:** +86-29-83375261
Received: 2004-02-21 **Accepted:** 2004-04-13

Abstract

AIM: To construct pEGFP-hepatocyte growth factor (HGF) expression vector, the to detect its expression in transfected human hepatocytes, and to investigate the influence of autocrine HGF expression on the proliferative potential and cytoprotective effects in human hepatocytes.

METHODS: Human HGF cDNA was ligated to the pEGFP vector. Recombinant plasmid was transfected into human hepatocyte line QZG with liposome. Expression of HGF protein was observed by fluorescence microscopy and immunohistochemistry. Hepatic cells were collected 24, 48, and 72 h after transfection to detect the number of [^{3}H]-TdR uptake in DNA. DNA synthesis was observed by using PCNA stain immunohistochemistry. Acute liver cell damage was induced by carbon tetrachloride. Cytoprotective effect was observed by examining the survival rate of hepatocytes and leakage of intracellular alanine transaminase (ALT) and potassium ions.

RESULTS: HGF identification of pEGFP-HGF by enzyme digestion showed that HGF fragment was cloned into *BamH* I and *Sal* I sites of pEGFP-N3. Expression of GFP in transfected hepatocytes was observed with fluorescence microscopy. The [^{3}H]-TdR uptake became 7 times as many as in the control group 96 h after transfection. After HGF transfection, the survival rate of hepatocytes poisoned by CCl_4 significantly increased (83% *vs* 61%, $P<0.05$), and the leakage of intracellular alanine transaminase and potassium ions decreased (586 nkat/L *vs* 1089 nkat/L, $P<0.01$; and 5.59 mmol/L *vs* 6.02 mmol/L, $P<0.01$ respectively). Culture of transfected hepatic cells promoted the proliferation of other non-transfected cells.

CONCLUSION: Transfected HGF is expressed in hepatic cells and has the activity of promoting cell division and protecting hepatic cells against poisoning.

He Y, Zhou J, Dou KF, Chen Y, Yan QG, Li HM. Autocrine expression of hepatocyte growth factor and its cytoprotective effect on hepatocyte poisoning. *World J Gastroenterol* 2004; 10(19): 2827-2830
http://www.wjgnet.com/1007-9327/10/2827.asp

INTRODUCTION

Hepatocyte growth factor (HGF) was originally isolated as the most potent mitogen for primary hepatocytes. HGF has subsequently been revealed to be a multifunctional cytokine in a wide variety of epithelial cells, endothelial cells, and some mesenchymal cells during the past two decades[1-7]. In addition to mitogenic activity, HGF has some unique morphogenic activities such as an induction of epithelial tubulogenesis including in cells derived from the kidney, liver and mammary gland[8,9]. Characterization of scatter factor, which enhances epithelial cell motility, revealed that it had the same molecule as HGF. HGF is a heterodimeric glycoprotein composed of a 69 ku α-chain and a 34 ku β-chain, and has four homologous kringle domains in the α-chain[10]. The receptor capable of signal transduction of HGF is a c-met protooncogene product of heterodimeric tyrosine kinase[11,12]. Extensive studies on the physiological function of HGF have established that the growth factor functions as a potent hepatotrophic factor for liver injuries, but elevated plasma HGF levels have not been noted in patients with hepatic diseases[13-19].

HGF and its receptor MET, ordinarily constitute a paracrine signaling system in which cells of mesenchymal origin produce the ligand (HGF) which binds to its receptor (MET) that is predomanantly expressed in cells of epithelial origin[10]. While the effects of exogenous HGF on promoting normal hepatocyte growth have been well characterized, there appears to have a controversy on effect of autocrine HGF on hepatocytes. In this study, the effects of forced autocrine expression of HGF in hepatocytes were examined. huHGF was expressed by transducing hepatocytes with a vector containing huHGF cDNA. It was demonstrated that the forced expression of HGF in hepatocytes led to an increase in the population of transduced hepatocytes compared to non-transduced hepatocytes in the same cultures. The results suggest that autocrine expression presents an advantage for the proliferation and survival of hepatocytes poisoning.

MATERIALS AND METHODS

Materials

PBS-7 vector containing human HGF cDNA was donated by Professor Toshikazu Nakamura (Division of Biochemistry, Osaka University Medical School, JaPan). The transfer vector $pEGFPN_3$ containing a humanized green fluorescence protein (GFP) cDNA was purchased from Clontech Biology Company (USA).

Culture of hepatocytes

Human hepatocyte QZG (donated by the Department of Pathology, Fourth Military Medical University) was cultured in RPMI1640 medium (Gibco) supplemented with 150 mL/L fetal bovine serum (100 kU/L penicillin, 100 kU/L streptomycin) and incubated at 37 ℃ in humidified atmosphere of 50 mL/L CO_2 incubator.

Construction of pEGFP-HGF vectors

Construction of pEGFP-HGF vector was previously described[20]. The human HGF cDNA was isolated from pBluescript SK$^-$ as a 2.3 kb *Bam*H I- *Sal* I fragment. The resulting cDNA fragment

was then inserted into the *Sal* I and *Bam*HI-sites of the pEGFP-N_3 vector.

Transduction of rat hepatocytes

Exponentially growing QZG cells were seeded into 35 mm tissue culture dishes and grown to 60-70% confluency in culture medium. Each culture dish was then transfected with 5 μg pEGFP-HGF constructs by using lipofectamine according to the instructions of the manufacturer (Gibco BRL, Eggenstein, Germany). Encapsulated pEGFP-HGF was incubated for 5 h on cells in serum free medium, then in medium containing 15 mL/L bovine serum. After a further incubation of the cells for 24 h, the culture medium was discarded and replaced by normal culture medium. Seventy-two hours after transfection, the QZG cells and their media were harvested for further analysis.

Analysis for HGF expression in hepatocyte

After transfected with pEGFP-HGF, the cells were examined for the presence of green fluorescence by using an inverted fluorescent light microscope. Immunocytochemical staining was performed by using HGF antibody on logarithmically growing cell lines. Firstly, the cells were plated onto coverslips, adhered overnight. Then, after rinsed three times with PBS, the cells were fixed in cold acetone for 8-10 min. Endogenous peroxidase was blocked with 10 mL/L hydrogen peroxide in absolute methanol for 30 min. The primary antibodies were applied for 2 h at 37 ℃ at 1:50 dilution in a humidified chamber. Then the typical SABC strategy followed.

Assay of DNA synthesis by ^{3}H-TdR incorporation

The cells were cultured in an appropriate medium for 24 h prior to beginning the experiment, and incubated with [^{3}H] thymidine (18.5 MBq/L, 37 kBq/well). After 6 h the cells were harvested with trysin/EDTA, and collected from the acetic fiber filter with a cellular collector and washed three times with PBS. The filter was dried overnight at 37 ℃, and transferred into a liquid scintillation counter (containing 10 g/L PO and 20 g/L POP in xylene) and cpm value was determined by the liquid scintillation counter (LS6500, Beckmen Co.)

Cell proliferation

The level of expression of proliferating cell nuclear antigen (PCNA) was used as a marker of cell proliferation. In the present study PCNA was measured by ABC immunohistochemical method.

Cytoprotective effects on CCl_4-intoxicated human hepatocytes

For assaying cytoprotective effect of autocrine HGF, hepatocyte QZG was poisoned by carbon tetrachloride (CCl_4). After treated with 15 mmol/L CCl_4 for 40 min, survival rate of cells was measured by trypan blue method. Aspartate aminotransferase (AST) and alanine aminotransferase (ALT) in supernatant were measured by using a biochemical analyzer. Leakage of intracellular potassium ions was measured by using an ion analyzer.

In situ hybridisation

This was performed as previously described. Hepatocytes were transduced with pEGFP-HGF, trypsinized after 48 h and centrifuged onto slides (roughly 40 000 cells/cm^2). These slides were used for *in situ* hybridization. Results were evaluated by counting at least 3 viewing fields per slide at a magnification ×200.

Statistical analysis

The results are expressed as mean±SE. Statistical analysis was performed by the Student's *t*-test. $P<0.05$ was considered statistically significant.

RESULTS

Identification of recombinant pEGFP-HGF expression vector

The recombinant pEGFP-HGF vector was digested by *Bam*H I and *Sal* I. pEGFP-HGF contained a 2300-bp and a 4700-kb gene fragments separated by electrophoresis in 12 g/L agarose gel (Figure 1). It proved that the HGF gene was correctly inserted inpEGFP-HGF.

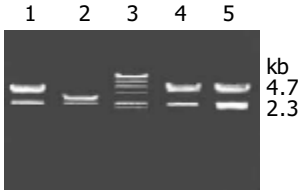

Figure 1 Identification of recombinant plasmids digested with restriction enzymes *Bam*H I and *Sal* I. 1, 4, 5: pEGFP-HGF plasmid digested with *Bam*H I and *Sal* I; 2: pBS-7 plasmid digested with *Bam*H I+*Sal* I; 3: λDNA / *Hin*dIII marker.

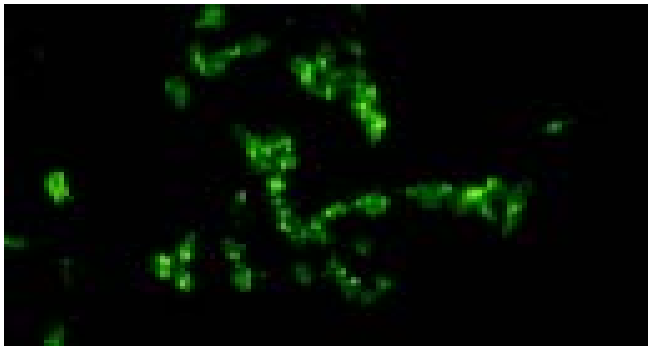

Figure 2 Green fluorescence in QZG cells transfected with pEGFP-HGF fusion constructs, Inverted fluorescent light microscope ×200.

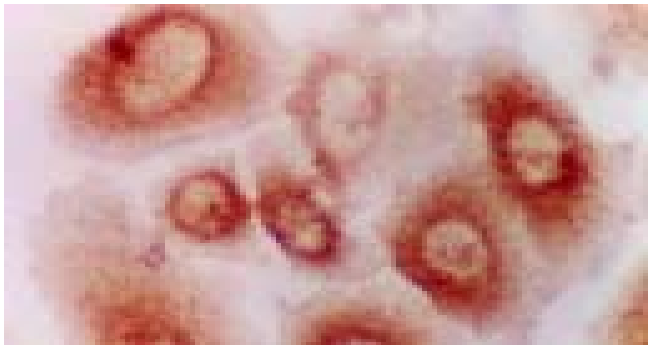

Figure 3 Expression of HGF protein in QZG cells transfected with pEGFP-HGF. SABC ×400.

Expression of pEGFP-HGF fusion proteins in QZG cell line

Green fluorescence was visible after transfection with pEGFP-HGF fusion constructs (Figure 2). The pEGFP-HGF fusion proteins were localized primarily in cytoplasm. The expression of HGF in the transfected QZG cells was also detected by immunohistochemical staining. A lot of brown granules were seen in HGF transfected QZG cell cytoplasms (Figure 3) proving that HGF gene could be expressed in QZG cells.

Effect on DNA synthesis

DNA synthesis as mirrored by [^{3}H]thymidine uptake of QZG cells was determined after transfection with pEGFP-HGF. DNA synthesis in QZG cells transfected by pEGFP-HGF was accelerated

in a time-dependent fashion increased by 7-fold compared to control group after 96 h transfection with pEGFP-HG F (Figure 4).

Cell proliferation

As shown in Figure 5, the expression rate of PCNA on QZG cells increased after transfection with pEGFP-HGF.

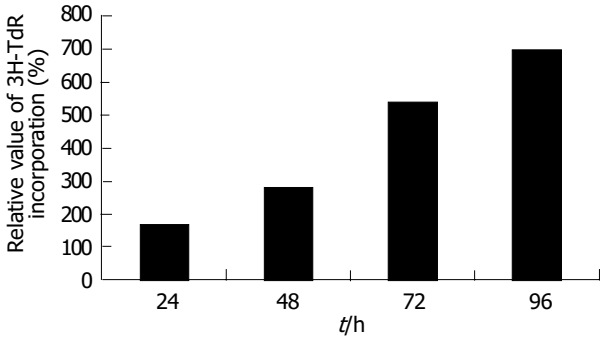

Figure 4 Relative values of ^{3}H-TdR incorporation in QZG cells transferred with pEGFP-HGF (relative to QZG cells transferred with pEGFP).

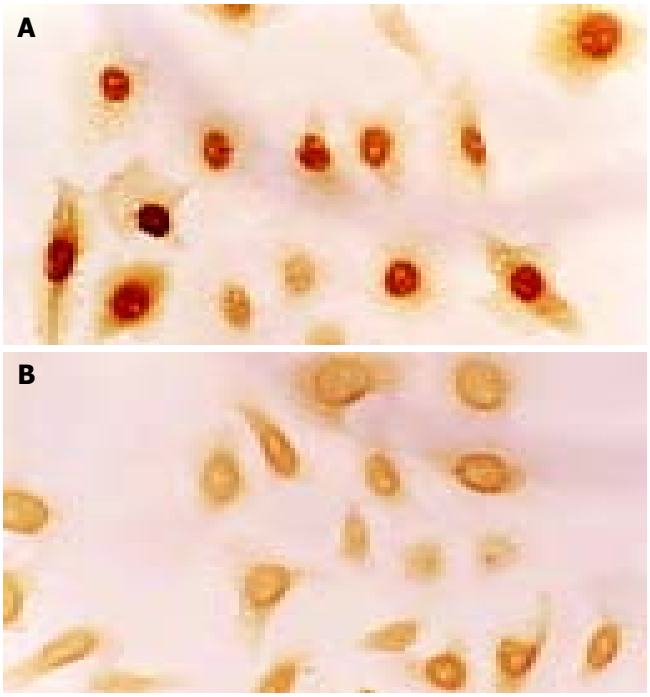

Figure 5 Expression of PCNA protein in QZG cells transferred with pEGFP-HGF (A) and transferred with pEGFP (B). ×200.

Table 1 Survival rate of hepatocytes and leakage of intracellular ALT and K^+

Group	Survival rate (%)	ALT (nkat/L)	K^+ (mmol/L)
QZG	96±2	403±70	5.21±0.04
pEGFP-HGF	98±1	429±80	5.18±0.02
QZG intoxicated by CCL_4	61±7[a]	1 089±223[b]	6.02±0.17[b]
pEGFP-HGF intoxicated by CCL_4	83±6[c]	586±124[d]	5.59±0.07[d]

[a]P<0.05, [b]P<0.01, *vs* QZG group; [c]P<0.05, [d]P<0.01, *vs* QZG intoxicated by CCL_4 group.

Cytoprotective effect on hepatocytes injuried by CCl_4

After pEGFP-HGF was transfected, the survival rate of QZG cells intoxicated by CCl_4 was significantly increased (83% *vs* 61%, t = 3.89, P<0.05). The leakage of intracellular alanine transaminase (ALT) (586 nkat/L *vs* 1 089 nkat/L, t = 13.07, P<0.01) and potassium ions (5.59 mmol/L *vs* 6.02 mmol/L, t = 12.91, P<0.01) was decreased (Table 1).

DISCUSSION

Hepatocyte growth factor (HGF) is well known as a pleiotropic substance with mitogenic, motogenic, morphogenic, and tumor suppressoion activities. HGF was found in the serum of partially hepatectomized rat and in rat platelets as the most potent stimulator of hepatocyte growth and DNA synthesis *in vitro*[21]. The mitogenic function of HGF was confirmed *in vivo*. In normal rats as well as partially hepatectomized rats, infusion of HGF stimulated a 6-fold increase in the mitotic labeling index of hepatocytes. It also stimulated protein synthesis, seen as increased hepatic messenger RNA content and serum albumin levels. HGF has been intensively investigated in terms of its beneficial effects on hepatic injury[22-24]. It has been documented that HGF reduced the hepatotoxicity of alpha-naphthylisothiocyanate, D-galactosamine, and carbon tetrachloride in rats[25,26]. Moreover, HGF increased survival of cirrhotic rats subjected to a major hepatic resection and treatment with dimethylnitrosamine[27-29]. These results suggest that HGF may play important roles in protection from and regeneration of hepatic injury and serve as a therapeutic agent.

HGF and its receptor MET, ordinarily constitute a paracrine signaling system in which cells of mesenchymal origin produce the ligand (HGF) which binds to its receptor (MET) that is predominantly expressed in cells of epithelial origin. In the present study, we demonstrated that HGF gene transfer into hepatocytes caused increased proliferation of hepatocytes by method of PCNA stain and increased DNA synthesis by method of [^{3}H]thymidine uptake. Forced HGF expression by cultured human hepatocytes had a mitogenic effect. The detection of HGF protein assessed by immunocytochemical staining confirmed the successful transfection of HGF gene.

Accumulated evidence has revealed that HGF has a cytoprotective effect on various types of liver cells. In hepatocytes, HGF attenuated the liver injury induced by lipopolysaccharide and D-galactosamine[30]. Moreover, HGF abrogated Fas-induced massive liver apoptosis and lethal hepatic failure by inducing Bcl-xL expression, with subsequent blockage of a Fas-mediated signaling pathway upstream of CPP32 in the liver, suggesting that HGF has an inhibitory effect on Fas-mediated apoptosis. HGF could also ameliorate hepatocellular dysfunction and posthepatectomy hyperbilirubinemia in an α-naphthylisothiocyanate-induced cholestasis model, in which the epithelia of bile ducts, as well as hepatocytes, became necrotic. This finding indicates that HGF could promote tissue repair of both epithelial cells and hepatocytes[31,32]. In the present study we demonstrated the cytoprotective effect of HGF transgene on hepatocyte injury by CCl_4. HGF transgene markedly increased the survival rate of hepatocytes against CCl_4 injury, decreased the leakage of intracellular alanine transaminase and potassium ions.

Since its introduction into cell biological research, the green fluorescent protein (GFP) of jellyfish *Aequorea victoria* has become a versatile tool for the analysis of protein function and dynamics at the cellular level. GFP, consisting of 238 amino acids, has been used as a tag for localization of a broad range of proteins in a wide variety of eukaryotic cells. A mutant of GFP, S65T with an excitation peak of 489 nm and an emission peak of 511 nm, could emit 4 to 6 times more fluorescence energy compared with wild-type GFP. GFP may be fused generically to

a target protein, and the fluorophore of GFP forms spontaneously in the presence of oxygen, thus rendering it an ideal probe for *in vivo* applications. The *in vivo* expression of GFP could obviate the fixation and permeablization of cells for immunofluorescence or the mirojijection of labeled proteins. GFP fusion proteins constitute a major advance in the study of the dynamics of intracelluar processes in living cells[33-37]. A major concern in the application of GFP as a fluorescent tag relates to whether the distribution of GFP fluorescence is identical to that of the protein to which it is fused. We have constructed GFP- HGF fusion gene and transfected into hepatocytes. The results indicate that the fusion protein can still be expressed in the nuclei of hepatocytes. Because liver disease, especially viral liver diseases are common in China, our study is of much more significance.

REFERENCES

1 **Yu SL,** Yang FH. Molecular biological progress of hepatocyte growth factor (HGF). *Shengwu Gongcheng Xuebao* 2002; **18**: 1-4

2 **Morishita R,** Aoki M, Yo Y, Ogihara T. Hepatocyte growth factor as cardiovascular hormone: role of HGF in the pathogenesis of cardiovascular disease. *Endocr J* 2002; **49**: 273-284

3 **Ricci G,** Catizone A, Galdieri M. Pleiotropic activity of hepatocyte growth factor during embryonic mouse testis development. *Mech Dev* 2002; **118**: 19-28

4 **Skibinski G.** The role of hepatocyte growth factor/c-met interactions in the immune system. *Arch Immunol Ther Exp* 2003; **51**: 277-282

5 **Liu Y**. Hepatocyte growth factor promotes renal epithelial cell survival by dual mechanisms. *Am J Physiol* 1999; **277**: F624-633

6 **Natsume M**, Tsuji H, Harada A, Akiyama M, Yano T, Ishikura H, Nakanishi I, Matsushima K, Kaneko S, Mukaida N. Attenuated liver fibrosis and depressed serum albumin levels in carbon tetrachloride-treated IL-6-deficient mice. *J Leukoc Biol* 1999; **66**: 601-608

7 **He Y,** Zhou J, Dou K. Autocrine expression of hepatocyte growth factor and its cytoprotective effect on hepatocyte poisoning *Zhonghua Yixue Zazhi* 2002; **82**: 275-278

8 **Ohnishi T,** Daikuhara Y. Hepatocyte growth factor/scatter factor in development, inflammation and carcinogenesis: its expression and role in oral tissues. *Arch Oral Biol* 2003; **48**: 797-804

9 **Kokuzawa J**, Yoshimura S, Kitajima H, Shinoda J, Kaku Y, Iwama T, Morishita R, Shimazaki T, Okano H, Kunisada T, Sakai N. Hepatocyte growth factor promotes proliferation and neuronal differentiation of neural stem cells from mouse embryos. *Mol Cell Neurosci* 2003; **24**: 190-197

10 **Funakoshi H,** Nakamura T. Hepatocyte growth factor: from diagnosis to clinical applications. *Clin Chim Acta* 2003; **327**: 1-23

11 **Zhang YW,** Vande Woude GF. HGF/SF-met signaling in the control of branching morphogenesis and invasion. *J Cell Biochem* 2003; **88**: 408-417

12 **Sun W,** Funakoshi H, Nakamura T. Localization and functional role of hepatocyte growth factor (HGF) and its receptor c-met in the rat developing cerebral cortex. *Brain Res Mol Brain Res* 2002; **103**: 36-48

13 **Nozato E**, Shiraishi M, Nishimaki T. Up-regulation of hepatocyte growth factor caused by an over-expression of transforming growth factor beta, in the rat model of fulminant hepatic failure. *J Surg Res* 2003; **115**: 226-234

14 **Hata J,** Ikeda E, Uno H, Asano S. Expression of hepatocyte growth factor mRNA in rat liver cirrhosis induced by N-nitrosodimethylamine as evidenced by in situ RT-PCR. *J Histochem Cytochem* 2002; **50**: 1461-1468

15 **Chijiiwa K,** Saiki S, Tanaka M. Serum interleukin-6 and hepatocyte growth factor levels in patients after hepatectomy. *Hepatogastroenterology* 2002; **49**: 467-471

16 **Borawski J,** Mysliwiec M. Serum hepatocyte growth factor is associated with viral hepatitis, cardiovascular disease, erythropoietin treatment, and type of heparin in haemodialysis patients. *Nephrol Dial Transplant* 2002; **17**: 637-644

17 **Chen P**, Li K, Dong JH, Han BL. Changes of TGF-α, HGF, PCNA and IGFBP-1s mRNA after partial hepatectomy in rat liver. *Shijie Huaren Xiaohua Zazhi* 2003; **11**: 434-437

18 **Xu W**, Wu SG. The possible relationship between hepatomegaly and release of HGF into plasma induced by clofibrate in rats. *World J Gastroenterol* 1999; **5**: 440-442

19 **Yamagami H**, Moriyama M, Tanaka N, Arakawa Y. Detection of serum and intrahepatic human hepatocyte growth factor in patients with type C live diseases. *Intervirology* 2001; **44:** 36-42

20 **He Y**, Zhou J, Dou KF. Construction of hepatocyte growth factor expression vector and detection of expression in human hepatocytes. *Shijie Huaren Xiaohua Zazhi* 2001; **9**: 1143-1146

21 **Luo YQ**, Wu MC. Hepatocyte growth factor. *Xin Xiaohuabingxue Zazhi* 1997; **5**: 198-199

22 **Okamoto K,** Suzuki S, Kurachi K, Sunayama K, Yokoi Y, Konno H, Baba S, Nakamura S. Beneficial effect of deletion variant of hepatocyte growth factor for impaired hepatic regeneration in the ischemically damaged liver. *World J Surg* 2002; **26**: 1260-1266

23 **Takeda Y,** Arii S, Kaido T, Imamura M. The impairment of hepatocytes and sinusoidal endothelial cells during cold preservation in rat fatty liver induced by alcohol and the beneficial effect of hepatocyte growth factor. *Transpl Int* 2003; **16**: 241-249

24 **Yamashita Y,** Fujise N, Imai E, Masunaga H. Reduction of monocrotaline-induced hepatic injury by deleted variant of hepatocyte growth factor (dHGF) in rats. *Liver* 2002; **22**: 302-307

25 **Otsuka T,** Takagi H, Horiguchi N, Toyoda M, Sato K, Takayama H, Mori M. CCl4-induced acute liver injury in mice is inhibited by hepatocyte growth factor overexpression but stimulated by NK2 overexpression. *FEBS Lett* 2002; **532**: 391-395

26 **Xue F,** Takahara T, Yata Y, Minemura M, Morioka CY, Takahara S, Yamato E, Dono K, Watanabe A. Attenuated acute liver injury in mice by naked hepatocyte growth factor gene transfer into skeletal muscle with electroporation. *Gut* 2002; **50**: 558-562

27 **Matsuno Y**, Iwata H, Umeda Y, Takagi H, Mori Y, Kosugi A, Matsumoto K, Nakamura T, Hirose H. Hepatocyte growth factor gene transfer into the liver via the portal vein using electroporation attenuates rat liver cirrhosis. *Gene Ther* 2003; **10**: 1559-1566

28 **Ueki T**, Kaneda Y, TsuTsui H, Nakanishi K, Sawa Y, Morishita R, Matsumoto K, Nakamura T, Takahashi H, Fujimoto J. Hepatocyte growth factor gene therapy of live cirrhosis in rats. *Nature Med* 1999; **5**: 226-230

29 **Oe S,** Fukunaka Y, Hirose T, Yamaoka Y, Tabata Y. A trial on regeneration therapy of rat liver cirrhosis by controlled release of hepatocyte growth factor. *J Control Release* 2003; **88**: 193-200

30 **Kosai K**, Matsumoto K, Funakoshi H, Nakamura T. Hepatocyte growth factor prevents endotoxin-induced lehal hepatic failure in mice. *Hepatology* 1999; **30**: 151-159

31 **Kondo H**, Tani T, Kodama M. Effects of deletion-type human hepatocyte growth factor on murine septic model. *J Surg Res* 1999; **85**: 88-95

32 **Zeng C**, Pesall JE, Gilkerson KK, McFarland DC. The effect of hepatocyte growth factor on turkey satellite cell proliferation and differentiation. *Poult Sci* 2002; **81**: 1191-1198

33 **Cheng H,** Liu YF, Zhang HZ, Shen WA, Zhang SZ. Construction and expression of anti-HCC immunotoxin of sFv-TNF-α and GFP fusion proteins. *Shijie Huaren Xiaohua Zazhi* 2001; **9**: 640-644

34 **Lin T,** Ding J, Meng FP, Han QL, Yu ZC, Guo CC, Liu ZG, Fan DM. Construction and identification of recombinant adenovirus vaccines of gastric cancer MG7-Ag mimotope. *Shijie Huaren Xiaohua Zazhi* 2003; **11**: 14-17

35 **Fujikawa T**, Hirose T, Fujii H, Oe S, Yasuchika K, Azuma H, Yamaoka Y. Purification of adult hepatic progenitor cells using green fluorescent protein(GFP)-transgenic mice and fluorescence-activated cell sorting. *J Hepatol* 2003; **39**: 162-170

36 **Scarff KL**, Ung KS, Sun J, Bird PI. A retained selection cassette increases reporter gene expression without affecting tissue distribution in SPI3 knockout/GFP knock-in mice. *Genesis* 2003; **36**: 149-157

37 **Waldo GS**. Improving protein folding efficiency by directed evolution using the GFP folding reporter. *Methods Mol Biol* 2003; **230**: 343-359

Edited by Chen WW and Wang XL **Proofread by** Xu FM

PO Box 2345, Beijing 100023, China
Fax: +86-10-85381893
E-mail: wjg@wjgnet.com www.wjgnet.com

World J Gastroenterol 2004;10(19):2831-2835
World Journal of Gastroenterology
Copyright © 2004 by The WJG Press ISSN 1007-9327

• BASIC RESEARCH •

Effects of herbal compound 861 on human hepatic stellate cell proliferation and activation

Lin Wang, Jian Wang, Bao-En Wang, Pei-Gen Xiao, Yan-Jiang Qiao, Xue-Hai Tan

Lin Wang, Yan-Jiang Qiao, School of Chinese Materia Medica, Beijing University of Chinese Medicine, Beijing 100102, China
Xue-Hai Tan, Jian Wang, Beijing Genomic Institute, Beijing 101300, China
Bao-En Wang, Liver Research Center, Beijing Friendship Hospital, Capital University of Medical Sciences, Beijing 100050, China
Pei-Gen Xiao, Institute of Medicinal Plant Development, Chinese Academy of Medical Sciences, Beijing 100094, China
Supported by the Fund of One Hundred Scientist Plan of Chinese Academy of Sciences and the Knowledge Innovation Program Foundation of Chinese Academy of Sciences, No. KSCX2-SW-207
Co-correspondents: Jian Wang
Correspondence to: Dr. Xue-Hai Tan, Beijing Genomic Institute, Beijing 101300, China. tanxh@genomics.org.cn
Telephone: +86-10-80481755 **Fax:** +86-10-80498676
Received: 2004-03-23 **Accepted:** 2004-04-16

Abstract

AIM: To investigate the effects of herbal compound 861 (Cpd 861) on cell proliferation in human hepatic stellate cells (LX-2) and human hepatocellular liver carcinoma cells (HepG2), and expression of α-smooth muscle actin (α-SMA) in LX-2 cells.

METHODS: LX-2 and HepG2 cells were incubated with various concentrations of Cpd 861 (0.1-0.003 mg/mL) for 1, 2, 3, 5 and 7 d. Cell proliferation was analyzed by 3-(4, 5-dimethylthiazol-2-yl)-5-(3-carboxymethoxyphenyl)-2-(4-sulfophenyl)-2H-tetrazolium (MTS) assay. Effects of Cpd861 on the expression of α-SMA mRNA in LX-2 cells were measured by real-time quantitative PCR method using SYBR Green I technology.

RESULTS: Cpd 861, at 0.1 mg/mL, significantly inhibited LX-2 cell proliferation (15% decrease relative to control, $P<0.05$) after 3 d of incubation. The inhibitory effects seemed to increase with the treatment time (25% decrease after 5 d of incubation and 35% decrease after 7 d of incubation, $P<0.01$). However, Cpd 861 did not affect HepG2 cell proliferation at the same concentration used for LX-2 cells. The expression levels of α-SMA mRNA decreased significantly when LX-2 cells were exposed to Cpd 861 for 48 h (59% decrease relative to control, $P<0.05$) or 72 h (60% decrease relative to control, $P<0.01$).

CONCLUSION: Cpd 861 can significantly inhibit LX-2 cell proliferation in a dose-dependant manner, and reduce the expression levels of α-SMA mRNA in LX-2 cells. Since hepatic cell proliferation and high level of α-SMA are associated with liver fibrosis, the results suggest that Cpd 861 may be useful in the treatment of this disease.

Wang L, Wang J, Wang BE, Xiao PG, Qiao YJ, Tan XH. Effects of herbal compound 861 on human hepatic stellate cell proliferation and activation. *World J Gastroenterol* 2004; 10 (19): 2831-2835
http://www.wjgnet.com/1007-9327/10/2831.asp

INTRODUCTION

Hepatic fibrosis is a reversible wound healing response to chronic liver injury due to a variety of insults, including viral hepatitis (especially hepatitis B and C), alcohol abuse, drugs, metabolic diseases, autoimmune attack of hepatocytes or congenital abnormalities[1,2]. As shown in many recent studies, hepatic stellate cells (previously called Ito cells, lipocytes, perisinusoidal cells, or fat-storing cells) are primary cell types to mediate fibrogenesis[1,2]. In normal liver, hepatic stellate cells (HSCs) are nonparenchymal quiescent cells with functions to store vitamin A. Following liver injury of any etiology, HSCs undergo a process of activation, transform from quiescent vitamin A-rich cells to proliferative, fibrogenic, contractile myofibroblasts. Activated HSCs lose lipid droplets, feature high level expression of α-smooth muscle actin (α-SMA), and also are responsible for the deposition of the majority of excess extracellular matrix (ECM, predominantly types I and III collagen), which leads to form action of scar tissue in the fibrotic liver[1-4].

Herbal compound 861 (Cpd 861) is an extract of 10 herbs with *Salvia miltiorrhiza*, *Astragalus membranaceus* and *Spatholobus suberectus* as its chief components. The recipe of this mixed compound was based on the therapeutically indications of Chinese medicine. Clinical studies showed Cpd 861 could significantly improve clinical symptoms in hepatic fibrosis patients as well as the biochemical parameters associated with diseases in clinical tests for patients[5,6]. Experimental researches also showed that Cpd 861 could inhibit cell proliferation, reduce the level of α-SMA and reverse the process of liver fibrosis on rat model[5-7]. In this study, we aimed to investigate the effects of Cpd 861 on LX-2 and HepG2 cell proliferation and expression of α-SMA in LX-2 cells.

MATERIALS AND METHODS

Materials

Human activated hepatic stellate cell line LX-2 was a gift from Dr. Friedman of Mount Sinai School of Medicine. LX-2 cells were a low-passaged human cell line from normal human stellate cells that were spontaneously immortalized[8,9]. The cells exhibited typical features of stellate cells and expressed α-SMA under all culture conditions and were regarded as at least partially activated even after immediate replating. LX-2 cells underwent further activation during growth and expansion on plastic surfaces[8].

Human hepatocellular carcinoma cell line HepG2 was purchased from the Chinese Academy of Medical Sciences (Beijing, China). Dulbecco's modified Eagle's medium (DMEM), *L*-glutamine and streptomycin were purchased from Gibco, Invitrogen, Carlsbad, CA. Fetal bovine serum (FBS) was from Hyclone, USA. Penicillin and phenazine methosulfate (PMS) were from Sigma, USA. MTS and oligo $(dT)_{15}$ primers were acquired from Promega, USA. TRIzol reagent and Moloney murine leukemia virus reverse transcriptase (M-MLV RT) were the products of Invitrogen, CA. SYBR Green I was purchased from OPE Technology Development Company, Shanghai, China. Hotstar Taq DNA polymerase was purchased from TW-Biotech, China.

Cell culture and cell proliferation assay

LX-2 cells were cultured in DMEM supplemented with 50 mL/L heat-inactivated FBS, 200 mmol/L *L*-glutamine, 100 U/mL penicillin and 100 μg/mL streptomycin. HepG2 cells were cultured in DMEM containing 100 mL/L FBS, 200 mmol/L *L*-glutamine, 100 U/mL penicillin and 100 μg/mL streptomycin.

MTS assay was used to determine the effect of Cpd 861 on the proliferation of LX-2 and HepG2 cells. In metabolically active cells, MTS was reduced by dehydrogenase enzymes into an aqueous, soluble formazan product. The absorbance was measured directly at 490 nm from 96-well assay plates without additional processing. The quantity of formazan was considered to be directly proportional to the number of viable cells in the culture[10,11].

LX-2 and HepG2 cells were seeded into 96-well tissue culture plates containing 100 μL DMEM containing 50 mL/L FBS (5000 LX-2 cells/well and 8000 HepG2 cells/well). After 24 h of incubation (37 ℃, 50 mL/L CO_2), the medium was carefully removed and 100 μL fresh medium containing various concentrations of Cpd 861 was added into the wells. The cells were treated continuously with Cpd 861 for 1, 2, 3, 5 and 7 d and the medium containing Cpd 861 was changed every other day. At the end of experiments, 20 μL/well of combined MTS/PMS solution was added. After 3 h of incubation at 37 ℃ in a humidified incubator, the absorbance was analyzed on a VERSAmax microplate reader at 490 nm. Absorbance values were the mean±SE of 3 replicates for each treatment. The cells in only controls and compound controls were included.

RNA isolation and reverse transcription

LX-2 cells were seeded into 60 mm dishes in DMEM containing 50 mL/L FBS. After 3 d of seeding, the medium was carefully removed and fresh medium containing Cpd 861 (0.01 mg/mL) was added. After 24, 48 and 72 h of Cpd 861 treatment, total RNA was extracted from LX-2 cells using TRIzol reagent as the lysis buffer. Complementary DNA (cDNA) was synthesized using oligo $(dT)_{15}$ primers and M-MLV RT.

Real-time quantitative PCR using SYBR Green I

After the reverse-transcription reaction, cDNA templates were amplified by quantitative real-time PCR. The reaction was performed using the iCycler iQ real-time PCR detection system (Bio-Rad, USA) with SYBR Green I. Human α-SMA and G3PDH (glyceraldehyde-3-phosphate dehydrogenase) primers were designed using Primer 3 software (Table 1).

Each experiment was performed in 25 μL of reaction volume [1.25 μL of 20× SYBR Green, 1 μL of first strand cDNA (50 ng RNA), 2 μL of each 5 nmolar primer, 0.75 U Hotstar Taq DNA polymerase, 2.5 μL of 10× amplification buffer (Mg^{++} free), 2.5 μL of 25 mmol/L $MgCl_2$, 0.5 μL of 10 mmol/L solution of four dNTP and 15.1 μL of dH_2O]. In the last tube, 1 μL of ddH_2O was added as a non-template control. The conditions of amplification cycles were as follows: 40 cycles consisting of denaturation at 95 ℃ for 40 s, annealing at 59 ℃ (for α-SMA) or at 60 ℃ (for G3PDH) for 40 s, and extension at 72 ℃ for 30 s.

The iCycler apparatus was used to measure the fluorescence of each sample in every cycle at the end of the extension[12]. A series of consecutive 10 fold dilution of α-SMA and G3PDH plasmid DNA ranging from 10^9 copies/μL to 10^3 copies/μL were used as the templates for the standard curves. The iCycler software was used to construct the calibration curve by plotting the Ct (threshold cycle) *vs* the logarithm of the number of copies for each calibrator. The number of copies in unknown samples was calculated by comparing their Cts with the standard calibration curve. The quality and quantities of samples were normalized based on that of G3PDH.

After PCR, a melting curve was obtained by increasing the temperature from 55 ℃ to 95 ℃ with a temperature transition rate of 0.1 ℃/s. The melting curves of all final PCR products were analyzed. The differences in melting temperature of PCR products allowed us to distinguish genuine products from nonspecific products, and primer dimers. To ensure that the correct product was amplified in the reaction, all samples were also separated on 20 g/L agarose gel electrophoresis. All PCR conditions and primers were optimized to produce a single product of the correct basepair size.

Table 1 Oligonucleotide PCR primers for human α-SMA and G3PDH

Oligonucleotide	Oligonucleotide primer sequence	Fragment size
α-SMA		
sense	ACT GGG ACG ACA TGG AAA AG	265 bp
antisense	TAG ATG GGG ACA TTG TGG GT	
G3PDH		
sense	ACC CAG AAG ACT GTG GAT GG	125 bp
antisense	TTC AGC TCA GGG ATG ACC TT	

Statistical analysis

Data were expressed as mean±SE. Statistical analysis was performed using GraphPad Prism (version 3.0) software. The *t* test was used for comparison between the groups. $P<0.05$ was considered statistically significant.

RESULTS

Cell proliferation assay

We examined the effects of Cpd 861 on the proliferation of LX-2 and HepG2 cells (Figures 1, 2). Cells were incubated

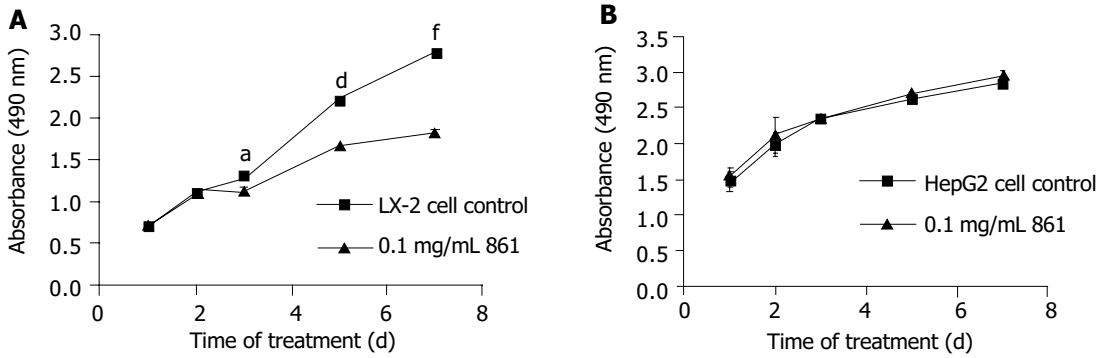

Figure 1 Regulation of proliferation in LX-2 and HepG2 cells by Cpd 861. A: Effect of 0.1 mg/mL Cpd 861 on LX-2 cell proliferation. B: Effect of 0.1 mg/mL Cpd 861 on HepG2 cell proliferation. Data are expressed as the mean±SE of 3 replicates. $^aP<0.05$ *vs* LX-2 cell controls after 3 d of incubation. $^dP<0.01$ *vs* LX-2 cell controls after 5 d of incubation. $^fP<0.01$ *vs* LX-2 cell controls after 7 d of incubation.

with 0.1 mg/mL, 0.03 mg/mL, 0.01 mg/mL and 0.003 mg/mL of Cpd 861 for different days (Figure 1). Cell proliferation was performed by MTS assay. As shown in Figure 2, the effects of Cpd 861 on LX-2 cell proliferation seemed to be correlated with the dose. A significant proliferation inhibition was observed when Cpd 861 concentration was over 0.03 mg/mL (Figure 2). As shown in Figure 1A, 0.1 mg/mL Cpd 861 significantly inhibited LX-2 cell proliferation (15% decrease relative to control, $P<0.05$) after 3 d of incubation. The inhibition effects seemed to increase with the treatment time (25% decrease after 5 d of incubation and 35% decrease after 7 d of incubation, $P<0.01$). The inhibition of cell proliferation Cpd 861 at 0.03 mg/mL concentration was also observed on d 3 (15% decrease relative to control) and on d 5 (21% decrease relative to control) (data not shown), and still could be observed on d 7 (18% decrease relative to control) (Figure 2). However, Cpd 861, at 0.01 mg/mL and 0.003 mg/mL concentrations, did not inhibit LX-2 proliferation evidently. The effects of Cpd 861 on LX-2 cell proliferation seemed low at early time points (on day 1 and day 2). We also examined the effects of Cpd 861 on the proliferation of HepG2 cells. As shown in Figures 1B and 2, Cpd 861 did not affect HepG2 cell proliferation.

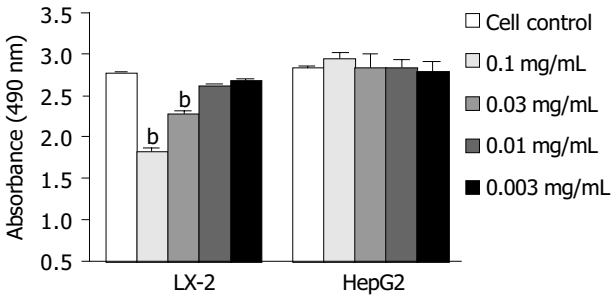

Figure 2 Dose dependent effects of Cpd 861 on cell proliferation in LX-2 and HepG2 7 d after incubation. Data are expressed as the mean±SE of 3 replicates. $^bP<0.01$ *vs* LX-2 cell controls.

Quantification of expression of α-SMA mRNA in Cpd 861-treated LX-2 cells

We examined the effect of Cpd 861 on the expression of α-SMA, a phenotypic marker of activated HSCs. The PCR amp/cycle graph and standard curve graph of α-SMA are shown in Figure 3. The standard curve showed a correlation coefficient

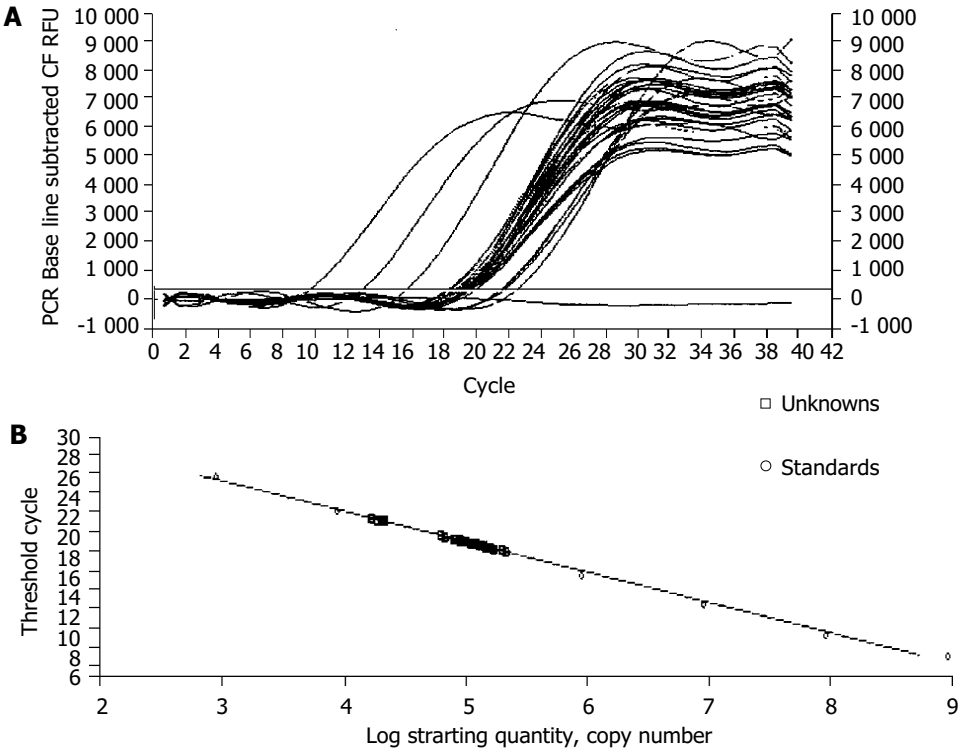

Figure 3 Fluorescence data (A) and standard curve (B) for α-SMA generated on iCycler iQ real-time PCR detection system. Plasmids containing the fragments for α-SMA were diluted from 10^9 to 10^3 copies.

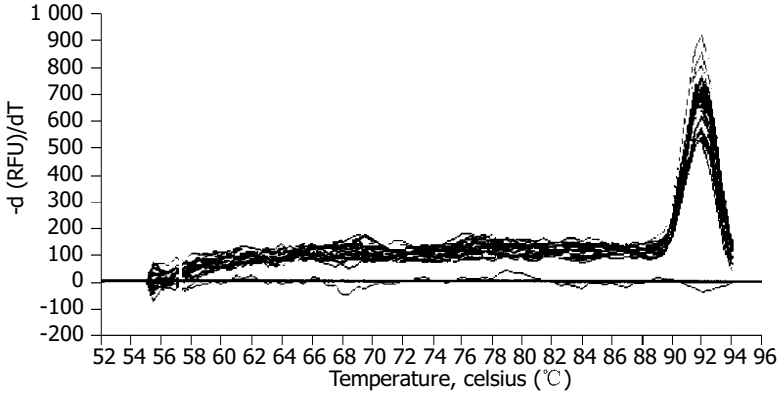

Figure 4 Melting curve for all PCR products after amplification.

>0.99, indicating a precise log-linear relationship. As shown in melt curve graph (Figure 4), single and sharply defined melting curves with narrow peaks were obtained for PCR products of α-SMA gene. Bands visible after electrophoresis on 2% agarose gel and ethidium bromide staining correlated well with the quantitative PCR results. As shown in Figure 5, Cpd 861 could reduce the expression levels of α-SMA in LX-2 cells after treatment. When LX-2 cells were exposed to Cpd 861 for 48 or 72 h, the expression levels of α-SMA decreased significantly (59% decrease relative to control at 48 h, $P<0.05$, and 60% decrease relative to control at 72 h, $P<0.01$) (Figure 5).

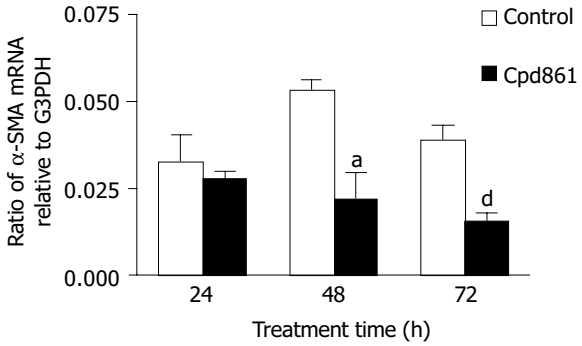

Figure 5 Effects of Cpd 861 on expression of α-SMA mRNA in LX-2 cells. LX-2 cells were incubated with 0.01 mg/mL Cpd 861 for different time. The relative number of molecules of α-SMA mRNA after normalization to G3PDH was calculated. The data represent mean±SE of 4 replicates for each treatment. $^{a}P<0.05$ *vs* LX-2 cell controls after 48 h of incubation. $^{d}P<0.01$ *vs* LX-2 cell controls after 72 h of incubation.

DISCUSSION

In the liver, activated stellate cells are the key mediators of fibrosis[4]. During hepatic fibrogenesis, HSCs undergo an activation process, becoming highly proliferative and α-SMA positive myofibroblast-like cells.

Cpd 861 is an effective herbal compound for treatment of patients with hepatic fibrosis[5]. Its function to effectively reverse hepatic fibrosis has been confirmed by liver biopsies[5-7]. In other studies, data showed that Cpd 861 also could suppress inflammation and fibrogenesis of the liver tissue[7, 13, 14] and reduce expression of collagens and fibrosis related cytokines[14-19]. It could also inhibit rat hepatic stellate cell proliferation in a dose-dependent manner and decrease activation of rat HSCs *in vivo* and *in vitro*[20,21].

Our results suggested that Cpd 861 could significantly inhibit human hepatic stellate cell LX-2 proliferation in a dose-dependant manner when its concentration was over 0.03 mg/mL. The inhibition function increased obviously with the incubation time. However, the results showed that Cpd 861 did not inhibit HepG2 cell proliferation at the same concentration, indicating that Cpd 861 probably could specifically inhibit hepatic stellate cell proliferation, although further study is needed.

RT-PCR is a technique that has been wildly used to quantify physiological changes in gene expression[22]. However, there is lack of accurate quantification in most of the cases[22,23]. Real-time PCR techniques developed during the last decade could offer much more accurate and precise quantitation of DNA and RNA[23,24]. In our study a reliable and accurate real-time PCR method using SYBR Green I technology[25,26] was taken to measure the effects of Cpd 861 on expression of α-SMA mRNA in LX-2 cells. To quantify the number of molecules of α-SMA mRNA, standard curves were constructed with plasmids containing the fragments for α-SMA and G3PDH as the templates. A high linearity was observed over a dynamic range of at least 5 orders of magnitude (from 10^9 to 10^3 copies). All PCR conditions and primers were optimized to produce the target products of the correct basepair size just as shown in melt curves. Quantities of α-SMA were expressed as relative ratio to the copy number of G3PDH. The results indicated that the expression levels of α-SMA mRNA decreased significantly when LX-2 cells were exposed to Cpd 861 at 0.01 mg/mL concentration for 48 or 72 h. Although at the same concentration, Cpd 861 did not inhibit LX-2 cell proliferation.

In conclusion, Cpd 861 can significantly inhibit LX-2 proliferation in a dose-dependant manner when its concentration is over 0.03 mg/mL. Additionally, Cpd 861 can reduce the expression levels of α-SMA mRNA in LX-2 cells and this function seems independent of its effects on inhibition of cell proliferation.

ACKNOWLEDGEMENT

We thank Dr. Friedman and Mount Sinai, School of Medicine, for their help in providing the LX-2 cell line.

REFERENCES

1 **Friedman SL.** Molecular regulation of hepatic fibrosis, an integrated cellular response to tissue injury. *J Biol Chem* 2000; **275**: 2247-2250
2 **Iredale JP**. Hepatic stellate cell behavior during resolution of liver injury. *Semin Liver Dis* 2001; **21**: 427-436
3 **Bataller R,** Brenner DA. Hepatic stellate cells as a target for the treatment of liver fibrosis. *Semin Liver Dis* 2001; **21**: 437-451
4 **Reeves HL,** Friedman SL. Activation of hepatic stellate cells –a key issue in liver fibrosis. *Front Biosci* 2002; **7**: d808-826
5 **Wang BE,** Wang TL, Jia JD, Ma H, Duan ZP, Li XM, Li J, Wang AM, Qian LX. Experiment and clinical study on inhibition and reversion of liver fibrosis with integrated Chinese and Western Medicine. *CJIM* 1999; **5**: 6-11
6 **Yin SS,** Wang BE, Wang TL. The effect of Cpd 861 on chronic hepatitis B related fibrosis and early cirrhosis: A randomized, double blind, placebo controlled clinical trial. *Zhonghua Ganzangbing Zazhi* 2004; **12**: 467-470
7 **Wang TL,** Wang BE, Zhang HH, Liu X, Duan ZP, Zhang J, Ma H, Li XM, Li NZ. Pathological study of the therapeutic effect on HBV –related liver fibrosis with herbal compound 861. *Weichangbingxue He Ganbingxue Zazhi* 1998; **7**: 148-153
8 **Taimr P,** Higuchi H, Kocova E, Rippe RA, Friedman SL**,** Gores GJ. Activated stellate cells express the TRAIL Receptor-2/Death receptor-5 and undergo TRAIL-mediated apoptosis. *Hepatology* 2003; **37**: 87-95
9 **Cao Q,** Mak KM, Ren C, Lieber CS. Leptin stimulates tissue inhibitor of metalloproteinase-1 in human hepatic stellate cells: respective roles of the JAK/STAT and JAK-mediated H2O2-dependant MAPK pathways. *J Biol Chem* 2004; **279**: 4292-4304
10 **Sutherland MW,** Learmonth BA. The tetrazolium dyes MTS and XTT provide new quantitative assays for superoxide and superoxide dismutase. *Free Radic Res* 1997; **27**: 283-289
11 **Dunigan DD,** Waters SB, Owen TC. Aqueous soluble tetrazolium/formazan MTS as an indicator of NADH- and NADPH-dependent dehydrogenase activity. *Biotechniques* 1995; **19**: 640-649
12 **Stagliano KE,** Carchman E, Deb S. Real-time polymerase chain reaction quantitation of relative expression of genes modulated by p53 using SYBR Green I. *Methods Mol Biol* 2003; **234:** 73-91
13 **Zhang FK,** Wang BE, Wang TL, Jia JD, Dong Z, Zhang J. Effect of different pharmaceutics of herbal compound 861 on experimental liver fibrosis. *Zhonghuo Zhongxiyi Jiehe Zazhi* 2000; **10**: 15-16
14 **Jia JD,** Wang BE, Dong Z, Cui L, Zhu JX, Che JT. The effect of herbal compound 861 on mRNA levels for type I, III, and IV collagens and TGF-β in immune complex rat liver fibrosis. *Zhonghua Ganzangbing Zazhi* 1996; **4**: 214-216
15 **Ma H,** Wang BE, Ma XM, Jia JD. Effect of herbal compound

861 on rat hepatic stellate cell collagen synthesis and degradation *in vitro*. *Zhonghua Ganzangbing Zazhi* 1999; **7**(Suppl): 30-32

16 **Ding HG,** Tang SZ, Wang BE, Jia JD, Zhao CH. Effects of herbal compound 861 in hepatic stellate cell expressing endothelin-1 protein and mRNA. *Zhonghua Ganzangbing Zazhi* 2003; **11**: 308

17 **Yin CH,** Ma H, Wang AM, Ma XM, Jia JD, Wang BE. Effect of compound 861 on tissue inhibitor of metalloprotenase 1 gene expression of HSC-T6 cells. *Zhonghua Ganzangbing Zazhi* 2002; **10**: 197-199

18 **Ding HG,** Wang BE, Shang HW. Effect of herbal compound 861 on expression and activity of nitric oxide synthase in hepatic stellate cells. *Zhonghuo Zhongxiyi Jiehe Zazhi* 2002; **22**: 362-364

19 **Yin CH,** Ma H, Wang AM, Ma XM, Jia JD, Wang BE. Effect of compound 861 on stromelysin gene expression of HSC-T6 cell. *Linchuang Ganzangbing Zazhi* 2002; **18**: 168-170

20 **You H,** Wang EN, Wang TL, Ma XM, Zhang J. Proliferation and apoptosis of hepatic stellate cells and effects of compound 861 on liver fibrosis. *Zhonghua Ganzangbing Zazhi* 2000; **8**: 78-80

21 **Ma H,** Wang BE, Ma XM, Jia JD. Effect of compound 861 on hepatic stellate cell proliferation and collagen synthesis. *Zhongguo Linchuang Yaolixue Yu Zhiliaoxue Zazhi* 1998; **3**: 172-175

22 **Wall SJ,** Edwards DR. Quantitative reverse transcription-polymerase chain reaction (RT-PCR): a comparison of primer-dropping, competitive, and real-time RT-PCRs. *Anal Biochem* 2002; **300**: 269–273

23 **Pérez C,** Vandesompele J, Vandenbroucke I, Holtappels G, Speleman F, Gevaert P, Cauwenberge PV, Bachert C. Quantitative real time polymerase chain reaction for measurement of human Interleukin - 5 receptor alpha spliced isoforms mRNA. *BMC Biotechnol* 2003; **3**: 17-23

24 **Ginzinger DG.** Gene quantification using real-time quantitative PCR: an emerging technology hits the mainstream. *Exp Hematol* 2002; **30**: 503-512

25 **Ponchel F,** Toomes C, Bransfield K, Leong FT, Douglas SH, Field SL, Bell SM, Combaret V, Puisieux A, Mighell A, Robinson PA, Inglehearn CF, Isaacs JD, Markham AF. Real-time PCR based on SYBR-Green I fluorescence: An alternative to the TaqMan assay for a relative quantification of gene rearrangements, gene amplifications and micro gene deletions. *BMC Biotechnol* 2003; **3**: 18-31

26 **Ramos-Payan R,** Aguilar-Medina M, Estrada-Parra S, Gonzalez-Y-Merchand JA, Favila-Castillo L, Monroy-Ostria A, Estrada-Garcia IC. Quantification of cytokine gene expression using an economical real-time polymerase chain reaction method based on SYBR Green I. *Scand J Immunol* 2003; **57**: 439-445

Edited by Kumar M and Wang XL **Proofread by** Xu FM

PO Box 2345, Beijing 100023, China
Fax: +86-10-85381893
E-mail: wjg@wjgnet.com www.wjgnet.com

World J Gastroenterol 2004;10(19):2836-2841
World Journal of Gastroenterology
Copyright © 2004 by The WJG Press ISSN 1007-9327

• BASIC RESEARCH •

Tegaserod inhibits noxious rectal distention induced responses and limbic system c-Fos expression in rats with visceral hypersensitivity

Hong-Mei Jiao, Peng-Yan Xie

Hong-Mei Jiao, Peng-Yan Xie, Department of Gastroenterology, First Hospital of Peking University, Beijing 100034, China
Correspondence to: Peng-Yan Xie, Department of Gastroenterology, First Hospital of Peking University, Beijing 100034, China. pengyanx2002@yahoo.com
Telephone: +86-10-66551122 Ext. 2581
Received: 2004-03-15 **Accepted:** 2004-04-17

Abstract

AIM: To examine the effects of tegaserod, a serotonin (5-HT) 4 receptor partial agonist, on abdominal withdrawal reflex (AWR) to rectal distention (RD) and c-Fos expression in limbic system.

METHODS: Neonatal Sprague-Dawley rats randomly received colonic irritation by acetic acid from postnatal day 8 to d 21 as a visceral hypersensitive model (group H) or by intrarectal saline as a control group (group C). When they became adults, rectal distention (RD) was performed by a balloon (6F; Fogarty arterial embolectomy catheter; length, 20 mm; diameter, 2 mm) which was rapidly inflated with increasing volumes of saline (0.4, 0.8 and 1.2 mL) for 20 s at five-minute intervals. Five subgroups of group H (H-saline, H-vehicle, H-Teg0.1, H-Teg0.3 and H-Teg1.0) were injected randomly with saline, vehicle (1-methyl-2-thpyrrolidone) or tegaserod at doses of 0.1, 0.3 and 1.0 mg/kg ip, respectively. Two subgroups of group C (C-Saline and C-Teg1.0) were injected with saline or tegaserod (1.0 mg/kg) ip. RD was performed 10 min after injection, AWR was recorded and c-Fos expression in limbic system was analyzed quantitatively by immunohistochemistry.

RESULTS: Compared to saline, tegaserod significantly inhibited AWR in group H (0.4 mL: from 2.0 to 0.5; 0.8 mL: from 3.5 to 1.5; 1.2 mL: from 4.0 to 3.0, $P<0.01$), but had no significant effect on group C. Tegaserod dose-dependently attenuated the number of c-Fos positive neurons in limbic structures, anterior cingulate cortex (ACC) showed the greatest attenuation. In group H, tegaserod (1.0 mg/kg) resulted in a significant overall decrease to 57% of H-saline (283±41 *vs* 162±16, $P<0.01$), in ACC to 42% of H-saline (72±10 *vs* 31±8, $P<0.01$). In group C, tegaserod (1.0 mg/kg) resulted in an overall decrease to 77% of C-saline (214±13 *vs* 164±22, $P<0.01$), in ACC to 65% of C-saline (48±8 *vs* 31±7, $P<0.01$).

CONCLUSION: Tegaserod inhibits the response to rectal distention in rats with visceral hypersensitivity and dose-dependently attenuates c-Fos expression in limbic system, especially in anterior cingulate cortex.

Jiao HM, Xie PY. Tegaserod inhibits noxious rectal distention induced responses and limbic system c-Fos expression in rats with visceral hypersensitivity. *World J Gastroenterol* 2004; 10(19): 2836-2841
http://www.wjgnet.com/1007-9327/10/2836.asp

INTRODUCTION

Irritable bowel syndrome (IBS) is a common disorder characterized by abdominal pain and altered bowel habits, consisting of constipation, diarrhea, or both. Several pathophysiological mechanisms have been suggested to play a role in the genesis of symptoms in patients with IBS, among others visceral hypersensitivity, autonomic nervous system dysregulation[1], alterations of gastrointestinal (GI) motility[2], and abnormalities in neurotransmitter systems[3]. It has been shown that at least a subgroup of IBS patients shows a hyperalgesic response to visceral stimuli, and discomfort in response to colorectal balloon distension under experimental conditions[3,4]. Abnormalities which upregulate afferent (sensory) signal intensity anywhere in the "brain-gut axis" could induce visceral hypersensitivity[5].

It has been shown in experimental rats that rectal distention is a non-invasive, reproducible visceral stimulus, which can induce a range of pseudoaffective responses, including vasomotor, visceromotor, and respiratory responses[3]. Abdominal withdrawal reflex (AWR) is an involuntary motor reflex similar to the visceromotor reflex[6]. Intestinal distention can be considered to as an appropriate stimulus for studies of visceral nociception[7].

In previous studies, it has been shown that noxious distension of hollow viscera induces a specific pattern of c-Fos expression in rat limbic brain structures[3,8], which involved in higher cognitive functions (*i.e.* emotion, memory, motivation) and led to the perception of visceral pain[9]. Induction of c-Fos expression is a well established marker of neuronal activation, and immunohistological detection of c-Fos-like immunoreactivity allows a mapping of activated brain nuclei on a single cell level[3].

Serotonin (5-HT) is thought to play a role in visceral nociceptive mechanisms. There is considerable evidence that serotonin is involved in the regulation of motility and sensation in the gut[3]. In animal studies, tegaserod was reported to inhibit abdominal contraction response to noxious intestinal distention[10]. Tegaserod, a 5-HT4 receptor partial agonist, could relieve symptoms in irritable bowel syndrome patients with abdominal pain, bloating and constipation[11]. However, little is known about the effect of tegaserod on neuronal activity in limbic structures at noxious rectal distention. Therefore, in the present study, we established a rat model to investigate the role of 5-HT4 receptors in mediating activation of limbic structures at rectal distention, as assessed by c-Fos expression. We aimed to establish a mechanism of the action of 5-HT4 receptors specific to visceral nociceptive neurotransmission.

MATERIALS AND METHODS

Animals

Experiments were performed using Sprague-Dawley rats obtained as preweanling neonates (younger than 8 d) from the Animal Center in the First Hospital of Peking University. Rats were housed in plastic cages containing corn chip bedding and maintained on a 12:12-h light-dark cycle (lights on at 7 AM) at 22 to 23 ℃ and in 60-65% humidity. The irritation procedure and the experimental testing were conducted during the light component of the cycle. The neonates were housed

12 in a cage with their mothers until they were 25 d old. Mothers had access to food and water *ad libitum*. After separation, the rats were housed 4 in a cage with access to food and water *ad libitum*. The animals were deprived of food but water 18 h before rectal distention (RD). Animal care and experimental procedures were followed institutional ethics guidelines and conformed to the requirements of the State Authority for Animal Research Conduct.

Weight

Each rat was weighed every 3 d from days 9 to 40.

Colon irritation

Neonatal Sprague-Dawley rats (8 d old) were divided into 2 groups (group C: control and group H: hypersensitivity) undergoing different treatments. Forty-eight rats in group H received intracolonic injections of 5 mL/L acetic acid (0.5 mL) daily between the ages of 8 and 21 d. Acetic acid was injected into the colon via the PE90 tube inserted to 2 cm from the anus. Twenty-four rats in group C received intracolonic injections of 9 g/L saline (0.5 mL) daily between the ages of 8 and 21 d[12].

Drug administration protocol

Because tegaserod (HTF 919; Novartis Pharma AG, Basel, Switzerland) is poorly soluble in water, the fractions were made up using 0.1 mL of 1-methyl-2-pyrrolidinone (vehicle)[10]. After dissolved in the vehicle, distilled water was added to make the solution up to 0.5 mL. According to the drugs injected intraperitoneally 10 min before RD, 48 rats in group H were divided into 6 subgroups (H0, H-saline, H-vehicle, H-Teg0.1, H-Teg0.3, and H-Teg1.0), and 24 rats in group C were divided into 3 subgroups (C0, C-saline, and C-Teg1.0), eight rats in each subgroup. Rats in group C-saline and H-saline were injected with saline (0.5 mL), in group C-Teg1.0 with tegaserod (1.0 mg/kg), in group H-vehicle with vehicle (0.1 mL and distilled water 0.4 mL) and in group H-Teg0.1, H-Teg0.3, and H-Teg1.0 with tegaserod at a dose of 0.1, 0.3 or 1.0 mg/kg, respectively. Groups H0 and C0 were not distended and only histological examination and myeloperoxidase (MPO) activity assay were done.

Histological examination and myeloperoxidase (MPO) activity assay

Three weeks after cessation of the irritation protocol, in groups H0 and C0, the distal 4-5 cm of the descending colon and rectum was removed and histological analysis and MPO activity assay were performed. MPO activity assay was performed as described previously[13,14]. MPO activity was expressed as U/g protein.

Behavioral testing[6,12]

Behavioral responses to RD were assessed in all groups 3 wk after cessation of the irritation protocol by measuring the abdominal withdrawal reflex (AWR) using a semiquantitative score. AWR is an involuntary motor reflex similar to the visceromotor reflex. However, the advantage of AWR over the visceromotor reflex is that the latter requires additional surgery to implant recording electrodes and wires in the abdominal muscles, which may cause additional sensitization in an already sensitized system. Distention balloons (described below) were placed in the rectum of lightly sedated adult rats (ether) and secured by taping the attached tube to the rat's tail. The rats were then housed in small Lucite cubicles (20 cm×8 cm×8 cm) on an elevated Plexiglas platform and allowed to wake up and adapt (20 min). Measurement of the AWR consisted of visual observation of animal response to graded RD (0.4, 0.8 and 1.2 mL) by blinded observers and assignment of AWR scores: 0, no behavioral response to RD; 1, brief head movement followed by immobility; 2, contraction of abdominal muscles; 3, lifting of abdomen; 4, body arching and lifting of pelvic structures. The rats were given RD for 20 s every 5 min. To achieve an accurate measure, distensions were repeated 5 times for each volume. The data for each animal were averaged for analysis. The results obtained were compared among groups. A change in the magnitude of an evoked response indicated a change in visceral pain processing.

Colon stimuli [12]

Colon stimulation consisted of graded RD produced by inflating a balloon inside the rectum. The balloon, 2 cm in length and 2 mm in diameter (6F, Fogarty arterial embolectomy catheter, Baxter, USA), was carefully inserted intrarectally and fixed at a distance of 1 cm with an adhesive tape at the tail of the rat. Distension was produced by rapidly inflating the balloon to the desired volumes with saline (0.4, 0.8 or 1.2 mL) for 20 s at 5-min intervals. Before they were used, the balloons were blown up and left overnight so the latex stretched and the balloons became compliant. Tegaserod (0.1, 0.3 or 1.0 mg/kg) or saline or vehicle was administered 10 min prior to RD. Only a single dose was tested in each animal.

c-Fos immunohistochemistry[15]

Within 30 min following the end of the distention procedure, the animals were deeply anesthetized with an overdose of sodium pentobarbitone (60 mg/kg intraperitoneally) and then perfused through the ascending aorta with saline (9 g/L), followed by 500 mL of cold 0.1 mol/L phosphate buffer (PB, 4 ℃) containing 40 g/L paraformaldehyde (pH 7.4). The brain was immediately removed and postfixed in the same fixative at 4 ℃ overnight, and then placed in 300 g/L sucrose with 0.1 mol/L PB for 72 h at 4 ℃. Coronal sections (40 μm thick) were cut from frozen blocks at the levels of brain regions of interest (1.5 mm to 5 mm posterior to bregma, according to the atlas of Paxinos and Watson). Every fifth section was stained for c-Fos-like immunoreactivity (c-Fos-ir) using the method of free floating for immunohistochemistry. Briefly, sections were first washed 3 times in phosphate buffered saline plus 3 g/L Triton X-100 (PBS-T) (5 min each time) at room temperature, and incubated for 10 min with PBS-T containing 50 mL/L normal goat serum to block nonspecific binding sites and facilitate tissue penetration. Then sections were washed with PBS-T and incubated for 24 h at room temperature with PBS-T containing rabbit polyclonal anti-Fos protein antiserum (Zhongshan, China) (diluted 1:200). After washed with PBS-T, sections were incubated with biotinylated anti-rabbit IgG (1:300, Zhongshan, China) for 120 min. The sections were then incubated with strepta-vidin-peroxidase conjugate (1:300) for 120 min and subsequently visualized using diaminobenzidine (DAB) as chromogen. Sections were mounted on gelatin-coated glass slides, air dried, dehydrated in ethanol, and xylene, then coverslipped with DePeX. Brain sections were examined using bright-field microscopy. The same lot of antibody was used for each study outlined below. The primary c-Fos antibody was omitted in one well of each immunohistological reaction as a negative control. In each study, every staining process included free-floating sections of all groups using the same buffers and solutions.

Fos-like immunoreactive nuclei

The number of c-Fos-like immunoreactive (c-Fos-ir) nuclei was counted in 5 sections of each rat as identified by morphology using an image analysis package (Leica Q550CW running QWIN software; Leica UK Ltd, Milton Keynes, UK). In the anterior cingulate cortex (ACC), thalamus (TH), hippocampus (HP), hypothalamus (HypoTH) and amygdala (Amy), c-Fos-ir nuclei were counted individually and expressed as the number per 600×500 pixel. All brain regions were counted bilaterally in

each section. The total number of c-Fos-ir nuclei in five sections was used for subsequent data analysis. The counts comprising all those nuclear immunoreactive signals could be clearly distinguished from the background.

Data and statistical analysis

Statistical analysis was done using SPSS for windows 11.0. The results of weight, MPO activity and the number of c-Fos-ir were expressed as mean±SD, and statistical significances were determined using Student's paired *t* test or one way analysis of variance (ANOVA), followed by Dunnett's post hoc test. The median values of the AWR scores among all groups at each volume of RD were compared using the Mann-Whitney *U*-test. $P<0.05$ was considered statistically significant.

RESULTS

Comparision of body masses of rats in each group

Masses on d 9 and 40 were not statistically different between groups H and C (18.9±3.2 g *vs* 19.6±3.2 g, 154.4±12.7 g *vs* 149.3±16.5 g, respectively). The model did not alter the growth rate of the rats.

Histological analysis and MPO activity assay

The identifiable histopathology was absent in the adult colons. The tissues showed no significant structural damage or loss of crypts. Mucin depletion or increase in intraepithelial lymphocytes was not seen in any of the tissues examined. MPO activity was not statistically different between groups H and C (20.49±1.64 U/g protein and 17.49±6.35 U/g protein, respectively).

Table 1 AWR scores in group H (median, min-max) (n = 8)

	0.4 mL	0.8 mL	1.2 mL
H-saline	2.0 (1-3)	3.5 (3-4)	4.0 (4-4)
H-vehicle	2.0 (0-3)	3.0 (2-4)	4.0 (3-4)
H-Teg0.1	1.0 (0-2)^b	2.0 (1-3)$^{a, b}$	3.0 (3-4)^{a,b}
H-Teg0.3	1.0 (0-1)^b	1.5 (0-3)^b	3.0 (3-4)^{a,b}
H-Teg1.0	0.5 (0-1)^b	1.5 (1-2)^b	3.0 (1-3)^b

$^bP<0.01$ *vs* H-saline; Difference between H-Teg0.1and H-Teg0.3 was not significant at all volumes; $^aP<0.05$ H-Teg0.1, H-Teg0.3 *vs* H-Teg1.0.

Table 2 AWR scores in group C (median, min-max, n = 8)

	0.4 mL	0.8 mL	1.2 mL
C-saline	1.0 (0-2)	2.5 (2-3)	3.0 (3-4)
C-Teg1.0	0.0 (0-2)	2.0 (2-2)	3.0 (3-4)
Z value	1.465	2.236	0
P value	0.195	0.105	1.000

The differences between C-saline and C-Teg1.0 were not significant at all volumes.

Comparison of tegaserod effects on AWR (Tables 1, 2)

H-saline *vs* C-saline Median AWR scores at volumes of 0.4, 0.8, and 1.2 mL were significantly higher in H-saline than in C-saline (2.0, 3.5, and 4.0, *vs* 1.0, 2.5, and 4.0, respectively) ($P<0.05$). These results suggested that the model of visceral hypersensitivity in this study was reliable (Figure 1A).

AWR in subgroups of group H Median AWR scores were similar in H-saline and in H-vehicle, so the effect of vehicle could be negligible. AWR scores were significantly higher in H-saline than in H-Teg0.1, H-Teg0.3, and H-Teg1.0. The 5-HT4 receptor agonist tegaserod (0.1, 0.3, and 1.0 mg/kg) significantly inhibited the response to rectal distention in rats with hypersensitivity ($P<0.01$). The difference between H-Teg0.1 and H-Teg0.3 was not significant at all volumes. The difference between H-Teg0.1 and H-Teg1.0 was significant at the volumes of 0.8 mL and 1.2 mL ($P<0.05$). The difference between H-Teg0.3 and H-Teg1.0 was significant only at 1.2 mL ($P<0.05$). At the volume of 0.4 mL, differences of AWR scores in H-Teg0.1, H-Teg0.3, and H-Teg1.0 were not significant (Figure 1B, Table 1).

C-saline *vs* C-Teg1.0 Median AWR scores were similar in C-saline and in C-Teg1.0 at all volumes. These results suggested that tegaserod (1.0 mg/kg) had little effect on the AWR response to RD in control rats (Figure 1C, Table 2).

C-Teg1.0 *vs* H-Teg1.0 At 1.2 mL, AWR scores were higher in C-Teg1.0 than in H -Teg1.0 ($P<0.05$). While at 0.4 mL and 0.8 mL, the differences between H-Teg1.0 and C-Teg1.0 were not significant. It seemed that the inhibitory effect on AWR at largest volume (1.2 mL) was stronger in hypersensitive condition than in normal condition (Figure 1D).

Table 3 Number of c-Fos positive neurons in limbic structures in group H (mean±SD, n = 8)

	ACC	Hippocampus	HypoTH	Amygdala	Thalamus	Overall
H-saline	72±10	54±13	51±17	44±16	62±19	283±41
H-vehicle	72±10	54±13	49±15	43±15	62±19	281±37
H-Teg0.1	53±14^b	48±10	47±13	42±11	50±13	239±31^a
H-Teg0.3	40±11^b	45±7	41±11^a	37±11	45±11^a	208±25^b
H-Teg1.0	31±8^b	36±9^b	31±10^b	30±8^b	34±10^b	162±16^b
F value	60.583	11.605	8.199	5.362	14.574	61.989
P value	0.000	0.000	0.000	0.000	0.000	0.000

$^aP<0.05$, $^bP<0.01$ *vs* H-saline.

Table 4 Number of c-Fos positive neurons in limbic structures in group C (mean±SD, n = 8)

	ACC	Hippocampus	HypoTH	Amygdala	Thalamus	Overall
C-saline	48±8	46±7	36±8	39±7	45±11	214±13
C-Teg1.0	31±7^b	36±8^b	30±9	33±10	34±7^a	164±22^b

$^aP<0.05$, $^bP<0.01$ *vs* C-saline.

Comparison of tegaserod effects on c-Fos expression in limbic structures (Tables 3, 4)

Repetitive RD significantly induced changes in neuronal activity in all animals, as determined by increased density of c-Fos-ir cells (Figure 2). c-Fos expression was located bilaterally in discrete areas of limbic structures. The overall number of c-Fos-ir cells in H-saline was significantly more than that in C-saline (283±41 *vs* 214±13, $P<0.001$), but the difference was not significant in hippocampus (54±13 *vs* 46±7, $P = 0.374$). Tegaserod given ip 10 min prior to RD produced a significant, dose-dependent attenuation in the total number of c-Fos-ir nuclei in limbic brain compared with saline. These effects were especially clear in anterior cingulate cortex (ACC). In the hippocampus and amygdala, the effect of tegaserod was significant only at the high-dose (1.0 mg/kg). Tegaserod (0.1 mg/kg) decreased the overall c-Fos-ir to 85% of saline ($P<0.05$). The greatest attenuation was in ACC (74% of H-saline), while amygdala was least affected (95% of H-saline). Tegaserod (0.3 mg/kg) significantly attenuated c-Fos expression in ACC, hypothalamus, and thalamus (to 56%, 80% and 73% of saline, respectively). A high dose of tegaserod (1.0 mg/kg) resulted in a significant ($P<0.01$) overall decrease of c-Fos in five areas, the overall number was decreased to 57% of saline. Similar to the low dose, ACC showed the greatest attenuation (42% of H-saline), while other regions were decreased to approximately 60% of H-saline (Figure 3A).

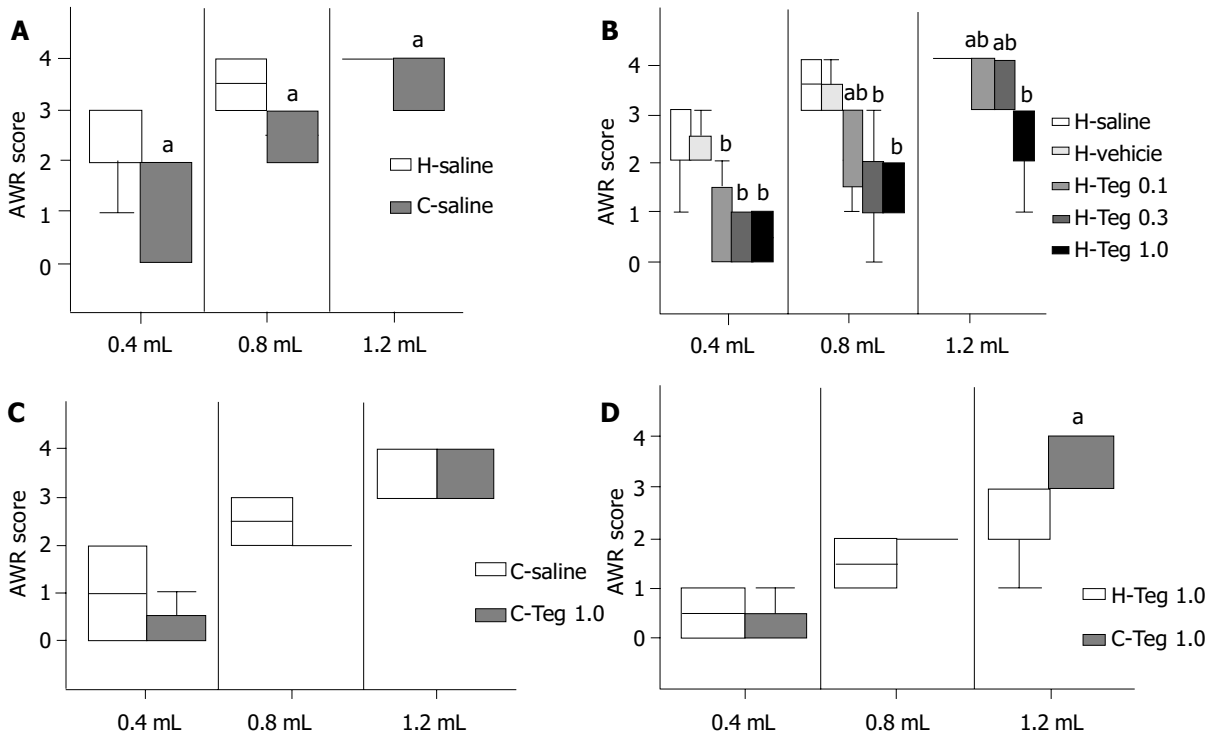

Figure 1 AWR scores of H-saline and C-saline, group H, group C, H-Teg1.0 and C-Teg1.0, [a]$P<0.05$; [b]$P<0.01$. A: AWR scores of H-saline and C-saline. B: AWR scores of group H. C: AWR scores of group C. D: AWR scores of H-Teg1.0 and C-Teg1.0.

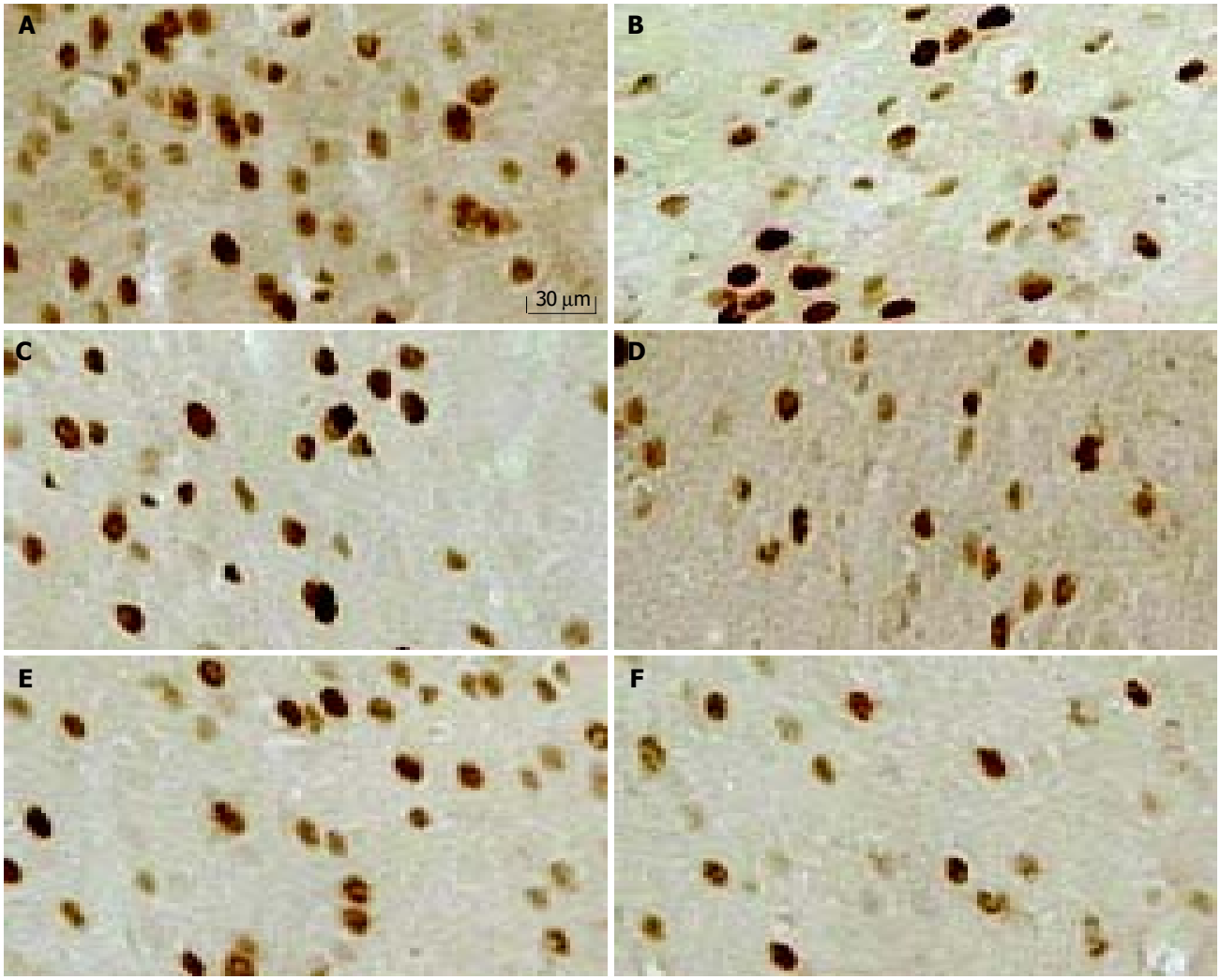

Figure 2 c-Fos-ir nuclei in anterior cingulate cortex (ACC) (200×). A: H-saline; B: H-Teg0.1; C: H-Teg0.3; D: H-Teg1.0; E: C-saline; F: C-Teg1.0.

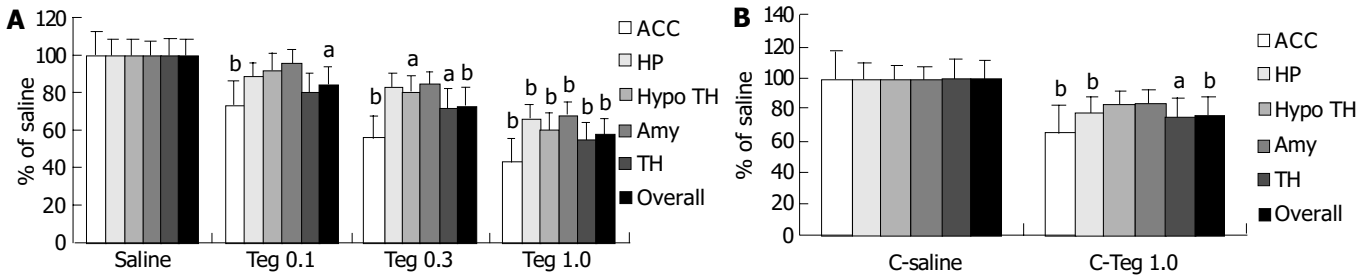

Figure 3 Number of overall c-Fos-ir nuclei and in each of the 5 areas as a percent of H-saline and C-saline. A: Number of overall c-Fos-ir nuclei and in each of the 5 areas as a percent of H-saline. B: Number of overall c-Fos-ir nuclei and in each of the 5 areas as a percent of C-saline.

In group C, although the inhibitory effect of tegaserod on AWR was not significant, the attenuation effect on c-Fos expression was also observered. Tegaserod (1.0 mg/kg) resulted in a significant overall decrease in c-Fos to 77% of C-saline. Similarly, ACC also was the greatest attenuation (65% of C-saline). In addition, tegaserod could decrease c-Fos in thalamus and hippocampus (76% and 78% of C-saline, respectively) (Figure 3B).

DISCUSSION

Experimental data suggested that patients with IBS had visceral sensory dysfunction so that physiological stimuli could induce their symptoms. Visceral afferent input is modulated by a variety of mechanisms operating between the gastrointestinal tract and the brain, and dysfunction of these regulatory mechanisms could distort gastrointestinal perception[16]. Intestinal discomfort reaches awareness via neural connections termed the "brain-gut axis". Abnormalities which upregulate afferent (sensory) signal intensity anywhere in this system could induce hypersensitivity, pain, and discomfort. Several features of IBS suggest involvement of the brain's emotional limbic system, such as higher prevalence of anxiety and psychosocial stressors, augmented intestinal and stress responses and response to centrally acting medication. Recent brain imaging data suggested that pathways involved in visceral pain perception overlapped with limbic pathway[17,18]. In the brain, increased thalamic activation has been seen in IBS, which could indicate increased afferent output from lower levels. Activation of the anterior cingulate cortex, the limbic center that encodes pain suffering, appeared to be enhanced in IBS, especially under the influence of anxiety[5].

Colonic irritation with acetic acid in neonatal rats could lead to a state of chronic visceral hypersensitivity in adults[19-21]. This model did not alter the growth rate of the rats. This hypersensitivity occurs in the absence of identifiable histopathology in the adult colon and does not change MPO activity of colonic tissue. Myeloperoxidase (MPO), a hydrogen peroxide (H_2O_2) oxidoreductase, is specifically found in mammalian granulocytic leukocytes, including polymorphonuclear leukocytes (PMNs), monocytes, basophils and eosinophils. MPO activity has been widely accepted as an enzyme marker to measure and quantitate the PMN content in a variety of tissues. It has been suggested that measurement of MPO provides a simple and specific method to quantitate PMN accumulation or infiltration in a variety of pathological processes accompanied with inflammation[22].

5-HT4 receptors have been found to be involved in regulating the sensitivity of rectal mechanoreceptive afferents[23]. Tegaserod is a 5-HT4 receptor partial agonist with a relatively long half-life (approximate 11 h in dogs and humans)[24]. It could dose-dependently inhibit the abdominal contraction response to noxious intestinal distention not linked to alterations in compliance[10]. In our study, in rats with hypersensitivity but not in control rats, tegaserod potently inhibited AWR at all volumes of distention. It seemed that the inhibitory effect on AWR at the highest volume (1.2 mL) was more powerful in hypersensitive condition than in normal condition. The results are inconsistent with the study of Coelho *et al.*[10]. Two reasons may have been responsible for these phenomena. One reason might be that the patterns of intestinal distention were different. In the study of Coelho *et al.*, the balloon was an inflated 5 min step of 15 mmHg, from 0 to 60 mmHg. The other reason might be that 5-HT4 receptors played a relatively modest role in modulating visceral sensation under basal physiological condition[25]. Thus, we tentatively suggest that the number of 5-HT4 receptors may be upregulated and/or the effect followed by the activity of 5-HT4 receptor may be increased under hypersensitive status. The exact mechanisms of its action need to be further researched.

c-fos, an immediate-early gene, could be expressed within the neurons following voltage-gated calcium entry into the cells[26]. *c-fos* was induced by noxious stimulus, generally as the result of an injury[27]. c-Fos protein encoded by *c-fos*, has been regarded as a third messenger molecule which couples the short term extracellular signals with the long term alteration in cell function when neurons are excited[28]. c-Fos could be interpreted as an increase in activity of those neurons expressing the protein[27], so it is usually used as a marker to indicate the activation of neurons[29]. Following injury there was a correlation between the expression of c-Fos and magnitude of hyperalgesia, and c-Fos expression following noxious intensities of intestinal distention could reflect the intensity of stimuli and the degree of discomfort[27]. Previous study has demonstrated that c-Fos is expressed in limbic brain structures in response to noxious rectal distention[9]. Limbic structures play an important role in visceral pain processing. The present report provided quantitative data on expression of c-Fos protein induced by rectal distention and the effect of tegaserod at different doses on c-Fos expression in brain nuclei, such as hypothalamus, thalamus, amygdala, hippocampus, and anterior cingulate cortex following noxious rectal distension. Functional brain imaging researches have demonstrated that colorectal distention could cause abnormal activation in ACC[17] and thalamus in IBS patients compared with control[17,18]. From our results, we conclude that tegaserod dose-dependently attenuates c-Fos expression in limbic structures. Especially in ACC and thalamus, the effect of tegaserod is more evident. This may do good for IBS patients.

5-HT4 receptors are widely distributed in peripheral and central sites. In gut, 5-HT4 receptors are located primarily on the enterochromaffin cells and less on smooth muscle cells, enterocytes, and neurons[24]. 5-HT4 receptors are highly expressed in several brain regions, such as limbic areas, periaqueductal grey matter and sensory terminals[30] and in spinal cord and dorsal root ganglion neurons[25]. The site of action of tegaserod was not established in the present study, but could be at the level of enteric or primary sensory neurons,

or via spinal or supraspinal neuronal circuits concerned with the modulation of nociceptive transmission. A study by Schikowski *et al*.[23] demonstrated that tegaserod might have a direct effect on the mechanoreceptive afferents. We supposed that 5-HT4 receptors might directly decrease the signals ascending to the central nervous system (CNS) or might decrease the activity of CNS (as demonstrated by c-Fos-ir nuclei), which would benefit for IBS patients. Little is known about the effect of tegaserod on response following intracerebroventricular injection. Further studies are needed to determine the central action of 5-HT4 receptors.

In conclusion, tegaserod inhibits response to noxious distention, and the effect is more evident in hypersensitive condition than in control. Tegaserod dose-dependently attenuates c-Fos expression in limbic structures, especially in anterior cingulate cortex. Therefore, tegaserod decreases central sensitization. Tegaserod may be of potential use in the treatment of visceral pains.

ACKNOWLEDGMENTS

The authors are grateful to Professor Xin-Guang Liu and Hua-Hong Wang for advice, and to Novartis Pharmaceuticals Corp for providing the drugs for this study.

REFERENCES

1 **Tougas G**. Irritable bowel syndrome: new approaches to its pharmacological management. *Can J Gastroenterol* 2001; **15** (Suppl B): 12B-13B

2 **Monnikes H**, Tebbe JJ, Hildebrandt M, Arck P, Osmanoglou E, Rose M, Klapp BF, Wiedenmann B, Heymann-Monnikes I. Role of stress in functional gastrointestinal disorders. Evidence for stress-induced alterations in gastrointestinal motility and sensitivity. *Dig Dis* 2001; **19**: 201-211

3 **Monnikes H,** Ruter J, Konig M, Grote C, Kobelt P, Klapp BF, Arnold R, Wiedenmann B, Tebbe JJ. Differential induction of c-fos expression in brain nuclei by noxious and non-noxious colonic distension: role of afferent C-fibers and 5-HT3 receptors. *Brain Res* 2003; **966**: 253-264

4 **Miura M**, Lawson DC, Clary EM, Mangel AW, Pappas TN. Central modulation of rectal distension-induced blood pressure changes by alosetron, a 5-HT3 receptor antagonist. *Dig Dis Sci* 1999; **44**: 20-24

5 **Mertz H.** Role of the brain and sensory pathways in gastrointestinal sensory disorders in humans. *Gut* 2002; **51**(Suppl 1): i29-i33

6 **Al-Chaer ED,** Kawasaki M, Pasricha PJ. A new model of chronic visceral hypersensitivity in adult rats induced by colon irritation during postnatal development. *Gastroenterology* 2000; **119:** 1276-1285

7 **Ness TJ**. Intravenous lidocaine inhibits visceral nociceptive reflexes and spinal neurons in the rat. *Anesthesiology* 2000; **92**: 1685-1691

8 **Monnikes H**, Lauer G, Arnold R. Peripheral administration of cholecystokinin activates c-fos expression in the locus coeruleus/subcoeruleus nucleus, dorsal vagal complex and paraventricular nucleus via capsaicin-sensitive vagal afferents and CCK-A receptors in the rat. *Brain Res* 1997; **770**: 277-288

9 **Traub RJ,** Silva E, Gebhart GF, Solodkin A. Noxious colorectal distention induced-c-Fos protein in limbic brain structures in the rat. *Neurosci Lett* 1996; **215**: 165-168

10 **Coelho AM,** Rovira P, Fioramonti J, Bueno L. Antinociceptive properties of HTF 919 (Tegaserod), a 5-HT4 receptor partial agonist, on colorectal distension in rats. *Gastroenterology* 2000; **118**(4 Suppl 2): A835

11 **Muller-Lissner SA,** Fumagalli I, Bardhan KD, Pace F, Pecher E, Nault B, Ruegg P. Tegaserod, a 5-HT4 receptor partial agonist, relieves symptoms in irritable bowel syndrome patients with abdominal pain, bloating and constipation. *Aliment Pharmacol Ther* 2001; **15**: 1655-1666

12 **Liu YB,** Yuan YZ, Tao RJ, Zhai ZK, Chen HZ. Establishment of a rat model of gut hypersensitivity and for evaluation of visceral sensitivity. *Chin J Dig* 2003; **23**: 34-37

13 **Al-Awadi FM,** Khan I. Studies on purine enzymes in experimental colitis. *Mol Cell Biochem* 1999; **194**: 17-22

14 **Bradford MM.** A rapid and sensitive method for the quantitation of microgram quantities of protein utilizing the principle of protein-dye binding. *Anal Biochem* 1976; **72**: 248-254

15 **Chowdhury GM,** Fujioka T, Nakamura S. Induction and adaptation of Fos expression in the rat brain by two types of acute restraint stress. *Brain Res Bull* 2000; **52**: 171-182

16 **Azpiroz F.** Hypersensitivity in functional gastrointestinal disorders. *Gut* 2002; **51**(Suppl 1): i25-i28

17 **Mertz H,** Margan V, Tanner G, Pickens D, Price R, Shyr Y, Kessler R. Regional cerebral activation in irritable bowel syndrome and control subjects with painful and nonpainful rectal distention. *Gastroenterology* 2000; **118**: 842-848

18 **Yuan YZ,** Tao RJ, Xu B, Sun J, Chen KM, Miao F, Zhang ZW, Xu JY. Functional brain imaging in irritable bowel syndrome with rectal b alloon-distention by using fMRI. *World J Gastroenterol* 2003; **9**: 1356-1360

19 **Lin C**, Al-Chaer ED. Long-term sensitization of primary afferents in adult rats exposed to neonatal colon pain. *Brain Res* 2003; **971**: 73-82

20 **Lidow MS**, Song ZM, Ren K. Long-term effects of short-lasting early local inflammatory insult. *Neuroreport* 2001; **12**: 399-403

21 **Ruda MA**, Ling QD, Hohmann AG, Peng YB, Tachibana T. Altered nociceptive neuronal circuits after neonatal periphera inflammation. *Science* 2000; **289**: 628-631

22 **Xia Y,** Zweier JL. Measurement of myeloperoxidase in leukocyte-containing tissues. *Anal Biochem* 1997; **245**: 93-96

23 **Schikowski A,** Thewissen M, Mathis C, Ross HG, Enck P. Serotonin type-4 receptors modulate the sensitivity of intramural mechanoreceptive afferents of the cat rectum. *Neurogastroenterol Motil* 2002; **14**: 221-227

24 **Lacy BE,** Yu S. Tegaserod: a new 5-HT4 agonist. *J Clin Gastroenterol* 2002; **34**: 27-33

25 **Bharucha AE,** Camilleri M, Haydock S, Ferber I, Burton D, Cooper S, Tompson D, Fitzpatrick K, Higgins R, Zinsmeister AR. Effects of a serotonin 5-HT(4) receptor antagonist SB-207266 on gastrointestinal motor and sensory function in humans. *Gut* 2000; **47**: 667-674

26 **Premkumar DR,** Adhikary G, Overholt JL, Simonson MS, Cherniack NS, Prabhakar NR. Intracellular pathways linking hypoxia to activation of c-fos and AP-1. *Adv Exp Med Biol* 2000; **475**: 101-109

27 **Traub RJ,** Stitt S, Gebhart GF. Attenuation of c-Fos expression in the rat lumbosacral spinal cord by morphine or tramadol following noxious colorectal distention. *Brain Res* 1995; **701**: 175-182

28 **Saria A,** Fischer HS, Humpel C, Pfattner A, Schatz DS, Schuligoi R. Margatoxin and iberiotoxin, two selective potassium channel inhibitors, induce c-fos like protein and mRNA in rat organotypic dorsal striatal slices. *Amino Acids* 2000; **19**: 23-31

29 **Harris JA.** Using c-fos as a neural marker of pain. *Brain Res Bull* 1998; **45**: 1-8

30 **Espejo EF,** Gil E. Antagonism of peripheral 5-HT4 receptors reduces visceral and cutaneous pain in mice, and induces visceral analgesia after simultaneous inactivation of 5-HT3 receptors. *Brain Res* 1998; **788**: 20-24

Edited by Kumar M and Wang XL **Proofread by** Xu FM

PO Box 2345, Beijing 100023, China
Fax: +86-10-85381893
E-mail: wjg@wjgnet.com www.wjgnet.com

World J Gastroenterol 2004;10(19):2842-2845
World Journal of Gastroenterology
Copyright © 2004 by The WJG Press ISSN 1007-9327

• BASIC RESEARCH •

Inhibitory effects of berberine on ion channels of rat hepatocytes

Fang Wang, Hong-Yi Zhou, Gang Zhao, Li-Ying Fu, Lan Cheng, Jian-Guo Chen, Wei-Xing Yao

Fang Wang, Hong-Yi Zhou, Li-Ying Fu, Lan Cheng, Jian-Guo Chen, Wei-Xing Yao, Department of Pharmacology, Tongji Medical College of Huazhong University of Science and Technology, Wuhan 430030, Hubei Province, China
Gang Zhao, Pancreatic Surgery Center, Union Hospital, Tongji Medical College of Huazhong University of Science and Technology, Wuhan 430022, Hubei Province, China
Correspondence to: Dr. Fang Wang, Department of Pharmacology, Tongji Medical College of Huazhong University of Science and Technology, Wuhan 430030, Hubei Province, China. wangfang0322@yahoo.com.cn
Telephone: +86-27-83691760
Received: 2004-02-03 **Accepted:** 2004-02-18

Abstract

AIM: To examine the effects of berberine, an isoquinoline alkaloid with a long history used as a tonic remedy for liver and heart, on ion channels of isolated rat hepatocytes.

METHODS: Tight-seal whole-cell patch-clamp techniques were performed to investigate the effects of berberine on the delayed outward potassium currents (I_K), inward rectifier potassium currents (I_{K1}) and Ca^{2+} release-activated Ca^{2+} currents (I_{CRAC}) in enzymatically isolated rat hepatocytes.

RESULTS: Berberine 1-300 μmol/L reduced I_K in a concentration-dependent manner with EC_{50} of 38.86±5.37 μmol/L and n_H of 0.82±0.05 (n = 8). When the bath solution was changed to tetraethylammonium (TEA) 8 mmol/L, I_K was inhibited. Berberine 30 μmol/L reduced I_K at all examined membrane potentials, especially at potentials positive to +60 mV (n = 8, P<0.05 or P<0.01 *vs* control). Berberine had mild inhibitory effects on I_{K1} in rat hepatocytes. Berberine 1-300 μmol/L also inhibited I_{CRAC} in a concentration-dependent fashion. The fitting parameters were EC_{50} = 47.20±10.86 μmol/L, n_H = 0.71±0.09 (n = 8). The peak value of I_{CRAC} in the I-V relationship was decreased by berberine 30 μmol/L at potential negative to -80 mV (n = 8, P<0.05 *vs* control). But the reverse potential of I_{CRAC} occurred at voltage 0 mV in all cells.

CONCLUSION: Berberine has inhibitory effects on potassium and calcium currents in isolated rat hepatocytes, which may be involved in hepatoprotection.

Wang F, Zhou HY, Zhao G, Fu LY, Cheng L, Chen JG, Yao WX. Inhibitory effects of berberine on ion channels of rat hepatocytes. *World J Gastroenterol* 2004; 10(19): 2842-2845
http://www.wjgnet.com/1007-9327/10/2842.asp

INTRODUCTION

Many natural drugs for liver diseases are currently used in popular medicine. For example, quaternary protoberberine alkaloids from *Flissitigma* and *Goniothalamus* have been used in popular medicine for hepatomegaly and hepatosplenomegaly[1,2]. The use of alkaloids from *Berberis aristata* for liver injury induced by chemical carcinogenesis and alkaloids from *Enantica* for disorders of bilirubin has also been reported[3,4].

Berberine is an isoquinoline alkaloid with a long history in both Ayurvedic and Chinese medicine. It exists in *Hydrastis canadensis* (golden seal), *Coptis chinensis* (Coptis or golden thread), *Berberis aquifolium* (Oregon grape), *Berberis vulgaris* (barberry), and *Berberis aristata* (tree turmeric). Berberine alkaloid can be found in roots, rhizomes, and stem bark of plants[5]. Berberine has been extensively studied and is known to exhibit multiple pharmacological activities such as antiprotozoal, antihypertensive[6], antibacterial[7], anti-inflammatory, anticholinergic[8] and antiarrhythmic activities[9]. Hwang *et al*. reported that berberine inhibited hepatotoxicity induced by *tert*-butyl hydroperoxide (*t*-BHP) via its antioxidant potential and could function as a chemopreventive agent in living systems[10]. Previous studies have shown that berberine could block delayed rectifier potassium currents, inward rectifier potassium currents (I_{K1}) and L-type calcium currents ($I_{Ca,L}$) in guinea pig ventricular myocytes[11,12]. So far, however, its hepatoprotective mechanism still remains unknown. No data are available on the relationship between ion currents in hepatocytes and the hepatoprotective effect of berberine.

Therefore, this study used patch-clamp techniques to record the whole-cell currents in isolated rat hepatocytes in order to investigate the hepatoprotective mechanism of berberine.

MATERIALS AND METHODS

Cell preparation

Rat hepatocytes were enzymatically isolated from Sprague-Dawley (SD) rats of either sex (150-200 g) by using slightly modified procedures described previously[13]. Briefly, adult animals were anesthetized with an intraperitoneal injection of pentobarbital sodium (30 mg/kg) in strict accordance to the guidelines established by the Institutional Animal Care and Use Committee, which follow all applicable state and federal laws. Portal vein and inferior vena cava were cannulated. The liver was initially perfused at a flow rate of 25 mL/min via a constant-flow system with modified oxygenated Ca^{2+}, Mg^{2+}-free Hanks' solution for several minutes, followed by perfusion with a Ca^{2+}, Mg^{2+}-free Hanks' solution containing collagenase (0.3 g/L, type I) for 10 min. The solutions were gassed with 950 mL/L O_2+50 mL/L CO_2 and heated to 37 ℃. After these perfusions, the liver was excised and then minced in Ca^{2+}, Mg^{2+}-free Hanks' solution at 0 ℃. The cells were filtered through a 200 μm nylon mesh, and washed 3 times by centrifugation at 50 g for 2 min. The cell pellets were resuspended in KB medium that yielded approximately 85% to 95% viable hepatocytes. A small aliquot of the medium containing single cells was transferred into a 1-mL chamber mounted on the stage of an inverted microscope (IX-70, Olympus, Japan). Spherical and smooth cells were used for the whole-cell patch-clamp studies. All experiments were performed at room temperature (20 ℃ to 22 ℃).

Voltage-clamp recording

A programmable vertical puller (pp-83, Narishige, Japan) was used to pull the electrodes. The resistance of capillary glass electrodes (GC150TF-10, Clark Electromedical Instruments, UK) used was 2 to 4 MΩ when filled with internal solution. A patch-clamp amplifier (EPC-9, Germany) was used to record the whole-cell currents with four-pole Bessel filter set at 1 kHz, digitized at 5 kHz. The protocols for voltage-clamp and data analysis were established with routines using pClamp 6.0 software (Axon Instrument, USA), and data

were stored in computer for subsequent analysis. Drug actions were measured only after steady-state conditions reached, which were judged by the amplitudes and time courses of currents remaining constant with further perfusion of drugs.

Drugs and solutions

Berberine hydrochloride was obtained from Yichang Pharmaceutical Company of China as base powders, dissolved in distilled water and made into a stock solution at 0.1 mol/L. Berberine was added to bath solutions for extracellular application. All drugs were purchased from Sigma (USA) unless otherwise indicated.

Ca^{2+}, Mg^{2+}-free Hanks' solution for cell-isolation (mmol/L) contained NaCl 137, KCl 5.4, NaH_2PO_4 0.5, Na_2HPO_4 0.58, $NaHCO_3$ 4.16 and glucose 5.5 (pH 7.3). Kraft-bruhe (KB) medium for cell-preservation (mmol/L) contained L-glutamic acid 70, KCl 130, taurine 15, KH_2PO_4 10, $MgCl_2$ 0.5, glucose 11, N-(hydroxyethyl) piperazine-N'-2-ethanesulphonic acid (HEPES) 10 and ethylene glycol-O-O'-bis (2-aminoethyl) -N,N,N',N'-tetraacetic acid (EGTA) 0.5 (pH 7.4).

In studies of I_K, the bath solution was a modified Tyrode's solution (mmol/L) containing NaCl 144, KCl 4.0, $CaCl_2$ 1.8, $MgCl_2$ 0.53, Na_2HPO_4 0.33, HEPES 5 and glucose 5.5 (pH 7.3). The patch pipette solution contained (mmol/L) KCl 130, K_2ATP 5.0, creatine phosphate 5.0 and HEPES 5.0 (pH 7.4).

For experiments on I_{K1}, both the bath solution and the pipette solution contained (mmol/L) KCl 7, $MgCl_2$ 2, EGTA 1, K-glutamate 130 and HEPES 10 (pH 7.4).

For I_{CRAC} recording, the bath solution (mmol/L) contained NaCl 140, KCl 2.8 $CaCl_2$ 10, $MgCl_2$ 0.5, glucose 11 and HEPES 10 (pH 7.4). The pipette solution used (mmol/L) contained K-glutamate 145, NaCl 8, $MgCl_2$ 1, MgATP 0.5, EGTA 10 and HEPES 10 (pH 7.2).

Data analysis

All the data were expressed as mean±SD and error bars were plotted as SD. Statistical significance was evaluated by a *t* test. Statistical differences were considered to be significant when *P* value was less than 0.05.

RESULTS

Effects of berberine on I_K

Under conventional whole-cell patch-clamp mode, the membrane potential was clamped at -50 mV, and I_K was elicited in isolated rat hepatocytes by depolarizing pulse to +140 mV for 900 ms. The current at the end point of the test pulse was measured as the amplitude of I_K.

The percentage block of I_K was defined as $(I_{Control}-I_{berberine})/I_{Control}$ and plotted as a function of logarithm [berberine] in

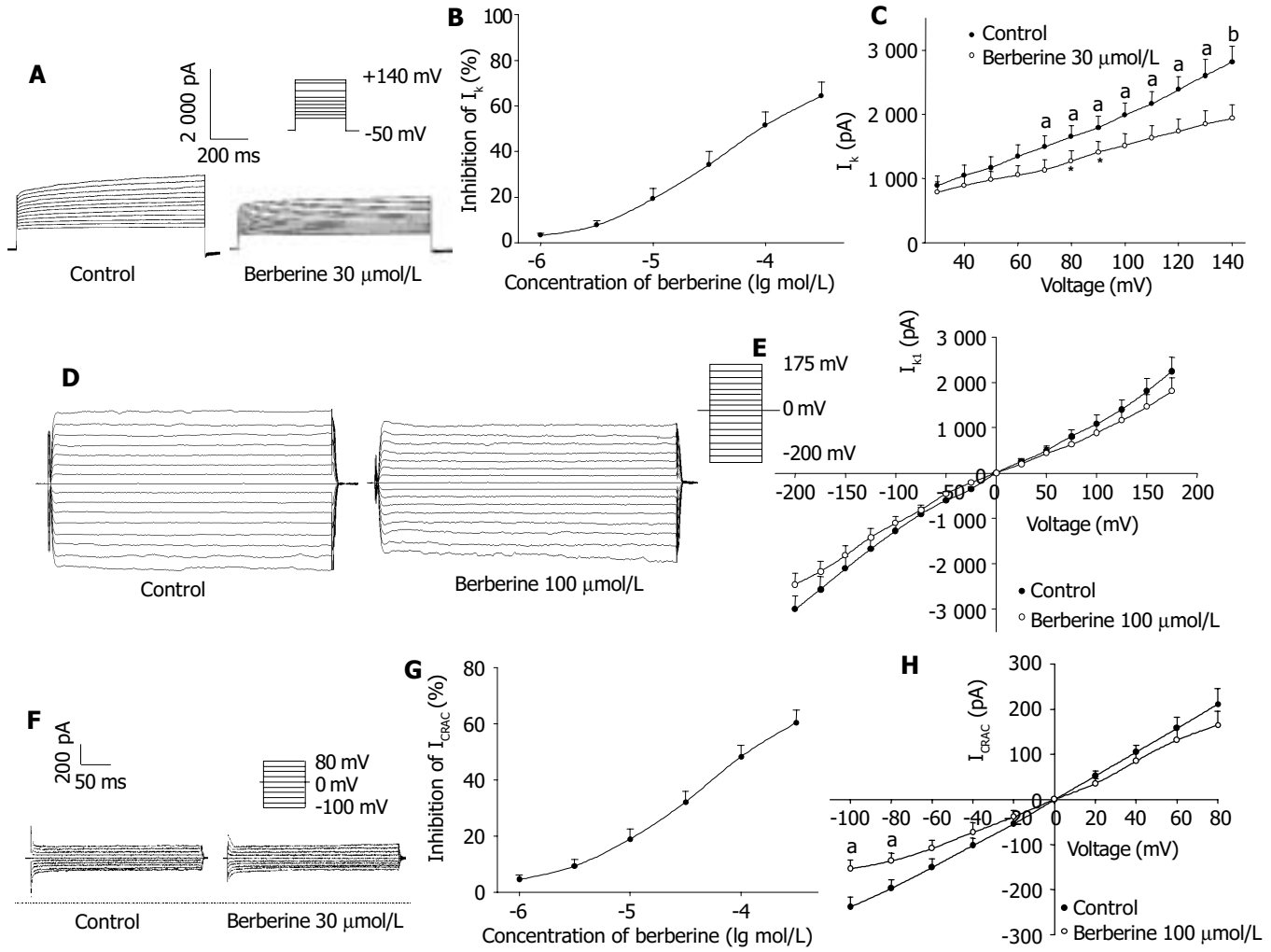

Figure 1 Effects of berberine on I_K. A: Families of I_K recorded with changes in the absence or presence of berberine 30 μmol/L and 100 μmol/L. Dotted line indicates zero current level; B: Dose-response curve for effects of berberine on I_K; C: I-V relationship of I_K under control (●) and berberine 30 μmol/L (○). D: Families of I_{K1} recorded with changes in the absence or presence of berberine 100 μmol/L. Dotted line indicates zero current level; E: I-V relationship of I_{K1} under control (●) and berberine 100 μmol/L (○). F: Families of I_{CRAC} recorded with changes in the absence or presence of berberine 30 μmol/L. Dotted line indicates zero current level; G: Dose-response curve for effects of berberine on I_{CRAC}; H: I-V relationship of I_{CRAC} under control (●) and berberine 30 μmol/L (○). The voltage steps used to elicit I_K are shown in the inset. n = 8, mean±SD, $^aP<0.05$, $^bP<0.01$ *vs* control.

Figure 1B. At +140 mV, berberine 1-300 μmol/L decreased the I_K amplitude concentration-dependently in all cells tested, which was poorly reversible after washout. The data points were fitted according to the Hill equation: Inhibition of current (%) = 100/ [1+ (EC_{50}/C) ^{nH}], and an EC_{50} value of 38.86±5.37 μmol/L and n_H of 0.82±0.05 were obtained (n = 8). When the bath solution was changed to tetraethylammonium (TEA) 8 mmol/L, I_K was inhibited.

Figure 1A shows the effects of berberine 30 μmol/L on the steady-state I-V relationship for I_K generated by applying 12 steps voltage command pulse from +30 mV to +140 mV for 900 ms with a 10 mV increment from a holding potential of -50 mV. By comparing these two I-V curves shown in Figure 1C, I_K was reduced by berberine 30 μmol/L at all membrane potentials examined, especially at potentials positive to +60 mV (n = 8, P<0.05 or P<0.01 *vs* control). The results clearly indicated that berberine had a depressant action on I_K in rat hepatocytes.

Effects of berberine on I_{K1}

Hyperpolarizing and depolarizing potentials over a range from -200 mV to +175 mV with a 25 mV increment for 40 ms were applied from a holding level of 0 mV. The absolute value at the end of test pulse was measured as the amplitude of I_{K1}. After administration of berberine 100, 300 μmol/L, the I_{K1} amplitude at -200 mV was decreased from -3 044.75±262.06 pA to -2 451.33±226.45 pA and -2 310.66±182.65 pA, respectively. The inhibition rates were 17.49±2.51% and 24.11±3.60%, respectively. Figures 1D and 1E shows the I-V relations of berberine 100 μmol/L on I_{K1}. As shown in Figures 1D and 1E, berberine only had mild inhibitory effects on I_{K1} in isolated rat hepatocytes.

Effects of berberine on I_{CRAC}

When the holding potential was 0 mV, and the cells were depolarized to -100 mV for 200 ms at a frequency of 0.2 Hz, I_{CRAC} was evoked. As shown in Figure 1G, I_{CRAC} also was blocked by berberine in a concentration-dependent fashion, with an EC_{50} value of 47.20±10.86 μmol/L and n_H of 0.71±0.09 (n = 8). Figure 1H shows the effect of berberine 30 μmol/L on the steady-stated I-V relationships generated by applying a series depolarizing pulses from a holding potential of 0 mV to different membrane potentials (-100 mV to +80 mV) with a 20 mV increment. The peak value of I_{CRAC} was reduced on either inward or outward components, especially from -100 mV through -80 mV (n = 8, P<0.05 *vs* control). But the reverse potential of I_{CRAC} occurred at voltage 0 mV in all cells.

DISCUSSION

In this study, for the first time, we characterized the effects of berberine on I_K, I_{K1} and I_{CRAC} by patch-clamp techniques and demonstrated that berberine mainly inhibited I_K, I_{CRAC} and I_{K1} in isolated rat hepatocytes.

Potassium channels are ubiquitous in eukaryotic cells and could play roles in resting membrane potential, frequency of action potential, membrane potential repolarization rates and cell functions. It has been found that membrane potential is important in regulating metabolic processes in the liver, including gluconeogenesis, amino acid transport, and the rate of uptake of bile salts[14,15]. Changes in K^+ permeability could affect the transmembrane potential. Bile formation was involved in anion accumulation within the apical lumen of hepatocytes. Potassium flux through hepatocellular basolateral membrane channels might provide the counterion for apical anion efflux[16]. Transcellular bile acid transport could be integrated in the regulation of intracellular pH, K^+ homeostasis and membrane potential. Hepatocellular K^+-depletion could result in the inhibition of bile acid secretion despite increasing the intracellular concentration[17-19].

During ischemia and hypoxia, hepatocellular volume and K^+ conductance were increased and would lead to cell death[20,21]. Nietsch *et al*. demonstrated TNF (25 ng/mL) elicited a 2- and 5-fold increase in K^+ current in hepatoma tissue culture cells. K^+ channel activation might participate in pathways that leading to TNF-mediated cell death, thus representing potential therapeutic targets to attenuate liver injury from TNF[22]. The inhibition of K^+ channels could delay hepatocyte apoptosis and death. Churchill *et al*. reported that potassium channel antagonists had protective effects on rat liver via regulating the energy metabolism[23].

Previous studies showed that berberine (0.5, 5 mg/kg, i.p.) protected rat liver from hepatotoxicity induced by *t*-BHP[10]. As shown previously, *t*-BHP could shrink hepatocytes by release of cellular K^+. Single-channel patch-clamp studies demonstrated *t*-BHP activated a 35-pS K^+ channel and contributed to the K^+ release of hepatocytes following exposure to *t*-BHP[24]. In this study, we observed that the concentration of berberine on I_K was consistent with the dose reported by Hwang[10]. The hepatoprotective effect of berberine on *t*-BHP may have some relations with the inhibitory effect on potassium channel.

However, as we reported previously, AP-Q had a protective effect on CCl_4-induced liver injury, probably by selectively increasing I_K. In this experiment, we observed that berberine had a protective effect on *t*-BHP induced liver injury by decreasing I_K. The contradiction may be due to the different mechanism of CCl_4-induced and *t*-BHP induced liver injury. CCl_4-induced hepatocyte injury paralleled with membrane depolarization by blocking the potassium channel in damaged hepatocytes[25-27]. However, *t*-BHP-induced liver injury is concerned with the release of cellular K^+ by activating potassium channel. A previous study showed that berberine had not any protective effects on CCl_4-induced liver injury[28].

Calcium has been demonstrated to play an important role in hepatocyte damage. An increase in calcium ion concentration in cytoplasm due to the influence of various toxic agents caused disturbances in the structure and function of hepatocytes, leading to their damage and even death[29]. Previous studies showed that hepatocellular Ca^{2+} overload and impaired Ca^{2+} signaling were related to hemorrhage/resuscitation liver injury. Increased Ca^{2+} uptake could result from a receptor-gated Ca^{2+} influx and/or oxygen-free radical induced membrane Ca^{2+} leaks. A protective effect of calcium channel blockers on hepatotoxins has been reported[30].

Calcium ions could enter the cells mostly through calcium channels. However, hepatocytes as the nonexcitable cells were short of the voltage-dependent Ca^{2+} channels but possessed plasma membrane Ca^{2+} channels that had a high selectivity for Ca^{2+}, and were activated by a decrease in the concentration of Ca^{2+} in intracellular stores, which was named I_{CRAC}[31,32]. Berberine inhibited I_{CRAC} with EC_{50} of 47.20 μmol/L, which was different from the EC_{50} of $I_{Ca,L}$ in cardiac myocytes[33]. The differential drug sensitivity of the two currents also provided further support for the idea that I_{CRAC} is different from voltage-gated Ca^{2+} channel.

Berberine inhibited I_K, I_{K1} and I_{CRAC} concentration-dependently in isolated rat hepatocytes and the inhibitory extent was I_K>I_{CRAC} >I_{K1}. Therefore, berberine could block K^+ channel and decrease the extracellular K^+ to regulate the metabolic processes in the liver. Berberine could also inhibit I_{CRAC} effectively and protect hepatocytes from calcium overload via the inhibition of I_{CRAC}. The inhibitory effects on potassium and calcium current may partly contribute to the hepatoprotective action of berberine. As berberine has already been used for liver damage in human beings[34], it may be a good candidate for further study and used in treatment of liver damage.

REFERENCES

1 **Virtanen P,** Lassila V, Njimi T, Mengata DE. Natural protoberberine alkaloids from Enantia chlorantha, palmatine,

columbamine and jatrorrhizine for thioacetamide-traumatized rat liver. *Acta anat* 1988; **131:** 166-170

2 **Virtanen D,** Lassila V, Njimi T, Ekotto Mengata D. Regeneration of D-galactosamine-traumatized rat liver with natural protoberberine alkaloids from Enantia chlorantha. *Acta Anat* 1988; **132:** 159-163

3 **Virtanen D,** Lassila V, Njimi T, Mengata DE. Effect of splenectomy on hepasor treatment in allyl-alcohol-traumatized rat liver. *Acta Anat* 1989; **134:** 301-304

4 **Anis KV**, Rajeshkumar NV, Kuttan R. Inhibition of chemical carcinogenesis by berberine in rats and mice. *J Pharm Pharmacol* 2001; **53:** 763-768

5 **Lau CW**, Yao XQ, Chen ZY, Ko WH, Huang Y. Cardiovascular actions of berberine. *Cardiovasc Drug Rev* 2001; **19:** 234-244

6 **Bova S**, Padrini R, Goldman WF, Berman DM, Cargnelli G. On the mechanism of vasodilating action of berberine: possible role of inositol lipid signaling system. *J Pharmacol Exp Ther* 1992; **261**: 318-323

7 **Amin AH**, Subbaiah TV, Abbasi KM. Berberine sulfate: antimicrobial activity, bioassay, and mode of action. *Can J Microbiol* 1969; **15:** 1067-1076

8 **Tsai CS**, Ochillo RF. Pharmacological effects of berberine on the longitudinal muscle of the guinea-pig isolated ileum. *Arch Int Pharmacodyn Ther* 1991; **310:** 116-131

9 **Wang YX**, Zheng YM. Ionic mechanism responsible for prolongation of cardiac action-potential duration by berberine. *J Cardiovasc Pharmacol* 1997; **30:** 214-222

10 **Hwang JM**, Wang CJ, Chou FP, Tseng TH, Hsieh YS, Lin WL, Chu CY. Inhibitory effect of berberine on *tert*-butyl hydroperoxide-induced oxidative damage in rat liver. *Arch Toxicol* 2002; **76:** 664-670

11 **Li BX**, Yang BF, Zhou J, Xu CQ, Li YR. Inhibitory effects of berberine on I_{K1}, I_K, and HERG channels of cardiac myocytes. *Acta Pharmacol Sin* 2001; **22:** 125-131

12 **Li Y**, Fu LY, Yao WX, Xia GJ, Jiang MX. Effects of benzyltetrahydropalmatine on potassium currents in guinea pig and rat ventricular myocytes. *Acta Pharmacol Sin* 2002; **23:** 612-616

13 **Seglen PO**. Preparation of isolated rat liver cells. *Methods Cell Biol* 1976; **13:** 29-83

14 **Bernardi P**, Azzone GF. Regulation of Ca^{2+} efflux in rat liver mitochondria. Role of membrane potential. *Eur J Biochem* 1983; **134:** 377-383

15 **Einarsson C**, Ellis E, Abrahamsson A, Ericzon BG, Björkhem I, Axelson M. Bile acid formation in primary human hepatocytes. *World J Gastroenterol* 2000; **6:** 522-525

16 **Roman R**, Feranchak AP, Troetsch M, Dunkelberg JC, Kilic G, Schlenker T, Schaack J, Fitz JG. Molecular characterization of volume-sensitive SK (Ca) channels in human liver cell lines. *Am J Physiol Gastrointest Liver Physiol* 2002; **282:** G116-G122

17 **vom Dahl S**, Hallbrucker C, Lang F, Haussinger D. Regulation of cell volume in the perfused rat liver by hormones. *Biochem J* 1991; **280**(Pt 1): 105-109

18 **Devin A**, Espie P, Guerin B, Rigoulet M. Energetics of swelling in isolated hepatocytes: a comprehensive study. *Mol Cell Biochem* 1998; **184:** 107-121

19 **Kiss L**, Immke D, LoTurco J, Korn SJ. The interaction of Na^+ and K^+ in voltage-gated potassium channels. Evidence for cation binding sites of different affinity. *J Gen Physiol* 1998; **111:** 195-206

20 **Hill CE**, Jacques JE. Cholestatic effects of the K^+ channel blockers Ba^{2+} and TEA occur through different pathways in the rat liver. *Am J Physiol* 1999; **276**(1 Pt 1): G43-G48

21 **Hill CE**, Briggs MM, Liu J, Magtanong L. Cloning, expression, and localization of a rat hepatocyte inwardly rectifying potassium channel. *Am J Physiol Gastrointest Liver Physiol* 2002; **282:** G233-G240

22 **Nietsch HH**, Roe MW, Fiekers JF, Moore AL, Lidofsky SD. Activation of potassium and chloride channels by tumor necrosis factor α. Role in liver cell death. *J Biol Chem* 2000; **275:** 20556-20561

23 **Churchill TA**, Fuller BJ. Effects of sodium and potassium channel antagonists on the energy metabolism of rat liver during cold storage. *Transplantation* 1995; **59:** 904-907

24 **Breit S**, Kolb HA, Haussinger D, Lang F. Effects of tetrabutylhydroperoxide on hepatocyte ion channels. *Cell Physiol Biochem* 1999; **9:** 133-138

25 **Wands JR**, Smuckler EA, Woodbury WJ. Transmembrane potential changes in liver cells following CCl_4 intoxication. *Am J Pathol* 1970; **58:** 499-508

26 **Olson JR**, Hosko MJ, Fujimoto JM. Alterations in the liver cell transmembrane potential following $CC1_4$ and bile salt treatment of rats. *Life Sci* 1979; **25:** 2043-2050

27 **Burczynski FJ**, Wang GQ, Minuk GY, Rosser B. Altered transmembrane ionic flux in hepatocytes isolated from cirrhotic rats. *J Hepatol* 1999; **30:** 492-497

28 **Janbaz KH**, Gilani AH. Studies on preventive and curative effects of berberine on chemical-induced hepatotoxicity in rodents. *Fitoterapia* 2000; 71: 25-33

29 **Isozaki H**, Fujii K, Nomura E, Hara H. Calcium concentration in hepatocytes during liver ischaemia-reperfusion injury and the effects of diltiazem and citrate on perfused rat liver. *Eur J Gastroenterol Hepatol* 2000; **12:** 291-297

30 **Farghali H**, Kmonickova E, LotKova H, Martinek J. Evaluation of calcium channel blockers as potential hepatoprotective agents in oxidative stress injury of perfused hepatocytes. *Physiol Res* 2000; **49:** 261-268

31 **Takanashi H**, Sawanobori T, Kamisaka K, Maezawa H, Hiraoka M. Ca^{2+}-activated K^+ channel is present in guinea-pig but lacking in rat hepatocytes. *Jpn J Physiol* 1992; **42:** 415-430

32 **Rychkov G**, Brereton HM, Harland ML, Barritt GJ. Plasma membrane Ca^{2+} release-activated Ca^{2+} channels with a high selectivity for Ca^{2+} identified by patch-clamp recording in rat liver cells. *Hepatology* 2001; **33:** 938-947

33 **Xu SZ**, Zhang Y, Ren JY, Zhou ZN. Effects of berberine on L- and T-type calcium channels in guinea pig ventricular myocytes. *Zhongguo Yaoli Xuebao* 1997; **18:** 515-518

34 **Brunton CC**. In pharmacological basis of therapeutics edited by Hardman JG, Limbird LE, Molinoff PB, Ruddon RW, Gilman AG. *New York: McGraw Hill* 1996: 917-936

Edited by Wang XL **Proofread by** Xu FM and Chen WW

PO Box 2345, Beijing 100023, China
Fax: +86-10-85381893
E-mail: wjg@wjgnet.com www.wjgnet.com

World J Gastroenterol 2004;10(19):2846-2849
World Journal of Gastroenterology
Copyright © 2004 by The WJG Press ISSN 1007-9327

• CLINICAL RESEARCH •

Surgical management of esophageal strictures after caustic burns: A 30 years of experience

Yong Han, Qing-Shu Cheng, Xiao-Fei Li, Xiao-Ping Wang

Yong Han, Qing-Shu Cheng, Xiao-Fei Li, Xiao-Ping Wang, Department of Thoracic Surgery, Tangdu Hospital, the Fourth Military Medical University, Xi'an 710038, Shaanxi Province, China
Correspondence to: Dr. Yong Han, Department of Thoracic Surgery, Tangdu Hospital, the Fourth Military Medical University, Xi'an 710038, Shaanxi Province, China. han2003002@vip.sina.com
Telephone: +86-29-83377736 **Fax:** +86-29-83246270
Received: 2004-02-14 **Aceepted:** 2004-03-02

Abstract

AIM: To analyze a 30-year historical series of patients treated in our hospital, who ingested corrosive substances, and to assess the effectiveness of surgical therapy administered in patients with strictures after caustic injury in esophagus during this period.

METHODS: A total of 79 cases of caustic burns in esophagus were treated in Tangdu Hospital from 1971 to 2001. Their clinical and pathological data were reviewed, and collected from the medical records of patients and interviews with them.

RESULTS: More men (n = 61) than women (n = 18) ingested caustic substances with a sex ratio of 3.4:1 during the 30-year period. The caustic materials were liquid lye and acids (54 cases and 25 cases, respectively). Sixty-eight patients were given esophageal replacement in more than three months after caustic injury with no postoperative death, of which 17 cases developed postoperative complications making a complication rate of 25%. The most common one was cervical anastomotic leakage. All patients had improvement in swallowing afterwards.

CONCLUSION: The presence and severity of injuries are correlated with the amount of caustic substances ingested. Surgical treatment is a good option in patients with severe strictures, and colonic interposition might be the best surgical process. The most important factors to guarantee a successful outcome for surgery are good vascular supply and absence of tension in the anastomosis.

Han Y, Cheng QS, Li XF, Wang XP. Surgical management of esophageal strictures after caustic burns: A 30 years of experience. *World J Gastroenterol* 2004; 10(19): 2846-2849
http://www.wjgnet.com/1007-9327/10/2846.asp

INTRODUCTION

Potentially catastrophic presentation and life long complications resulting from caustic ingestion make it one of the most challenging clinical situations in gastroenterology. Caustic material ingestion is most frequently encountered in children who accidentally swallowed caustic materials or in adults who ingested caustic materials for suicidal purposes[1,2]. Alkaline caustics and acids are the commonest chemicals implicated in caustic burns. Burns from ingestion of such agents may include the oral, pharynx, larynx, esophagus and stomach. Destruction of tissues or of these organs may lead to complications, of which respiratory compromise, esophageal and gastric perforation, septicemia, or even death might occur. Stricture formation with inability to swallow food after the injury is inevitable in some cases. Many different therapies have been recommended. The literature regarding the treatment of these patients is quite controversial and inconclusive. Repeated dilations to maintain an adequate lumen diameter were given in patients with chronic strictures. As for the complications and ineffectiveness of the dilation in more severe strictures, surgical replacement of esophagus may be required. The objective of this study was to analyze a 30-year historical series of patients treated in our hospital who ingested caustic substances, and to assess the effectiveness of surgical therapy administered in patients with strictures after caustic injury in esophagus as well as the best time for operation.

MATERIALS AND METHODS

Subjects

From 1971 to 2001, 79 cases of caustic burns in esophagus were treated in Tangdu Hospital. Their clinical and pathological data were reviewed, and collected from the medical records of patients and interviews with them. Sixty-one men and 18 women ingested caustic substances (sex ratio 3.4:1), respectively. Patients aged from 2 to 72 years (mean, 20.8 ± 2.5 years). The caustic materials for injuries were liquid lye and acids (54 cases and 25 cases, respectively). Ingestion was associated with suicidal intent in 70% of cases and accidental in 29% of cases. The amount of substances ingested ranged from 5-15 mL to as much as 40 mL, with the amount tending to be larger in the suicide attempts. To determine the amount of caustic substances ingested, patients or witnesses were asked to compare the amount ingested to the amount of water in a cup. The time intervals the patient came to our hospital after ingestion varied from several hours to several days. A total of 73 cases presented lesions of the esophagus. Two patients, who ingested a large amount of more than 60 mL caustic substances, died of stomach and esophageal perforation during the acute phase as a result of generalized infection and bleeding. Four patients, who ingested less than 15 mL, did not present severe complications. Esophageal strictures were found in 72 cases, the presence of stenosis was determined 2 wk after ingestion (chronic phase) by endoscopy and radiological signs.

Treatment

All the patients were given early emergency managements including early administration of an appropriate neutralizing agent such as ingesting water or milk after the ingestion, although it did not seem to prevent stenosis[3], and antibiotics, as well as the correction of any apparent hydration deficiency or acid-base imbalance, and corticosteroid treatment to the patients with signs of esophagitis. Forty-eight patients of 77 cases underwent emergent endoscopy to assess the degree of damage after patients were stabilized, which was very important for the diagnosis and evaluation of the degree of injuries. Patients with ulceration, blisters, even areas of extensive

necrosis always tended to develop esophageal strictures[4,5]. Among the 79 patients, 72 might undergo a long period of dysphagia, and gastrostomy or jejunostomy was performed for feed routinely soon after the injury except 4 patients who were lucky enough to escape severe injury and suffered from only oral burn, and 1 patient refused for further treatment because of economical reasons. No emergency thoracotomy was performed for the esophagectomy or gastrectomy in this group. Sixteen patients were performed repeated dilations 1-2 mo after ingestion (Table 1).

Table 1 Previous management before esophagus replacement (n = 79)

Procedures	n	%
Gastrostomy	25	31.6
Jejunostomy and pyloroplasty	12	15.2
Jejunostomy	19	24.1
Repeated dilation after gastrostomy or jejunostomy	15	19.0
Dilation and stent placement after gastrostomy or jejunostomy	1	1.2
No surgery	7	8.8

Esophageal replacement

Sixty-eight patients, among whom 12 had been given repeated dilation with failure therapy, were performed esophagus replacement for diffuse or multiple caustic esophageal strictures and 3 patients were cured after corticosteroid treatment and repeated dilations, 1 patient was performed stent placement. Among the 68 patients, 65 underwent the operation 6 mo and 3 three months after the injury. Stomach, jejunum and colon were used for esophageal replacement (Table 2). The colon (63/68) was commonly used as an esophageal substitute in reconstruction, and all went through the substernal route.

Table 2 Operation procedure of esophageal replacement (n = 68)

Procedure	n	%
Colonic interposition	63	92.6
Esophagogastrostomy	3	4.4
Jejunal interposition	2	3.0

Surgical procedure of colonic interposition

As colonic interposition was mostly used in our study, the surgical procedure was prescribed. The operation was carried out through an upper abdominal incision and a cervical oblique incision along the inner border of the sternocleidomastoid muscle in 62 patients and in 1 patient with a right thoracotomy respectively. The cervical esophagus was explored. It was transected in the level that esophagus was normal. In case the cervical esophagus was thickened and stiff in consistency, indicating that the organ was too extensively injured, a hypopharyngocolostomy had to be performed. This was occurred in 7 cases in this series.

A sufficient colon segment for graft was mobilized from colonic mesentery. The middle and left colonic arteries were identified and freed respectively. The root of the vessels elected was clamped with bulldog clamps for about 15 min. In the same time, the estimated ends of graft were clamped with intestinal clamps and watched. If the colon acted as replacement expressed normal in color, peristalsis and marginal arterioles would be pulsating (especially those in both ends of the segment), it would be transected. The colonic segment used in this group consisted of left colon in 30 cases, right colon and transverse colon in 33 cases. The peristaltic orientation of graft consisted of isoperistalsis in 40 cases and antiperistalsis in 23 cases.

The substernal tunnel in 61 cases and the subcutaneous tunnel in 2 were prepared. The proximal end of graft was elevated gently from abdomen up to the neck through the tunnel. A proximal esophagocolic or hypopharyngocolic anastomosis was performed in an end-to-end or end-to-side fashion with hand-suturing single-layer technique in 56 and 7 cases, respectively.

Cologastric anastomosis was performed over the midportion of the anterior wall of the stomach without extensively injuring the stomach, and the anastomosis between the distal portion of graft and a Rouxeny loop of jejunum was performed.

Additional procedure included resection of upper portion of sternum in 5 patients in order to avoid or decrease compression on the proximal colonic graft at the level of the thoracic inlet.

RESULTS

After early emergency management in these patients, 2 patients who ingested more than 60 mL of caustic substances died of stomach and esophageal perforation during the acute phase as a result of generalized infection and bleeding. Four patients, who ingested less than 10 mL, did not present complications in the present study. On this basis, we believed that the presence and severity of injuries were correlated with the amount of caustic substances ingested, which was similar with the result of Chien *et al*.[6]. Sixteen patients were performed repeated dilation 1-2 mo after ingestion in fear of perforation in earlier dilations and 12 patients needed further surgical treatment.

Sixty-eight cases were performed esophageal replacement because of the later stricture, which caused persistent dysphagia and weight loss in these patients. Results of operation were satisfactory with no postoperative death and improved swallowing ability, among which 17 cases developed postoperative complications making a complication rate of 25% (Table 3). The most common one was cervical anastomotic leakage, which occurred in 9 cases in this series. Postoperatively, swallow ability was considered good in 65 patients (95.7%) after an average of 22-mo follow-up (six months to eight years). The swallow ability was determined through the questionnaire about the sorts and amounts of food that could be swallowed compared with the condition before injury and operation in a general analysis.

Table 3 Postoperative complications (n = 17)

Complication	n	%
Cervical anastomostic leakage	9	52.9
Cervical wound infection	2	11.7
Anastomotic stenosis	3	17.6
Intestinal obstruction	1	5.8
Pneumothorax	1	5.8
Aspiration pneumonitis	1	5.8

DISCUSSION

A successful management of corrosive injury involves prompt recognition and early treatment. Unfortunately, it is sometimes not possible to maintain an esophageal lumen despite all the measures. Clinically apparent esophageal strictures occurred in 10-30% of patients with a caustic injury[7], even higher in some other reports[8,9]. In our study, 68 patients (85%) presented strictures that needed replacement, which might be due to the ingestion of relatively large amount of caustic substances for suicidal intent. Treatment of the strictures after esophageal injury was very difficult, and dilation has been used in many hospitals[10]. Even after many times of dilation, strictures were

found in about 48% cases[11], and although the danger of severe complications, such as perforation of the esophagus per procedure, was low (0.9-1.5%)[12,13], a significant number of people, especially children were at risk with a relatively high mortality[14,15]. Dilatation therapy, furthermore, required frequent admissions to hospital and multiple anesthetics with inherent risks. Surgical intervention, which is a good way to solve the problem of strictures, in the form of esophageal replacement, was carried out in more than half patients with established esophageal strictures[16].

Most beneficial time for surgery

The time for operation of esophageal replacement after corrosive injury is still under controversy. Certainly, emergency surgical exploration is indicated if perforation or penetration is demonstrated.

Bassiouny *et al.*[17] found in rats that collagen deposition peaked during the second week but continued for a long time after corrosive injury of esophagus. Scar retraction began as early as the end of the second week, and lasted for about six months. It took about 6-12 mo before full fibrosis stopped to develop after the injury[18], which showed that the edge of the stricture in the esophagus might not be confirmed until then. A too earlier operation, when the scar has not completely formed, may promote the risk of anastomostic stenosis. So, it is believed that the chance of successful surgical management is greater if the operation is carried out at least six months after the injury. In our study, 3 patients with strictures in the lower segment of esophagus, who developed severe dysphagia and refused gastrostomy, were performed partial esophagectomy and esophagogastrostomy about 90 d after caustic injury. However, anastomostic stenosis occured in 2 patients (67%) 2 mo after operation, a higher incidence of stenosis. The other 65 patients were performed operation 6 mo after injury with only one esophageal stenosis occured.

Although it was reported that esophageal replacement could be performed even 2-3 mo after injury[19], but many conditions must be met and the mucosa in the pharynx must be normal. So we think that the most beneficial time for surgery is no less than six months after the injury.

Choice of replacement organs

The organs used for esophageal replacement in patients after caustic injuries included stomach, jejunum and colon in previous studies[20,21]. Stomach has the disadvantages of long-term gastroesophageal reflux, possible ulceration, anastomostic stenosis and progressive dysfunctional propulsion[22]. The stomach is always not long enough to reestablish a continuity of esophagus when anastomosis had to be performed in the neck because the diffused injuries of esophagus, when patients had to be given partial gastrectomy after caustic injuries. In our study partial esophagectomy and esophagogastrostomy were performed only in 3 patients on the condition that strictures were located in the lower segment of esophagus. Jejunal interposition is seldom used because of the difficulty for operation since blood vessels of jejunum are too thin and easier to be affected after anastomosis. Furthermore, the jejunum is fragile to the erosion of acid in a long run, so the jejunum should not be the first choice. In our study, only 2 cases of jejunal interposition were performed, because the patients had undergone abdominal operation before and the stomach and colon were unable to be mobilized. With good blood supply and improved somatic growth, colon is long enough for esophageal replacement, and it causes fewer late complications of esophagitis and stricture because of the resistance to acid. So colon could offer potential advantages over other organs[20,23], and is believed to be an ideal organ for the replacement. We used colon for replacement in 63 cases, and the result was satisfactory. Our experiences support the idea that colon interposition is the best process for reconstruction of esophagus in caustic injury strictures.

Choice of colon segment as a graft is also a key point for reconstruction of esophagus. The left colon has been considered by many surgeons to be a preferable conduit for several reasons. But left colon interposition could always be used in an antiperistalic fashion, which may cause inflammation of the anatomosis, and affect the healing process. In our study, leakage of cervical anastomosis appeared in 7 cases of the antiperistalic anastomosis group, which was much higher than the isoperistaltic groups. So, it is suggested that the reversed peristalsis might cause more complications of anastomosis than isoperistalsis. The choice of a colon segment for substitution in our study was also affected by the supply of blood vessels during operation, and the color of intestine, and pulsation of marginal arteries after the supplying artery of colon was clamped. The mortality and morbidity in the literature after colonic interposition was very high[24]. The most severe complication was complete necrosis of the transplanted colon. When it happened, a more complex reconstruction procedure should be considered. We had no experience in facing such a catastrophy. In 1 case, local necrosis in the proximal end of transplanted colon was observed when anastomotic leakage was diagnosed 3 d after the procedure. The anastomotic leakage was the most common complication in 9 of 63 cases, making an incidence as high as 13.3%. Considering the fact that most patients in whom esophageal disease was caused by caustic injury accompanied with bad nutritional status, this rate of postoperative complication after colon interposition is acceptable. Anastomotic leakage of the patients was managed by opening the cervical wound, and it seemed to have no effect on the late swallow ability of patients after anastomotic leakage compared with the patients without leakage in the follow up interviews. There was no death in the group. The outcome was favorable when compared with published literature[24].

Residual esophagus

It is still a subject of a controversy whether the residual esophagus should be resected after colonic interposition. Many studies have focused on the relation between esophageal injury and carcinoma. Although the scarred and damaged esophagus might have an increased incidence of carcinoma[25,26], there is no evidence that has been reported. In our study, esophagectomy was only performed in the esophagogastrostomy and jejunal interposition groups, and no residual esophagus was resected in the colonic interposition group. In our follow-up study, no carcinoma of residual esophagus occurred even 8 years after operation. In our experience, an additional thoracotomy or esophagectomy to resect the injuried esophagus is a big burden for patients, when an abdominal incision is enough in colonic interposition procedure. Adhesion and inflammation of the residual esophagus after long time caustic injuries may be a great strike for patients to receive esophagectomy, with a higher risk of complications, even death than expected. It is therefore suggested that a long term follow-up and observation for the residual esophagus may be a preferable option for the treatment of caustic injuries of esophagus. Resection of the residual esophagus should be seriously considered anyhow.

Keys for success of surgical procedure

Certainly good nutrition and careful peri-operation treatment are important for the healing process of anastomosis. Gastrostomy or jejunostomy must be performed for the nutrition of patients. In addition to an effective nutritional support, the pivotal keys for a successful surgical procedure are the adequate and good vascular supply for the esophageal replacement, as well as the absence of tension at the anastomosis. Thus, an

enough length of substitutes must be prepared. Resection of parts of the sternum should be considered for colonic interposition to allow a spacious room for the graft colon, if the sternum exerts pressure upon the graft colon .

REFERENCES

1 **Havanond C.** Clinical features of corrosive ingestion. *J Med Assoc Thai* 2003; **86:** 918-924

2 **Rodriguez MA,** Meza Flores JL. Clinical-epidemiological characteristics in caustics ingestion patients in the Hipolito Unanue National Hospital. *Rev Gastroenterol Peru* 2003; **23**: 115-125

3 **Ramasamy K,** Gumaste VV. Corrosive ingestion in adults. *J Clin Gastroenterol* 2003; **37:** 119-124

4 **Tseng YL,** Wu MH, Lin MY, Lai WW. Massive upper gastrointestinal bleeding after acid-corrosive injury. *World J Surg* 2004; **28:** 50-54

5 **Havanond C.** Is there a difference between the management of grade 2b and 3 corrosive gastric injuries? *J Med Assoc Thai* 2002; **85:** 340-344

6 **Chien WC,** Pai L, Lin CC, Chen HC. Epidemiology of hospitalized burns patients in Taiwan. *Burns* 2003; **29:** 582-588

7 **Schaffer SB,** Hebert AF. Caustic ingestion. *J La State Med Soc* 2000; **152:** 590-596

8 **de Jong AL,** Macdonald R, Ein S, Forte V, Turner A. Corrosive esophagitis in children: a 30-year review. *Int J Pediatr Otorhinolaryngol* 2001; **57:** 203-211

9 **Lopez Vallejos P,** Garcia Sanchez MV, Naranjo Rodriguez A, Galvez Calderon C, Hervas Molina A, Chicano Gallardo M, Mino Fugarolas G. Endoscopic dilatation of caustic esophageal strictures. *Gastroenterol Hepatol* 2003; **26:** 147-151

10 **Shao YX,** Chen ZH, Ning JW. Treatment of esophageal stricture and leakage with dilation stents. *Shijie Huaren Xiaohua Zazhi* 2002; **10:** 249-251

11 **Ogunleye AO,** Nwaorgu GB, Grandawa H. Corrosive oesophagitis in Nigeria: clinical spectrums and implications. *Trop Doct* 2002; **32:** 78-80

12 **Lan LC,** Wong KK, Lin SC, Sprigg A, Clarke S, Johnson PR, Tam PK. Endoscopic balloon dilatation of esophageal strictures in infants and children: 17 years' experience and a literature review. *J Pediatr Surg* 2003; **38:** 1712-1715

13 **Poddar U,** Thapa BR. Benign esophageal strictures in infants and children: results of Savary-Gilliard bougie dilation in 107 Indian children. *Gastrointest Endosc* 2001; **54:** 480-484

14 **Erdogan E,** Eroglu E, Tekant G, Yeker Y, Emir H, Sarimurat N, Yeker. Management of esophagogastric corrosive injuries in children. *Eur J Pediatr Surg* 2003; **13:** 289-293

15 **Lew RJ,** Kochman ML.A review of endoscopic methods of esophageal dilation. *J Clin Gastroenterol* 2002; **35:** 117-126

16 **Adegboye VO,** Brimmo A, Adebo OA. Transhiatal esophagectomy in children with corrosive esophageal stricture. *Afr J Med Med Sci* 2000; **29:** 223-226

17 **Bassiouny IE,** Al-Ramadan SA, Al-Nady A. Long-term functional results of transhiatal oesophagectomy and colonic interposition for caustic oesophageal stricture. *Eur J Pediatr Surg* 2002; **12:** 243-247

18 **Demirbilek S,** Aydin G, Yucesan S, Vural H, Bitiren M. Polyunsaturated phosphatidylcholine lowers collagen deposition in a rat model of corrosive esophageal burn. *Eur J Pediatr Surg* 2002; **12:** 8-12

19 **Munoz-Bongrand N,** Gornet JM, Sarfati E. Diagnostic and therapeutic management of digestive caustic burns. *J Chir* 2002; **139**: 72-76

20 **Erdogan E,** Emir H, Eroglu E, Danismend N, Yeker D. Esophageal replacement using the colon: a 15-year review. *Pediatr Surg Int* 2000; **16:** 546-549

21 **Hirschl RB,** Yardeni D, Oldham K, Sherman N, Siplovich L, Gross E, Udassin R, Cohen Z, Nagar H, Geiger JD, Coran AG. Gastric transposition for esophageal replacement in children: experience with 41 consecutive cases with special emphasis on esophageal atresia. *Ann Surg* 2002; **236:** 531-539

22 **Helardot P.** Caustic burns of the esophagus, esophagectomy and replacement with gastric tube: comparative study with other procedures. *Saudi Med J* 2003; **24:** S39

23 **Deschamps C.** History of esophageal surgery for benign disease. *Chest Surg Clin N Am* 2000; **10:** 135-144

24 **Ma QF,** Liu K, Wang YJ, Cheng QS, Wang XP, Zhou YA. Colonic interposition for 40 patients with benign esophageal disease. *Disi Junyi Daxue Xuebao* 2001; **22:** 708-713

25 **Kim YT,** Sung SW, Kim JH. Is it necessary to resect the diseased esophagus in performing reconstruction for corrosive esophageal stricture? *Eur J Cardiothorac Surg* 2001; **20:** 1-6

26 **Davids PH,** Bartelsman JF, Tilanus HW, van Lanschot JJ. Consequences of caustic damage of the esophagus. *Ned Tijdschr Geneeskd* 2001; **145:** 2105-2108

Edited by Kumar M and Wang XL **Proofread by** Xu FM

PO Box 2345, Beijing 100023, China
Fax: +86-10-85381893
E-mail: wjg@wjgnet.com www.wjgnet.com

World J Gastroenterol 2004;10(19):2850-2853
World Journal of Gastroenterology
Copyright © 2004 by The WJG Press ISSN 1007-9327

• CLINICAL RESEARCH •

Laparoscopic resection of submucosal tumor on posterior wall of gastric fundus

Zhong-Wei Ke, Cheng-Zhu Zheng, Ming-Gen Hu, Dan-Lei Chen

Zhong-Wei Ke, Cheng-Zhu Zheng, Ming-Gen Hu, Dan-Lei Chen, Department of Minimally Invasive Surgery, Changhai Hospital, Second Military Medical University, Shanghai 200433, China
Correspondence to: Dr. Zhong-Wei Ke, Department of Minimally Invasive Surgery, Changhai Hospital, Second Military Medical University, 174 Changhai Road, Shanghai 200433, China. weiz@miscenter.cn
Telephone: +86-21-25072014 **Fax:** +86-21-25074527
Received: 2004-02-14 **Accepted:** 2004-03-04

Abstract

AIM: Laparoscopic resection of tumors on the posterior wall of gastric fundus, especially when they are next to the esophagocardiac junction (ECJ), is both difficult and time-consuming. Furthermore, it can lead to inadvertent esophagus stenosis and injury to the spleen. In order to overcome these difficulties, laparoscopically extraluminal resection of gastric fundus was designed to manage submucosal tumors located on the posterior wall of gastric fundus and next to ECJ.

METHODS: From January 2001 to September 2003, laparoscopically extraluminal resection of gastric fundus was successfully carried out on 15 patients. There were 11 males and 4 females with an average age of 58 years (range, 38 to 78 years). The mean diameter of the tumors was 4.8 cm. The distance of the tumor border from ECJ was about 1.5-2.5 cm. The four-portal operation procedures were as follows: localization of the tumor, dissection of the omentum, mobilization of the gastric fundus and the upper polar of spleen, exposure of ECJ, and resection of the gastric fundus with Endo GIA.

RESULTS: The laparoscopic operation time averaged (66.2±10.4) min, the average amount of bleeding was (89.4±21.7) mL. The mean post-operative hospital stay was (5.3±1.1) d. Within 36 h post-operation, 73.3% of all the patients recovered their gastrointestinal function and began to eat something and to walk. In all the operations, no apparent tumor focus was left and no complication or conversion to open surgery occurred.

CONCLUSION: Our newly designed procedure, laparoscopically extraluminal resection of the gastric fundus, can avoid contamination of the abdominal cavity, injury to the spleen and esophageal stenosis. The procedure seems to be both safe and effective.

Ke ZW, Zheng CZ, Hu MG, Chen DL. Laparoscopic resection of submucosal tumor on posterior wall of gastric fundus. *World J Gastroenterol* 2004; 10(19): 2850-2853
http://www.wjgnet.com/1007-9327/10/2850.asp

INTRODUCTION

Malignant gastric tumors are still considered a contraindication for laparoscopic surgery by many surgeons. However, the removal of benign tumors laparoscopically has been widely accepted as a feasible alternative to laparotomy[1-6]. The most frequent benign gastric tumor is leiomyoma, and extensive resection is indicated because it is difficult to differentiate it from leiomyosarcoma only by biopsy. When a gastric submucosal tumor is laparoscopically removed, it is recommended to resect a sufficient margin of the surrounding normal tissues in the event that the tumor is malignant[5,7-14].

Laparoscopic resection of a gastric fundus tumor on the anterior wall is relatively easy, in which a wedge of stomach can be resected under laparoscopic vision using an Endo GIA after the lesion is marked endoscopically. However, laparoscopic resection of tumors on the posterior wall of gastric fundus, especially when they are next to the esophagocardiac junction (ECJ), is both difficult and time-consuming. Furthermore, it can lead to inadvertent esophagus stenosis and injury to the spleen[14-18]. In order to overcome these difficulties, we proposed a new technique for the management of submucosal tumors located on the posterior wall of gastric fundus and next to ECJ, which was *laparoscopically extraluminal resection of the gastric fundus*.

MATERIALS AND METHODS

Materials

From January 2001 to September 2003, 15 procedures of laparoscopically extraluminal resection of the gastric fundus were carried out for the submucosal tumors located on the posterior wall of gastric fundus and next to EJC. There were 11 male and 4 female patients with an average age of 58 years (range, 38 to 78 years). The complaints at admission included upper gastrointestinal bleeding (10 cases, 66.7%) and abdominal pain (4 cases, 26.7%). The remaining one (6.7%) was diagnosed when having a physical checkup. Preoperative examinations included gastroscopy, ultrasonic gastroscopy, and barium swallow examination of the upper gastrointestinal tract, all of which revealed a submucosal lesion on the posterior wall of gastric fundus near the ECJ with a regular margin. Since these tumors could not be lifted by intrasubmucosal injection of normal saline, gastroscopic local tumor resections were not indicated. Besides, gastroscopy suggested the presence of ulcers at the center of tumor surfaces in 11 patients. The neoplasm diameter ranged 3.0-6.5 cm with a mean value of 4.8 cm. The distance of the neoplasm margin from ECJ was about 1.5-2.5 cm (Figure 1).

Surgical Methods

Anesthesia and position After general anesthesia under bronchial intubation, the patient was placed in a supine position with both legs abducted 30°. The surgeon stood between the patient's legs while the laparoscopic holder and the operative assistant on the right and left sides of the patient, respectively.
Portal positions Trocars with 5 mm or 10-12 mm in diameter were placed in the umbilicus, the left or right midclavicular line, and under the xiphoid (Figure 2).
Localization of tumors Under laparoscopy, three methods could be used for neoplasm localization: naked eye inspection, instrument exploration, and intra-operative gastroscopy[19]. In

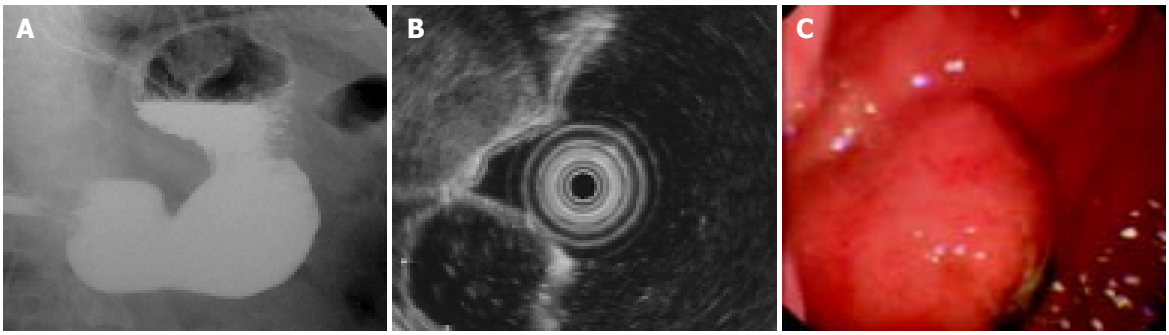

Figure 1 Submucosal tumors on gastric fundus diagnosed in preoperative examinations. A: A lesion near to ECJ with a clear-cut margin shown in barium swallow examination of upper gastrointestine; B: A lesion with a clear-cut margin protruded into gastric lumen shown in ultrasonic gastroscopy; C: A hemisphere-like projection in the posterior wall of gastric fundus and an ulcer in its center shown in gastroscopy.

this series, the neoplasms had a relative large diameter. So the localization was realized via naked eye inspection and instrument exploration except in four cases under the help of gastroscopy. To perform this operation, it was also important to confirm the distances between tumors and ECJ after the tumors were localized.

Dividing omentum, entering omental bursa, and dividing splenogastric ligament Omentum dissection was begun from the middle-inferior pole of spleen and proceeded along outside of gastroepiploic vascular arch. After entering the omental bursa, the gastric posterior wall was turned to right by three-finger forceps. Next, the short gastric vessels were coagulated and cut with the ultrasonically activated scalpel to completely divide the gastric fundus from the superior pole of spleen.

Dissection of the left side of cardiac orifice to expose ECJ

Resection of gastric fundus using Endo GIA Figure 3A shows the cutting line of Endo GIA. The firing times of Endo GIA depended on the size of tumors. Complete resection of tumors with a sufficient margin usually required 2-3 sequential firings. When Endo GIA was placed near the left side of cardia, special care was taken to ensure that ECJ was not involved to avoid postoperative esophagus stenosis (Figure 3B).

Taking out of specimens Specimens were taken out through portal B after they were put in the specimen bag. Pathological examination was routinely carried out during the procedure.

The surgical field was irrigated and drainage tube was placed under the left diaphragm.

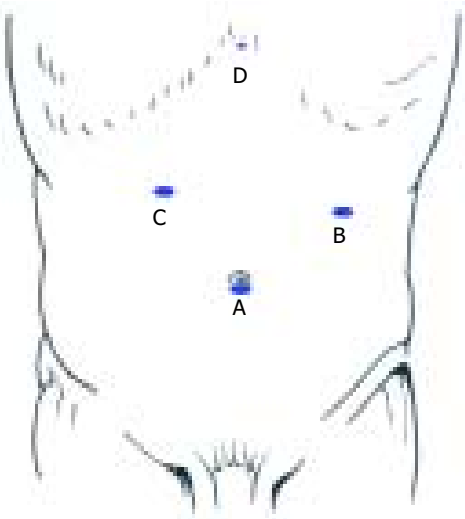

Figure 2 Trocar positions for laparoscopically extraluminal resection of gastric fundus. A: Endoscope portal (10 mm); B, C: Main working portals (10-12 mm); D: Assisting working portal (5 mm).

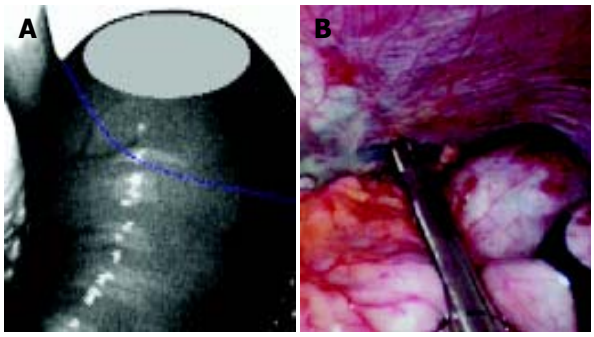

Figure 3 Resection of gastric fundus with Endo GIA. A: The blue line represents the Endo GIA resection line; B: When Endo GIA was placed near the cardia, special care was taken to ensure that ECJ was not involved.

Figure 4 Resected specimens. Line a: the distance of the tumor to ECJ.

RESULTS

In this series, the mean operative time, blood loss, and postoperative hospital stay were 66.2±10.4 min (range, 55 to 90 min), 89.4±21.7 mL (range, 50-200 mL), and 5.3±1.1 d (range, 4-7 d), respectively. On the first postoperative day, the abdominal drainage was 40-180 mL (average, 60.7±14.3 mL). Of all the patients, 73.3% recovered their gastrointestinal function within 36 h after operation and began to eat and to walk. The slowest recovery of gastrointestinal function occurred 60 h post-operation.

Figure 4 shows the resected specimens. The distance of the tumor to the section edge was: (1) 1-1.5 cm to ECJ, with an average of 1.1±0.3 cm; (2) 2.5-6 cm to the other three edges, with an average of 3.9±1.2 cm. The intra-operative frozen sections suggested that all the tumors were benign. But the postoperative paraffin-embedded sections revealed two cases of mesenchymoma with a low malignancy. In these two cases, the distance of the tumor to ECJ was 1.3 cm and 1.5 cm respectively, and the distance to the other three edges was greater than 3 cm. The

extensive salvage operation was not carried out, and a follow-up period of 18 mo and 22 mo, respectively, did not find any recurrence and metastasis. In the other 13 cases, leiomyoma was diagnosed in 8 cases, mesenchymoma in 4 cases, and neurofibroma in 1 case.

All the 15 laparoscopic surgeries were carried out successfully with no apparent lesion left, and no complication and conversion to open surgery occurred. Follow-up was continued for 3.5-33 mo and revealed no abnormality.

DISCUSSION

Clinically, gastric benign tumors are difficult to differentiate into malignancy. Even in benign tumors, canceration and severe complications of obstruction and bleeding may take place latter. So, active measures should be taken to surgically resect the tumors. As to the resection depth, the tendency was to remove the total layer of gastric wall[20-22]. Under gastroscopy, some gastric tumors could be excised via the intrasubmucosal injection of normal saline. However, this technique is applied mainly to the resection of mucosal tumors and not effective on submucosal neoplasms. Furthermore, the whole thickness of gastric wall could not be removed using this method. In the past, laparotomy was primarily performed to resect gastric submucosal tumors. With the advent of minimally invasive surgery, laparoscopic resection has become the first choice of many surgeons[23-26].

Submucosal tumors in the fundus or cardia of stomachs can be managed via laparoscopic proximal gastrectomy. However, postoperative reflux esophagitis is common. For most benign gastric submucosal tumors, the range of excision is too large and the procedure is too invasive[27-31]. Laparoscopic wedge resection of stomachs is the most commonly seen procedure for submucosal tumors of gastric fundus[31-34]. The tumor on the anterior wall of fundus is easy to excise with Endo GIA[20]. But for submucosal tumors on the posterior wall of gastric fundus, especially when next to ECJ, the wedge resection of stomachs is quite difficult, and caution should be taken to protect ECJ from postoperative esophageal stenosis and the spleen from injury, especially its superior polar.

In our early experience, we managed to resect submucosal tumors on the posterior wall of gastric fundus through the window of gastrotomy on the anterior gastric wall. The procedure was performed as follows: to cut open the anterior wall of the gastric body or fundus firstly (gastrotomy on the anterior gastric wall), to extract the posterior wall of gastric fundus through this cut, and to excise the tumor on the posterior gastric wall with Endo GIA or the method of stripping plus endoscopic suturing[35]. This method, though relatively easy to carry out and with quite a good outcome, has the disadvantage of seriously intra-operative abdominal contamination of gastric juice. Furthermore, this method cannot achieve good exposure of ECJ and has not been used in the excision of tumors on the posterior wall near ECJ. Sekimoto *et al*.[20] reported that intraluminal resection of the full thickness of posterior gastric wall lesion was performed to manage submucosal tumors on the posterior wall of gastric fundus near ECJ. In this study, balloon-tip trocars were inserted directly into the gastric lumen and gas was charged into the stomach through the trocars, then wedge resection of the posterior wall tumor was completed under direct vision with Endo GIA. The authors believe that the procedure has fewer traumas to patients and less opportunity of intraperitoneal contamination by gastric juice than gastrotomy on the anterior gastric wall. ECJ was always in the surgeon's sight, so the distance between the resection line and ECJ could be continously monitored, which means less morbidity of postoperative esophageal stenosis. However, we think that the above two methods have the same disadvantage of a limited range of resection and a higher incidence of spleen injury in that the short gastric vessels were not cut and especially that the superior pole of the spleen was not completely divided from gastric fundus. Moreover, care must be taken that the lateral tension to the gastric wall from gas inflation cannot be excessive, otherwise, injury of splenic capsule or gastric wall laceration might occur[15-18,20].

In order to solve these problems, we proposed a new laparoscopic approach to surgical resection of submucosal tumors on the posterior wall of gastric fundus. In this technique, the omentum is dissected to get access to the omental bursa. So, the splenogastric ligament could be severed to completely dissect the gastric fundus away from the superior pole of spleen. Then the left side of cardiac orifice is dissected to expose ECJ, and the gastric fundus is resected with the Endo GIA. Through these measures, the newly designed approach, *laparoscopically extraluminal resection of gastric fundus*, could avoid intraperitoneal contamination, the spleen injury and the postoperative esophagus stenosis. Meanwhile, it could also provide a sufficient range of gastric resection. The main disadvantage is the increased steps required. However, with necessary training and skills in the laparoscopic surgery, the procedure can be accomplished not quite both difficult and time consuming. The average operation time in our series was only 66.2±10.4 min. The procedure, we think, is both safe and effective in that the ECJ and the superior pole of spleen are under the continuous supervision of the operator when resecting the gastric fundus, and that the procedure can provide a more sufficient range of resection.

When the laparoscopically extraluminal resection of gastric fundus is performed, two key points must be stressed. One is that the interspace between gastric fundus and superior pole of spleen must be adequately dissected. The other is that when Endo GIA is placed near the cardia, special care must be taken to ensure that ECJ is not involved. So long as the above key points are fulfilled, our method is safe, easy and beneficial to the laparoscopic resection of submucosal tumors on the posterior wall of gastric fundus.

REFERENCES

1 **Shimizu S**, Noshiro H, Nagai E, Uchiyama A, Tanaka M. Laparoscopic gastric surgery in a Japanese institution: analysis of the initial 100 procedures. *J Am Coll Surg* 2003; **197**: 372-378

2 **Cuschieri A**. Laparoscopic gastric resection. *Surg Clin North Am* 2000; **80**: 1269-1284

3 **Giger U**, Schafer M, Krahenbuhl L. Technique and value of staging laparoscopy. *Dig Surg* 2002; **19**: 473-478

4 **Croce E**, Olmi S, Magnone S, Russo R. Laparoscopic surgery of the stomach: state of the art. *Chir Ital* 2003; **55**: 811-820

5 **Ludwig K**, Weiner R, Bernhardt J. Minimally invasive resections of gastric tumors. *Chirurg* 2003; **74**: 632-637

6 **Saikawa Y**, Kumai K, Otani Y, Yoshida M, Furukawa T, Kitagawa Y, Kubota T, Kitajuma M. Present status of laparoscopic surgery for gastrointestinal neoplasms. *Nippon Naika Gakkai Zasshi* 2003; **92**: 53-57

7 **Yang W**, Wu YL, Chu Y, Sheng H, He JH, Xiong FB, Wang Y, Cheng SD. Difference of tumor size between endoscopic estimation and postoperative pathological measurement in early gastric carcinoma. *Shijie Huaren Xiaohua Zazhi* 2003; **11**: 51-53

8 **Avital S**, Brasesco O, Szomstein S, Liberman M, Rosenthal R. Technical considerations in laparoscopic resection of gastric neoplasms. *Surg Endosc* 2003; **17**: 763-765

9 **Yuan Y**, Lin HZ, Zhang YC, Wang XJ, Wu YQ, Gao H, Wang L, Liu YH, Lu F, Lou SQ. Study on the pathogenetic effect of salted pork from a high risk area of stomach cancer in China. *China Nati J New Gastroenterol* 1997; **3**: 93-94

10 **Qin DX**, Wang GQ, Yuan FL, Tang MZ, Li MS, Zhang ZL. Screening for upper digestive tract cancer with an occult blood bead detector. Investigation of a normal north China population.

Cancer 1988; **62**: 1030-1034
11 **Cheng YS**, Li MH, Chen WX, Zhuang QX, Chen NW, Shang KZ. Follow-up evaluation for benign stricture of upper gastrointestinal tract with stent insertion. *World J Gastroenterol* 2003; **9**: 2609-2611
12 **Hsieh CC**, Shih CS, Wu YC, Huang BS, Hsu WH, Huang MH, Wang LS. Leiomyosarcoma of the gastric cardia and fundus. *Zhonghua Yixue Zazhi* 1999; **62**: 418-424
13 **Alecu L**, Costan I, Vitalariu A, Obrocea F, Pacuraru E, Gulinescu L. Gastric stromal tumor treated by laparoscopic surgery. *Chirurgia* 2002; **97**: 297-304
14 **Pross M**, Wolff S, Nestler G, Schubert D, Kahl S, Lippert H. A technique for endo-organ resection of gastric wall tumors using one intragastric trocar. *Endoscopy* 2003; **35**: 613-615
15 **Motson RW**, Fisher PW. A new technique for laparoscopic resection of a submucosal tumor on the posterior wall of the gastric fundus. *Surg Endosc* 2000; **14**: 205-206
16 **Pross M**, Wolff S, Schubert D, Meyer L, Lippert H. Combined minimal-invasive procedures for resection of benign gastric wall tumors. *Zentralbl Chir* 2003; **128**: 191-194
17 **Bouillot JL**, Bresler L, Fagniez PL, Samama G, Champault G, Parent Y. Laparoscopic resection of benign submucosal stomach tumors. A report of 65 cases. *Gastroenterol Clin Biol* 2003; **27**(3 Pt 1): 272-276
18 **Moesta KT**, Hunerbein M, Schlag PM. Treatment procedures for adenocarcinoma of the esophagogastric junction. *Chirurg* 2003; **74**: 381-392
19 **Ke ZW**, Zheng CZ, Qiu M, Li JH, Yin K, Hua JD. Laparoscopic small bowel resection. *Zhonghua Weichang Waike Zazhi* 2002; **5**: 92-94
20 **Sekimoto M**, Tamura S, Hasuike Y, Yano M, Murata A, Inoue M, Shiozaki H, Monden M. A new technique for laparoscopic resection of a submucosal tumor on the posterior wall of the gastric fundus. *Surg Endosc* 1999; **13**: 71-74
21 **Xu GW**. The gastric tumor. In: Wu JP, Qiu FZ, eds. Huang Jia-Si Waike Xue. 6th Edition. *Beijing: Renmin WeiSheng Press* 1999: 1031-1052
22 **Tangoku A**, Yamamoto K, Hirazawa K, Takao T, Mori N, Tada K, Oka M. Laparoscopic resection of large leiomyomas of the gastric fundus. *Surg Endosc* 1999; **13**: 1050-1052
23 **Rohatgi A**, Singh KK. Laparoendoscopic management of gastrointestinal stromal tumors. *J Laparoendosc Adv Surg Tech A* 2003; **13**: 37-40
24 **Tonouchi H**, Mohri Y, Tanaka K, Konishi N, Ohmori Y, Kobayashi M, Watanabe Y, Matsumura K, Takeda K, Kusunoki M. Lymphatic mapping and sentinel node biopsy during laparoscopic gastrectomy for early cancer. *Dig Surg* 2003; **20**: 421-427
25 **Kobayashi T**, Kazui T, Kimura T. Surgical local resection for early gastric cancer. *Surg Laparosc Endosc Percutan Tech* 2003; **13**: 299-303
26 **Nguyen NT**, Jim J, Nguyen A, Lee J, Chang K. Laparoscopic resection of gastric stromal tumor: a tailored approach. *Am Surg* 2003; **69**: 946-950
27 **Uyama I**, Ogiwara H, Takahara T, Kikuchi K, Iida S. Laparoscopic and minilaparotomy proximal gastrectomy and esophagogastrostomy: technique and case report. *Surg Laparosc Endosc* 1995; **5**: 487-491
28 **Zhang G**, Miao L, Zhang H, Lu J. Clinical study on reservation of part of stomach for patients with cardiac cancer of the gastric stump. *Chin Med J* 1998; **111**: 630-633
29 **Usui S**, Inoue H, Yoshida T, Fukami N, Kudo SE, Iwai T. Hand-assisted laparoscopic total gastrectomy for early gastric cancer. *Surg Laparosc Endosc Percutan Tech* 2003; **13**: 304-307
30 **Dostalik J**, Martinek L, Satinsky I, Richter V, Stigler J. Laparoscopic total gastrectomy-initial experience. *Rozhl Chir* 2003; **82**: 353-356
31 **Walsh RM**, Ponsky J, Brody F, Matthews BD, Heniford BT. Combined endoscopic/laparoscopic intragastric resection of gastric stromal tumors. *J Gastrointest Surg* 2003; **7**: 386-392
32 **Jess P**, Jensen KH. Laparoscopic wedge resection of stromal gastric tumor guided by laparoscopic ultrasonographic scanning. *Ugeskr Laeger* 2003; **165**: 1038-1039
33 **Ozmen MM**, Zulfikaroglu B, Ozalp N, Ziraman I, Hengirmen S, Sahin B. Staging laparoscopy for gastric cancer. *Surg Laparosc Endosc Percutan Tech* 2003; **13**: 241-244
34 **Onate-Ocana LF**, Ochoa-Carrillo FJ. The role of minimal invasion surgery in the management of patients with gastric carcinoma. *Cir Cir* 2003; **71**: 324-328
35 **Ke Z**, Zheng C, Qiu M, Shen Y, Hua J. Laparoscopic gastric resection. *Zhonghua Waike Zazhi* 2000; **38**: 680-682

Edited by Kumar M and Wang XL **Proofread by** Xu FM

PO Box 2345, Beijing 100023, China
Fax: +86-10-85381893
E-mail: wjg@wjgnet.com www.wjgnet.com

World J Gastroenterol 2004;10(19):2854-2858
World Journal of Gastroenterology
Copyright © 2004 by The WJG Press ISSN 1007-9327

• CLINICAL RESEARCH •

First two cases of living related liver transplantation with complicated anatomy of blood vessels in Beijing

Wen-Han Wu, Yuan-Lian Wan, Long Lee, Yin-Mo Yang, Yan-Ting Huang, Chao-Long Chen, Sheung-Tat Fan

Wen-Han Wu, Yuan-Lian Wan, Long Lee, Yin-Mo Yang, Yan-Ting Huang, Department of Surgery, The First Hospital, Peking University, Beijing 100034, China
Chao-Long Chen, Department of Surgery, Chang Gung Memorial Hospital, 123 Ta-Pei Road, Niao-Sung, Kaohsiung, Taiwan, China
Sheung-Tat Fan, Department of Surgery, Queen Mary Hospital, University of Hong Kong Medical Centre, 102 Pokfulam Road, Hong Kong, China
Correspondence to: Dr. Wen-Han Wu, Department of Surgery, The First Hospital, Peking University, Beijing 100034, China
Received: 2003-07-17 **Accepted:** 2003-10-12

Abstract

AIM: Living related liver transplantation (LRLT) has been developed in response to the paediatric organ donor shortage. Though it has been succeeded in many centers worldwide, the safety of the donor is still a major concern, especially in donors with anatomy variation. We succeeded in performing the first two cases of living related liver transplantation with complicated anatomy of blood vessels as a way to overcome cadaveric organ shortage in Beijing.

METHODS: Two patients, with congenital liver fibrosis and congenital biliary atresia were performed with living donor liver transplantation in our hospital and then followed up from November 12 to December 13, 2001. The two living donors, mother and father, were healthy aged 34 and 35 years. One right lobe (segment V, VI, VII, VIII) and one left lateral lobe (segment II and III) were used. The grafts weighed 394 g and 300 g. The ratio of graft weight to the standard liver volume (SLV) of donors was 68% and 27%. The graft weight to recipient body weight ratio was 3.2% and 4.4%. The graft weight to recipient estimated standard liver mass (ESLM) ratio was 63% and 85%. The two donors had complicated blood vessel variation.

RESULTS: Two patients undergone living donor liver transplantation had good results. Abnormal liver function with high bilirubin level appeared in a few days after operation, but liver function returned to normal one month after operation with bilirubin level almost decreased to near normal. No bleeding, thrombosis, infection and bile leakage occurred. One had an acute rejection and recovered. The two donors recovered in two weeks. One had slight fever because of a little collection in abdomen and recovered after paracentesis and drainage.

CONCLUSION: Living donor liver transplantation has been proved to be a good way that offers a unique opportunity of getting a timely liver graft as a response to shortage of pediatric donors, though it could be a technically difficult operation if there is anatomical variation.

Wu WH, Wan YL, Lee L, Yang YM, Huang YT, Chen CL, Fan ST. First two cases of living related liver transplantation with complicated anatomy of blood vessels in Beijing. *World J Gastroenterol* 2004; 10(19): 2854-2858
http://www.wjgnet.com/1007-9327/10/2854.asp

INTRODUCTION

Orthotopic liver transplantation is an effective therapy for end-stage liver disease and has been proved to be a major advance in the treatment of children with liver disease. But the development of liver transplantation in infants and young children has been hampered by the shortage of donors, especially the scarcity of size-matched donors. Though reduced-size liver transplantation (RLT) was used in some centers, it does not expand the pool of potential donors and the mortality rate of recipients on the waiting list has remained high.

From November 12 to December 13 of 2001, the first two cases of living related liver transplantation in Beijing were successfully performed in our hospital. The donors were mother and father. The recipients were their 12-year-old and 31-month-old daughters. The donors and recipients all recovered about two months after operation. These two cases indicate the potential benefit of living related liver transplantation in Beijing.

MATERIALS AND METHODS

Patients

Between November 12 and December 13 of 2001, living related liver transplantation was successfully performed on two cases in the First Hospital, Peking University. They were two girls. Underlying diseases were congenital liver fibrosis and congenital biliary atresia.

Donor selection and evaluation

The living donors were mother and father with ABO identical blood group to the patients. There was no biochemical or serologic evidence of liver disease. Computerized tomography (CT) with volumetric measurement was performed to assess the volume of the right lobe and the left lateral lobe in order to determine the graft to be harvested. Angiographies to assess the vascular anatomy were performed in both donors. We found that both donors had blood vessel variations. In donor 1, the right hepatic artery (RHA) was from the superior mesenteric artery (SMA) (Figure 1A). The two branches of right portal veins (anterior and posterior right portal vein, ARPV and PRPV) of the mother were combined to the left portal veins (LPV) separately inside the liver parenchyma, no common trunk of right portal vein was found (Figure 1B). In donor 2, the left hepatic artery was derived from the right anterior hepatic artery, which was nearly inside the liver parenchyma (Figure 1C).

Donor operation

Laparotomy was performed via bilateral subcostal incision with an upward midline extension to the xiphoid process. Cholecystectomy was performed and the cystic duct was cannulated for cholangiography using undiluted radiographic contrast in order to delineate the ductal anatomy.

In donor 1, the cholangiography showed that it had the similar variation to the portal vein, the two branches of right bile ducts (anterior and posterior right bile ducts, ARBD and PRBD) of the mother were combined to the left bile duct separately which were inside the liver parenchyma (Figure 2).

Intraoperative ultrasonography was then performed to

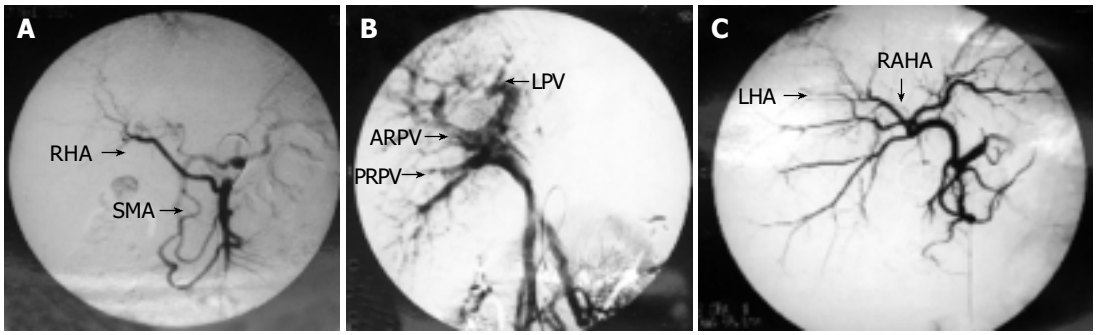

Figure 1 Angiography of the donors. A: Right hepatic artery (RHA) from superior mesenteric artery (SMA). B: Two branches of right portal veins (anterior and posterior right portal veins, ARPV and PRPV) of the mother. C: Left hepatic artery (LHA) derived from right anterior hepatic artery (RAHA).

determine the configuration of the right hepatic vein, the junction of the middle hepatic vein with the left hepatic vein and to mark on the liver surface the position of the middle hepatic vein, which would be the liver transection plane. No right inferior hepatic veins were found in these two donors. The transection line was determined by the optimal graft volume and the anatomy of its drainage veins. The entire drainage area of the right and left hepatic veins were also identified by intra-operative ultrasonography. All of the right and left hepatic venous branches were traced to the periphery in the medial segment and marked with electrocautery on the liver surface. Hilar dissection was performed to free the right hepatic artery and portal vein. Branches of the right and left portal veins supplying the caudate process were divided and ligated.

In donor 1, dissection of the right portal veins (ARPV and PRPV) and the right hepatic ducts (ARBD and PRBD) was not made until the liver was transected, because they were inside the liver parenchyma due to anatomical variation. Parenchymal transection was performed by intraoperative ultrasonography with an ultrasonic dissector without vascular occlusion. The right hepatic ducts (the anterior and posterior ducts) were divided near the confluence of the bile ducts. The defect on the left hepatic duct was closed with 5-0 PDS monofilament absorbable sutures. After mobilization of the right liver, the right portal veins (the anterior and posterior veins), the right hepatic artery (from superior mesenteric artery) and vein were clamped at the junction with the main trunks and divided. At the back table, the graft was immersed in ice sludge and flushed with University of Wisconsin (UW) solution through the right portal venous cannula. The stumps of the right hepatic artery, the right hepatic vein and portal vein on the donor liver remnant were sutured.

In donor 2, The left hepatic artery, portal vein and hepatic vein were freed and hepatic parenchymal transection was accomplished using an ultrasonic dissector without vascular occlusion. Because the left hepatic artery was from the anterior right hepatic artery, the dissection of the left hepatic artery was partly inside the liver parenchyma when the liver transection was finished. The left duct was divided close to the cut surface of the liver, with an intact Glissonian sheath. The left hepatic duct was divided near the confluence of the bile ducts. The isolated graft was perfused in situ with the left portal vein clamped and cannulated by a catheter connected with cold lactated Ringer's solution followed by a cold UW solution, when the left hepatic vein was opened.

Recipient operation

The abdomen was entered through a bilateral subcostal incision with midline extension. Hilar dissection was performed to isolate and divide branches of the hepatic artery and portal vein. Then, total hepatectomy was performed with the inferior vena cava preserved.

In recipient 1, the graft right hepatic vein (RHV-D) was anastomosed end-to-end to the recipient right hepatic vein (RHV-R). The graft anterior right portal vein (ARPV-D) was anastomosed end-to-end to the recipient left portal vein (LPV-R) and the graft posterior right portal vein (PRPV-D) was anastomosed end-to-end to the recipient right portal vein (RPV-R). The similar method was used to reconstruct the bile duct without stenting after the hepatic artery anastomosis (Figure 3).

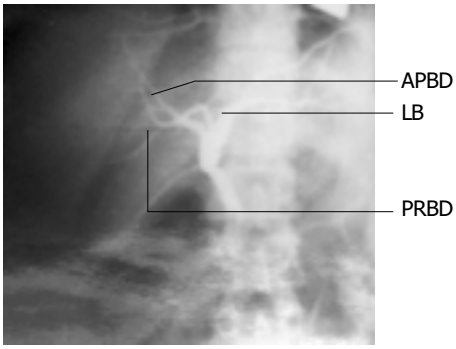

Figure 2 Chlangiography of the donor 1 Two branches of right bile duct (anterior and posterior right bile ductS, ARBD and PRBD) of the mother.

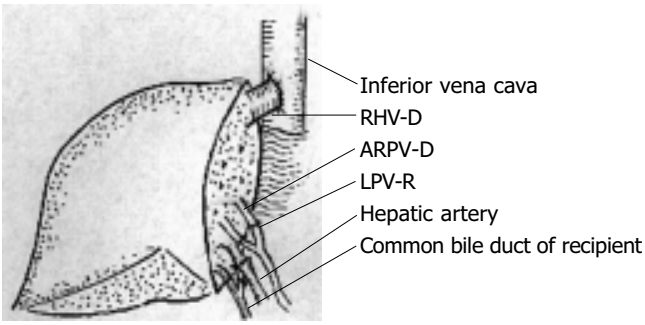

Figure 3 End-to-end anastomosis of the graft right hepatic vein (RHV-D) to the recipient right hepatic vein (RHV-R).

In recipient 2, the graft left hepatic vein was anastomosed end-to-end to the confluence of the recipient left and middle hepatic veins. The graft left portal vein was anastomosed end-to-end to the truncated bifurcation of the recipient portal vein. The left hepatic duct was anastomosed to the Roux-en-Y limb of jejunum with an internal stent after the hepatic artery anastomosis.

The hepatic artery of the graft was anastomosed to the recipient hepatic artery using microvascular techniques.

Postoperative immunosuppression

Induction and maintenance immunosuppressive therapy consisted of a triple-drug regimen of steroid, cyclosporine A, and azathioprine. Acute rejection episode suspected on clinical and biochemical features and confirmed by percutaneous liver biopsy, was treated by intravenous bolus of methyl-predimetholone.

RESULTS

There was no operative mortality in the two living donors. One donor had postoperative complication of abdominal collection about two weeks after operation and recovered by percutaneous drainage about three weeks afteroperation. Blood losses during the donor operations were 150 mL and 70 mL respectively, and no blood transfusion was required in these two donor operations. Blood losses during the recipient operations were 50 mL and 100 mL respectively, and recipient 2 received 200 mL blood transfusion in the operation. The first warm ischaemia time of the grafts was 30 s and almost 0 s. The cold ischaemia time of the grafts was 120 min and 180 min. The second warm ischaemia time of the graft was 40 min and 50 min. The portal and arterial reperfusion interval time was 70 min and 90 min.

Table 1 Laboratory findings of donor 1

Content	Pre-operation	1 d post-operation	3 d post-operation	7 d post-operation	14 d post-operation
ALT (IU/L)	12	372	110	48	45
AST (IU/L)	9	404	105	43	40
TBIL (ug/L)	10.5	80.2	32.5	7.4	8.2
DBIL (ug/L)	3.8	37.5	4	3.94	2.1
PTA (%)	78.0	32.0	29.0	56.0	72.0

Table 2 Laboratory findings of donor 2

Content	Pre-operation	1 d post-operation	3 d post-operation	7 d post-operation	14 d post-operation
ALT (IU/L)	37	816	305	42	
AST (IU/L)	30	817	58	37	
TBIL (ug/L)	7.7	21.8	9.7	5.0	
DBIL (ug/L)	3.5	3.24	2.3	0.78	
PTA (%)	82	127	151	127	

The weight of grafts was 394 g and 300 g, respectively. The ratio of graft weight to the standard liver volume (SLV) of donor was 68% and 27%, respectively. The graft weight to recipient body weight ratio was 3.2% and 4.4% respectively, and the graft weight to recipient estimated standard liver mass (ESLM) was 63% and 85%.

The duration of postoperative hospital stay of the donors was 7 d and 21 d. Most laboratory profiles returned to normal about two weeks after operation. The two donors had normal liver function and were able to return to their preoperative activities 3 mo after the operation.

Both patient and graft survived well 3 mo after operation. No postoperative complication occurred in recipient 1. Recipient 2 had an attack of acute rejection one week after the operation, and recovered after bolus treatment of methylprednisolone (1 g methylprednisolone per day for three days, iv).

Data on the postoperative serum total bilirubin (TBIL), direct bilirubin (DBIL), alanine aminotransferase (ALT), aspartate aminotransferase (AST) and prothrombin activities (PTA) are shown in Tables 1-4.

DISCUSSION

The well-known inverse relationship between the availability of cadaveric pediatric organs and the epidemiology of pediatric liver disease has resulted in a substantial mortality rate among children on the waiting list[1,2]. Although RLT could alleviate the shortage of small donor organs, it did not expand the pool of potential donors, but induced a shift of grafts from a limited pool of adult cadaveric donors to pediatric recipients[3]. The use of liver donors has providesd a means for increasing the overall supply of livers[4,5].

Though liver consists of paired structures anatomically, safe separation of liver into its right and left halves requires considerable experience[6,7]. Fan *et al.*[14] identified the reasons for unsatisfactory outcomes such as the presence of necrotic tissue on the liver transection surface, inadequate hepatic venous drainage, missed right posterior hepatic duct, and more than one right hepatic duct orifice on the graft.All these made its reconstruction difficult[8]. We followed the procedure "living donor liver transplantation using right lobe graft" by preferring the division of liver parenchyma along the Cantlie line[9]. To define the Cantlie line, we used the middle hepatic vein as a reference by using the intraoperative ultrasonogram[10,11]. To reduce the bleeding in the operation, we also decreased the central venous pressure to about 5 cm H_2O[12].

The blood supply to the hepatic duct is dependent on a peribiliary plexus[13]. In the harvesting of the right or the left

Table 3 Laboratory findings of recipient 1

Content	Pre-operation	1 d post-operation	3 d post-operation	7 d post-operation	14 d post-operation	21 d post-operation	28 d post-operation
ALT (IU/L)	40	372	189	103	80	24	28
AST (IU/L)	44	418	78	53	19	17	22
TBIL (ug/L)	17.4	73.4	63.3	80.6	58.6	53.6	23.8
DBIL (ug/L)	5.0	45.28	30.6	46.6	30.2	26.6	6.6
PTA (%)	89	18	31	43	41	73	81

Table 4 Laboratory findings of recipient 2

Content	Pre-operation	1 d post-operation	3 d post-operation	7 d post-operation	14 d post-operation	21 d post-operation	28 d post-operation
ALT (IU/L)	105	1 054	1 397	496	185	47	42
AST (IU/L)	250	3 028	414	107	70	35	31
TBIL (ug/L)	480.4	87.7	209.3	216.2	205.4	96.7	44.2
DBIL (ug/L)	373.8	44.79	124.4	178.1	161.1	82.1	30.7
PTA (%)	92	7	16	58	72	76	78

lobe graft, the blood supply is mainly from tiny arterial arcades from the right or the left portion of the caudate lobe[13]. So, the liver tissue cranial to the hepatic duct was cleared by ultrasonic dissector down to the caudate process and care was taken to avoid thinning the wall of the hepatic duct with ultrasonic dissector. We also noticed to maintain the blood pressure stable in the operation because hypotensive episodes would render the hepatic duct stump vulnerable to ischemia and necrosis[14].

In our group, the two donors had complicated anatomy variation. In donor 1, ARPV and PRPV were parallelly combined to the left portal vein, which were inside the liver parenchyma, no common trunk of right portal vein was found in extraparenchyma of the liver. The right hepatic duct had the similar anatomical variation with two parallel branches. This was rare in our past experiences and made the operation quite complicated. A series of 990-arterioportographic studies and 3 000-endoscopic retrograde cholangio-pancreatic-graphic studies of the liver showed that the incidence of this kind of portal vein variation and hepatic bile duct variation was 0.15% and 5.08%, respectively[15-17]. When we tried to expose the ARPV and PRPV, we did not follow the main trunk of portal vein from the hilum, but dissected the hepatic parenchyma with intraoperative ultrasonography by an ultrasonic dissector without vascular occlusion in combination with hilar dissection to free the ARPV and PRPV[11]. Dissection of right hepatic ducts was not carried out until the liver was transected. Chen *et al*.[4] reported that 83.33% intrahepatic ducts had the similar anatomy variation as the portal veins[18]. We paid more attention to intraoperative cholangiography and certified the similar anatomical variation in our group. We performed the same procedure to finish the dissection of anterior right hepatic duct and posterior right hepatic vein[19,20].

In donor 2, angiographic study showed that the left hepatic artery was from the anterior right hepatic artery. To avoid ischemia due to excessive hepatic artery dissection, which might cause biliary stricture or leakage[21], we dissected the left hepatic artery just on the left side of the common hepatic duct and carefully preserved the posterior right hepatic artery from the left side of the left hepatic artery. We also performed a little dissection in liver parenchyma with an ultrasonic dissector to get enough length of left hepatic artery for anastomosis[4]. It is important not to isolate the left hepatic artery too far into the left side of the liver parenchyma to avoid devascularization of the left hepatic duct[22].

Since these are the first two cases of living related liver transplantation in Beijing, ethical issues need to be considered when one contemplates liver transplantation from parent to child. These issues are similar to those associated with the transplantation of renal grafts from living related donors[23]. With the experience in liver resection, we conclude that the surgical risk is low enough to be acceptable for a parent or other close relatives if they volunteer to be an organ donor. Sure, it is an ethical dilemma of subjecting a healthy person to major hepatic resection to obtain a graft for a patient with end-stage liver disease[24-26]. We all agree with the congsensus that living-donor liver transplantation is not justified when there are sufficient cadaveric donors. However, the procedure could be justified for a patient with fulminant hepatic failure when no cadaver donor was available and when the recipient had a reasonable chance of a successful outcome[27].

The success of these first two cases has led to the acceptance of living related liver transplantation (LRLT) for clinical application in our center. With the excellent results in many centers and our present study[28,29], we consider that LRLT should be a good way for the care of patients with end-stage liver diseases or fulminant liver failure, particular in countries where cadaveric organ donation is limited or not available[30,31]. Though it might be very difficult technically, we should not give it up when we consider safety of the donor as our absolute priority first.

REFERENCES

1 **Kelly D,** Sibal A. Current status of liver transplantation. *Indian J Pediatr* 2003; **70**: 731-736

2 **Ogura Y,** Kaihara S, Haga H, Kozaki K, Ueda M, Oike F, Fujimoto Y, Ogawa K, Tanaka K. Outcomes for pediatric liver retransplantation from living donors. *Transplantation* 2003; **76**: 943-948

3 **Abouljoud M,** Yoshida A, Dagher F, Moonka D, Brown K. Living donor and split-liver transplantation: an overview. *Transplant Proc* 2003; **35**: 2772-2774

4 **Chen CL**, Chen YS, Liu PP, Chiang YC, Cheng YF, Huang TL, Eng HL. Living related donor liver transplantation. *J Gastroenterol Hepatol* 1997; **12**: S342-345

5 **Malago M,** Testa G, Frilling A, Nadalin S, Valentin-Gamazo C, Paul A, Lang H, Treichel U, Cicinnati V, Gerken G, Broelsch CE. Right living donor liver transplantation: an option for adult patients: single institution experience with 74 patients. *Ann Surg* 2003; **238**: 853-863

6 **Kamel IR,** Lawler LP, Fishman EK. Variations in anatomy of the middle hepatic vein and their impact on formal right hepatectomy. *Abdom Imaging* 2003; **28**: 668-674

7 **Yersiz H,** Renz JF, Farmer DG, Hisatake GM, McDiarmid SV, Busuttil RW. One hundred in situ split-liver transplantations: a single-center experience. *Ann Surg* 2003; **238**: 496-505

8 **Fan ST**, Lo CM, Liu CL. Technical refinement in adult-to-adult living donor liver transplantation using right lobe graft. *Ann Surg* 2000; **231**: 126-131

9 **Akamatsu N,** Sugawara Y, Kaneko J, Sano K, Imamura H, Kokudo N, Makuuchi M. Effects of middle hepatic vein reconstruction on right liver graft regeneration. *Transplantation* 2003; **76**: 832-837

10 **Cheng YF**, Huang TL, Chen CL, Chen TY, Huang CC, Ko SF, Lee TY. Variations of the left and middle hepatic veins: application in living related hepatic transplantation. *J Clin Ultrasound* 1996; **24**: 11-16

11 **Ko EY,** Kim TK, Kim PN, Kim AY, Ha HK, Lee MG. Hepatic vein stenosis after living donor liver transplantation: evaluation with doppler US. *Radiology* 2003; **229:** 806-810

12 **Johnson M**, Mannar R, Wu AV. Correlation between blood loss and inferior vena caval pressure during liver resection. *Br J Surg* 1998; **85**: 188-190

13 **Stapleton GN**, Hickman R, Terblanche J. Blood supply of the right and left hepatic ducts. *Br J Surg* 1998; **85**: 202-207

14 **Fan ST**, Lai EC, Lo CM, Chu KM, Liu CL, Wong J. Hepatectomy with an ultrasonic dissector for hepatocellular carcinoma. *Br J Surg* 1996; **83**: 117-120

15 **Cheng YF**, Huang TL, Lee TY, Chen TY, Chen CL. Variation of the intrahepatic portal vein; angiographic demonstration and application in living-related hepatic transplantation. *Transplant Proc* 1996; **28**: 1667-1668

16 **Huang TL**, Cheng YF, Chen CL, Chen TY, Lee TY. Variants of the bile ducts: clinical application in the potential donor of living-related hepatic transplantation. *Transplant Proc* 1996; **28**: 1669-1670

17 **Kornasiewicz O**, Krawczyk M, Paluszkiewicz R, Zieniewicz K, Hevelke P, Grzelak I, Pacho R, Rowinski O, Kalicinski P, Kaminski A, Pawlowska J. Anatomical alteration of the vascular tree observed during living related liver transplantation. *Transplant Proc* 2003; **35**: 2245-2247

18 **Cheng YF**, Huang TL, Shen CL, Sheen-Chen SM, Liu CC, Chen TY, Lee TY. Anatomic dissociation between the intrahepatic bile duct and portal vein: risk factors for left hepatectomy. *World J Surg* 1997; **21**: 297-300

19 **Kornberg A,** Heyne J, Schotte U, Hommann M, Scheele J. Hepatic venous outflow reconstruction in right lobe living-donor liver graft using recipient's superficial femoral vein. *Am J Transplant* 2003; **3**: 1444-1447

20 **Hisatsune H,** Yazumi S, Egawa H, Asada M, Hasegawa K, Kodama Y, Okazaki K, Itoh K, Takakuwa H, Tanaka K, Chiba T. Endoscopic management of biliary strictures after duct-to-duct biliary reconstruction in right-lobe living-donor liver

transplantation. *Transplantation* 2003; **76**: 810-815

21 **Sanchez-Urdazpal L**, Gores GJ, Ward EM, Maus TP, Buckel EG, Steers JL, Wiesner RH, Krom RAF. Diagnostic features and clinical outcome of ischemic-type biliary complications after liver transplantation. *Hepatology* 1993; **17**: 605-609

22 **Kanazawa A,** Kubo S, Tanaka H, Takemura S, Yamazaki K, Hirohashi K, Shiomi S. Bile leakage after living donor liver transplantation demonstrated with hepatobiliary scan using 9mTc-PMT. *Ann Nucl Med* 2003; **17**: 507-509

23 **D'Alessandro AM**, Sollinger HW, Knechtle SJ, Kalayoglu M, Kishen WA, Uehling DT, Moon TD, Messing EM, Bruskewitz RC, Pirsch JD. Living related and unrelated donors for kidney transplantation. A 28-year experience. *Ann Surg* 1995; **222**: 353-362

24 **Broelsch CE**, Whitington PF, Emond JC, Heffron TG, Thistlethwaite JR, Stevens L, Piper J, Whitington SH, Lichtor JL. Liver transplantation in Children from living related donors. Surgical techniques and results. *Ann Surg* 1991; **214**: 428-437

25 **Basaran O,** Karakayali H, Emiroglu R, Tezel E, Moray G, Haberal M. Donor safety and quality of life after left hepatic lobe donation in living-donor liver transplantation. *Transplant Proc* 2003; **35**: 2768-2769

26 **Lan AK,** Luk HN, Goto S, Chen SM, Eng HL, Chen YS, de Villa VH, Wang CC, Cheng YF, Chen CL, Lee JH, Jawan B. Stress response to hepatectomy in patients with a healthy or a diseased liver. *World J Surg* 2003; **27**: 761-764

27 **Majno P,** Mentha G, Berney T, Buhler LH, Giostra E, Gelez P, Morard I, Bednarkiewicz M, Huber O, Morel P. Adult-to-adult living-donor liver transplantation. A summary of current status and an outline of the program in Geneva. *Swiss Surg* 2003; **9**: 227-236

28 **Imamura H,** Seyama Y, Kokudo N, Maema A, Sugawara Y, Sano K, Takayama T, Makuuchi M. One thousand fifty-six hepatectomies without mortality in 8 years. *Arch Surg* 2003; **138**: 1198-1206

29 **Ghobrial RM,** Busuttil RW. Future of adult living donor liver transplantation. *Liver Transpl* 2003; **9**(10 Suppl 2): S73-79

30 **Zimmerman MA**, Trotter JF. Living donor liver transplantation in patients with hepatitis C. *Liver Transpl* 2003; **9**: S52-57

31 **Sugawara Y,** Makuuchi M, Kaneko J, Akamatsu N, Imamura H, Kokudo N. Living donor liver transplantation for hepatitis B cirrhosis. *Liver Transpl* 2003; **9**: 1181-1184

Edited by Xu JY and Wang XL **Proofread by** Xu FM

PO Box 2345, Beijing 100023, China
Fax: +86-10-85381893
E-mail: wjg@wjgnet.com www.wjgnet.com

World J Gastroenterol 2004;10(19):2859-2863
World Journal of Gastroenterology
Copyright © 2004 by The WJG Press ISSN 1007-9327

• BRIEF REPORTS •

Transcutaneous perianal sonography: A sensitive method for the detection of perianal inflammatory lesions in Crohn's disease

Jochen Wedemeyer, Timm Kirchhoff, Gernot Sellge, Oliver Bachmann, Joachim Lotz, Michael Galanski, Michael P. Manns, Michael J. Gebel, Jörg S. Bleck

Jochen Wedemeyer, Gernot Sellge, Oliver Bachmann, Michael P. Manns, Michael J. Gebel, Jörg S. Bleck, Department of Gastroenterology, Hepatology and Endocrinology, Medical School of Hannover, Carl Neuberg Str. 1, 30623 Hannover, Germany
Timm Kirchhoff, Joachim Lotz, Michael Galanski, Department of Diagnostic Radiology, Medical School of Hannover, Carl Neuberg Str. 1, 30623 Hannover, Germany
Correspondence to: Jochen Wedemeyer M.D., Department of Gastroenterology, Hepatology and Endocrinology, Medical School of Hannover, Carl Neuberg Str. 1, 30625 Hannover, Germany. wedemeyer.jochen@mh-hannover.de
Telephone: +49-511-5323157 **Fax:** +49-511-5328157
Received: 2004-03-18 **Accepted:** 2004-04-29

Abstract

AIM: Pelvic magnetic resonance imaging (MRI) and endoanal ultrasound which are established imaging methods for perianal inflammatory lesions in patients with Crohn's disease require expensive specialized equipments and expertise. We investigated the feasibility and sensitivity of transcutaneous perianal ultrasound (PAUS) using regular ultrasound probes in the imaging of perianal inflammatory lesions. The sonographic findings were correlated to pelvic MRI-scans.

METHODS: We performed PAUS in 25 patients with Crohn's disease and clinical signs of perianal inflammatory disease. Within a median of 10 d (range 0-75) these patients underwent MRI of the pelvis. Regular convex and linear high resolution probes were used for PAUS. The sonographic findings were correlated to the MRI findings by blinded investigators.

RESULTS: The sonographic investigations were well tolerated by all patients. Fistulae typically presented as hypoechoic tracks. Twenty-nine fistulae were detected in 22 patients. Abscesses were detected in 7 patients and presented as hypo- or anechoic formations. Twenty-six of 29 fistulae and 6 of 7 abscesses could be confirmed by MRI. Kappa statistics showed an excellent agreement (kappa>0.83) between the two imaging methods.

CONCLUSION: PAUS is a simple, painless, feasible, real-time method that can be performed without specific patient preparation which is comparable in its sensitivity to pelvic MRI in the detection of perianal fistulae and/or abscesses. PAUS can especially be recommended as a screening tool in acute perianal disorders such as perianal abscess and for follow-up studies of perianal inflammatory disease.

Wedemeyer J, Kirchhoff T, Sellge G, Bachmann O, Lotz J, Galanski M, Manns MP, Gebel MJ, Bleck JS. Transcutaneous perianal sonography: A sensitive method for the detection of perianal inflammatory lesions in Crohn's disease. *World J Gastroenterol* 2004; 10(19): 2859-2863
http://www.wjgnet.com/1007-9327/10/2859.asp

INTRODUCTION

Perianal disease is a common complication in Crohn's disease. Approximately 20% of patients with Crohn's disease would suffer from perianal fistulae and/or sinus tracks[1,2]. The diagnosis and treatment of perianal fistulae can be difficult and represent a challenge for physicians. Treatment modalities include conservative as well as surgical approaches. Therefore comprehensive imaging is necessary in order to develop adequate treatment strategies and to evaluate treatment outcomes[3]. Endoanal ultrasound (EAUS) as well as MRI of the pelvis are frequently used for imaging of perianal fistulae, sinus tracks or abscesses. The combination of MRI and EAUS is capable of detecting perianal fistulae with a sensitivity of 100%[4,5]. Recent studies for the medical treatment of perianal disease used either MRI of the pelvis or transanal ultrasound as a follow-up tool to evaluate the therapy outcomes after infliximab treatment[6-8].

However, both imaging methods require specialized and fairly expensive equipments as well as an experienced investigator. The use of a rigid EAUS probe can be painful or even impossible in patients with inflammatory perianal disease due to anal stenosis. Furthermore, EAUS does not allow the assessment of pathological changes extending to the gluteal region. MRI allows the evaluation of the whole pelvic region, however, it lacks the real time capacity of ultrasound and the high resolution of high frequency linear ultrasound probes.

Transcutaneous perineal/perianal ultrasound (PAUS) represents another method to detect perianal inflammatory disease which can be performed using regular ultrasound probes without special patient preparation. Furthermore, it can be used in patients with anal stenosis. However, despite its methodical simplicity, PAUS is not yet widely used in the detection of perianal fistulae and/or abscesses. Several investigators have applied perineal ultrasound in female patients for diagnosis of incontinence including postpartum anal sphincter tears[9-15]. These investigations were regularly performed in the lithotomy position and supplemented or compared with transvaginal or transrectal ultrasound. Rubens *et al*.[16] described PAUS as a valuable tool to image perianal inflammatory disease in their pictorial essay, while Stewart *et al*.[17] recently described PAUS using a combination of transvaginal and transperineal ultrasound in female and transperineal ultrasound in male patients to detect perianal fistulas and abscesses. Beside a linear probe, Parks *et al*.[18] used a transvaginal probe for the PAUS to take advantage of its small footprints and they were able to classify fistulae according to the Parks classification. In their recent published study Mallouhi *et al*.[19] showed a high correlation of perineal ultrasound findings and surgical examination. However, as Mallouhi *et al*.[19] pointed out correctly surgical exploration in some cases, might not allow the detection of every perianal fistula. Despite the obvious advantages of perianal/perineal ultrasound no studies exist so far that compared the effectiveness of PAUS with the established imaging methods such as MRI and/or EAUS. Therefore, we investigated patients with clinical signs of perianal fistulae or abscesses using PAUS and compared the detected pathology with results of MRI scans of the pelvis as the gold standard. Also, we performed follow-up

studies in certain patients to monitor the treatment effectiveness.

MATERIALS AND METHODS

Patients were recruited either from the inflammatory bowel disease outpatient clinic or from the gastroenterology wards of our institution. Ultrasound examinations were performed in 25 patients (17 females, 8 males) with a mean age of 36.2±2.5 years. All patients had prediagnosed Crohn's disease confirmed by biopsy and presented with complaints suspicious of perianal disease. No specific preparations of the patients such as enemas were performed. Either a Toshiba Aplio (3.3 Mhz [Tissue Harmonic Imaging, THI] and 12 Mhz transducer), a Toshiba Powervision (6 Mhz and 12 Mhz transducer, Toshiba, Neuss, Germany) or a Siemens Elegra (3.75 [THI] and 9 Mhz transducer, Siemens, Erlangen, Germany) was used depending on availability for the ultrasound examination. Colour Doppler ultrasound was applicable with all probes. The ultrasound probe was covered with contact gel, and introduced into a regular latex examination glove with the fingers of the glove tied up in knots for hygienic reasons (Figure 1A). For sufficient contact, contact gel was spread on the outside of the glove before the examination was performed. PAUS was performed with the patient in the left lateral position by placing the probe directly above the anus in the sagittal plane (Figure 1B). For better orientation, the examination was started with a convex transducer identifying bladder, rectum and prostate/vagina (Figure 2). Details and pathological findings were imaged and further investigated using the linear high resolution probes. The maximal penetration for good visualisation using linear transducers was 6 cm. Depending on the specific findings the probe was turned or shifted in the perianal area. The probe was placed above any pathological opening. Colour Doppler was used to distinguish blood vessels from other anechoic/ hypoechoic lesions such as fistulae. All ultrasound examinations were checked by either J.S.B. or M.J.G. who both held the highest DEGUM (German society for ultrasound in medicine) ultrasound certificates (DEGUM III, Seminarleiter). Colour Doppler ultrasound was applicable with all probes. Fistulae were catagorized as superficial, intersphincteric, transsphincteric suprasphincteric, extrasphincteric, recto-vaginal fistulae and/or abscesses.

Within a median of 10 d (range 0-75) the patients were also examined by pelvic MRI. MRI was performed to identify inflammatory changes, abscess formations and fistulae. A 1.5 Tesla MR scanner (GE Signa Horizon Echospeed, Milwaukee, Wisconsin) was used. A phased array surface coil was placed on the pelvis. Transverse and sagittal T1-spin echo (T1SE), fat-saturated T2-fast spin echo (fsT2FSE) sequences were applied. Also, transverse and oblique coronal (angulated adjacent to the anal canal) T2FSE sequences without fat saturation were applied in order to detect fistulous tracks. Either respiratory compensation or respiratory trigger was used to avoid artefacts from respiratory motion. After intravenous gadolinium administration (0.1 mmol/kg Gd-DTPA, Magnevist, Schering, Berlin, Germany) transverse and oblique coronal fat-saturated T1-spin echo (fsT1SEpostGd) sequences were performed. Raised signal intensity in the T2-weighted images and an increased uptake of Gd-DTPA served as markers for active inflammatory changes, whereas low signal intensity bands distorting normal fibrofatty tissue in both T1 and T2 weighted images were considered to be fibrous scarring. The results were reviewed by two radiologists in consensus reading. The investigators of either method were not aware of the results generated by the other.

Results were compared by calculating the kappa coefficient according to Cohen.

RESULTS

General Images

PAUS was well tolerated in all patients. In cases of subcutaneous perianal abscesses or significant inflammatory changes, slight local pain was reported during the examination when pressure was applied with the ultrasound probe. Two patients who had a history of significant anal stenosis and repeated surgical anal dilations were included in the study and evaluated with PAUS, because endoanal ultrasound could not be performed in these cases.

A general view was achieved using a regular convex probe (as listed in the Materials and Methods section) that showed rectum, bladder, prostate gland and urethra or vagina and uterus (Figure 2). Small intestinal bowel loops could be shown as well as pathological pelvic intraabdominal fluid collections. However, for comprehensive imaging of perianal inflammatory disease, a high frequency linear probe provided a much more detailed imaging. The penetration that could be achieved using a linear transducer (as listed in Materials and Methods) was sufficient to detect most of the perianal inflammatory changes. The anal canal presented as an anechoic area (Figure 3A,B). The external anal sphincter presented with hyperechoic striped bands while the internal sphincter had a homogenic hypoechoic texture (Figure 3B).

Pathological findings were detected in 96% (24/25) of the patients examined with PAUS. Pathological findings included entero-cutaneous perianal fistulae, sinus tracts without cutaneous openings, bifurcated complex perianal fistulae, perianal or subcutaneous abscesses, rectovaginal fistulae and inflammatory remnants post perianal abscess.

Fistulas

In 88% (22/25) of patients investigated, fistulae and/or sinus tracts could be visualized by PAUS. A total of 29 fistulae were detected. Fistulae and sinus tracks presented as hypo/anechoic tracks. Figure 3 shows typical PAUS images of entero-cutaneous perianal fistulae. Regularly small hyperechoic dots could be detected representing air bubbles within the fistulous tracks. In 45% (10/22) of the fistulae, it was possible to trace small hyperechoic dots which would move within the fistulae and therefore enabling the investigator to detect even minor fistulous tracks indicating active fistulae.

MRI confirmed 90% (26/29) fistulae in 91% (20/22) of these patients. All fistulae detected by MRI were also detected by PAUS. The kappa coefficient for fistulae was calculated as 0.83 resembling an excellent agreement. In two patients both methods described incomplete fistulae (sinus tracks with no visible cutaneous opening). Figure 4 shows a perianal enterocutaneous fistula imaged by PAUS and MRI.

As PAUS included inspection of the anoderm, cutaneous openings of fistulae could easily be detected. In two cases MRI was not able to confirm perianal fistulae that were detected by PAUS. However, discharge from a cutaneous opening proved the presence of a perianal fistula in both of these cases, which could be visualized with PAUS. Both of these fistulae were short intersphincteric fistulae of type 1 according to the Parks classification[18]. In one of these cases the fistula described in PAUS could be detected in a repeat MRI performed using a vaginal tampon for better anatomical differentiation. However, the investigators were aware of the findings made in the PAUS in this second examination.

Follow-up PAUS investigations were performed in 8 of the 25 patients. Improvement under therapy was noted in 4 cases, no change in 2 cases and progressive disease in 2 patients. The sonographical improvement was consistent with clinical findings. In one case follow-up MRI was performed confirming the PAUS findings as both imaging methods described an abscess within the fistulous track.

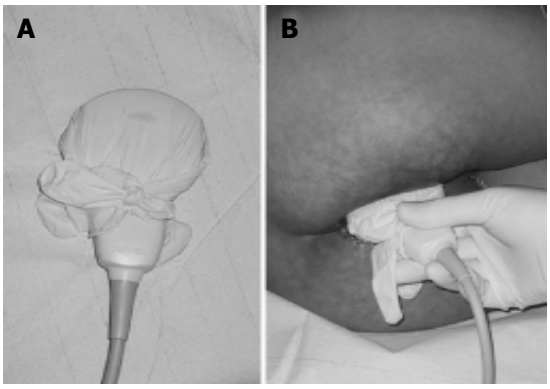

Figure 1 A regular latex examination glove filled with ultrasound contact gel was used to cover the probes for hygienic reasons (A). The examinations were performed in the left lateral position with the probe placed above the anus (B).

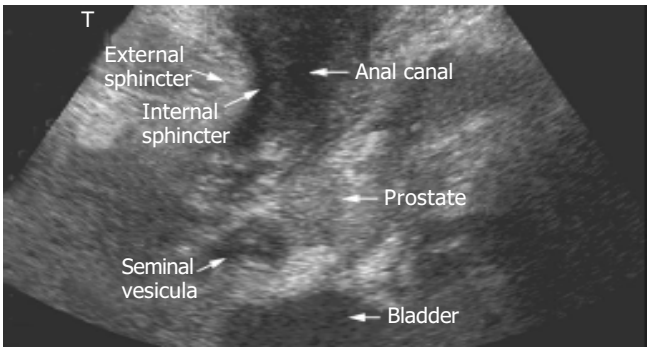

Figure 2 A general overview over perianal anatomy and pathology can be obtained using a regular convex 3.5 Mhz probe.

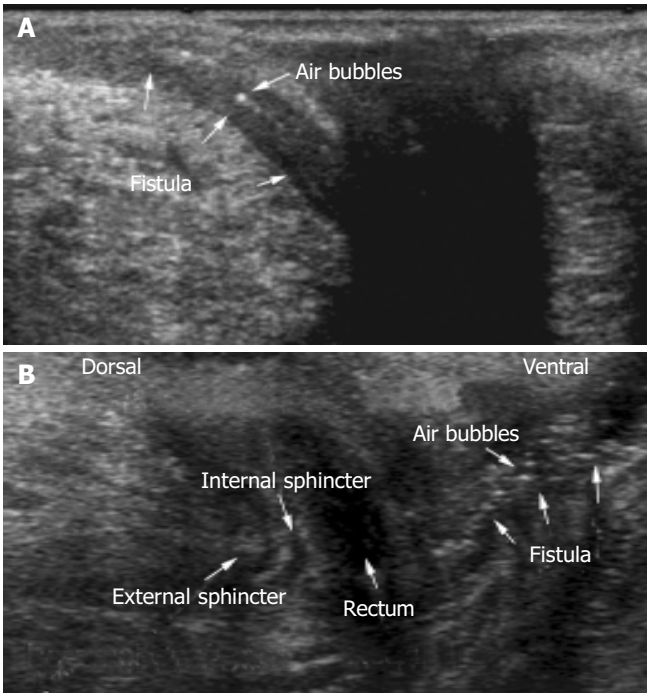

Figure 3 Perianal imaging of entero-cutaneous fistulae using a 10 MHz ultrasound probe. Hyperechoic dots resemble air bubbles within the fistulous track. The rectum represents as hypo- anechoic structure. External and internal anal sphincter can be distinguished.

Recto-vaginal fistulae

PAUS was able to visualize rectovaginal fistulae in 3 cases. MRI confirmed recto-vaginal fistulae in two of the three cases. In the remaining case MRI showed a fistula from the sigmoid colon to the vagina, in contrast, PAUS described a recto-vaginal fistula. While gynaecological examination did not confirm the presence of any fistula, drainage of blue stain into the vagina after the introduction of a methylene blue soaked swab into the rectum finally proved the presence of a recto-vaginal fistula as was described by PAUS. The sigmoid-vaginal fistula was not detected in the PAUS examination.

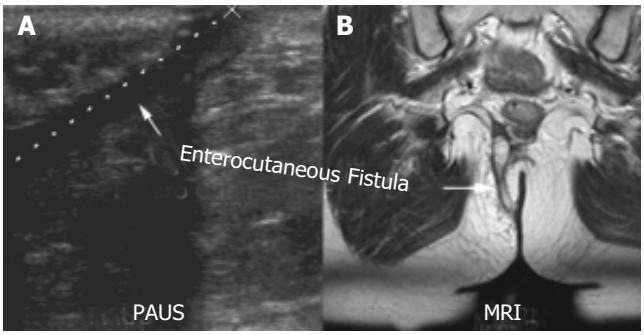

Figure 4 Enterocutaneous fistula detected with PAUS (A) was confirmed using MRI (oblique coronary T2-FSE sequence without fat saturation) (B).

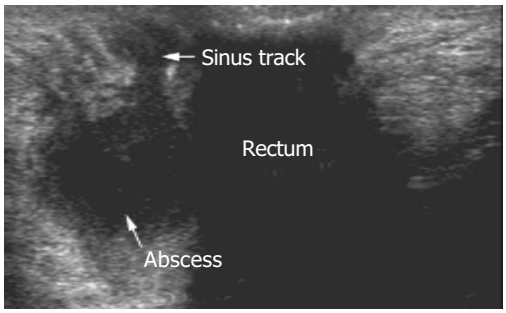

Figure 5 Typical appearance of a pararectal abscess, dorsal of the rectum. Furthermore a sinus track could be detected that perforated the external sphincter and ceased in multiple small sinus tracks that did not have a cutaneous opening.

Abscesses

Perianal fluid collections/abscesses were detected by PAUS in 28% (7/25) of the patients. Abscesses presented as oval shaped hypo- to anechoic masses which were demarcated off the regular tissue by a hypoechoic seam (Figure 5). In 5 cases a direct association of a fistulous and/or sinus track to the abscess formation could be demonstrated. Figure 5 shows a perianal sonographic scan of a male patient that presented to our outpatient clinic with severe perianal discomfort. While inspection and digital examination of the anus were inconspicuous, the transcutaneous perianal ultrasound examination revealed hypoechoic fluid collections dorsal of the rectum in this patient. The abscess shown in Figure 5 had a fistulous track connecting the rectum and a complex intrasphincteric fistulous system. In 6 cases fluid collections could be confirmed using MRI, and no fluid collection detected in MRI was missed by PAUS. In one case MRI could not confirm a fluid collection. However the two examinations were performed at an interval of 23 d. The smallest abscess detected in PAUS measured 14 mm×12 mm× 8 mm. In three of the cases with significant, drainable abscesses examination under anaesthesia (EUA) could confirm PAUS/MRI findings.

Figure 6 shows an example of a perianal abscess as imaged by PAUS and MRI. Clinical inspection of the anal region did not show any abnormalities in this patient. However anal

discharge upon digital examination was observed and further imaging was initiated. Both PAUS and MRI showed a significant fluid collection with a diameter of approximately 4.5 cm. In contrast to MRI, PAUS detected a fistulous connection to the rectum. In addition to the abscess, a sinus track was detected that emanated from the abscess, and ended within the gluteal fat. The sinus tract could clearly be visualized by both methods (Figure 6). Interestingly, EUA failed to reproduce the pathological findings in the first place and had to be repeated to confirm the PAUS/MRI findings and to achieve appropriate drainage of the abscess. In Figure 7 a small subcutaneous abscess was imaged by PAUS and MRI. Both methods were able to show an active fistulous track reaching from the rectum to the subcutaneous fluid collection.

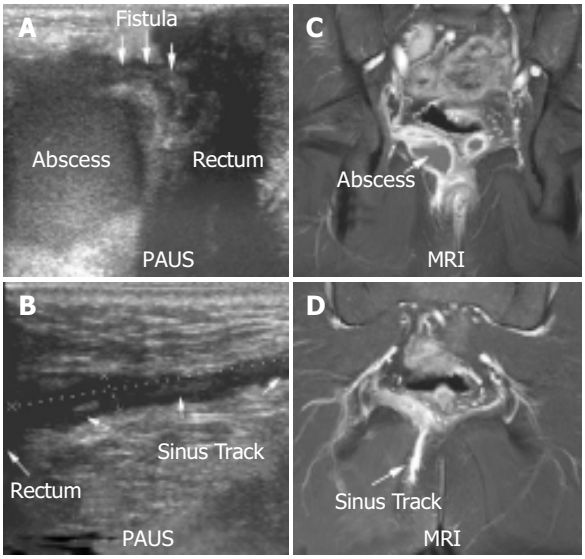

Figure 6 PAUS (A+B) and MRI (C+D) imaging (coronary fat-saturated T1-SE sequence after gadolinium administration) of a perianal abscess. In contrast to MRI, PAUS was able to clearly identify a connection between the rectum and the abscess (A+C). Both methods could identify a sinus track that began within the abscess and ended in the gluteal fat (B+D). A scale (cm) is shown on the left side of the PAUS images for orientation.

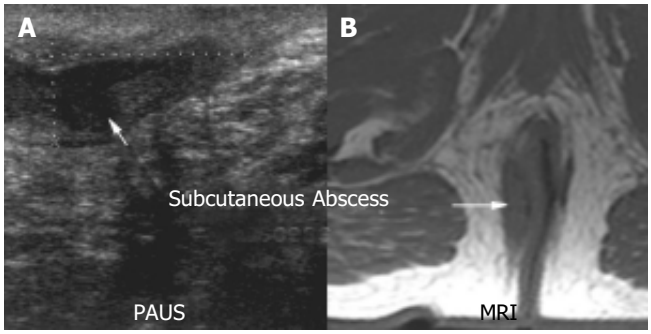

Figure 7 Comparison of PAUS (A) and MRI (B) imaging (transverse T1-SE sequence) of a subcutaneous abscess. A small fistula from the rectum to the abscess could be detected with PAUS and MRI.

DISCUSSION

In this study we investigated the feasibility of transcutaneous PAUS for the evaluation of perianal inflammatory disorders in patients with Crohn´s disease.

We showed that perianal fistulae, complex fistulous systems as well as perianal abscesses could be detected with high sensitivity using PAUS. The results were comparable to pelvic MRI that currently represents in combination with EAUS, the gold standard for the imaging of perianal inflammatory disease. However, PAUS still has certain limitations when performed in the left lateral position compared to EAUS and MRI. The localization of fistulae within the sphincter apparatus is important when surgical interventions are indicated. While imaging of the internal anal sphincter is difficult using PAUS, the external sphincter can be clearly distinguished due to its hyperechoic striped appearance. In terms of impact on treatment, the definite description of the anatomical relationship of pathological changes to the external anal sphincter according to the Parks classification is most important[18]. Still, accurate localization of pathological changes to the internal/external sphincter requires an experienced investigator.

Despite the limitations stated above, we believe that PAUS has several advantages compared to EAUS and MRI. PAUS is as effective as MRI in the detection of perianal fistulae, but the detection of air bubbles within a fistulous track can clearly indicate active fistulae. Real time imaging in sonography is an advantage that can be helpful in detecting possible connection to the rectal lumen. In two cases investigated by MRI and PAUS, MRI was not able to detect a short perianal fistulae, while the cutaneous openings of the fistulae were obvious on clinical inspection. While EAUS is limited to pathological changes associated to the rectal lumen, perianal ultrasound can be used to identify fistulous tracks in the gluteal region. PAUS therefore combines the high resolution and real time capabilities of EAUS and the panoramic view generated by MRI.

The presence of perianal abscesses is an important condition for surgical interventions in patients with perianal Crohn´s disease. Abscesses were detected by PAUS with the same sensitivity as by MRI. PAUS therefore is a valuable tool in the screening for perianal disease. Especially when immediate action is necessary and sophisticated diagnostic imaging could delay diagnosis due to limited availability, PAUS might be a feasible alternative to EAUS and MRI. For example, we were able to detect perianal abscesses in two patients that presented with severe perianal discomfort using PAUS. These patients did not have a history of perianal inflammatory disease and neither inspection of the anus nor digital rectal examination revealed pathological findings. These two patients underwent immediate surgical drainage of their abscesses without further imaging and therefore had to be excluded from this study. Vice versa a perianal abscess was suspected in a patient that presented with a painful perianal swelling with typical redness and induration. An abscess was ruled out using PAUS and the patient was spared a surgical intervention and had complete remission of symptoms. Again no further imaging was performed in this patient. In the future, a mobile application of PAUS in the operating room to guide drainage operations is conceivable. This, however, has not been tested in this study yet.

With more advanced imaging techniques in medicine, the costs of diagnosis and treatment have become a serious and important issue. Especially in chronic diseases, such as Crohn´s disease which require regular examination for follow-up and treatment-evaluation alternative, easily available methods to EAUS and MRI as rather expensive diagnostic tools are more than welcome. We believe that PAUS represents such an alternative for it can be performed with regular ultrasound probes and is therefore widely available. It is fast and does not require special patient preparations such as enemas or injection of contrast agents. Basically it can be performed in any outpatient radiology or internal medicine practice. Depending on on-site experience additional imaging of perianal disease with EAUS or MRI might be necessary. However, after initial comparison with the established methods, follow-up can easily be performed with PAUS alone. In follow-up studies the application of more sophisticated imaging methods such as

EAUS or MRI would then be limited to investigate significant clinical changes not detectable by the transcutaneous approach.

In general PAUS was well tolerated by our patients. As a matter of fact one of the reasons to perform this study was that several patients refused diagnosis with EAUS. As perianal inflammatory disease can result in fibrosis and consecutive anal stenosis, EAUS might not be applicable at all in some patients.

The use of contrast agents such as hydrogen peroxide or Levovist might improve the imaging quality of perianal ultrasound[20-23]. However, the main goal of this study was to determine whether a simple alternative approach was helpful in the imaging of perianal disorders.

We would like to encourage the readers of this article who perform EAUS to employ PAUS using regular ultrasound probes. Since PAUS has been established in our department, the use of EAUS for inflammatory disease has been drastically reduced and is now limited to very few cases that can not be clarified with PAUS and/or MRI.

In conclusion, PAUS represents a sensitive, non-invasive tool that can be used for initial screening and follow-up in the detection of perianal inflammatory disease.

REFERENCES

1 **Hellers G**, Bergstrand O, Ewerth S, Holmstrom B. Occurrence and outcome after primary treatment of anal fistulae in Crohn's disease. *Gut* 1980; **21**: 525-527

2 **Schwartz DA**, Loftus EV Jr, Tremaine WJ, Panaccione R, Harmsen WS, Zinsmeister AR, Sandborn WJ. The natural history of fistulizing Crohn's disease in Olmsted County, Minnesota. *Gastroenterology* 2002; **122**: 875-880

3 **Sandborn WJ**, Fazio VW, Feagan BG, Hanauer SB. AGA technical review on perianal Crohn's disease. *Gastroenterology* 2003; **125**: 1508-1530

4 **Orsoni P**, Barthet M, Portier F, Panuel M, Desjeux A, Grimaud JC. Prospective comparison of endosonography, magnetic resonance imaging and surgical findings in anorectal fistula and abscess complicating Crohn's disease. *Br J Surg* 1999; **86**: 360-364

5 **Schwartz DA**, Wiersema MJ, Dudiak KM, Fletcher JG, Clain JE, Tremaine WJ, Zinsmeister AR, Norton ID, Boardman LA, Devine RM, Wolff BG, Young-Fadok TM, Diehl NN, Pemberton JH, Sandborn WJ. A comparison of endoscopic ultrasound, magnetic resonance imaging, and exam under anesthesia for evaluation of Crohn's perianal fistulas. *Gastroenterology* 2001; **121**: 1064-1072

6 **van Bodegraven AA**, Sloots CE, Felt-Bersma RJ, Meuwissen SG. Endosonographic evidence of persistence of Crohn's disease-associated fistulas after infliximab treatment, irrespective of clinical response. *Dis Colon Rectum* 2002; **45**: 39-45

7 **Bell SJ**, Halligan S, Windsor AC, Williams AB, Wiesel P, Kamm MA. Response of fistulating Crohn's disease to infliximab treatment assessed by magnetic resonance imaging. *Aliment Pharmacol Ther* 2003; **17**: 387-393

8 **Van Assche G**, Vanbeckevoort D, Bielen D, Coremans G, Aerden I, Noman M, D'Hoore A, Penninckx F, Marchal G, Cornillie F, Rutgeerts P. Magnetic resonance imaging of the effects of infliximab on perianal fistulizing Crohn's disease. *Am J Gastroenterol* 2003; **98**: 332-339

9 **Roche B**, Deleaval J, Fransioli A, Marti MC. Comparison of transanal and external perineal ultrasonography. *Eur Radiol* 2001; **11**: 1165-1170

10 **Bernstein I**, Juul N, Gronvall S, Bonde B, Klarskov P. Pelvic floor muscle thickness measured by perineal ultrasonography. *Scand J Urol Nephrol Suppl* 1991; **137**: 131-133

11 **Cornelia L**, Stephan B, Michel B, Antoine W, Felix K. Transperineal versus endo-anal ultrasound in the detection of anal sphincter tears. *Eur J Obstet Gynecol Reprod Biol* 2002; **103**: 79-82

12 **Kiilholma PJ**, Makinen JI, Pitkanen YA, Varpula MJ. Perineal ultrasound: an alternative for radiography for evaluating stress urinary incontinence in females. *Ann Chir Gynaecol Suppl* 1994; **208**: 43-45

13 **Piloni V**. Dynamic imaging of pelvic floor with transperineal sonography. *Tech Coloproctol* 2001; **5**: 103-105

14 **Pregazzi R**, Sartore A, Bortoli P, Grimaldi E, Troiano L, Guaschino S. Perineal ultrasound evaluation of urethral angle and bladder neck mobility in women with stress urinary incontinence. *BJOG* 2002; **109**: 821-827

15 **Schaer GN**, Koechli OR, Schuessler B, Haller U. Perineal ultrasound for evaluating the bladder neck in urinary stress incontinence. *Obstet Gynecol* 1995; **85**: 220-224

16 **Rubens DJ**, Strang JG, Bogineni-Misra S, Wexler IE. Transperineal sonography of the rectum: anatomy and pathology revealed by sonography compared with CT and MR imaging. *Am J Roentgenol* 1998; **170**: 637-642

17 **Stewart LK**, Mc Gee J, Wilson SR. Transperineal and transvaginal sonography of perianal inflammatory disease. *Am J Roentgenol* 2001; **177**: 627-632

18 **Parks AG**, Gordon PH, Hardcastle JD. A classification of fistula-in-ano. *Br J Surg* 1976; **63**: 1-12

19 **Mallouhi A**, Bonatti H, Peer S, Lugger P, Conrad F, Bodner G. Detection and characterization of perianal inflammatory disease: accuracy of transperineal combined gray scale and color Doppler sonography. *J Ultrasound Med* 2004; **23**: 19-27

20 **Chew SS**, Yang JL, Newstead GL, Douglas PR. Anal fistula: Levovist-enhanced endoanal ultrasound: a pilot study. *Dis Colon Rectum* 2003; **46**: 377-384

21 **Kruskal JB**, Kane RA, Morrin MM. Peroxide-enhanced anal endosonography: technique, image interpretation, and clinical applications. *Radiographics* 2001; **21**: S173-S189

22 **Poen AC**, Felt-Bersma RJ, Eijsbouts QA, Cuesta MA, Meuwissen SG. Hydrogen peroxide-enhanced transanal ultrasound in the assessment of fistula-in-ano. *Dis Colon Rectum* 1998; **41**: 1147-1152

23 **Sloots CE**, Felt-Bersma RJ, Poen AC, Cuesta MA, Meuwissen SG. Assessment and classification of fistula-in-ano in patients with Crohn's disease by hydrogen peroxide enhanced transanal ultrasound. *Int J Colorectal Dis* 2001; **16**: 292-297

Edited by Zhang JZ and Wang XL **Proofread by** Xu FM

PO Box 2345, Beijing 100023, China
Fax: +86-10-85381893
E-mail: wjg@wjgnet.com www.wjgnet.com

World J Gastroenterol 2004;10(19):2864-2866
World Journal of Gastroenterology
Copyright © 2004 by The WJG Press ISSN 1007-9327

• BRIEF REPORTS •

Low plasma apolipoprotein A-I level is not a reliable marker of fibrosis in children with chronic hepatitis B

Mukadder Ayse Selimoglu, Rasit Vural Yagcl, Gül Yüce

Mukadder Ayse Selimoglu, Department of Pediatric Gastroenterology, Hepatology and Nutrition, Faculty of Medicine, Atatürk University, Erzurum, Turkey
Rasit Vural Yagcı, Department of Pediatric Gastroenterology, Hepatology and Nutrition, Faculty of Medicine, Ege University, İzmir, Turkey
Gül Yüce, Department of Pathology, Faculty of Medicine, Ege University, İzmir, Turkey
Correspondence to: Dr. Mukadder-Ayse Selimoglu, Atatürk Üniversitesi, Tlp Fakültesi, Çocuk Saglıgı ve Hastalıkları AD, Erzurum 25240, Turkey. ayseselimoglu@hotmail.com
Telephone: +90-442-2361212 Ext. 1635 **Fax:** +90-442-2361301
Received: 2004-02-14 **Accepted:** 2004-04-29

Abstract

AIM: To evaluate the clinical value of plasma apolipoprotein A-I (Apo A-I) as a marker of fibrosis in children with chronic hepatitis B (CHB).

METHODS: Liver biopsy specimens from 49 children with CHB were evaluated by using Knodell index. Plasma Apo A-I level was measured after 12-h fasting. Student's *t* test, Spearman's correlation test and receptor-operating characteristic (ROC) curve were used for statistical evaluation.

RESULTS: Mean Apo A-I level of the patients was not different from that of controls (P>0.05). Six (8.7%) children had fibrosis score of more than 2 (severe fibrosis). No difference in the level of mean plasma Apo A-I was found among children with and without severe fibrosis (P>0.05). No correlation between Apo A-I level and fibrosis scores was found (P>0.05). The area under the ROC curve was 0.407±0.146 (P>0.05).

CONCLUSION: Severe fibrosis is not common in children with CHB and plasma Apo A-I level is not a reliable indicator of fibrosis.

Selimoglu MA, Yagcı RV, Yüce G. Low plasma apolipoprotein A-I level is not a reliable marker of fibrosis in children with chronic hepatitis B. *World J Gastroenterol* 2004; 10(19): 2864-2866
http://www.wjgnet.com/1007-9327/10/2864.asp

INTRODUCTION

Apolipoprotein A-I (Apo A-I) is produced mainly by hepatocytes and its level varies according to the degree of liver fibrosis[1-4]. In our previous study, we demonstrated the inverse correlation of Apo A-I with the Child-Pugh score[3] in children with cirrhosis. Data of Apo A-I levels in chronic hepatitis were mainly from studies performed in adults with hepatitis C[5,6]. A recent study showed that serum Apo A-I level was inversely correlated with liver fibrosis in adult patients with chronic hepatitis B (CHB)[7].

Liver biopsy is an invasive procedure especially for children. It is well known that serum alanine transaminase (ALT) is a good indicator of portal inflammation in chronic hepatitis[8], but a reliable biochemical fibrosis index is not available for children. The aim of this study was to determine if low plasma Apo A-I level was a reliable indicator of fibrosis in childhood CHB.

MATERIALS AND METHODS

Forty-nine hepatitis Be antigen (HBeAg) positive children (13 females and 36 males) with pathology verified chronic HBV infection were included in this study. Their mean age was 9.1±4.1 years (3 to 18 years). Patients were excluded if they had hepatitis D or C or HIV infection. No patient had evidence of decompensated liver diseases or autoimmune hepatitis. Parents of the patients were required to give written informed consent before entering the study.

Pretreatment liver biopsy specimens were obtained from all patients and scored with the use of the Knodell index[9], which grades the histological activity of hepatitis on a scale from 0 to 22, with higher scores indicating more severe abnormalities. The overall Knodell score is the sum of the scores for periportal/bridging necrosis (0 to 10), intralobular degeneration and focal necrosis (0 to 4), portal inflammation (0 to 4), and fibrosis (0 to 4). Before the patients entered the study, blood samples were taken for the test of blood cell counts, serum alanine aminotransferase (ALT), Apo A-I, hepatitis B surface antigen (HBsAg), HBeAg, antibody to HBeAg, antibody to HBsAg and HBV DNA.

Plasma Apo A-I levels of 20 gender- and age-matched healthy children were used as controls. Student's *t* test, Spearmen's correlation test and ROC curve were used for statistical analysis.

RESULTS

Pre treatment ALT, Apo A-I, hepatic activity index (HAI), portal fibrosis, inflammation and necrosis scores, and HBV DNA levels of the children are shown in Table 1. Mean plasma Apo A-I level of 49 children with CHB was not different from that of controls (39.3±5.8 μmol/L *vs* 40.71±4.8 μmol/L, P>0.05).

Table 1 Some pretreatment biochemical, pathological and serological findings in children with chronic hepatitis B

Parameter	mean±SD	Range
ALT (IU/l)	80±80	21-396
Apo A-I (μmol/L)	39.3±5.8	29.2-57.5
Hepatic activity index	7.0±3.0	3-17
Portal fibrosis	1.4±0.9	0-4
Portal inflammation	2.0±1.2	0-4
Focal necrosis	1.6±0.9	0-4
Bridging necrosis	2.0±1.6	0-6
HBV DNA (ng/L)	1 537±712	118-3 111

Children with CHB were divided into 2 groups according to their fibrosis stage: group 1, whose portal fibrosis scores were 0, 1 or 2; group 2, whose portal fibrosis scores were 3 or 4. In groups 1 and 2, the mean Apo A-I levels were 39.6±5.6 μmol/L

and 36.9±6.8 μmol/L, respectively (P> 0.05). Only 6 (8.7%) children had a fibrosis score of more than 2.

No correlation among Apo A-I and HAI, portal inflammation, portal fibrosis, focal necrosis, bridging necrosis scores was found (P>0.05). A positive correlation between ALT and portal inflammation scores and between ALT and HAI was found (P< 0.05 and P<0.01, respectively).

The area under the ROC curve of Apo A-I was 0.407±0.146 (P>0.05, Figure 1).

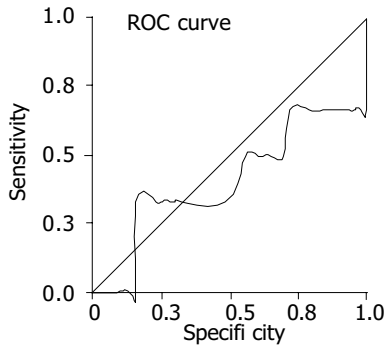

Figure 1 ROC curve of Apo A-I.

DISCUSSION

Fibronectin, a major liver extracellular matrix component, can interact with Apo A-I both by downregulating its mRNA level in liver cells and by binding to this molecule after its secretion in the extracellular space[1,2]. Since fibronectin is the first matrix component to be produced in excess and deposited in liver fibrosis, it has been thought to be involved in the decrease in Apo A-I in alcoholic patients with liver fibrosis and cirrhosis[1,2].

Because liver biopsy is an invasive method with a 1/10 000 mortality rate, noninvasive serum markers of liver fibrosis are under investigation[10]. Furthermore, although histological analysis is considered to be the gold standard for the diagnosis of extensive fibrosis and cirrhosis, the rate of false-negative results was approximately 15-20%[10]. Clinical investigations on fibrosis markers were generally focused on hepatitis C rather than hepatitis B[5,6]. One of the few studies performed of patients with CHB was the study Huang *et al*.[7]. They investigated the value of serum biochemical markers in the diagnosis of liver fibrosis of patients with hepatitis B and observed that levels of ALT, total bilirubin, alpha 2-macroglobulin, GGT and Apo A-I were signi-ficantly correlated with the clinical staging of liver fibrosis, and concluded that a combined assessment of these indices might help obtain an accurate diagnosis of liver cirrhosis with less need of pathological biopsy in this population[7].

Besides noninvasive biochemical markers, some studies strongly recommended using some historical features such as sex, age at biopsy and alcohol consumption as independent predictors of fibrosis in chronic hepatitis C adults[5]. They demonstrated that a simple index including age, sex, and five biochemical markers could accurately predict significant hepatitis C-related fibrosis[5].

Teare *et al*.[11]. compared aminoterminal type III procollagen propeptide (PIIIP) with the PGA index, which combines the prothrombin time, gamma-glutamyl transpeptidase activity, and serum Apo A-I concentration, in predicting liver fibrosis in patients with alcoholic liver disease, primary biliary cirrhosis, and CHB. They stated that PGA and PIIIP values were increased in all patients with CHB in comparison with controls. For the detection of cirrhosis they found that PGA was 91% sensitive and 81% specific[11]. Similarly Ding *et al*.[12] evaluated the diagnostic value of serum liver fibrosis markers by analyzing the correlation between liver fibrosis stage in patients with CHB and serum liver fibrosis markers, such as hyaluronate, type III procollagen, laminin, and type IV collagen in 278 patients. They found that liver fibrosis stage was correlated to inflammation degree and that serum hyaluronate, type III procollagen, laminin, and type IV collagen could reflect the state of liver fibrosis[12].

The difference between mean Apo A-I level of children with CHB and controls was not significant (39.3±5.8 μmol/L *vs* 40.71±4.8 μmol/L). In 2002, we reported similar figures for children with chronic hepatitis, most of them had CHB[4]. However, Norton *et al*.[13] reported that Apo A-I and apo C-III steady-state mRNA levels were suppressed by HBV replication and/or gene expression. Other studies revealed that the levels of Apo A-I and Apo A-II were reduced during acute hepatitis, when virus levels were high, and normalized after viral clearance[14,15]. Similar results were reported for chronic HBV infection. Reduced levels of circulating lipoproteins and apolipoproteins have been correlated with increased viral replication[16-18]. In our study no correlation between HBV DNA and Apo A-I levels was detected.

Of the 49 children, only 8.7% had significant fibrosis according to Knodell index (>2), suggesting that fibrosis is not prevalent in this age group. Although the mean plasma Apo A-I level was lower in this small population compared to children with mild/no fibrosis (36.9±6.8 μmol/L *vs* 39.6±5.6 μmol/L), statistical significance was not detected.

Recently it has been recommended to use ROC curves in determ-ination of the indices of hepatic fibrosis in clinical practice[19,20]. In this study, plasma Apo A-I level as a fibrosis marker was measured in children with CHB and compared with Knodell scores to determine if it had any clinical value as a marker of fibrosis. In conclusion, severe fibrosis and Knodell score higher than 2, are not common in CHB children and plasma Apo A-I level is not a reliable indicator of fibrosis.

REFERENCES

1 **Paradis V,** Laurent A, Mathurin P, Poynard T, Vidaud D, Vidaud M, Bedossa P. Role of liver extracellular matrix in transcriptional and post-transcriptional regulation of apolipoprotein A-I by hepatocytes. *Cell Mol Biol* 1996; **42**: 525-534

2 **Paradis V**, Mathurin P, Ratziu V, Poynard T, Bedossa P. Binding of apolipoprotein A-I and acetaldehyde-modified apolipoprotein A-I to liver extracellular matrix. *Hepatology* 1996; **23**: 1232-1238

3 **Selimoglu MA,** Aydogdu S, Yagci RV. Low plasma apolipoprotein A-I level: new prognostic criterion in childhood cirrhosis? *Turk J Pediatr* 2001; **43**: 307-311

4 **Selimoglu MA,** Aydogdu S, Yagci RV. Lipid parameters in childhood cirrhosis and chronic liver disease. *Pediatr Int* 2002; **44**: 400-443

5 **Myers RP,** Ratziu V, Imbert-Bismut F, Charlotte F, Poynard T. Biochemical markers of liver fibrosis: a comparison with historical features in patients with chronic hepatitis C. *Am J Gastroenterol* 2002; **97**: 2419-2425

6 **Poynard T,** Imbert-Bismut F, Ratziu V, Chevret S, Jardel C, Moussalli J, Messous D, Degos F. Biochemical markers of liver fibrosis in patients infected by hepatitis C virus: longitudinal validation in a randomized trial. *J Viral Hepat* 2002; **9**: 128-133

7 **Huang W,** Gong FY. Diagnostic value of serum biochemical markers for liver fibrosis in patients with hepatitis B virus. *Diyi Junyi Daxue Xuebao* 2002; **22**: 1034-1036

8 **Tang TJ,** Kwekkeboom J, Laman JD, Niesters HG, Zondervan PE, de Man RA, Schalm SW, Janssen HL. The role of intrahepatic immune effector cells in inflammatory liver injury and viral control during chronic hepatitis B infection. *J Viral Hepat* 2003; **10**: 159-167

9 **Knodell RG,** Ishak KG, Black WC, Chen TS, Craig R, Kaplowitz N, Kiernan TW, Wollman J. Formulation and application of a numerical scoring system for assessing histological activity in asymptomatic chronic active hepatitis. *Hepatology* 1981; **1**: 431-435

10 **Cadranel JF,** Mathurin P. Prothrombin index decrease: a use-

ful and reliable marker of extensive fibrosis? *Eur J Gastroenterol Hepatol* 2002; **14**: 1057-1059

11 **Teare JP,** Sherman D, Greenfield SM, Simpson J, Bray G, Catterall AP, Murray-Lyon IM, Peters TJ, Williams R, Thompson RP. Comparison of serum procollagen III peptide concentrations and PGA index for assessment of hepatic fibrosis. *Lancet* 1993; **342**: 895-898

12 **Ding H,** Chen Y, Feng X, Liu D, Wu A, Zhang L. Correlation between liver fibrosis stage and serum liver fibrosis markers in patients with chronic hepatitis B. *Zhonghua Ganzangbing Zazhi* 2001; **9**: 78-80

13 **Norton PA,** Gong Q, Mehta AS, Lu X, Block TM. Hepatitis B virus-mediated changes of apolipoprotein mRNA abundance in cultured hepatoma cells. *J Virol* 2003; **77**: 5503-5506

14 **Vergani C,** Trovato G, Delu A, Pietrogrande M, Dioguardi N. Serum total lipids, lipoprotein cholesterol, and apolipoprotein A in acute viral hepatitis and chronic liver disease. *J Clin Pathol* 1978; **31**: 772-778

15 **Vergani C,** Trovato G, Pietrogrande M, Crocchiolo P, Dioguardi N. Behavior of total lipids, cholesterol, lipoproteins and apolipoprotein A in the blood of subjects with acute hepatitis and chronic hepatopathy. *Minerva Med* 1978; **69**: 2081-2094

16 **Chen Z,** Keech A, Collins R, Slavin B, Chen J, Campbell TC, Peto R. Prolonged infection with hepatitis B virus and association between blood cholesterol and liver cancer. *BMJ* 1993; **306**: 890-894

17 **Cordova C,** Musca A, Violi F, Alessandri C, Iuliano L. Apolipoproteins A-I, A-II and B in chronic active hepatitis and in liver cirrhotic patients. *Clin Chim Acta* 1984; **137**: 61-66

18 **Fehér J,** Romics L, Jakab L, Fehér E, Szilvási I, Papp G. Serum lipids and lipoproteins in chronic liver disease. *Acta Med Acad Sci Hung* 1976; **33**: 217-223

19 **Zheng M,** Cai WM, Weng HL, Liu RH. ROC curves in evaluation of serum fibrosis indices for hepatic fibrosis. *World J Gastroenterol* 2002; **8**: 1073-1076

20 **Walsh KM,** Timms P, Campbell S, Macsween RNM, Morris AJ. Plasma levels of matrix metalloproteinases-2 (MMP-2) and tissue inhibitors of metalloproteinases-1 and -2 (TIMP-1,2) as noninvasive markers of liver disease in chronic hepatitis C disease in chronic hepatitis C comparison using ROC analysis. *Dig Dis Sci* 1999; **44**: 624-630

Edited by Chen WW and Wang XL **Proofread by** Xu FM

PO Box 2345, Beijing 100023, China
Fax: +86-10-85381893
E-mail: wjg@wjgnet.com www.wjgnet.com

World J Gastroenterol 2004;10(19):2867-2869
World Journal of Gastroenterology
Copyright © 2004 by The WJG Press ISSN 1007-9327

• BRIEF REPORTS •

Prospective study in 142 cases of hepatitis C virus infection

Wen-Mei Fan, Wan-Fu Zhu, Li-Min Yin, Lai Wei, Xiao-Yuan Xu, Hui Zhuang

Wen-Mei Fan, **Wan-Fu Zhu, Li-Min Yin, Hui Zhuang**, Department of Microbiology, School of Basic Medicine, Peking University Health Science Center, Beijing 100083, China
Lai Wei, Hepatology Institute, People's Hospital, Peking University, Beijing 100044, China
Xiao-Yuan Xu, Department of Infectious Diseases, First Hospital, Peking University, Beijing 100034, China
Supported by the National Key Technologies Research and Development Program of China during the 10th Five-Year period, No. 2001BA705B06
Correspondence to: Professor Wan-Fu Zhu, Department of Microbiology, School of Basic Medicine, Health Science Center, Peking University, Beijing 100083, China. zhuwanfu@sun.bjmu.edu.cn
Telephone: +86-10-82801599 **Fax:** +86-10-82801599
Received: 2004-03-05 **Accepted:** 2004-04-05

Abstract

AIM: There is limited information on the natural history of HCV infection in China. We investigated the outcome of HCV infection after nine-year follow-up and the risk factors in blood donors in China in order to provide the foundation for prevention and therapy.

METHODS: A total of 172 cases of HCV infection with anti-HCV positive and ALT abnormality were enrolled in the archives when was screened blood in Hebei Province in 1993. In them 142 blood donors were followed up till July 2002. No antiviral treatment was applied to them during the period of infection. In the present study, anti-HCV, HCV-RNA and aminotransferase were detected and genotyping was conducted by the method of restriction fragment length polymorphism(RFLP). B-type ultrasound detection was performed in all the patients. Age, sex, alcohol consumption and clinical symptoms were questioned.

RESULTS: After nine years' follow-up, 10.56% (15/142) of the cases were negative for anti-HCV and 16.42% (12/134) of them were negative for HCV-RNA. The genotypes 1b, 2a and 1b/2a were 91.07%, 6.25% and 2.68% respectively. Twelve cases (8.45%) were negative for both HCV RNA and anti-HCV. The rate of chronicity in this group was 83.58% (112/134), and the rate of viral spontaneous resolution was 16.42% (22/134). The mean level of ALT, AST, γ–GT in HCV RNA positive cases was significantly higher than that in HCV RNA negative cases (P<0.001). The abnormal rate of ALT and/or AST in male donors was significantly higher than that in female donors (P = 0.005). The rate of progression to liver cirrhosis from chronic hepatitis C was significantly higher in the cases of super-infection with HBV than that in the cases of single HCV infection. Overdose alcohol consumption promoted the progression to chronicity.

CONCLUSION: This area (Hebei Province) has a higher rate of chronicity in HCV infection, and measures should be taken to prevent its progression to serious liver diseases, especially for patients super-infected with HCV and HBV.

Fan WM, Zhu WF, Yin LM, Wei L, Xu XY, Zhuang H. Prospective study in 142 cases of hepatitis C virus infection. *World J Gastroenterol* 2004; 10(19): 2867-2869
http://www.wjgnet.com/1007-9327/10/2867.asp

INTRODUCTION

Hepatitis C virus is the major cause of post-transfusion hepatitis. It has been estimated that nearly 170 million people are infected with HCV in the world. High chronicity is an obvious characteristic of HCV infection. Eighty-five percent of infected patients developed chronic infection and 8-45% of them could resolve. Liver cirrhosis developed in 10-50%, hepatocellular carcinoma in 1-23%, liver disease related mortality in 4-15%[1-3] in twenty years of natural infection. There is limited information about the long-term follow-up study in China. Many donors were infected with HCV by means of plasmapheresis in the 1990 s[4]. In the present study, 172 cases of blood donors infected with HCV were diagnosed in August of 1993, and 142 of them were followed up till July 2002. The outcome in natural history of HCV infection and related factors affecting the outcome were investigated.

MATERIALS AND METHODS

Patients

A total of 172 cases of blood donors from a rural area of Zhao Country in Hebei Province were diagnosed as HCV infection by etiology and biochemistry detection (including anti-HCV and hepatitis B surface antigen) in August of 1993. Thirteen cases of them were co-infected with hepatitis C virus and hepatitis B virus. Nine years later, only 142 persons (66 men and 76 women with a mean age of 36.67±9.10 years at time of infection and 45.70±9.11 years at time of investigation) were followed up. Additionally, three children with aged of 2 to 8 years at the time of infection were checked-up in our series. It was noted that all of the donors received no antiviral treatment during the nine years of infection.

Methods

Anti-HCV antibodies Five-milliliter peripheral vein blood was collected for biochemical and etiology detection. All patients were tested for the presence of anti-HCV antibodies with Abbott diagnostic test kit (Abbott, USA) according to the manufacturer's instructions in 1993 and 2002. The rest of the blood samples were stored at -80 ℃.

HCV RNA detection and genotyping Primers were designed from the conserved 5'-noncoding (5'-NC) region of the HCV genome. P1:5'-GTGTGAGGAACTACTGTGTT-3', P1':5'-AACACTACTCGGCTAGCAGT-3', and P2:5'-TTCACGCAGAAAGCGTCTAG-3', P2':5'-GTTTATCAAGAAAGGACCCG-3'. RT-PCR procedure was performed as previously described[5]. PCR products positive for HCV RNA were genotyped with restriction fragment length polymorphism (RFLP) method[5].

Risk factors for HCV chronicity All data of risk factors for HCV chronicity were collected by using special questionnaires, including sex, age, symptoms, alcohol consumption, alanine aminotransferase (ALT), aspartate aminotransferase (AST), γ-glutamyltransferase (γ-GT), alkaline phosphatase (ALP), total bilirubin (Tbil), direct bilirubin (Dbil), total protein (TP) and

albumin (ALB) in 12 by using fully automatic biochemical analysis compliance 7071A (Hitachi, Japan). HBV markers were also detected by Abbott diagnostic kit.

Diagnostic criterion Chronic hepatitis C and liver cirrhosis were diagnosed based on the critera modified at the Sixth (Xi' an) National Convention of Infectious, Parasitic and Liver Diseases[6].

Statistical analysis

Quantitative values were expressed as mean±SE. Unpaired Student's *t* test, χ^2 and Fisher's exact test were used for statistical comparison of the data. $P<0.05$ was considered statistically significant.

RESULTS

Outcome of HCV infection

In the172 cases enrolled in this study in 1993, seven cases were already died at the time of investigation. Two (1.16%) out of seven cases died of suspected hepatocellular carcinoma. Twenty-three cases were out of follow-up. In the present study, only 142 cases were followed-up under the investigation. Out of the 142 cases, HCV RNA was detected in 134 cases. The result showed that 112 cases (83.58%) of the donors were positive for HCV RNA and 16.42% were negative for HCV RNA; 89.44% were positive for anti-HCV and 10.56% were negative for anti-HCV ; 8.45% of them were negative for both anti-HCV and HCV RNA. Out of the 142 infected persons, most but one (who was with chronic moderate hepatitis C) with mild chronic hepatitis C had no obvious clinical symptoms according to the viral hepatitis prevention project. In the cases with persistent infection, B-type ultrosound detection showed 2.68% with liver cirrhosis, 86.61% with chronic hepatitis and 10.71% with fatty liver.

Anti-HCV, HCV RNA and abnormity of liver function

Ninety-one point sixty percent of the cases were positive for HCV RNA in the positive group of anti-HCV. Eight cases of severe hepatitis and three cases of liver cirrhosis were positive for both anti-HCV and HCV RNA. Another two patients with liver cirrhosis and severe hepatitis were co-infected with both HCV and HBV in 1993 and turned positive for anti-HCV, negative for HCV RNA and positive for hepatitis B surface antigen in the present study. The rate of ALT and/or AST abnormalities in the positive group of anti-HCV was 28.57% (34/119), while that in the negative group of anti-HCV was zero (Table 1). The average level of ALT, AST and γ-GT in the positive group of HCV RNA was significantly higher than that in the negative group ($P<0.001$) (Table 2). On the other hand, the abnormal rate of ALT and / or AST in the positive group was also significantly higher than that in negative group (29.46% *vs* 4.55%, $P = 0.014$).

Clinical symptoms

Fifty out of 112 cases (44.64%) of chronic HCV infection had mild symptoms, including abdominal pain (18.75%), fatigue (17.86%), and arthralgia (16.96%). The rates of cases with symptoms in the group of liver cirrhosis was 50.0%. Surprisingly, six cases with negative viral markers had fatigue.

Table 1 Abnormal of serum alanine aminotransferase in patients infected with HCV after 9 years' follow-up in different groups

Group	Liver function	
	Normal cases (%)	Abnormal cases (%)
Anti-HCV(+)HCV RNA(+)	76 (69.72)	33 (30.28)
Anti-HCV(+)HCV RNA(-)	9 (90.00)	1 (10.00)
Anti-HCV(-)HCV RNA(+)	3 (100.0)	0
Anti-HCV(-)HCV RNA(-)	12 (100.0)	0
Anti-HCV(+)HCVRNA(undetected)	4 (50.00)	4 (50.00)
Total	104 (73.24)	38 (26.76)

Note: The number in the bracket is the percentage of normal and abnormal cases in each group.

Co-infection with HBV and alcohol consumption

Thirteen of 142 cases had co-infection with HBV in 1993. Twelve cases of them were positive for hepatitis B surface antigen (HBsAg) and the rest were negative for HBsAg and positive for anti-hepatitis B core (anti-HBc). Nine years later, three of them turned negative for HbsAg, suggesting that spontaneous resolution of HBsAg per year was 2.77% similar to the of standard rate of resolution (2.01%) in our country[7]. The rate of spontaneous resolution of anti-HCV was 7.69% in the group of co-infection with HBV while 8.53% in the group of single HCV infection. There was no significant difference between the two groups. Thirty point seventy-seven percent lost their HCV RNA in the group super-infected with HCV and HBV and 14.88% lost their HCV RNA in the group with single HCV infection. However, there was no significant difference between them. Two (15.38%) out of thirteen cases with co-infection developed liver cirrhosis while two (1.55%) out of 129 cases with single HCV infection also developed liver cirrhosis. The progression to liver cirrhosis due to co-infection was significant faster than that due to single infection ($P<0.05$). Thirteen of 142 cases had alcohol consumption of more than 100 g every day and all developed persistent infection. We also found that all cases with viral resolution had no history of excessive alcohol consumption, suggesting that alcohol consumption might promote the progression of HCV infection to chronicity.

Age at the time of primary infection

We divided the donors into three groups according to the age of infection: 18-30 years, 31-40 years and ⩾41 years. The rate of spontaneous viral resolution in the three groups was 17.95%, 15.09% and 16.67% respectively. There was no significant difference. There was no linear correlation between the age of infection and the viral load (r = -0.144). Liver function was normal in the three investigated children. One of them was negative for viral markers and the other two developed persistent infection.

Influence of sex on the viral resolution

Sixty-two male cases and seventy-two female cases were detected for HCV RNA. The rate of viral resolution was 12.90% in the male group and 19.44% in the female group. No significant

Table 2 Comparison of ALT, AST, ALP, γ-GT, TBIL and DBIL between positive (+) and negative (-) HCV RNA patients (mean±SE)

HCV RNA	Case	ALT (IU/L)	AST (IU/L)	ALP (IU/L)	γ-GT (IU/L)	Tbil (μmol/L)	DBiL (μmol/L)
+	112	31.2±32.6[b]	34.8±27.0[b]	82.0±36.6	20.0±17.6[b]	13.2±5.6	6.0±2.3
-	22	16.1±8.6	22.9±6.5	78.9±40.1	12.4±5.8	12.1±7.4	5.4±2.2

[b]$P<0.001$ *vs* the negative group of HCV RNA.

difference was found between them. Four cases of liver cirrhosis were all male cases. The rate of ALT and/or AST abnormalities was significantly higher in male donors than in female donors ($P = 0.005$).

Related factors affecting the outcome of HCV might include co-infection with HBV and long-term excessive alcohol consumption, which could promote the progression of HCV infection to chronicity and liver cirrhosis. In the present study, we could not find the significant correlation between the outcome of HCV and age of infection and sex.

DISCUSSION

The harm of hepatitis C is only next to hepatitis B in our country. The epidemic rate is 3.2% in Chinese population and it is estimated that 41 million people were infected[8]. Economic burden for HCV is 11.7-21.6 billion RMB per year in China. New cases have been decreased through the detection of blood donors since 1990 s, but part of patients would progress to chronic hepatitis, liver cirrhosis and hepatocellular carcinoma. Although there are many reports on this aspect in Western countries[9-13], few similar researches have been carried out in China. So it is very necessary to summarize the natural outcome of HCV in China.

Chronicity rate

The rate of spontaneous resolution in the present study was 16.42%, lower than 29.01%[14] reported before in China after 12-25 years of infection. It may be because the qualitative method used in the study was more sensitive than quantitative method used in another area. Additionally, during our investigation, the infection was spontaneously resolved in some cases, which might be one of the causes of high chronicity in HCV infection in this study. Two patients died of suspected liver disease, and the case fatality rate was 1.16% in the group studied, which was lower than the previously reported[10]. B-type ultrasound detection reflected liver inflammation in some degree under the condition that liver biopsy was not taken. After nine years of infection, 2.68% of the patients developed liver cirrhosis, which was lower than 7-16% after 8-16 years of infection[1]. Our results showed that the clinical symptoms were latent in the donors studied. Compared with the patients with HBV infection, higher chronicity and faster progression to liver cirrhosis were observed in the patients with HCV infection.

Factors affecting the outcome

Age As described previously[15-17], age appear to be an important determinant of progression. The data suggest that the younger the age at infection, the lower the rate of progression. In the present study, no difference was found in the rate of viral resolution in the different age groups, which is consistent with a previous report[14]. The rate of chronicity was higher in the group than in children and young women of other countries.

Sex Regarding sex, there is evidence that the rate of progression of liver disease was lower in women than in men. The cases who progressed to liver cirrhosis in our study were all males. The rate of ALT and/or AST abnormalities in males was significantly higher than that in females, indicating that males might relate with the more serious liver disease.

Super-infection with HBV The rate of viral resolution in the donors super-infected with HBV was a little higher than in the donors without HBV infection, but there was no significant difference. The rate of progression to liver cirrhosis in the cases super-infected with HCV and HBV was significantly higher than that in the cases only infected with HCV, which is consistent with previous reports.

Alcohol consumption Several reports showed that overdose alcohol consumption might contribute to the progression to liver cirrhosis and hepatocellular carcinoma. In the present study, alcohol consumption was shown the progression to chronicity. Whether alcohol consumption affects the progression of liver diseases, needs to be further studied.

In summary, this area (Hebei province) has a higher rate of chronicity in HCV infection, and measures should be taken to prevent the progression to serious liver diseases, especially for the patients super-infected by HCV and HBV.

REFERENCES

1 **Alberti A**, Chemello L, Benvegnu L. Natural history of hepatitis C. *J Hepatol* 1999; **31**(Suppl 1): 17-24

2 **Seeff LB**. Natural history of chronic hepatitis C. *Hepatology* 2002; **36**(5 Suppl 1): S35-46

3 **Hoofnagle JH.** Course and outcome of hepatitis C. *Hepatology* 2002; **36**(5 Suppl 1): S21-S29

4 **Wang SP**, Ding H, Zhang HQ, Lu YZ, Yang JC, Zhao XK, Geng HH, Zhu WF. Hepatitis C virus infection in the plasmapheresis donors. *Zhonghua Liuxingbing Zazhi* 1994; **15**: 71-73

5 **Du SC**, Tao QM, Zhu L. Typing on 5'-terminal noncoding region of hepatitis C virus genome with restrict endonuclease. *Zhonghua Yixue Zazhi* 1993; **73**: 7-9

6 Modified at the Sixth (Xi' an) National Convention of Infectious, Parasitic and Liver Disease. Viral hepatitis prevention project. *Zhonghua Chuanranbing Zazhi* 2001; **19**: 56-62

7 **Luo KX.** Hepatitis B basic biology and clinical science. 1sted. *Beijing: People's Medical Publishing House* 1997: 159

8 **Cheng JM**. Modern epidemiology. 1sted. *Beijing: People's Military Medical Publishing House* 1999: 269

9 **Bellentani S**, Pozzato G, Saccoccio G, Crovatto M, Croce LS, Mazzoran L, Masutti F, Cristianini G, Tiribelli C. Clinical course and risk factors of hepatitis C virus related liver disease in the general population: report from the Dionysos study. *Gut* 1999; **44**: 874-880

10 **Seeff LB**, Miller RN, Rabkin CS, Buskell-Bales Z, Straley Eason KD, Smoak BL, Johnson LD, Lee SR, Kaplan EL. 45-year follow-up of hepatitis C virus infection in healthy young adults. *Ann Intern Med* 2000; **132**: 105-111

11 **Datz C,** Cramp M, Haas T, Dietze O, Nitschko H, Froesner G, Muss N, Sandhofer F, Vogel W. The natural course of hepatitis C virus infection 18 years after an epidemic outbreak of non-A, non-B hepatitis in a plasmapheresis centre. *Gut* 1999; **44**: 563-567

12 **Yokosuka O**, Kojima H, Imazeki F, Tagawa M, Saisho H, Tamatsukuri S, Omata M. Spontaneous negativation of serum hepatitis C virus RNA is a rare event in type C chronic liver diseases: analysis of HCV RNA in 320 patients who were followed for more than 3 years. *J Hepatol* 1999; **31**: 394-399

13 **Mazzeo C**, Azzaroli F, Giovanelli S, Dormi A, Festi D, Colecchia A, Miracolo A, Natale P, Nigro G, Alberti A, Roda E, Mazzella G. Ten year incidence of HCV infection in northern Italy and frequency of spontaneous viral clearance. *Gut* 2003; **52**: 1030-1034

14 **Wei L**, Wang QX, Xu XY, Wan H, Gao Y, Tian XL, Yu M, Sun DG, Fan CL, Jin J, Fan WM, Yi LM, Zhu WF, Chen HS, Zhuang H, Wang Y. 12-25-year follow-up of hepatitis C virus infection in a rural area of Hebei province, China. *Beijing Daxue Xuebao* 2002; **34**: 574-578

15 **Minola E**, Prati D, Suter F, Maggiolo F, Caprioli F, Sonzogni A, Fraquelli M, Paggi S, Conte D. Age at infection affects the long-term outcome of transfusion-associated chronic hepatitis C. *Blood* 2002; **99**: 4588-4591

16 **Bellentani S**, Tiribelli C. The spectrum of liver disease in the general population: lesson from the Dionysos study. *J Hepatol* 2001; **35**: 531-537

17 **Alter MJ,** Kruszon-Moran D, Nainan OV, McQuillan GM, Gao F, Moyer LA, Kaslow RA, Margolis HS. The prevalence of hepatitis C virus infection in the United States, 1988 through 1994. *N Engl J Med* 1999; **341**: 556-562

Edited by Kumar M and Wang XL **Proofread by** Xu FM

PO Box 2345, Beijing 100023, China
Fax: +86-10-85381893
E-mail: wjg@wjgnet.com www.wjgnet.com

World J Gastroenterol 2004;10(19):2870-2873
World Journal of Gastroenterology
Copyright © 2004 by The WJG Press ISSN 1007-9327

• BRIEF REPORTS •

Ability of luteinizing hormone releasing hormone-*Pseudomonas aeruginosa* exotoxin 40 binding to LHRH receptor on human liver cancer cells

Shou-Liang Gong, Gang Zhao, Hong-Guang Zhao, Wen-Tian Lü, Guang-Wei Liu, Ping Zhu

Shou-Liang Gong, Gang Zhao, Hong-Guang Zhao, Wen-Tian Lü, Guang-Wei Liu, Radiobiology Research Unit of Ministry of Public Health, School of Public Health, Jilin University, Changchun 130021, Jilin Province, China
Ping Zhu, Institute of Military Veterinary Medicine, Quartermaster University of Chinese PLA, Changchun 130062, Jilin Province, China
Supported by the Key Programs of National Science and Technology, No. 96-901-05-101
Correspondence to: Shou-Liang Gong, Radiobiology Research Unit of Ministry of Public Health, School of Public Health, Jilin University, Changchun 130021, Jilin Province, China. gongsl@163.com
Telephone: +86-431-5622028 **Fax:** +86-431-5645486
Received: 2003-11-18 **Accepted:** 2003-12-16

Abstract

AIM: To explore the ability of recombinant toxin luteinizing hormone releasing hormone-*Pseudomonas aeruginosa* exotoxin 40 (LHRH-PE40) and LHRH binding to LHRH receptor (LHRHR) on the membrane surface of human liver cancer HEPG cells.

METHODS: LHRH was labeled by using ^{125}I with enzymatic reaction. The affinity and receptor volume of LHRH-PE40 and LHRH binding to LHRHR on the membrane surface of human liver cancer cells were measured with radioligand receptor assay.

RESULTS: The specific activity of LHRH labeled with ^{125}I was 2.7×10^4 kBq/μL, and its radiochemical purity reached to 99.2-99.7%. The binding of ^{125}I to LHRH was maximal for 240 min in the warm cultivation, and this binding was stabilized. The inhibiting rates of ^{125}I-LHRH and LHRH on the proliferation of human liver cancer HEPG cells were not significantly different. On the basis of the saturation curve of ^{125}I-LHRH binding to the membrane LHRHR of HEPG cells, ^{125}I-LHRH of 1×10^5 cpm was selected for radioligand receptor assay. The affinity constants (Kd) of LHRH-PE40 and LHRH binding to the membrane LHRHR of HEPG cells were 0.43±0.12 nmol/L and 4.86±1.47 nmol/L, respectively, and their receptor volumes were 0.37±0.15 μmol/g and 0.42±0.13 μmol/g, respectively. The binding of LHRH-PE40 to the membrane protein of normal liver cells was not observed.

CONCLUSION: The recombinant toxin LHRH-PE40 binding to the membrane surface of LHRHR of human liver cancer HEPG cells was very strong, while the specific binding of it to normal liver cells was not observed. The results provide an important experimental basis for the clinical application of LHRH-PE.

Gong SL, Zhao G, Zhao HG, Lü WT, Liu GW, Zhu P. Ability of luteinizing hormone releasing hormone-*Pseudomonas aeruginosa* exotoxin 40 binding to LHRH receptor on human liver cancer cells. *World J Gastroenterol* 2004; 10(19): 2870-2873
http://www.wjgnet.com/1007-9327/10/2870.asp

INTRODUCTION

Guide medicine is currently one of the focuses in the field of medicine and biology. We can couple some tumor specific antibodies, cytokines or hormones, *etc.* with toxins (such as animal and plant toxin, radiotherapy and chemotherapy medicines or bacterial toxins, *etc.*) through chemical method or connection by gene fusing technology, and then express fusing protein to make a guide medicine with specific target characteristics and killing cell toxicity, that is biological missile, which can selectively kill homologous antigen-associated cells or antibody-associated cells, while exerts little effect on irrespective cells[1]. So far, a series of recombined immune toxins have shown perfect effects through *in vitro* and animal experiment[2-4], moreover the results in some clinic investigations are also satisfactory[5,6]. DAB389IL-2 which IL-2 receptor used as a guide medicine of target has passed FAD's warrant and come into use[7].

Luteinizing hormone-releasing hormone (LHRH) is also termed gonadotropin-releasing hormone (GnRH). It is a peptide hormone synthesized and secreted mostly from hypothalamus. *Pseudomonas aeruginosa* exotoxin 40 (PE40) was obtained by removing I a region of PE. A fusing protein LHRH-PE40 was recombined by the fusion of both LHRH gene and PE40 gene with genetic engineering *in vitro*. LHRH-PE40 is a guide medicine to treat cancer. PE40 has effect on antitumor and immune regulation. The key of LHRH-PE40 biological effect is selectively to kill carcinoma cells. This effect is gained by the distributing difference of membrane surface LHRH receptor (LHRHR) in live cancer cells and normal liver cells. Many experimental results showed that LHRHR expressed greatly in the membrane surface of some carcinoma cells, but not in that of normal liver cells[8-13]. The results provide an important basis for studying and preparing guide medicine to treat cancer[14]. Therefore, LHRHR is acted as a sign to distinguish carcinoma cells from normal cells. The abilities of LHRH-PE40 binding to the membrane surface LHRHR of liver cancer cells and normal liver cells were observed with radioligand receptor assay for providing an important experimental basis for LHRH-PE40 clinical application.

MATERIALS AND METHODS

Liver cancer cell line and normal liver tissues

Human liver cancer HEPG cell line was bought from the Cell Center, Institute of Cell Biology, Chinese Academy of Medical Sciences (Beijing, China). Human liver tissues (3 cases) were provided by the Center of Medicolegal Examination, Criminal and Police Team, Liaoyuan City, Jilin, China.

Human liver cancer HEPG cell line was maintained in 75 cm^2 culture flasks at 37 ℃ in a humidified 50 mL/L CO_2-in-air mixture. The cells were passed weekly. After cells were harvested in exponential growth phase, they were dissociated with a non-enzymatic cell dissociation solution (Sigma, USA), and then counted by a hemacytometer. The cells were washed twice with phosphate-buffered saline (PBS) before cell membrane protein was prepared.

Reagents and hormones

^{125}I was from Amersham, UK. LHRH and thyrotropin releasing hormone (TRH) were bought from Institute of Biochemistry, Shanghai. LHRH-PE40 was synthesized by the Institute of Military Veterinary Medicine, Quartermaster University of PLA. Lactoperoxidase, glucoseoxidase and Sephadex G-25 gel were made in Sigma, USA.

LHRH labeled with ^{125}I of enzymatic reaction

The lactoperoxidase-glucoseoxidase method by Piyachaturawata *et al*.[15] was slightly modified to label LHRH using ^{125}I with enzymatic reaction. Half mol/L PBS of 20 μL (pH 7.6), LHRH of 5 μg (dissolved in 0.1 mol/L NaAc of 5 μL), 2.3 mU lactoperoxidase (dissolved in 0.1 mol/L NaAc of 10 μL, pH 5.6), 2.8 mU glucoseozidase (dissolved in 0.1 mol/L NaAc of 10 μL, pH 5.6) and 5 g/L β-D (+) glucose of 5 μL in proper order were added into the test tube with 3.7×10^4 kBq fresh ^{125}I of non-reducer, oscillated and mixed, to make ^{125}I quickly labeling to LHRH. After the reaction for 5 min at 22-25 ℃, 0.1 mol/L boric acid buffer of 50 μL was added into the test tube to stop the reaction. The reactant of LHRH labeled with ^{125}I in test tube was separated and purified by column chromatography (the column of 1 cm×25 cm) with Sephadex G-25 gel to removing free ^{125}I, eluted with o.1 mol/L boric acid buffer (containing 1 g/L gelatin and 0.2 g/L sodium azide, pH 9.2, flow rate: 3 mL/3 min, 3 mL/tube). Thirty-six tubes were collected. The radioactivity (counts per minute, cpm) of ^{125}I-LHRH of 10 μL in each tube was determined. The specific activity of ^{125}I-LHRH determined with self-displacement curve was $2.69\text{-}3.7\times10^4$ GBq/g LHRH.

Inhibiting rate of liver cancer cell proliferation measured with MTT

Inhibiting rates of both ^{125}I-LHRH and LHRH on the proliferation of human liver cancer HEPG cells were measured using enzyme-linked immunosorbent assay meter (Bio-Rad, USA) with MTT (thiazolyl blue) method[16].

Preparation of cell membrane protein

The preparation of the membrane protein in human liver cancer HEPG cells: The cells were centrifuged in culture fluid, counted, washed once with PBS and centrifuged (500 r/min, 4 ℃, 5 min). The centrifuged sediment was suspended in ice-cold sucrose buffer for 20 min. The suspension was again centrifuged (300 r/min, 4 ℃, 5 min) after the cells in the suspension were ground with ultrasonic meter at ice bath. The centrifuged supernatant was further centrifuged (18 000 *g*, 4 ℃, 30 min). The centrifuged sediment was a membrane protein. Then the purer membrane protein of liver cancer cells was gained after the membrane protein was washed once with PBS.

Preparation of membrane protein in normal human liver cells: The liver tissue was sheared into fragments with ophthalmic scissors after the frozen tissue was thawed in sucrose buffer. The fragments were homogenized at ice bath for 1 min and centrifuged (1 500 r/min, 4 ℃, 10 min). The centrifuged supernatant was again centrifuged (31 000 *g*, 4 ℃, 15 min). Then the purer membrane protein of normal liver cells was gained after the membrane protein was washed once with PBS.

Competitive binding of LHRH-PE40 and LHRH to LHRHR of HEPG cell membrane

Polypropylene test tubes dried after soak with 10 g/L bovine serum albumin (BSA) were used as the reactive tubes. The tri-tube was used as a determined value. LHRH-PE40 or LHRH of different concentrations and ^{125}I-LHRH (1×10^5 cpm) of 100 μL in proper order were added into the reactive tube in ice bath, respectively, and mixed. Then, 100 μL suspension of the cell membrane (containing 180-220 μg protein) was added into the reactive tube. The reactive tubes were cultivated at 4 ℃ for 4 h after oscillation. Excessive LHRH-PE40 or LHRH (200 μg) was added into the non-specific binding tube. The total volume in the reactive tube was 0.3 mL. The reactant was filtrated by using a microfilter with 32# glass fiber filter paper at 93.3 kPa negative pressure vacuum. The reactive tube and filter pore were washed 3 times with 0.5 mL of precolded 0.5 mol/L PBS (pH 7.4): physiological saline at 1:50. The radioactivity of the sediment on the filter paper filtered at vacuum and dried for 5 min was measured with ^{125}I automatic radio-immunity analyzer. The protein was measured with Lowry modification, and its standard curve was done with human serum albumin.

RESULTS

Characteristics of LHRH labeled with ^{125}I

The specific activity of LHRH labeled with ^{125}I of enzymatic reaction was 2.7×10^4 kBq/μg. Its radiochemical purity measured using paper chromatography with the developer of 5% KI and 1 mol/L HCl (1:1) reached 99.2-99.7%. ^{125}I-LHRH did not produce free ^{125}I 3 and 7 d after preservation at -80 ℃, and produced 5% free ^{125}I after 10 d. The inhibiting rate of ^{125}I-LHRH on the proliferation of cancer cells was not significantly different as compared with that of LHRH (Figure 1).

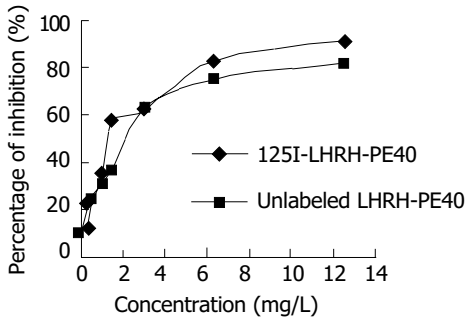

Figure 1 Inhibitory rates of unlabeled LHRH and ^{125}I–LHRH on human liver cancer HEPG cell proliferation.

Warm cultivation time of ^{125}I-LHRH binding to HEPG cell membrane protein

The ^{125}I-LHRH binding to HEPG cell membrane protein was observed for 60, 90, 120, 150, 180, 240 and 300 min in warm cultivation. The binding increased with the prolongation of warm cultivation time, and reached the peak value at 240 min. If the time in the warm cultivation was prolonged further, the binding decreased.

Radioligand receptor assay of competitive binding of LHRH-PE40 and LHRH to HEPG cell membrane protein with ^{125}I-LHRH

The specific binding of HEPG cell membrane protein to ^{125}I-LHRH increased with the protein concentration. The increase of the binding was not obvious as protein concentration exceeded 250 μg per 0.3 mL, while the non-specific binding increased obviously. According to the experimental results, the protein concentration of 180-220 μg per 0.3 mL was used as radioligand receptor assay.

The saturation curve of ^{125}I-LHRH binding to LHRHR of HEPG cells was firstly done. ^{125}I-LHRH of 1×10^5 cpm in 50% linear range of the saturation curve was selected as radioligand receptor assay (Figure 2). Figure 3 shows the inhibiting curve of competitive binding of non-labeled LHRH-PE40 and LHRH to HEPG cell membrane protein LHRHR with ^{125}I-LHRH. ^{125}I-LHRH binding to LHRHR reduced with increase of the non-labeled ligands to demonstrate a specific inhibiting curve of competitive binding. LHRH-PE40 could bind to HEPG cell surface LHRHR, while TRH could not. Figure 4 was drawn with Scatchard method

to gain two straight lines. The affinity constants (Kd) of binding of LHRH-PE40 and LHRH to LHRHR of HEPG cells were 0.43±0.12 μmol/g and 4.86±1.47 μmol/g, respectively, and their receptor volumes were 0.37±0.15 μmol/g and 0.42±0.13 μmol/g, respectively.

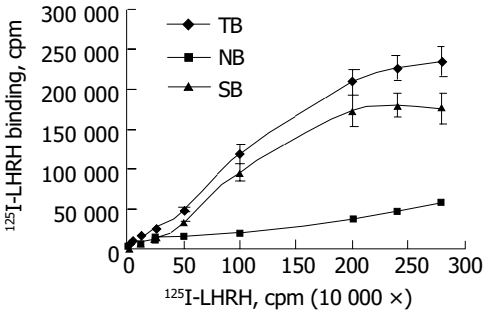

Figure 2 Saturation curve of ^{125}I-LHRH binding to LHRHR of human liver cancer HEPG cells. TB: total binding, NB: non-specific binding, SB: specific binding.

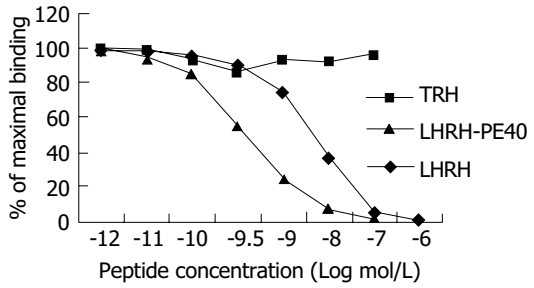

Figure 3 Inhibiting curve of competitive binding of non-labeled LHRH-PE40, LHRH and TRH to human liver cancer HEPG cell LHRHR with ^{125}I-LHRH.

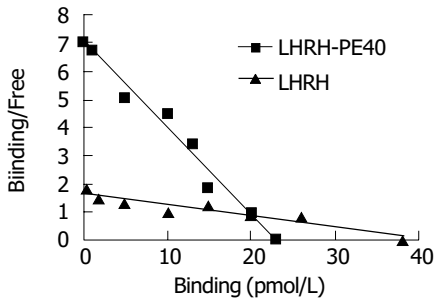

Figure 4 Scatchard analysis of LHRH-PE40 and LHRH binding to LHRHR of human liver cancer HEPG cells.

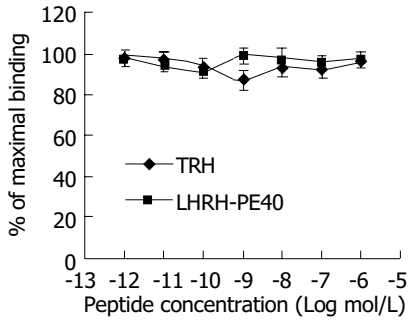

Figure 5 Inhibiting curve of competitive binding of non-labeled LHRH-PE40 and TRH to normal human liver cell LHRHR with ^{125}I-LHRH.

The binding curve of LHRH-PE40 to the membrane protein of normal liver cells was not significantly different from that of negative control TRH (Figure 5). The labeled ligand ^{125}I-LHRH binding to the membrane protein of normal liver cells did not change with increase of the non-labeled ligand LHRH-PE40. The result suggested that LHRH-PE40 binding to trace LHRHR in the membrane of normal human liver cells could not be examined.

DISCUSSION

The specific activity of LHRH labeled with ^{125}I of enzymatic reaction was 2.7×10^4 kBq/μL, and its radiochemical purity reached 99.2-99.7%. The ^{125}I binding to LHRH was maximal at 240 min in the warm cultivation. This binding was stabilized, i.e. ^{125}I-LHRH did not produce free ^{125}I 3 and 7 d after preservation at -80 ℃, and produced 5% free ^{125}I after 10 d. The inhibiting rates of ^{125}I-LHRH and LHRH on the proliferation of human liver cancer HEPG cells measured with MTT (thiazolyl blue) method were not significantly different. The results suggest that LHRH satisfactorily labeled with ^{125}I of enzymatic reaction may be used as radioligand receptor assay.

LHRH-PE40 is a guide medicine to treat cancer. It is composed of the guide fraction of LHRH peptides and the toxicity fraction of PE40 protein. The active principle of LHRH-PE40 is that its toxicity fraction PE40 enters in cells through transmembrane transport to kill cancer cells after its guide fraction LHRH binds to LHRHR of cancer cell membrane surface. The expression of LHRH and its receptor as a part of a negative autocrine regulatory system of cell proliferation has been demonstrated in a number of human malignant tumors. Moreover, the dose-dependent antiproliferative effects of LHRH agonists on cell lines derived from these cancers have been observed by various investigators[17-19]. The effect exerts through the signal transduction in cancer cells[20, 21]. So, the specific binding of guide fraction LHRH to LHRHR of cancer cell membrane surface becomes the key in the treatment of carcinoma. It has been currently demonstrated that there also are LHRH and its receptor LHRHR in some tissues besides hypothalamus and pituitary. Some literatures indicated that there was LHRHR in the membrane surface of normal liver cells, but its content was very low[8,9]. The fact brings forward a challenge against the LHRHR specificity of killing cancer cells. However, our experimental results showed that specific binding of LHRH-PE40 to the membrane surface LHRHR of human liver cancer HEPG cells occurred, while did not to normal human liver cell membrane surface where there may be trace LHRHR. Of course, the negative result of this non-specific binding may be affected by the precision limitation in the experimental method itself. For example, some methods could be used only when the Kd of sample was less than 10^{-8} nmol/L[22]. Both epidermal growth factor (EGF) and interleukin-2 (IL-2) used as the guide medicines are also faced with the same problem that their trace receptors exist on the surface of normal liver and kidney cells, but they have been used in clinic. Although this kind of medicines may also have a weak liver toxicity, their side effects are less as compared with chemotherapy. So, LHRH-PE40 has some value in curing liver cancer with numeric proliferation of LHRHR.

The binding of hormone to its receptor was limited by many factors[23]. Among these factors the space of hormone protein can directly affect the binding to its receptor. LHRH is a decapeptide without free amino and carboxyl. The amino acids at its 4-6 sites can form β-sheet like a barrette, which makes it binding to receptor. Furthermore, the amino acids at this hormone's first and 4-10 sites can bind to its receptor too. LHRH of LHRH-PE40 replaces I a section of PE. A linking bridge of both His and Met amino acids added between two molecules maintains the primary structure of LHRH. But whether LHRH's space configuration of this fusing protein changes should be

further explored. The results from this experiment were that the affinity constants (Kd) of LHRH-PE40 and LHRH binding to LHRHR of HEPG cells were 0.43±0.12 nmol/g and 4.86±1.47 nmol/L, respectively, and their receptor volumes were 0.37±0.15 μmol/g and 0.42±0.13 μmol/g, respectively. The affinity constant of LHRH-PE40 is nearly one-tenth of LHRH. Therefore, we can infer that LHRH-PE40 maintains the characteristics of LHRH binding to its receptor, and its binding capacity is stronger than LHRH itself. The result is identical with the report published elsewhere[6]. This enhancing binding capacity may be caused by its molecular mass being larger than LHRH, which makes itself more stable and decomposed difficultly *in vitro*. These results proved that LHRH-PE40 can bind to LHRHR on the surface of liver cancer cells, and then exerts its guide action.

Up till now, some problems still need to be resolved on the guide medicine for the treatment of cancer. Somebody testified that positive rate of LHRHR in adjacent tissues of cancers was even higher than that in cancer tissues[24], which should be attached importance. The articles demonstrated that the signal transduction pathways mediated by LHRHR were different[25], LHRHR of cancer cell surface could mediate cell apoptosis[26,27].

ACKNOWLEGEMENTS

We are grateful to Dr. Zhang PY and Dr. Li JZ for their excellent technical assistance, and Dr. Wu GM and Dr. Zhang GL for their providing experimental materials.

REFERENCES

1 **Panchal RG**. Novel therapeutic strategies to selectively kill cancer cells. *Biochem Pharmacol* 1998; **55**: 247-252

2 **Reiter Y**, Pastan I. Recombinant Fv immunotoxins and Fv fragments as novel agents for cancer therapy and diagnosis. *Trends Biotechnol* 1998; **16**: 513-520

3 **Perentesis JP**, Gunther R, Waurzyniak B, Yanishevski Y, Myers DE, Ek O, Messinger Y, Shao Y, Chelstrom LM, Schneider E, Evans WE, Uckun FM. *In vivo* biotherapy of HL-60 myeloid leukemia with a genetically engineered recombinant fusion toxin directed against the human granulocyte macrophage colony-stimulating factor receptor. *Clin Cancer Res* 1997; **3**(12 Pt l): 2217-2227

4 **Saleh MN**, LeMaistre CF, Kuzel TM, Foss F, Platanias LC, Schwartz G, Ratain M, Rook A, Freytes CO, Craig F, Reuben J, Sams MW, Nichols JC. Antitumor activity of DAB389IL-2 fusion toxin in mycosis fungoides. *J Am Acad Dermatol* 1998; **39**: 63-73

5 **Kreitman RJ**, Wilson WH, Robbins D, Margulies I, Stetler-Stevenson M, Waldmann TA, Pastan I. Responses in refractory hairy cell leukemia to a recombinant immunotoxin. *Blood* 1999; **94**: 3340-3348

6 **Haggerty HG**, Warner WA, Comereski CR, Peden WM, Mezza LE, Damle BD, Siegall CB, Davidson TJ. BR96 sFv-PE40 immunotoxin: nonclinical safety assessment. *Toxicol Pathol* 1999; **27**: 87-94

7 **Duvic M**, Kuzel TM, Olsen EA, Martin AG, Foss FM, Kim YH, Heald PW, Bacha P, Nichols J, Liepa A. Quality-of-life improvements in cutaneous T-cell lymphoma patients treated with denileukin diftitox (ONTAK(R)). *Clin Lymphoma* 2002; **2**: 222-228

8 **Zhao G**, Gong SL, Yue Y, Zhu P. Distribution of human LHRH receptors in normal and carcinomatous tissues outside pituitary. *Jilin Daxue Xuebao* 2002; **28**: 445-447

9 **Zhao G**, Gong SL, Zhu P. Binding ability of LHRH-PE40 to LHRH receptors on the surface of cancer cell line. *Jilin Daxue Xuebao* 2003; **29**: 5-8

10 **Dharap SS**, Qiu B, Williams GC, Sinko P, Stein S, Minko T. Molecular targeting of drug delivery systems to ovarian cancer by BH3 and LHRH peptides. *J Control Release* 2003; **91**: 61–73

11 **Grundker C**, Gunthert AR, Millar RP, Emons G. Expression of gonadotropin-releasing hormone II (GnRH-II) receptor in human endometrial and ovarian cancer cells and effects of GnRH-II on tumor cell proliferation. *J Clin Endocrinol Metab* 2002; **87**: 1427–1430

12 **Volker P**, Grundker C, Schmidt O, Schulz KD, Emons G. Expression of receptors for luteinizing hormone-releasing hormone in human ovarian and endometrial cancers: frequency, autoregulation, and correlation with direct antiproliferative activity of luteinizing hormone-releasing hormone analogues. *Am J Obstet Gynecol* 2002; **186**: 171–179

13 **Halmos G**, Arencibia JM, Schally AV, Davis R, Bostwick DG. High incidence of receptors for luteinizing hormone-releasing hormone (LHRH) and LHRH receptor gene expression in human prostate cancers. *J Urol* 2000; **163**: 623–629

14 **Plonowski A**, Schally AV, Nagy A, Groot K, Krupa M, Navone NM, Logothetis C. Inhibition of *in vivo* proliferation of MDA-PCa-2b human prostate cancer by a targeted cytotoxic analog of luteinizing hormone-releasing hormone AN-207. *Cancer Lett* 2002; **176**: 57–63

15 **Piyachaturawata P**, Pedroza E, Huang WY, Arimura A, Schally AV. Studies on the iodination of LH-RH and the biological and immunological activities of the products. *Life Sci* 1980; **26**: 1309-1318

16 **Xu N**, Shi AP, Wang YD, Wang CX, Guo WH. Effect of telomerase oligonucleotides on the inhibition of telomerase activity and cell growth in bladder. *Jilin Daxue Xuebao* 2003; **29**: 630-633

17 **Gunthert AR**, Grundker C, Hollmann K, Emons G. Luteinizing hormone-releasing hormone induces JunD–DNA binding and extends cell cycle in human ovarian cancer cells. *Biochem Biophys Res Commun* 2002; **294**: 11–15

18 **Grundker C**, Gunthert AR, Westphalen S, Emons G. Biology of the gonadotropin-releasing homone system in gynecological cancers. *Eur J Endocrinol* 2002; **146**: 1–14

19 **Shacham S**, Cheifetz MN, Lewy H, Ashkenazi IE, Becker OM, Seger R, Naor Z. Mechanism of GnRH receptor signaling: from the membrane to the nucleus. *Ann Endocrinol* 1999; **60**: 79–88

20 **Grundker C**, Schlotawa L, Viereck V, Emons G. Protein kinase C -independent stimulation of activator protein-1 and c-Jun N-terminal kinase activity in human endometrial cancer cells by the LHRH agonist triptorelin. *Eur J Endocrinol* 2001; **145**: 651–658

21 **Grundker C**, Volker P, Schulz KD, Emons G. Luteinizing hormone–releasing hormone agonist triptorelin and antagonist cetrorelix inhibit EGF-induced c-fos expression in human gynecological cancers. *Gynecol Oncol* 2000; **78**: 194–202

22 **Lü BZ**, Tian Y. Receptorology outline. 1st Ed. *Beijing Sciences Press* 1991: 27-32

23 **Luo HB**, Zhu P, Li LJ. Bacterial toxin and clinic. 1st Ed. *Beijing People Health Press* 1999: 91-99

24 **Zhang JS**, Huang GS, Huang WQ, Zhang YQ. Immunohisochemical localization of gonadotropin releasing hormone and its receptor in hepatocellular carcinoma tissues. *Disi Junyi Daxue Xuebao* 1998; **19**: 235-236

25 **Limonta P**, Moretti RM, Marelli MM, Dondi D, Parenti M, Motta M. The luteinizing hormone-releasing hormone receptor in human prostate cancer cells: messenger ribonucleic acid expression, molecular size, and signal transduction pathway. *Endocrinology* 1999; **140**: 5250-5256

26 **Imai A**, Tamaya T. GnRH receptor and apoptotic signaling. *Vitam Horm* 2000; **59**: 1-33

27 **Grundker C**, Schulz K, Gunthert AR, Emons G. Luteinizing hormone–releasing hormone induces nuclear factor κB-activation and inhibits apoptosis in ovarian cancer cells. *J Clin Endocrinol Metab* 2000; **85**: 3815–3820

Edited by Xu CT and Wang XL **Proofread by** Pan BR and Xu FM

PO Box 2345, Beijing 100023, China
Fax: +86-10-85381893
E-mail: wjg@wjgnet.com www.wjgnet.com

World J Gastroenterol 2004;10(19):2874-2877
World Journal of Gastroenterology
Copyright © 2004 by The WJG Press ISSN 1007-9327

• BRIEF REPORTS •

Human endostatin gene transfer, either naked or with liposome, has the same inhibitory effect on growth of mouse liver tumor cells *in vivo*

Chun-Hong Ma, Yan Zhang, Xiao-Yan Wang, Li-Fen Gao, Hua Liu, Chun Guo, Su-Xia Liu, Ying-Lin Cao, Li-Ning Zhang, Wen-Sheng Sun

Chun-Hong Ma, Yan Zhang, Xiao-Yan Wang, Li-Fen Gao, Hua Liu, Chun Guo, Su-Xia Liu, Ying-Lin Cao, Li-Ning Zhang, Wen-Sheng Sun, Institute of Immunology, Medical College of Shandong University, Jinan 250012, Shandong Province, China
Supported by the National Natural Science Foundation of China, No. 30100078 and Huo Yingdong Educational Fund, No.81035
Correspondence to: Dr. Chun-Hong Ma, Institute of Immunology, Medical College of Shandong University, Jinan 250012, Shandong Province, China. machunhong@sdu.edu.cn
Telephone: +86-531-8382038
Received: 2003-11-21 **Accepted:** 2003-12-22

Abstract

AIM: To explore a safe and efficient strategy of tumor therapy using anti-angiogenetic agents.

METHODS: Endostatin gene with a signal sequence of human IgG γ chain was amplified by PCR and cloned into pVAX1 plasmid which was the only vector authorized by FDA in clinical trial to construct a recombinant plasmid named as pVAX-sEN. The recombinant plasmid was detected with *Eco*RI/*Kpn*I and DNA sequencing. BALB/c mice bearing hepatocarcinoma cell line H22 were treated with naked pVAX-sEN or liposome-DNA complex in which the dose of DNA and the ratio of DNA and liposome were different from each other. To compare the efficiency of gene transfection, expression of endostatin at the treated tumor site was assayed with ELISA. To investigate the effect of pVAX1-sEN on hepatocellular carcinoma, pVAX-sEN either naked or in liposome-DNA complex was injected into BALB/c mice bearing H22, then the diameter of tumors was measured, microvessel density was detected by immunohistochemistry, endostatin expression *in vivo* was assayed at different time points.

RESULTS: DNA sequencing showed the endostatin gene with the signal peptide was correctly cloned. *In situ* gene expression assay indicated that both the ratio of DNA and liposome and the dose of DNA could affect the gene transfection efficiency. Interestingly, naked pVAX-sEN had a similar *in situ* endostatin expression to pVAX-sEN with liposome. Animal experiments showed that pVAX-sEN together with pVAX-sEN-liposome complex could efficiently suppress the growth of mouse hepatoma cells.

CONCLUSION: Naked endostatin plasmid intratumoral injection can get a similar gene transfection efficiency to liposome-DNA complex when used *in situ*.

Ma CH, Zhang Y, Wang XY, Gao LF, Liu H, Guo C, Liu SX , Cao YL, Zhang LN, Sun WS. Human endostatin gene transfer, either naked or with liposome, has the same inhibitory effect on growth of mouse liver tumor cells *in vivo*. *World J Gastroenterol* 2004; 10(19): 2874-2877
http://www.wjgnet.com/1007-9327/10/2874.asp

INTRODUCTION

Tumor neovascularization is necessary to the growth and metastasis of tumors[1]. Anti-angiogenesis is an effective method to treat cancer[2,3]. Endostatin, an endogenous angiogenesis inhibitor, was found in 1997[4].It can specifically suppress endothelial cell proliferation. Animal experiments have demonstrated that endostatin can strikingly inhibit the growth of many kinds of tumor cells without drug resistance and toxicity. Endostatin is a promising agent to treat cancer [5,6]. However, to produce a large quantity of biologically active proteins has been proven difficult, the treatment requires repeated administration and high doses of recombinant protein, which limits endostatin's clinical application. Gene therapy can overcome the above disvantages and become a potential method for cancer therapy. In this article, we constructed the recombinant eukaryotic plasmid using pVAX1 which is the only vector authorized by FDA in clinical trial. It can express secretive endostatin *in vivo*. Efficient gene transfer and expression are the key to gene therapy. In order to explore an efficient and easy gene transfer method, we also compared the inhibitory effect of liposome and naked DNA transfection on mouse hepatoma cells *in vivo*.

MATERIALS AND METHODS

Plasmids

Eukaryotic expression vector pVAX1 authorized by FDA in clinical trial was purchased from Invitrogen(USA). Cloning vector pGEM-T-EN containing human endostatin genes was constructed and preserved in our laboratory[7].

Cells and cultures

Mouse hepatoma cell line H22 was purchased from Shandong Medical Science Institute and grown in BALB/c abdominal cavity.

Animals

BALB/c female mice, 5-6 wk of age, were provided by Experimental Animal Center of Shandong University. A total of 1×10^6 H22 cells were transplanted subcutaneously into mice. Treatment began 1 wk later, when tumor volume ranged between 0.4 to 0.5 cm^3.

Primer design

According to the sequences in GeneBank, primers were designed to amplify endostatin genes. In order to get a secretary protein, signal sequence of human IgG γ chain was added to the 5' end of forward primer, and sequences recognized by *KpnI* and *EcoRI* were respectively added to the forward primer and reverse primer: forward(P1): 5' TTAGGTACCATGGAAGCCCCAGCTCAG CTTCTCTTCCTCCTGCTACTCTGGCTCCCAGATACCACC GGACACAGCCACCGC 3' ; reverse(P2): 5' CGGCGAATTCC TTGGAGG CAGTC 3'. All of these oligonucleotide primers were synthesized by Shanghai BioAsia Bio-technology Co.Ltd.

PCR

The endostatin gene containing signal sequence of human

IgG γ chain was amplified by PCR taking pGEM-T-EN as template and P1 and P2 as primers. PCR reaction was performed in 25 μL volume containing: 1μL of plasmid DNA, 2.5 μL of 10×buffer, 0.5 mmoL Mg^{++}, 5 nmol/L dNTP, 3 units of Taq polymerase,10 nmol/L primers (forward and reverse). Reaction conditions were at 95 ℃ for 5 min, then 30 cycles each at 95 ℃ for 1 min, at 62 ℃ for 1 min, at 72 ℃ for 3 min, followed by a final extension at 72 ℃ for 5 min. PCR products were purified by UNIQUE-10 Kit (Shanghai Shenggong Biological Co.Ltd) after 20 g/L agarose gel electrophoresis.

Construction of recombinant eukaryotic plasmid expressing secretive endostatin

PCR products and pVAX1 were digested by *Eco*RI and *Kpn*I (TaKaRa Biotechnology, Dalian) respectively, then purifed and ligased with T4DNA ligase (TaKaRa Biotechnology, Dalian) at room temperature overnight. *E.coli*, DH5α, competent cells were transfected using $CaCl_2$. Recombinant clones were detected by *Eco*RI and *Kpn*I and then sequenced by Shanghai BioAsia Bio technology Co.Ltd.

In situ expression of secretary endostatin

Five-to-six week old female BALB/c mice were injected subcutaneously with 1×10^6 logarithmically growing H22 cells to axillary. One week later, when tumor volume was about 0.4 to 0.5 cm^3, naked plasmid or liposome-DNA complex (Lipofectamine™2000 from Invitrogen) was administered intratumorly. The ratio of liposome and recombinant plasmid in liposome-DNA complex was 1:1, 1:3, 1:8 respectively. Animals were sacrificed 3 d after injection and about 0.5 cm^3 of tumor was separated and cut into pieces ,then cultured in 0.5 mL MEM medium with 100 mL/L of FCS at 37 ℃, 50 mL/L CO_2 atmosphere for 24 h. Supernatants were collected and centrifuged at 1 000 r/min for 5 min, then stored at -20 ℃ for gene expression assay.

In vivo inhibition assay

One week after BALB/c mice were injected subcutaneously with 1×10^6 logarithmically growing H22 cells to axillary, naked recombinant plasmid (20 μg) or the liposome-DNA complex containing 20 μg recombinant plasmid was administered intratumorly once a week for two weeks. The ratio of liposome and recombinant plasmid in liposome-DNA complex was 1:1. pVAX1 and NS were respectively injected into animals as control. The length (a) and width (b) of tumor were measured twice a week. The tumor volumes were then calculated using the formula: $Volume=a\times b^2\times0.52$.

The experiment was done in triplicate with 5 animals in each group.

In vivo expression assay of endostatin

In order to determine the association of anti-tumor effects and the expression level of endostatin, peripheral blood was prepared from tail at different time point and serum was used to detect the expression of endostatin with ELISA.

ELISA

Expression of endostatin was detected with human endostatin™ protein accucyte® EIA kit (Oncogene) following the manufacturer's instructions.

Immunohistochemistry

Mice were killed 3 d after the fourth administration. Tumors were excised, fixed in formalin and prepared for paraffin-embedded sections. Factor VIII-related antigen was detected with S-P immunohistochemistory kit (Beijing Zhongshan Biocompany) according to the manufacturer's instructions. Tumor microvessel density (MVD) was evaluated as described by Weidner[8].

Statistical analysis

All data were expressed as mean±SD. Student's *t* -test was used for statistical analysis. A *P* value <0.05 was considered statistically significant.

RESULTS

Plasmid construction

Endostatin gene with signal sequence of human IgG γ chain was amplified by PCR and cloned into eukaryotic vector pVAX1 named as pVAX-sEN. Two percent agarose gel electrophoresis demonstrated two binds about 3 kb and 610 bp in size as expected after the recombinant plasmid was digested by *Kpn*I and *Eco*RI (Figure 1). DNA sequencing analysis indicated both the sequence of endostatin and signal peptide were in accordance with those in the GenBank.

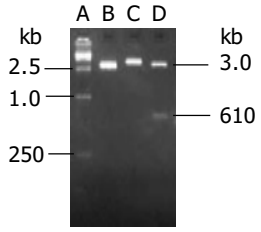

Figure 1 Detection of the recombinant plasmid pVAX-sEN using *Eco*RI and *Kpn*I digestion. A: Marker15 000; B: pVAX1 digested by *Eco*RI; C: Recombinant plasmid pVAX-sEN digested by *Eco*RI; D: Recombinant plasmid pVAX-sEN digested by *Eco*RI and *Kpn*I.

In situ gene expression assay of naked DNA and liposome-DNA complex

To compare the efficiency of gene transfection, expression of endostatin transgenic protein at the tumor site of the treated group was assayed with ELISA. Endostatins were detected in all samples treated with naked or liposome-DNA complex but not in the control groups (Figure 2). Endostatin expression was about 30 ng/mL when the ratio of liposome and DNA was 1:1. With the addition of the liposome into complex the expression of endostatin was increased gradually. When the ratio reached 1:8, the endostatin was 92 ng/mL. Interestingly, naked DNA administration could get a pretty high gene expression which was about 86 ng/mL.

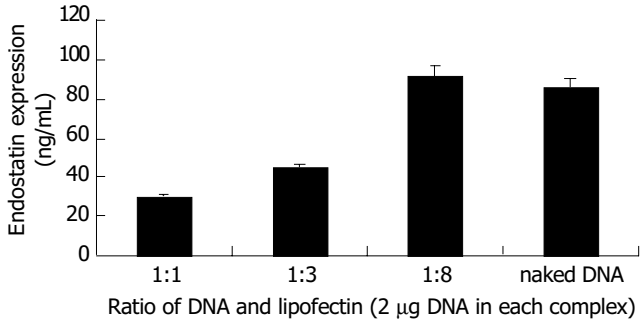

Figure 2 Comparison of *in vivo* transfection using different ratios of liposome and DNA in liposome-DNA complex and naked DNA.

To compare gene transfection using liposome-DNA complex containing different doses of DNA *in vivo*, liposome-DNA

complex was prepared with the ratio of liposome and DNA 1:1 which contained different doses of DNA. Twenty-four hours after transfection endostatins were detected by ELISA (Figure 3). The result indicated that when DNA was less than 20 μg , with the elevation of DNA doses, the expression of endostatin increased. When the DNA dose reached 20 μg, endostatin reached 152 ng/mL, the peak expression. On the contrary, when the DNA reached 50 μg, the expression of endostatin dropped to 80 ng/mL.

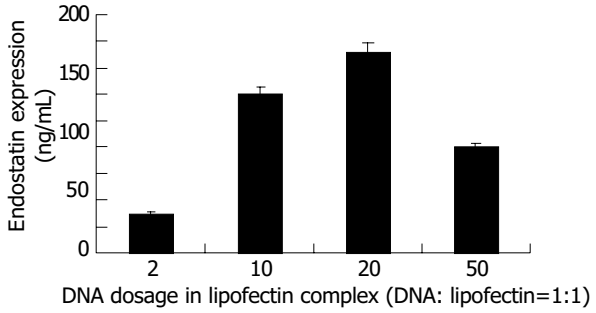

Figure 3 Comparison of *in vivo* transfection using liposome complex (the ratio of liposome and DNA is 1:1) containing different doses of DNA.

In vivo inhibitory effect of pVAX-sEN on mouse hepatoma cells

Changes of tumor volumes indicated pVAX-sEN-liposome complex could obviously inhibit the growth of mouse hepatoma cells when administered intratumorly (Figure 4). The tumor volume was only 0.451±0.26 cm^3, obviously less than that in NS treated group (1.86±0.62 cm^3) and pVAX1 treated group (1.56±0.37 cm^3) (P<0.05). The inhibition rate was about 73%. Interestingly, pVAX-sEN alone could produce an inhibitory effect. The tumor size in pVAX-sEN treated group was 0.4±0.25 cm^3, and the inhibitory rate was about 80%, which was not significant from pVAX-sEN-liposome complex treated group (P>0.05).

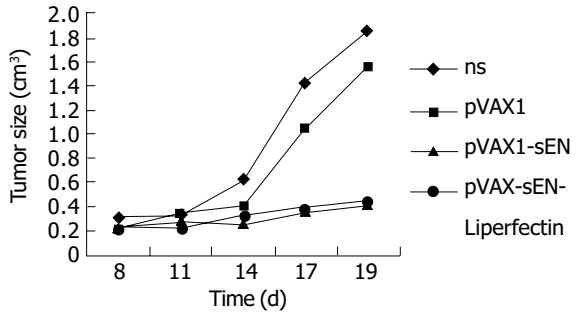

Figure 4 Inhibitory effect of recombinant secretive endostatin on mouse hepatoma cells.

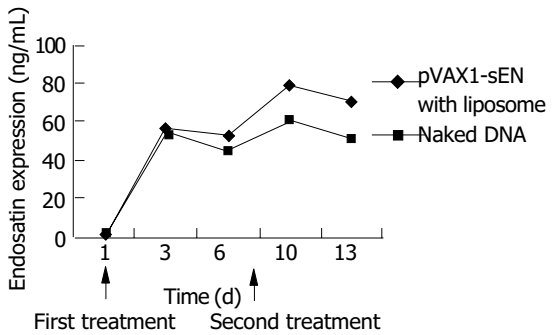

Figure 5 *In vivo* endostatin expression in peripheral blood of treated mice.

In vivo expression of endostatin

ELISA showed that the expression of endostatin in peripheral blood varied with the administration of recombinant plasmid. Three days after the first treatment of recombinant plasmid, both naked and in combination with liposome, the expression of endostatin could be detected (56.8±3.8 ng/mL and 54±5.8 ng/mL, respectively. P>0.05) and then the expression decreased 2 d later. After the second administration the expression raised to 79.8±6.1 ng/mL and 60.43±8.3 ng/mL and it could be lasted for another 3 d. The expression level in naked plasmid treated mice was lower than that in DNA-liposome complex treated mice (50.1±6.3 ng/mL *vs* 70.4±6.4 ng/mL, P<0.05) (Figure 5).

Inhibition of tumor angiogenesis by pVAX-sEN

Immunohistochemical analysis showed a potent inhibition of angiogenesis in tumors treated by pVAX-sEN. The MVD was counted and results are shown in Figure 6. Expression of endostatin mediated by naked pVAX-sEN or liposome-DNA complex injection caused a significant reduction in MVD compared with the NS control group or the pVAX1 treated group (P<0.05). However, the difference in MVD between naked DNA and liposome-DNA complex injection groups was not statistically significant.

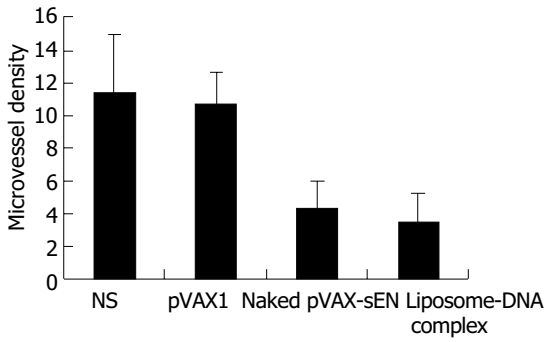

Figure 6 Inhibition of tumor neovascularization by injecting recombinant plasmid.

DISCUSSION

Growth and metastasis of tumor depend on the neuvascularization. Anti-angiogenesis can effectively suppress tumor growth. Endostatin was found to specifically inhibit endothelial cell proliferation but not actively proliferating cells such as carcinoma cells, intestinal cells, epithelial cells, bone marrow cells[4]. So the application of endostatin did not cause bone marrow ablation, stomach and intestinal reaction, and other side effects[5]. Moreover, endostatin could be used for a long time without drug resistance since its target cells, endothelial cells have a relatively stable gene structure and low mutation rate[5,6]. Consequently endostatin is an attractive new strategy in cancer therapy.

Recombinant endostatin protein has been used in clinical trials at present[9]. However poor solubility of recombinant endostatin protein and its high effective dose have limited its wide spread application[4]. Gene therapy by which endostatin can express *in vivo* is an efficient method for anti-angiogenesis cancer therapy[10-12].

The key point of gene therapy is to establish an effective gene delivering system. Vectors used to deliver genes nowadays mainly include viral and non-viral vectors. Because of limitations of viral vectors such as potent danger, immune response and limitations of the gene length[13-15], more and more researchers have payed their attention to non-viral vectors. In this paper, a highly safe vector pVAX1 authorized by FDA in clinical trial was selected to construct a recombinant vector expressing

secretive endostatin which was named as pVAX-sEN. DNA sequencing indicated endostatin gene together with a signal peptide was correctly cloned. Animal experiments showed pVAX-sEN could efficiently suppress the growth of mouse hepatoma cells. This study provides an experimental basis for further study on safe and efficient gene therapy with endostatin.

Non-viral gene can be transferred by physical and chemical methods. The cationic liposome-mediated gene transfer system is popular because of its low immunity, high safety, easy preparation, no limitation to gene sequence and potential to be used repeatedly[16,17]. Gene transfer efficiency of liposome can be affected by many factors. Studies indicated that a suitable quantity ratio of DNA and liposome was one of the essential factors[18]. Naked DNA injection is another simple safe gene transfer method. Many researchers have verified that naked DNA administration could induce a high gene expression level[19,20]. In 2003 VEGF administered into cardiac muscle using naked DNA was applied to clinical trial[21]. In our study, cationic liposome was used to transfer endostatin DNA into mouse hepatoma cells *in vivo*. It showed that when the quantity ratio of liposome and DNA was 1:1, the expression of endostatin was pretty high. When the quantity ratio was 1:8, endostatin reached the highest expression (92 ng/mL). With the elevation of DNA dose, the expression of endostatin increased. When the DNA dose reached 20 μg, the expression of endostatin amounted to 152 ng/mL. However, if DNA dose reached 50 μg, the expression of endostatin dropped to 80 ng/mL. The possible reason was that the high dose of liposome in the complex might be deposited[18]. So the transfection efficiency was lower. Results also indicated that naked DNA could also get a pretty high gene expression (86 ng/mL). Our *in vivo* inhibition assay even showed that naked DNA could get an inhibition as efficient as DNA-liposome complex.In 2002, Shi *et al*.[22] compared the transfection rate of naked DNA with liposome-DNA complex and found the expression of IL-12 was equal. Their result is in accordance with ours. However, *in vivo* gene expression assay indicated that the peripheral expression of endostatin in naked DNA treated mice decreased more quickly than that in DNA-liposome complex treated mice.

In conclusion, we successfully constructed the recombinant vector secretively expressing endostatin using highly safe vector pVAX1 named pVAX-sEN. Animal experiments showed it could efficiently suppress the growth of hepatoma cells. It is a promising method in cancer therapy. At the same time we compared the transfection efficiency of naked pVAX-sEN DNA with liposome-DNA complex. Results indicated naked DNA could produce both a high endostatin gene expression and a good tumor inhibition effect when used *in situ*, strongly suggesting that naked DNA administration is a simple, safe and efficient gene transfer method.

REFERENCES

1 **Folkman J**. What is the Evidence that tumors are angiogenesis dependent. *J Natl Cancer Inst* 1990; **82**: 4-6

2 **Marx J**. Angiogenesis. A boost for tumor starvation. *Science* 2003; **301**: 452-454

3 **Brem S**, Brem H, Folkman J, Finkelstein D, Patz A. Prolonged tumor dormancy by prevention of neovascularization in the vitreous. *Cancer Res* 1976; **36**: 2807-2812

4 **O'Reilly MS**, Boehm T, Shing Y, Fukai N, Vasios G, Lane WS, Flynn E, Birkhead JR, Folkman J, Fukai N, Vasios G, Lane WS, Elynn E, Birkhead JR, Folkman J. Endostatin: an endogenous inhibitor of angiogenesis and tumor growth. *Cell* 1997; **88**: 277-285

5 **Boehm T**, Folkman J, Browder T, O'Reilly MS. Antiangiogenic therapy of experomantal cancer does not induce acquired drug resistance. *Nature* 1997; **390**: 404-407

6 **Kerbel RS**. A cancer therapy resistant to resistance. *Nature* 1997; **390**: 335-336

7 **Ma CH**, Sun WS, Zhang LN, Wang XY, Li X. Expression of human endostatin in picha yeast and its inhibition effect on tumor. *J Shandong Med University* 2001; **39**: 334-336

8 **Weidner N.** Current pathologic methods for measuring intratumoral microvessel density within breast carcinoma and other solid tumors. *Breast Cancer Res Treat* 1995; **36**: 169-180

9 **Eder JP Jr**, Supko JG, Clark JW, Puchalski TA, Garcia-Carbonero R, Ryan DP, Shulman LN, Proper J, Kirvan M, Rattner B, Connors S, Keogan MT, Janicek MJ, Fogler WE, Schnipper L, Kinchla N, Sidor C, Phillips E, Folkman J, Kufe DW. Phase I clinical trial of recombinant human endostatin administered as a short intravenous infusion repeated daily. *J Clin Oncol* 2002; **20**: 3772-3784

10 **Wang X**, Liu F, Li X, Li J, Xu G. Anti-tumor effect of human endostatin mediated by retroviral gene transfer in nude mice. *Chin Med J* 2002; **115:** 1664-1669

11 **Nakashima Y**, Yano M, Kobayashi Y, Moriyama S, Sasaki H, Toyama T, Yamashita H, Fukai I, Iwase H, Yamakawa Y, Fujii Y. Endostatin gene therapy on murine lung metastases model utilizing cationic vector-mediated intravenous gene delivery. *Gene Ther* 2003; **10**: 123-130

12 **Li X**, Fu GF, Fan YR, Shi CF, Liu XJ, Xu GX, Wang JJ. Potent inhibition of angiogenesis and liver tumor growth by administration of an aerosol containing a transferrin-liposome-endostatin complex. *World J Gastroenterol* 2003; **9**: 262-266

13 **Bramson JL**, Hitt M, Gauldie J, Graham FL. Pre-existing immunity to adenovirus does not prevent tumor regression following intratumoral administration of a vector expressing IL-12 but inhibits virus dissemination. *Gene Ther* 1997; **4**: 1069-1076

14 **Lehrman S**. Virus treatment questioned after gene therapy death. *Nature* 1999; **401**: 517-518

15 **Rochlitz CF**. Gene therapy of cancer. *Drugs Today* 2000; **36**: 619-629

16 **Ota T**, Maeda M, Tatsuka M. Cationic liposomes with plasmid DNA influence cancer metastatic capability. *Anticancer Res* 2002; **22**: 4049-4052

17 **Kaiser S**, Toborek M. Liposome-mediated high-efficiency transfection of human endothelial cells. *J Vasc Res* 2001; **38**: 133-143

18 **Clark PR**, Stopeck AT, Ferrari M, Parker SE, Hersh EM. Studies of direct intratumoral gene transfer using cationic lipid-complexed plasmid DNA. *Cancer Gene Ther* 2000; **7**: 853-860

19 **Kim JM**, Jeong JG, Ho SH, Hahn W, Park EJ, Kim S, Yu SS, Lee YW, Kim S. Protection against collagen-induced arthritis by intramuscular gene therapy with an expression plasmid for the interleukin-1 receptor antagonist. *Gene Ther* 2003; **10**: 1543-1550

20 **Imboden M**, Shi F, Pugh TD, Freud AG, Thom NJ, Hank JA, Hao Z, Staelin ST, Sondel PM, Mahvi DM. Safety of interleukin-12 gene therapy against cancer: a murine biodistribution and toxicity study. *Hum Gene Ther* 2003; **14**: 1037-1048

21 **Fortuin FD**, Vale P, Losordo DW, Symes J, DeLaria GA, Tyner JJ, Schaer GL, March R, Snell RJ, Henry TD, Van Camp J, Lopez JJ, Richenbacher W, Isner JM, Schatz RA. One-year follow-up of direct myocardial gene transfer of vascular endothelial growth factor-2 using naked plasmid deoxyribonucleic acid by way of thoracotomy in no-option patients. *Am J Cardiol* 2003; **92**: 436-439

22 **Shi F**, Rakhmilevich AL, Heise CP, Oshikawa K, Sondel PM, Yang NS, Mahvi DM. Intratumoral injection of interleukin-12 plasmid DNA, either naked or in complex with cationic lipid, results in similar tumor regression in a murine model. *Mol Cancer Ther* 2002; **1**: 949-957

Edited by Zhu LH and Wang XL **Proofread by** Xu FM

PO Box 2345, Beijing 100023, China
Fax: +86-10-85381893
E-mail: wjg@wjgnet.com www.wjgnet.com

World J Gastroenterol 2004;10(19):2878-2882
World Journal of Gastroenterology
Copyright © 2004 by The WJG Press ISSN 1007-9327

• BRIEF REPORTS •

Expression of plasma vascular endothelial growth factor in patients with hepatocellular carcinoma and effect of transcatheter arterial chemoembolization therapy on plasma vascular endothelial growth factor level

Xin Li, Gan-Sheng Feng, Chuan-Sheng Zheng, Chen-Kai Zhuo, Xi Liu

Xin Li, Gan-Sheng Feng, Chuan-Sheng Zheng, Chen-Kai Zhuo, Xi Liu, Department of Interventional Radiology, Union Hospital, Tongji Medical College, Huazhong University of Science and Technology, Wuhan 430022, Hubei Province, China
Supported by the National Natural Science Foundation of China, No. 39770839
Correspondence to: Xin Li, M.D., Department of Radiology, the Affiliated Union Hospital, Tongji Medical College, Huazhong University of Science and Technology, Wuhan 430022, Hubei Province, China. wxyao2001@yahoo.com.cn
Telephone: +86-27-85726373
Received: 2004-03-27 **Accepted:** 2004-04-05

Abstract

AIM: To investigate the expression level of plasma vascular endothelial growth factor (P-VEGF) in patients with hepatocellular carcinoma (HCC) and its relationship with the clinicopathologic characteristics, and to examine the changes of P-VEGF in the course of transcatheter arterial chemoembolization (TACE).

METHODS: Peripheral blood samples were taken from 45 HCC patients before and 1, 3, 7 d, and 1 mo after TACE. Plasma VEGF level was measured with the quantitative sandwich enzyme-linked immunosorbent assay (ELISA). Twenty patients with benign liver lesions and 17 healthy control subjects were also included in this study.

RESULTS: Plasma VEGF levels in HCC patients were significantly elevated as compared to those in patients with benign liver lesions (P = 0.006) and in the normal controls (P = 0.003). Significant differences were observed when P-VEGF was categorized by tumor size (P = 0.006), portal vein thrombosis (P = 0.011), distant metastasis (P = 0.017), arterial-portal vein shunting (P = 0.026), and International Union Against Cancer (UICC) TNM stage (P = 0.044). There was no correlation between plasma level of VEGF and the level of alpha fetoprotein (α-FP) (r = 0.068, P = 0.658) and weakly correlated with the number of platelets (r = 0.312, P = 0.038). P-VEGF levels increased significantly and reached the peak value on the first day after TACE, and then decreased gradually. The change rate of P-VEGF concentration (one month post-TACE/pre-TACE×100%) was correlated with the retention rate of lipiodol oil (rs = 0.494, P = 0.001) and the tumor volume change (rs = 0.340, P = 0.034). The patients who achieved a partial or complete response to TACE therapy showed significantly less pre-treatment P-VEGF than those nonresponders (P = 0.025). A high pre-therapeutic P-VEGF level was associated with poor response to treatment (P = 0.018).

CONCLUSION: A high pre-treatment P-VEGF level is a useful marker for tumor progression, especially for vascular invasion. TACE increases the level of P-VEGF only temporarily which may be associated with tumor ischemia. P-VEGF may be useful in predicting treatment response, monitoring disease course after TACE and judging the effect of different TACE regimens.

Li X, Feng GS, Zheng CS, Zhuo CK, Liu X. Expression of plasma vascular endothelial growth factor in patients with hepatocellular carcinoma and effect of transcatheter arterial chemoembolization therapy on plasma vascular endothelial growth factor level. *World J Gastroenterol* 2004; 10(19): 2878-2882
http://www.wjgnet.com/1007-9327/10/2878.asp

INTRODUCTION

Transcatheter arterial chemoembolization (TACE) is the most frequently applied palliative treatment in HCC patients who are considered to be unsuitable candidates for surgery. But the indications and outcome of TACE are not clearly defined in the literature[1,2]. TACE therapy is invasive and associated with high financial costs[3]. To predict which patients are likely to benefit from TACE would be useful to both oncologists and patients.

Tumor angiogenesis is essential for solid tumorigenesis, growth, invasion and metastasis[4-6]. Tumor angiogenesis is mediated by angiogenic factors and vascular endothelial growth factor (VEGF) is one of the most potent factors. Strong VEGF expression has been demonstrated in various solid tumor types. In HCC, VEGF expression in tumor tissue has been reported to be correlated with aggressive behavior, early metastasis spread, and poor prognosis[7,8]. Recently, the expression of VEGF in patients with various malignancies has been made possible by measuring circulating VEGF concentrations with the enzyme-linked immunosorbent assay (ELISA)[9]. The elevation of VEGF in blood implies a promotion of tumor angiogenesis, and several studies have revealed the predictive value of circulating VEGF level in disease progression and prognosis in various types of cancer[10,11]. Raised pre-treatment circulation VEGF levels in small-cell lung carcinoma, esophageal carcinoma, gastrointestinal cancer and non-Hodgkin's lymphoma have been associated with a poor outcome[12-15].

Although elevated circulation VEGF levels have been measured in patients with various tumors. To our knowledge few data are available with regard to plasma VEGF (P-VEGF) levels in patients with HCC[16]. Data concerning the change of P-VEGF in the course of TACE therapy and its significance in prediction of patient's response to chemoembolization have not been reported to date.

Therefore, in this prospective study, we analyzed the P-VEGF level in patients with HCC prior to treatment to determine the clinicopathologic significance of P-VEGF, and to assess the clinical usefulness of pre-treatment P-VEGF as a predictor of outcome in patients undergoing TACE therapy for HCC.

MATERIALS AND METHODS

Patients and treatment design

The study consisted of 45 patients (37 males, 8 females, mean age 50 years, range 29-77 years) with unresectable HCC who underwent TACE at the Department of Interventional Radiology, Wuhan Union Hospital between October 2000 and February 2002. HCC was diagnosed by distinctive radiographic findings, serum alpha fetoprotein, and with (n = 8) or without histological proof. All patients were treated with TACE therapy alone without any other therapies such as surgery, percutaneous ethanol injection, or systemic chemotherapy. The chemoembolization agents consisted of 100 mg/m^2 of carboplatin, 50 mg/m^2 of doxorubicin hydrochloride, 1 g of 5-fluorouracil and 5-25 mL of iodized oil (Lipiodol; Guerbet, Aulnay-sous-Bois, France). For those with hepatic arterial-portal vein fistula, gelfoam piece was used to block the fistula before iodized oil was used.

Twenty patients underwent TACE therapy for benign diseases (ten patients underwent partial hepatic artery embolization for hepatic cavernous angioma, ten patients underwent partial spleen artery embolization for hypersplenism) and seventeen healthy volunteers were also involved in this study, served as control to evaluate the P-VEGF cut-off level.

Clinicopathologic data

Physical examination, chest X-ray, routine liver function test were performed. Complete blood count, hepatitis B surface antigen status and serum alpha fetoprotein (α-FP) were prospectively collected from each patient. Tumor characteristics such as size, location, capsular, portal vein involvement, lymph node or extrahepatic metastasis, were assessed on the basis of radiographic findings. Tumor vascularity and arteio-portal vein shunting (A-V shunting) were studied by superselective digital subtraction angiography (DSA). Tumor staging was performed using the International Union Against Cancer (UICC) TNM classification[17].

Blood sampling and enzyme immunoassay of P-VEGF concentration

Peripheral venous blood was taken before (n = 45) and 1 (n = 30), 3 (n = 44), 7 (n = 18) and 1 mo (n = 45) after TACE therapy. Blood samples were collected in sterile glass tubes containing 0.057 mL of 15% EDTA. Plasma was separated by centrifugation at 2000 r/min for 15 min to eliminate platelets and stored at -70 ℃ till use.

Plasma VEGF was measured in duplicate by commercially available ELISA kits (Quantikine human VEGF, R&D System, Minneapolis, MN, USA). According to the manufacturer the minimal detectable dose of VEGF was <5.0 ng/L, the intra-assay and the inter-assay variabilities were 6.7-5.1% and 8.8-6.2%, respectively. Absorbance was determined using a biokinetics reader EL312e (Bio-Tek Instruments, Winooski, VT, USA) at 450 nm.

Definition of response to TACE treatment

Response to treatment was assessed by image examinations one month after TACE Therapy. Treatment was evaluated according to the tumor volume change and retention rate of the iodized oil. The tumor volume was calculated using the summed products of the longest dimensions of the lesion, and patients were categorized as responding group (tumor size decrease or stable, no new-born nest) and non-responding group (enlargement of the tumor or the presents of new-born nest). According to the retention rate of the oil, patients were categorized as groups >75%, 50-75%, 25-50% and <25%.

Statistical analysis

Statistical analysis was carried out by the SPSS 10.0 packed program. To investigate the relationships between P-VEGF levels and other variables, t test, ANOVA test, Chi-square test, Fisher exact probability test, correlation coefficient (r) and spearman's rank correlation (rs) were used when appropriate. P<0.05 based on a two-tailed test was considered statistically significant.

RESULTS

Pre-TACE P-VEGF in patients with HCC

The pre-operative P-VEGF levels were significantly higher in HCC patients (63.83±51.09 ng/L) than those in benign liver diseases (28.99±6.67 ng/L) (P = 0.006) and in healthy controls (25.60±5.47 ng/L) (P = 0.003). There was no significant difference in P-VEGF levels between the patients with benign liver diseases and healthy control. The sensitivity of P-VEGF in detecting HCC, using the mean P-VEGF of the patients with benign liver diseases (28.99 ng/L) as cut-off level, was found to be 73.3% with 62.2% specificity.

Correlation between pre-TACE P-VEGF and clinicopathologic features

There was no significant association between pre-TACE P-VEGF levels and various clinical and laboratory variables, except the gender (t = 4.111, P = 0.003). There was a weak correlation between P-VEGF levels and the platelet number (PLT) (r = 0.312, P = 0.038) and no correlation with the levels of α-FP (r = 0.068).

There was no significant association between the P-VEGF level and the presence of cirrhosis, tumor location, tumor capsule, ascites, lymph node metastasis, or the tumor vascularity. Significant differences were observed when P-VEGF was categorized by tumor size (P = 0.006), distant metastasis (P = 0.017), portal vein thrombosis (P = 0.011), arterio-portal vein shunting (P = 0.026), and advanced TNM stage (P = 0.044) (Table 1, Figure 1).

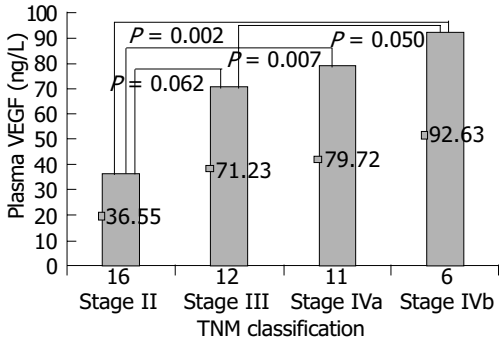

Figure 1 Mean plasma vascular endothelial growth factor levels at each disease stage in patients with hepatocellular carcinoma.

Using mean concentration of TII tumors as cut-off level, P-VEGF was able to predict TIII/TIV tumors with 75.9% sensitivity and 62.5% specificity. Using mean concentration of portal vein thrombosis of negative tumors as cut-off level, P-VEGF was found to have a sensitivity of 62.5% and a specificity of 64.9% in detecting portal vein thrombosis of positive tumors. Using mean concentration of the distant metastasis-free group as cut-off level, P-VEGF was able to exclude distant metastasis with a negative predictive value of 89.3%, a sensitivity of 50% and a specificity of 64.1%. P-VEGF could predict the presence of A-V shunting with 75% sensitivity and 67.6% specificity by using mean concentration of the non-A-V shunting patients as cut-off level (Table 2).

Change of P-VEGF levels during TACE course

P-VEGF levels were significantly elevated in patients with HCC

Table 1 Pre-TACE plasma VEGF levels in patients categorized by radiological parameters

	Group	No. of patients	Median plasma VEGF (ng/L)	Statistic value	*P* value
Cirrhotic liver	No	13	80.15	t = 1.380	0.175
	Yes	32	57.19		
Tumor location	Left lobe	4	77.82	F = 0.275	0.843
	Right lobe	26	66.62		
	Spiegel's lobe	5	50.38		
	Multiple lobe	10	57.68		
Tumor capsule	No	32	68.15	t = 0.888	0.379
	Yes	13	53.18		
Ascites	No	37	62.81	t = 1.151	0.280
	Yes	8	82.60		
Lymph node involvement	No	39	61.68	t = 1.677	0.101
	Yes	6	101.31		
Tumor vascularity	Hypervascularity	31	75.59	F = 0.922	0.406
	Median	9	55.31		
	Hypovascularity	3	39.1		
Tumor size	<5 cm	7	27.57	F = 5.804	0.006
	5-10 cm	22	55.59		
	>10 cm	11	101.54		
Portal vein thrombosis	No	37	57.97	t = 2.669	0.011
	Yes	8	104.79		
Extra hepatic metastasis	No	39	59.39	t = 2.483	0.017
	Yes	6	116.18		
TNM classification	Stage II	16	36.55	F = 2.937	0.044
	Stage III	12	71.23		
	Stage Iva	11	79.72		
	Stage Ivb	6	92.63		
Arterio-portal vein shunting	No	37	56.03	t = 2.283	0.026
	Yes	8	99.9		

TNM: tumor-node-metastasis. Tumor vascularity and arterial-portal vein shunting were studied by superselective digital subtraction angiographic (DSA).

Table 2 Effect of different VEGF levels on specificity and sensitivity in predicting tumor load in patients with HCC

	Cut-off VEGF value (ng/L)	Sensitivity (%)	Specificity (%)	Positive predictive value (%)	Negative predictive value (%)
TII and TIII/IV	36.55	75.9	62.5	78.6	58.8
Portal vein thrombosis	57.97	62.5	64.9	27.8	88.8
Extra hepatic metastasis	59.39	50	64.1	17.6	89.3
Arterio-portal vein shunting	56.03	75	67.6	33.3	92.6

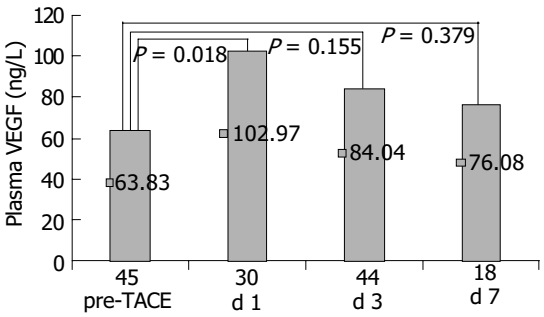

Figure 2 Effect of TACE on mean plasma vascular endothelial growth factor levels.

on the first post-TACE day (102.97±89.26 ng/L) compared to pre-TACE (63.83±51.09) (P = 0.018). Then VEGF level decreased gradually to 84.04±79.16 ng/L on the third day and 76.08±45.38 ng/L on the seventh day post-TACE, showing no statistical difference with pre-TACE P-VEGF levels (Figure 2).

A similar change of P-VEGF was found in patients who underwent TACE for treatment of benign liver diseases (data not shown).

One month after TACE, the P-VEGF level was 71.47±50.87 ng/L, no statistical difference was found between them and pre-TACE P-VEGF levels.

Correlation between P-VEGF and response to TACE therapy

Treatment response was evaluated according to the change in tumor volume and retention of the oil. Forty five patients were categorized as responding group (18 cases) and non-responding group (27 cases). The change rate of P-VEGF levels was associated with the change in tumor volume (rs = 0.340, P = 0.034). No statistic difference was found between changes in α-FP levels and tumor volume (rs = 0.230, P = 0.138).

The pre-TACE P-VEGF level in non-responding group (73.33±70.32 ng/L) was significantly higher than that in the responding group (49.52±25.33 ng/L, P = 0.025). The response rate of the low VEGF group (P-VEGF<49.5 ng/L) was significantly higher than that of the high VEGF group (P-VEGF>49.5 ng/L) (51.6% *vs* 14.29%; P = 0.018, Fisher exact probability test) (Table 3).

Table 3 Correlation between plasma VEGF concentration and response to treatment

Clinical response	Plasma VEGF (ng/L)		No. of patients		
			Low VEGF	High VEGF	
Responder	49.52±25.33	t = 2.285	16	2	χ^2 = 5.599
Non-responder	73.33±70.32	P = 0.025	15	12	P = 0.018

According to the retention rate of the iodized oil, 45 patients were classified as follows: 11 cases >75%, 16 cases 50 - 75%, 9 cases 25 - 50% and 9 cases <25%. The change rate of P-VEGF levels was strongly associated with oil retention (rs = 0.494, P = 0.001). No statistical difference was found between the change rate of α-FP and oil retention (rs = 0.209, P = 0.179).

DISCUSSION

By alternate splicing of the VEGF gene, VEGF could exist at least in one of the four forms, namely, VEGF206 (tissue bound), VEGF189 (tissue bound), VEGF165 (the most abundant form, soluble, and partly tissue bound) and VEGF121 (soluble)[18]. Compared with bioassays, detection of soluble VEGF isoforms with immunoassay was characterized by low detection limits and greater specificity, reproducibility, and practicability[19,20].

Recently, serum VEGF was measured by an enzyme-linked immunosorbent assay (ELISA) in patients with various types of cancer[20]. Increased levels of VEGF were demonstrated in most patients with cancer and closely related to tumor progression and metastasis[21,22]. However, some studies have shown that VEGF is not only secreted from tumor cells but also from a variety of $CD34^+$ hematological cells (including platelets, megakaryocytes, monocytes, T-lymphocytes and leukocytes) during clotting[23]. Serum VEGF concentrations could reflect blood platelet counts rather than VEGF synthesis by tumor tissues, and plasma rather than serum should be considered suitable for the measurement of circulating VEGF[24]. So in our study, plasma VEGF concentrations were analyzed and ethylenediamine tetraacetic acid (EDTA) was used as anticoagulant.

Hepatocellular carcinoma (HCC) is a highly vascular tumor characterized by neovascularization and a high propensity for venous invasion. A strong VEGF expression was observed in the tissue of HCC and closely associated with tumor progression and metastasis[6]. Recently, Poon *et al*.[25] reported that serum VEGF level was significantly elevated in patients with HCC, and significantly high serum VEGF levels were associated with the absence of tumor capsule, the presence of venous invasion and microsatellite modules, and advanced TNM stage. Li *et al*.[26] also considered that serum VEGF was a predictor of invasion and metastasis of HCC. To our knowledge, only one previous study measured P-VEGF changes in HCC patients. Jinno *et al*.[16] reported that P-VEGF was a promising tumor marker for remote metastasis of HCC and its specificity, sensitivity and overall accuracy were high enough to be clinically useful.

In the current study, pre-TACE P-VEGF was found to be markedly elevated in the majority of patients with HCC and the increase was closely related to a more advanced stage of diseases. This finding suggested that HCC cells were an important source of P-VEGF. But the lower P-VEGF levels in HCC patients overlapped considerably with those in normal controls, thus limiting the application of VEGF as a tumor marker in early detection of HCC.

We found that high P-VEGF levels were associated with the presence of extrahepatic metastasis and portal vein involvement. Because vascular invasion by tumor cells is indispensable for remote metastasis, metastasis, portal vein involvement and A-V shunting can reflect the ability of tumor cells to invade blood vessels. These results indicated that P-VEGF could be used as a tumor marker in detecting vascular invasive phenotypes of HCC. It is clinically important to search for the metastasis radiologically in patients with high P-VEGF levels.

In the present study, there was a weak correlation of PLT number with P-VEGF level. It has been suggested that platelets aggregate at metastatic sites, due to factors released from metastatic cells and vascular invasion, resulting in microthrombosis, tumor adhesion, and may release VEGF to the circulation[27,28]. Therefore, we considered that in metastatic HCC patient platelet activation was a part of the sources of plasma VEGF.

The finding that there was no significant association between the P-VEGF level and tumor vascularity shown by DSA is of great interest. This might suggest that circulation VEGF levels could reflect the formation of new vessels rather than the degree of existing tumor vascularity.

No correlation was found between P-VEGF and serum α-FP, suggesting that they had different mechanisms of production, and P-VEGF might be an independent predictive factor.

Suzuki *et al*.[29] found serum VEGF increased significantly and reached the peak value 7 d after TACE, suggesting that VEGF might play a role as a sensitive marker for tumor ischemia. We observed that P-VEGF increased and reached the peak value on the first day after TACE and then decreased gradually. We thought that the changes of serum VEGF during TACE might be associated with chemotherapy-induced thrombocytopenia and a subsequent rebound increase in platelet number[30]. Although the exact mechanism is currently unknown, hypoxia caused by TACE, clotting and platelets aggregation after TACE, tumor cell lysis (and release of VEGF)[31], elevation of VEGF in acute hepatitis[32], and tissue trauma[33] might contribute to the increase of P-VEGF in the early post-TACE period.

It has been reported that high pre-treatment levels of circulating VEGF are correlated with a poor response to the conventional chemotherapy[12-15]. Similar results were found that the mean P-VEGF of the responding group was significantly higher than that of the non-responding group. Two treatment response indicators (tumor volume change and retention of the iodized oil) were associated with the change rate of P-VEGF levels rather than the change rate of α-FP. These results indicated that P-VEGF might act as a follow-up marker for post-TACE monitoring of the disease course and evaluation of curative effect, especially in α-FP negative patients. It may be useful in predicting treatment response and judging the effect of different TACE regimens.

In summary, P-VEGF level is an independent predictive factor of tumor progression, especially vascular invasion. TACE increases the level of P-VEGF only temporarily which may be associated with tumor ischemia. P-VEGF may be useful in predicting treatment response, monitoring disease course after TACE and judging the effect of different TACE regimens.

REFERENCES

1 **Okada S**. Transcatheter arterial embolization for advanced hepatocellular carcinoma: the controversy continues. *Hepatology* 1998; **27**: 1743-1744

2 **Llad Inverted Question Marko L**, Virgili J, Figueras J, Valls C, Dominguez J, Rafecas A, Torras J, Fabregat J, Guardiola J, Jaurrieta E. A prognostic index of the survival of patients with unresectable hepatocellular carcinoma after transcatheter arterial chemoembolization. *Cancer* 2000; **88**: 50-57

3 **Katyal S**, Oliver JH, Peterson MS, Chang PJ, Baron RL, Carr BI. Prognostic significance of arterial phase CT for prediction of response to transcatheter arterial chemoembolization in unresectable hepatocellular carcinoma: a retrospective analysis. *Am J Roentgenol* 2000; **175**: 1665-1672

4 **Hanahan D**, Folkman J. Patterns and emerging mechanisms of the angiogenic switch during tumorigenesis. *Cell* 1996; **86**: 353-364

5 **Kirsch M**, Schackert G, Black PM. Metastasis and angiogenesis. *Cancer Treat Res* 2004; **117**: 285-304

6 **Gupta MK**, Qin RY. Mechanism and its regulation of tumor-induced angiogenesis. *World J Gastroenterol* 2003; **9**: 1144-1155

7 **Yamaguchi R**, Yano H, Iemura A, Ogasawara S, Haramaki M, Kojiro M. Expression of vascular endothelial growth factor in human hepatocellualr carcinoma. *Hepatology* 1998; **28**: 68-77

8 **Poon RT**, Lau CP, Ho JW, Yu WC, Fan ST, Wong J. Tissue factor expression correlates with tumor angiogenesis and invasiveness in human hepatocellular carcinoma. *Clin Cancer Res* 2003; **9**: 5339-5345

9 **Kondo S**, Asano M, Matsuo K, Ohmori I, Suzuki H. Vascular endothelial growth factor/vascular permeability factor is detectable in the sera of tumor-bearing mice and cancer patients. *Biochim Biophys Acta* 1994; **1221**: 211-214

10 **Kraft A,** Weindel K, Ochs A, Marth C, Zmija J, Schumacher P, Unger C, Marme D, Gastl G. Vascular endothelial growth factor in the sera and effusions of patients with malignant and nonmalignant disease. *Cancer* 1999; **85**: 178-187

11 **Fuhrmann-Benzakein E**, Ma MN, Rubbia-Brandt L, Mentha G, Ruefenacht D, Sappino AP, Pepper MS. Elevated levels of angiogenic cytokines in the plasma of cancer patients. *Int J Cancer* 2000; **85**: 40-45

12 **Salven P**, Teerenhovi L, Joensuu H. A High pretreatment serum VEGF concentration is associated with poor outcome in non-Hodgkin's lymphoma. *Blood* 1997; **90**: 3167-3172

13 **Salven P**, Ruotsalainen T, Mattson K, Joensuu H. High pretreatment serum level of vascular endothelial growth factor (VEGF) is associated with poor outcome in small-cell lung cancer. *Int J Cancer* 1998; **79**: 144-146

14 **Shimada H**, Takeda A, Nabeya Y, Okazumi SI, Matsubara H, Funami Y, Hayashi H, Gunji Y, Kobayashi S, Suzuki T, Ochiai T. Clinical significance of serum vascular endothelial growth factor in esophageal squamous cell carcinoma. *Cancer* 2001; **92**: 663-669

15 **Hyodo I**, Doi T, Endo H, Hosokawa Y, Nishikawa Y, Tanimizu M, Jinno K, Kotani Y. Clinical significance of plasma vascular endothelial growth factor in gastrointestinal cancer. *Eur J Cancer* 1998; **13**: 2041-2045

16 **Jinno K**, Tanimizu M, Hyodo I, Nishikawa Y, Hosokawa Y, Doi T, Endo H, Yamashita M, Okada Y. Circulating vascular endothelial growth factor (VEGF) is a possible tumor marker for metastasis in human hepatocellular carcinoma. *J Gastroenterol* 1998; **33**: 376-382

17 **Zhang ZJ**, Wu MC, Shen F, He J, Chen H, Yang GS, Cong WM, Zong M. Significance of TNM classification in prognostic evaluation of hepatocellular carcinoma following surgical resection. *Zhonghua Zhongliu Zazhi* 1999; **21**: 293-295

18 **Houck KA**, Ferrara N, Winer J, Cachianes G, Li B, Leung DW. The vascular endothelia growth factor family: Identification of a fourth molecular species and characterization of alternative splicing of RNA. *Mol Endocrinol* 1991; **5**: 1806-1814

19 **Bienvenu JA**, Monneret G, Gutowski MC, Fabien N. Cytokine assays in human sera and tissues. *Toxicology* 1998; **129**: 55-61

20 **Yamamoto Y**, Toi M, Kondo S, Matsumoto T, Suzuki H, Kitamura M, Tsuruta K, Taniguchi T, Okamoto A, Mori T, Yoshida M, Ikeda T, Tominaga T. Concentrations of vascular endothelial growth factor in the sera of normal controls and cancer patients. *Clin Cancer Res* 1996; **2**: 821-826

21 **Zhao J**, Hu J, Cai J, Yang X, Yang Z. Vascular endothelial growth factor expression in serum of patients with hepatocellular carcinoma. *Chin Med J* 2003; **116**: 772-776

22 **Dirix LY**, Vermeulen PB, Pawinski A, Prove A, Benoy I, De Pooter C, Martin M, Van Oosterom AT. Elevated levels of the angiogenic cytokines basic fibroblast growth factor and vascular endothelial growth factor in sera of cancer patients. *Br J Cancer* 1997; **76**: 238-243

23 **Lee JK**, Hong YJ, Han CJ, Hwang DY, Hong SI. Clinical usefulness of serum and plasma vascular endothelial growth factor in cancer patients: which is the optimal specimen? *Int J Oncol* 2000; **17**: 149-152

24 **Jelkmann W**. Pitfalls in the measurement of circulating vascular endothelial growth factor. *Clin Chem* 2001; **47**: 617-623

25 **Poon RT**, Ng IO, Lau C, Zhu LX, Yu WC, Lo CM, Fan ST, Wong J. Serum vascular endothelial growth factor predicts venous invasion in hepatocellular carcinoma: a prospective study. *Ann Surg* 2001; **233**: 227-235

26 **Li XM**, Tang ZY, Qin LX, Zhou J, Sun HC. Serum vascular endothelial growth factor is a predictor of invasion and metastasis in hepatocellular carcinoma. *J Exp Clin Cancer Res* 1999; **18**: 511-517

27 **Pinedo HM**, Verheul HM, D'Amato RJ, Folkman J. Involvement of platelets in tumor angiogenesis? *Lancet* 1998; **352**: 1775-1777

28 **Mohle R**, Green D, Moore MA, Nachman RL, Rafii S. constitutive production and thrombin-induced release of vascular endothelial growth factor by human megakaryocytes and platelets. *Proc Natl Acad Sci U S A* 1997; **94**: 663-668

29 **Suzuki H,** Mori M, Kawaguchi C, Adachi M, Miura S, Ishii H. Serum vascular endothelial growth factor in the course of transcatheter arterial embolization of hepatocellular carcinoma. *Int J Oncol* 1999; **14**: 1087-1090

30 **Verheul HM**, Hoekman K, Luykx-de Bakker S, Eekman CA, Folman CC, Broxterman HJ, Pinedo HM. Platelet: transporter of vascular endothelial growth factor. *Clin Cancer Res* 1997; **3**: 2187-2190

31 **Nasu R**, Kimura H, Akagi K, Murata T, Tanaka Y. Blood flow influences vascular growth during tumor angiogenesis. *Br J Cancer* 1999; **79**: 780-786

32 **Akiyoshi F**, Sata M, Suzuki H, Uchimura Y, Mitsuyama K, Matsuo K, Tanikawa K. Serum vascular endothelial growth factor levels in various liver diseases. *Dig Dis Sci* 1998; **43**: 41-45

33 **Bondestam J**, Salven P, Jaaskela-Saari H, Ikonen T, Lepantalo M, Mattila S, Joensuu H. Major surgery increases serum levels of vascular endothelial growth factor only temporarily. *Am J Surg* 2000; **179**: 57-59

Edited by Kumar M and Wang XL **Proofread by** Xu FM

PO Box 2345, Beijing 100023, China
Fax: +86-10-85381893
E-mail: wjg@wjgnet.com www.wjgnet.com

World J Gastroenterol 2004;10(19):2883-2885
World Journal of Gastroenterology
Copyright © 2004 by The WJG Press ISSN 1007-9327

• BRIEF REPORTS •

Quantifying anti-HBV effect of targeted ribonuclease by real-time fluorescent PCR

Jun Liu, Ying-Hui Li, Jin Ding, Wei-Dong Gong, Cai-Fang Xue, Ya Zhao, Yu-Xiao Huang

Jun Liu, Ying-Hui Li, Jin Ding, Wei-Dong Gong, Cai-Fang Xue, Ya Zhao, Yu-Xiao Huang, Department of Etiology, Fourth Military Medical University, Xi'an 710032, Shaanxi Province, China
Supported by the National Natural Science Foundation of China, No. 30100157; Medical Research Fund of Chinese PLA, No. 01MA184; Innovation Project of FMMU, No. CX99005
Co-correspondents: Cai-Fang Xue
Correspondence to: Dr. Jun Liu, Department of Etiology, Fourth Military Medical University, Xi'an 710033, Shaanxi Province, China. etiology@fmmu.edu.cn
Telephone: +86-29-83374536 **Fax:** +86-29-83374594
Received: 2004-03 -11 **Accepted:** 2004-04 -13

Abstract

AIM: To quantify the inhibition of HBV replication by targeted ribonuclease by using real-time fluorescent PCR.

METHODS: Targeted ribonuclease was introduced into 2.2.15 cells by liposome-mediated transfection or HIV-TAT mediated protein transduction. Forty-eight hours after the transfection and 24 h after the transduction, supernatants of 2.2.15 cells were collected and HBV DNA in the supernatants was quantified by real-time fluorescent PCR with a commercial kit.

RESULTS: HBV DNA concentrations in the supernatants of 2.2.15 cells transfected or transducted with targeted ribonuclease were $4.9\pm2.4\times10^8$ copies/L and $8.3\pm4.0\times10^8$ copies/L, respectively. Compared with controls, transfection or transduction of targeted ribonuclease reduced HBV DNA concentration in the supernatants of 2.2.15 cells by 90.4% and 90.1%, respectively ($P<0.05$).

CONCLUSION: Targeted ribonuclease can inhibit HBV replication in 2.2.15 cells.

Liu J, Li YH, Ding J, Gong WD, Xue CF, Zhao Y, Huang YX. Quantifying anti-HBV effect of targeted ribonuclease by real-time fluorescent PCR. *World J Gastroenterol* 2004; 10 (19): 2883-2885
http://www.wjgnet.com/1007-9327/10/2883.asp

INTRODUCTION

Chronic hepatitis B virus (HBV) infection is a major health problem worldwide. Globally, more than 350 million people are infected with HBV, and some of them will evolve into liver cirrhosis and hepatocellular carcinoma (HCC). Current treatment regimens for chronic HBV infection, including interferon-γ, lamivudine, adefovir, or different combinations of these drugs, have only a limited long-term efficacy, but many adverse effects and drug resistance[1,2]. Therefore, the exploration of novel treatment strategies for HBV infection is both necessary and urgent. In fact, many ingenious treatment strategies have been tested for inhibition of HBV replication, such as antisense nucleotides, ribozymes, intracellular antibodies, targeted nucleases, RNA interference[3-13]. All of them can inhibit HBV replication to various degrees.

To explore alternative treatment methods against HBV infection, targeted ribonuclease (TN), a fusion protein of HBVc and human eosinophil-derived neurotoxin (hEDN), was constructed and its effect on HBV replication was tested. After the targeted ribonuclease was introduced by transfection or transduction into 2.2.15 cells, a cell model of HBV infection, we found that it significantly reduced the serological markers of HBV replication, namely HBsAg and HBeAg, in the supernatants of 2.2.15 cells, suggesting that the targeted ribonuclease could inhibit HBV replication.

To further characterize the anti-HBV effect of the targeted ribonuclease, the HBV DNA was quantified in the supernatants of 2.2.15 cells treated by the targeted ribonuclease. Our results showed that the targeted ribonuclease markedly reduced HBV DNA concentration in the supernatants, which together with our previous findings, demonstrate that HBV replication can be inhibited by targeted ribonuclease.

MATERIALS AND METHODS

Cell culture

2.2.15 cells, a human hepatoblastoma Hep G2 cell line stably transfected by HBV genome, were cultured in Dulbecco's modified Eagle's medium (DMEM, purchased from Gibco Life Technologies, Grand Island, NY) supplemented with 100 mL/L fetal calf serum (Sijiqing Biotech Company, Hangzhou, China).

Transfection

The transfection methods were previously described[14]. Briefly, twenty-four hours before transfection, 2.2.15 cells were seeded into a culture plate at the density of 2×10^8/L. Lipofectamine™ 2000 reagent (Gibco Life Technologies) was used for the transfection of 2.2.15 cells by p/TN, p/TNm, p/hEDN, p/HBVc, pcDNA3.1 (-), or mock solution (DMEM plus Lipofectamine™ 2000 reagent containing no plasmid) according to the manufacturer's protocol. p/TN, p/TNm, p/hEDN and p/HBVc are the eukaryotic expression plasmids for targeted ribonuclease, point-mutated targeted ribonuclease without ribonuclease activity, human eosinophil-derived neurotoxin, and HBV core protein, respectively.

Transduction

2.2.15 cells were seeded into a culture plate at the density of 2×10^8/L. Twenty-four hours later, purified recombinant proteins with protein transduction domain, TAT-TN, TAT-TNm, TAT-hEDN, and TAT-HBVc were added into the culture medium. For mock transduction, an equal volume of DMEM instead of protein was added into the culture medium.

Real-time fluorescent PCR

Forty-eight hours after transfection and 24 h after transduction, the supernatants of 2.2.15 cells were collected and HBV DNA in the supernatants was quantified by using fluorescent PCR kit for quantification of HBV DNA (Daan Gene Company, Guangzhou, China) according to the manufacturer's protocol. PCR primers were: P1: 5'ATCCTGCTGCTATGCCTCATCTT3', P2: 5' ACAGTGGGGAAAGCCCTACGAA3'. The probe was 5'TGGCTAGTTTACTAGTGCCATTTTG3'. PCR reaction was analyzed by PE 5700 (Perkin Elmer, USA).

Statistical analysis

All data were analyzed by SPSS 10.0 software. Differences were considered statistically significant when $P<0.05$.

RESULTS

HBV DNA in the supernatants of 2.2.15 cells transfected or transducted with the targeted ribonuclease and controls was quantified by real-time fluorescent PCR. The results are shown in Figure 1. Compared with the controls, HBV DNA concentration in the supernatant of 2.2.15 cells was markedly reduced by the targeted ribonuclease, which was introduced into the cells by both pathways, *i.e.* transfection and transduction. The transfected targeted ribonuclease reduced HBV DNA concentration by 90.4% and the transducted targeted ribonuclease by 90.1% ($P<0.05$). Either hEDN or HBVc alone had no such an effect, indicating that it was the fusion protein itself, *i.e.* the targeted ribonuclease, but not its constituent molecules that exerted the anti-HBV effect. Interestingly, TNm which was mutated at just one amino acid residue (Lys113→Arg) but had no ribonuclease activity as compared with TN, did not decrease HBV DNA concentration either, suggesting that the ribonuclease activity was needed in the anti-HBV effect of the targeted ribonuclease. To exclude the possibility that the anti-HBV effect of the targeted ribonuclease was due to nonspecific killing of 2.2.15 cells, we also detected cell viability of the transfected and transducted cells by MTT assay. The results showed that the targeted ribonuclease had no adverse effects on cell viability and proliferation as compared with controls ($P>0.05$, data not shown).

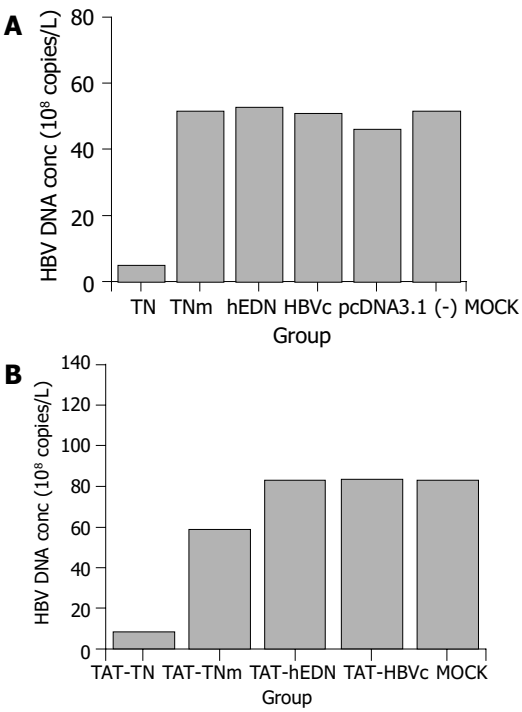

Figure 1 HBV DNA concentration in the supernatants of tranfected and transducted 2.2.15 cells. A: HBV DNA concentration in the supernatants of transfected 2.2.15 cells. TN, TNm, hEDN, HBVc, pcDNA3.1 (-), and MOCK represent the supernatants collected from 2.2.15 cells transfected by p/TN, p/TNm, p/hEDN, p/HBVc, pcDNA3.1 (-), or mock solution (DMEM plus Lipofectamine™ 2000 reagent containing no plasmid), respectively. B: HBV DNA concentrations in the supernatants of transducted 2.2.15 cells. TAT-TN, TAT-TNm, TAT-hEDN, TAT-HBVc, and MOCK represent the supernatants collected from 2.2.15 cells transducted by purified proteins of TAT-TN, TAT-TNm, TAT-hEDN, TAT-HBVc, or mock solution (DMEM), respectively.

DISCUSSION

Real-time fluorescent PCR is a simple, sensitive, specific and precise method to quantitate nucleic acids over a vast dynamic range[15]. Due to these advantages, real-time fluorescent PCR has been widely used in both basic research and clinical diagnosis to measure the quantity of nucleic acids. As for HBV, real-time fluorescent PCR has been used in monitoring viral load during the course of antiviral treatment to evaluate the efficacy of the treatment and predict the possibility of emergence of drug-resistant variants, in the analysis of anti-HBV effect of small interfering RNA transfected into HBV-producing cell lines, and in the study of HBV pathogenesis[10,16-19]. In the current research, we also used real-time fluorescent PCR to precisely quantify HBV DNA in the supernatants of 2.2.15 cells to detect the effect of the targeted ribonuclease on HBV replication. The targeted ribonuclease reported here is a fusion protein against HBV infection constructed by us, based on the principle of capsid-targeted viral inactivation (CTVI)[5,20]. Our previous studies showed that it significantly reduced HBsAg and HBeAg in the supernatants of 2.2.15 cells, suggesting that the targeted ribonuclease could inhibit HBV replication. In consistent with our previous findings, in this study we observed the targeted ribonuclease notably reduced HBV DNA in the supernatants of 2.2.15 cells. Taken together, these results demonstrate that the targeted ribonuclease strongly inhibits HBV replication. The targeted ribonuclease may therefore be one of the promising alternative anti-HBV agents which are being studied in the pursuing of a satisfactory treatment for chronic HBV infection.

Although the precise mechanism of anti-HBV effect of targeted ribonuclease still remains unknown and awaits further study, the principle of capsid-targeted viral inactivation (CTVI) implies that it may specifically recognize pregenomic RNA (pgRNA) of HBV, the template for HBV replication, intracellularly by the HBVc domain of fusion protein, and then degrades pgRNA by the hEDN domain. This will in turn lead to a decrease in the replication of HBV DNA and synthesis of viral proteins, which finally results in a reduction of extracellular HBV DNA and viral proteins (HBsAg and HBeAg). In fact, we have found that purified targeted ribonuclease can degrade RNA *in vitro* (unpublished data) which supports this mechanism. Experiments are ongoing in this laboratory to clarify the mechanism and to apply the targeted ribonuclease to small animal models.

REFERENCES

1 **Conjeevaram HS,** Lok AS. Management of chronic hepatitis B. *J Hepatol* 2003; **38**(Suppl 1): S90-S103

2 **Jaboli MF,** Fabbri C, Liva S, Azzaroli F, Nigro G, Giovanelli S, Ferrara F, Miracolo A, Marchetto S, Montagnani M, Colecchia A, Festi D, Reggiani LB, Roda E, Mazzella G. Long-term alpha interferon and lamivudine combination therapy in non-responder patients with anti-HBe-positive chronic hepatitis B: Results of an open, controlled trial. *World J Gastroenterol* 2003; **9:** 1491-1495

3 **Li JG,** Lian JQ, Jia ZS, Feng ZH, Nie QH, Wang JP, Huang CX, Bai XF. Effect of ribozymes on inhibiting expression of HBV mRNA in HepG2 cells. *Shijie Huaren Xiaohua Zazhi* 2003; **11:** 161-164

4 **Lu YY,** Wang L, Liu Y, Yu M, Li K, Wang YD, Zhang LX, Cheng J. Inhibitory effect of HBcAg ScFv on hepatitis B virus. *Shijie Huaren Xiaohua Zazhi* 2002; **10:** 765-769

5 **Beterams G,** Nassal M. Significant interference with hepatitis B virus replication by a core-nuclease fusion protein. *J Biol Chem* 2001; **276:** 8875-8883

6 **Giladi H,** Ketzinel-Gilad M, Rivkin L, Felig Y, Nussbaum O, Galun E. Small interfering RNA inhibits hepatitis B virus replication in mice. *Mol Ther* 2003; **8:** 769-776

7 **McCaffrey AP,** Nakai H, Pandey K, Huang Z, Salazar FH,

Xu H, Wieland SF, Marion PL, Kay MA. Inhibition of hepatitis B virus in mice by RNA interference. *Nat Biotechnol* 2003; **21:** 639-644

8 **Shlomai A,** Shaul Y. Inhibition of hepatitis B virus expression and replication by RNA interference. *Hepatology* 2003; **37:** 764-770

9 **Hamasaki K,** Nakao K, Matsumoto K, Ichikawa T, Ishikawa H, Eguchi K. Short interfering RNA-directed inhibition of hepatitis B virus replication. *FEBS Lett* 2003; **543:** 51-54

10 **Ying C,** De Clercq E, Neyts J. Selective inhibition of hepatitis B virus replication by RNA interference. *Biochem Biophys Res Commun* 2003; **309:** 482-484

11 **Chen Y,** Du D, Wu J, Chan CP, Tan Y, Kung HF, He ML. Inhibition of hepatitis B virus replication by stably expressed shRNA. *Biochem Biophys Res Commun* 2003; **311:** 398-404

12 **Konishi M,** Wu CH, Wu GY. Inhibition of HBV replication by siRNA in a stable HBV-producing cell line. *Hepatology* 2003; **38:** 842-850

13 **Klein C,** Bock CT, Wedemeyer H, Wustefeld T, Locarnini S, Dienes HP, Kubicka S, Manns MP, Trautwein C. Inhibition of hepatitis B virus replication *in vivo* by nucleoside analogues and siRNA. *Gastroenterology* 2003; **125:** 9-18

14 **Liu J,** Li YH, Xue CF, Ding J, Gong WD, Zhao Y, Huang YX. Targeted ribonuclease can inhibit replication of hepatitis B virus. *World J Gastroenterol* 2003; **9**: 295-299

15 **Klein D.** Quantification using real-time PCR technology: applications and limitations. *Trends Mol Med* 2002; **8:** 257-260

16 **Werle B,** Cinquin K, Marcellin P, Pol S, Maynard M, Trepo C, Zoulim F. Evolution of hepatitis B viral load and viral genome sequence during adefovir dipivoxil therapy. *J Viral Hepat* 2004; **11:** 74-83

17 **Kohmoto M,** Enomoto M, Yano Y, Otani S, Minamitani S, Tamori A, Habu D, Takeda T, Shiomi S, Seki S, Arakawa T, Nishiguchi S. Detection of serum hepatitis B virus DNA by real-time quantitative polymerase chain reaction (TaqMan PCR) during lamivudine treatment: comparison with three other assays. *Hepatol Res* 2003; **26:** 125-133

18 **Ide T,** Kumashiro R, Koga Y, Tanaka E, Hino T, Hisamochi A, Murashima S, Ogata K, Tanaka K, Kuwahara R, Sata M. A real-time quantitative polymerase chain reaction method for hepatitis B virus in patients with chronic hepatitis B treated with lamivudine. *Am J Gastroenterol* 2003; **98:** 2048-2051

19 **Wieland SF,** Spangenberg HC, Thimme R, Purcell RH, Chisari FV. Expansion and contraction of the hepatitis B virus transcriptional template in infected chimpanzees. *Proc Natl Acad Sci U S A* 2004; **101:** 2129-2134

20 **Natsoulis G,** Boeke JD. New antiviral strategy using capsid-nuclease fusion proteins. *Nature* 1991; **352:** 632-635

Edited by Zhang JZ and Wang XL **Proofread by** Xu FM

PO Box 2345, Beijing 100023, China
Fax: +86-10-85381893
E-mail: wjg@wjgnet.com www.wjgnet.com

World J Gastroenterol 2004;10(19):2886-2889
World Journal of Gastroenterology
Copyright © 2004 by The WJG Press ISSN 1007-9327

• BRIEF REPORTS •

Expression of survivin and its significance in colorectal cancer

Wei-Chang Chen, Qiang Liu, Jian-Xin Fu, Su-Ya Kang

Wei-Chang Chen, Qiang Liu, Department of Gastroenterology, The First Affiliated Hospital of Suzhou University, Suzhou 215006, Jiangsu Province, China
Jian-Xin Fu, Jiangsu Institute of Hematology, The First Affiliated Hospital of Suzhou University, Suzhou 215006, Jiangsu Province, China
Su-Ya Kang, Department of Pathology, The First Affiliated Hospital of Suzhou University, Suzhou 215006, Jiangsu Province, China
Supported by 135 Medical Important Talent Foundation of Jiangsu Province, No. 37RC 2002037
Correspondence to: Dr. Wei-Chang Chen, Department of Gastroenterology, The First Affiliated Hospital of Suzhou University, Suzhou 215006, Jiangsu Province, China. cwc-sz@hotmail.com
Telephone: +86-512-65223637 Ext. 8374
Received: 2003-11-21 **Accepted:** 2003-12-22

Abstract

AIM: To study the expression of survivin,a novel member of inhibitors of apoptosis protein (IAP) and its significance in colorectal carcinoma.

METHODS: Survivin mRNA expression was evaluated by semi-quantitative reverse transcriptase polymerase chain reaction (RT-PCR) in 52 colorectal carcinoma samples and 48 adjacent normal colorectal tissue samples. PCR product was sequenced to verify the desired result. Expressions of survivin protein, proliferating cell nuclear antigen labelling index (PI) and apoptotic index (AI) were detected immunohistochemically in 52 human colorectal carcinomas.

RESULTS: The expression of survivin mRNA was detected in a significantly greater proportion of colorectal carcinoma samples than in adjacent normal colorectal tissues (67.3% *vs* 25%; $P<0.01$). There was no relationship between survivin mRNA expression in colorectal carcinomas and sex, tumor size, histological types, lymphnode metastasis, distant metastasis and Dukes' stage. The PCR product shared 99% of homology with human counterparts. Survivin expression was observed immunohistochemically in 27 of 52 cases of colorectal carcinoma (51.9%). The AI was significently lower in survivin positive group than in survivin negative group (0.67±0.18% *vs* 1.14±0.42%; $P<0.001$), while the PI was greater in survivin positive group than in survivin negative group (51±22% *vs* 27±18%, $P<0.001$).

CONCLUSION: Survivin is a special tumor marker independent of histopathological characteristics. It may play an important role during human colorectal tumorigenesis by inhibiting apoptosis and accelerating proliferative activity of colorectal tumor cells.

Chen WC, Liu Q, Fu JX, Kang SY. Expression of survivin and its significance in colorectal cancer. *World J Gastroenterol* 2004; 10(19): 2886-2889
http://www.wjgnet.com/1007-9327/10/2886.asp

INTRODUCTION

Apoptosis is an evolutionally conserved genetic program of cellular suicide and also central to the homeostasis of adult tissues by maintaining the balance between cell production and cell elimination. There is compelling evidence that defects in apoptosis contribute to human diseases such as malignancies. In the evolution of colorectal cancer (CRC) the imbalance between cell proliferation and cell apoptosis may be an important potential factor. A large number of evidences show that many molecules such as p53 and bcl-2 are involved in the regulation of apoptosis during colorectal tumorigenesis. The inhibitor of apoptosis proteins(IAPs), which are widely expressed in all kinds of malignacies, is encoded by the highly-conservative anti-apoptosis gene family and plays an important role in the regulation of apoptosis. IAP molecules contain 1-3 copies of a -70 amino acid zinc-finger fold, and designate the baculovirus IAP repeat (BIR) and their mechanism of action has been directly attributed to the binding of Caspases,thus preventing enzyme activity of the Caspases[1,2]. Among molecules of the IAP family, survivin, a novel anti-apoptosis gene is prominently expressed in CRC and several other malignancies[3,13-18]. The role of survivin in blocking apoptosis is unclear and its ability to inhibit Caspase-3 activity has been widely debated[3-5]. Survivin may paly an important role in the development of CRC. The present study was to examine the expression of survivin in CRC and to evaluate the association between expression of survivin and clinicopathological characteristics of patients with CRC. We also investigated the significence of survivin expression in CRC.

MATERIALS AND METHODS

Patients

Specimens used for this study were obtained from 52 carcinomas and 48 adjacent normal tissures from the resection margins at the First Affiliated Hospital of Suzhou Univercity. The suspected de novo cancers and patients with a known familial colon cancer syndrome history were excluded. All patients had received neither chemotherapy nor radiation therapy before tumor resection. The diagnosis and histopathologic classification were determined according to the General Rules for Pathologic Studies of National CRC Cooperation Group. In CRC patients, there were 31 males and 21 females, and the mean age of the patients was 61.1 years. According to histological differentiation grade, 52 cases of CRC were classified as well, moderately and poorly differentiated subgroups which included 6, 39 and 7 cases respectively. Seven, 19, 17 and 9 cases were staged as Dukes' A, B, C and D respectively. After washed with physiological saline, all cancer tissue samples were cut into two pieces by sterile blade.One piece was fixed with formalin for H&E, the other was frozen in liquid nitrogen immediately after the lesion was resected and stored at -80 ℃ for subsequent assay.

Semi-quantitative RT-PCR

Briefly, total RNAs were extracted from colorectal cancer and normal mucosae, using TRIzol reagent (Life Technologies, Rockville, MD). Prepared RNA (2 μg) was mixed with the random hexamer (100 ng) ,incubated for 5 min at 70 ℃, and then quickly chilled at 4 ℃ for 5 min. RNA samples were reverse-transcriped at 37 ℃ for 60 min into first-strand cDNA in reverse transcription solution [50 mmol/L Tris-HCl (pH8.3), 40 mmol/L KCl, 8 mmol/L

$MgCl_2$, 0.5 mmol/L each dNTP, 225 mg/mL BSA, 5 mmol/L DTT, 25 units of RNasin (Promega, Madison, WI), and 200 units of Mo-MLV reverse transcriptase (Life Sciences, Rockville, MD)] with a total volume of 40 μL. The cDNA samples were incubated at 95 ℃ for 5 min to inactivate the reverse transcriptase and then chilled. The samples were amplified by adding of 50 μL of PCR mixture [50 mmol/L Tris-HCl (pH 8.3), 40 mmol/L KCl, 2 mmol/L $MgCl_2$, 0.2 mmol/L each dNTP, 10 pmoL of each sense and antisense primer, and 1.5 units of Taq polymerase(MBI,)]. Amplification of β_2-microglobulin (β_2-MG) gene was performed 28 cycles, each for 30 s at 94 ℃, for 30 s at 58 ℃, and 60 s at 72 ℃, followed by an extension at 72 ℃ for 7 min. Amplification of survivin gene was performed 32 cycles,each for 45 s at 94 ℃, 45 s at 61 ℃, and for 60 s at 72 ℃, followed by an extension at 72 ℃ for 7 min. The products were electrophoresed on 15 g/L agarose gels and then scanned. Specific primers for survivin gene, targeting a 528-bp fragment, were: 5'-TTGAA TCGCG GGACC CGTTG G-3' (sense) and 5'-CAGAG GCCTC AATCC ATGGC A-3'(antisense). As internal standards, β_2-microglobulin (β_2-MG) gene was used. Primer pairs specific to β_2-MG gene, targeting a 330-bp fragment, were used sense: 5'-CTCGC GCTAC TCTCT CTTTC-3' and antisense: 5'-CATGT CTCGA TCCCA CTTAA-3'.

Sequencing of survivin

The PCR products of survivin were isolated and purified using UNIQ-10 purification kit (MBI) and then ligated with pGEM easy T vector by T4 DNA ligase and transformed *E. coli* JM109. Recombinant vectors were identified through *Eco*RI digestion and agarose gel electrophoresis. Positive plasmids were sequenced by an ABI PRISM 377 DNA sequencer (Perkin-Elmer Company).

Immunohistochemistry

Immunohistochemical staining of survivin was performed by SP method. For PCNA, SABC method was performed. TUNEL assay was used to detect apoptosis. In brief, paraffin sections (4 μm thick) were dewaxed, dehydrated, and then immersed in a 10^{-3}mol/L sodium citrate buffer (pH 6.0). For detection of survivin, antigen retrieval was performed by boiling the sections for 20 min in a pressure cooker. For detection of PNCA, the sections were heated in a microwave oven for 10 min to retrieve the antigens. Endogenous peroxidase was inactivated by incubating the sections with 30 mL/L hydrogen peroxide.Nonspecific reactions were blocked by bovine serum. The sections were incubated with a primary antibody overnight at 4 ℃. The antibody used was an 8E2 monoclonal antibody(Chemcon, USA) at 1:5 dilution. Rinsed with PBS, the sections were incubated for 30 min at 37 ℃ with biotinylated secondary antibody and streptavidin conjugated to horseradish peroxidase, respectively. After three rinse with PBS, the sections were incubated with diaminobenzidine substrate, then rinsed with distilled water and counterstained with hematoxylin. As a negative control, PBS was used instead of the primary antibody. PCNA (Maxim, USA) and TUNEL(Roche, USA) assay were performed according to the manufacturer's instructions.

Scoring criteria

The mean percentage of positive tumor cells for the expression of survivin was determined in at least five areas at 400-fold magnification, and cases with less than 10% positively stained cells were defined as negative. Cases with 10-29% positively stained cells were defined as "+", 30-59% as "++", and 60% or more as "+++".These scorings were performed in a blind fashion.

PI and AI were expressed as the ratio of positively stained tumor cells to all tumor cells. If possible, five areas were randomly selected for counting under 400-fold magnification. Otherwise, the whole section underwent assessment.

Statistical analysis

All results were analyzed by software of SPSS 10.00. $P<0.05$ was considered statistically significant.

RESULTS

Expressions of survivin mRNA in colorectal carcinoma samples and adjacent normal mucosa samples

Fifty two CRC samples and forty eight normal mucosa samples were available for analyses. The expressions of survivvin mRNA were detected in a significantly greater proportion of CRC than in normal mucosa samples (67.3% *vs* 25% $P<0.01$). Survivin mRNA was not detected in normal tissue when the associated cancer was survivin negative (Figure 1).

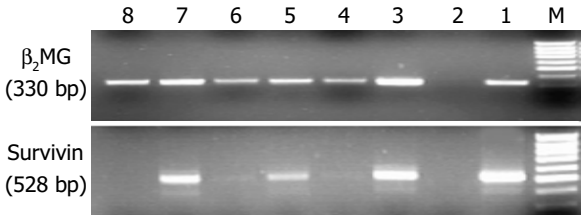

Figure 1 RT-PCR products of paired samples from normal colonic mucosae (lanes 4, 6, 8) and CRC (lanes 3, 5, 7) from three different resection specimens. Lane 1: positive control (U937 cell line) , lane 2: negative control, lane M: DNA mark. Expression of β_2MG confirmed the fidelity of reverse transcription.

Relationship between expressions of survivin mRNA and clinicopathological characteristics of patients with CRC

No relationship was found between survivin mRNA expression in CRC and sex, tumor size, histological types, lymphnode metastasis, distant metastasis and Dukes' stage (Table 1).

Table 1 Correlation between expression of survivin mRNA and clinicopathological characteristics of patients with CRC

Variable	Total No β_2MG	Survivin	*P* Valur
Sex			
Male	31	0.74±0.63	>0.05
Female	21	0.77±0.56	
Tumor size			
⩾5 cm	20	0.71±0.59	>0.05
<5 cm	32	0.78±0.61	
Histological type			
High	7	0.62±0.51	>0.05
Middle	39	0.75±0.59	
Low	6	0.92±0.74	
Lymphnode metastasis			
Positive	22	0.80±0.65	>0.05
Negative	30	0.72±0.57	
Distant metastasis			
Positive	9	0.93±0.18	>0.05
Negative	43	0.72±0.65	
Duke stage			
A	7	0.55±0.57	>0.05
B	19	0.73±0.62	
C	17	0.77±0.73	
D	9	0.93±0.18	

Correlations between expression of survivin, AI and PI

The expression of survivin protein was observed in cytoplasm of malignant tumor cells. Survivin expression was observed immunohistochemically in 27 of 52 cases of colorectal carcinoma (51.9%). To examine whether the expression of survivin correlated with AI and PI, tissure samples obtained from

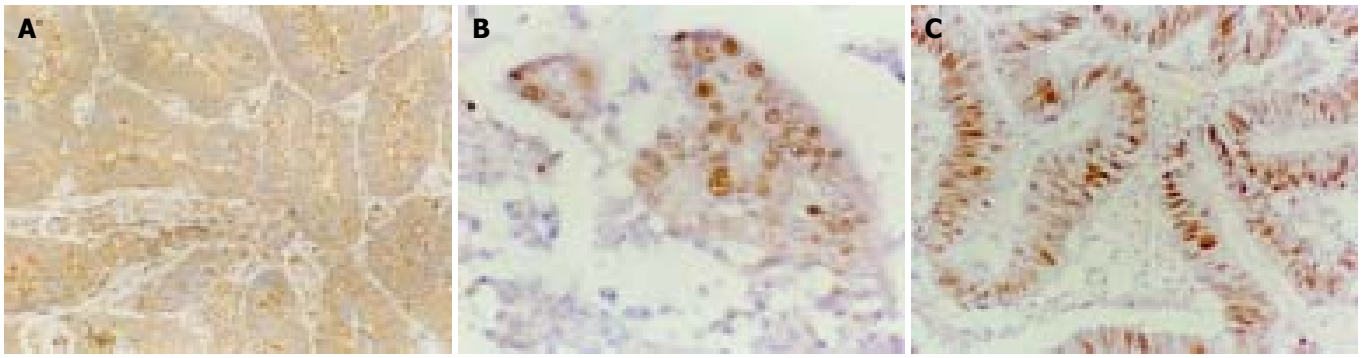

Figure 3 Immunohistochemical analysis of apoptosis,proliferation,and survivin in CRC. Survivin expression was restricted to the cytoplasm of cancer cells (brown staining, ×400 fold). Apoptotic cells and proliferative cells were detected in the nucleoli of cancer cells (brown staining, ×400 fold).

carcinoma were divided into two groups according to the expression of survivin and compared to AI and PI (Figure 2). Survivin positive tumors had significantly lower values for AI than survivin negative tumors (P<0.001), and PI in survivin positive tumors was higher than in survivin negative tumors ($P \leqslant 0.001$, Figure 3).

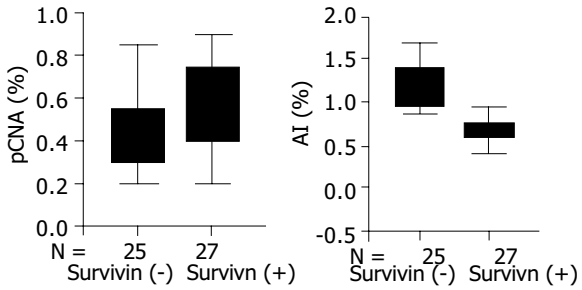

Figure 2 Correlations between survivin expression and AI and PI. P<0.001 as PI in survivin positive tumors (51±22%) compared with survivin negative tumors (27±18%), P<0.001 as AI in survivin positive tumors (0.67±0.18%) compared with survivin negative tumors (1.14±0.42%).

DISCUSSION

Hybridization screening of a human P1genomic library with the cDNA of effector cell protease recepor-1 (EPR-1) yielded a new gene spanning -15 kb containing four exons and three introns, and located to band 17q25 by Ambrosini *et al.* in 1997[6].Survivin is the smallest member of the IAP gene family,structurally characterized by a single BIR module and a -COOH-terminus α-helix coiled domain, substituting a canonical ring finger[6]. Prominently expressed in a variety of apoptosis-regulated organs during embryonic and fatal development[7], survivin is undetectable in most normal adult tissues,and becomes abundantly reexpressed in a variety of human cancers. The PCR based approach used in our study is exqusitely sensitive and may detect gene transcripts even in a single cell or cell cluster with a comparable specificity. The present study showed that expression of survivin mRNA was detected in a significantly greater proportion of CRC samples than in adjacent normal colorectal tissues (67.3% *vs* 25%, P<0.01). The data were consistent with a study by Adida *et al.*[8]. Furthermore, the prevalence of survivin mRNA expression in the present study correlated well with the expression of survivin protein (unpublished data). Recent studies demonstrated that the novel splice variants survivin-△Ex3 and survivin-2B were expressed in malignancies[9,10]. Survivin-△Ex3, which lacks exon 3, exhibited a pronounced anti-apoptotic activity, whereas survivin-2B containing a part of intron 2 as an additional cryptic exon, largely lost its anti-apoptotic activity. These alternative splice variants have not been explored so far. In gastric carcinomas, Mahotka *et al.*[10] showed that survivin-2B might act as a naturally occurring antagonist of survivin and might play a role in tumor progression. We found that CRC also expressed survivin-△Ex3, survivin-2B and survivin. The latter was a dominant transcrip (Figure 1), and shared 99% of homology with human counterparts by sequencing.

The expression of survivin mRNA was independent of clinical pathological characteristics. The result was consistent with previous studies[8,11]. However, in endometrial carcinoma, survivin expression correlated with clinical stage, histological grade, invasive behavior and survival rate[12]. The expression of survivin has been proved as a prognostic mark in non-small cell lung cancer[13], breast carcinoma[14], oesophageal carcinoma[15] and hepatocellular carcinoma[16]. In CRC, Adida *et al.*[8] reported that the predictive value of survivin expression was limited to patients with stage II CRC, those with survivin negative tumors had a five year survival rate of 94.4% compared with 44.8% for patients with survivin positive tumors. Recent studies showed the phenomena of chemo-radioresistance were prevalent in survivin positive tumors and molecular manipulation of survivin expression might enhance chemotherapy and radiation therapy[17-22]. These findings indicate that survivin may play an important role in chemoresistance of cancer cells. However, the clinical importance of survivin expression remains unclear in patients with cancer.

We found that survivin positive tumors had significantly lower values for AI than survivin negative tumors, and PI was higher in survivin positive tumors than in survivin negative tumors (P<0.001 for both). These findings indicate that the overexpression of survivin not only inhibits cell death but also reflects the presence of a greater number of proliferating cells. By inhibiting apoptosis and promoting proliferation, survivin plays an important role in colorectal tumorigenesis.

There has been a considerable interest in survivin biomedical researches. The exploitation of survivin might provide important predictive and prognostic clues in diagnosis, and offer new therapeutic alternatives for cancer. Further studies are required to identify the potential role and mechanism of survivin in the development of CRC.

REFERENCES

1 **Miller LK**. An exegesis of IAPs: salvation and surprises from BIR motifs. *Trends Cell Biol* 1999; **9**: 323–328

2 **Altieri DC**. The molecular basis and potential role of survivin in cancer diagnosis and therapy. *Trends Mol Med* 2001; **7**: 542-547

3 **Zhu XD,** Lin GJ, Qian LP, Chen ZQ. Expression of survivin in human gastric carcinoma and gastric carcinoma model of rats.

World J Gastroenterol 2003; **9**: 1435-1438
4 **Kasof GM,** Gomes BC. Livin, a novel inhibitor of apoptosis protein family member. *J Biol Chem* 2001; **276**: 3238-3246
5 **Shin S,** Sung BJ, Cho YS, Kim HJ, Ha NC, Hwang JI, Chung CW, Jung YK, Oh BH. An anti-apoptotic protein human survivin is a direct inhibitor of caspase-3 and –7. *Biochemistry* 2001; **40**: 1117-1123
6 **Shankar SL,** Mani S, O'Guin KN, Kandimalla ER, Agrawal S, Shafit-Zagardo B. Survivin inhibition induces human neural tumor cell death through caspase-independent and -dependent pathways. *J Neurochem* 2001; **79**: 426-436
7 **Ambrosini G,** Adida C, Altieri DC. A novel anti-apoptosis gene, survivin, expressed in cancer and lymphoma. *Nat Med* 1997; **3**: 917-921
8 **Adida C,** Crotty PL, McGrath J, Berrebi D, Diebold J, Altieri DC. Developmentally regulated expression of the novel cancer anti-apoptosis gene survivin in human and mouse differentiation. *Am J Pathol* 1998; **152**: 43-49
9 **Sarela AI,** Macadam RC, Farmery SM, Markham AF, Guillou PJ. Expression of the antiapoptosis gene, survivin, predicts death from recurrent colorectal carcinoma. *Gut* 2000; **46**: 645-650
10 **Mahotka C,** Wenzel M, Springer E, Gabbert HE, Gerharz CD. Survivin-△Ex3 and survivin-2B: two novel splice variants of the apoptosis inhibitor survivin with different antiapoptotic properties. *Cancer Res* 1999; **59**: 6097-6102
11 **Krieg A,** Mahotka C, Krieg T, Grabsch H, Muller W, Takeno S, Suschek CV, Heydthausen M, Gabbert HE, Gerharz CD. Expression of different survivin variants in gastric carcinomas: first clues to a role of survivin-2B in tumour progression. *Br J Cancer* 2002; **86**: 737-743
12 **Lin LJ,** Zheng CQ, Jin Y, Ma Y, Jiang WG, Ma T. Expression of survivin protein in human colorectal carcinogenesis. *World J Gastroenterol* 2003; **9**: 974-977
13 **Takai N,** Miyazaki T, Nishida M, Nasu K, Miyakawa I. Survivin expression correlates with clinical stage, histological grade, invasive behavior and survival rate in endometrial carcinoma. *Cancer Lett* 2002; **184**: 105-116
14 **Monzo M,** Rosell R, Felip E, Astudillo J, Sanchez JJ, Maestre J, Martin C, Font A, Barnadas A, Abad A. A novel anti-apoptosis gene: Re-expression of survivin messenger RNA as a prognosis marker in non-small- cell lung cancers. *J Clin Oncol* 1999; **17**: 2100-2104
15 **Tanaka K,** Iwamoto S, Gon G, Nohara T, Iwamoto M, Tanigawa N. Expression of survivin and its relationship to loss of apoptosis in breast carcinomas. *Clin Cancer Res* 2000; **6**: 127-134
16 **Ikeguchi M,** Kaibara N. survivin messenger RNA expression is a good prognostic biomarker for oesophageal carcinoma. *Br J Cancer* 2002; **87**: 883-887
17 **Ikeguchi M,** Hirooka Y, Kaibara N. Quantitative analysis of apoptosis-related gene expression in hepatocellular carcinoma. *Cancer* 2002; **95**: 1938-1945
18 **Asanuma K,** Moriai R, Yajima T, Yagihashi A, Yamada M, Kobayashi D, Watanabe N. Survivin as a radioresistance factor in pancreatic cancer. *Jpn J Cancer Res* 2000; **91**: 1204-1209
19 **Ikeguchi M,** Liu J, Kaibara N. Expression of survivin mRNA and protein in gastric cancer cell line (MKN-45) during cisplatin treatment. *Apoptosis* 2002; **7**: 23-29
20 **Kato J,** Kuwabara Y, Mitani M, Shinoda N, Sato A, Toyama T, Mitsui A, Nishiwaki T, Moriyama S, Kudo J, Fujii Y. Expression of survivin in esophageal cancer: correlation with the prognosis and response to chemotherapy. *Int J Cancer* 2001; **95**: 92-95
21 **Ambrosini G,** Adida C, Sirugo G, Altieri DC. Induction of apoptosis and inhibition of cell proliferation by survivin gene targeting. *J Biol Chem* 1998; **273**: 11177-11182
22 **O'Connor DS,** Grossman D, Plescia J, Li F, Zhang H, Villa A, Tognin S, Marchisio PC, Altieri DC. Regulation of apoptosis at cell division by p34cdc 2 phosphorylation of survivin. *Proc Natl Acad Sci U S A* 2000; **97**: 13103-13107

Edited by Wang XL and Xu FM

PO Box 2345, Beijing 100023, China
Fax: +86-10-85381893
E-mail: wjg@wjgnet.com www.wjgnet.com

World J Gastroenterol 2004;10(19):2890-2893
World Journal of Gastroenterology
Copyright © 2004 by The WJG Press ISSN 1007-9327

• BRIEF REPORTS •

Expression of toll-like receptor 4 and MD-2 gene and protein in Kupffer cells after ischemia-reperfusion in rat liver graft

Yong Peng, Jian-Ping Gong, Chang-An Liu, Xu-Hong Li, Ling Gan, Shou-Bai Li

Yong Peng, Jian-Ping Gong, Chang-An Liu, Xu-Hong Li, Ling Gan, Shou-Bai Li, Department of Hepatobiliary Surgery, the Second Affiliated Hospital of Chongqing Medical University, Chongqing 400010, China
Supported by the National Natural Science Foundation of China, No. 30300337, 30200278, 30170919
Correspondence to: Dr. Jian-Ping Gong, Department of Hepatobiliary Surgery, the Second Affiliated Hospital of Chongqing Medical University, 74 Linjiang Road, Chongqing 400010, China. gongjianping11@hotmail.com
Telephone: +86-23-63766701 **Fax:** +86-23-63829191
Received: 2004-03-11 **Accepted:** 2004-04-13

Abstract

AIM: To investigate the expression of toll-like receptor 4 (TLR4) and MD-2 gene and protein in Kupffer cells (KCs) and their role in ischemia-reperfusion (IR) injury of rat liver graft.

METHODS: KCs were isolated at 0 (control group), 2, 12, 24 h (IR group) following IR in rat liver graft. mRNA expression of TLR4 and MD-2 was detected by RT-PCR analysis, protein expression of TLR4/MD-2 was detected by flow cytometric (FCM) analysis, and tumor necrosis factor-α (TNF-α) level in supernatant was measured by ELISA. Then isolated KCs were incubated with anti-TLR4 polyclonal antibody (anti-TLR4 group), and TNF-α level was measured again.

RESULTS: The mRNA and protein expression of TLR4/MD-2 and the level of TNF-α in IR group increased significantly at 2 h following IR, and reached the maximum at 12 h, and slightly decreased at 24 h, but were still significantly higher than those in the control group ($P<0.01$). The expression of these factors was markedly decreased after anti-TLR4 antibody treatment as compared with the IR group ($P<0.01$).

CONCLUSION: Lipopolysaccharide (LPS) following IR can up-regulate TLR4/MD-2 gene and protein expression in KCs, and synthesize cytokine TNF-α. Anti TLR4 antibody can inhibit the production of TNF-α induced by LPS. TLR4 and its partner molecule MD-2 may play an important role in Kupffer cell activation and IR injury.

Peng Y, Gong JP, Liu CA, Li XH, Gan L, Li SB. Expression of toll-like receptor 4 and MD-2 gene and protein in Kupffer cells after ischemia-reperfusion in rat liver graft. *World J Gastroenterol* 2004; 10(19): 2890-2893
http://www.wjgnet.com/1007-9327/10/2890.asp

INTRODUCTION

Toll-like receptor 4 (TLR4) is a transmembrane protein, mainly existed in monocytes/macrophages[1-3]. It plays an important role in recognizing endotoxin (lipopolysaccharide, LPS) or LPS-CD14 complex, and mediating monocyte/macrophage activation and pro-inflammatory cytokine release[2,4,5]. MD-2 molecule is a secreting protein, linking with the exocytic area of TLR4, and facilitating the binding of TLR4 and LPS to enhance cell activation induced by LPS[6-10]. Kupffer cells (KCs) are not only the biggest residing macrophages in the body, but also are the main participant of ischemia-reperfusion injury (IRI) in liver transplantation[11-14]. Therefore, studying the expression of TLR4 and MD-2 gene and protein in KCs following IR is very important to clarify the source of cytokines involved in IRI. The aim of the current study was to investigate the expression of TLR4 and MD-2 gene and protein, and the production of cytokines in liver graft by isolating and culturing KCs following IRI, and to probe the role of TLR4 and MD-2 in IRI injury.

MATERIALS AND METHODS

Establishment of animal model of IRI following liver transplant in rat

Male Wistar rats weighing 210-250 g, supplied by Chongqing Medical University, were used as donors and recipients. Orthotopic liver transplantation was performed with improved two-cuff technique introduced by Peng *et al*.[15] as following: (1) Graft procurement: portal vein (PV), hepatic artery (HA), infrahepatic vena cava (IHVC), and bile duct were divided. Then the graft was infused and harvested for preparation. PV and IHVC were prepared by cuff technique, and a drainage Teflon catheter was inserted into the bile duct. (2) Implantation of graft: the graft was placed orthotopically in the recipient's abdominal cavity after the original liver was removed. The suprahepatic vena cava was sutured end to end, and the portal vein was anastomosed by cuff method, then the liver was perfused. After the anastomosis of IHVA and HA was completed, the bile duct was reestablished end to end by Teflon catheter.

KC isolation and culture

KCs were isolated at 0, 2, 12, 24 h following IR with *in situ* collagenase perfusion technique described by Gong *et al*.[16]. In brief, the liver was removed with portal vein perfusion with Hank's balance salt solution (HBSS) and digested in a solution of 0.5 g/L collagenase (type IV, Sigma, USA). The digest was washed thoroughly and plated on plastic dishes in RPMI medium containing 100 mL/L fetal calf serum (FCS). After 6 h incubation at 37 ℃ in humidified atmosphere containing 50 mL/L CO_2 in air, the nonadherent cells were removed by pipet. The adherent cells were collected with a rubber policeman. KC purity exceeded 90% as assessed by light microscopy, and viability was greater than 95% as determined by trypan blue exclusion assay. The KCs at 0 h were regarded as control group, and those at 2, 12 and 24 h were as IR group.

RNA isolation and complementary DNA synthesis

Total RNA was isolated from rat KCs using the TRIZOL reagent (Life Technologies, USA). The quality of RNA was controlled by the intactness of ribosomal RNA bands. A total of 5 μg of each intact total RNA sample was reverse-transcribed to complementary DNA (cDNA) using AMV reverse transcriptase (Roche, USA).

Determination of TLR4 and MD-2 mRNA by RT-PCR

The PCR primers used are shown in Table 1. The conditions for

amplification were as follows: denaturation at 94 ℃ for 1 min, annealing at 58 ℃ for 1 min, and extension at 72 ℃ for 1 min for 30 cycles, and extension at 72 ℃ for 7 min again. The PCR products were electrophoresed on 20 g/L agarose gels containing ethidium bromide, and video photographed on an ultraviolet transilluminator, and the results were shown as the ratio of relative absorbance of TLR4 or MD-2/β-actin analyzed with Quantity one 4.1.0 software.

Table 1 Primer used for PCR amplification of TLR4 and MD-2 gene

	Primer sequence	Size (bp)
TLR4	5' TGGATACGTTTCCTTATAAG 3'	311
	5' GAAATGGAGGCACCCCTTC3'	
MD-2	5'ATGGTCTTCCTGGCGAGTTT3'	332
	5'CCATGGCACAGAACTTCCTT3'	
β-actin	5'ATCATGTTTGAGACCTTCAACA 3'	300
	5'CATCTCTTGCTCGAAGTCCA 3'	

Flow cytometric analysis

Expression of TLR4 and MD-2 membrane protein in KCs was determined by flow cytometric analysis. In brief, KCs were incubated with rabbit anti-rat TLR4 polyclonal antibody (1 μg/mL) labeled with FITC and goat anti-rat MD-2 polyclonal antibody (1 μg/mL) labeled with PE (Sigma, USA). After washed three times, 10 000 cells were analyzed by flow cytometry (Coulter, USA), and the percentage and mean fluorescence intensity (MFI) of TLR4 and MD-2-positive cells were taken as the indexes.

TNF-α level in supernatant

Supernatants were collected to measure the levels of TNF-α with ELISA kit (Jingmei Biotechnology Company, China) following the manufacturer's instructions.

Blocking test of anti-TLR4 antibody

To determinate the role of TLR4 and MD-2 in LPS-induced KC activation, KCs were harvested and adjusted to the concentration of 1×10^6/(mL·well). Then, 0.2 mL of anti-TLR4 antibody (1: 100) was added to the medium, and incubated for 30 min at 37 ℃. The supernatants were collected again for measuring the levels of TNF-α by ELISA analysis following the manufacturer's instructions.

Statistical analysis

All results were expressed as mean±SD. Statistical difference between means was determined by Student's *t* test using SigmaPlot 2000 software (SPSS Inc., USA). A *P* value <0.01 was considered statistically significant.

RESULTS

Expression of TLR4 and MD-2 mRNA in KCs

RT-PCR analysis showed that KCs from control group had low but detectable levels of TLR4 and MD-2 mRNA. The mRNA level was significantly increased with time, reaching its maximum of nine-fold at 12 h following IR, and slightly declined 24 h after IR, but was still significantly higher than that in the control group (P<0.01) (Figure 1).

Binding of FITC, PE to KCs

To confirm the expression of TLR4 and MD-2 membrane protein on KCs, we examined the binding of FITC/PE to the cells. TLR4 and MD-2 positive cells were 7.94% and 6.51% in control group. But in the rats with IR, the mean fluorescence intensity (MFI) was significantly increased, and TLR4 positive cells were 45.71%, 78.46%, and 61.72% and PE positive cells were 38.64%, 74.15%, and 58.47%, respectively, at 2 h, 12 h and 24 h following IR, which were significantly higher compared with the control group (P<0.01) (Figure 2).

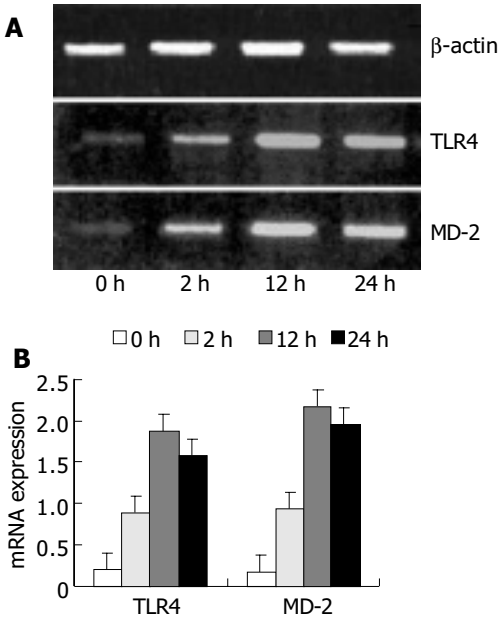

Figure 1 Expression of TLR4 and MD-2 mRNA by RT-PCR analysis. A: PCR products were electrophoresed on agarose gels and photographed. B: Quantitative data of mRNA levels were shown as the ratio of relative absorbance and expressed as mean±SD. Expression of TLR4 and MD-2 mRNA were significantly increased in the IR group compared with the control group (P<0.01).

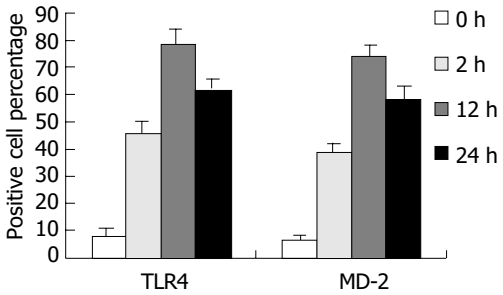

Figure 2 Percentage of TLR4 and MD-2 positive cells. The percentage of TLR4 and MD-2 positive cells was significantly increased after IR compared with the control group.

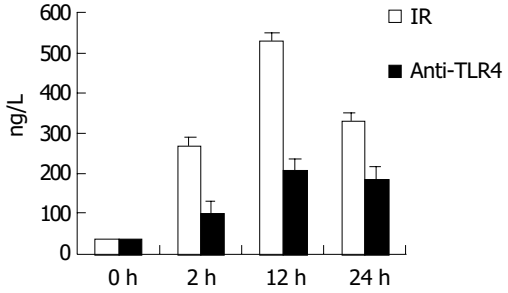

Figure 3 Comparison of TNF-α production in supernatant of KCs. In IR group, the TNF-α level in supernatant was increased with time, and reached the maximum (529.1±30.9 ng/mL) at 12 h. But in anti-TLR4 group, the production of TNF-α was obviously inhibited by Ab against TLR4 compared with the IR group (P<0.01).

Decrease of TNF-α levels after anti-TLR4 treatment

In IR group, the level of TNF-α in supernatant of KCs was 267.4±24.1, 529.1±30.9, and 329.7±24.6 ng/mL at 2, 12 and 24 h after IR, respectively. In group of anti-TLR4 antibody blockade, the production of TNF-α in supernatant was obviously inhibited by Ab against TLR4 when compared with that in IR group ($P<0.01$), and it was 102.5±10.4, 207.6±18.4, and 185.3±12.7 ng/mL at 2, 12 and 24 h after IR, respectively (Figure 3).

DISCUSSION

Toll protein is a transmembrane protein which mainly acts as a necessary tool for immune defence to microorganism[6,17-20]. The first toll-like protein in human cells was reported by Janeway, and named toll-like receptor (TLR)[3,21]. About ten members of TLR superfamily in mammals have been reported in recent years. Among them, TLR4 plays a key role in LPS signal transduction[4,22,23].

When LPS enters blood, it first binds to LBP (LPS binding protein), forming a LPS-LBP compound, and then binds to TLR4 on cell membranes leading to activation of cells[18,24,25]. Recent studies have confirmed that the activation of cells induced by LPS needs another important molecule, namely MD-2. MD-2 is a key regulator protein, which could promote LPS signal transduction through connecting with TLR4 on cell membranes and forming the TLR4/MD-2 compound[26-28].

Kupffer cells are special macrophages residing in hepatic sinusoids, which constitute 80% to 90% of total fixed macrophages in the body[13,29]. Because of their special location, KCs act as an important defensive barrier for gut-derived endotoxemia. A large amount of endotoxins contact with KCs through portal circulation following ischemia- reperfusion after liver transplantation, and activate the KCs[30,31]. Thus, it is very important to study the expression of TLR4 and MD-2 in KCs to clarify the origin of cytokines and the mechanism of IRI.

In our study, we found there were weak expressions of TLR4 and MD-2 gene and protein in resting KCs, which might play a critical role in maintaining the normal function of KCs, and might be essential for keeping KCs to be ready for activation after stress. But after IR, a large mount of LPS entered liver sinusoids, activated KCs, resulting in increased release of harmful cytokines such as TNF-α, which reached the maximum at 12 h after IR. To correctly illuminate the relation between TLR4 and MD-2 and downstream cytokines, we used anti-TLR4 antibody to inhibit the binding function of TLR4, and found that the production of TNF-α was greatly decreased, suggesting that the expression of TLR4 and MD-2 protein is indispensable to the secretion of downstream cytokines.

In summary, the present data suggest that there are weak expressions of TLR4 and MD-2 mRNA and protein in Kupffer cells. Expressions of TLR4 and MD-2 can significantly increase following ischemia-reperfusion in rat liver transplantation. LPS can induce activation of KCs by combining with TLR4 and MD-2, and subsequently release harmful cytokines, which ultimately attack the graft. Further studies are needed for elucidating TLR4/MD-2-mediated signal transduction pathways which lead to the secretion of cytokines during IRI on liver graft.

ACKNOWLEDGEMENT

This work was supported by the Key Laboratory of Hepatobiliary Surgery Department of Chongqing Medical University.

REFERENCES

1 **Latz E,** Visintin A, Lien E, Fitzgerald KA, Espevik T, Golenbock DT. The LPS receptor generates inflammatory signals from the cell surface. *J Endotoxin Res* 2003; **9:** 375-380

2 **Espevik T,** Latz E, Lien E, Monks B, Golenbock DT. Cell distributions and functions of Toll-like receptor 4 studied by fluorescent gene constructs. *Scand J Infect Dis* 2003; **35:** 660-664

3 **Kimoto M,** Nagasawa K, Miyake K. Role of TLR4/MD-2 and RP105/MD-1 in innate recognition of lipopolysaccharide. *Scand J Infect Dis* 2003; **35**: 568-572

4 **Harada K,** Ohira S, Isse K, Ozaki S, Zen Y, Sato Y, Nakanuma Y. Lipopolysaccharide activates nuclear factor-kappaB through toll-like receptors and related molecules in cultured biliary epithelial cells. *Lab Invest* 2003; **83:** 1657-1667

5 **Fujihara M,** Muroi M, Tanamoto K, Suzuki T, Azuma H, Ikeda H. Molecular mechanisms of macrophage activation and deactivation by lipopolysaccharide: roles of the receptor complex. *Pharmacol Ther* 2003; **100:** 171-194

6 **Re F,** Strominger JL. Separate functional domains of human MD-2 mediate Toll-like receptor 4-binding and lipopolysaccharide responsiveness. *J Immunol* 2003; **171:** 5272-5276

7 **Guillot L,** Medjane S, Le-Barillec K, Balloy V, Danel C, Chignard M, Si-Tahar M. Response of human pulmonary epithelial cells to lipopolysaccharide involves Toll-like receptor 4 (TLR4)-dependent signaling pathways: evidence for an intracellular compartmentalization of TLR4. *J Biol Chem* 2004; **279:** 2712-2718

8 **Asai Y,** Hashimoto M, Ogawa T. Treponemal glycoconjugate inhibits Toll-like receptor ligand-induced cell activation by blocking LPS-binding protein and CD14 functions. *Eur J Immunol* 2003; **33:** 3196-3204

9 **Totemeyer S,** Foster N, Kaiser P, Maskell DJ, Bryant CE. Toll-like receptor expression in C3H/HeN and C3H/HeJ mice during Salmonella enterica serovar Typhimurium infection. *Infect Immun* 2003; **71:** 6653-6657

10 **Akashi S,** Saitoh S, Wakabayashi Y, Kikuchi T, Takamura N, Nagai Y, Kusumoto Y, Fukase K, Kusumoto S, Adachi Y, Kosugi A, Miyake K. Lipopolysaccharide interaction with cell surface Toll-like receptor 4-MD-2: higher affinity than that with MD-2 or CD14. *J Exp Med* 2003; **198:** 1035-1042

11 **Schauer RJ,** Gerbes AL, Vonier D, Meissner H, Michl P, Leiderer R, Schildberg FW, Messmer K, Bilzer M. Glutathione protects the rat liver against reperfusion injury after prolonged warm ischemia. *Ann Surg* 2004; **239:** 220-231

12 **Cavalieri B,** Perrelli MG, Aragno M, Ramadori P, Poli G, Cutrin JC. Ischaemic preconditioning modulates the activity of Kupffer cells during *in vivo* reperfusion injury of rat liver. *Cell Biochem Funct* 2003; **21**: 299-305

13 **Carini R,** Albano E. Recent insights on the mechanisms of liver preconditioning. *Gastroenterology* 2003; **125:** 1480-1491

14 **Giakoustidis DE,** Iliadis S, Tsantilas D, Papageorgiou G, Kontos N, Kostopoulou E, Botsoglou NA, Gerasimidis T, Dimitriadou A. Blockade of Kupffer cells by gadolinium chloride reduces lipid peroxidation and protects liver from ischemia/reperfusion injury. *Hepatogastroenterology* 2003; **50:** 1587-1592

15 **Peng Y,** Gong JP, Yan LN, Li SB, Li XH. Improved two-cuff technique for orthotopic liver transplantation in rat. *Hepatobiliary Pancreat Dis Int* 2004; **3:** 33-37

16 **Gong JP,** Wu CX, Liu CA, Li SW, Shi YJ, Yang K, Li Y, Li XH. Intestinal damage mediated by Kupffer cells in rats with endotoxemia. *World J Gastroenterol* 2002; **8:** 923-927

17 **Visintin A,** Latz E, Monks BG, Espevik T, Golenbock DT. Lysines 128 and 132 enable lipopolysaccharide binding to MD-2, leading to Toll-like receptor-4 aggregation and signal transduction. *J Biol Chem* 2003; **278:** 48313-48320

18 **Tamai R,** Asai Y, Hashimoto M, Fukase K, Kusumoto S, Ishida H, Kiso M, Ogawa T. Cell activation by monosaccharide lipid A analogues utilizing Toll-like receptor 4. *Immunology* 2003; **110**: 66-72

19 **Uehori J,** Matsumoto M, Tsuji S, Akazawa T, Takeuchi O, Akira S, Kawata T, Azuma I, Toyoshima K, Seya T. Simultaneous blocking of human Toll-like receptors 2 and 4 suppresses myeloid dendritic cell activation induced by Mycobacterium bovis bacillus Calmette-Guerin peptidoglycan. *Infect Immun* 2003; **71:** 4238-4249

20 **Vives-Pi M,** Somoza N, Fernandez-Alvarez J, Vargas F, Caro P, Alba A, Gomis R, Labeta MO, Pujol-Borrell R. Evidence of expression of endotoxin receptors CD14, toll-like receptors TLR4 and TLR2 and associated molecule MD-2 and of sensitivity to

endotoxin (LPS) in islet beta cells. *Clin Exp Immunol* 2003; **133:** 208-218

21 **Tamai R,** Sugawara S, Takeuchi O, Akira S, Takada H. Synergistic effects of lipopolysaccharide and interferon-gamma in inducing interleukin-8 production in human monocytic THP-1 cells is accompanied by up-regulation of CD14, Toll-like receptor 4, MD-2 and MyD88 expression. *J Endotoxin Res* 2003; **9:** 145-153

22 **Suzuki M,** Hisamatsu T, Podolsky DK. Gamma interferon augments the intracellular pathway for lipopolysaccharide (LPS) recognition in human intestinal epithelial cells through coordinated up-regulation of LPS uptake and expression of the intracellular Toll-like receptor 4-MD-2 complex. *Infect Immun* 2003; **71:** 3503-3511

23 **Thompson PA,** Tobias PS, Viriyakosol S, Kirkland TN, Kitchens RL. Lipopolysaccharide (LPS)-binding protein inhibits responses to cell-bound LPS. *J Biol Chem* 2003; **278:** 28367-28371

24 **Ohnishi T,** Muroi M, Tanamoto K. MD-2 is necessary for the toll-like receptor 4 protein to undergo glycosylation essential for its translocation to the cell surface. *Clin Diagn Lab Immunol* 2003; **10:** 405-410

25 **Miyake K,** Nagai Y, Akashi S, Nagafuku M, Ogata M, Kosugi A. Essential role of MD-2 in B-cell responses to lipopolysaccharide and Toll-like receptor 4 distribution. *J Endotoxin Res* 2002; **8:** 449-452

26 **Medvedev AE,** Vogel SN. Overexpression of CD14, TLR4, and MD-2 in HEK 293T cells does not prevent induction of *in vitro* endotoxin tolerance. *J Endotoxin Res* 2003; **9:** 60-64

27 **Okamoto M,** Sato M. Toll-like receptor signaling in anti-cancer immunity. *J Med Invest* 2003; **50:** 9-24

28 **Schroder NW,** Morath S, Alexander C, Hamann L, Hartung T, Zahringer U, Gobel UB, Weber JR, Schumann RR. Lipoteichoic acid (LTA) of Streptococcus pneumoniae and Staphylococcus aureus activates immune cells via Toll-like receptor (TLR)-2, lipopolysaccharide-binding protein (LBP), and CD14, whereas TLR-4 and MD-2 are not involved. *J Biol Chem* 2003; **278:** 15587-15594

29 **Zhu X,** Qiu Y, Shi M, Ding Y. Matrine protects sinusoidal endothelial cells from cold ischemia and reperfusion injury in rat orthotopic liver transplantation. *Ann Clin Lab Sci* 2003; **33:** 216-225

30 **Kojima Y,** Suzuki S, Tsuchiya Y, Konno H, Baba S, Nakamura S. Regulation of pro-inflammatory and anti-inflammatory cytokine responses by Kupffer cells in endotoxin-enhanced reperfusion injury after total hepatic ischemia. *Transpl Int* 2003; **16:** 231-240

31 **Kiemer AK,** Gerwig T, Gerbes AL, Meissner H, Bilzer M, Vollmar AM. Kupffer-cell specific induction of heme oxygenase 1 (hsp32) by the atrial natriuretic peptide-role of cGMP. *J Hepatol* 2003; **38:** 490-498

Edited by Kumar M and Wang XL **Proofread by** Xu FM

PO Box 2345, Beijing 100023, China
Fax: +86-10-85381893
E-mail: wjg@wjgnet.com www.wjgnet.com

World J Gastroenterol 2004;10(19):2894-2897
World Journal of Gastroenterology
Copyright © 2004 by The WJG Press ISSN 1007-9327

• BRIEF REPORTS •

Protective effects of recombinant human growth hormone on cirrhotic rats

Shuang Chen, Hong-Tao Wang, Bin Yang, Yu-Ru Fu, Qing-Jia Ou

Shuang Chen, Hong-Tao Wang, Bin Yang, Qing-Jia Ou, Department of General Surgery, Sun Yat-Sen Memorial Hospital, the Second Affiliated Hospital, Sun Yat-Sen University, Guangzhou 510120, Guangdong Province, China
Yu-Ru Fu, Medical Research Center, Sun Yat-Sen Memorial Hospital, the Second Affiliated Hospital, Sun Yat-Sen University, Guangzhou 510120, Guangdong Province, China
Supported by the Natural Science Foundation of Guangdong Province, No. 984213 and Academic Foundation of Sun Yat -Sen University and Ministry of Public Health for Project 211, No. F000099075
Correspondence to: Dr. Shuang Chen, M.D., Ph.D., Department of General Surgery, Sun Yat-Sen Memorial Hospital, the Second Affiliated Hospital, Sun Yat-Sen University, Guangzhou 510120, Guangdong Province, China. mdchens@yahoo.com
Telephone: +86-20-81332539 **Fax:** +86-20-81332853
Received: 2004-03-11 **Accepted:** 2004-04-05

Abstract

AIM: To investigate the effects and molecular mechanisms of recombinant human growth hormone (rhGH) on protecting liver function and alleviating portal hypertension of liver cirrhotic rats.

METHODS: Liver cirrhosis of male Sprague-Dawley rats was induced by administration of thioacetamide. The rats with or without liver cirrhosis were randomly divided into four groups. Group A consisted of the normal rats was treated with normal saline (NS), group B consisted of the normal rats was treated with rhGH, group C consisted of cirrhotic rats was treated with NS, and group D consisted of cirrhotic rats was treated with rhGH. The rats of different groups were subcutaneously injected with 0.5 mL of NS or 333 ng/kg of rhGH daily for 7 d. After treatments, the following parameters were examined, including GH-binding capacity (R_T) by ^{125}I-hGH binding, growth hormone receptor mRNA(GHR mRNA) expression by RT-PCR, relative content of collagen (RCC) by histomorphomertry, and level of malon-dialdehyde (MDA) and superoxide dismutase (SOD) in liver tissue by thiobarbituric acid reaction and pyrogallic acid self-oxidation, respectively. Serum albumin (ALB), alanine transaminase (ALT) and portal vein pressure (PVP) were also examined.

RESULTS: rhGH up-regulated both the GH-binding capacity (R_T) and the expression of GHR mRNA *in vivo.* R_T in group A (72±12 fmol/mg protein) was significantly higher than that in group C (31±4 fmol/mg protein) (P<0.05). R_T in group B (80±9 fmol/mg protein) increased markedly compared to group A (P<0.05). R_T in group D (40±7 fmol/mg protein) raised remarkably compared with group C (P<0.05), but less than that in group A, and there was no significant GH binding affinity contrast (Kd) change. The GHR mRNA level (iOD, pixel) in group A (29±3) was significantly higher than that in group C (23±3) (P<0.05). GHR mRNA levels were significantly raised in group B (56±4) and group D (42±8) compared with groups A and C (29±3 and 23±3, respectively) (P<0.05). Compared with the normal liver, MDA level was higher and SOD level was lower in cirrhotic livers. After rhGH treatment, MDA level was significantly declined to 12.0±2.2 nmol/mg protein and SOD was raised to 1029±76 U/mg protein in group D (P<0.05). ALB levels in groups B and D (42±7 g/L and 37±7 g/L, respectively) were significantly raised compared with those in groups A and C (35±5 g/L and 29±4 g/L, respectively) (P<0.05). ALT level was markedly lower in group D (69±7 U/L) compared to group C (89±15 U/L) (P<0.05), and close to group A (61±10 U/L). RCC in group C (22.30±3.86%) was significantly higher than that in group A (1.14±0.21%) and group D (14.70±2.07%) (P<0.05). In addition, rhGH markedly alleviated portal hypertension in liver cirrhotic rats (group D *vs* C, 9.3±1.5 cmH_2O *vs* 14.4±2.0 cmH_2O) (P<0.05).

CONCLUSION: Pharmacological doses of rhGH can increase R_T and GHR mRNA expression, ameliorate liver functions, repress fibrosis and decline portal hypertension, suggesting it has potentially clinical usage as a hepatotropic factor.

Chen S, Wang HT, Yang B, Fu YR, Ou QJ. Protective effects of recombinant human growth hormone on cirrhotic rats. *World J Gastroenterol* 2004; 10(19): 2894-2897
http://www.wjgnet.com/1007-9327/10/2894.asp

INTRODUCTION

Liver cirrhosis is a common pathway of a variety of chronic liver diseases[1], and is associated with high protein catabolism, low anabolism and negative nitrogen balance[2], resulting in hypoproteinemia which contributes to ascites, dysfunction of coagulation and suppression of immune response[3]. Early reports showed that cirrhotic patients undergone emergency abdominal surgery exhibited a higher mortality[4]. In retrospective studies of liver transplant recipients, protein-calorie malnutrition has been associated with adverse outcomes in patients with end-stage liver diseases[5,6]. A prospective study showed that cirrhotic patients with hypermetabolism and emaciation had a much higher mortality rate after liver transplantation than those with normal metabolism[7]. It is critical for patients with hepatic cirrhosis to correct malnutrition. To date, studies have shown that nutritional support is always not effective enough to prevent protein loss and optimize the care of these patients in severe catabolic illnesses, including cirrhosis[8,9].

Growth hormone (GH) is essential for body growth in children. In adults, GH continues to stimulate many anabolic processes. GH secreted by the pituitary gland is pulsatile, and its action depends on its binding to growth hormone receptor on cell membrane[10-13]. New insights have initiated new applications and a growing potential for GH replacement therapy in adults. Recombinant human growth hormone (rhGH) has been clinically used in many states, such as after abdominal operation[14], organ transplantation[15], major trauma[16] and severe burns[17], to enable the patients to survive an aggressive surgery[18]. After treatment with rhGH, donor site healing rate

in children with severe burns was enhanced and hospitalization time was decreased[19-21]. It significantly enhanced cell-mediated immunity and decreased wound infection rates and length of hospitalization in a large group of postoperative patients[22]. Some clinical trials reported that growth hormone enhanced nitrogen retention of patients with chronic obstructive lung diseases[23], severe sepsis[24,25] and emaciated AIDS[26,27], in addition to fasted adult volunteers. Although there are many controversies[28-32], it has been confirmed that rhGH is an effective drug to accelerate protein anabolism[33] and plays a central role in metabolic intervention with a significant cost-effect benefit[34].

In this study, we investigated the effects and molecular mechanism of pharmacological doses of recombinant human growth hormone (rhGH) on expression of growth hormone receptor (GHR) in liver tissue, liver function and portal vein pressure in a rat cirrhotic model with portal hypertension.

MATERIALS AND METHODS

Induction of liver cirrhosis

Male SD rats were purchased from Medical Animal Center of Sun Yat-Sen University. Rat liver cirrhosis was induced by daily intraperitoneal injection of 30 g/L thioacetamide (TAA, 50 mg/kg for 9 to 12 wk). Twenty normal rats (body mass 200-300 g) were randomly divided into two groups: group A (n = 10) was treated with normal saline (NS), and group B (n = 10) was treated with rhGH. Twenty cirrhotic rats (body mass, 200-300 g) were randomly divided into two groups: group C (n = 10) was treated with NS and group D (n = 10) was treated with rhGH. The rats were injected subcutaneously with 0.5 mL of NS or 333 ng/kg of rhGH daily for 7 d.

Experimental methods and observation indexes

Rats were anesthetized with pentobarbital (30 mg/kg, subcutaneous injection), weighed, antisepsised. Then peritoneum was incised to explore the liver.

Measurement of portal vein pressure (PVP) After the portal vein was punctured, PVP was measured directly.

Estimation of liver function Blood samples from inferior vena cava were collected to measure serum albumin (ALB) and alanine transaminase (ALT) levels by biochemical autoanalyzers.

Tissue sampling Partial liver tissue samples were frozen in liquid nitrogen immediately, then stored at -80 ℃ for use, The rest part was fixed in 100 g/L formaldehyde solution and stained with Masson trichrome stain for regular pathological examination.

GH binding capacity (R_T) analysis One hundred μL (approximately 20 000 cpm) of ^{125}I-hGH (NEN inc, USA) with a specific activity of about 108 μCi/μg, 100 μL of unlabelled hGH with various concentrations (0-3 nmol/L was divided into 7-9 concentration gradients, standard samples were bought from Northern Biological Technical Company), and 100 μL of liver membrance microsomes (preparation with gradient centrifugation technique) were mixed and incubated at 4 ℃ overnight. Dissociated ligands were eliminated by filtration. The precipitates were subjected to a radioactive counter, and then ^{125}I-GH binding capacity (R_T, fmol/mg protein) and binding affinity contrast (kd, nmol/L) were calculated by Scatchard analysis.

Expression of GHR mRNA in liver tissue Self-designed primers were as follows: forward, 5'-ATGTGAGATCCAGACAACG-3', and reverse, 5'-ATGTCAGGGTCATAACAGC-3'. The amplification segment containing introns was supposed to be 499 bp in length. Total RNA of the rats' liver tissues was extracted with Trizol following the manufacturer's instructions. RT-PCR was performed with RT-PCR kits (Epicedure inc. USA) as previously described[35]. After thirty amplification cycles were performed, the PCR products were detected by gel electrophoresis. The level of GHR mRNA was expressed as iOD (pixel, the integral optical density of amplification segment).

Level of malon-dialdehyde (MDA) and superoxide dismutase (SOD) Thiobarbituric acid reaction and pyrogallic acid self oxidation method were adopted to measure the amount of MDA (the degradation products of peroxide lipid in liver) and the activity of SOD, respectively.

Measurement of relative content of collagen (RCC) in liver Liver fibrosis levels was expressed as RCC. After stained with Masson's trichrome stain, liver collagen content was calculated by histomorphometric measurement. Three random areas were chosen and analyzed by computers with Kontron IBAS2.5 system (Germany) for digital image analysis. The total area and the fibrotic area with positive staining were automatically selected, outlined and evaluated by planimetry. RCC was calculated as a percentage of positive staining area in the total area.

Statistical analysis

The data were processed with duplex factor χ^2 analysis by software statistica 5.0. Least significant difference (LSD) was adopted to compare the inter-group variance. Values were expressed as mean±SD. P<0.05 was considered statistically significant.

RESULTS

GH-binding capacity (R_T) analysis

As shown in Table 1, R_T in group A was significantly higher than that in group C (P<0.05). R_T in group B increased markedly compared with group A (P<0.05). It significantly increased in group D compared with group C (P<0.05), but was lower than that in group A. There was no significant difference in Kd.

GHR mRNA expression in liver tissue

As shown in Table 1 and Figure 1, the expression of GHR mRNA (iOD, pixel) in group A was significantly higher than that in group C (P<0.05). It was significantly raised in groups B and D after rhGH treatment, which was 1.9 and 1.8 times higher than that in groups A and C, respectively (P<0.05). It was higher in group D than in group A.

Serum ALB and ALT level

Without rhGH treatment, ALB level in cirrhotic rats (group C)

Table 1 Effects of rhGH treatment on various parameters (mean±SD)

Group	R_T (fmol/mg protein)	GHR mRNA (iOD)	ALB (g/L)	ALT (U/L)	MDA (nmol/mg protein)	SOD (U/mg)	RCC (%)	PVP (cmH_2o)
A	72±12	29±3	35±5	61±10	10.2±1.4	1078±185	1.14±0.21	5.6±0.7
B	80±9^c	56±4^c	42±7^c	55±11	9.4±1.2	1057±159	1.13±0.18	5.8±0.7
C	31±4^a	23±3^a	29±4^a	89±15^a	18.7±3.2^a	824±108^a	22.30±3.86^a	14.4±2.0^a
D	40±7^{ac}	42±8^{ac}	37±7^c	69±7^{ac}	12.0±2.2^{ac}	1029±76^c	14.70±2.07^{ac}	9.3±1.5^{ac}

^aP<0.05 *vs* control groups A and B, ^cP<0.05 *vs* before rhGH treatment (group A or C).

was significantly lower than that in normal rats (group A), and ALT in cirrhotic rats was markedly higher than that in normal rats (P<0.05) (Table 1). After rhGH administration, ALB in groups B and D increased significantly (P<0.05), ALT in group D decreased remarkably (P<0.05), which was close to normal rats (Table 1).

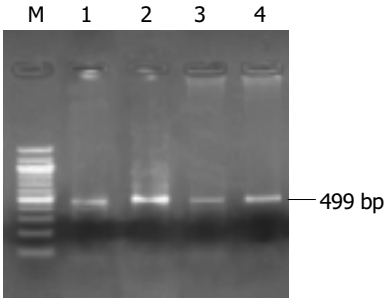

Figure 1 Expression of GHR mRNA in normal and cirrhotic liver tissues after NS or rhGH administration. Lane 1: control group +NS (group A); Lane 2: control group +rhGH (group B); Lane 3: cirrhotic group +NS (group C); Lane 4: cirrhotic group +rhGH (group D); and Lane M: DNA standard marker of 100, 200, 300, 400, 500, 600, 700, 800, 900, 1 000, 1 100 and 1 200 bp, respectively.

Changes of MDA and SOD in liver tissue

Before the treatment with rhGH, the amount of MDA in cirrhotic rats (group C) was significantly higher than that in normal rats (group A) (P<0.05), and SOD in cirrhotic rats was significantly lower than that in normal rats (P<0.05). After rhGH administration, MDA and SOD in group B were not obviously changed, but in group D, MDA was significantly lower than that in group C (P<0.05), while SOD was significantly higher than that in group C (P<0.05). The curve correlation analysis manifested a significant correlation between SOD and MDA (P<0.01). (Table 1, Figure 2).

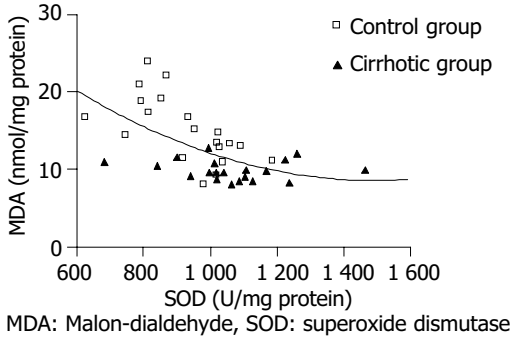

MDA: Malon-dialdehyde, SOD: superoxide dismutase

Figure 2 Correlation analysis of SOD and MDA.

RCC in liver tissue

As shown in Table 1, RCC in group C was significantly higher than that in group A (P<0.05). Compared with group C, it was significantly lower in group D (P<0.05).

Changes of PVP

As shown in Table 1, PVP in cirrhotic rats (group C) was significantly higher than that in normal rats (group A) (P<0.05). After rhGH administration, no significant change was found in normal rats, however PVP in cirrhotic rats (group D) was significantly lower than that in group C (P<0.05).

DISCUSSION

In cirrhotic patients, nutritional status was an important predictor of morbidity, mortality, and survival after transplantation[36]. The poor status of these patients was associated with the state of acquired GH resistance[37,38], which is common in conditions associated with malnutrition and protein catabolism, trauma or surgery, organ failure and critical illness. Much has been done regarding the expression of GHR and signal transduction[10-13], but the expression of GHR and GHR mRNA in some pathological states such as cirrhotic hepatocytes, malignant cells, remains to be established. Chang *et al*.[39] reported that ^{125}I-rhGH binding activity in 6 cases of hepatocellular carcinoma and adjacent cirrhotic liver tissues could not be detected and they believed that GHR in cirrhotic hepatic tissues disappeared although the study only examined one aspect of the GHR and GH binding. Another study[40] showed that specific binding of ^{125}I-hGH in liver tissues from liver transplant of 17 patients with end-stage liver diseases was lower than that in normal controls, but only in 3 cirrhotic livers Scatchard analysis was performed for calculation of GH binding capacity and affinity. In this setting of tissue-based GH binding assay, there was still a controversy about the expression of GHR on cirrhotic liver cells.

Our study showed that rhGH could significantly increase serum ALB and SOD levels, decrease ALT and MAD to nearly the normal level in liver cirrhotic rats. In addition, after rhGH treatment, both the liver fibrosis level and PVP were remarkably decreased.

In our study, the expression of GHR mRNA in cirrhotic liver tissue was lower than that in normal liver tissue, suggesting that liver cirrhosis could down-regulate GHR gene transcription and result in decrease of GHR, which might be an important reason of malnutrition in liver cirrhosis.

Simultaneously, we found that rhGH up-regulated GHR and its mRNA in both cirrhotic and normal liver tissues. in normal liver, the changes before and after rhGH treatment were not obvious. We hypothesized that the up-regulation of GHR and its mRNA in cirrhotic rats could improve liver function, and decrease liver fibrosis levels and PVP. This implied that the effects of rhGH on the expression of GHR and GHR mRNA in cirrhotic liver tissues might play an important role in ameliorating the sensibility of cirrhotic liver tissues to rhGH, thereby exerting a therapeutic effect on liver cirrhosis.

In conclusion, rhGH can up-regulate the expression of GHR and its mRNA in livers, particularly in cirrhotic livers, which can increase the sensibility of cirrhotic liver tissue to growth hormones. Thus, rhGH can protect liver function, repress fibrosis, alleviate portal hypertension of cirrhotic livers.

REFERENCES

1 **Strong RW**. Liver transplantation: current status and future prospects. *J R Coll Surg Edinb* 2001; **46**: 1-8

2 **Dichi JB**, Dichi I, Maio R, Correa CR, Angeleli AY, Bicudo MH, Rezende TA, Burini RC. Whole-body protein turnover in malnourished patients with child class B and C cirrhosis on diets low to high in protein energy. *Nutrition* 2001; **17**: 239-242

3 **Sobhonslidsuk A**, Roongpisuthipong C, Nantiruj K, Kulapongse S, Songchitsomboon S, Sumalnop K, Bussagorn N. Impact of liver cirrhosis on nutritional and immunological status. *J Med Assoc Thai* 2001; **84**: 982-988

4 **Maull KI**, Turnage B. Trauma in the cirrhotic patient. *South Med J* 2001; **94**: 205-207

5 **Moukarzel AA**, Najm I, Vargas J, McDiarmid SV, Busuttil RW, Ament ME. Effect of nutritional status on outcome of orthotopic liver transplantation in pediatric patients. *Transplant Proc* 1990; **22**: 1560-1563

6 **Harrison J**, McKiernan J, Neuberger JM. A prospective study on the effect of recipient nutritional status on outcome in liver transplantation. *Transpl Int* 1997; **10**: 369-374

7 **Muller MJ**, Lautz HU, Plogmann B, Burger M, Korber J, Schmidt FW. Energy expenditure and substrate oxidation in patients with cirrhosis: the impact of cause, clinical staging

and nutritional state. *Hepatology* 1992; **15**: 782-794
8 **Streat SJ**, Beddoe AH, Hill GL. Aggressive nutritional support does not prevent protein loss despite fat gain in septic intensive care patients. *J Trauma* 1987; **27**: 262-266
9 **Le Cornu KA**, McKiernan FJ, Kapadia SA, Neuberger JM. A prospective randomized study of preoperative nutritional supplementation in patients awaiting elective orthotopic liver transplantation. *Transplantation* 2000; **69**: 1364-1369
10 **Carter-Su C**, Schwartz J, Smit LS. Molecular mechanism of growth hormone action. *Annu Rev Physiol* 1996; **58**: 187-207
11 **Hocquette JF**, Postel-Vinay MC, Kayser C, de Hemptinne B, Amar-Costesec A. The human liver growth hormone receptor. *Endocrinology* 1989; **125**: 2167-2174
12 **Husman B**, Andersson G, Norstedt G, Gustafsson JA. Characterization and subcellular distribution of somatogenic receptor in rat liver. *Endocrinology* 1985; **116**: 2605-2611
13 **van Neste L**, Husman B, Moller C, Andersson G, Norstedt G. Cellular distribution of somatogenic receptors and insulin-like growth factor-I mRNA in the rat liver. *J Endocrinol* 1988; **119**: 69-74
14 **Wong WK**, Soo KC, Nambiar R, Tan YS, Yo SL, Tan IK. The effect of recombinant growth hormone on nitrogen balance in malnourished patients after major abdominal surgery. *Aust N Z J Surg* 1995; **65**: 109-113
15 **Rodeck B**, Kardorff R, Melter M, Ehrich JH. Improvement of growth after growth hormone treatment in children who undergo liver transplantation. *J Pediatr Gastroenterol Nutr* 2000; **31**: 286-290
16 **Petersen SR**, Holaday NJ, Jeevanandam M. Enhancement of protein synthesis efficiency in parenterally fed trauma victims by adjuvant recombinant human growth hormone. *J Trauma* 1994; **36**: 726-733
17 **Singh KP**, Prasad R, Chari PS, Dash RJ. Effect of growth hormone therapy in burn patients on conservative treatment. *Burns* 1998; **24**: 733-738
18 **Iglesias P**, Diez JJ. Clinical applications of recombinant human growth hormone in adults. *Expert Opin Pharmacother* 1999; **1**: 97-107
19 **Herndon DN**, Hawkins HK, Nguyen TT, Pierre E, Cox R, Barrow RE. Characterization of growth hormone enhanced donor site healing in patients with large cutaneous burns. *Ann Surg* 1995; **221**: 649-656
20 **Aili Low JF**, Barrow RE, Mittendorfer B, Jeschke MG, Chinkes DL, Herndon DN. The effect of short-term growth hormone treatment on growth and energy expenditure in burned children. *Burns* 2001; **27**: 447-452
21 **Hart DW**, Herndon DN, Klein G, Lee SB, Celis M, Mohan S, Chinkes DL, Wolf SE. Attenuation of posttraumatic muscle catabolism and osteopenia by long-term growth hormone therapy. *Ann Surg* 2001; **233**: 827-834
22 **Vara-Thorbeck R**, Guerrero JA, Rosell J, Ruiz-Requena E, Capitan JM. Exogenous growth hormone: effects on the catabolic response to surgically produced acute stress and on postoperative immune function. *World J Surg* 1993; **17**: 530-537
23 **Pape GS**, Friedman M, Underwood LE, Clemmons DR. The effect of growth hormone on weight gain and pulmonary function in patients with chronic obstructive lung disease. *Chest* 1991; **99**: 1495-1500
24 **Koea JB**, Breier BH, Douglas RG, Gluckman PD, Shaw JH. Anabolic and cardiovascular effects of recombinant human growth hormone in surgical patients with sepsis. *Br J Surg* 1996; **83**: 196-202
25 **Li W**, Li J, Xu B, Yin L, Wang L, Gu J, Ren J, Quan Z. Effect of recombinant human growth hormone with total parenteral nutrition on albumin synthesis in patients with peritoneal sepsis. *Zhonghua Waike Zazhi* 1998; **36**: 643-645
26 **Schambelan M**, Mulligan K, Grunfeld C, Daar ES, LaMarca A, Kotler DP, Wang J, Bozzette SA, Breitmeyer JB. Recombinant human growth hormone in patients with HIV-associated wasting. A randomized, placebo-controlled trial. Serostim Study Group. *Ann Intern Med* 1996; **125**: 873-882
27 **Waters D**, Danska J, Hardy K, Koster F, Qualls C, Nickell D, Nightingale S, Gesundheit N, Watson D, Schade D. Recombinant human growth hormone, insulin-like growth factor 1, and combination therapy in AIDS-associated wasting. A randomized, double-blind, placebo-controlled trial. *Ann Intern Med* 1996; **125**: 865-872
28 **O'Leary MJ**, Ferguson CN, Rennie M, Hinds CJ, Coakley JH, Preedy VR. Effect of growth hormone on muscle and liver protein synthesis in septic rats receiving glutamine-enriched parenteral nutrition. *Crit Care Med* 2002; **30**: 1099-1105
29 **Losada F**, Garcia-Luna PP, Gomez-Cia T, Garrido M, Pereira JL, Marin F, Astorga R. Effects of human recombinant growth hormone on donor-site healing in burned adults. *World J Surg* 2002; **26**: 2-8
30 **Carroll PV**, Van den Berghe G. Safety aspects of pharmacological GH therapy in adults. *Growth Horm IGF Res* 2001; **11**: 166-172
31 **Takala J,** Ruokonen E, Webster NR, Nielsen MS, Zandstra DF, Vundelinckx G, Hinds CJ. Increased mortality associated with growth hormone treatment in critically ill adults. *N Engl J Med* 1999; **341**: 785-792
32 **Jeschke MG**, Barrow RE, Herndon DN. Recombinant human growth hormone treatment in pediatric burn patients and its role during the hepatic acute phase response. *Crit Care Med* 2000; **28**: 1578-1584
33 **Raguso CA**, Genton L, Kyle U, Pichard C. Management of catabolism in metabolically stressed patients: a literature survey about growth hormone application. *Curr Opin Clin Nutr Metab Care* 2001; **4**: 313-320
34 **Wilmore DW**. Postoperative protein sparing. *World J Surg* 1999; **23**: 545-552
35 **Zhao J**, van Tol HT, Taverne MA, van der Weijden GC, Bevers MM, van den Hurk R. The effect of growth hormone on rat preantral follicles *in vitro*. *Zygote* 2000; **8**: 275-283
36 **Mendenhall CL,** Tosch T, Weesner RE, Garcia-Pont P, Goldberg SJ, Kiernan T, Seeff LB, Sorell M, Tamburro C, Zetterman R. VA cooperative study on alcoholic hepatitis. II: Prognostic significance of protein-calorie malnutrition. *Am J Clin Nutr* 1986; **43**: 213–218
37 **Moller S,** Becker U, Gronbaek M, Juul A, Winkler K, Skakkebaek NE. Short-term effect of recombinant human growth hormone in patients with alcoholic cirrhosis. *J Hepatol* 1994; **21**: 710–717
38 **Donaghy A,** Ross R, Gimson A, Hughes SC, Holly J, Williams R. Growth hormone, insulin like growth factor-1, and insulin like growth factor binding proteins 1 and 3 in chronic liver disease. *Hepatology* 1995; **21**: 680–688
39 **Chang TC,** Lin JJ, Yu SC, Chang TJ. Absence of growth-hormone receptor in hepatocellular carcinoma and cirrhotic liver. *Hepatology* 1990; **11**: 123-126
40 **Shen XY,** Holt RI, Miell JP, Justice S, Portmann B, Postel-Vinay MC, Ross RJ. Cirrhotic liver expresses low levels of the full-length and truncated growth hormone receptors. *J Clin Endocrinol Metab* 1998; **83**: 2532-2538

Edited by Kumar M and Wang XL **Proofread by** Xu FM

PO Box 2345, Beijing 100023, China
Fax: +86-10-85381893
E-mail: wjg@wjgnet.com www.wjgnet.com

World J Gastroenterol 2004;10(19):2898-2900
World Journal of Gastroenterology
Copyright © 2004 by The WJG Press ISSN 1007-9327

• BRIEF REPORTS •

Tumor necrosis factor α antibody prevents brain damage of rats with acute necrotizing pancreatitis

Yan-Ling Yang, Ji-Peng Li, Kai-Zong Li, Ke-Feng Dou

Yan-Ling Yang, Ji-Peng Li, Kai-Zong Li, Ke-Feng Dou, Department of Hepatobiliary Surgery, Xijing Hospital, Fourth Military Medical University, Xi'an 710032, Shaanxi Province, China
Correspondence to: Ke-Feng Dou, Department of Hepatobiliary Surgery, Xijing Hospital, Fourth Military Medical University, Xi'an 710032, Shaanxi Province, China. gdwk@fmmu.edu.cn
Telephone: +86-29-3375259 **Fax:** +86-29-3375561
Received: 2003-12-12 **Accepted:** 2004-02-20

Abstract

AIM: To study the protective effects of tumor necrosis factor α (TNFα) antibody on pancreatic encephalopathy in rats.

METHODS: One hundred and twenty SD rats were randomly divided into normal control group, acute necrotizing pancreatitis group and TNFα antibody treated group. Acute hemorrhage necrotizing pancreatitis model in rats was induced by retrograde injection of 50 g/L sodium taurocholate into the pancreatobiliary duct. Serum TNFα was detected and animals were killed 12 h after drug administration. Changes in content of brain water, MDA and SOD as well as leucocyte adhesion of brain microvessels were measured.

RESULTS: In TNFα antibody treated group, serum TNFα level was decreased. Content of brain water, MDA and SOD as well as leucocyte adhesion were decreased significantly in comparison with those of acute necrotizing pancreatitis group (P<0.05).

CONCLUSION: TNFα antibody can alleviate the brain damage of rats with acute hemorrhage necrotizing pancreatitis.

Yang YL, Li JP, Li KZ, Dou KF. Tumor necrosis factor α antibody prevents brain damage of rats with acute necrotizing pancreatitis. *World J Gastroenterol* 2004; 10(19): 2898-2900 http://www.wjgnet.com/1007-9327/10/2898.asp

INTRODUCTION

Pancreatic encephalopathy, a syndrome of mental retardation induced by severe acute pancreatitis, has been greatly concerned by clinicians. Unfortunately, the pathogenesis and mechanism of pancreatic encephalopathy are still unclear although many factors are thought to be related to it, such as pancreatin, epiphyte infection, electrolyte disturbance, lack of vitamin, alcoholism, hypoxemia[1-3]. Recent reports have shown that overactivation of leucocytes and overexpression of cytokines play important roles in the pathogenesis of pancreatic encephalopathy. Moreover, the high level of TNFα in patients has a remarkable correlation with pancreatic encephalopathy[4-9]. In the present study, we attempted to block or relieve pancreatic encephalopathy by using TNF α antibody.

MATERIALS AND METHODS

Animals

One hundred and twenty male Spargue-Dawley (SD) rats weighing 230±20 g, were obtained from Animal Research Center of Shaanxi Academy of Traditional Medicine, and fed with standard rat chow.

Drugs

Sodium taurocholate (Sigma) was diluted to 50 g/L with saline prior to use. TNFα monoclonal antibody (Jingmei Co.Ltd., Guangdong, China) was diluted at 1:100 with saline prior to use.

Experimental grouping

One hundred and twenty SD rats were randomly divided into three groups: Group I: normal control group (n = 40), sham operation was performed and saline was retrograde injected into the pancreatobiliary duct of the rats; Group II: acute necrotizing pancreatitis group (n = 40), in which an acute hemorrhage necrotizing pancreatitis model was induced by retrograde injection of 50 g/L sodium taurocholate into the pancreatobiliary duct; Group III: TNFα antibody treated group (n = 40), in which 1 mL TNFα antibody (2.0 mg/kg) was injected into the rats through dorsum veins of penis 5 min prior to operation. Blood samples (2 mL) were taken from inferior vena cava of all animals in each group 12 h after operation. Then the rats were killed and samples were obtained for analysis.

Operation

The animals were fasted but free to drink water 12 h before operation. Then the rats were intraabdominally anesthetized by 100 g/L pentobarbital sodium (30 mg/kg), and incised through median incision of the abdomen. After the common bile duct was clamped in hepatoduodenal ligament by small artery clamps, a cannula was inserted into pancreatobiliary duct through mammary papilla from anterior wall of duodenum. Then sodium taurocholate (50 g/L) was injected by the cannula with even speed of 0.1 mL/min, the scatheless vascular clamp was removed 10 min later. Finally, the abdomen incisions were closed and the animals were given gentamicin to prevent infection[10,11].

Evaluation of TNFα in serum

Evaluation of serum TNFα was performed by sandwich ELISA method with double antibodies. The kit was purchased from Endogen Company (USA) and the procedures were made according to the manufacturer's instructions.

Evaluation of water content in brain

Evaluations of water content in brain of 20 rats in each group were completed by the methods of dry and wet weight estimation. Water content in brain = (wet weight - dry weight) ÷ wet weight ×100%.

Evaluation of brain MDA and SOD content

Skulls of 20 rats in each group were opened to get frontal lobe of the brain. Then brain tissues were homogenized and centrifuged. MDA and SOD contents were gained by chemical colorimetry (kit purchased from Bioengineer Institute of Nanjing Jiancheng, China).

Congregation of leucocytes and mural counting in blood capillary

After stained by HE, the whole number of leucocytes in 20 sections

Table 1 Serum TNFα level, content of brain water, MDA and SOD as well as leucocyte mural counting in brain blood capillary in three groups

Group	Serum TNFα level (pg/mL)	Brain water content (%)	Brain MDA content (nmol/mL)	Brain SOD content (nmol/mL)	Mural leucocytes (per 20 capillary)
I[a]	25.17±2.26	77.09±0.51	5.32±1.40	13.40±2.77	6.12±1.60
II	264.58±4.39	83.17±1.42	17.26±3.18	35.52±3.10	62.15±5.18
III[c]	74.33±1.78	81.41±1.52	11.71±3.26	23.65±1.93	38.37±3.43

[a]$P<0.05$ *vs* II, [c]$P<0.05$ *vs* II.

of brain tissues was counted under light microscope to obtain the mean number.

Statistical analysis

The data were expressed as mean±SD and analyzed by software of SPSS10.0. $P<0.05$ was considered statistically significant.

RESULTS

Serum TNFα level

The level of TNFα in blood serum in acute necrotizing pancreatitis group (264.58±4.39 pg/mL) was increased markedly ($P<0.05$) compared with that in the normal control group (25.17±2.26 pg/mL). But the level of TNFα in blood serum in the TNFα antibody treated group (74.33±1.78 pg/mL) was decreased markedly ($P<0.05$) compared with that in acute necrotizing pancreatitis group.

Brain water content

Brain water content in the acute necrotizing pancreatitis group (83.17±1.42%) was significantly higher than that in the normal control group (77.09±0.51%). But it was significantly lower in the TNFα antibody treated group (81.41±1.52%) than in the acute necrotizing pancreatitis group ($P<0.05$).

Brain MDA content

Brain MDA content of in the acute necrotizing pancreatitis group (17.26±3.18 nmol/mL) was increased remarkably ($P<0.05$) compared with that in the normal control group (5.32±1.40 nmol/mL). It was decreased remarkably in the TNFα antibody treated group (11.71±3.26 nmol/mL) in comparison with acute necrotizing pancreatitis group ($P<0.05$).

Brain SOD content

Brain SOD content in the acute necrotizing pancreatitis group (35.52±3.10 nmol/mL) was increased remarkably compared with that in the normal control group (13.40±2.77 nmol/mL). It was decreased remarkably in the TNFα antibody treated group (23.65±1.93 nmol/mL) in comparison with acute necrotizing pancreatitis group ($P<0.05$).

Leucocyte mural counting of brain blood capillary

The number of leucocyte mural counts in blood capillary in every 20 blood capillaries in the TNFα antibody treated group (38.37±3.43) was significantly lower ($P<0.05$) than that in the acute necrotizing pancreatitis group (62.15±5.18).

DISCUSSION

Cytokines, mainly excreted by immunocytes in human body, are soluble peptides, which play important roles in immune activation and inflammatory reactions. In normal conditions, the content of cytokines is very low. However, the expression of cytokines is increased remarkably following multiple stimulations, such as infection and trauma. It is well known that the overactivation of cytokines could induce or even aggravate tissue damage[12-16]. Acute severe pancreatitis could always lead to systemic inflammatory response syndrome (SIRS) and multiple organ dysfunction syndrome (MODS)[17-24]. The present studies have focused on the pathogenesis and therapy of respiratory failure, kidney failure, hepatic failure and cardiovascular function failure complicated by acute severe pancreatitis. However, investigations on mechanism of brain damage and related preventive measures after acute severe pancreatitis remain ineffective.

TNFα is excreted by activated macrophages, endothelial cells and B lymphocytes with multiple functions. It can play important roles in inflammatory reactions. Animal experiments suggested that serum TNFα in patients with acute severe pancreatitis could induce pancreatic and other organs' damages. In the early period of acute severe pancreatitis, TNFα was involved in occurrence and progress of acute severe pancreatitis. On the other hand, TNFα was closely related with the severity and mortality of this disease[25-31].

In acute severe pancreatitis, the mechanisms of TNFα -induced brain damage included[32-40]: (1) TNFα could stimulate differentiation of phospholipase A2 or directly activate phospholipase, aggregate and activate leucocytes to release cellular media, thus reinforcing permeability of blood capillary including platelet active factor (PAF), leukotriene B4 (LTB4), nitrogen monoxide (NO), thromboxane A2 (TXA2), prostaglandin (PG) and oxygen-derived free radidicals. The media in positive feedback could accelerate the yield of TNFα , and thereby form "waterfall" cascade reaction. (2) TNFα could directly increase the permeability of blood endothelial cells, and also act through leukocytes, up-regulate adhesive factors of endothelial cells, such as ELAM-l and ICAM-l, thus facilitating adhesiveness and contraction of leukocytes to cause leakage of blood capillary and tissue damage. (3) TNFα could induce inflammatory injuries of myelin sheath by direct toxicity or activating immune cells.

In the present study, we attempted to relieve pancreatic encephalopathy by using TNF α antibody. The results showed that the level of serum TNFα, content of brain water, MDA and SOD as well as mural leucocyte count of the rats in TNFα antibody treated group, reduced significantly compared with those in acute necrotizing pancreatitis group. The present data suggest that TNFα antibody plays an important protective role in pancreatic encephalopathy in rats. But the optimal concentration of TNFα antibody and its influence on body immune system still need further investigation.

REFERENCES

1 **Chan C**, Fryer J, Herkes G, Prelog K, Harrington T. Fatal brain stem event complicating acute pancreatitis. *J Clin Neurosci* 2003; **10**: 351-358

2 **Ruggieri RM**, Lupo I, Piccoli F. Pancreatic encephalopathy: a 7-year follow-up case report and review of the literature. *Neurol Sci* 2002; **23**: 203-205

3 **Chen L**, Zhang X. Pancreatic encephalopathy and Wernicke encephalopathy. *Zhonghua Neike Zazhi* 2002; **41**: 94-97

4 **Ammori BJ**. Role of the gut in the course of severe acute pancreatitis. *Pancreas* 2003; **26**: 122-129

5 **Nam JH**, Murthy S. Acute pancreatitis-the current status in management. *Expert Opin Pharmacother* 2003; **4**: 235-241

6 **Demols A**, Deviere J. New frontiers in the pharmacological prevention of post-ERCP pancreatitis: the cytokines. *JOP* 2003; **4**: 49-57

7 **Algul H**, Tando Y, Schneider G, Weidenbach H, Adler G, Schmid RM. Acute experimental pancreatitis and NF-kappaB/Rel activation. *Pancreatology* 2002; **2**: 503-509

8 **Noji T**, Karasawa A, Kusaka H. Pharmacological study on the effects of the adenosine uptake inhibitor KF24345 on inflammatory diseases. *Nippon Yakurigaku Zasshi* 2003; **122**: 121-134

9 **Park BK**, Chung JB, Lee JH, Suh JH, Park SW, Song SY, Kim H, Kim KH, Kang JK. Role of oxygen free radicals in patients with acute pancreatitis. *World J Gastroenterol* 2003; **9**: 2266-2269

10 **Dib M**, Zhao X, Wang X, Andersson E, Drewsen G, Andersson R. Acute phase response in acute pancreatitis: a comparison with abdominal sepsis. *Scand J Gastroenterol* 2003; **38**: 1072-1077

11 **Strate T**, Mann O, Kleinhans H, Schneider C, Knoefel WT, Yekebas E, Standl T, Bloechle C, Izbicki JR. Systemic intravenous infusion of bovine hemoglobin significantly reduces microcirculatory dysfunction in experimentally induced pancreatitis in the rat. *Ann Surg* 2003; **238**: 765-771

12 **Nakane A**, Sasaki S. Effect of cytokines on the expression of Shiga toxin toxicity. *Nippon Rinsho* 2002; **60**: 1089-1094

13 **Klar E**, Werner J. New pathophysiologic knowledge about acute pancreatitis. *Chirurg* 2000; **71**: 253-264

14 **Ogawa M**. Acute pancreatitis and cytokines: "second attack" by septic complication leads to organ failure. *Pancreas* 1998; **16**: 312-315

15 **Miller AP**, Chen YF, Xing D, Feng W, Oparil S. Hormone replacement therapy and inflammation: interactions in cardiovascular disease. *Hypertension* 2003; **42**: 657-663

16 **Herrera MT**, Toledo C, Valladares F, Muros M, Diaz-Flores L, Flores C, Villar J. Positive end-expiratory pressure modulates local and systemic inflammatory responses in a sepsis-induced lung injury model. *Intensive Care Med* 2003; **29**: 1345-1353

17 **Bhatia M**. Novel therapeutic targets for acute pancreatitis and associated multiple organ dysfunction syndrome. *Curr Drug Targets Inflamm Allergy* 2002; **1**: 343-351

18 **Fang BW**, Qiu Q, Wu XZ, Kong L, Qin MF, Zhou ZL, Cui NQ. Changes in pro-inflammatory cytokines and media and peptide hormones during multiple organ dysfunction syndrome following acute abdominal diseases. *Zhongguo Weizhongbing Jijiu Yixue* 2003; **15**: 19-22

19 **Austrums E**, Pupelis G, Snippe K. Postoperative enteral stimulation by gut feeding improves outcomes in severe acute pancreatitis. *Nutrition* 2003; **19**: 487-491

20 **Isenmann R**, Rau B, Zoellner U, Beger HG. Management of patients with extended pancreatic necrosis. *Pancreatology* 2001; **1**: 63-68

21 **Buter A**, Imrie CW, Carter CR, Evans S, McKay CJ. Dynamic nature of early organ dysfunction determines outcome in acute pancreatitis. *Br J Surg* 2002; **89**: 298-302

22 **Zhang Q**, Ni Q, Cai D, Zhang Y, Zhang N, Hou L. Mechanisms of multiple organ damages in acute necrotizing pancreatitis. *Chin Med J* 2001; **114**: 738-742

23 **Gloor B**, Uhl W, Tcholakov O, Roggo A, Muller CA, Worni M, Buchler MW. Hydrocortisone treatment of early SIRS in acute experimental pancreatitis. *Dig Dis Sci* 2001; **46**: 2154-2161

24 **Desiateryk VI**, Kryvyts'kyi IuM, Shapovaliuk VV. Inflammation response syndrome, sepsis and multi-organ insufficiency in patients operated for destructive pancreatitis. *Klin Khir* 2001; **4**: 24-26

25 **Makhija R**, Kingsnorth AN. Cytokine storm in acute pancreatitis. *J Hepatobiliary Pancreat Surg* 2002; **9**: 401-410

26 **Bhatia M**, Brady M, Shokuhi S, Christmas S, Neoptolemos JP, Slavin J. Inflammatory mediators in acute pancreatitis. *J Pathol* 2000; **190**: 117-125

27 **Holtmann MH**, Schutz M, Galle PR, Neurath MF. Functional relevance of soluble TNF-alpha, transmembrane TNF-alpha and TNF-signal transduction in gastrointestinal diseases with special reference to inflammatory bowel diseases. *Z Gastroenterol* 2002; **40**: 587-600

28 **Farrow B**, Evers BM. Inflammation and the development of pancreatic cancer. *Surg Oncol* 2002; **10**: 153-169

29 **Bhatia M**, Neoptolemos JP, Slavin J. Inflammatory mediators as therapeutic targets in acute pancreatitis. *Curr Opin Investig Drugs* 2001; **2**: 496-501

30 **Reinheckel T**, Deussing J, Roth W, Peters C. Towards specific functions of lysosomal cysteine peptidases: phenotypes of mice deficient for cathepsin B or cathepsin L. *Biol Chem* 2001; **382**: 735-741

31 **Yamauchi J**, Shibuya K, Sunamura M, Arai K, Shimamura H, Motoi F, Takeda K, Matsuno S. Cytokine modulation in acute pancreatitis. *J Hepatobiliary Pancreat Surg* 2001; **8**: 195-203

32 **Brady M**, Christmas S, Sutton R, Neoptolemos J, Slavin J. Cytokines and acute pancreatitis. *Baillieres Best Pract Res Clin Gastroenterol* 1999; **13**: 265-289

33 **Markert R**, Modzelewski B. Inflammatory mediators in the acute pancreatitis. *Pol Merkuriusz Lek* 1999; **6**: 100-103

34 **Zang GQ**, Zhou XQ, Yu H, Xie Q, Zhao GM, Wang B, Guo Q, Xiang YQ, Liao D. Effect of hepatocyte apoptosis induced by TNF-alpha on acute severe hepatitis in mouse models. *World J Gastroenterol* 2000; **6**: 688-692

35 **Silveira RC**, Procianoy RS. Interleukin-6 and tumor necrosis factor-alpha levels in plasma and cerebrospinal fluid of term newborn infants with hypoxic-ischemic encephalopathy. *J Pediatr* 2003; **143**: 625-629

36 **Gimenez F**, Barraud de Lagerie S, Fernandez C, Pino P, Mazier D. Tumor necrosis factor alpha in the pathogenesis of cerebral malaria. *Cell Mol Life Sci* 2003; **60**: 1623-1635

37 **Kawada J**, Kimura H, Ito Y, Hara S, Iriyama M, Yoshikawa T, Morishima T. Systemic cytokine responses in patients with influenza-associated encephalopathy. *J Infect Dis* 2003; **188**: 690-698

38 **Miura Y**, Koyanagi Y, Mizusawa H. TNF-related apoptosis-inducing ligand (TRAIL) induces neuronal apoptosis in HIV-encephalopathy. *J Med Dent Sci* 2003; **50**: 17-25

39 **Ichiyama T**, Isumi H, Ozawa H, Matsubara T, Morishima T, Furukawa S. Cerebrospinal fluid and serum levels of cytokines and soluble tumor necrosis factor receptor in influenza virus-associated encephalopathy. *Scand J Infect Dis* 2003; **35**: 59-61

40 **Okamoto M**, Ono M, Baba M. Suppression of cytokine production and neural cell death by the anti-inflammatory alkaloid cepharanthine: a potential agent against HIV-1 encephalopathy. *Biochem Pharmacol* 2001; **62**: 747-753

Edited by Wang XL and Zhang JZ **Proofread by** Xu FM

PO Box 2345, Beijing 100023, China
Fax: +86-10-85381893
E-mail: wjg@wjgnet.com www.wjgnet.com

World J Gastroenterol 2004;10(19):2901-2904
World Journal of Gastroenterology
Copyright © 2004 by The WJG Press ISSN 1007-9327

• BRIEF REPORTS •

Effects of narcotic analgesic drugs on human Oddi's sphincter motility

Shuo-Dong Wu, Zhen-Hai Zhang, Jun-Zhe Jin, Jing Kong, Wei Wang, Qiang Zhang, Dong-Yan Li, Min-Fei Wang

Shuo-Dong Wu, Zhen-Hai Zhang, Jun-Zhe Jin, Jing Kong, Wei Wang, Qiang Zhang, Dong-Yan Li, Min-Fei Wang, Department of Hepatobiliary Surgery, the Second Affiliated Hospital, China Medical University, Shenyang 110004, Liaoning Province, China
Correspondence to: Dr. Shuo-Dong Wu, Department of Hepatobiliary Surgery, the Second Affiliated Hospital, China Medical University, Shenyang 110004, Liaoning Province, China
Telephone: +86-24-83955062
Received: 2004-02-11 **Accepted:** 2004-02-26

Abstract

AIM: To assess the effects of intramuscular analgesics (morphine, Ap-237, pethidine and tramadol) on human Oddi's sphincter motility with choledochoscope manometry.

METHODS: A total of 70 patients having T tubes after cholecystectomy and choledochotomy were assessed by choledochoscope manometry. They were randomly divided into morphine group, Ap-237 group, pethidine group and tramadol group. Basal pressure of Oddi's sphincter (BPOS), amplitude of phasic contractions (SOCA), frequency of phasic contractions (SOF), duration of phasic contractions (SOD), duodenal pressure (DP) and common bile duct pressure (CBDP) were scored and analyzed. All narcotic analgesic drugs were administered intramuscularly.

RESULTS: Levels of BPOS, SOCA and SOF were increased after injection of morphine and Ap-237 (P<0.05), level of CBDP was increased from 4.97±3.87 mmHg to 8.62±7.43 mmHg (10 min later) and 7.32±5.95 mmHg (20 min later) after injection of morphine (P<0.01). No apparent change occurred after intramuscular injection of pethidine. Level of BPOS was increased from 7.01±5.50 mmHg to 2.87±2.78 mmHg 10 min after injection of tramadol and SOCA was decreased from 63.34±35.29 mmHg to 45.90±27.86 mmHg (10 min later, P<0.05) and 35.97±24.30 (20 min later, P<0.01) after administration of tramadol.

CONCLUSION: All these findings indicate that Oddi's sphincter manometry via choledochoscope is a practical and new way to study the dynamics of Oddi' s sphincter. The regular dose of morphine and Ap-237 could increase BPOS, SOF and SOCA. Morphine could increase the level of CBDP, demonstrating an excitatory effect on the sphincter of Oddi. Pethidine had no effect on Oddi's sphincter motility. Tramadol shows an inhibitory effect on the motility of the sphincter of Oddi and decreases levels of BPOS and SOCA.

Wu SD, Zhang ZH, Jin JZ, Kong J, Wang W, Zhang Q, Li DY, Wang MF. Effects of narcotic analgesic drugs on human Oddi's sphincter motility. *World J Gastroenterol* 2004; 10(19): 2901-2904
http://www.wjgnet.com/1007-9327/10/2901.asp

INTRODUCTION

Morphine can cause excitatory effect on Oddi's sphincter motility and therefore induces upper abdominal pain with characteristics of biliary colic in some patients. Morphine could increase intrabiliary duct pressure[1-3], and delay bile flow to the duodenum[4], for this reason, other opioid analgesics rather than morphine are recommended clinically to relieve the pain, especially biliary pain. It is believed that pethidine has less effect on the sphincter than morphine and therefore is usually the drug of choice for pain relief in acute pancreatitis. Pethidine is also commonly used during endoscopic retrograde cholangiopancreatography (ERCP). Because of potential interference, all narcotic analgesic drugs, including pethidine, are proscribed during Oddi's sphincter manometry (OSM). However, the performance of OSM with only diazepam sedation was difficult as pethidine markedly improves ERCP tolerance.

The aim of this study was to evaluate the effects of four analgesic drugs on human Oddi's sphincter motility by choledochoscope manometry, and to understand the different clinical responses to analgesics.

MATERIALS AND METHODS

Patients

OSM was performed for 70 patients (25 men, 45 women, and mean age 55.5 years, range 35-77 years) with PENTAX choledochoscope at the Second Affiliated Hospital of China Medical University between November 2001 and December 2003. All patients underwent cholecystectomy and choledochotomy, at least 1.5 mo (mean 2.5 mo) after T tube drainage. The patients were fasted overnight before manometry.

Methods

A triple lumen polyethylene manometry catheter 200 cm in length with an outer diameter of 1.7 mm was used for manometry. The three side holes in the distal end were located 2 mm apart. Sterile water was infused through the catheter at a flow rate of 0.5 mL/min by a hydraulic capillary infusion system. PC polygraph HR (Swedish CTD-Synetics medical company) and relevant program were used to record and analyze the tracings. Manometry was performed after all the stones were removed from the common bile duct. The catheter was introduced via the side-pore of choledochoscope into duodenum directly, when the pressure was stable, duodenal pressure-curve was recorded. It was then withdrawn in a stepwise fashion, the position of catheter in the sphincter could be confirmed by direct observation through choledochoscope or by the characteristic pressure changes on the screen. The Oddi's sphincter and common bile duct motility tracings were recorded respectively. Drugs were administered intramuscularly at 10 min intervals.

Patients were randomly administered one of the four different drugs. Morphine was administered in a dose of 0.1 mg/kg after the first measurement, the second and third manometries were performed respectively 10 min and 20 min later. Each of the other three analgesics was administered in a dose of 1 mg/kg. The procedures were same as in morphine group.

Basal pressure of Oddi's sphincter (BPOS), amplitude of phasic contractions (SOCA), frequency of phasic contractions (SOF), duration of phasic contractions (SOD), duodenal pressure (DP) and common bile duct pressure (CBDP) were recorded and analyzed with a special computer program. Statistical analysis was carried out using the Student's t- test.

Data were expressed as mean±SD. A single-tailed *P* value <0.05 was considered statistically significant.

RESULTS

Seventy patients with T-tubes had no evidence of ampullary abnormality underwent OSM. Clear tracings of pressure and phasic contractions were acquired. Data were compared.

Effect of morphine on Oddi's sphincter motility

Morphine at the dose of 0.1 mg/kg produced an immediate and marked stimulatory effect on the sphincter of Oddi and bile duct, which was obvious 10 min after injection. Levels of BPOS, SOCA, SOF and CBDP were all significantly increased ($P<0.01$) and the effect persisted for 20 min (Table 1). Ten patients (25%) had an increased BPOS between 30-40 mmHg, four patients had an increased BPOS over 40 mmHg after drug administration.

Effect of pethidine on Oddi's sphincter motility

No statistical difference before and after administration of pethidine (1 mg/kg). Pethidine showed no apparent effect on Oddi's sphincter motility (Table 2).

Effect of Ap-237 on Oddi's sphincter motility

Marked increased levels of BPOS, SOCA and SOF were observed 10 min after injection of Ap-237, and high levels of BPOS and SOF persisted for 20 min, which showed an excitatory effect on Oddi's sphincter motility (Table 3).

Effect of tramadol on Oddi's sphincter motility

Levels of BPOS and SOCA were obviously reduced 10 min after administration of tramadol, which maintained at low levels for 20 min and showed an inhibitory effect of tramadol on Oddi's sphincter motility. (Table 4)

DISCUSSION

The most important development in our understanding of Oddi's sphincter motility came with the advent of Oddi's sphincter manometry (OSM) in the mid-1970s. Then, it was considered as the gold standard method for evaluating the function of Oddi's sphincter. OSM could be directly performed during surgery, or

Table 1 Manometric data before and after administration of morphine in 40 patients (mean±SD)

	Before morphine administration (n = 40)	10 min after morphine administration (n = 40)	20 min after morphine administration (n = 10)
Oddi's sphincter basal pressure (mmHg)	8.90±9.11	22.23±16.04[b]	20.51±13.46[b]
Amplitude of phasic contractions (mmHg)	50.85±36.66	104.97±49.15[d]	89.04±62.37[d]
Frequency of phasic contractions (n/min)	7.22±2.89	9.29±1.93[f]	8.85±2.42[f]
Common bile duct pressure (mmHg)	4.97±3.87	8.62±7.43[h]	7.32±5.95[h]

[b]P, [d]P, [f]P, [h]$P<0.01$ *vs* themselves, n represents the number of patients involved in the research.

Table 2 Manometric data before and after administration of pethidine in 10 patients (mean±SD)

	Before pethidine administration (n = 10)	10 min after pethidine administration (n = 10)	19 min after pethidine administration 20 (n = 10)
Oddi's sphincter basal pressure (mmHg)	7.06±5.07	11.24±6.11	6.68±4.32
Amplitude of phasic contractions (mmHg)	78.52±40.23	95.65±45.49	70.35±31.67
Frequency of phasic contractions (n/min)	7.31±1.95	6.49±2.81	7.92±2.07
Common bile duct pressure (mmHg)	4.23±2.83	4.70±3.87	3.91±3.36

n represents the number of patients involved in the research.

Table 3 Manometric data before and after administration of Ap-237 in 10 patients (mean±SD)

	Before Ap-237 administration (n = 10)	10 min after Ap-237 administration (n = 10)	20 min after Ap-237 administration (n = 10)
Sphincter of Oddi basal pressure (mmHg)	6.42±5.10	11.33±9.39[a]	11.34±8.40[a]
Amplitude of phasic contractions (mmHg)	52.56±30.99	87.03±51.72[c]	50.06±29.11
Frequency of phasic contractions (n/min)	5.62±1.34	7.72±2.16[e]	9.28±3.98[f]
Common bile duct pressure (mmHg)	4.20±3.97	4.82±2.30	3.25±2.30

[a]P, [c]P, [e]$P<0.05$, [f]$P<0.01$ *vs* themselves, n represents the number of patients involved in the research.

Table 4 Manometric data before and after administration of tramadol in 10 patients (mean±SD)

	Before tramadol administration (n = 10)	10 min after tramadol administration (n = 10)	20 min after tramadol administration (n = 10)
Sphincter of Oddi basal pressure (mmHg)	7.01±5.50	2.87±2.78[a]	6.39±5.37
Amplitude of phasic contractions (mmHg)	63.34±35.29	45.90±27.86[c]	35.97±24.30[d]
Frequency of phasic contractions (n/min)	7.24±2.52	8.14±2.54	7.07±3.70
Common bile duct pressure (mmHg)	4.41±2.65	3.97±4.69	4.96±2.82

[a]P, [c]$P<0.05$, [d]$P<0.01$ *vs* themselves, n represents the number of patients involved in the research.

indirectly during ERCP, via a T-tube or percutaneously. A basal pressure and phasic contractions of Oddi's sphincter could be obtained with OSM.

OSM during ERCP is a useful tool in the evaluation of patients with unexplained pancreaticobiliary pain or recurrent idiopathic pancreatitis[5-7]. However, it might provoke serious pancreatitis[8,9]. It is a technical procedure, because it requires selective deep bile duct and/or pancreatic duct cannulation during active duodenal peristalsis and in suboptimally anesthetized patients. These features account for the relatively high failure rate (up to 20%) even in expert hands[10].

OSM *via* choledochoscopic approach allows easy and accurate recording of Oddi's sphincter pressure and makes a long time maneuver of manometry possible. The position of manometric catheter in the sphincter can be monitored on the screen with the characteristic phasic contractions. It also could be confirmed by direct observation through choledochofiberoscopy. And it is easy to get enough patients for manometry. However, it is difficult to get a relative normal value of the sphincter of Oddi via choledochoscope manometry, for patients with a T-tube tract often suffer from hepatobiliary or pancreatic diseases. Furthermore, whether irrigation of natural cold saline and the semi-closed state of bile duct during choledochoscopic procedure affect the motility of the sphincter of Oddi is unknown.

Morphine and pethidine are the two most commonly used analgesic drugs. Their effects on the sphincter of Oddi have well been researched. Helm *et al.*[11] studied the effect of morphine on SO using OSM during ERCP. In a small cumulative dose of 2.5-5 μg/kg, morphine increased the frequency of phasic contractions to a maximum of 10-12/min, but it did not affect the mean amplitude of phasic contractions and the mean SO basal pressure. As the cumulative dose was increased from 10 to 20 μg/kg, no further increase in the frequency of phasic pressure waves was seen. Instead, the phasic wave amplitude and the mean SO basal pressure increased. Blaut *et al.*[12] found that morphine increased the intraductal biliary pressure (IDP) with OSM via a T-tube, but the high intraductal biliary pressure caused by morphine could be counteracted by transcutaneous electrical nerve stimulation (TENS). Elta *et al.*[13] performed ERCP manometry to evaluate the effect of pethidine at therapeutic doses on SO manometry, and found that after administration of pethidine the frequency of phasic contractions increased, but the mean SO basal pressure did not change. Using the same method, Sherman *et al.*[14], found that biliary sphincter basal pressure and phasic wave amplitude were not significantly altered by pethidine, but phasic frequency increased and phasic duration decreased slightly after administration of pethidine, sphincter basal pressure of the pancreatic and the common channel's sphinctures was not significantly altered, but their phasic wave amplitude decreased, phasic frequency increased, and phasic duration decreased.

The only study directly comparing morphine to pethidine with OSM was done in 1990 by Thune *et al.*[15] They compared the effect of morphine and pethidine on patients intraoperatively after surgical placement of a catheter across the SO. Morphine was associated with an increase in phasic wave frequency, but no change was found in basal sphincter pressure, amplitude, or wave propagation direction. Pethidine showed a dose-dependent decrease in phasic wave frequency but without significant changes in the basal sphincter pressure, contraction amplitude or wave propagation direction.

We found that morphine could increase the basal pressure of Oddi' sphincter, common bile duct pressure, frequency and amplitude of phasic contractions. Morphine showed an excitatory effect on the sphincter of Oddi, and might be a cause of Oddi's sphincter dysfunction(SOD). SO may function as a peristaltic pump to actively expel fluid from the sphincter segment into the duodenum. The SO segment fills with fluid from the common bile duct (CBD) only during the diastolic interval between phasic contractions. Outflow of fluid from the CBD is reduced or arrested when (1) the frequency of phasic contractions increases sufficiently to compromise diastolic filling of the sphincter segment, (2) phasic contractions propagate retrograde or occur simultaneously along the sphincter segment, or (3) passive filling of the sphincter segment is prevented by a BPOS that exceeds the CBDP. Morphine could cause functional obstruction of the SO by all three of these mechanims[11]. OSM shows a diagnotic value for Oddi's sphincter dysfunction. Elevated basal pressure (>40 mmHg) was the most important manometric finding in Oddi's sphincter dysfunction and its borderline was about 30-40 mmHg. Our study found that 10 patients (25%) had an increased BPOS between 30-40 mmHg, four patients had an increased BPOS over 40 mmHg. So morphine can cause spasm of SO and should not be used during ERCP manometry or choledochoscope examination. After administration of pethidine, no patients had an elevated BPOS up to 30 mmHg. Pethidine could be used for an additional analgesia during OSM. This may improve both patient's tolerance and the success rate of the procedure. But we should be cautious in patients with renal failure, hepatic failure or central nervous system diseases. For the pethidine metabolite, normeperidine, might invoke seizures at high doses or in patients with renal failure. Hubbard[16] reports that pethidine invoked seizures in a patient with Oddi's sphincter dysfunction.

Tramadol has the same analgesic effect as morphine. But it has little effect on the respiratory system and circulation system, and can be used in old patients with respiratory system diseases. There were only a few researches about its effect on the sphincter of Oddi. Staritz *et al.*[17] and Brandstatter *et al.*[18] performed ERCP manometry to evaluate the effect of tramadol on SO manometry, and found that it had no apparent effect on Oddi's sphincter motility. Our study indicated that tramadol could decrease BPOS and the amplitude of phasic contractions, showing an inhibitory effect on the sphincter of Oddi, and tramadol could be used during ERCP manometry and choledochoscope examination.

As a fast acting analgesic, Ap-237 has little effect on visceral pain. A MEDLINE search found no report about its effect on the sphincter of Oddi. We found that Ap-237 could increase BPOS, amplitude and frequency of phasic contractions, showing an excitatory effect on the sphincter of Oddi, and Ap-237 should not be used in patients with hepatobiliary and pancreatic diseases.

REFERENCES

1 **Sarles JC**, Midejean A, Devaux MA. Electromyography of the sphincter of Oddi. Technic and experimental results in the rabbit: Effect of certain drugs. *Am J Gastroenterol* 1975; **63**: 221-231

2 **Dedrick DF**, Tanner WW, Bushkin FL. Common bile duct pressure during enflurane anesthesia. Effects of morphine and subsequent naloxone. *Arch Surg* 1980; **115**: 820-822

3 **Radnay PA**, Duncalf D, Novakovic M, Lesser ML. Common bile duct pressure changes after fentanyl, morphine, meperidine, butorphanol, and naloxone. *Anesth Analg* 1984; **63**: 441-444

4 **Joehl RJ**, Koch KL, Nahrwold DL. Opioid drugs cause bile duct obstruction during hepatobiliary scans. *Am J Surg* 1984; **147**: 134-138

5 **Coyle WJ**, Pineau BC, Tarnasky PR, Knapple WL, Aabakken L, Hoffman BJ, Cunningham JT, Hawes RH, Cotton PB. Evaluation of unexplained acute and acute recurrent pancreatitis using endoscopic retrograde cholangiopancreatography, sphincter of Oddi manometry and endoscopic ultrasound. *Endoscopy* 2002; **34**: 617-623

6 **Lehman GA**. Acute recurrent pancreatitis. *Can J Gastroenterol* 2003; **17**: 381-383

7 **Mariani A**, Curioni S, Zanello A, Passaretti S, Masci E, Rossi M, Del Maschio A, Testoni PA. Secretin MRCP and endoscopic

pancreatic manometry in the evaluation of sphincter of Oddi function: a comparative pilot study in patients with idiopathic recurrent pancreatitis. *Gastrointest Endosc* 2003; **58**: 847-852

8 **Rolny P**, Anderberg B, Ihse I, Lindstrom E, Olaison G, Arvill A. Pancreatitis after sphincter of Oddi manometry. *Gut* 1990; **31**: 821-824

9 **Maldonado ME**, Brady PG, Mamel JJ, Robinson B. Incidence of pancreatitis in patients undergoing sphincter of Oddi manometry (SOM). *Am J Gastroenterol* 1999; **94**: 387-390

10 **Kowalski T**, Kanchana T, Pungpapong S. Perceptions of gastroenterology fellows regarding ERCP competency and training. *Gastrointest Endosc* 2003; **58**: 412-414

11 **Helm JF**, Venu RP, Geenen JE, Hogan WJ, Dodds WJ, Toouli J, Arndorfer RC. Effects of morphine on the human sphincter of Oddi. *Gut* 1988; **29**: 1402-1407

12 **Blaut U,** Marecik J, Hartwich A, Herman RM, Laskiewicz J, Thor PJ. The effect of transcutaneous nerve stimulation on intraductal biliary pressure in post-cholecystectomy patients with T-drainage. *Eur J Gastroenterol Hepatol* 2003; **15**: 21-26

13 **Elta GH**, Barnett JL. Meperidine need not be proscribed during sphincter of Oddi manometry. *Gastrointest Endosc* 1994; **40**: 7-9

14 **Sherman S**, Gottlieb K, Uzer MF, Smith MT, Khusro QE, Earle DT, Brunelle RL, Hawes RH, Lehman GA. Effects of meperidine on the pancreatic and biliary sphincter. *Gastrointest Endosc* 1996; **44**: 239-242

15 **Thune A**, Baker RA, Saccone GT, Owen H, Toouli J. Differing effects of pethidine and morphine on human sphincter of Oddi motility. *Br J Surg* 1990; **77**: 992-995

16 **Hubbard GP**, Wolfe KR. Meperidine misuse in a patient with sphincter of Oddi dysfunction. *Ann Pharmacother* 2003; **37**: 534-537

17 **Staritz M,** Poralla T, Manns M, Meyer Zum Buschenfelde KH. Effect of modern analgesic drugs (tramadol, pentazocine and buprenorphine) on the bile duct sphincter in man. *Gut* 1986; **27**: 567-569

18 **Brandstatter G**, Schinzel S, Wurzer H. Influence of spasmolytic analgesics on motility of sphincter of Oddi. *Dig Dis Sci* 1996; **41**: 1814-1818

Edited by Wang XL and Ren SY **Proofread by** Xu FM

PO Box 2345, Beijing 100023, China
Fax: +86-10-85381893
E-mail: wjg@wjgnet.com www.wjgnet.com

World J Gastroenterol 2004;10(19):2905-2907
World Journal of Gastroenterology
Copyright © 2004 by The WJG Press ISSN 1007-9327

• BRIEF REPORTS •

Angiographic findings of gastrointestinal stromal tumor

Song-Hua Fang, Dan-Jun Dong, Shi-Zheng Zhang, Mei Jin

Song-Hua Fang, Dan-Jun Dong, Shi-Zheng Zhang, Department of Radiology, Sir Run Run Shaw Hospital, Zhejiang University, Hangzhou 310016, Zhejiang Province, China
Mei Jin, Department of Pathology, Sir Run Run Shaw Hospital, Zhejiang University, Hangzhou 310016, Zhejiang Province, China
Correspondence to: Song-Hua Fang, Department of Radiology, Sir Run Run Shaw Hospital, Zhejiang University, Hangzhou 310016, Zhejiang Province, China. fangsonghua@163.com
Telephone: +86-571-86090073 Ext. 4609
Received: 2004-02-06 **Accepted:** 2004-03-04

Abstract

AIM: To discuss the angiographic features of gastrointestinal stromal tumor (GIST) and to evaluate their diagnostic role.

METHODS: Twelve patients with pathologically proved GIST underwent angiography (DSA)1 wk before operation, using Puck and digital subtraction DSA. The origin, size, morphology and angiographic appearance of the lesions were reviewed.

RESULTS: Two tumors arose from stomach, 8 from jejunum, and 2 from ileum. Seven cases were benign and 5 were malignant. Obviously thickened supplying arteries were detected in 8 tumors, and early-developed veins were found in 3. Two types of angiographic changes of GIST were observed. Four cases had twisted irregular neoplastic vessels with partially coarse and indistinct margins, which were all malignant. Eight cases had ball-like neoplastic vessels with uniform tumor staining, of which 7 were benign and 1 was malignant.

CONCLUSION: Angiography facilitates localization and diagnosis of GIST, helps define their size, range and location, and is especially valuable to patients suffering from melena with unknown reasons.

Fang SH, Dong DJ, Zhang SZ, Jin M. Angiographic findings of gastrointestinal stromal tumor. *World J Gastroenterol* 2004; 10(19): 2905-2907
http://www.wjgnet.com/1007-9327/10/2905.asp

INTRODUCTION

Gastrointestinal stromal tumor and its imaging features have been reported[1-3]. However, to our knowledge, the appearance of GIST at angiography has been seldom discussed. We analyzed retrospectively the angiographic appearance of 12 cases of GIST, which was proved by surgical pathology (immunohistochemistry), and the diagnostic value of angiography was discussed.

MATERIALS AND METHODS

Subjects

Twelve patients (4 women and 8 men, aged 40-70 years with a mean age of 53.3 years) with pathologically proved GIST (immunohistochemistry) who underwent angiography 1 wk before surgery were included. All the patients suffered from recurrent melena for 3 mo to 3 years, with syncope in 2 cases, a palpable abdominal mass in 1 case, and concomitant abdominal pain in another case.

After routine preparations, Seldinger's puncture of femoral artery and super selective catherization, angiographies of superior mesenteric artery, inferior mesenteric artery and coeliac trunk were performed sequentially using 6-7 F catheters. Omnipaque (iodine content: 350 mg/mL) as contrast medium was administered with a dose of 30 mL and at a rate of 8 mL/s for superior mesenteric artery, 20 mL/s and 6 mL/s for inferior mesenteric artery, and 40 mL/s and 8 mL/s for celiac trunk. Puck changer was used in all angiographies (with the sequence 2 films/s×3 s, 1 film/s×4 s, 1 film/2 s×4 s), and DSA was selected necessarily (with acquisition sequence 3.1 films/s×5 s, 1.6 films/s×5 s, 1 film/s×2 s). The dose and rate of contrast medium were same in two methods. The apparatus was GE medical systems, Hiline.

RESULTS

Size origin and morphology of the tumors

Two tumors arose from stomach, 8 from jejunum (Figures 1,2), and 2 from ileum. Most of them were originated from the jejunum with a percentage of 66.7% (8/12). The lesions had different sizes, ranged from 3 cm×3 cm×2 cm to 5 cm×6 cm×4 cm (mean 4 cm×4.5 cm×3 cm) in 7 benign lesions, of which 5 lesions were malignant (Figure 3). The smallest was 5.5 cm×4.5 cm×3 cm and the largest was 6.5 cm×10 cm×7 cm. All tumors were round or oval in shape, except an irregular malignant tumor and another dumbbell-shaped benign tumor growing endophytically and exophytically from the intestinal lumen at the same time.

Angiographic appearance

Thickened supplying arteries were observed in 8 tumors (Figure 1), of which 6 were benign and 2 were malignant. Early-developed veins were found in 3 cases (Figure 1), all of which were benign. Four cases having irregular twisted neoplastic vessels with different vessel size and partially coarse and obscure vessel margin were all malignant (Figure 3). Eight cases have ball-like neoplastic vessels with clear margins, included 7 benign and 1 malignant cases. However, the 7 benign cases all had predominantly homogeneous tumor staining with distinct margins (Figures 1, 2).

Boundary of tumors and relationship to surrounding structures

Four malignant tumors had an indistinct border, and the others had a clear margin. The surrounding organs were pushed by the tumors. Intestinal intussusception was found in 1 patient with recurrent abdominal pain.

Pathology

The neoplastic cells were fusiform or polygon in shape, and arranged in interlacing or swirl or fence-like. LSAB label was used in immunohistochemistry. Leiomyomas or leiomyosarcomas of other organs (uterus and soft tissue) and shwannomas of soft tissue were chosen for comparisons. High positive presentation of Vim, CD_{117} and CD_{34} was found in 12 cases of GIST. Negative presentation of CD_{34} was found in leiomyomas or leiomyosarcomas, and positive S-100 and negative CD_{34} were found in shwannomas.

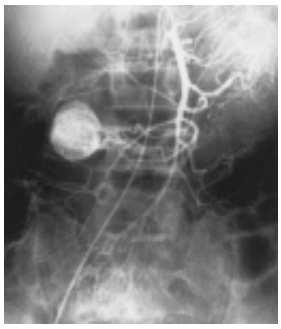

Figure 1 Benign stromal tumor in a 54-year-old male.

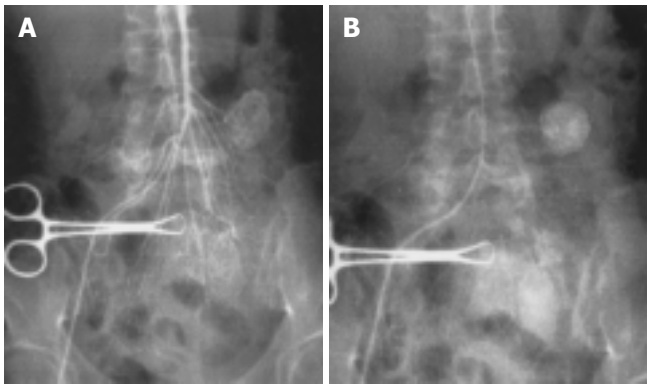

Figure 2 Benign stromal tumor and marked homogeneous tumor-staining in a 41-year-old male. A: Benign stromal tumor; B: Marked homogeneous tumor staining.

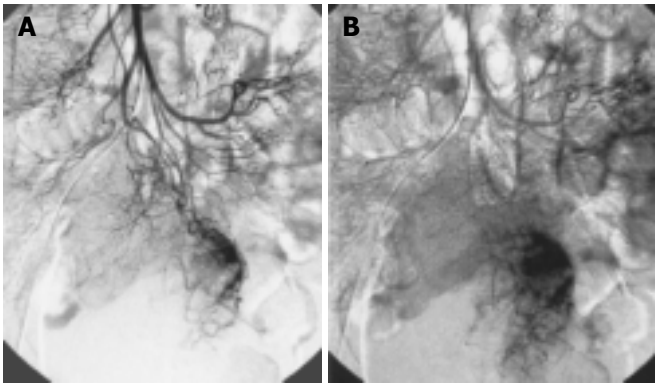

Figure 3 Malignant stromal tumor and heterogeneous tumor staining in a 35-year-old female. A: Malignant stromal tumor; B: Heterogeneous tumor staining with irregular morphology.

Others

Five malignant tumors contained necrotic or cystic changes with different degrees and two possessed central hemorrhage. Six patients in this study underwent CT at the same time. Masses were revealed by CT in 4 cases, only intestinal intussusception was seen in 1 patient, and diagnosis could not be established with confidence in the other case because of the relatively small size. Of the 3 patients who underwent barium examinations, one was normal, one had an intestinal filling defect and another had his intestines pushed away. No metastasis was found before surgery and no lymphadenopathy was demonstrated during operation.

DISCUSSION

GIST included the majority of primary non-epithelial tumors of gastrointestinal (GI) tract. These tumors were originated from cells located in the wall of the organ and showed a remarkable variability in their differentiation pathways. They can be divided into 4 major categories on the basis of their phenotypical features: tumors showing differentiation toward smooth muscle, tumors showing apparent differentiation toward neural elements, tumors showing dual differentiation toward smooth muscle and neural elements, tumors lacking differentiation toward either cell type even after exhaustive immunohistochemical and ultrastructural probing[4,5]. However, with the development in immunohistochemistry and ultrastructural probing, it has been agreed generally that GIST is an independent kind of tumors originated from primitive mesenchymal cells of GI tract with non-directive differentiation, some of which have incomplete differentiation parts of smooth muscles and/or nerve sheath cells[1,6-8]. Micro superstructures of these tumors are similar to those of primitive mesenchymal cells without any characteristics of differentiated cellularity. Vim, CD_{117} and CD_{34} are highly presented in immunohistochemistry. The standards were all compliant in this study.

GIST could be localized in any portion of the GI tract, but was most often found in the gastric part[9,10]. The jejunum as the most frequent place (66.7%) in this group did not reflect the fact, because it is not necessary for gastric lesion to do angiography when endoscopy, endoluminal ultrasonogrphy or barium study was available and effective.

CT and MR imaging features have been reported previously[1-3,10]. To our knowledge, however, few articles included a description of the appearance of GIST on angiography. According to our study, tdwo types of angiographic changes could be concluded. First, abnormally distributed twisted neoplastic vessels with different thickness and obscure margin were one of the malignant features, and heterogeneous tumor blush with ill-defined border in capillary phase was another. Second ball like vessels with a clear margin, well defined homogeneous tumor staining in round or oval shape, and early-developed veins, suggested a benign GIST. The differentiation points have been described in many previous documents already, including that the malignant tumor was characterized by a larger size more than 5 cm, necrosis, hemorrhage, an indistinct border, and adherence to or direct invasion of the structures nearby[5,11]. The tumors in our group with first type of manifestations were all malignant, but they were found in a relatively small number of patients.

There are many diagnostic approaches for GIST, including barium meal, double-contrast barium study, ultrasonography, fibro-endoscopy, endoluminal ultrasonography, CT, MR imaging and angiography. The sensitivity of these procedures varied according to the different sites of lesions. CT has been considered as the most effective method[1,9]. Therefore, angiography is used less and less in diagnosing tumors of GI, as a result, angiography is only recommended for patients with melena when no abdominal mass is palpable and the examination of upper GI is negative. It helps indicate the supplying arteries, differentiate benign from malignant tumors, and define their size, range and origin, despite the tumors grow exophytically or endophytically. On the other hand, we do not suggest routine use of this procedure because of its traumatic property, high risk and relative complicated technique.

REFERENCES

1 **Belloni M,** De Fiori E, Mazzarol G, Curti A, Crosta C. Endoscopic ultrasound and computed tomography in gastric stromal tumours. *Radiol Med* 2002; **103**: 65-73

2 **Pisanu A,** Ambu R, Uccheddu A. Uncommitted gastrointestinal stromal tumour. Case report. *G Chir* 2001; **22**: 217-221

3 **Kitabayashi K**, Seki T, Kishimoto K, Saitoh H, Ueno K, Kita I, Takashimas, Kurose N, Nojima T. A spontaneously ruptured

gastric stromal tumor presenting as generalized peritonitis: report of a case. *Surg Today* 2001; **31**: 350-354

4 **LaRock RG,** Ginn PE. Immunohistochemical staining characteristics of canine gastrointestinal stromal tumors. *Vet Pathol* 1997; **34**: 303-311

5 **Rosai J**. Gastriointestinal tract. In: Rosai J, ed. Ackerman's surgical pathology. 8th ed. *Mosby-year Book Inc U S A* 1996: 645-648

6 **Tworek JA,** Appelman HD, Singleton TP, Greenson JK. Stromal tumors of the jejunum and ileum. *Mod Pathol* 1997; **10**: 200-209

7 **Spivach A,** Zanconati F, Bonifacio Gori D, Pellegrino M, Sinconi A. Stromal tumors of the small intestine (GIST). Prognostic differences based on clinical, morphological and immunophenotypic features. *Minerva Chir* 1999; **54**: 717-724

8 **Mignon F,** Julie C, Izzillo R, Luciani A, Guichoux F, Mesurolle B, El Hajam M, Qanadli SD, Chagnon S, Lacombe P. Imaging features of gastric stromal tumors: radiologic-pathologic correlation. Report of 4 cases. *J Radiol* 2000; **81**: 874-881

9 **Wiener Y,** Gold R, Zehavy S, Sandbank J, Halevy A. Primary gastrointestinal stromal tumors. *Harefuah* 2001; **14**: 377-380

10 **Hasegawa S,** Semelka RC, Noone TC, Woosley JT, Marcos HB, Kenney PJ, Siegelman ES. Gastric stromal sarcomas: correlation of MR imaging and histopathologic findings in nine patients. *Radiology* 1998; **208**: 591-595

11 **Lin SC,** Huang MJ, Zeng CY, Wang TI, Liu ZL, Shiay RK. Clinical manifestations and prognostic factors in patients with gastrointestinal stromal tumors. *World J Gastroenterol* 2003; **9**: 2809-2812

Edited by Wang XL and Chen WW **Proofread by** Xu FM

PO Box 2345, Beijing 100023, China
Fax: +86-10-85381893
E-mail: wjg@wjgnet.com www.wjgnet.com

World J Gastroenterol 2004;10(19):2908-2910
World Journal of Gastroenterology
Copyright © 2004 by The WJG Press ISSN 1007-9327

• BRIEF REPORTS •

Expression of growth hormone and its receptor in chronic atrophic gastritis and its clinical significance

Jian-Min Si, Qian Cao, Min Gao

Jian-Min Si, Qian Cao, Min Gao, Gastroenterology Laboratory, Institute of Clinical Medicine, Sir Run Run Shaw hospital, School of Medicine, Zhejiang University, Hangzhou 310016, Zhejiang Province, China
Correspondence to: Dr. Qian Cao, Department of Gastroenterology of Sir Run Run Shaw Hospital, Zhejiang University, School of Medicine, Hangzhou 310016, Zhejiang Province, China. wcjd@public.bta.net.cn
Telephone: +86-571-86090073-4503 **Fax:** +86-571-86044718
Received: 2002-11-30 **Accepted:** 2003-03-16

Abstract

AIM: To investigate the growth hormone (GH) and growth hormone receptor (GHR) expression of and its clinical significance in patients with chronic atrophic gastritis (CAG).

METHODS: A total of 90 cases were enrolled in the study. Thirty were healthy controls, the other 60 patients were divided into two groups according to the endoscopical and histological diagnosis. Blood samples were drawn in the morning (menarche did not occur during the blood extraction in female patients), gastric mucosa was obtained by endoscopy. Serum GH and gastrice mucosal GHR levels were measured using radioimmunoassay (RIA) and En Vinsion technique.

RESULTS: The average GH level was 1.021±0.132 μg/L in CAG patients, in controls it was 2.869±0.512 μg/L. There was a significant difference between these two groups (P<0.01). The positive rate of GHR in CAG patients was 10%, in controls the rate was 100%. There was a significant difference (P<0.01). There was no significant change of GH level (3.176±0.421 μg/L) in patients with gastric carcinoma compared with controls (P>0.05).

CONCLUSION: The study shows that levels of GH and GHR expression are low in CAG patients. CAG pathogenesis has a correlation with mucosal nutrient deficiency, decreased levels of GH and GHR have an adverse effect on the repair and regeneration of CAG. There is no significant change of GH in gastric carcinorma patients, GH dose not play a role in the pathogenesis of gastric cancer.

Si JM, Cao Q, Gao M. Expression of growth hormone and its receptor in chronic atrophic gastritis and its clinical significance. *World J Gastroenterol* 2004; 10(19): 2908-2910
http://www.wjgnet.com/1007-9327/10/2908.asp

INTRODUCTION

Growth factor family is a group of protein hormones discovered during the 20th century. This family includes growth hormone (GH), insulin-like growth factor (ILGF), epidermal growth factor (EGF), transfer growth factor (TGF), and vascular endothelial growth factor (VEGF), *etc*. These factors can stimulate cell DNA, RNA and protein synthesis, control cell growth and differentiation, and promote regeneration of injured epithelia[1-7]. Studies in recent years have shown that there is an intimate relationship between growth factor and gastric mucosal disease[6]. Growth hormone (GH) is a type of monopeptide strain hormone released from anterior pituitary eosinophilic cells. In the gastrointestinal (GI) tract, GH is known to promote water and electrolyte transport and calcium absorption. The proliferative functions of GH have been reported as well. Administration of GH restores the intestinal and gastric mucosal weight after hypophysectomy in rats, it is regarded as an important nutrient factor[8].

Chronic atrophic gastritis (CAG) is a gastric precancerous lesion and has a high morbidity in China[9]. Gastric mucosal malnutrient is considered as an important factor in the pathogenesis of CAG[10-13].

Since CAG was recognized as a precancerous condition of the stomach by the World Health Organization in the early 1980 s, a number of methods have been tested for their ability to reverse and prevent the development of cancer. Most gastric mucosa protectors promote the growth and repair of gastric mucosa by promoting the aggregation and secretion of growth factors such as EGF, TGF. In a previous animal study, GH/GHR expression was measured on atrophic gastritis rats. The levels of GH and GHR expression in rats with CAG were low[14]. However, the effect and safety of GH in clinical use are uncertain in CAG. The purpose of the present study was to investigate the expression of GH/GHR in patients with CAG and gastric cancers.

MATERIALS AND METHODS

Research subjects

Ethical approval for this study was given by the Sir Run Run Shaw Hospital in May 1999. Clinical data were obtained by review of case records for all patients. Patients were selected at random from adult out-patients attending the gastroenterology clinics. Diagnosis was made on the basis of clinical, endoscopical and histological data according to standard criteria. We excluded the patients who had abnormal findings in other vital organs (such as the heart, liver, lung, pancreas and pituitary). Patients were divided in two groups. Thirty patients in group B were diagnosed as moderate-severe gastritis and 30 patients in group C were diagnosed as gastric cancer, 30 unrelated individuals served as controls. Characteristics of the research subjects are shown in Table 1.

Sample collection and processing

After an overnight fast, 3 mL of blood was taken from cubital vein. Blood samples were set for two hours, then centrifuged at 3 500 rpm for 15 min. Supernatant was saved and stored at -20 ℃. Two samples were taken from gastric antrum tissue and two from gastric body tissue, or four from the primary focus, and immediately immersed in 10% buffered formalin and embedded in paraffin wax using standard techniques. Five μm thick sections were cut and stained with hematoxylin and eosin for histopathological analysis. Each slide was assessed.

Analytical methods

The level of serum GH was measured by radioimmunoassay

(RIA) (Reagents were from DPC Company in Tianjing). The detection of gastric mucosal GHR expression was carried out by immunohistochemistry and En Vinsion assay (reagents from Biogenesis Company).

Table 1 Base-line characteristics of the patients

Characteristic	Group A (n = 30)	Group B (n = 30)	Group C (n = 30)
Age (yr)	48±7	50±6	52±9
Male	19	17	20
Female	11	13	10
Endoscopical finding	normal gastric mucosa	chronic atrophic gastritis(CAG)	gastric cancer
Pathologic finding	mild superficial gastritis(non-active)	moderate-severe CAG with or without intestinal malplasia	gastric cancer

Statistical analysis

Concentrations of serum GH were expressed as mean±SD. Differences between the two groups were evaluated by *t*-test. Significance was shown as $P<0.05$. The expression of GHR was expressed as positive rate. Differences between groups were evaluated by χ^2 test. Significance was shown as $P<0.05$. All experimental data were analyzed with Spss-pc+ software.

RESULTS

The average level of serum GH was lower in group B than in groups A and C. There were significant differences between them, but there was no significant difference between groups A and C.

Table 2 Serum GH Level (ng/mL) in the studied groups (mean±SD)

Group	A group (n = 30)	B group (n = 30)	C group (n = 30)
GH level	$2.869\pm0.512^{1,2}$	1.021 ± 0.132^{1}	3.176 ± 0.421^{2}

$^1t_{AB} = 3.135$ $P<0.01$ $^1t_{BC} = 3.537$ $P<0.01$ $^2t_{AC} = 1.893$ $P>0.05$.

Table 3 Positive rate of gastric mucosal GHR expression in the studied groups (%)

Group	A group (n = 30)	B group (n = 30)	C group (n = 30)
GHR expression	100 (30/30)^1	10 (3/30)^2	13 (4/30)^{1,2}

$^1\chi^2_{AB}=49$ $P<0.01$ $^1\chi^2_{AC}=45$ $P<0.01$ $^2\chi^2_{BC} = 0.16$ $P>0.05$.

The positive rate of gastric mucosal GHR expression in groups B and C was lower than that in group A. There were significant differences between them, but there was no difference between groups B and C.

DISCUSSION

Growth hormone (GH) is a type of monopeptide strain hormones released from anterior pituitary eosinophilic cells. Growth hormone receptor (GHR) is widely distributed in the gastrointestinal tracts. GH takes its effect on target tissues by combining with GHR. In the stomach, GHR is mainly distributed among parietal and chief cells. In 1995, Nagano *etc* by using reverse transcription PCR technology and Southern blot analysis, found the wide distribution of GHR in the gastrointestinal tract especially in epidermal cells, suggesting that GH and GHR could play an important role in the regulation of metabolism, growth, and differentiation of gastric mucosal cells. GH and GHR could improve protein synthesis, promote wound healing, stimulate gastrointestinal tract proliferation and repair, regulate immunological responses, and improve absorption of nutrients[8]. Presently, clinical applications of recombinant human growth hormone (rhGH) in various gastrointestinal ailments such as malabsorption and short bowel syndrome were reported[15-19].

Chronic atrophic gastritis (CAG) is a gastric precancerous lesion and listed as the first of cancer prevention by WTO. CAG pathogenesis has a correlation with mucosal nutrient deficiency. CAG patients had a decreased serum level of trace elements and beta-carotene with malnutrition[20-21].

During the last several years, we have focused on exploring the correlation between CAG and GH. In a previous animal study, we measured the GH/GHR expression in atrophic gastritis rats, and found the levels of GH and GHR expression in rats with CAG were rather low. After removing the pituitary glands from rats, Crean GP discovered that there were gastric mucosal atrophy, shrinkage and decreased expression of parietal and chief cells. Increased secretion of gastric acid and pepsin, and exogenous GH have been shown to promote protein synthesis and increase gastrointestinal absorption of nutrients. We have considered using GH to treat CAG[14].

Our present study showed the same results as before[14]. The levels of GH/GHR expression in patients with CAG were significantly lower than normal. GH and GHR could regulate the metabolism, growth and differentiation of gastrointestinal epidermal cells, therefore, a decreased GH/GHR level would hinder the repair and recovery of CAG. Decreased levels of GH and GHR had an adverse effect on the progression of CAG. This study suggests that when CAG is treated, GH or GH-like drugs may be considered in the treatment regimen to promote mucosal repair and stop the progression of CAG.

Exogenous GH has been shown to significantly increase the expression of c-myc oncogene[22]. Watanabe *et al*.[23] showed that by using N-methyl-N-nitrosourea solution to induce gastric cancer in F344 rats, GH levels were elevated, suggesting that high concentrations of GH play a role in the pathogenesis of gastric cancer. Studies have shown that acromegalic patients, had an increased risk of developing gastrointestinal tumor and carcinoma[24-28]. Therefore, cautions should be taken to monitor the possibilities of gastrointestinal cancers. Whether clinical usage of growth hormone and medicine which stimulates the release of growth hormone causes the carcinogenesis of atrophic gastritis is concerned. Our study showed that the serum GH level in gastric cancer patients and normal individuals was similar, the positivity rate of GHR expression was not high, suggesting that GH dose not play a role in the development of gastric cancer. Lobie *et al*.[29] investigated the effect of GH on gastric structure and function in GH-deficient Lewis (dwarf) rats, Bovine GH (65 micrograms/100 g body wt), was administered twice daily to adult male dwarf rats for 6 d (DW+) while control animals received vehicle only (DW-). Administration of GH produced a significant increase in body ,stomach wt and stomach to body wt ratio. GH administration also resulted in an increase of total gastric DNA, RNA, and protein. The density of differentiated (parietal and chief) cell types was not significantly different in DW- and DW+ animals. They demonstrated that GH could stimulate proliferation and enlargement of the gastric mucosae without significant alterations in cellular composition. So we recommend using GH as a treatment agent for CAG, but a definite conclusion needs further clinical observations.

REFERENCES

1 **Arzt E**, Pereda MP, Castro CP, Pagotto U, Renner U, Stalla GK. Pathophysiological role of the cytokine network in the an-

terior pituitary gland. *Front Neuroendocrinol* 1999; **20**: 71-95
2 **Li HW**, Wang JB. Study on TGFβ_1, TGFβ_2, TGFβ_3 expression in the chick basilar papilla following gentamicin toxicity. *Lingchuang Erbiyanhouke Zazhi* 1998; **12**: 463-465
3 **Shirakata Y**, Komurasaki T, Toyoda H, Hanakawa Y, Yamasaki K, Tokumaru S, Sayama K, Hashimoto K. Epiregulin, a novel member of the epidermal growth factor family, is an autocrine growth factor in normal human keratinocytes. *J Biol Chem* 2000; **275**: 5748-5753
4 **Kobayashi T**, Hashimoto K, Okumura H, Asada H, Yoshikawa K. Endogenous EGF-family growth factors are necessary for the progression from the G1 to S phase in human keratinocytes. *J Invest Dermatol* 1998; **111**: 616-620
5 **Zushi S**, Shinomura Y, Kiyohara T, Miyazaki Y, Tsutsui S, Sugimachi M, Higashimoto Y, Kanayama S, Matsuzawa Y. Role of heparin-binding EGF-related peptides in proliferation and apoptosis of activated ras-stimulated intestinal epithelial cells. *Int J Cancer* 1997; **73**: 917-923
6 **Abe S,** Sasano H, Katoh K, Ohara S, Arikawa T, Noguchi T, Asaki S, Yasui W, Tahara E, Nagura H, Toyota T. Immunohistochemical studies on EGF family growth factors in normal and ulcerated human gastric mucosa. *Dig Dis Sci* 1997; **42**: 1199-1209
7 **Ono I**, Gunji H, Zhang JZ, Maruyama K, Kaneko F. Studies on cytokines related to wound healing in donor site wound fluid. *J Dermatol Sci* 1995; **10**: 241-245
8 **Nagano M**, Chastre E, Choquet A, Bara J, Gespach C, Kelly PA. Expression of prolactin and growth hormone receptor genes and their isoforms in the gastrointestinal tract. *Am J Physiol* 1995; **268**(3 Pt 1): G431-G442
9 **Pan GZ**, Chao SZ, Liu TH, Lu XH, Chen YF, Chen SP. Contemporary Gastroenterology. 1st ed. Beijing: *Science Pub* 1998: 991
10 **You WC**, Blot WJ, Li JY, Chang YS, Jin ML, Kneller R, Zhang L, Han ZX, Zeng XR, Liu WD. Precancerous gastric lesions in a population at high risk of stomach cancer. *Cancer Res* 1993; **53**: 1317-1321
11 **Fukao A**, Hisamichi S, Ohsato N, Fujino N, Endo N, Iha M. Correlation between the prevalence of gastritis and gastric cancer in Japan. *Cancer Causes Control* 1993; **4**: 17-20
12 **Jin GQ**, Yao JS, Jiang YN, Zhu HW, Ye YG, He MJ, Xiao SD. Observasion on gastric mucosa of the healthy elderly. *Zhonghua Xiaohua Zazhi* 1984; **4**: 18-19
13 **Krasinski SD**, Russell RM, Samloff IM, Jacob RA, Dallal GE, McGandy RB, Hartz SC. Fundic atrophic gastritis in an elderly population. Effect on hemoglobin and several serum nutritional indicators. *J Am Geriatr Soc* 1986; **34**: 800-806
14 **Cao Q**, Si JM, Li XL. GH/GHR expression on atrophic gastritis in rats. *Zhonghua Xiaohua Zazhi* 2001; **21**: 627-628
15 **Jeppesen PB**, Mortensen PB. Enhancing bowel adaptation in short bowel syndrome. *Curr Gastroenterol Rep* 2002; **4**: 338-347
16 **Zhu WM**, Li N, Ren JA, Gu J, Jiang J, Li JS. Rehabilitation therapy for short bowel syndrome. *Chin Med J* 2002; **115**: 776-778
17 **Scolapio JS**. Treatment of short-bowel syndrome. *Curr Opin Clin Nutr Metab Care* 2001; **4**: 557-560
18 **Gu Y**, Wu ZH, Xie JX, Jin DY, Zhou HC. Effects of growth hormone (rhGH) and glutamine supplemented parenteral nutrition on intestinal adaptation in short bowel rats. *Clin Nutr* 2001; **20**: 159-166
19 **Ukleja A**, Tammela LJ, Lankisch MR, Scolapio JS. Nutritional support for the patient with short-bowel syndrome. *Curr Gastroenterol Rep* 1999; **1**: 331-334
20 **Bukin YV**, Zaridze DG, Draudin-Krylenko VA, Orlov EN, Sigacheva NA, Dawei F, Kurtzman MYA, Schlenskaya IN, Gorbacheva ON, Nechipai AM. Effect of beta-carotene supplementation on the activity of ornithine decarboxylase (ODC) in stomach mucosa of patients with chronic atrophic gastritis. *Eur J Cancer Prev* 1993; **2**: 61-68
21 **Palli D**, Decarli A, Cipriani F, Forman D, Amadori D, Avellini C, Giacosa A, Manca P, Russo A, Salkeld RM. Plasma pepsinogens, nutrients, and diet in areas of Italy at varying gastric cancer risk. *Cancer Epidemiol Biomarkers Prev* 1991; **1**: 45-50
22 **Murphy J**, Bell GI, Friesen HG. Growth hormone stimulates sequential induction of c-myc and insulin-like growth factor I expression *in vivo*. *Endocrinology* 1987; **120**: 1806-1812
23 **Watanabe H**, Fujimoto N, Kawamoto K, Ando Y, Yamada K, Okamoto T, Kanin GN, Ito A. Elevated serum growth hormone accelerates gastric tumorigenesis in F344 rats after treatment with N-methyl-N-nitrosourea in their drinking water. *Jpn J Cancer Res* 1995; **86**: 631-637
24 **Ezzat S**, Strom C, Melmed S. Colon polyps in acromegaly. *Ann Intern Med* 1991; **114:** 754-755
25 **Pines A**, Rozen P, Ron E, Gilat T. Gastrointestinal tumors in acromegalic patients. *Am J Gastroenterol* 1985; **80**: 266-269
26 **Asai K**, Shimoyama S, Sanno N, Kaminishi M, Oohara T. A rare case of gastric cancer in an acromegalic patient. *J Gastroenterol* 1997; **32**: 528-532
27 **Kojima K**, Miyake M, Nakagawa H, Yunoki Y, Ogurusu K, Saino S, Wani T, Kawaguchi Y. Multiple gastric carcinoids and pituitary adenoma in type A gastritis. *Intern Med* 1997; **36**: 787-789
28 **Papotti M**, Cassoni P, Volante M, Deghenghi R, Muccioli G, Ghigo E. Ghrelin-producing endocrine tumors of the stomach and intestine. *J Clini Endocrinol Metab* 2001; **86**: 5052-5059
29 **Lobie PE**, Garcia-Aragon J, Waters MJ. Growth hormone (GH) regulation of gastric structure and function in the GH-deficient rat: up-regulation of intrinsic factor. *Endocrinology* 1992; **130**: 3015-3024

Edited by Wang XL and Zhu L **Proofread by** Xu FM

PO Box 2345, Beijing 100023, China
Fax: +86-10-85381893
E-mail: wjg@wjgnet.com www.wjgnet.com

World J Gastroenterol 2004;10(19):2911-2915
World Journal of Gastroenterology
Copyright © 2004 by The WJG Press ISSN 1007-9327

• BRIEF REPORTS •

Clinical and experimental study of oxaliplatin in treating human gastric carcinoma

Wan-Long Lin, Ding-Guo Li, Qiang Chen, Han-Ming Lu

Wan-Long Lin, Ding-Guo Li, Qiang Chen, Han-Ming Lu, Department of Gastroenterology, Affiliated Xinhua Hospital, Shanghai Second Medical University, Shanghai 200092, China
Correspondence to: Dr. Wan-Long Lin, Department of Gastroenterology, Affiliated Xinhua Hospital, Shanghai Second Medical University, Shanghai 200092, China. linwanlong155@sohu.com
Telephone: +86-21-56748087
Received: 2003-09-18 **Accepted:** 2003-10-27

Abstract

AIM: To evaluate the therapeutic effectiveness of oxaliplatin on human gastric carcinoma and to explore its mechanisms.

METHODS: Twenty-two cases of stage IV gastric carcinoma received 4-6 (mean 4.6) cycles of first line combined chemotherapy with oxaliplatin (oxaliplatin 85 mg/m^2, iv, gtt, 1 h, d 1; leukovorin 200 mg/m^2, iv, gtt, 1 h, d 1 and d 2; 5-FU 300 mg/m^2,iv, d 1 and d 2, 5-FU, continuous iv, gtt, 48 h; 1 cycle/2 wk). Response rate, progression-free survival (PFS), total survival time, toxic side effects were evaluated. The inhibitory effect of oxaliplatin on human gastric cell line SGC-7901 was detected and IC_{50} was calculated by MTT. Transmission electron microscopy, flow cytometry and TUNEL were performed to evaluate the apoptosis of cell line induced by the drug. The expression of Caspase-3 m-RNA was detected by RT-PCR. AC-DEVD-CHO, a Caspase-3 specific inhibitor, was used to elucidate the role of activated Caspase-3 in the process of apoptosis induced by oxaliplatin.

RESULTS: Total response (complete and partial) occurred in 9 (40.9%) patients. Mean PFS was 4.2 mo and mean total survival time was 7.2 mo. Cumulative neurotoxicity (all grade I-II), vomiting and diarrhea, myelosuppression appeared in 93.5%, 20%, 32.9% patients, respectively. IC_{50} was calculated to be 0.71 mg/L by MTT assay. A maximal inhibitory rate reached 85.3%. Apoptosis index was elevated after incubated with 1 mmol/L oxaliplatin for 30 min, but without statistic significance (P>0.05). However it could be detected at a much higher degree both by flowcytometry and by TUNEL with a statistical significance (68.47±7.92% and 8.23±2.67%, respectively, P<0.05) after incubated with 1 mmol/L oxaliplatin for 2 d. By means of RT-PCR, we detected an enhancement of Caspase-3 m-RNA expression induced by oxaliplatin which was also in positive correlation with the apoptotic level. AC-DEVD-CHO, a Caspase-3 specific inhibitor, could significantly inhibit and delay apoptosis induced by oxaliplatin.

CONCLUSION: Oxaliplatin is effective and well-tolerated in patients with advanced gastric carcinoma. Oxaliplatin could significantly inhibit the growth of human gastric cell line SGC-7901. The induction of Caspase-3 m-RNA expression, activation of Caspase-3 and promotion of apoptosis may be some of the therapeutic mechanisms of oxaliplatin on gastric carcinoma. Annexin-V-fluorescein labeling flow cytometry is much more sensitive than TUNEL in detecting early stage apoptosis.

Lin WL, Li DG, Chen Q, Lu HM. Clinical and experimental study of oxaliplatin in treating human gastric carcinoma. *World J Gastroenterol* 2004; 10(19): 2911-2915
http://www.wjgnet.com/1007-9327/10/2911.asp

INTRODUCTION

Gastric cancer is one of the common carcinomas in human being. Drug treatment draws more and more attention as an essential part of comprehensive treatment of gastric malignancy. Gastric carcinoma is relatively sensitive to chemotherapy. It is generally considered that chemotherapy may prolong patient's life and decrease relapse. Oxaliplatin (L-OHP) is an innovative third generation platinum compound with powerful anti-neoplasm competence, lack of cross drug resistance with CDDP, with a synergistic effect with 5-FU and satisfactory safety profile. This new anticancer drug provides us more choices in fighting against malignancy, especially colon cancer. At present, treating gastric cancer with oxaliplatin and the relationship between chemotherapy and cancer cell apoptosis draw more and more attention. The discovery of Caspase family (cysteine proteases) that is implicated in the execution of programmed cell death in organisms ranging from nematodes to humans, brings the fresh air to the research of malignant cell apoptosis. The Caspase family is big and family members interact with each other to promote or inhibit the process of apoptosis. Caspase-3 locates in the downstream of the Caspase cascade. The proteolytic activation of Caspase-3 plays a key role in apoptotic process. This article summarizes the effect and side effects of chemotherapy with oxaliplatin on 22 cases of stage IV human gastric cancer, and tries to elucidate the mechanisms of chemotherapy by detecting apoptosis of cancer cells and evaluating the role Caspase-3 plays in apoptotic process.

MATERIALS AND METHODS

Patients

A total of 22 cases of stage IV human gastric cancer patients who underwent chemotherapy in the Affiliated Xinhua Hospital of Shanghai Second Medical University from January 1999 to September 2002 were enrolled in this study. There were 17 men and 5 women, and their age ranged from 25 to 70 years (mean, 60±10 years). Among the 22 patients, 16 had poorly differentiated adenocarcinoma and 6 had signet ring cell carcinoma.

Methods

Each case received a combination chemotherapy containing L-OHP (L-OHP 85 mg/m^2 by continuous intravenous infusion for 2 h on d 1, leucovorin 200 mg/m^2 by continuous intravenous infusion for 1 h on d 1 and d 2, 5-FU 300 mg/m^2 by bolus intravenous injection on d 1 and d 2, 5-FU 1200 mg/m^2 by continuous intravenous infusion for 48 h, one course lasting 2 wk for 4-6 courses).

Cell culture

Human gastric adenocarcinoma cell line SGC-7901, purchased

from the Shanghai Institute of Cell Biology, Chinese Academy of Sciences, was routinely maintained in RPMI 1640 containing 100 mL/L fetal bovine serum (FBS), 100 U/mL penicillin, 100 U/mL streptomycin at 37 ℃ in a humidified atmosphere containing 50 mL/L CO_2.

MTT assay

Cells were seeded at the density of 5×10^3 per well in 96-well plates in RPMI-1640 containing 100 mL/L FBS. After 24 h, fresh medium was added, containing oxaliplatin at concentrations of 0 to 10 mg/L. After 48 h incubation, MTT assay was performed, 150 μL of stock MTT (0.5 mg/mL) was added to each well, and the cells were further incubated at 37 ℃ for 4 h. The supernatant was removed and 150 μL DMSO was added to each well. An ELISA reader was used to measure the absorbance at a wavelength of 525 nm.

Transmission electron microscopy

The cells treated with 0.1 mg/L oxaliplatin were trypsinized and harvested after 24 h. Subsequently the cells were fixed in 40 g/L glutaral and immersed with Epon 821, embedded in capsules and converged for 72 h at 60 ℃, then prepared into ultrathin sections (60 nm) and stained with uranyl acetate and lead citrate. Cell morphology was examined by transmission electron microscopy.

Flow cytometry

SGC-7901 cells were treated with oxaliplatin or oxaliplatin plus AC-DEVD-CHO at oxaliplatin concentrations of 0 to 10 mg/L for 30 min. Cells were digested by 2.5 g/L trypsin, washed in 0.01 mol/L PBS, fixed by cold alcohol at 4 ℃ and dyed with annexin-V (according to the description of annexin-V kit), and then analyzed by flow cytometry.

TUNEL

SGC-7901 cells were added to 6-well plates with cover glass-slides at 6×10^4 cells/well, after incubated with oxaliplatin or oxaliplatin plus AC-DEVD-CHO at different oxaliplatin concentrations of 0 to 10 mg/L and fixed in 40 g/L formaldehydum polymerisatum for 1 h. After washed in 0.01 mol/L PBS twice, the cells were treated with reaction buffer, labeled with fluorescein dUTP in a humid box for 1 hour at 37 ℃, then combined with anti-fluorescein antibody, colorized with NBT/BCIP. Cells were visualized with light microscopy. The apoptotic index (AI) was calculated as follows: AI = (number of apoptotic cells/total number) ×100%.

RT-PCR

Total RNA was extracted from cells using an RNA extraction reagent, TR IZOL (Life Technologies, USA), according to standard acid-guanidium-phenol-chloroform method[17]. About 4 μg of total RNA as reversely transcribed at 42 ℃ for 60 min in a total of 30 μL reaction volume using a first-strand cDNA synthesis kit (Boehringer Mannheim, Germany). cDNA was incubated at 95 ℃ for 5 min to inactivate the reverse transcriptase, and served as template DNA for 28 rounds of amplification using the GeneAmp PCR system 2400 (Perkin-Elmer Applied Biosystems, CA, USA). PCR was performed in a standard 25 μL reaction mixture consisting of 1.5 mmol/L magnesium chloride (pH 8.3), 2.5 mmol/L dNTPs, 12.5 pmoL each of sense and antisense primers and 2.5 U of Taq DNA polymerase (M BI, Canada). Amplification was performed for 1 min at 94 ℃, for 1 min at 62 ℃ and for 1 min at 72 ℃ after heat-start for 5 min. Finally, an additional extension step was carried out for 10 min at 72 ℃. As control, the DNA template of Caspase-3 was replaced by that of β-actin in the reaction. The amplification products were separated on 12 g/L agarose gels and visualized by ethidium bromide staining. PCR primers for Caspase-3 were as follows: forward primer, 5'- ATG GAG AAC ACT GAA AAC TCA -3'; reverse primer , 5'- TTA GTG ATA AAA ATA GAG TTC -3': according to the Caspase-3 gene structure in GeneBank. An 834 bp PCR product of Caspase-3 and a 315 bp product of β-actin were obtained.

Statistical analysis

The difference between each two groups was analyzed by ANOVA. $P<0.05$ was considered statistically significant.

RESULTS

Clinical results

Nine cases achieved objective responses (including 1 complete response and 8 partial responses), the response rate was 40.9% progression-free survival (PFS) 4.2 mo, and total survival time 7.2 mo. The rate of accumulative neurotoxicity, vomiting and diarrhea, bone marrow depression was 93.5%, 20% and 32.9%, respectively (Table 1).

Inhibitory effect of oxaliplatin on SGC-7901

Taking the means of data from MTT assay, we got a smooth inhibition curve, which was a typical inverse 'S', and the IC_{50} was calculated to be 0.71 mg/L by GrapHpaol Prism software (Figure 1). The inhibition of L-OHP on SGC-7901 cell line was typically dose dependent. A maximal inhibitory rate reached 85.3%.

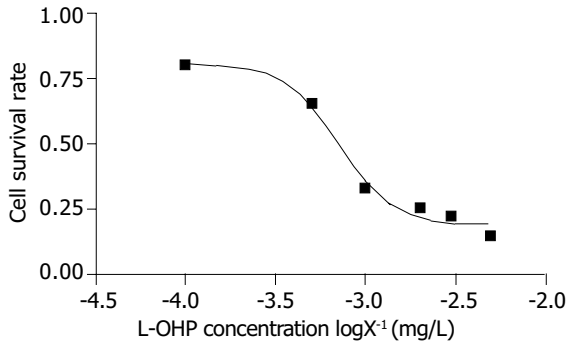

Figure 1 Relationship between SGC-7901 cell survival rate and L-OHP concentration.

Apoptosis induced by L-OHP

We used transmission electron microscopy, TUNEL and

Table 1 Side effects of combined chemotherapy with oxaliplatin in treating stage IV gastric carcinoma (cycles, n = 102)

Side effects	Anemia	Neutropenia	Thrombo-cytopenia	Nausea& vomiting	Diarrhea	Mucositis	Dysaesthesia
I	27	17	7	14	16	9	89
II	7	6	3	6	3	1	6
III	0	0	0	0	1	0	0
IV	0	0	0	0	0	0	-
Incidence (%)	32.9	22.9	10	20	20	10	93.5

Annexin-V labeling flowcytometry to quest for the mechanism of its anti-neoplastic effect. After treatment of SGC-7901 cells with oxaliplatin (0.1 mg/L) for 24 h, some cells showed apoptotic characteristics including chromatin condensation, chromatin crescent formation, nucleus fragmentation and apoptotic body formation by transmission electron microscopy (Figure 2). Apoptotic index was 0.38% in the control group. In the experimental group, the apoptotic index determined by the TUNEL method was 7.35% while receiving L-OHP 1mg/L (slightly higher than IC_{50}) for 4 h and 14.35% while increasing the L-OHP concentration to 5 mg/L. As time went on, the apoptotic index remained stable in the control group, and was significantly increased in two experimental groups (0.5 mg/L and 1 mg/L) which reached a peak of 7.93% and 10.15%, respectively on the 4th d and decreased slightly on the 7th d. The two experimental groups had a similar trend. We could conclude that the increase in apoptotic index correlated with the L-OHP concentration and time. The apoptotic level was positively correlated with L-OHP at a concentration within 0-2.0 mg/L, as detected by Annexin-V labeling flowcytometry. The apoptotic index reached a peak of 76.47% when the concentration of L-OHP was 2 mg/L. On the contrary, the apoptotic index dropped when the concentration reached 5 mg/L.

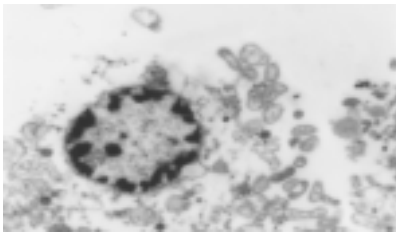

Figure 2 Oxaliplatin-induced apoptosis in SGC-7901 cells with transmission electron microscopy. It shows apoptotic cells with chromatin condensation, chromatin crescent formation, nucleus fragmentation (×4 000).

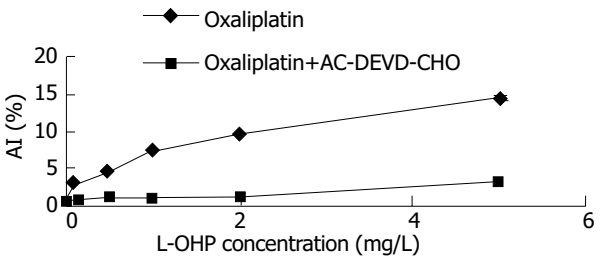

Figure 3 Inhibitory effect of AC-DEVD-CHO on apoptosis detected by TUNEL.

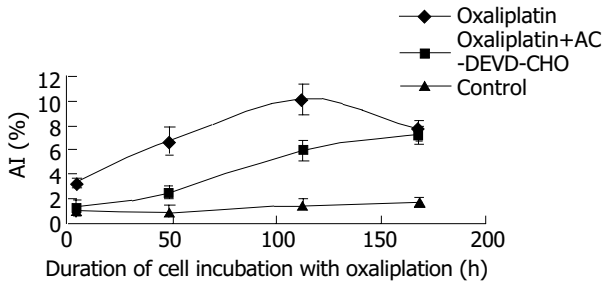

Figure 4 Effect of AC-DEVD-CHO on apoptosis at different times detected by TUNEL.

Expression of Caspase-3 m-RNA

By means of RT-PCR, we detected an enhancement of Caspase-3 m-RNA expression (0.48±0.47 *vs* 0.18±0.20, $P<0.05$) induced by L-OHP which was also in positive correlation with the apoptotic level.

Role of activated Caspase-3 in apoptotic process induced by oxaliplatin

AC-DEVD-CHO, a Caspase-3 specific inhibitor, could significantly inhibit and delay apoptosis induced by L-OHP (Figures 3, 4).

DISCUSSION

Gastric carcinoma is one of the major causes of cancer morbidity and mortality in China. The natural history shows a high metastatic potential since many patients with gastric carcinoma at advanced stage will relapse or initially present with metastasis. One of the first issues solved by clinical research over the last decade is the value of chemotherapy in the metastatic setting. Indeed, chemotherapy has been shown to have a favorable impact on survival and quality of life compared with supportive care alone. However, in this disease some traditional chemotherapy regimens were considered as poorly tolerated or less effective[1-4]. Oxaliplatin is an innovative platinum compound indicated as a first-line therapy in combination with 5-FU and folinic acid for metastatic colorectal cancer[5-8]. Oxaliplatin has a powerful anti-neoplasm competence, little cross drug resistance with CDDP, a synergistic effect with 5-FU and a satisfactory safety profile[9-11]. We replaced CDDP with oxaliplatin in a traditional FLP protocol, trying to explore its anti-neoplasm activity and side effects in treating advanced gastric carcinoma. In 22 patients, 9 cases achieved objective responses (including 1 complete response and 8 partial responses), the overall response rate reached 40.9%, PFS 4.2 mo, and overall survival time 7.2 mo. The toxicity was tolerable, the rate of vomiting and diarrhea (1 case with grade III diarrhea), bone marrow depression was 20% and 32.9%, respectively. No alopecia and skin toxicity were encountered. Although the incidence of accumulative neurotoxicity was as high as 93.5%, all of them were grade I-II. Acute symptoms manifesting as transient dysaesthesia and/or paraesthesia of the extremities were commonly observed, their occurrence was triggered or enhanced by exposure to cold. No patient experienced pharyngolaryngeal dysaesthesia characterized by a transient sensation of difficulty in breathing or swallowing without any objective evidence of respiratory distress, which was encountered during the multi-center research in treating colorectal cancer after 9 cycles[12-14]. In all the cases in this study, symptoms improved after treatment discontinuation. It is suggested that oxaliplatin is effective and well-tolerated in patients with stage IV gastric carcinoma.

We chose human gastric cancer cell line SGC-7901 for experimental study. First, we used MTT to prove if L-OHP could inhibit SGC-7901 growth. using the means of our data from the experiments, we obtained a smooth inhibition curve, which was a typical inversed 'S'. IC_{50} was 0.71 mg/L and the maximal inhibitory rate reached 85.3%.The inhibition of L-OHP on SGC-7901 cell line was typically dose dependent.

Naturally occurring or programmed cell death can regulate cell number, facilitate morphogenesis, remove harmful or otherwise abnormal cells, and eliminate cells that have already performed their functions during the life development as well as in tissue homeostasis and aging. The role of apoptosis in the process of carcinogenesis, development of cancer and malignancy treatment has drawn more and more attention in recent years[15-17]. In this study, we tried to evaluate the level of apoptosis induced by oxaliplatin. Transmission electron microscopy could reveal the changes of cell ultrastructure during the apoptotic process. TUNEL assay is a traditional method for detecting apoptosis, but its selectivity is poor. It could hardly differentiate the apoptotic cells from the necrotic ones.

Phosphatidylserine (PS) only exists in the cytoplasm side of cell plasma membrane, and externalization of PS occurs in the early stage of apoptosis. Annexin-V could specifically conjugate to the PS to detect the apoptotic cells[18]. So we combined traditional transmission electron microscopy and TUNEL assay with relatively highly selective annexin-V labeling flowcytometry to detect SGC-7901 cell line apoptosis induced by oxaliplatin. After treatment of SGC-7901 cells with oxaliplatin, some cells showed typical morphologic changes of apoptosis including chromatin condensation, chromatin crescent formation, nucleus fragmentation and apoptotic body formation under transmission electron microscope, TUNEL assay showed the AI positively correlated with drug concentration and treatment time. Annexin-V-fluorescein labeling flowcytometry was much more sensitive than TUNEL in detecting the early stage apoptosis. The apoptotic level positively correlated with L-OHP at a concentration within 0-2.0 mg/L, as detected by annexin-V labeling flowcytometry. The apoptotic index reached a peak, when the concentration of L-OHP was 2 mg/L. On the contrary, the apoptotic index dropped while the concentration reached 5 mg/L. To put these results together, we believed that the induction of apoptosis played a key role in inhibiting malignant cells at a low drug concentration of L-OHP, and that cytotoxicity and apoptosis coexisted while the drug concentration was high. This discovery may provide a theoretical basis for this type of treatment.

The discovery of cytosolic aspartate-specific proteases, called Caspases, which are responsible for the deliberate disassembly of a cell into apoptotic bodies, brings the fresh air to the research of malignant cell apoptosis. The Caspase family is big and dozens of family members interact with each other to promote or inhibit the process of apoptosis. Caspases are present as inactive pro-enzymes, most of which are activated by proteolytic cleavage. There are two pathways of Caspase activation, namely the cell surface death receptor pathway and the mitochondria-initiated pathway. In the cell surface death receptor pathway, activation of Caspase-8 following its recruitment to the death-inducing signaling complex (DISC) is the critical event that transmits the death signal. This event is regulated at several different levels by various viral and mammalian proteins. Activated Caspase-8 can activate downstream Caspases, such as Caspase-3 by direct cleavage or by indirectly cleaving bid and inducing cytochrome C release from the mitochondria. In the mitochondrial-initiated pathway, Caspase activation is triggered by the formation of an Apaf-1/cytochrome C complex that is fully functional in recruiting and activating proCaspase-9. Activated Caspase-9 will then cleave and activate downstream Caspases such as Caspase-3, -6, and -7[19-23]. So we can find out that Caspase-3 locates in the downstream of the Caspase cascade. The proteolytic activation of Caspase-3 has been found to play a key role in apoptotic process[24-26]. Caspase-3 may then cleave vital cellular proteins or activate additional Caspases by proteolytic cleavage. In this study, we detected an enhancement of Caspase-3 m-RNA expression induced by oxaliplatin by means of RT-PCR. Caspase-3 m-RNA expression was also positively correlated with the apoptotic level. AC-DEVD-CHO, a Caspase-3 specific inhibitor, could significantly inhibit and delay apoptosis induced by oxaliplatin. Taken together, we believe that Caspase-3 synthesis and activation play a key role in the apoptotic process of SGC-7901 cell line induced by oxaliplatin.

Our research demonstrates that oxaliplatin is effective and well tolerable in treating gastric cancer. Inducing cancer cell apoptosis may be one of the anti-neoplasm mechanisms. This apoptosis may be mediated by up-regulation of Caspase-3 synthesis and activation. The efficacy and safety profile of oxaliplatin as a chemotherapeutic drug in combined anti-gastric carcinoma chemotherapy regimen should be further confirmed by double blind multi-center clinical studies.

REFERENCES

1 **Cascinu S**, Scartozzi M, Labianca R, Catalano V, Silva RR, Barni S, Zaniboni A, D'Angelo A, Salvagni S, Martignoni G, Beretta GD, Graziano F, Berardi R, Franciosi V. High curative resection rate with weekly cisplatin, 5-fluorouracil, epidoxorubicin, 6S-leucovorin, glutathione, and filgastrim in patients with locally advanced, unresectable gastric cancer: a report from the Italian Group for the Study of Digestive Tract Cancer (GISCAD). *Br J Cancer* 2004; **90**: 1521-1525

2 **Park YH**, Ryoo BY, Choi SJ, Kim HT. A phase II study of capecitabine and docetaxel combination chemotherapy in patients with advanced gastric cancer. *Br J Cancer* 2004; **90**: 1329-1333

3 **Yamamura Y**, Kodera Y, Tanemura H, Oshita H, Miyashita K, Fujimura T. A phase I study of combination chemotherapy using TS-1 and pirarubicin (THP) for advanced gastric cancer. *Gan To Kagaku Ryoho* 2004; **31**: 361-365

4 **Ramos-De La Medina A**, Salgado-Nesme N, Torres-Villalobos G, Medina-Franco H. Clinicopathologic characteristics of gastric cancer in a young patient population. *J Gastrointest Surg* 2004; **8**: 240-244

5 **Braun AH**, Achterrath W, Wilke H, Vanhoefer U, Harstrick A, Preusser P. New systemic frontline treatment for metastatic colorectal carcinoma. *Cancer* 2004; **100**: 1558-1577

6 **Santini D**, Massacesi C, D'Angelillo RM, Marcucci F, Campisi C, Vincenzi B, Pilone A, Bianco V, Bonsignori M, Tonini G. Raltitrexed plus weekly oxaliplatin as first-line chemotherapy in metastatic colorectal cancer: a multicenter non-randomized phase ii study. *Med Oncol* 2004; **21**: 59-66

7 **Di Leo A**, Buyse M, Bleiberg H. Is overall survival a realistic primary end point in advanced colorectal cancer studies? A critical assessment based on four clinical trials comparing fluorouracil plus leucovorin with the same treatment combined either with oxaliplatin or with CPT-11. *Ann Oncol* 2004; **15**: 545-549

8 **Link K**, Happich K, Schirner I, Jungert B, Bruckl V, Mannlein G, Bruckl WM, Merkel S, Gohl J, Hohenberger W, Hahn EG, Wein A. Palliative second-line treatment with weekly high-dose 5-fluorouracil as 24-hour infusion and folinic acid (AIO) plus oxaliplatin after pre-treatment with the AIO-regimen in colorectal cancer (CRC). *Anticancer Res* 2004; **24**: 385-391

9 **Arnould S**, Hennebelle I, Canal P, Bugat R, Guichard S. Cellular determinants of oxaliplatin sensitivity in colon cancer cell lines. *Eur J Cancer* 2003; **39**: 112-119

10 **Marchetti P**, Galla DA, Russo FP, Ricevuto E, Flati V, Porzio G, Ficorella C, Cifone MG. Apoptosis induced by oxaliplatin in human colon cancer HCT15 cell line. *Anticancer Res* 2004; **24**: 219-226

11 **Ravaioli A**, Marangolo M, Pasquini E, Rossi A, Amadori D, Cruciani G, Tassinari D, Oliverio G, Giovanis P, Turci D, Zumaglini F, Nicolini M, Panzini I. Bolus fluorouracil and leucovorin with oxaliplatin as first-line treatment in metastatic colorectal cancer. *J Clin Oncol* 2002; **20**: 2545-2550

12 **Chiara S**, Nobile MT, Gozza A, Taveggia P, Heouaine A, Pastrone I, Percivale PL, Lionetto R, Sanguineti O, Rosso R. Phase II study of weekly oxaliplatin and high-dose infusional 5-fluorouracil plus leucovorin in pretreated patients with metastatic colorectal cancer. *Anticancer Res* 2004; **24**: 355-360

13 **Lehky TJ**, Leonard GD, Wilson RH, Grem JL, Floeter MK. Oxaliplatin-induced neurotoxicity: acute hyperexcitability and chronic neuropathy. *Muscle Nerve* 2004; **29**: 387-392

14 **Cavaletti G**, Petruccioli MG, Marmiroli P, Rigolio R, Galbiati S, Zoia C, Ferrarese C, Tagliabue E, Dolci C, Bayssas M, Griffon Etienne G, Tredici G. Circulating nerve growth factor level changes during oxaliplatin treatment-induced neurotoxicity in the rat. *Anticancer Res* 2002; **22**: 4199-4204

15 **Onizuka S**, Kawakami S, Taniguchi K, Fujioka H, Miyashita K. Pancreatic carcinogenesis: apoptosis and angiogenesis. *Pancreas* 2004; **28**: 317-319

16 **Correa P**. The biological model of gastric carcinogenesis. *IARC Sci Publ* 2004; **157**: 301-310

17 **Schrenk D**, Schmitz HJ, Bohnenberger S, Wagner B, Worner W. Tumor promoters as inhibitors of apoptosis in rat hepatocytes. *Toxicol Lett* 2004; **149**: 43-50

18 **Kim SJ**, Kim JE, Moon IS. Paraquat induces apoptosis of cultured rat cortical cells. *Mol Cells* 2004; **17**: 102-107
19 **Del Bello B**, Valentini MA, Comporti M, Maellaro E. Cisplatin-induced apoptosis in melanoma cells: role of caspase-3 and caspase-7 in Apaf-1 proteolytic cleavage and in execution of the degradative phases. *Ann N Y Acad Sci* 2003; **1010**: 200-204
20 **Twiddy D**, Brown DG, Adrain C, Jukes R, Martin SJ, Cohen GM, MacFarlane MM, Cain K. Pro-apoptotic proteins released from the mitochondria regulate the protein composition and caspase-processing activity of the native Apaf-1/caspase-9 apoptosome complex. *J Biol Chem* 2004; **279**: 19665-19682
21 **Cain K**. Chemical-induced apoptosis: formation of the Apaf-1 apoptosome. *Drug Metab Rev* 2003; **35**: 337-363
22 **Del Bello B**, Valentini MA, Mangiavacchi P, Comporti M, Maellaro E. Role of caspases-3 and -7 in Apaf-1 proteolytic cleavage and degradation events during cisplatin-induced apoptosis in melanoma cells. *Exp Cell Res* 2004; **293**: 302-310
23 **Jazirehi AR**, Gan XH, De Vos S, Emmanouilides C, Bonavida B. Rituximab (anti-CD20) selectively modifies Bcl-xL and apoptosis protease activating factor-1 (Apaf-1) expression and sensitizes human non-Hodgkin's lymphoma B cell lines to paclitaxel-induced apoptosis. *Mol Cancer Ther* 2003; **2**: 1183-1193
24 **Dong ML**, Zhu YC, Hopkins JV. Oil A induces apoptosis of pancreatic cancer cells via caspase activation, redistribution of cell cycle and GADD expression. *World J Gastroenterol* 2003; **9**: 2745-2750
25 **Fu YG**, Qu YJ, Wu KC, Zhai HH, Liu ZG, Fan DM. Apoptosis-inducing effect of recombinant Caspase-3 expressed by constructed eukaryotic vector on gastric cancer cell line SGC7901. *World J Gastroenterol* 2003; **9**: 1935-1939
26 **Boulares AH**, Ren T. Mechanism of acetaminophen-induced apoptosis in cultured cells: roles of caspase-3, DNA fragmentation factor, and the Ca2+ and Mg2+ endonuclease DNAS1L3. *Pharmacol Toxicol* 2004; **94**: 19-29

Edited by Wang XL **Proofread by** Zhu LH and Xu FM

PO Box 2345, Beijing 100023, China
Fax: +86-10-85381893
E-mail: wjg@wjgnet.com www.wjgnet.com

World J Gastroenterol 2004;10(19):2916-2918
World Journal of Gastroenterology
Copyright © 2004 by The WJG Press ISSN 1007-9327

• BRIEF REPORTS •

A new method of preventing bile duct injury in laparoscopic cholecystectomy

Fang Xu, Cheng-Gang Xu, De-Zheng Xu

Fang Xu, Cheng-Gang Xu, De-Zheng Xu, Department of General Surgery, Hangzhou Second Hospital, Hangzhou 310015, Zhejiang Province, China
Correspondence to: Fang Xu, Department of General Surgery, Hangzhou Second Hospital, Hangzhou 310015, Zhejiang Province, China. xufangsurg@zj165.com
Telephone: +86-571-88303636 **Fax:** +86-571-88021730
Received: 2003-12-12 **Accepted:** 2004-02-01

Abstract

AIM: Of all the complications of laparoscopic cholectecystomy, bile duct injury (BDI) is the most serious complication. The prevention of injury to the common bile duct (CBD) remains a significant concern in laparoscopic cholecystectomy (LC). Different kinds of methods have been advanced to avoid this injury but no single method has gained wide acceptance. Because of various limitations of current methodologies we began a study using cold light illumination of the extrahepatic biliary system (light cholangiography LCP) to better visualize this area and thereby reduce the risk of bile duct injury.

METHODS: Thirty-six patients with cholelithiasis were divided into two groups. Group I (16 cases) received LCP and group II (20 cases) received methelenum coeruleum cholangiography (MCCP). In group I cold light was used to illuminate the common bile duct by leading an optical fiber into the common duct with a duodenoscope at the time of LC. The light coming from the fiber in the CBD could clearly illuminate the location of CBD and hepatic duct establishing its location relative to the cystic duct. This method was compared with the dye injection technique using methelenum coeruleum.

RESULTS: In group I thirteen cases were successfully illuminated and three failed. The cause of three failed cases was due to the difficulty in inserting the fiber into the ampulla of Vater. No complications occurred in the thirteen successful cases. In each of these successful cases the location of the common and hepatic ducts was clearly seen differentiating the ductal system from surrounding anatomy. In ten cases both the left and right hepatic ducts could be seen and in three only the right hepatic ducts were seen. In four of the thirteen cases, cystic ducts were also seen. In group II, eighteen of the twenty cases were successful. The location of extrahepatic ducts became blue differentiating the ductal system from surrounding anatomy. Two cases failed due to a stone obstructing the cystic duct, and extravisation of the dye turned the entire area blue. LCP showed the common and hepatic ducts more clearly than MCCP.

CONCLUSION: LCP is the only technique that can clearly and directly show the location of the extrahepatic biliary system and may be useful in selecting cases of uncertain anatomy in the prevention of bile duct injury.

Xu F, Xu CG, Xu DZ. A new method of preventing bile duct injury in laparoscopic cholecystectomy. *World J Gastroenterol* 2004; 10(19): 2916-2918
http://www.wjgnet.com/1007-9327/10/2916.asp

INTRODUCTION

Bile duct injury continues to be one of the most serious complications of LC. The principal cause is the difficulty in recognition of the junction of the cystic duct to the hepatic duct. A number of methods have been advanced to avoid this error but no single method has gained wide acceptance. From March 2001 to October 2003 we used LCP for illumination of the biliary system in 36 cases and believe it is quite useful.

MATERIALS AND METHODS

Patients

Thirty-six patients with cholelithiasis, including 16 males and 20 females aged 41 to 66 years (mean age: 56 years) were selected for the procedure and divided into two groups. Group I (16 cases) received LCP and group II (20 cases) received MCCP.

Materials

Laparoscopic equipments were produced by Stryker and duodenoscopes with a channel diameter of 3.5 cm and 4.2 cm respectively were from Olympus. Optical fibers were specially produced according to our own design.

Methods

All patients drank 500 mL 100 g/L mannitol 15 h before operation and were fasted during this period. All cases received general anesthesia. In group I, Calot's triangle was dissected carefully and the relationship of the cystic duct to the hepatic and common bile ducts was noted. Duodenoscope was then introduced and the optic fiber was advanced into the common duct. When the light was turned on, the extra hepatic ducts were clearly seen. In group II, instead of placing the duodenoscope, a needle guided with the laparoscope was percutaneously punctured into the gall bladder. Five mL of bile was aspirated from the gall bladder. After that 5 mL of MCCP dye was injected. The bile ducts became blue.

RESULTS

In group I, thirteen cases were successfully illuminated and three failed. The cause of three failed cases was due to the difficulty in inserting the fiber into the ampulla of Vater. The time required for this examination ranged from 15 to 100 min with a median time of 35 min. No complications occurred in the thirteen successful cases. In each of these cases, the location of the common and hepatic ducts was seen clearly differentiating the ductal system from surrounding anatomy. In ten cases both the left and right hepatic ducts could be seen and in three only the right hepatic ducts were seen. In four of the thirteen cases, the cystic ducts were also seen. In two cases the ducts were clearly seen in spite of considerable fat over Calot's triangle.

In group II, eighteen of the twenty cases were successful.

The extrahepatic duct became blue differentiating the ductal system from surrounding anatomy. Two cases failed due to a stone obstructing the cystic duct, and extravisation of the dye turned the entire area blue.

DISCUSSION

Prevention of injury to the ductal system continues to be a matter of considerable concern of surgeons performing laparoscopic cholecystectomy. The accurate incidence of bile duct injury (BDI) during laparoscopic cholecystectomy (LC) is not known[1]. The principal causes of CBD in LC are the uncertain anatomy and the laparoscopic view that is quite different from open cholecystectomy. A few methods have been practiced, *e.g.* using 30° laparoscope, applying three dimensional laparoscope and inserting laparoscope through the right side of umbilicus were used. Greater efforts have been concentrated on dealing with the uncertain anatomy. The key point continues to be how to best identify the anatomy and thereby avoid injury. Currently the primary means of preventing injury resulted from uncertain anatomy include careful dissection, the judgment of an experienced surgeon, conversion to open cholecystectomy and intraoperative cholangiography (IOC).

The major causes of uncertain anatomy are anatomic variation and unclear anatomy. Kurumi *et al.*[2] classified confluent forms of the cystic duct and the bile duct into five different types, including four abnormal types. Sixteen instances (3.13%) of anatomic variation of the biliary tract were found among 511 patients, and four cases (4.35%) were found in 92 cadavers. Anatomic variation of the biliary tract is both common and complicated and can create a pitfall during laparoscopic cholecystectomy. Unclear anatomy resulted from inflammation and adhesion at Calot's triangle is an important factor associated with injury[3-5]. The judgment of an experienced surgeon[1,4,6] and conversion from laparoscopic to open cholecystectomy[5,7] are now considered the primary means of preventing bile duct injury resulted from uncertain anatomy. Unfortunately these means do not always work effectively. Injuries are likely to occur despite better procedures and increased experience[4]. Calvete *et al.* believed that no relation could be found between the experience of surgeons and the number of BDI over different periods of time[8]. Therefore, BDI during LC can not be attributed solely to the learning curve. One approach is to convert to open cholecystectomy when the anatomy is uncertain. But even open cholecystectomy can not avoid CBD injury due to the uncertain anatomy. Yang *et al.*[9] reported iatrogenic extrahepatic bile duct injury in 182 patients. Bile duct injury occurred in 152 patients during open cholecystectomy and in 30 patients during laparoscopic cholecystectomy. The incidence of BDI after LC was similar to that in the open procedure[1].

Cautious dissection is necessary and essential to prevent BDI in LC[4,6,10-12]. Illegible anatomy often poses dissection difficultly to operators and rends them quite helpless. Surgeons are seeking assisting measures to help them identify the anatomy during LC. Some surgeons recommended that IOC be attempted on all patients undergoing LC. They deemed that the routine use of IOC during laparoscopic cholecystectomy could not prevent bile duct injuries, but minimized the extent of the injuries so that they could be repaired easily, thus decreasing the rate of BDI[13-16]. But its routine use during LC remains controversial. Routine IOC yields very little useful clinical information compared to selective policies. A large number of unnecessary IOC were performed under routine IOC policy, and therefore a selective policy has been advocated[17]. IOC depends on the radiopaque dye introduced into the ductal system via the cystic duct and displayed by either a static film or fluoroscopy which does not always identify the relationship of the ductal system to adjacent anatomy. The primary purpose of IOC is to identify anatomy and any aberration as well as to identify stones. The image of IOC obtained from static film or fluoroscopy is completely different from that obtained from the monitor and can not really tell where the cystic duct or common bile duct is. The information afforded by IOC can only help operators realize if there are continuity, stones, tumor and injury of the ducts but can not help them dissect easily and safely. Thus it is of limited value during dissection of the area. Nevertheless it has become the most common method of visualizing the area.

The use of MCCP has been advocated by Xu *et al.*[18]. This technique does give a direct image but it is blurry. A mixture is got by injecting methylenum coeruleum into gall bladder. The color of the mixture is close to that of the tissue surrounding the extrahepatic duct, so that the bile ducts can not be identified clearly. The image is even more indistinct when there is much fatty tissue over the ducts. If there is extravasation, the entire area turns blue making dissection more difficult since the dye is not easily washed away. CBD does not keep the dye long enough. The dye diluted by the bile flows into duodenum soon, so that the operator can not observe Calot's triangle repeatedly. Finally, the procedure can not be used if the duct is blocked by a stone.

Because of these limitations of current methodologies, we advocated the new method of direct illumination of the extrahepatic ductal system (LCP). By adjusting the optic fiber, it can go into right or left hepatic duct and cystic duct. The movement of the fiber must be slow and soft. It is not very easy sometimes to insert the fiber into cystic duct for the duct may pass behind the common hepatic duct to enter on its posterior wall or on its left lateral aspect. If the inserting was difficult, we gave the attempt up in case that the duct wall was injured by the fiber. We do not think the illumination of cystic duct is absolutely necessary. The important thing is to know the locations of CBD and common hepatic duct, though the illumination of cystic duct may make the image of Calot's triangle appear completely.

Table 1 Comparison between group I and group II

	Group I (n=16)	Group II (n=20)
Examine method	LCP	MCCP
Examine time (min)		
Range	15-100	5-10
Median	35	7
Examination cost	$ 200	$ 5
Image	direct	direct
Legibility	clear	blurry
Observed time	unlimited	limited

Additional observations we made during this study revealed the importance of releasing any adhesions in the area of the ductal system to straighten the ductal system out facilitating the introduction of the optical fiber. The initial dissection of the ductal system along with our observations as to the probable location of the various elements was also helpful. In our opinion it is best to keep the optical fiber in the right hepatic duct until the dissection of the gall bladder and cystic duct is completed. This is particularly true in the occasional case when the cystic duct comes off the right hepatic duct. We do not feel routine LCP examination of the ductal system is indicated but in selected cases. The examination with LCP is extremely rewarding and not terrifically difficult in any hospital where the intraoperative endoscopic retrogarde cholangiopancreatography (ERCP) is practiced. As far as the cost is concerned, the increase is quite acceptable (Table 1). Of course, if there is any reason

for intraoperative ERCP to be done, it can be easily accomplished during LCP, though it needs not to be done as a routine. LCP can not help operators realize if there are continuity, stones, tumor and injury of the ducts. When the forgoing conditions are suspected, cholangiography should be done with intraoperative ERCP.

LCP is currently the most effective way to directly observe the extrahepatic ductal system during laparoscopic cholecystectomy and may play a useful role in clarifying uncertain anatomy in selected cases. As a useful assisting measure, it plays an important role in preventing extrahepatic duct injury in LC.

REFERENCES

1 **Savassi-Rocha PR**, Almeida SR, Sanches MD, Andrade MA, Frerreira JT, Diniz MT, Rocha AL. Iatrogenic bile duct injuries. *Surg Endosc* 2003; **17**: 1356-1361

2 **Kurumi Y,** Tani T, Hanasawa K, Kodama M. The prevention of bile duct injury during laparoscopic cholecystectomy from the point of view of anatomic variation. *Surg Laparosc Endosc Percutan Tech* 2000; **10**: 192-199

3 **Mahatharadol V.** Bile duct injuries during laparoscopic cholecystectomy: an audit of 1522 cases. *Hepatogastroenterology* 2004; **51**: 12-14

4 **Francoeur JR,** Wiseman K, Buczkowski AK, Chung SW, Scudamore CH. Surgeons' anonymous response after bile duct injury during cholecystectomy. *Am J Surg* 2003; **185**: 468-475

5 **Bingener-Casey J,** Richards ML, Strodel WE, Schwesinger WH, Sirinek KR. Reasons for conversion from laparoscopic to open cholecystectomy: a 10-year review. *J Gastrointest Surg* 2002; **6**: 800-805

6 **Panpimanmas S,** Kanyaprasit K. Complications of laparoscopic cholecystectomy and their management. *Hepatogastroenterology* 2004; **51**: 9-11

7 **Fathy O,** Zeid MA, Abdallah T, Fouad A, Eleinien AA, el-Hak NG, Eleibiedy G, el-Wahab MA, Sultan A, Anwar N, Ezzat F. Laparoscopic cholecystectomy: a report on 2000 cases. *Hepatogastroenterology* 2003; **50**: 967-971

8 **Calvete J,** Sabater L, Camps B, Verdu A, Gomez-Portilla A, Martin J, Torrico MA, Flor B, Cassinello N, Lledo S. Bile duct injury during laparoscopic cholecystectomy: myth or reality of the learning curve? *Surg Endosc* 2000; **14**: 608-611

9 **Yang FQ,** Dai XW, Wang L, Yu Y. Iatrogenic extrahepatic bile duct injury in 182 patients: causes and management. *Hepatobiliary Pancreat Dis Int* 2002; **1**: 265-269

10 **Panzera F,** Ghisio S, Grosso A, Vigezzi P, Vitale M, Cariaggi RM, Mistrangelo M. Laparoscopic cholecystectomy. Our experience. *Minerva Chir* 2000; **55**: 489-492

11 **Luo D,** Chen XR, Mao JX, Li SH, Zhou ZD, Yu SM. Three-dimensional identification of the cystic infundibulum-cystic duct junction: a technique for identification of the cystic duct in laparoscopic cholecystectomy. *Hepatobiliary Pancreat Dis Int* 2003; **2**: 441-444

12 **Bassi M**. Bile duct injuries due to unwarranted duct catheterization during cholangiography (prevention and treatment). *Chir Ital* 2003; **55**: 41-44

13 **Polat FR,** Abci I, Coskun I, Uranues S. The importance of intraoperative cholangiography during laparoscopic cholecystectomy. *JSLS* 2000; **4**: 103-107

14 **Ludwig K,** Bernhardt J, Steffen H, Lorenz D. Contribution of intraoperative cholangiography to incidence and outcome of common bile duct injuries during laparoscopic cholecystectomy. *Surg Endosc* 2002; **16**: 1098-1104

15 **Flum DR**, Dellinger EP, Cheadle A, Chan L, Koepsell T. Intraoperative cholangiography and risk of common bile duct injury during cholecystectomy. *JAMA* 2003; **289**: 1639-1644

16 **Vezakis A**, Davides D, Ammori BJ, Martin IG, Larvin M, McMahon MJ. Intraoperative cholangiography during laparoscopic cholecystectomy. *Surg Endosc* 2000; **14**: 1118-1122

17 **Metcalfe MS,** Ong T, Bruening MH, Iswariah H, Wemyss-Holden SA, Maddern GJ. Is laparoscopic intraoperative cholangiogram a matter of routine? *Am J Surg* 2004; **187**: 475-481

18 **Xu JJ**, Xiong XH, Yu HL, Xi JS, Bu YB, Jin SS. The effect of methylenum coeruleum in laparoscope cholecystectomy. *Zhonghua Waike Zazhi* 2000; **38**: 756-757

Edited by Wang XL and Zhang JZ **Proofread by** Xu FM

PO Box 2345, Beijing 100023, China
Fax: +86-10-85381893
E-mail: wjg@wjgnet.com www.wjgnet.com

World J Gastroenterol 2004;10(19):2919-2921
World Journal of Gastroenterology
Copyright © 2004 by The WJG Press ISSN 1007-9327

• CASE REPORT •

An unusual presentation of "silent" disseminated pancreatic neuroendocrine tumor

Dragomir Marisavljevic, Natasa Petrovic, Nikola Milinic, Vesna Cemerikic, Miodrag Krstic, Olivera Markovic, Dragoljub Bilanovic

Dragomir Marisavljevic, Natasa Petrovic, Nikola Milinic, Olivera Markovic, Dragoljub Bilanovic, Medical Center "Bezanijska kosa", Belgrade, Yugoslavia
Vesna Cemerikic, Miodrag Krstic, Clinical Center Serbia, Belgrade, Yugoslavia
Correspondence to: Petrovic Natasa, Medical Center "Bezanijska kosa", Bezanijska kosa bb, 11080 Belgrade, Yugoslavia. naca@infosky.net
Telephone: +381-11-3010748 **Fax:** +381-11-606520
Received: 2003-06-30 **Accepted:** 2003-11-06

Abstract

To present a patient diagnosed with pancreatic carcinoid that was extremely rare and produced an atypical carcinoid syndrome. We reported a 58-year old male patient who presented with long standing, prominent cervical lymphadenopathy and occasional watery diarrhea. Pathohistological and immunohistochemical examination of lymph node biopsy showed a metastatic neuroendocrine tumor, which was histological type A of carcinoid (EMA+, cytokeratin+, CEA-, NSE+, chromogranin A+, synaptophysin+, insulin-). Bone marrow biopsy showed identical findings. Primary site of the tumor was pancreas and diagnosis was made according to cytological and immunocytochemical analysis of the tumor cells obtained with aspiration biopsy of pancreatic mass (12 mm in diameter) under endoscopic ultrasound guidance. However, serotonin levels in blood and urine samples were normal. It is difficulty to establish the precise diagnosis of a "functionally inactive" pancreatic carcinoid and aspiration biopsy of pancreatic tumor under endoscopic ultrasound guidance can be used as a new potent diagnostic tool.

Marisavljevic D, Petrovic N, Milinic N, Cemerikic V, Krstic M, Markovic O, Bilanovic D. An unusual presentation of "silent" disseminated pancreatic neuroendocrine tumor. *World J Gastroenterol* 2004; 10(19): 2919-2921
http://www.wjgnet.com/1007-9327/10/2919.asp

INTRODUCTION

In 1907, Obendorfer applied the term "karzinoide" to describe a set of ileal tumors that behaved in a more benign manner than carcinomas. Since then, carcinoid tumors have been found to be relatively uncommon neuroendocrine tumors arising from neural crest cells known as "amine precursor uptake and decarboxylation cells" (APUD), which are derived from gut endoderm. Recent consensus meetings suggested that a more appropriate term "neuroendocrine tumor" should be used for all endocrine tumors of the digestive system, because these tumors derive from the diffuse neuroendocrine system[1]. Pancreas, mucosa of the gastrointestinal tract[2] and endocrine cells scattered in other endodermal sites (such as thyroid, lung, biliary tree and the urogenital tract) belong to APUD system. Neuroendocrine tumors can be subclassified into those with or without clinical syndromes and are termed "functionally active" and "functionally inactive" pancreatic carcinoid, respectively[3]. Carcinoid of the pancreas is extremely rare and the diagnosis may puzzle physicians and pathologists[4]. Pancreatic carcinoids produce an atypical carcinoid syndrome, skin flushing was reported in only 34%, the main symptom is pain, followed by diarrhea and weight loss.

We hereby described a patient with disseminated "functionally inactive" neuroendocrine tumor who presented with lymph node metastases, but without characteristic symptoms of carcinoid syndrome. The primary site of the tumor was pancreas.

CASE REPORT

A 58-years old male was admitted to Hematology Department in June 2001 with complaint of a left anterior neck mass and occasional massive, watery diarrhea. The patient noticed slow enlargement of neck mass for two years prior to admission, and also stated that in the last 12 mo he had episodes of diarrhea 1-2 times/wk. Diarrhea was massive and watery (up to 1 L/d) without visible blood or mucous and usually self-limited. Diarrhea was not associated with abdominal pain, tenesmus or with food intake. He lost 5 kg in 3-4 mo, inspite of good appetite. His previous medical history was unremarkable. Physical examination showed a left anterior neck mass (7 cm×6 cm in diameter), painless and movable in all directions. Chest X-ray showed paratracheal infiltrate. On bronchoscopy, external compression on posterior and lateral tracheal walls was seen. CT of chest showed enlarged mediastinal lymph nodes (up to 40 mm). CT of abdomen showed an enlarged pancreatic head (46 mm) with a mild hypodense area (12 mm in diameter). Pathohistological findings of tissue samples from the neck tumor (cuneiform biopsy) and bone marrow (trephine biopsy) were identical, namely a metastatic neuroendocrine tumor, which was histological type A of carcinoid. Immunophenotyping of cells from the neck tissue sample showed well-differentiated neuroendocrine tumor (APUDOMA) that was immunostained as follows: EMA+, cytokeratin 8+, CEA-, *NSE+*, *chromogranin A+*, *synaptophysin+*, insulin-. In an effort to find the primary site of APUDOMA, esophagogastroduodenoscopy, endoscopic enteroscopy, colonoscopy, small bowel barium enema, radial endoscopic ultrasound (radial EUS - Olympus device) were done (Figure 1). Ultrasound (linear EUS) guided aspiration biopsy of the pancreatic mass was performed (Figure 2). Cytological examination showed solid nodular nests of small uniform, epitheloid cells of dense heterochromatin. Immunocytochemical analysis revealed groups of epithelial cells with positive cytoplasmatic staining on NSE and chromogranin A that implied on tumor with neuroendocrine differentiation (Figure 3). Pathohistological examination of aspiration liver biopsy was normal, excluding possible liver micro-metastasis. To exclude MEN syndrome, X-ray and MRI of sellar region as well as thyroid US were done and all tests were normal. On 2D ultrasound the right heart was anatomically and functionally within normal limits. Blood count and biochemistry were normal except for occasional hypokalemia and mild hypoproteinaemia (with proportional decrease in all electrophoresis fractions). CEA was significantly increased (535.5 ng/mL), but pancreatic tumor marker (CA 19-9) and alpha-feto protein were within normal

limits. Serotonin level in blood and urine was normal (0.25 mmol/L and 359 mmol/24 h, respectively). 5-HIAA in the urine sample was increased (84 μmol/L, reference range: 10.4-41.6 μmol/L). Periodical diarrhea was controlled with loperamid and oral potassium supplementation. During hospitalization, patient developed urinary retention. Rectal examination and US revealed a prostatic adenoma (size 44 mm×54 mm×54 mm, 60 g weight) with normal values of prostate serum antigen. Transvesical adenectomy was performed, and pathohystologic findings confirmed it to be an adenoma. Postoperative period was complicated with prolonged wound healing and vesicodermal fistula. The patient also had changes of mental status, but CT of the head did not show any abnormalities. The patient was regularly followed up. In December 2001 he was doing well, still complaining of frequent diarrhea and minimal enlargement of the neck mass. Blood tests continued to show hypoproteinemia and hypokalemia, easily controlled with potassium supplementation. However, the patient died in January 2002 at home. His family recorded no particular circumstances related to his death.

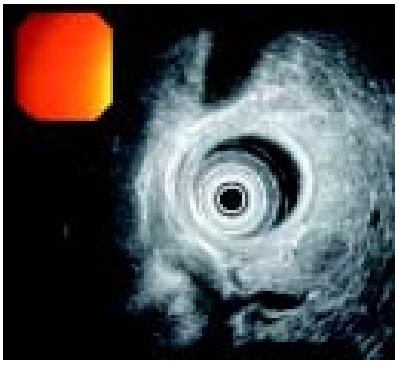

Figure 1 Pancreatic mass (radial endoscopic ultrasound, Olympus device).

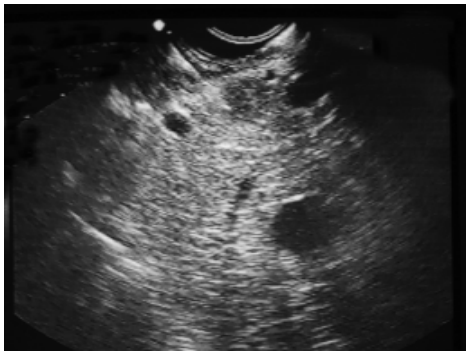

Figure 2 Ultrasound (linear EUS) guided aspiration biopsy of the pancreatic mass.

DISCUSSION

Functionally active neuroendocrine tumors are presented with clinical symptoms because of excessive hormone release from the tumor cells as in insulinoma, gastrinoma, VIPoma, glucagonoma and carcinoid syndrome[5]. Carcinoid tumors, except those originating from rectum, produced a variety of endocrine substances, the most frequent one was serotonin and kallikrein[6-8]. Carcinoid syndrome that includes diarrhea, flushing, wheezing, and right-sided heart disease[9] is caused by systemic serotonin release. Less than 10% of carcinoids had some of these symptoms[10]. Explanation is efficient hepatic metabolism of vasoactive amines, and that is also the reason why carcinoid syndrome rarely occurred in the absence of liver metastasis. Exceptions are circumstances in which venous blood from a large tumor was drained directly into systemic circulation[11].

Functionally inactive neuroendocrine tumors can be diagnosed in several ways: a) accidentally during routine ultrasonography performed for unexplained abdominal complaints, b) when a large tumor of the pancreatic head is causing obstruction and consequently extrahepatic jaundice, c) when a patient presents with abdominal pain secondary to bowel pseudo-obstruction, and d) as complications of the tumor such as bleeding. Our patient had occasional diarrhea that was not significant (less than 1L per day). Besides he had no other symptoms, and his blood tests failed to show any endocrine abnormalities. Histopathological and imunohistochemical analyses of the tissue sample from the neck mass showed a well-differentiated neuroendocrine tumor, which was histological type A of carcinoid (APUDOMA). At the time of diagnosis, metastatic disease of cervical and mediastinal lymph nodes, and bone marrow already existed which was confirmed by histopathological finding. Aspiration liver biopsy was done to exclude micro-metastases, that otherwise could not be visualized by imaging methods, and the result was negative. Primary site of the tumor was unknown. Because the most frequent localization of carcinoid was in the gastrointestinal tract, it was explored in whole, but primary tumor was not found. Aspiration biopsy of the pancreatic mass under endoscopic ultrasound guidance was done for the first time in Yugoslavia. Immunocytochemical report confirmed that the pancreatic mass was the primary site that only occurred in 2-3% of all cases[4,12,13]. Also, carcinoid tumors up to 1 cm rarely metastaze, but that was not the case with our patient.

The slow growth rate and late invasion of adjacent organs rendered local resection of pancreatic carcinoid tumor possible, but the high incidence of distant metastases (69%) prevented long-term survival in the majority of patients[4]. Diarrhea with hypokalemia and hypoproteinemia, as a manifestation of carcinoid syndrome in this case could be explained by increased release of vasoactive substances most probably from the

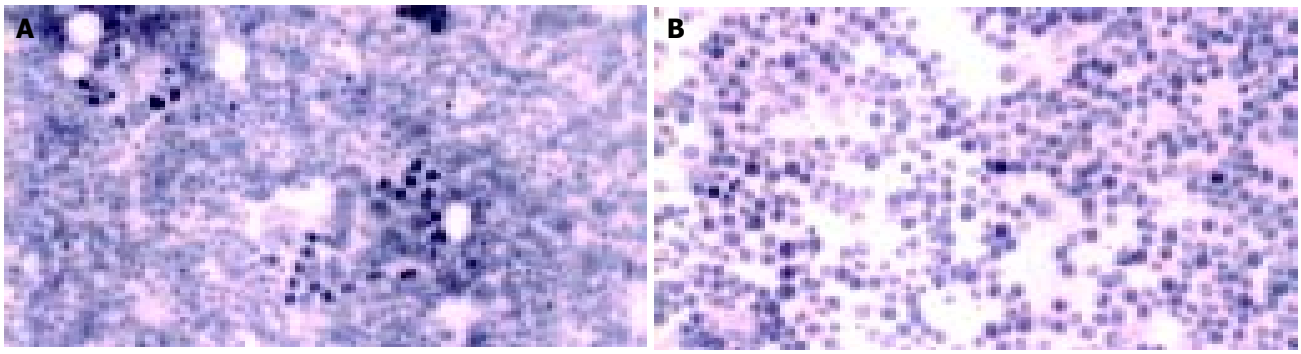

Figure 3 Groups of epithelial cells with positive cytoplasmic staining on chromogranin (A) and NSE (B) (immunocytochemical analysis).

extensive metastasis in the bone marrow, and lymph nodes. However, these metabolic abnormalities were well controlled and could not be the main cause of his death.

In summary, atypical presentation in this and other reported cases of pancreatic carcinoids suggests that metastatic potential of functionally inactive neuroendocrine cells is originated from the pancreas.

REFERENCES

1 **Polak JM**. Diagnostic histopathology of neuroendocrine tumors. *Edinburgh: Churchill-Livingstone* 1993

2 **Solcia E**, Capella C, Riocca R. Disorders of the endocrine system. In: Ming SC, Goldman H, eds. Pathology of the gastrointestinal tract. *Philadelphia:Williams and Wilkins* 1998: 295-322

3 **Arnold R**. Diagnosis and Management of Neuroendocrine Tumors. 8th United European Gastroenterology Week, Brussels, *Belgium* 2001

4 **Maurer CA**, Baer HU, Dyong TH, Mueller-Garamvoelgyi E, Friess H, Ruchti C, Reubi JC, Buchler MW. Carcinoid of the pancreas: clinical characteristics and morphological features. *Eur J Cancer* 1996; **32A**: 1109-1116

5 **Eriksson B**, Oberg K, Stridsberg M. Tumor markers in neuroendocrine tumors. *Digestion* 2000; **62**: 33-38

6 **Sweeney JF**, Rosemurgy AS. Carcinoid tumors of the gut. *Cancer Control* 1997; **4**: 18-24

7 **Shebani KO**, Souba WW, Finkelstein DM, Stark PC, Elgadi KM, Tanabe KK, Ott MJ. Prognosis and survival in patients with gastrointestinal tract carcinoid tumors. *Ann Surg* 1999; **229**: 815-821

8 **Kulke MH**, Mayer RJ. Carcinoid tumors. *N Engl J Med* 1999; **340**: 858-868

9 **Anderson AS**, Krauss D, Lang R. Cardiovascular complications of malignant carcinoid disease. *Am Heart J* 1997; **134**: 693-702

10 **Vinik AI**, Thompson N, Eckhauser F, Moattari AR. Clinical features of carcinoid syndrome and the use of somatostatin analogue in its management. *Acta Oncol* 1989; **28**: 389-402

11 **Onaitis MW**, Kirshbom PM, Hayward TZ, Quayale FJ, Feldman JM, Seigler HF, Tyler DS. Gastrointestinal Carcinoids: Characterization by site of origin and hormone production. *Ann Surg* 2000; **232**: 549-556

12 **Varshney S,** Johnson CD. Neuroendocrine tumors of the pancreas. *Indian J Gastroenterol* 2000; **19**: 181-183

13 **Jensen RT**. Pancreatic endocrine tumors: recent advances. *Ann Oncol* 1999; **10**: 170-176

Edited by Wang XL and Xu JY **Proofread by** Xu FM

• LETTERS@WJGNET.COM •

Regulation of plasma erythropoietin in chronic liver disease

Frank Tacke, Tom Luedde, Michael P. Manns, Christian Trautwein

Frank Tacke, Tom Luedde, Michael P. Manns, Christian Trautwein, Department of Gastroenterology, Hepatology and Endocrinology, Hannover Medical School 30625 Hannover, Germany
Correspondence to: Christian Trautwein, M.D., Professor of Medicine, Hannover Medical School, Department of Gastroenterology, Hepatology and Endocrinology, Carl-Neuberg-Strasse 1, D-30625, Hannover, Germany. trautwein.christian@mh-hannover.de
Telephone: +49-511-5326620 **Fax:** +49-511-5324896
Received: 2004-05-25 **Accepted:** 2004-06-22

Tacke F, Luedde T, Manns MP, Trautwein C. Regulation of plasma erythropoietin in chronic liver disease. *World J Gastroenterol* 2004; 10(19): 2922
http://www.wjgnet.com/1007-9327/10/2922.asp

To the Editor:

In a May-issue of the *World Journal of Gastroenterology*, there is a very interesting study by Bruno *et al*. on erythropoietin (EPO) levels in patients with chronic liver disease[1]. We have very recently reported a similar, but much larger study by Tacke *et al.*[2] on the role of EPO in chronic liver disease. By comparing Bruno's results with our patient cohort and applying their criteria in a re-evaluation of our study population, we uncovered interesting differences between the two studies and could answer some of the key questions in the article raised by Bruno *et al*., e.g. on the correlation of EPO with liver dysfunction and potential regulating factors in the clinical setting of liver cirrhosis.

Therefore, we would like to briefly present our data and compare the results with Bruno's recent study. We think the role of EPO is important in the pathophysiology of chronic liver disease, and the recent studies provided new insights into its regulation in liver cirrhosis.

Chronic anemia is a common clinical complication in patients with liver cirrhosis and is regarded as an important prognostic factor[3]. The great progress in the understanding of cytokine alterations in chronic liver diseases as well as the discovery and clinical application of different hematopoietic growth factors have raised attention to the potential pathophysiological role of erythropoietin (EPO) in liver diseases[4,5]. In a recent issue of the World Journal of Gastroenterology, Bruno *et al.* reported that increased EPO plasma levels were only detected in cirrhotic patients with hemoglobin concentrations below 12 g/dL and that this EPO response was inadequate compared to patients with iron-deficiency anemia[1]. Furthermore, the authors did not observe an association between EPO levels and the stage of liver cirrhosis or liver synthesis function. The regulating factors in the pathophysiological setting of advanced liver diseases as well as possible clinical consequences remained an open question.

We analyzed 111 patients with chronic liver diseases who were evaluated for potential liver transplantation and 220 healthy (non-anemic) controls with the same EPO ELISA (R&D Systems, Wiesbaden, Germany) kit. In contrast to Bruno *et al.* who studied mainly patients with viral hepatitis and advanced stages of cirrhosis, our much larger cohort comprised all Child's stages of cirrhosis in a fairly equal number of patients as well as different etiology subgroups. As we reported recently, EPO plasma levels clearly increased with Child's stage of liver cirrhosis, independent of the disease etiology (Figure 1)[2]. EPO also correlated directly with the markers of liver synthesis function, e.g. cholinesterase activity (r = -0.448, P<0.001), albumin concentration (r = -0.358, P<0.001), or prothrombin time (r = 0.300, P = 0.001). Interestingly, the absolute values of measured EPO levels in Bruno *et al*. and our studies were relatively similar (e.g. mean EPO 11.6 U/L for chronic hepatitis by Bruno *et al*., median EPO 11.3 U/L for our "non cirrhosis" group), thereby raising the question whether the clear association between EPO and stage of liver cirrhosis could have been observed if the number of patients included in Bruno *et al*. study was high enough. Furthermore, it is hard to believe that EPO was normally distributed in anemic or non-anemic cirrhotic patients as the mean±SD values suggested by Bruno *et al*., thus a different statistical analysis using median and *U*-test could possibly uncover these important correlations.

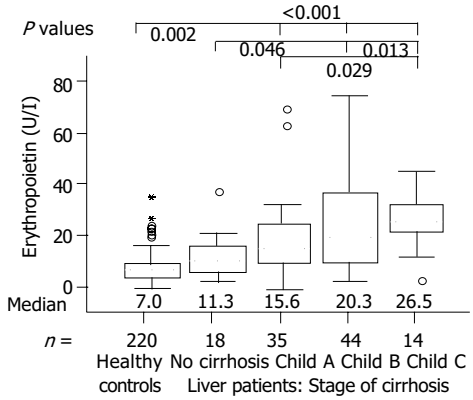

Figure 1 Erythropoietin plasma levels and stage of cirrhosis. EPO was significantly higher in patients with liver cirrhosis than in healthy controls and increased with Child's stages of cirrhosis.

We also found a significant inverse correlation between EPO levels and hemoglobin in patients with chronic liver diseases (r = -0.498, P<0.001, Spearman rank correlation analysis). As this was described by Bruno *et al.* only for patients with iron-deficiency anemia, this correlation could not be observed when we divided our liver disease patient group by the criteria of Bruno *et al*. into so-called anemic or non-anemic patients (hb$\leqslant$12, n = 48, *vs* hb>120 g/L, n = 63). However, in accordance with Bruno *et al.*, we also found significantly elevated EPO levels in anemic *vs* non-anemic liver disease patients (median EPO 29.3 *vs* 11.4 U/L, P<0.001, U-test). In contrast, the non-anemic liver disease patients also had elevated EPO levels as compared with controls (P<0.05), which could be possibly explained by the much larger control group in our study.

In further investigating the potential regulating factors, one should consider the complex clinical picture of advanced liver cirrhosis. As we could show, the degrees of anemia and liver dysfunction not only were independent parameters associated with elevated EPO in chronic liver disease, but also impaired pulmonary function[2]. Changes in pulmonary function test and blood gas analysis were commonly found in our study population, and EPO was inversely correlated with carbon dioxide tension (pCO_2) and elevated in patients with reduced (carbon monoxide) diffusion capacity. In addition, we noticed a positive correlation between interleukin-6 and EPO, thereby possibly linking the EPO response to a common protective cytokine response usually seen in liver cirrhosis[6].

In conclusion, the recent studies by Bruno *et al.* and our group provide some new important insights in the regulation of plasma EPO in chronic liver diseases. EPO plasma levels are apparently upregulated in patients with liver cirrhosis, and one might speculate whether this increase is sufficient in the setting of chronic anemia when compared with other forms of anemia,

e.g. iron-deficiency. However, the regulation of plasma EPO is complex and multifactorial, and the degrees of anemia, liver dysfunction, impaired pulmonary function and cytokine alterations are the major factors in regulating plasma erythropoietin in patients with chronic liver diseases.

REFERENCES

1 **Bruno CM**, Neri S, Sciacca C, Bertino G, Di Prima P, Cilio D, Pellicano R, Caruso L, Cristaldi R. Plasma erythropoietin levels in anaemic and non-anaemic patients with chronic liver diseases. *World J Gastroenterol* 2004; **10**: 1353-1356

2 **Tacke F**, Schoffski P, Luedde T, Meier PN, Ganser A, Manns MP, Trautwein C. Analysis of factors contributing to higher erythropoietin levels in patients with chronic liver disease. *Scand J Gastroenterol* 2004; **39**: 259-266

3 **Orrego H**, Israel Y, Blake JE, Medline A. Assessment of prognostic factors in alcoholic liver disease: toward a global quantitative expression of severity. *Hepatology* 1983; **3**: 896-905

4 **Pirisi M,** Fabris C, Falleti E, Soardo G, Toniutto P, Gonano F, Bartoli E. Evidence for a multifactorial control of serum erythropoietin concentration in liver disease. *Clin Chim Acta* 1993; **219**: 47-55

5 **Yang YY**, Lin HC, Lee WC, Huang YT, Hou MC, Lee FY, Chang FY, Lee SD. Plasma erythropoietin level in patients with cirrhosis and its relationship to the severity of cirrhosis and renal function. *J Gastroenterol Hepatol* 2003; **18**: 1156-1161

6 **Streetz KL**, Tacke F, Leifeld L, Wustefeld T, Graw A, Klein C, Kamino K, Spengler U, Kreipe H, Kubicka S, Muller W, Manns MP, Trautwein C. Interleukin 6/gp130-dependent pathways are protective during chronic liver diseases. *Hepatology* 2003; **38**: 218-229

Edited by Xu XQ, Wang XL and Zhang JZ

• LETTERS@WJGNET.COM •

Comment on "Eosinophilic gastroenteritis: Clinical experience with 15 patients"

Peter J Kerr

Peter J Kerr, BEng (Hons) CEng, MIEE, MIMechE
Correspondence to: Mr Peter J Kerr, 6 Middledyke Lane, Cottingham, East Yorkshire, HU16 4NH, United Kingdom. pkerr@pkerr.karoo.co.uk
Telephone: +44-1482-847201 **Fax:** +44-1482-847201
Received: 2004-06-15 **Accepted:** 2004-06-22

Kerr PJ. Comment on "Eosinophilic gastroenteritis: Clinical experience with 15 patients". *World J Gastroenterol* 2004; 10(19): 2923
http://www.wjgnet.com/1007-9327/10/2923.asp

To the Editor:

I recently read the paper by Chen *et al*.[1] published in your Journal. The paper shows that there have been a few cases where medications have caused eosinophilia. Clozapine is an antipsychotic medication that can cause eosinophilia. It is pointed out in your paper "The diagnostic criteria included . . . 5), exclusion of intestinal lymphoma, Crohn's disease or other tumors." Table 2 shows symptoms associated with eosinophilic gastroenteritis, which are very like those in Crohn's disease.

Miss Z, a 29 years old female received a diagnosis of Crohn's disease five years ago. It seemed to be the more aggressive fistulizing form of Crohn's disease. The inflammation seemed to be located in her colon. She had several perianal abscesses. Miss Z took the antipsychotic, clozapine. Clozapine can cause constipation, diarrhea[2-7], nausea[6,8], vomiting[3,6,8], allergic reactions, *etc*. Clozapine has also been linked with colitis[5,14], gastrointestinal symptoms[7], hepatotoxicity[12], eosinophilia[5,7,9], neutropenia[5,6], colon perforation[13], necrotizing colitis[13], perianal abscesses[9], and increased levels of TNF-alpha[10], *etc*.

When Miss Z was growing up, she had no prodromal symptoms that, even with the benefit of hindsight one might be able to say, this was the beginning of Crohn's disease. The sickness and diarrhea started 32 d after the clozapine was titrated to its full dose of 300 mg/d in November 1998.

Tumor necrosis factor α (TNF α) is a proinflammatory cytokine that has an important role in the pathogenesis of Crohn's disease. Infliximab-a chimeric anti-TNF α monoclonal antibodybinds to TNF α with high affinity, thereby neutralising its biological activity. Pollmacher *et al*.[10], found that clozapine significantly increased the plasma levels of TNF-alpha.

Miss Z responded very well to infliximab. Steroids (prednisolone) had little effect on the symptoms. Stopping clozapine was not an option unless we were to be reasonably sure that it was responsible for causing or exacerbating the inflammation in Miss Z's colon.

I am particularly interested in the effect of clozapine. If it were to cause eosinophilia it might have effects on the colon. I wondered if the symptoms of nausea, vomiting, *etc*, might persist all the time when clozapine was taken.

REFERENCES

1 **Chen MJ**, Chu CH, Lin SC, Shih SC, Wang TE. Eosinophilic gastroenteritis: Clinical experience with 15 patients. *World J Gastroenterol* 2003; **9**: 2813-2816

2 **Harvey RJ**, Bullock T, Montgomery SA. Diarrhoea during treatment with clozapine: association with lymphocyte count. *BMJ* 1992; **305**: 810

3 **Patterson BD**, Jennings JL. Spiking fever and profuse diarrhea with clozapine treatment. *American J Psychiatry* 1993; **150**: 1126

4 **Druss BG,** Mazure CM. Transient fever and hematologic abnormalities during clozapine use. *J Clin Psychopharmacol* 1993; **13**: 155-156

5 **Lucht MJ**, Rietschel M. Clozapine-induced eosinophilia: subsequent neutropenia and corresponding allergic mechanisms. *J Clin Psychiatry* 1998; **59**: 195-197

6 **Beck DA**, Miller DD. Clozapine-associated neutropenic enterocolitis. *Ann Clin Psychiatry* 1994; **6**: 185-188

7 **Galletly C**, Wilson D, McEwen S. Eosinophilia associated with decreasing neutrophil count in a clozapine treated patient. *J Clin Psychiatry* 1996; **57**: 40-41

8 **Maria DD**. Clozapine-induced gastrointestinal symptoms. Llorente, Annual Meeting - American Psychiatric Association. *New Research Abstracts* 1997; **150**: 132

9 **Amital D**, Gross R, Amital H, Zohar I. Coexistence of eosinophilia and agranulocytosis in a clozapine treated patient. *British J Psychiatry* 1997; **170**: 194

10 **Pollmacher T**, Hinze-Selch D, Mullington J. Effects of clozapine on plasma cytokine and soluble cytokine receptor levels. *J Clin Psychopharmacol* 1996; **16**: 403-409

11 **John JP,** Chengappa KN, Baker RW, Gupta B, Mortimer MT. Assessment of changes in both weight and frequency of use of medications for the treatment of gastrointestinal symptoms among clozapine-treated patients. *Ann Clin Psychiatry* 1995; **7**: 119-125

12 **Macfarlane B**, Davies S, Mannan K, Sarsam R, Pariente D, Dooley J. Fatal acute fulminant liver failure due to clozapine: a case report and review of clozapine-induced hepatotoxicity. *Gastroenterology* 1997; **112**: 1707-1709

13 **Freudenreich O**, Goff DC. Colon perforation and peritonitis associated with clozapine. *J Clin Psychiatry* 2000; **61**: 950-951

14 **Friedberg JW**, Frankenburg FR, Burk J, Johnson W. Clozapine-caused eosinophilic colitis. *Ann Clin Psychiatry* 1995; **7**: 97-98

Edited by Xu XQ, Wang XL and Zhang JZ

e.g. iron-deficiency. However, the regulation of plasma EPO is complex and multifactorial, and the degrees of anemia, liver dysfunction, impaired pulmonary function and cytokine alterations are the major factors in regulating plasma erythropoietin in patients with chronic liver diseases.

REFERENCES

1 **Bruno CM**, Neri S, Sciacca C, Bertino G, Di Prima P, Cilio D, Pellicano R, Caruso L, Cristaldi R. Plasma erythropoietin levels in anaemic and non-anaemic patients with chronic liver diseases. *World J Gastroenterol* 2004; **10**: 1353-1356

2 **Tacke F**, Schoffski P, Luedde T, Meier PN, Ganser A, Manns MP, Trautwein C. Analysis of factors contributing to higher erythropoietin levels in patients with chronic liver disease. *Scand J Gastroenterol* 2004; **39**: 259-266

3 **Orrego H**, Israel Y, Blake JE, Medline A. Assessment of prognostic factors in alcoholic liver disease: toward a global quantitative expression of severity. *Hepatology* 1983; **3**: 896-905

4 **Pirisi M,** Fabris C, Falleti E, Soardo G, Toniutto P, Gonano F, Bartoli E. Evidence for a multifactorial control of serum erythropoietin concentration in liver disease. *Clin Chim Acta* 1993; **219**: 47-55

5 **Yang YY**, Lin HC, Lee WC, Huang YT, Hou MC, Lee FY, Chang FY, Lee SD. Plasma erythropoietin level in patients with cirrhosis and its relationship to the severity of cirrhosis and renal function. *J Gastroenterol Hepatol* 2003; **18**: 1156-1161

6 **Streetz KL**, Tacke F, Leifeld L, Wustefeld T, Graw A, Klein C, Kamino K, Spengler U, Kreipe H, Kubicka S, Muller W, Manns MP, Trautwein C. Interleukin 6/gp130-dependent pathways are protective during chronic liver diseases. *Hepatology* 2003; **38**: 218-229

Edited by Xu XQ, Wang XL and Zhang JZ

• LETTERS@WJGNET.COM •

Comment on "Eosinophilic gastroenteritis: Clinical experience with 15 patients"

Peter J Kerr

Peter J Kerr, BEng (Hons) CEng, MIEE, MIMechE
Correspondence to: Mr Peter J Kerr, 6 Middledyke Lane, Cottingham, East Yorkshire, HU16 4NH, United Kingdom. pkerr@pkerr.karoo.co.uk
Telephone: +44-1482-847201 **Fax:** +44-1482-847201
Received: 2004-06-15 **Accepted:** 2004-06-22

Kerr PJ. Comment on "Eosinophilic gastroenteritis: Clinical experience with 15 patients". *World J Gastroenterol* 2004; 10(19): 2923
http://www.wjgnet.com/1007-9327/10/2923.asp

To the Editor:

I recently read the paper by Chen *et al*.[1] published in your Journal. The paper shows that there have been a few cases where medications have caused eosinophilia. Clozapine is an antipsychotic medication that can cause eosinophilia. It is pointed out in your paper "The diagnostic criteria included . . . 5), exclusion of intestinal lymphoma, Crohn's disease or other tumors." Table 2 shows symptoms associated with eosinophilic gastroenteritis, which are very like those in Crohn's disease.

Miss Z, a 29 years old female received a diagnosis of Crohn's disease five years ago. It seemed to be the more aggressive fistulizing form of Crohn's disease. The inflammation seemed to be located in her colon. She had several perianal abscesses. Miss Z took the antipsychotic, clozapine. Clozapine can cause constipation, diarrhea[2-7], nausea[6,8], vomiting[3,6,8], allergic reactions, *etc*. Clozapine has also been linked with colitis[5,14], gastrointestinal symptoms[7], hepatotoxicity[12], eosinophilia[5,7,9], neutropenia[5,6], colon perforation[13], necrotizing colitis[13], perianal abscesses[9], and increased levels of TNF-alpha[10], *etc*.

When Miss Z was growing up, she had no prodromal symptoms that, even with the benefit of hindsight one might be able to say, this was the beginning of Crohn's disease. The sickness and diarrhea started 32 d after the clozapine was titrated to its full dose of 300 mg/d in November 1998.

Tumor necrosis factor α (TNF α) is a proinflammatory cytokine that has an important role in the pathogenesis of Crohn's disease. Infliximab-a chimeric anti-TNF α monoclonal antibodybinds to TNF α with high affinity, thereby neutralising its biological activity. Pollmacher *et al*.[10], found that clozapine significantly increased the plasma levels of TNF-alpha.

Miss Z responded very well to infliximab. Steroids (prednisolone) had little effect on the symptoms. Stopping clozapine was not an option unless we were to be reasonably sure that it was responsible for causing or exacerbating the inflammation in Miss Z's colon.

I am particularly interested in the effect of clozapine. If it were to cause eosinophilia it might have effects on the colon. I wondered if the symptoms of nausea, vomiting, *etc*, might persist all the time when clozapine was taken.

REFERENCES

1 **Chen MJ**, Chu CH, Lin SC, Shih SC, Wang TE. Eosinophilic gastroenteritis: Clinical experience with 15 patients. *World J Gastroenterol* 2003; **9**: 2813-2816

2 **Harvey RJ**, Bullock T, Montgomery SA. Diarrhoea during treatment with clozapine: association with lymphocyte count. *BMJ* 1992; **305**: 810

3 **Patterson BD**, Jennings JL. Spiking fever and profuse diarrhea with clozapine treatment. *American J Psychiatry* 1993; **150**: 1126

4 **Druss BG,** Mazure CM. Transient fever and hematologic abnormalities during clozapine use. *J Clin Psychopharmacol* 1993; **13**: 155-156

5 **Lucht MJ**, Rietschel M. Clozapine-induced eosinophilia: subsequent neutropenia and corresponding allergic mechanisms. *J Clin Psychiatry* 1998; **59**: 195-197

6 **Beck DA**, Miller DD. Clozapine-associated neutropenic enterocolitis. *Ann Clin Psychiatry* 1994; **6**: 185-188

7 **Galletly C**, Wilson D, McEwen S. Eosinophilia associated with decreasing neutrophil count in a clozapine treated patient. *J Clin Psychiatry* 1996; **57**: 40-41

8 **Maria DD**. Clozapine-induced gastrointestinal symptoms. Llorente, Annual Meeting - American Psychiatric Association. *New Research Abstracts* 1997; **150**: 132

9 **Amital D**, Gross R, Amital H, Zohar I. Coexistence of eosinophilia and agranulocytosis in a clozapine treated patient. *British J Psychiatry* 1997; **170**: 194

10 **Pollmacher T**, Hinze-Selch D, Mullington J. Effects of clozapine on plasma cytokine and soluble cytokine receptor levels. *J Clin Psychopharmacol* 1996; **16**: 403-409

11 **John JP,** Chengappa KN, Baker RW, Gupta B, Mortimer MT. Assessment of changes in both weight and frequency of use of medications for the treatment of gastrointestinal symptoms among clozapine-treated patients. *Ann Clin Psychiatry* 1995; **7**: 119-125

12 **Macfarlane B**, Davies S, Mannan K, Sarsam R, Pariente D, Dooley J. Fatal acute fulminant liver failure due to clozapine: a case report and review of clozapine-induced hepatotoxicity. *Gastroenterology* 1997; **112**: 1707-1709

13 **Freudenreich O**, Goff DC. Colon perforation and peritonitis associated with clozapine. *J Clin Psychiatry* 2000; **61**: 950-951

14 **Friedberg JW**, Frankenburg FR, Burk J, Johnson W. Clozapine-caused eosinophilic colitis. *Ann Clin Psychiatry* 1995; **7**: 97-98

Edited by Xu XQ, Wang XL and Zhang JZ

tinal dysfunction. *World J Gastroenterol* 2004; **10**: 875-880
2 **Reeve JR Jr**, Green GM, Chew P, Eysselein VE, Keire DA. CCK-58 is the only detectable endocrine form of cholecystokinin in rat. *Am J Physiol Gastrointest Liver Physiol* 2003; **285**: G255-G265
3 **Paloheimo PI**, Clemmesen O, Dalhoff O, Dalhoff K, Rehfeld JF. Plasma cholecystokinin and its precursors in hepatic cirrhosis. *J Hepatol* 1997; **27**: 299-305
4 **Xiao R**, Cui ZJ. Mutual dependence of VIP/PACAP and CCK receptor signaling for a physiological role in duck exocrine pancreatic secretion. *Am J Physiol Regul Integr Comp Physiol* 2004; **286**: R189-R198

Edited by Xu XQ, Wang XL and Zhang JZ

• LETTERS@WJGNET.COM •

Plagiarized and inaccurate papers in the *World Journal of Gastroenterology*

Thomas E. Adrian

Thomas E. Adrian, Northwestern University Feinberg School of Medicine, 303 E. Chicago Avenue, Tarry 4-711, Chicago, IL 60611, USA
Correspondence to: Professor Thomas E. Adrian, Edward Elcock Professor of Surgical Research, Northwestern University Feinberg School of Medicine, 303 E. Chicago Avenue, Tarry 4-711, Chicago, IL 60611, USA. tadrian@northwestern.edu
Telephone: +1-312-503 3493 **Fax:** +1-312-503 3491
Received: 2004-04-24 **Accepted:** 2004-06-22

Adrian TE. Plagiarized and inaccurate papers in the *World Journal of Gastroenterology*. *World J Gastroenterol* 2004; 10(19): 2925
http://www.wjgnet.com/1007-9327/10/2925.asp

To the Editor:

I was astonished to find this paper [Dong ML, Ding XZ, Collin P, Adrian TE. Red oil A5 inhibits proliferation and induces apoptosis in pancreatic cancer cells. *World J Gastroenterol* 2004; 10(1): 105-111] published in your journal. This has been done without my knowledge or the other coauthor, Dr. Ding. There are numerous errors. These include (1) the exclusion of an important collaborating contributor; (2) the appearance that the work was carried out in China, when it was actually carried out at Northwestern University in Chicago; (3) an incorrect name for the compound being used; (4) an incorrect company name where the compound originated from. The following are the correct information. The authors list should be: Dong ML[1], Ding XZ[1], Collin P[2], Adrian TE[1]. The title should have been: CR-A5 inhibits proliferation and induces apoptosis in pancreatic cancer cells (the term oil A5 is meaningless; the product is called CR-A5). The address where the work was carried out was: [1]"Department of Surgery and Robert H. Lurie Comprehensive Cancer Center, Northwestern Feinberg School of Medicine, Chicago, IL" and [2]"Coastside Research, Stonington, Maine". The funding sources that should have been acknowledged were: The American Institute of Cancer Research, the RAPID Program of the RAPID Program of the Chemoprevention Branch fo the National Cancer Institute, the Michael Rolfe Foundation and the Maine Technology Institute. Dr. Dong did carry out this work in my laboratory with the help of others, however, we never discussed where the work would be published and I certainly did not sanction its publication in your journal. I consider what Dr. Dong has done to be dishonest. Most journals require the signature of all authors before a paper can be accepted for publication, this would be a good policy for the World Journal of Gastroenterology to adopt. More seriously, regarding Dr. Dong, I have now found another paper that he has published in your journal [Dong ML, Zhu YC, Hopkins JV. Oil A induces apoptosis of pancreatic cancer cells via caspase activation, redistribution of cell cycle and GADD expression. *World J Gastroenterol* 2003; (9): 2745-2750]. Again this paper was published without my knowledge. The other authors are unknown to me and the name John V. Hopkins appears to have been fabricated. The contents of this paper have been almost entirely plagiarized from a previous publication from a Medical Oncologist, Dr. Xin-Quan Li who worked in my laboratory and Xian-Zhong Ding in the laboratory (Li X, Ding XZ, Adrian TE. Aresenic trioxide induces apoptosis in pancreatic cancer cells via changes in cell cycle, caspase activation, and GADD expression. Pancreas 27: 174-179, 2003). More disturbingly, at least some of the data have clearly been fabricated. The data in Figure 5 of the *World Journal of Gastrorenterology* paper have been entirely lifted from the arsenic trioxide data in Figures 6 and 7 in the Pancreas paper. Please find the enclosed MS Powerpoint file where I have indicated the stolen data in red. Furthermore, careful perusal of the data in Figures 3 and 7 has been assembled in the computer by cutting and pasting sections from different gels. Since some of the data have clearly been fabricated this sheds doubt on all of the other findings in the manuscript. I never saw the raw data for most of these experiments and doubt that they were ever performed. I request that this paper is immediately retracted from the journal with an explanation published. I am sure you will want to do this for the integrity of the journal. An internal committee will be set up at Northwestern University to investigate this matter. I will attempt to contact the Dean of Wenzhou Medical College to inform him of this situation with one of his faculty. Since my NIH grant number was also copied onto the WJG paper, I am informing the NIH of this matter. Please let me know if I should inform your editorial board of what has happened. Finally, as you have requested, I state that the contents of this letter represent my viewpoints rather than those of the journal.

Apology to Dr. Thomas E. Adrian

After we received the letter of Dr Thomas E. Adrian, Dr Mi-Lian Dong wrote a letter for Dr Thomas E. Adrian and the following is the statement from Dr Mi-Lian Dong (the letter was provided by Dr. Thomas E. Adrian). Statement from Dr Mi-Lian Dong for Dr Thomas E. Adrian. From: Mi-Lian Dong (mdong2@hotmail.com). Sent: Monday, June 28, 2004 8:54 AM. To: tadrian@northwestern.edu. Subject: Dear Dr. Thomas Adrian, I don't know how to start this letter, but I have to face it. I can imagine your anger and your disappointment for my unacceptable behavior. I feel very sorry and apologize for what stupid things I did. When I was in Chicago, my former supervisor-Dr. White from Lutheran General Hospital, a very nice gentleman, took care of me and introduced me to your lab. In your Lab, you and Dr. Ding trained me and I learned a lots new stuff, some I never heard before as a clinician in China. I believe I worked very hard and did my best in your lab to repay your generous help. I never forget those wonderful days. But now, I destroyed all those wonderful memories. Dr. Thomas Adrian, I already sent a letter to the journal to ask them to remove that article. Such stupid things never happened in my 40 years life. I cannot sleep well and cannot focus my daily work as a busy doctor. I took a few days off. I believe I got punishment from this, but I accept it. It is unforgettable lesson for my future life. But now, besides sorry and regret, I really don't know what else I can do. Again, I apologize for what I did. Sincerely, Mi-Lian Dong.

Edited by Xu XQ, Zhang JZ and Wang XL